Giusy Lofrano · Giovanni Libralato
Jeanette Brown *Editors*

Nanotechnologies for Environmental Remediation

Applications and Implications

Springer

Nanotechnologies for Environmental Remediation

giovanni.libralato@unina.it

Giusy Lofrano · Giovanni Libralato
Jeanette Brown
Editors

Nanotechnologies for Environmental Remediation

Applications and Implications

Springer

giovanni.libralato@unina.it

Editors
Giusy Lofrano
Department of Chemistry and Biology
University of Salerno
Fisciano, Salerno
Italy

Giovanni Libralato
Department of Biology
University of Naples Federico II
Naples
Italy

Jeanette Brown
Department of Civil and Environmental Engineering
Manhattan College
Bronx, NY
USA

ISBN 978-3-319-53161-8 ISBN 978-3-319-53162-5 (eBook)
DOI 10.1007/978-3-319-53162-5

Library of Congress Control Number: 2017930140

© Springer International Publishing AG 2017
This work is subject to copyright. All rights are reserved by the Publisher, whether the whole or part of the material is concerned, specifically the rights of translation, reprinting, reuse of illustrations, recitation, broadcasting, reproduction on microfilms or in any other physical way, and transmission or information storage and retrieval, electronic adaptation, computer software, or by similar or dissimilar methodology now known or hereafter developed.
The use of general descriptive names, registered names, trademarks, service marks, etc. in this publication does not imply, even in the absence of a specific statement, that such names are exempt from the relevant protective laws and regulations and therefore free for general use.
The publisher, the authors and the editors are safe to assume that the advice and information in this book are believed to be true and accurate at the date of publication. Neither the publisher nor the authors or the editors give a warranty, express or implied, with respect to the material contained herein or for any errors or omissions that may have been made. The publisher remains neutral with regard to jurisdictional claims in published maps and institutional affiliations.

Printed on acid-free paper

This Springer imprint is published by Springer Nature
The registered company is Springer International Publishing AG
The registered company address is: Gewerbestrasse 11, 6330 Cham, Switzerland

giovanni.libralato@unina.it

Foreword

Nanotechnology, the science of a few billionths of a meter, is today one of the fastest growing fields in engineering, being considered the emblem of the twenty-first century innovation. In particular, the feverish development of engineered nanoscale materials (NMs) represents a technological revolution for the development of innovative material and new productive sectors at the service of citizens. Because of their high surface area per unit mass and due to a high reactivity NMs that exhibit properties different from those exhibited on macroscale leading to extraordinary properties that enable unique applications. In this context, there is a strong belief that nanotechnology could provide solutions also to a number of environmental challenges including the use of nanosized reactive products to degrade or immobilize contaminants (environmental nanoremediation) by reacting with target contaminants at a faster rate than would larger particles and so leading to marked improvements in efficiency and ecocompatibility compared with conventional techniques. Environmental nanoremediation of various contaminants has been recently reported for the treatment of surface water, groundwater, wastewater, and for soil and sediment cleanup from toxic metal ions, organic and inorganic solutes, and emerging contaminants, such as pharmaceutical and personal care products. One emerging nanotechnology, nanosized zero valent iron and its derivatives, has reached the commercial market for field-scale remediation. Interestingly, nanoremediation technology had been documented in at least more than 40 cleanup sites around the world, predominantly in the United States. Unfortunately, in spite of the great excitement about the potential benefits offered by the introduction of environmental nanoremediation several safety-related questions, e.g. the induction of toxic effects due to uncontrolled release of NMs into the environment, remain unsolved and we must be careful about the potential risk of econanotoxicity.

This book comprises 12 state-of-the-art chapters concerning salient aspects of the use of NMs in environmental applications including nanoremediation and wastewater treatment. It represents a valuable reference source for nanotech industries as well as for practicing scientists, research professionals working in

giovanni.libralato@unina.it

research and development laboratories, graduate students and university professors working in the field of environmental sciences and engineering, ecology, econanotoxicology, public health and environmental control. I hope that it will be of interest not only to the international scientific community but also to the competent authorities and officers entrusted with responsibilities in regulatory issues concerning the environmental risk assessment of NMs.

There is a common feeling that the magnitude of the research effort in the development of environmentally friendly NMs throughout their lifecycle and their potential environmental effects is bound to increase greatly in the coming years. Thus, it is expected that this book will contribute to spur the interest of all those wishing the development of "green nanoproducts" and the application of such nanoproducts in supporting environmental sustainability in the pursuit of scientific and social ends. This book is addressed to everyone who is concerned about the use and the environmental impact of NMs.

Dr. Enrico Sabbioni
CeSI, Aging Research Center,
"G. d'Annunzio" University Foundation, Chieti, Italy

giovanni.libralato@unina.it

Preface

Nanotechnology holds a great potential in advancing water and wastewater treatment general performance boosting water supply through the safe use of unconventional water sources such as treated wastewater. Similarly, nanoremediation could drastically improve subsurface in situ remediation efficiency increasing the contaminant degradation and detoxification and minimizing off-site or ex situ activities.

The aims of developing nano-based techniques and later on technologies to remediate polluted waters, groundwater and soil/sediment are in growing harmony with the principles of Green Chemistry, and more broadly, Green Engineering and Technology. In the book framework, worldwide investigators present and discuss the continuing efforts to better understand the recent development in applying nanoscience, nano-engineering and nanotechnology for environmental remediation.

Candidate nanomaterials, properties and mechanisms that enable the applications, advantages and limitations as compared to existing processes, and barriers and research needs for commercialization are presented in the Chapters "Progress in Nanomaterials Applications for Water Purification"–"The Use of Al and Fe Nanoparticles for the Treatment of Micropollutants". Chapter "Environmental Nanoremediation and Electron Microscopies" will compile aspects related to electron microscopy applied to nanomaterials detection. The application of nanomaterials in photocatalysis processes and as adsorbents is discussed in Chapters "Adsorption and Desorption Properties of Carbon Nanomaterials, the Potential for Water Treatments and Associated Risks"–"Removal of Copper, Iron and Zinc from Soil Washing Effluents Containing Ethylenediaminedisuccinic Acid as Chelating Agent Through Sunlight Driven Nano-TiO_2-Based Photocatalytic Processes", whereas the effect of nanoparticles in the wastewater treatment and activated sludge is discussed in Chapters "Impact of Silver Nanoparticles on Wastewater Treatment" and "Use of Nanoparticles for Reduction of Odorant Production and Improvements in Dewaterability of Biosolids". Chapter "Environmental Effects of nZVI for Land and Groundwater Remediation" will present the environmental effects of nZVI for land remediation. Finally, the risk associated with the presence of nanoparticles in the environment will be evaluated in Chapter "Presence, Behavior and Fate of Engineered Nanomaterials in Municipal Solid Waste Landfills".

giovanni.libralato@unina.it

All chapters include fundamentals of the processes investigated that will offer students, technicians and academicians the opportunity to evaluate and select the technologies that lead to be aware of the risk and benefit related to the application of nanotechnologies for environmental remediation.

Fisciano, Italy — Giusy Lofrano
Naples, Italy — Giovanni Libralato
Bronx, USA — Jeanette Brown
December 2016

giovanni.libralato@unina.it

Contents

giovanni.libralato@unina.it

giovanni.libralato@unina.it

Progress in Nanomaterials Applications for Water Purification

Diana Sannino, Luigi Rizzo and Vincenzo Vaiano

Abstract The exploration on nanomaterials and their fascinating and enhanced properties has implicated the focusing on their applications embracing a wide range of processes on nanometer scale. In this perspective, nanotechnology in water treatment applications is offering and presenting now new approaches to overcome the limitations of the traditional treatment technologies. This chapter describes several types of nanomaterials that could be used in wastewater treatment underlining their advantages with respect the traditional systems.

Keywords Nanomaterials · Wastewater treatment · Innovative systems

1 Introduction

Nanomaterials have been synthesized and applied in scientific and technological fields since the end of 19th century. Nanomaterials and nanotechnologies investigations date back to 1989 when new instrumentations, like Scanning Tunneling microscope, lead to deep knowledge of "nanodimensions" of the materials. Subsequently several nanomaterials were introduced in medicine, biotechnology, computer science, and space exploration. Additionally, innovative nanotechnology materials and processes have contributed to the development of chemical industry through new nano-catalysts and products.

D. Sannino (✉) · V. Vaiano
Department of Industrial Engineering, University of Salerno,
Via Giovanni Paolo II, 132, 84084 Fisciano, SA, Italy
e-mail: dsannino@unisa.it

L. Rizzo
Department of Civil Engineering, University of Salerno,
via Giovanni Paolo II, 132, 84084 Fisciano, SA, Italy

© Springer International Publishing AG 2017

G. Lofrano et al. (eds.), *Nanotechnologies for Environmental Remediation*,
DOI 10.1007/978-3-319-53162-5_1

giovanni.libralato@unina.it

Nanoscale materials are classified with respect to their characteristic length scale, whose dimensions are in the nanometric range, starting from 1 nm up to several hundred nanometers. However the actual definition identifies nanomaterials as those having at least one size between 0 and 100 nm. According to Siegel,[1] nanostructured materials are classified as zero dimensional, one dimensional, two dimensional, three dimensional nanostructures.

From the start of the nanotechnology age, the exploration of nanomaterials and their fascinating and enhanced properties has focused on their applications; embracing a wide range of processes on nanometer scale, and becoming an "enabling key technology" of the century. Nanoscale properties also include "nanostructure induced effects" that can be found on electronic structures depending on size. Moreover the surface or interface induced effects are extremely favored by increased specific surface area. Due to the nanoscale, a particle system imparts an increase in the chemical reactivity and/or a change to the physical properties of the material.[2]

Nanotechnology development has brought a high level of innovation in the environmental sector.[3] Nanomaterials show interesting chemical and physical properties that make them suitable for several applications in the environmental field. The application of nanotechnology in solving different environmental issues in water/wastewater treatment through the transformation and detoxification of a wide range of contaminants like PCBs, heavy metals, organochlorine pesticides and solvents[4] has been well documented.

Nanomaterials typically investigated in water/wastewater treatment are iron-based nanoparticles, at different oxidation states, such as nanoscale zero-valent iron and magnetite (Fe_3O_4), metal, and metal oxide engineered nanomaterials that include other oxides such as TiO_2, Ag and ZnO. In addition, the recent production of nanomaterials at industrial scale has encouraged the development of new technologies based on them. In particular, carbon based nanomaterials, largely available now o at lower costs than that in the past, are under intensive investigation for their applications in water purification and environmental remediation.

The purpose of this chapter is to focus on the most interesting nanomaterials for use in the environmental field and present nanotechnologies that have high potential impact on innovation for water treatment technologies.

[1]Siegel (1994).

[2]Tang et al. (2013).

[3]Bavasso et al. (2016).

[4]OECD Report, Opportunities and risks of Nanotechnologies, www.oecd.org/science/nanosafety/37770473.pdf, Stevens and George (2005).

giovanni.libralato@unina.it

2 Metal Nanoparticles in Water Treatment/Environmental Remediation

One of the most applied nanomaterials is nanoscale zero-valent iron (nZVI),[5,6,7] due to its low toxicity and potential for environmental remediation. An large number of studies have demonstrated the efficacy of nano zero valent iron in groundwater remediation, in the reductive degradation of organic compounds, in the removal of poly-chlorinated compounds,[8,9,10] and as a high surface area adsorbent for hex-avalent Cr and potentially other heavy metals. Nano-ZVI acts as an electron donor, and promotes the transformation of high valence metals to nontoxic forms. Further abilities of these materials lie in the combined chemical transformation with adsorption and co-precipitation processes, resulting in the removal of contaminants present in low concentrations. Nano-ZVI has also shown effective in removing contaminants such as nitrates, phosphates and perchlorates[11] from groundwater.

The addition of functional groups to nZVI results in selectivity towards certain pollutants (or stabilization with organic compounds is achieved). Another nZVI modification which also enhances their ability to target contaminants is the coupling with further metals, yielding bimetallic nZVI nanoparticles. This is done by alloying or deposition of a second metal, especially noble metals like Pd or Pt, which have been demonstrated to significantly increase the nZVI degradation rate of contaminants.

nZVI has shown high efficacy in the removal of uranium in water, typically as UO_2^{2+} from both natural origin or industrial activities like mining. Crespi et al., reported 65% removal of U (VI) by nZVI.[12] Uranium removal from water is a function of the presence of dissolved oxygen, which reduces the removal action of nZVI. As a consequence these nanoparticles are a promising technology for the remediation of ground water, having very low level of solubilized oxygen.

Combined technologies (nZVI and bacteria) for the treatment of persistent and toxic halogenated organic compounds, have shown positive results. A sequential nano-bio treatment using nZVI and diphenyl ether-degrading bacteria was successfully used in the degradation of polybrominated diphenyl ethers (PBDEs), avoiding the formation of toxic byproducts,[13] and resulting in the formation of

[5]Mueller et al. (2012).
[6]Karn et al. (2009).
[7]Lacinova et al. (2012).
[8]Zhang (2003).
[9]Amin et al. (2014).
[10]Ghasemzadeh et al. (2014).
[11]Rajan (2011).
[12]Crespi et al. (2016).
[13]Kim et al. (2012).

giovanni.libralato@unina.it

bromophenols and other less toxic intermediates. At the same time, nZVI can be applied in water treatment under near anoxic conditions.

However, efforts to improve nZVI nanoparticles characteristics center on the limitation of their aggregation and stabilization to allow both maintaining reactivity during application and reducing treatment time. Due to strong attractive interparticle forces, nZVI tend to increase in size, yielding agglomeration up to the formation of micron size particles, resulting in limited mobility in porous media.[14] Coatings with organic compounds or various polymers can stabilize their size and dispersion.

Other types of nanometals can be used for water disinfection. The ability of silver compounds to inactivate microbes is well known and silver nanoparticles have found wide application in nanoengineering. Nanosilver disinfection works in different ways, by interactions with DNA, changing the membrane characteristic adhering to their surfaces, giving rise to the formation of reactive oxygen species or radicals able to damage the external walls of the biocells, and altering the enzymatic activity.[15,16,17,18] The low toxicity and the effectiveness in microbial inactivation in contaminated water are enhanced by regulating and controlling the size of the nanoparticles. In fact, higher antibacterial effect is shown by nanoparticles below the 10 nm compared to the larger ones (e.g., 11–20 nm). Moreover their morphology also plays a relevant role[19] in terms of antibacterial effect; for example rope-shaped silver nanoparticles are less effective compared to truncated triangular shaped nanosilver plates.[20] Silver nanoparticles are mostly derived from the reduction of aqueous soluble salts by reduction or photo reduction. Nanosilver embedded in polymers has been demonstrated to preserve the antibacterial properties so different nanocomposites have been developed. Nanosilver-fiber composites with polycaprolattone, polyurethane and cellulose acetate are very effective in the inactivation of Gram positive and negative bacteria.[21] Good nanoparticle dispersion in polyurethane foam can be obtained, yielding effective antibacterial filters.[22,23,24] When inserted in polymeric membranes, a reduction of biofouling as well as good pathogen removal efficiency is observed. Nanosilver is also used in the production of low-cost microfilters for producing potable water which is especially needed in remote areas.[25]

[14]O'Carroll et al. (2013).
[15]Kim et al. (2007).
[16]Xiu et al. (2011).
[17]Liau et al. (1997).
[18]Danilczuk et al. (2006).
[19]Pal et al. (2007).
[20]Makhluf et al. (2005).
[21]Morones et al. (2005).
[22]Balogh et al. (2001).
[23]Chen et al. (2003).
[24]Botes and Cloete (2010).
[25]Peter-Varbanets et al. (2009).

giovanni.libralato@unina.it

Expensive precious metal nanoparticles have been proposed for water treatment applications. An example is given by Pd nanoparticles, but also alloyed Pd nanoparticles with silver showed their efficiency in the trichloroethylene hydrodechlorination.[26] However the potential applications in the water treatment are limited considering the high costs of their precursors.

Metal nanoparticles have also been shown to promote activity of heterogeneous photocatalysts in the degradation of a wide range of contaminants, including dyes. The addition of noble nanometals improves the performance of TiO_2 as a wide bandgap semiconductor used in advanced oxidation processes for wastewater. The positive effects of noble metal nanoparticles can be understood when considering that, TiO_2, excited by photons of ultra-bandgap energy, typically energy higher than 3.2 eV belonging to UV range (365 nm), forms electron-hole pairs. These electron-hole pairs can interact with adsorbed species resulting in oxidation and/or reduction reactions, in particular by generating hydroxyls radicals with strong oxidizing power. The generation of electron-hole pairs occurs in femtoseconds, while hundreds of femtoseconds are needed for propagation toward the surface of photogenerated charges. The interaction of photogenerated electron holes pairs with surface species that give rise to oxidation and reduction reactions takes hundreds of picoseconds, so it is much slower, and some of the exciting photon energy harvested is lost due to the recombination of photoholes and photoelectrons as heat.[27] To limit the recombination of the separated charges generated under UV irradiation the presence of a co-catalyst with an electron-withdrawing feature favors the separation of photo induced positive and negative charges. The noble metal addition on TiO_2 surface with different metal particle sizes helps to decreases the electron-hole recombination rate, and greatly enhances the efficiency of photocatalysts for the photodegradation reactions of several pollutants.

For TiO_2 photo activity, the overall effect in the promotion of photo removal activity by noble metal addition depends on metal content, metal particle size and oxidation state. Nanometal particles are very suitable in yielding promoted photo activities. Apart from "classical" methods for depositing nanometals on the TiO_2 surface, photochemical deposition of gold and platinum is a viable method to achieve nanodispersed noble metal particles having very low size and good ability to spread on the oxide surface, resulting in lower costs due to a lower required load of noble metals.

Photoreduction of a noble metal precursor, typically a chloride salt or an acid, is conducted under different time and irradiation intensity,[28] resulting in higher photo performances with respect to photocatalysts obtained by chemical reduction of precursors. Furthermore this method allows photocatalysts enhanced with noble nanometals to be obtained directly without further thermal treatment. There are

[26]Han et al. (2016).

[27]Ohtani (2013).

[28]Vaiano et al. (2016).

giovanni.libralato@unina.it

significant differences in nanometal particle sizes and morphology between photocatalysts prepared by different methods. However the number and the size of gold and platinum particles increase with the deposition time, and with an increased distribution on the overall TiO_2 surface. The highest discoloration and mineralization rate in the case of Patent blue dye was found on the catalyst Au–TiO_2 prepared by photochemical deposition method, using high light intensity and short time of deposition. The superior removal of dye is attributed to a good balance between the action of gold nanoparticles as a sink for photoelectrons and the favorable tailoring of nanoparticles with an efficient heterogeneous distribution on the TiO_2 surface involving a limited part of the oxide surface; therefore preserving the adsorption ability of the photocatalyst.

For Pt–TiO_2 photocatalysts, metal nanoparticles of lowest sizes were transferred by photodepositon, and relevant discoloration and dye mineralization of patent blue were correspondently observed, confirming the photocatalytic reaction dependence from the noble metal nanoparticles sizing, dispersion, and number.

As alternatives to noble metals, other metal nanoparticles have been studied as co-catalysts in photocatalytic processes. In particular, it has been reported that copper zerovalent coadiuvated TiO_2 have important activity in the photocatalytic reforming of wastewater.[29] This treatment could represent an effective remediation technology for industrial segregated streams, when purification due to their stationarity in production, their high organic load, presence of refractory or slow biodegradable organic compounds, or presence of complex composition in organic compounds may not be achieved by conventional treatment processes and technologies. Valorization of the polluted stream can be achieved by photoreforming of liquid waste containing oxygenated organic compounds like alcohols, glycerol, sugars, short-chain organic acids and yielding hydrogen according to the general reaction[30,31]: $C_nH_mO_l + (2n - l)H_2O \rightarrow nCO_2 + (2n + m/2 - l)H_2$. The combined water photocatalytic system permits simultaneous organic carbon oxidation and hydrogen production, although dye molecules are also reported as electron donors. Copper nanozerovalent particles have shown relevant activity in this combined process, and photoreduction from copper salt leads to active photoreforming photocatalysts, greatly influenced by morphological and structural parameters. Copper nanoparticles undergo oxidation and reduction cycles during the H_2 photoproduction combined with oxygenated compounds photoxidaton, performing a central role in the overall reaction. The smaller copper particles (2 nm) exhibit high activity with respect to nanocopper (3.7 nm) meanwhile the different morphology exhibit a high influence in the Cu–TiO_2 interaction, enhancing the charge separation through the development of a more intimate contact among them.[32]

[29]Gombac et al. (2010).

[30]Vaiano et al. (2015).

[31]Carraro et al. (2014).

[32]Montini et al. (2011).

giovanni.libralato@unina.it

Photoreforming of organic species using copper-modified TiO_2 photocatalysts, prepared by in situ photodeposition processes, with nanometric sizes presents a promising strategy to improve the process efficiency.[33]

3 Magnetic and Magnetic Core Composites Nano/Micro Particles

Magnetic particles and nanoparticles are also an attractive option in water purification. Several studies discuss the application of magnetism to solve problems in water treatment, initially concerning the separation of solids through more efficient systems with respect to classical gravity settling. A well demonstrated and consolidated process is SIROFLOC, presented during the late 1970s, as a process for treatment of potable water supply based on the use of very fine particles of magnetite, Fe_3O_4.[34] Starting with the premise that the magnetite surface in the presence of dilute sodium hydroxide solutions changes their characteristic surface charge, this change allows them to interact with negatively charged colloidal particles in wastewater. The fine magnetite particles demonstrated a faster removal rate in the clarification process and by the application of a magnetic field the magnetic particles could easily be recovered and recycled. This process was commercialized in the early 1980s and it was installed in several plants around the world.

The magnetic nanoparticles largely studied and applied are based on iron oxide-materials, this focus is mainly due to their high natural abundance, low cost, and environmentally benign nature. Previously published reviews have thoroughly discussed iron oxide based magnetic materials for water treatment, describing bare and functionalized iron oxide materials for adsorption, their photocatalytic applications, and fate in the environment.

Nanomagnetite (Fe_3O_4) particles have been shown to be good nanoadsorbents for heavy metal and dye removal, offering an easy recovery option of magnetic nanoadsorbents. They have also been shown to be suitable for removal of radionuclides and interaction with cations and anions.[35,36,37,38,39] Depending on the surrounding conditions, such as low pH, Fe_3O_4 nanomagnetic particles, are subject to phase changes, losing the magnetic characteristics when the nanoparticles undergo aggregation.[40] The typical saturation magnetization of magnetite

[33]Clarizi et al. (2016).
[34]https://csiropedia.csiro.au/sirofloc/.
[35]Zhu et al. (2013).
[36]Ngomsik et al. (2005).
[37]Kaur et al. (2014).
[38]Ambashta et al. (2010).
[39]Mehta et al. (2015).
[40]Bae and Chung (2012).

giovanni.libralato@unina.it

nanometer microparticles was reported to be approximately 50 emu/g.[41] Organic surfactant or polymer coating has been demonstrated to limit these phenomena and to modify the surface properties of magnetic nanoparticles.[42] These magnetic nanoparticles could be prepared such in size to range from the nanoscale to several microns. The high pollutant removal capacity and rate of reaction of the magnetic nanoparticles is size dependent. Since the total surface area of particles can increase up to a thousand times for a set mass, decreasing the particle size to nano-scale and reaching a very high surface-area-to-volume ratio causes an increased number of active sites for reactions, and allows reduction in the mass required for treatment processes. Various studies showed that the removal capacity and reactivity of nanoparticles are highly size dependent[43] (Nurmi et al. 2005). It is reported[44] a seven times higher removal capacity for Fe_3O_4 nanoparticles (8 nm) with respect to coarse-grained counterparts (50 mm).

A relevant technology for the continuous production of nanoparticles by wet precipitation chemical synthesis is the spinning disk reactor (SDR).[45] High rotational speed of a disk allows for a very thin film with a thickness in the range 50–500 μm with numerous. The reagent solutions are fed at a short distance small distance (5 mm) from the disk surface through little tubes. The mean rotational velocity of the disk is controlled from 0 to 150 rad/s. The intense mixing and the contact between the two solutions at small liquid residence time give rise to local supersaturation, intense nucleation and limit the growth rate of the nanoparticles. So very small nanoparticles can be attained with nanoparticles a very narrow size distribution. The SDR has many advantages when compared with other mixing devices used for precipitation process: (i) a small liquid residence time, limiting the growth rate after nucleation, that leads to the production of narrow PDSs of nanoparticles at a specific target size; (ii) micro-mixing conditions attained by means of a limited energy consumption; (iii) continuous operation, compatible to industrial practice, can be performed. Strong influence on the particle size distribution of the nanoparticles is exerted by the operating conditions and the arrangement of the device, such as the rotation speed and the feeding point location Fe_3O_4 magnetic nanoparticles have been successfully synthesized with a spinning disk reactor[46]; then stabilized by the addition of tetraethyl orthosilicate (TEOS), in water-ethanol solutions to get magnetic nanoparticles embedded in a silica matrix. Nanocomposites with magnetic properties useful for core-shell application (Fig. 1) are obtained. The use of magnetic core Fe_3O_4 for different nanomaterials as shell is a viable solution to improve separation in several processes and applications. The removal and recycling of the nanomaterials by attracting the magnetic core with an

[41]Liu et al. (2012).
[42]Huang and Chen (2009).
[43]Nurmi et al. (2005).
[44]Shen et al. (2009).
[45]de Caprariis et al. (2012).
[46]Vaiano et al. (2016).

giovanni.libralato@unina.it

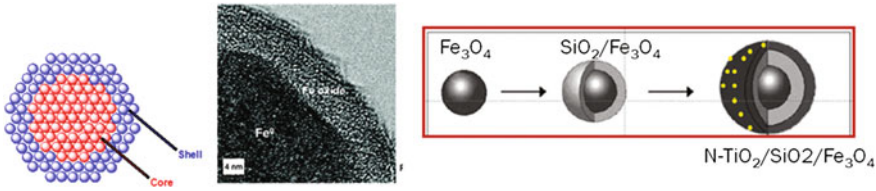

Fig. 1 Core-shell nanoparticles and their layered structure at 1 or 2 shells

external magnetic field is possible. Nanocomposites of photocatalysts such as visible active N-doped TiO_2 dispersed on SiO_2/Fe_3O_4 ferromagnetic nanoparticles were highly active in photocatalytic removal of phenol under visible irradiation.

It must be noted that commercial zerovalent iron nanoparticles are nanocomposite systems. The nanoparticles contain 14–18% Fe(0) and 2–6% Fe_3O_4 and exhibit a core-shell like structure with a Fe(0)-rich core surrounded by a magnetite-rich shell. The concentration of bivalent iron gradually decreases going from the external layer to the center of the nanoparticle.[47] Magnetic-core nano/micro particles (MPs) having cores made with magnetic elements like nickel, cobalt or their oxides and alloys, demonstrated ferromagnetic or super-paramagnetic properties.[48,49,50,51] Shells layer coating nanoparticles give improved particle chemical stability and resistance to the oxidation, however also offer specific functionalities, modifying the selectivity for ion uptake [62–65] or enhancing the affinity for hydrophobic contaminants. The most used[52,53] are silica or alumina polymers or surfactants.

An example is related to the removal of PAHs through a C18-functionalized Fe_3O_4 at enhanced hydrophobic interaction. The hydrophilicity and dispersibility of octadecyl-functionalized Fe_3O_4 in an aqueous solution improved because of the presence of hydrophilic alginate polymers.[54,55] A rapid separation of pollutant-laden particles from treated water via the external magnetic field, requiring less energy by applying small superparamagnetic nanoparticles, is one of the major benefits since their super-paramagnetic properties facilitate a high level of separation. Recently, superparamagnetic iron oxide nanoparticles were synthesized by co-precipitation and nanocomposited with polypropylene by an ex situ processing method involving a sequence of solvent casting and compression

[47]Montesinos et al. (2014).
[48]Ngomsik et al. (2005).
[49]Ambashta and Sillanpää (2010).
[50]Liu et al. (2008).
[51]Girginova et al. (2010).
[52]Clark and Keller (2012).
[53]Wang et al. (2008).
[54]Liu et al. (2009).
[55]Zhang et al. (2010).

giovanni.libralato@unina.it

molding.[56] Mechanical and magnetic properties have been tailored by the careful choice of compositions. Nanocomposites at percentage of Fe_3O_4 nanoparticles equal or higher than 5% appeared attractive for these applications, resulting in magnetic properties to be used at reasonable low fields such as 0.5 T, presenting more suitable nanocomposite materials which can be used more easily using less energy for recovery in these environmental applications.

The need for efficient adsorbents is confirmed by increasing water shortages and the higher need for water treatment. Magnetic nanoparticles as spinel ferrites like MFe_2O_4 (M=Mn, Cu, Co, Ni, Zn, Mg, Ca etc.) and their composites with tailored size, composition, magnetic characteristics and structure are reported as alternative to the more traditional Fe_3O_4 for water treatment applications.[57] Due to high adsorption capacity, low-cost and tunable features, their application in the removal of pollutants, such as metal ions, dyes, and pharmaceuticals, is very appealing. These compounds can be also regenerated by changing the pH of the solution, or with acid, bases or alcohols at low concentration. Accelerated and repeatable cyclic usage of these adsorbents over long time periods is based on their straight forward sorption-magnetic separation-regeneration properties, relevant when compared with several new generation adsorbents.

Because nanoparticles are highly reactive and mobile in an aqueous medium, toxicity is a concern, and it is essential to fully investigate possible toxic effects as well as the leaching of metal ions in dependence of environmental conditions. Stabilization of the nanoparticles is achieved by either coating or grafting with or with chelating agents. Water treatment can benefit from their variety of sizes, diverse structures, high surface areas, excellent chemical and thermal stabilities, ease of separation, and high adsorption performance at different pHs. Moreover they exhibit catalytic activity to promote organic reactions or for the degradation of organic pollutants. Simultaneously sustainable production from industrial waste should induce a decrease in their costs.

Conventional water treatment processes can be only a partial solution for uranyl removal due to low efficiency or high associated costs. In these cases, advanced reduction processes based on the use of iron nanostructured materials like nanozerovalent iron (nZVI) or nanomagnetite (nM) are a good alternative.

4 Nanometal Oxides in Advanced Water/Wastewater Treatment

Along with the nanometaloxides already mentioned, nanophotocatalysts have been widely investigated and there has been much recent advancement in their formulation and electronic, physical and chemical characteristics. The oldest and most

[56]Shirinova et al. (2016).

[57]Reddy and Yun (2016).

giovanni.libralato@unina.it

widely investigated photocatalyst is nanoporous TiO_2. The nanoporous TiO_2 allows for heterogeneous photocatalysis which has become an effective water purification technology to treat organic pollutants, even those hard to remove by conventional techniques. As mentioned in the previous paragraph, the band gap of anatase TiO_2 is 3.2 eV and the activation of the mineralization reactions of pollutants takes place under UV irradiation. Potentially photocatalyst activation by sunlight makes the process quite attractive because the energy cost of UV lamps can be saved, but only a small portion (5%) of the overall solar energy can be used which results in a great limitation in the use of photocatalysts for the conversion of solar energy into chemical energy.

As a consequence, up to recent years, photocatalytic processes using solar light where limited in their efficiency because of the ability of photocatalyst to work essentially with the UV-part of the solar spectrum, which is related to the absorption of photons of ultra-band gap energy. Several approaches have been investigated to promote the visible light activity of wide band gap semiconductors, including sensitization of semiconductors with organic molecules, metal ion doping, non-metallic elements doping, nanocompositing, or coupling with small band-gap semiconductors.

Very interesting results are obtained by doping TiO_2 with non-metallic elements such as nitrogen (N), sulfur (S), and carbon (C). In particular, studies on N-doped TiO_2 have shown both theoretically and experimentally that the nitrogen species localized N 2p states, results in relevant visible photoactivity.[58] Since the nanotitania and nanoxide based photocatalysts are largely described and reported in the scientific literature, this section will focus on recent progress in nanoengineering of the visible active TiO_2 and nanoxides.

For the synthesis of visible active nanophotocatalysts, different strategies such as sol-gel, micelle and inverse micelle, hydrothermal, solvothermal, direct oxidation, chemical vapour deposition, flame spray pyrolysis electrodeposition, sonochemical, and microwave methods have been proposed. Among all these techniques, the sol-gel method is the most commonly used due to its relatively low cost and great flexibility. The sol-gel method is based on inorganic polymerization reactions, involving four basic steps: photocatalysts precursor hydrolysis, polycondensation, drying, and thermal treatment. Several parameters, such as type of precursor, type of solvent, water content, pH, concentration of precursor and temperature, can influence both the structure of the initial gel, and, in turn, the properties of the resulting materials, including the crystal structure, particle size, shape and crystallinity, specific surface area, surface properties, aggregation, adsorption ability. High efficient N-doped titania has been obtained through the optimization of sol-gel method. Nanoparticellar N-doped TiO_2 photocatalysts can be obtained by sol gel method, via hydrolysis of titanium tetraisopropoxide by aqueous ammonia solution at 0 °C.[59] These nano doped photocatalyst were highly active in the presence of

[58]Sato (1986).

[59]Rizzo et al. (2014).

giovanni.libralato@unina.it

visible light for different water purification treatment. In particular, the photocatalytic degradation of some dyes, such as methylene blue, methyl orange, or emerging contaminants like spyramicin, atrazine,[60] or refractory compounds, such as phenol and terephtalic acid greatly improved on these nanomaterials. Furthermore, successful application in water disinfection[61] and high efficiency in the reduction of the total chemical oxygen demand (COD) of a highly polluted wastewater such as from oil mills and tannery wastewater, were observed.

The influence of the nanosize of N-doped titania has been shown by studying the effect of organic molecules on the aggregation and agglomeration of the powder. The control of the suspension and the aggregation of the nanoparticles are essential in maximizing the action of the N-doped TiO_2 particles properties in photocatalytic degradation of methylene blue.[62] However, the photocatalytic processes applied in slurry reactors has limited the industrial applications, because the necessary separation of photocatalyst nanopowder after liquid phase reactions is difficult and expensive.

Nanotechnology helps with the nanodimensions and improves another constraint of these photocatalysts, i.e. the insufficient quantum efficiency resulting from the relatively high recombination rate of photogenerated electron-hole pairs. Coupling N-doped TiO_2 to other suitable oxides or semiconductors having phosphor characteristics, an enhanced photon transfer was achieved. This effect was used realizing core-shell photocatalysts with photoluminescent core, able to absorb UV radiation and emitting a 440 nm centred radiation able to photoexcite the shell of N-doped titania catalyst. These photocatalysts N-doped TiO_2/phosphors exhibited a high photocatalytic activity for the removal of MB and emerging contaminants[63,64,65](Fig. 2).

A further approach investigated to improve nanodispersion of the photoactive doped nanoxide is to prepare nanocomposites with polymers. N-doped TiO_2 was dispersed in UV transparent syndiotactic polystyrene monolithic aerogel (s-Ps).[66] The accessibility of the catalytic surface to photons and reactants, limited by light scattering and shadowing of the nanoparticles themselves, were notably enhanced, strongly limiting the aggregation phenomena that typically occur when the catalyst is suspended in water solutions. These features increased the photocatalytic activity of the N-doped TiO_2 under visible light irradiation in comparison with the nanopowder sample dispersed in solution. The separation of photocatalyst from the purified wastewater after photocatalytic treatment can be achieved through the use of magnetic core of magnetite nanoparticles. Nanocomposites consisting of visible

[60]Vaiano et al. (2015).
[61]Miranda et al. (2016).
[62]Sacco (2015).
[63]Vaiano et al. (2015).
[64]Sacco et al. (2015).
[65]Sacco et al. (2015).
[66]Vaiano et al. (2014).

giovanni.libralato@unina.it

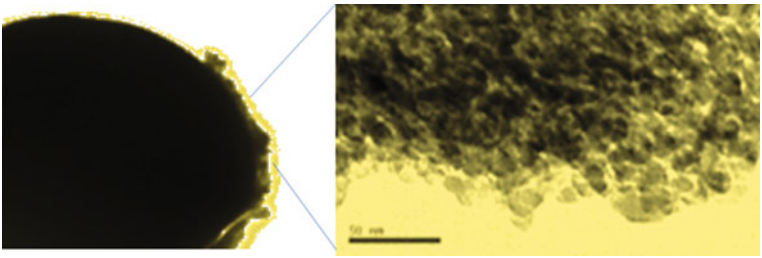

Fig. 2 Surface coating of phosphor (ZnS) particles with doped titanium nanoxide aggregates (N–TiO_2)

active N-doped TiO_2 supported on SiO_2/Fe_3O_4 ferromagnetic nanoparticles were stable and efficient in phenol degradation after four operation/regeneration cycles (de Caprariis et al. 2012).

Further wide band gap semiconductor photocatalyst that presents high chemical reactivity, low cost mild reaction conditions, and low toxicity is ZnO. Its use results in high photocatalytic activity in the removal of organic contaminants. Some examples include nanostructured ZnO semiconductor films used for degradation of organic contaminants (4-chlorocatechol),[67] $ZnO/ZnAl_2O_4$, Mn doped ZnO[68] and Ag_2O/ZnO nanorods heterostructure[69] which have been found effective in the photodegradation of some organics.

Other nanomaterials that demonstrated ability in visible light promoted photoactivity are the perovskites nanomaterials. In particular, high hydrogen production by $LaFeO_3$ prepared through combustion synthesis has been achieved during photocatalytic treatment of glucose containing wastewater (from food industry).[70]

5 Carbon Nanomaterials in the Water Treatment

Adsorbent materials are widely used in the treatment of contaminated streams containing organic compounds, heavy metals, microorganisms, and refractory compounds. To overcome several shortcomings attributable to the traditional adsorption systems based on activated carbon and/or polymers and ion exchange resin, carbon-based nanomaterials have emerged as a new generation of adsorbent materials, with increased adsorption capacity. Carbon nanomaterials, composed of carbon atoms, are allotropic forms of carbon, and include single-wall carbon nanotubes, multi-walled carbon nanotubes, carbon nanofibers, fullerene, graphene and

[67]Kamat et al. (2002).
[68]Ullah and Dutta (2008).
[69]Lam et al. (2013).
[70]Iervolino et al. (2016).

giovanni.libralato@unina.it

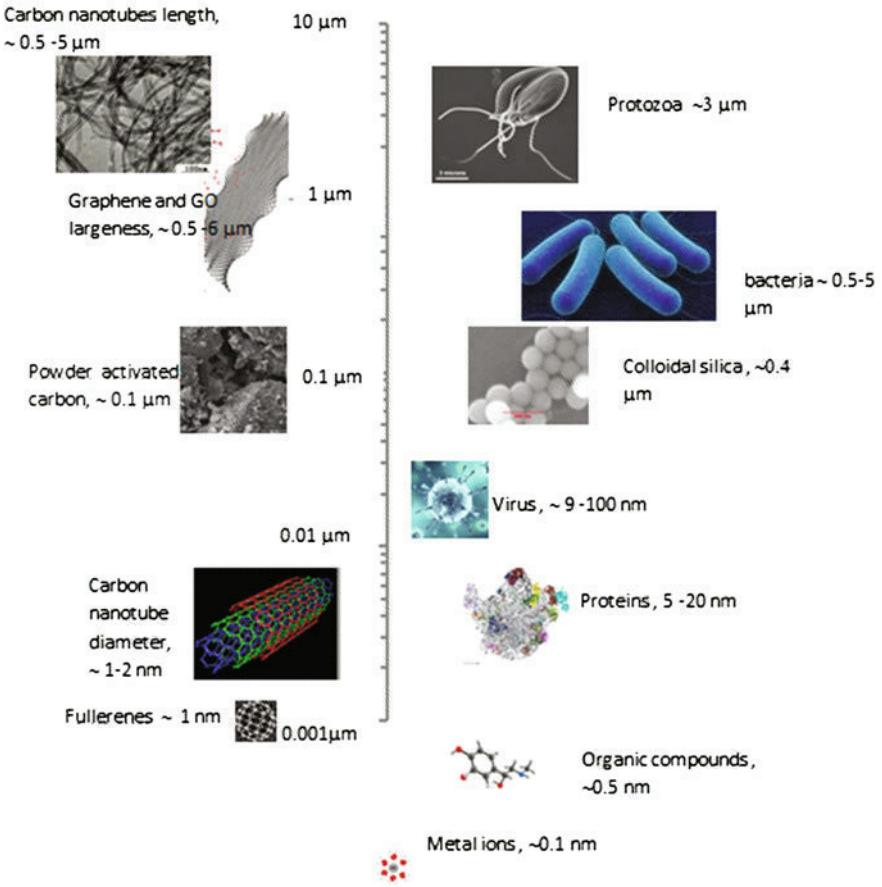

Fig. 3 Sizes of nanocarbons and some water pollutants

derivatives, and amorphous carbonaceous composites.[71,72,73] Carbon nanomaterials possess an exceptionally high surface area and high adsorption affinity for organic and inorganic pollutants (Fig. 3), so they show great application in adsorption processes.[74,75] Carbon nanomaterials, with inherently hydrophobic surfaces, can be modified by introducing large amounts of functional groups to target specific pollutants via chemical or electrical interactions.[76] Nanostructuring of nanomaterials

[71]Li et al. (2005).
[72]Wang et al. (2010).
[73]Wang et al. (2013).
[74]Musico et al. (2014).
[75]Santos et al. (2012).
[76]Smith et al. (2014).

giovanni.libralato@unina.it

can be easily accomplished. For example, they may be aligned to form efficient filters or mixed in membranes for removal of pollutants.[77,78]

These nanocarbons were able to reduce the biofouling and clogging of the adsorbent beds or to get modified selection in the adsorption.[79,80,81] They have shown efficacy also in the mechanical resistance enhancing of adsorbent beds, subjected to undesirable breakthrough with loss of efficiency and continuity of the process. The pure forms of major carbon-based nanomaterials, such as graphene (G), graphene oxide (GO), single-walled carbon nanotubes (SWNT), fullerenes and multi-walled carbon nanotubes (MWNT), are rarely present in advanced water purification systems.

Although they have shown superior adsorbents and disinfectants properties over the conventional methods,[82] their direct application as pure materials is restricted because of their high production costs. Compared with granular activated carbon, the price for 1 kg is three orders of magnitude higher for the cheapest carbon nanomaterial (MWNT) at several thousands of dollars per kilogram. Other nanocarbons are even more expensive than MWNT.

Development of cheaper production methods for carbon-based nanomaterials, reducing the costs of carbon precursor and of catalysts, could change the market in the future. Successful and greater application requires progress in their commercialization, with the reduction of cost and the implementation of large scale production. Moreover the management, human health, and ecological risk are issues that must be resolved for the development of their application in the water treatment field. Because of the high adsorption ability shown by carbon nanomaterials for emerging chemical contaminants, for which the traditional adsorbent are almost ineffective, as well as the capacity for a direct inactivation of biological contaminants in wastewater[83] makes them of great interest for wastewater treatment.

Even though further investigations are necessary to evaluate their fate in the environment, there are several technologies currently under development for the application of nanocarbon materials for water treatment. The main limitation is the extremely small size in some dimensions that hinder direct water treatment with carbon-based nanomaterials because it is difficult to separate them from purified water. Their recovery from the treated water is the main issue that must be solved for their application to become a accepted for water treatment.

Another possible process to improve separation is to modify carbon nanomaterials with magnetic particles and nanoparticles to permit magnetic field induced removal of the nanopurifying agent.

---

[77]Yang et al. (2011).

[78]Madadrang et al. (2012).

[79]Crini (2005).

[80]Bhatnagar and Sillanpa (2011).

[81]Eighmy et al. (1992).

[82]Brady-Estévez et al. (2008).

[83]Mauter and Elimelech (2008).

giovanni.libralato@unina.it

One of the most successful approaches of using nanocarbon is related to nanocompositing technology with polymeric materials to obtain membranes or polymer blending with carbon nanomaterials. The incorporation of carbon-based nanomaterials into polymeric membranes, have been successful for water treatment as well as nanocomposite membranes. The formation of covalent bonds among the functional groups occurring on nanomaterials and membranes has led to stable nanocomposite membranes. Physical systems have also been adopted, such as physisorption or embedding nanocarbons in polymer membranes during their preparation.[84,85]

Functionalized carbon nanomaterials can offer hydrophilic properties that can be conferred to the nanocomposite membrane. The nanomembrane becomes hydrophilic if the functionalized nanotubes bear groups such as –COOH, –OH and $–NH_2$, and hydrogen bonding between functional groups and water improves its permeability, favoring the rejection of hydrophobic pollutants.[86,87]

A further effect, as observed during the incorporation of NH_2-nanotubes is the generation of nano-channels on the surface.

The incorporation of carbon nanotubes into membranes resulted in improved membrane permeability, but consideration must be given to their orientation with respect to membrane surface.[88] Nanotubular cross porosity can be generated through the aligning of these nanomaterials parallel to the membrane section, allowing the passage of water through a non-porous polymeric layer. This kind of membrane involves multi-walled nanotubes, modified to favor specific removal of some contaminants, which permits rejection of the pollutants and leaves only water to transfer to the other side of the nanocomposite membrane. Because of the lower friction factors in the smooth inner cavities of the nanotubes, higher then theoretically expected water permeability is achieved. It worthwhile to note that nanochannels and the characteristic of hydrophobicity control the overall membrane performances, which presents a defined porosity related to the characteristic of nanotubes dimensionality.

If carbon nanomaterials are blended with the membrane polymer, the elongated carbon nanomaterials are randomly arranged and the mechanical properties of the membrane are enhanced as well as the affinity for water or the hydrophobicity of membrane. Some examples are mixed multi-walled nanotubes–polyvinyl alcohol (PVA) membranes, with relevant characteristic of water permeability and stiffness, at improved rejection of solutes in the presence of low load of nanotubes, up to 4wt %.[89] Interfacial polymerization of polyamide and nanotubes yields highly solvent-resistant nanofiltration membranes. The embedded nanomaterials are tightly

[84]Li et al. (2008).
[85]Upadhyayula and Gadhamshetty (2010).
[86]Vatanpour et al. (2011).
[87]Amini et al. (2013).
[88]Mauter and Elimelech (2008).
[89]Choi et al. (2006).

giovanni.libralato@unina.it

packed inside the polymer matrix, thus minimizing the risk of detachment. Increased carbon nanotube load (1–4 wt% functionalized nanotubes) was found to improve the water permeability and rejection of solutes. Other mixed carbon nanomaterial-polymer membrane has been obtained as PVK-GO coated onto a nitrocellulose membrane.

A further type of free-standing membranes is based on the pure graphene and GO, and was prepared by vacuum filtration.[90,91] Despite high biocompatibility, anti-microbial properties, extreme selectivity, and surprising speed only a few applications to water treatment can be found. A 3D GO nanosponge constructed by centrifugation was also obtained and it was found to effectively and rapidly adsorb some dyes [almost all methylene blue (99.1%) and methyl violet (98.8%)] from aqueous solutions. Reduced GO aerogels dispersed within the gel matrix of hydrophilic or hydrophobic amino acids, as lysine and cysteine, demonstrated increased capture of heavy metals or oils.[92]

Nanocomposite membranes, prepared by interactions through physiorption or covalent bonding between the functional groups on the nanomaterial and the membrane surface, have resulted in strong modification of filtering membrane surfaces, with higher ability to separate microbes from water,[93] due to both the reduction in the pore size caused by the membrane nanomaterial coatings, and bacterial adsorption properties. Improved inactivation of both Gram-negative and Gram-positive bacteria, are obtained by the nanomaterial/nanocomposite membrane.[94] For example, impregnation of chitosan beads with SWNT doubled adsorption rate from 223 to 450 mg/g.[95] Another study found that Pb^{2+} ion removal was removed very efficiently from solution by a magnetic chitosan/GO blend, with a maximum adsorption capability of 77 mg/g. In addition to its competitive adsorption rate and desirable separation properties, it could also be regenerated up to 90% of original capacity through four generations of washing, although it diminished in subsequent washings.

Mixing chitosan beads with nanocarbon produces a good adsorbent for the removal of several contaminants from water. This is due to the variety of functional groups, which improve biocompatibility and biodegradability, and good mechanical resistance due to the addition of the nanomaterials. The high use of chitosan for water treatment is due to its resistance to degradation, and the combination with nanomaterials greatly improves adsorption capacity.

The coupling of carbon-based nanomaterials with magnetic nanoparticles has been proposed to solve the separation problems. Nanocomposite of carbon nanomaterials with magnetic particles obtained by co-precipitation or intercalations of

[90]Joshi et al. (2014).
[91]Hu et al. (2010).
[92]Liu et al. (2012).
[93]Santos et al. (2011).
[94]Ahmed et al. (2012).
[95]Fan et al. (2013).

giovanni.libralato@unina.it

the magnetic nanoparticles within the graphene layers enabled a more favorable water purification from dyes and pesticides.[96,97] Adsorption properties of the nanomaterials can be so applied enabling the water recovery in a simpler and cheaper way.[98] Several other studies have reported successful synthesis of TiO_2, ZnO, Al_2O_3 on carbon based nanomaterials for separation of organic contaminants from aqueous solutions.[99,100,101]

Recent developments in membrane technology have resulted in higher energy saving in RO plants.[102] NF has also been evaluated for desalinating seawater.[103] Nanomaterials are very useful in developing more efficient and cheaper nanostructured and reactive membranes for water/wastewater treatment and desalination such as CNT filters.[104] The controlled synthesis of both the length and diameters of CNTs has enabled them to be used in RO membranes to achieve high water fluxes. Carbon nanomaterials offer opportunities to control the cost of desalination and increase its energy efficiency and among these are CNTs, zeolites,[105] and graphene.[106] Thin film nanocomposite membranes containing Ag and TiO_2 nanoparticles exhibited good salt rejection.[107] Membrane permeability and salt rejection are shown to be effective also in coatings of TiO_2/Al_2O_3 composite ceramic membranes with iron.

6 Perspectives in Water Treatment Improved by Nanotechnology

Nanotechnology in water treatment applications is showing new approaches to overcome traditional treatment technology limitations. The more effective processes for water purification need to meet further reduction in costs especially because the removal of pollutants is required even when they are present in low concentrations. These more stringent water standard limits are not and cannot be accomplished with conventional technologies. Moreover the generation of sludge and hazardous wastes connected to traditional treatment results in further treatment requiring high

[96]Wang et al. (2011).
[97]Wu et al. (2011).
[98]Tang et al. (2013).
[99]Li et al. (2011).
[100]Ma et al. (2014).
[101]Saleh et al. (2011).
[102]Fritzmann et al. (2007).
[103]Mohsen et al. (2003).
[104]Srivastava et al. (2004).
[105]Li et al. (2004).
[106]Jiang et al. (2009).
[107]Lee et al. (2008).

giovanni.libralato@unina.it

energy and/or costly solutions. Nano-based technologies are shown to perform well, by increasing removal efficiency of several pollutants compared to conventional processes and technologies. Moreover nanotechnologies can also be complementary to some traditional techniques. The application of nanomaterials for water treatment is strongly related to the lowering of their production costs and to the identification of specific applications where they can be competitive with conventional processes. Moreover, the synthesis on an industrial-scale is encouraging their use since they are expected to become cheaper in the next future.

The higher efficiencies largely reported for the nano-implemented technologies for water treatment result in a simplification of the water treatment train, and/or a reduction of energy, time, and cost for environmental remediation. Because of the high potential to achieve more economic treatment with an higher water quality, several researches are currently investigating the fate of the nanomaterials in the environment, transport features, toxicity, transformation of cumulated nanomaterials in natural hydric bodies, and long term effects of the nanotechnologies applications.

Nanohybrid materials have been shown to be safer for water treatment applications, permitting the easier recovery of nanomaterials after their use, decreasing the costs of water nanotreatment and avoiding any adverse environmental effect. For the most part, nanotechnologies appear to present limited environmental impact; however further studies and investigations devoted to recovery and recycle of these materials are necessary so that their high efficacy in the removal of diverse biological and chemical contaminants can be utilized. The unique properties of nanoparticles and nanostructured materials; high surface-area, chemical activity, high mobility and magnetic and mechanical properties among others are encouraging more and more interest in water nanobased treatment and in nanoenvironmental applications.

References

Ahmed F, Santos CM, Vergara RAMV, Tria MCR, Advincula R, Rodrigues DF (2012) Antimicrobial applications of electroactive PVK-SWNT nanocomposites. Environ Sci Technol 46(3):1804–1810

Ambashta RD, Sillanpää M (2010) Water purification using magnetic assistance: a review. J Hazard Mater 180:38–49

Amin MT, Alazba AA, Manzoor U (2014) A review of removal of pollutants from water/wastewater using different types of nanomaterials. Adv Mater Sci Eng 2014:1–24

Amini M, Jahanshahi M, Rahimpour A (2013) Synthesis of novel thin film nanocomposite (TFN) forward osmosis membranes using functionalized multi-walled carbon nanotubes. J Membr Sci 435(233–41):241

Bae ST, Chung KW (2012) Method for preparing engineered Mg doped ferrite superparamagnetic nano particle exhibiting Ac magnetic induction heating at high temperature and Mg doped ferrite superparamagnetic nano particles engineered by the method. In: PCT/KR 2009-007801, PCT/USA 13/141,844, PCT/Japan/2011-543434, PCTEurope/2011-234291, PCT/China/200980152546. 6, Nuri Vista Co., Ltd., Seoul, KR, 2012, assigned

giovanni.libralato@unina.it

Balogh L, Swanson DR, Tomalia DA, Hagnauer GL, McManus AT (2001) Dendrimer-silver complexes and nanocomposites as antimicrobial agents. Nano Lett 1(1):18–21
Bavasso I, Vilardi G*, Stoller M, Chianese A, Di Palma L (2016) Perspectives in nanotechnology based innovative applications for the environment. Chem Eng Trans 47:55–60
Bhatnagar A, Sillanpää M (2011) A review of emerging adsorbents for nitrate removal from water. Chem Eng J 168(2):493–504
Botes M, Cloete TE (2010) The potential of nanofibers and nanobiocides in water purification. Crit Rev Microbiol 36(1):68–81
Brady-Estévez AS, Kang S, Elimelech M (2008) A single-walled-carbon-nanotube filter for removal of viral and bacterial pathogens. Small 4(4):481–484
Mueller N, Braun J, Bruns, J, Cernik M, Rissing P, Rickerby D, Nowack B (2012) Application of nanoscale zero valent iron (NZVI) for groundwater remediation in Europe. Environ Sci Pollut Res 19(2012):550–558
Carraro G, Maccato C, Gasparotto A, Montini T, Turner S, Lebedev OI, Gombac V, Adami G, Van Tendeloo G, Barreca D, Fornasiero P (2014) Enhanced hydrogen production by photoreforming of renewable oxygenates through nanostructured Fe2O3 polymorphs. Adv Funct Mater 24:372–378
Chen Y, Wang L, Jiang S, Yu HJ (2003) Study on novel antibacterial polymer materials materials (I) preparation of zeolite antibacterial agents and antibacterial polymer composite and their antibacterial properties. J Polym Mater 20(3):279–284
Choi J-H, Jegal J, Kim W-N (2006) Fabrication and characterization of multi-walled carbon nanotubes/polymer blend membranes. J Membr Sci 284(1):406–415
Clarizi L, Vitiello G, Luciani G, Di Somma I, Andreozzi R, Marotta R (2016) In situ photodeposited nanoCu on TiO_2 as a catalyst for hydrogen production under UV/visible radiation. Appl Catal A: Gen 518:142–149. doi:10.1016/j.apcata.2015.07.044
Clark KK, Keller A (2012) Investigation of two magnetic permanently confined micelle array sorbents using nonionic and cationic surfactants for the removal of PAHs and pesticides from aqueous media. Water Air Soil Pollut 223:3647–3655
Crespi J, Quici N, Halac EB, Leyva AG, Ramosb CP, Mizrahi M, Requejo FG, Litter MI (2016) Removal of uranium (VI) with iron nanoparticles. CET 47
Crini G (2005) Recent developments in polysaccharide-based materials used as adsorbents in wastewater treatment. Prog Polym Sci 30(1):38–70
Danilczuk M, Lund A, Sadlo J, Yamada H, Michalik J (2006) Conduction electron spin resonance of small silver particles. Spectrochimica Acta—Part A: Mole Biomole Spectro 63(1):189–191
De Caprariis B, Di Rita M, Stoller M, Verdone N, Chianese A (2012) Reaction-precipitation by a spinning disc reactor: influence of hydrodynamics on nanoparticles production. Chem Eng Sci 76:73–80
Fan L, Luo C, Sun M, Li X, Qiu H (2013) Highly selective adsorption of lead ions by water-dispersible magnetic chitosan/graphene oxide composites. Colloids Surf B: Biointerface 103:523–959
Fritzmann C, Löwenberg T, Wintgens T, Melin T (2007) State-of-the-art of reverse osmosis desalination. Desalination 216(1–3):1–76
Ghasemzadeh G, Momenpour M, Omidi F, Hosseini MR, Ahani M, Barzegari A (2014) Applications of nanomaterials in water treatment and environmental remediation. Front Environ Sci Eng 8:471–482
Girginova PI, Daniel-da-Silva AL, Lopes CB, Figueira P, Otero M, Amaral VS, Pereira E, Trindade T (2010) Silica coated magnetite particles for magnetic removal of Hg2+ from water. J Colloid Interface Sci 345:234–240
Gombac V, Sordelli L, Montini T, Delgado JJ, Adamski A, Adami V, Cargnello V, Bernal S, Fornasiero P (2010) CuO_x−TiO_2 photocatalysts for H_2 production from ethanol and glycerol solutions. J Phys Chem A 114:3916–577
Han Y, Liu C, Horita J, Yan W (2016) Trichloroethene hydrodechlorination by Pd–Fe bimetallic nanoparticles: solute-induced catalyst deactivation analyzed by carbon isotope fractionation Appl. Catal. B: Environ 188:77–86

giovanni.libralato@unina.it

Hu W, Peng C, Luo W, Lv M, Li X, Li D et al (2010) Graphene-based antibacterial paper. ACS Nano 4(7):4317–234323

Huang SH, Chen DH (2009) Rapid removal of heavy metal cations and anions from aqueous solutions by an amino-functionalized magnetic nano-adsorbent. J Hazard Mater 163:174–179

Iervolino G, Vaiano V, Sannino D, Rizzo L, Ciambelli P (2016) Production of hydrogen from glucose by $LaFeO_3$ based photocatalytic process during water treatment (2016). Int J Hydrogen Energy 41(2):959–966. doi:10.1016/j.ijhydene.2015.10.085

Jiang D-E, Cooper VR, Dai S (2009) Porous graphene as the ultimate membrane for gas separation. Nano Lett 9(12):4019–4024

Joshi RK, Carbone P, Wang FC, Kravets VG, Su Y, Grigorieva IV et al (2014) Precise and ultrafast molecular sieving through graphene oxide membranes. Science 343(6172):752–754

Kamat PV, Huehn R, Nicolaescu R (2002) A "sense and shoot" approach for photocatalytic degradation of organic contaminants in water. J Phys Chem B 106(4):788–794

Karn B, Kuiken T, Otto M (2009) Nanotechnology and in situ remediation: a review of the benefits and potential risks. Environ Health Perspect 117(2009):1823–1831

Kaur R, Hasan A, Iqbal N, Alam S, Saini MK, Raza SK (2014) Synthesis and surface engineering of magnetic nanoparticles for environmental cleanup and pesticide residue analysis: a review. J Sep Sci 37(14):1805–1825

Kim JS, Kuk E, Yu KN et al (2007) Antimicrobial effects of silver nanoparticles. Nanomed: Nanotechnol Biol Med 3(1):95–101

Kim Y-M, Murugesan K, Chang Y-Y, Kim E-J, Chang YS (2012) Degradation of polybrominated diphenyl ethers by a sequential treatment with nanoscale zero valent iron and aerobic biodegradation. J Chem Technol Biotechnol 87:216–224

Lacinova L, Kvapil P, Cernik M (2012) A field comparison of two reductive dechlorination (zero-valent iron and lactate) methods. Environ Technol 33(2012):741–749

Lam SM, Sin JC, Abdullah AZ, Mohamed AR (2013) Efficient photodegradation of resorcinol with Ag2O/ZnO nanorods heterostructure under a compact fluorescent lamp irradiation. Chem. Pap 67:1277–1284

Lee HS, Im SJ, Kim JH, Kim HJ, Kim JP, Min BR (2008) Polyamide thin-film nanofiltration membranes containing TiO2 nanoparticles. Desalination 219(1–3):48–56

Li L, Dong J, Nenoff TM, Lee R (2004) Desalination by reverse osmosis using MFI zeolite membranes. J Membr Sci 243(1–2):401–404

Li Y-H, Di Z, Ding J, Wu D, Luan Z, Zhu Y (2005) Adsorption thermodynamic, kinetic and desorption studies of Pb^{2+} on carbon nanotubes. Water Res 39(4):605–609

Li Q, Mahendra S, Lyon DY, Brunet L, Liga MV, Li D et al (2008) Antimicrobial nanomaterials for water disinfection and microbial control: potential applications and implications. Water Res 42(18):4591–4602

Li Z, Gao B, Chen GZ, Mokaya R, Sotiropoulos S, Li Puma G (2011) Carbon nanotube/titanium dioxide (CNT/TiO2) core–shell nanocomposites with tailored shell thickness, CNT content and photocatalytic/photoelectrocatalytic properties. Appl Catal B 110:50–757

Liau SY, Read DC, Pugh WJ, Furr JR, Russell AD (1997) Interaction of silver nitrate with readily identifiable groups: relationship to the antibacterial action of silver ions. Lett Appl Microbiol 25(4):279–283

Liu J-F, Zhao Z-S, Jiang G-B (2008) Coating Fe3O4 magnetic nanoparticles with humic acid for high efficient removal of heavy metals in water. Environ Sci Technol 42:6949–6954

Liu Y, Li H, Lin JM (2009) Magnetic solid-phase extraction based on octadecyl functionalization of monodisperse magnetic ferrite microspheres for the determination of polycyclic aromatic hydrocarbons in aqueous samples coupled with gas chromatography-mass spectrometry. Talanta 77:1037–1042

Liu J, Bin Y, Matsuo M (2012) Magnetic behavior of Zn-doped Fe3O4 nanoparticles estimated in terms of crystal domain size. J Phys Chem C 116:134–143

Liu F, Chung S, Oh G, Seo TS (2012) Three-dimensional graphene oxide nanostructure for fast and efficient water-soluble dye removal. ACS Appl Mater Interfaces 4(2):922–927

giovanni.libralato@unina.it

Ma L, Chen A, Lu J, Zhang Z, He H, Li C (2014) In situ synthesis of CNTs/Fe–Ni/TiO_2 nanocomposite by fluidized bed chemical vapor deposition and the synergistic effect in photocatalysis. Particuology 14:24–32

Madadrang CJ, Kim HY, Gao G, Wang N, Zhu J, Feng H et al (2012) Adsorption behavior of EDTA-graphene oxide for Pb (II) removal. ACS Appl Mater 4(3):1186–1193

Makhluf S, Dror R, Nitzan Y, Abramovich Y, Jelinek R, Gedanken A (2005) Microwave-assisted synthesis of nanocrystalline MgO and its use as a bacteriocide. Adv Funct Mater 15(10): 1708–1715

Mauter MS, Elimelech M (2008) Environmental applications of carbon-based nanomaterials. Environ Sci Technol 42(16):5843–5859

Mehta D, Mazumdar S, Singh SK (2015) Magnetic adsorbents for the treatment of water/wastewater—a review. J Water Process Eng 7:244–265

Miranda AC, Lepretti M, Rizzo L, Caputo I, Vaiano V, Sacco O, Lopes WS, Sannino D (2016) Surface water disinfection by chlorination and advanced oxidation processes: inactivation of an antibiotic resistant *E. coli* strain and cytotoxicity evaluation (2016). Sci Total Environ 554–555:1–6. doi:10.1016/j.scitotenv.2016.02.189

Mohsen MS, Jaber JO, Afonso MD (2003) Desalination of brackish water by nanofiltration and reverse osmosis. Desalination 157(1–3):167

Montesinos VN, Quici N, Halac EB, Leyva AG, Custo G, Bengio S, Zampieri G, Litter MI (2014) Highly efficient removal of Cr(VI) from water with nanoparticulated zerovalent iron: understanding the Fe(III)-Cr(III) passive outer layer structure. Chem Eng J 244:569–575

Montini T, Gombac V, Sordelli L, Delgado JJ, Chen X, Adami G, Fornasiero P (2011) Nanostructured Cu/TiO2 photocatalysts for H2 production from ethanol and glycerol aqueous solutions. ChemCatChem 3:574

Morones JR, Elechiguerra JL, Camacho A et al (2005) The bactericidal effect of silver nanoparticles. Nanotechnology 16(10):2346–2353

Musico, YLF, Santos C, Dalida M, Rodrigues DF (2014) Surface modification of membrane filters using graphene and graphene oxide-based nanomaterials for bacterial inactivation and removal. ACS Sustain Chem Eng 2(7):1559–1565

Ngomsik A-F, Bee A, Draye M, Cote G, Cabuil V (2005) Magnetic nano-and microparticles for metal removal and environmental applications: a review. Comptes Rendus Chimie 8:963–970

Nurmi JT, Tratnyek PG, Sarathy V, Baer DR, Amonette JE, Pecher K, Wang C, Linehan JC, Matson DW, Penn RL, Driessen MD (2005) Characterization and properties of metallic iron nanoparticles: spectroscopy, electrochemistry, and kinetics. Environ Sci Technol 39: 1221–1230

O'Carroll D, Sleep B, Krol M, Boparai H, Kocur C (2013) Nanoscale zero valent iron and bimetallic particles for contaminated site remediation. Adv Water Resour 51:104–122

Ohtani B (2013) Titania photocatalysis beyond recombination: a critical review. Catalysts 3:942

Pal S, Tak YK, Song JM (2007) Does the antibacterial activity of silver nanoparticles depend on the shape of the nanoparticle? A study of the gram-negative bacterium *Escherichia coli*. Appl Environ Microbiol 73(6):1712–1720

Peter-Varbanets M, Zurbrügg C, Swartz C, Pronk W (2009) Decentralized systems for potable water and the potential of membrane technology. Water Res 43(2):245–265

Rajan CS (2011) Nanotechnology in groundwater remediation. Int J Environ Sci Dev 2:1–6

Reddy DHK, Yun Y-S (2016) Spinel ferrite magnetic adsorbents: alternative future materials for water purification? Coord Chem Rev 315:90–111

Rizzo L, Sannino D, Vaiano V, Sacco O, Scarpa A, Pietrogiacomi D (2014) Effect of solar simulated N-doped TiO_2 photocatalysis on the inactivation and antibiotic resistance of an *E. coli* strain in biologically treated urban wastewater. Appl Catal B 144:369–378. doi:10.1016/j.apcatb.2013.07.033

Sacco O (2015) Photocatalytic oxidation of organic pollutants under visible light irradiation: from n-doped TiO2 photocatalysts to the design of a continuous fixed bed reactor. Ph.D. Thesis in Chemical Engineering, University of Salerno

giovanni.libralato@unina.it

Sacco O, Vaiano V, Han C, Sannino D, Dionysiou DD, Ciambelli P (2015a) Long afterglow green phosphors functionalized with Fe-N doped TiO_2 for the photocatalytic removal of emerging contaminants (2015). Chem Eng Trans 43:2107–2112. doi:10.3303/CET1543352

Sacco O, Vaiano V, Han C, Sannino D, Dionysiou DD (2015b) Photocatalytic removal of atrazine using N-doped TiO_2 supported on phosphors (2015). Appl Catal B 164:462–474. doi:10.1016/j.apcatb.2014.09.062

Saleh TA, Gondal MA, Drmosh QA, Yamani ZH, Al-Yamani A (2011) Enhancement in photocatalytic activity for acetaldehyde removal by embedding ZnO nano particles on multiwall carbon nanotubes. Chem Eng J 166(1):407–412

Santos CM, Tria MCR, Vergara RAMV, Ahmed F, Advincula RC, Rodrigues DF (2011) Antimicrobial graphene polymer (PVK-GO) nanocomposite films. Chem Commun 47 (31):8892–8894

Santos CM, Mangadlao J, Ahmed F, Leon A, Advincula RC, Rodrigues DF (2012) Graphene nanocomposite for biomedical applications: fabrication, antimicrobial and cytotoxic investigations. Nanotechnology 23(39):395101

Sato S (1986) Photocatalytic activity of NOx-doped TiO2 in the visible light region. Chem Phys Lett 123:126–128

Shen YF, Tang J, Nie ZH, Wang YD, Ren Y, Zuo L (2009) Tailoring size and structural distortion of Fe_3O_4 nanoparticles for the purification of contaminated water. Bioresource Technol 100:4139–4146

Shirinova H, Di Palma L, Sarasini F, Tirillò J, Ramazanov MA, Hajiyeva F, Sannino D, Polichetti M, Galluzzi A (2016) Synthesis and characterization magnetic nanocomposites for environmental remediation. Chem Eng Trans 47:103–108

Siegel RW (1994) Nanophase materials. In: Trigg GL (ed) Encyclopedia of applied physics, vol 11. VCH, Weinheim, pp 1–27

Smith SC, Ahmed F, Gutierrez KM, Frigi Rodrigues D (2014) A comparative study of lysozyme adsorption with graphene, graphene oxide, and single-walled carbon nanotubes: potential environmental applications. Chem Eng J 240:147–154

Srivastava A, Srivastava ON, Talapatra S, Vajtai R, Ajayan PM (2004) Carbon nanotube filters. Nat Mater 3(9):610–614

Stevens MM, George JH (2005) Science, exploring and engineering the cell surface interface. Science 310:1135–1138

Tang SCN, Lo IMC (2013) Magnetic nanoparticles: essential factors for sustainable environmental applications. Wat Res 47:2613–2632

Tang Y, Guo H, Xiao L, Yu S, Gao N, Wang Y (2013) Synthesis of reduced graphene oxide/magnetite composites and investigation of their adsorption performance of fluoroquinolone antibiotics. Colloids Surf A Physicochem Eng Aspects 424:74–80

Taylor Eighmy T, Robin Collins M, Spanos SK, Fenstermacher J (1992) Microbial populations, activities and carbon metabolism in slow sand filters. Water Res 26(10):1319–1328

Ullah R, Dutta J (2008) Photocatalytic degradation of organic dyes with manganese-doped ZnO nanoparticles. J Hazard Mater 156:194–200

Upadhyayula VKK, Gadhamshetty V (2010) Appreciating the role of carbon nanotube composites in preventing biofouling and promoting biofilms on material surfaces in environmental engineering: a review. Biotechnol Adv 28(6):802–816

Vaiano V, Sacco O, Sannino D, Ciambelli P, Longo S, Venditto V, Guerra G (2014) N-doped TiO_2/s-PS aerogels for photocatalytic degradation of organic dyes in wastewater under visible light irradiation. J Chem Technol Biotechnol 89(8):1175–1181. doi:10.1002/jctb.4372

Vaiano V, Iervolino G, Sarno G, Sannino D, Rizzo L, Mesa JJM, Hidalgo MC, Navío JA (2015) Simultaneous production of CH4 and H2 from photocatalytic reforming of glucose aqueous solution on sulfated Pd-TiO2 catalysts. Oil Gas Sci Technol 70:891–902

Vaiano V, Sacco O, Sannino D, Ciambelli P (2015b) Photocatalytic removal of spiramycin from wastewater under visible light with N-doped TiO_2 photocatalysts. Chem Eng J 261:3–8. doi:10.1016/j.cej.2014.02.071

giovanni.libralato@unina.it

Vaiano V, Sacco O, Sannino D, Ciambelli P (2015c) Process intensification in the removal of organic pollutants from wastewater using innovative photocatalysts obtained coupling Zinc Sulfide based phosphors with nitrogen doped semiconductors (2015). J Clean Prod 100:208–211. doi:10.1016/j.jclepro.2015.03.041

Vaiano V, Iervolino G, Sannino D, Murcia JJ, Hidalgo MC, Ciambelli P, Navío JA (2016a) Photocatalytic removal of patent blue V dye on Au–TiO_2 and Pt–TiO_2 catalysts. Appl Catal B 188:134–146. doi:10.1016/j.apcatb.2016.02.001

Vaiano V*, Saccoa V, Sannino D, Stollerb M, Ciambelli P, Chianese A (2016) Photocatalytic removal of phenol ferromagnetic N-TiO2/SiO2/Fe3O4 nanoparticles in presence of visible light irradiation. Chem Eng Trans 47:235–240

Vatanpour V, Madaeni SS, Moradian R, Zinadini S, Astinchap B (2011) Fabrication and characterization of novel antifouling nanofiltration membrane prepared from oxidized multiwalled carbon nanotube/polyethersulfone nanocomposite. J Membr Sci 375(1):284–294

Wang S, Sun H, Ang H-M, Tadé MO (2013) Adsorptive remediation of environmental pollutants using novel graphene-based nanomaterials. Chem Eng J 226:336–47347

Wang P, Shi Q, Shi Y, Clark KK, Stucky GD, Keller AA (2008) Magnetic permanently confined micelle arrays for treating hydrophobic organic compound contamination. J Am Chem Soc 131:182–188

Wang L, Zhu D, Duan L, Chen W (2010) Adsorption of single-ringed N-and S-heterocyclic aromatics on carbon nanotubes. Carbon 48(13):3906–3915

Wang C, Feng C, Gao Y, Ma X, Wu Q, Wang Z (2011) Preparation of a graphene-based magnetic nanocomposite for the removal of an organic dye from aqueous solution. Chem Eng J 173 (1):92–97

Wu Q, Zhao G, Feng C, Wang C, Wang Z (2011) Preparation of a graphene-based magnetic nanocomposite for the extraction of carbamate pesticides from environmental water samples. J Chromatogr A 1218(44):7936–7942

Xiu Z-M, Ma JZ, Alvarez PJ (2011) Differential effect of common ligands and molecular oxygen on antimicrobial activity of silver nanoparticles versus silver ions. Environ Sci Technol 45 (20):9003–9008

Yang S-T, Chen S, Chang Y, Cao A, Liu Y, Wang H (2011) Removal of methylene blue from aqueous solution by graphene oxide. J Colloid Interface Sci 359(1):24–929

Zhang W (2003) Nanoscale iron particles for environmental remediation: an overview. J Nanopart Res 5:323–332

Zhang S, Niu H, Cai Y, Shi Y (2010) Barium alginate caged Fe3O4@C18 magnetic nanoparticles for the pre-concentration of polycyclic aromatic hydrocarbons and phthalate esters from environmental water samples. Anal Chim Acta 665:167–175

Zhu J, Wei S, Chen M, Gu H, Rapole SB, PallavkarS, Ho TC, Hopper J, Guo Z (2013) Magnetic nanocomposites for environmental remediation. Adv Powder Technol 24:459–467

giovanni.libralato@unina.it

Nanomaterials for Water Remediation: Synthesis, Application and Environmental Fate

Antonella De Luca and Bernardí Bayarri Ferrer

Abstract World Health Organization estimates that almost 1 billion people in the world have no access to potable water and that 2.6 billion people lack access to adequate sanitation (World Health Organization (WHO), in Meeting the MDG drinking water and sanitation target: a mid-term assessment of progress/WHO/UNICEF Joint Monitoring Programme, 2004). The high level of quality required to make possible the utilization of reclaimed water to fill this lack of resource leads into the necessity of adapting conventional treatment schemes to more restrictive requirements. Nanotechnology processes could represent one of the most useful options for the achievement of this goal. National Nanotechnology Initiative (NNI) defined nanotechnology as "the understanding and control of matter at dimension between approximately 1 and 100 nanometers (nm), where unique phenomena enable novel application not feasible when working with bulk materials or even single atoms or molecules". The knowledge achieved in this field offers the possibility of using novel material in the treatment of surface water, groundwater and wastewater especially for the removal of heavy metals, organic and inorganic solutes and microorganism. Due to the generally new ambit of research, the scientific community is actively involved in the development of new strategies and novel nanomaterials synthesis. Thousands of scientific articles related to nanotechnology applications in water sanitation have been published in the last decade. On the basis of their function, nanomaterials can be easily classified as: nanosorbents, nanocatalysts and redox active nanoparticles, nanostructured and reactive membranes, bioactive nanoparticles. Literature about current research on nanomaterials, methods of synthesis and characterization are reviewed in this chapter. Moreover, possible environmental impacts related with their application are also commented.

Keywords Nanomaterials · Water treatment · Synthesis methods · Characterization techniques · Environmental impact

A. De Luca (✉)
Chemical Engineering Department, University of Barcelona,
Marti i Franques, 1, 08028 Barcelona, Spain
e-mail: deluca.antonella85@gmail.com

B.B. Ferrer
Calle de Cervantes 35, 08912 Badalona, Spain

© Springer International Publishing AG 2017

G. Lofrano et al. (eds.), *Nanotechnologies for Environmental Remediation*,
DOI 10.1007/978-3-319-53162-5_2

giovanni.libralato@unina.it

1 Introduction

In response to the great percentage of world population that have no access to potable water and the often irresponsible use of water resources, the scientific community is doing formidable efforts in achieving the goal of reducing the water exploitation through alternative sources of water supply. Water reuse represents a valid option for the achievement of this goal. The possibility of providing potable water supply to huge areas of developing countries, such as finding a more environmentally friendly solution to the increasing water demand, is a global and actual issue. The high level of quality required to ensure proper utilization of reclaimed water lead to the necessity of adapting conventional wastewater treatment plants to the more advanced treatment and more restrictive discharge standards.

New approaches are continually being examined in order to find a solution which could be more effective and durable than the current options. The progress achieved in nanoscale science suggests that this technology could represent a good solution to the water quality problem. Nanocatalysts, nanosorbents, nanostructured catalytic membranes among others are possible products resulting from new developments in nanotechnologies that can be employed for this purpose.

Using the definition developed by the National Nanotechnology Initiative (NNI), the U.S. Government research and development (R&D) program, "nanotechnology" is identifiable as "the understanding and control of matter at dimension between approximately 1 and 100 nanometers (nm), where unique phenomena enable novel application not feasible when working with bulk materials or even single atoms or molecules". Furthermore, according to NNI "nanomaterials are all nanoscale materials or materials that contain nanoscale structures internally or on their surfaces. These can include engineered nano-objects, such as nanoparticles, nanotubes, nanoplates, and naturally occurring nanoparticles, such as volcanic ash, sea spray, and smoke". Finally, it's important to keep in mind that nanomaterials are not undiscovered materials but nanoscale form of well-known materials.

Since the history of nanotechnology conceptually started, with the speech that Richard Feynman gave on December 29th 1959 at the annual meeting of American Physical Society SWCNT (Feynman 1960), there have been a lot of advances. For the first time, his amazing vision focused attention on the possibility of working with tiny materials. Thus, nanotechnology became one of the latest challenges for humans, the control of materials at atomic level.

Scientists are now largely investigating the possible real application of nanomaterials in a wide range of fields, from the basic sciences to the engineering application. Among them, some really interesting ones are the application of nanomaterials in environmental sanitation, such as water and soil treatment.

Thousands of scientific articles related to nanotechnology applications in water sanitation have been published over the past several years. Figure 1 shows the increase of publications describing the application of nanomaterials for water remediation since the early 2000s.

giovanni.libralato@unina.it

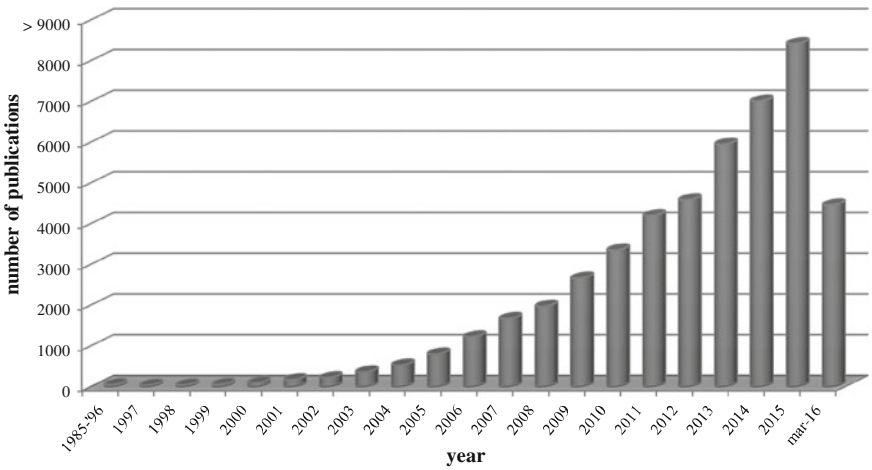

Fig. 1 Publications on nanomaterials application for water remediation per year (www.sciencedirect.com)

Advances in nanoscale science and engineering are providing important opportunities to develop more cost effective and environmentally acceptable water purification processes. In this chapter the use of nanotechnology in areas relevant to water purification (including separation and reactive media for water filtration, water bioremediation, and disinfection) has been reviewed.

2 Classes of Nanomaterials

Several classifications can be made of nanomaterials used in water treatment, especially on the basis of their use and their function. On the basis of their use, we can consider nanomaterials classified as: nanomaterials for water filtration, nanotechnologies for water remediation, and bioactive nanoparticles for water disinfection (Theron et al. 2008). On the basis of their function in water remediation, nanomaterials can be classified as: nanosorbents, nanocatalysts and redox active nanoparticles, nanostructured and nanoreactive membranes, bioactive nanoparticles (Savage and Diallo 2005). In this chapter, the classification suggested by Savage and Diallo is used.

2.1 Nanosorbents

Nanosorbents are nanoscale particles from organic and inorganic material that have high affinity to absorb substances (sorbate) by physical or chemical interactions. The very high surface area that characterizes nanoparticles is responsible of

giovanni.libralato@unina.it

significant enhancement of sorption potential compared to conventional material. Functionalizing the nanoparticles with chemical groups, it is sometimes possible to enhance the absorbent affinity towards target compounds. Activated carbon is one of the most common sorbent materials due to its good balance and cost-effectiveness. Moreover, different carbon-based materials and metal oxides have received great interest from the scientific community because of the possibility of a wide range of contaminants removal. Among them, great interest has been especially concentrated on carbon nanotubes (CNTs), Self-Assembled Monolayer on Mesoporous Supports (SAMMS), and zeolites. A brief description of these materials is shown below.

Carbon nanotubes (CNTs) are attractive due to their significant structural, mechanical and chemical properties (Popov 2004). They have cylindrical structures in which carbon-atom hexagons are arranged in a helical fashion about a needle axis (Iijima 1991). The unique properties of CNTs, listed below, make possible their use in several applications:

- High Electrical Conductivity;
- Very High Tensile Strength;
- High Flexibility;
- Great Elasticity;
- High Thermal Conductivity;
- Low Thermal Expansion Coefficient;
- High capability as Electron Field Emitters;
- Aspect Ratio.

According to several studies, CNTs present greater benefits than commercially available granular activated carbon (GAC) (Mukhopadhyay 2011). When using CNTs to remove natural organic matter (NOM) from water system, Su and Lu (2007) showed higher adsorption and desorption capacities than GAC filters. This capacity together with the lower reactivation temperature required and the lower weight loss exhibited by the CNTs indicate this technology could be probably function more economically than GAC for the removal of NOM from water system (Su and Lu 2007; Mukhopadhyay 2011). With regards to other contaminant removals such as cyanobacterial toxin (e.g., microcystins MCs), CNTs also showed sorption capacities superior to those of GAC. In particular, Yan et al. (2006) demonstrated that the amount of adsorption of MCs on the CNTs is determined by the specific surface area and the external diameter of the CNTs (Yan et al. 2006).

CNTs are essentially divided into single-wallet carbon nanotubes (SWCNTs) and multi-wallet carbon nanotubes (MWCNTs) depending of the hybridized carbon atom layers in the wall of CNTs (Theron et al. 2008). More in detail, SWCNTs consist of a single graphite sheet wrapped into a cylindrical tube while MWCNTs are instead composed of an array of concentrically nested nanotubes (Baughman et al. 2002) (Fig. 2).

giovanni.libralato@unina.it

Hyung and Kim (2008) studied the effects of NOM composition and water characteristics on the NOM adsorption to MWCNTs; finding a preferential adsorption of the higher molecular weight fraction of NOM. Moreover they also demonstrated that the degree of NOM adsorption depended on the nature of the

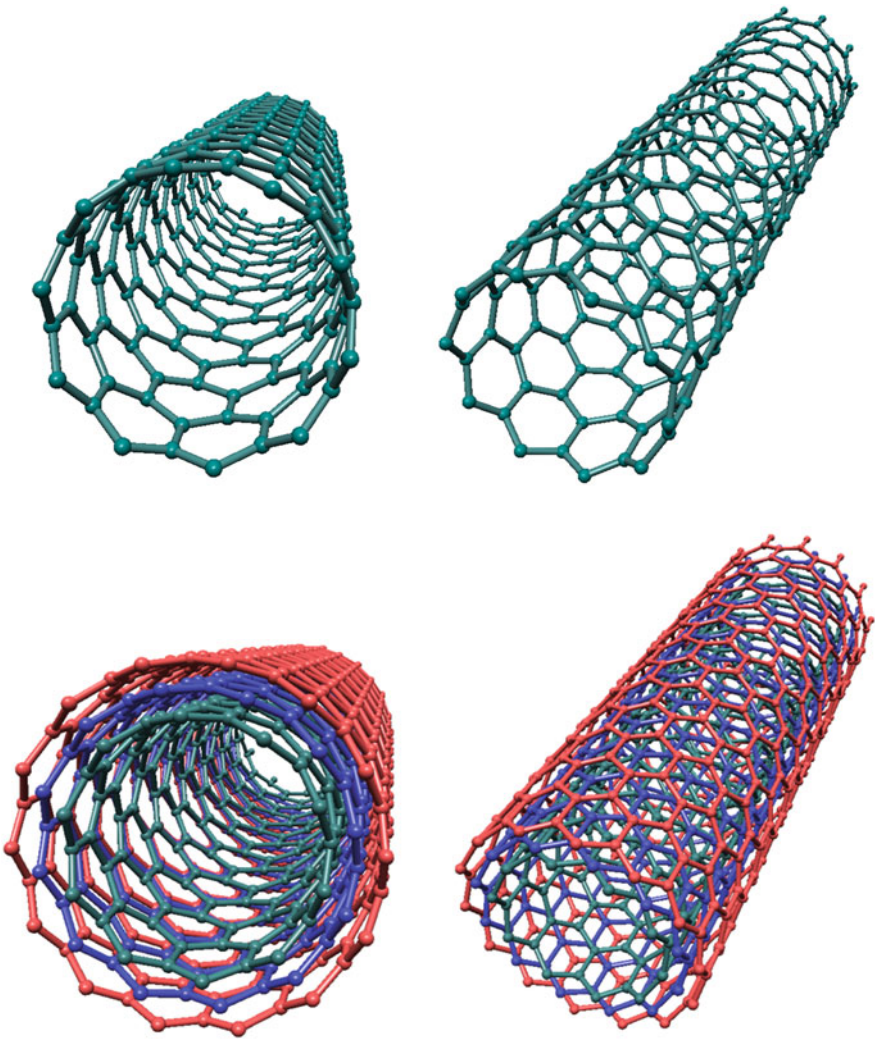

Fig. 2 Molecular representation of single-wallet carbon nanotubes (SWCNTs, *top*) and multi-wallet carbon nanotubes (MWCNTs, *below*)

giovanni.libralato@unina.it

NOM. In particular, the adsorption degree was proportional to the aromatic carbon content of NOM. From the point of view of water quality, it was also demonstrated the NOM adsorption increased as the pH decreased and the ionic strength increased (Hyung and Kim 2008).

The adsorption of trihalomethanes (THMs) by carbon nanotubes have also been tested (Lu et al. 2005). When testing two different initial concentrations (0.2 and 3.2 mg/L), Lu et al. observed that the adsorption quickly increased with time until equilibrium was reached. The contact time required to reach equilibrium was different for the two concentrations tested. That was equal to 180 min for C_0 = 0.2 mg/L and equal to 150 min for C_0 = 3.2 mg/L. Lu et al. justified the longer contact time to reach equilibrium for lower initial THMs concentration as consequence of the fact that diffusion mechanisms control the adsorption of THMs onto CNTs. In the case of initial concentration of 0.2 mg/L, the final adsorption capacities of $CHCl_3$, $CHBrCl_2$, $CHBr_2Cl$ and $CHBr_3$ set at 0.11, 0.06, 0.05 and 0.05 mg/g respectively while for C_0 = 3.2 mg/L they set at 1.51, 0.78, 0.72 and 0.64 mg/g respectively. The suitability of carbon nanotubes as means of pollution control for the sorption of divalent metal ions from aqueous solution has been deeply evaluated in a review published by Rao et al. (2007). After comparing the sorption performance of several systems, they suggested surface oxidized CNTs as promising sorbents for divalent metal ion removal from water and wastewater. They also pointed out the chemical interaction between the surface functional groups of CNTs and the divalent ions was the prevalent sorption mechanism. The drop in pH value, in fact, increased with a rise in initial metal ion concentration. This clearly indicates that sorption of more metal ion onto CNTs causes the release of more H^+ ions (the protons in the carboxylic and phenolic groups of CNTs) from the surface site of CNTs into the solution (Rao et al. 2007).

A new innovative class of environmental sorbents materials is also represented by **Self-Assembled Monolayer on Mesoporous Supports** (SAMMS) (Chen et al. 1999). The Pacific Northwest National Laboratory and Steward Environmental Solution is involved in the development of SAMMS, an award-winning technology created by attaching a monolayer of molecules to mesoporous ceramic support. Its high functional density and the surface area (up to 1000 m^2/g) make this sorbent material characterized by a really fast kinetics, high sorption capacity and excellent selectivity (Chen et al. 1999). Functional groups are introduced to the pore surface of mesoporous silica as the terminal groups of organic monolayers to selectively bind targeted molecules while the pore size, monolayer length, and density can be adjusted to give the material specific diffusive and kinetic properties (Feng 1997). Thiol-SAMMS, for example, was specifically developed for the removal of mercury from liquid media. Thiol-SAMMS has shown the unique ability to bind cationic, organic, metallic, and complexed forms of mercury. The adsorption by thiol-SAMMS occurred very rapidly, in fact, ~82–95% of total mercury adsorption already occurred within the first 5 min (Liu et al. 1998). Cesium selective SAMMS has been also synthesized in order to find out a new methodology for the cleanup of cesium-containing nuclear wastes and contaminated groundwater. Lin et al. (2001), for instance, achieved the complete removal of cesium in the presence of competing

giovanni.libralato@unina.it

metal ions for solutions containing 2 mg/L cesium under a variety conditions when using copper ferrocyanide immobilized within a mesoporous ceramic matrix as sorbent material (Lin et al. 2001).

Zeolites are hydrated aluminasilicate minerals with a three-dimensional highly ordered crystal structure built from the elements aluminum, oxygen, and silicon, with alkali or alkaline-Earth metals (such as sodium, potassium, and magnesium) plus water molecules trapped in the gaps between them (Breck 1974). Zeolites can be mainly considered as sorbents and ion-exchange media for metal ions. Additionally the high surface area, that makes zeolites really good sorbents, are also characterized by having high mechanical and chemical resistance that justify their use as catalyst and ion-exchanger as well. The scientific community is always trying to synthesize new materials with new novel zeolite framework structures. Nevertheless, 231 framework types code have been actually approved by the International Zeolite Association (IZA) Structure Commission (IZA-SC). Conventional synthesis methods allow the production of zeolites with dimensions ranging between 1 and 10 μm. New synthesis methods, successfully led to the production of nanoscale zeolites (dimensions ranging from 5 to 100 nm) (Landau et al. 2003; Cravillon et al. 2009; Nune et al. 2010). In 2004, Song et al., compared the adsorption capacity of nanocrystalline ZSM-5 with a Si/Al ratio of 20 and that of commercial ZSM-5. They showed that the ZSM-5 sample with a particle size of 15 nm adsorbed approximately 50% more toluene than the other ZSM-5 samples, most likely due to the adsorption of toluene on the external surface (Song et al. 2004). Again, Song et al. (2005) tested nanocrystalline NaY zeolites on the adsorption of toluene and nitrogen dioxide. They tested two samples synthesized with Si/Al ratios of 1.8 and crystal sizes of 23 and 50 nm and, for comparison, a commercial NaY sample as well. The authors demonstrated that, when using the nanocrystalline samples, the adsorption capacities increase of almost 10 and 30% for toluene and nitrogen dioxide removal respectively respect to the commercial NaY (Song et al. 2005).

Table 1 lists other examples of nanosorbents and their application in water remediation.

2.2 *Nanocatalysts and Redox Active Nanoparticles*

A nanocatalyst is a material with catalytic properties and at least one nanoscale dimension, either externally or in terms of internal structures. The small size of nanocatalysts is responsible of their higher catalytic activity. The porous nanostructure of the material, in fact, provides high surface to volume ratio, therefore more surface is available to interact with the reactants. Also really promising is the option of combining nanosorbents with catalyst (i.e. magnetic nanoparticles). In this case, the concentration of the contaminant at the particle surface, due to the adsorption potential of the particles, facilitates the decomposition of the contaminant by the catalyst.

giovanni.libralato@unina.it

Table 1 Examples of nanoparticles and nanomaterials as sorbents for water remediation

Nanosorbent	Pollutant	Reference
Carbon nanotubes (SWCNTs, MWCNTs)	NOM	Su and Lu (2007)
	Trihalomethanes (THMs)	Lu et al. (2005)
	Heavy metal ions	Lu and Liu (2006)
	Herbicides	Zhou et al. (2007b)
	Cyanobacterial toxins	Albuquerque et al. (2008)
	Microcystins (MCs)	Yan et al. (2006)
	Ethylbenzene	Bina et al. (2012)
	Roxarsone	Hu et al. (2012)
Self-Assembled Monolayer on Mesoporous Supports (SAMMS)	NOM	Majewski (2007)
	Inorganic ions	Feng et al. (1997), Kelly et al. (2001)
	Metal ions	Goyal et al. (2011)
– Thiol-SAMMS	Heavy metal ions	Chen et al. (1999), Yantasee et al. (2007), Fryxell et al. (2007)
– Cu(II)-EDA-SAMMS, Fe(II)-EDA-SAMMS	Phosphate ions	Chouyyok et al. (2010)
Poly (AAc/AM/SH)superabsorbent hydrogels	Phosphate ions	Singh and Singhal (2013)
Monodisperse manganese oxide nanospheres	Methylene blue and heavy metal ions	Chen and He (2008)
Functionalized iron oxide magnetic nanomaterials		
– magMCM-41, Fe^{3+}-magMCM-41	Chromium	Chen et al. (2011)
– maghemite nanoparticles	Chromium	Hu et al. (2005)
– Mesoporous SiO_2	Chromium	Wang and Lo (2009)
– Poly-l-cysteine coated Fe_2O_3 MNPs	Heavy metal ions	White et al. (2009)
– Humic acid coated Fe_3O_4 nanoparticles (Fe_3O_4/HA)	Heavy metal ions	Liu et al. (2008)
– Bionanocomposite for magnetic removal	Inorganic particles	Sousa et al. (2015)
Zeolites	Toluene	Song et al. (2004, 2005)
	Nitrogen dioxide	Song et al. (2005)
Zero-valent iron nanoparticles (nZVI)	Heavy metal ions	Kanel et al. (2005), Giasuddin et al. (2007), Boparai et al. (2011)
	Nitrobenzene	Ling et al. (2012)
	PCBs	Liu and Zhang (2010)

giovanni.libralato@unina.it

Between the wide selections of catalyst, **titanium dioxide** (TiO_2) is probably the most popular. In this case, photocatalytic reaction occurs when light absorption induces a charge separation. At this state, TiO_2 particle is very unstable and it may react with several pollutants adsorbed at the surface or even water producing the highly reactive hydroxyl radical (see Fig. 3). The reason for its popularity is attributed to its relatively high photoactivity under UV irradiation, high stability, low cost and safety to both humans and the environment (Gupta and Tripathi 2011). TiO_2 exists in three crystalline forms; anatase and rutile are the most common types, and the crystalline size of the rutile is always larger than the anatase phase. Brookite is the third structural form, an orthorhombic structure, which is rarely utilized (Bagheri et al. 2014). TiO_2 has had a long-standing use as direct application in form of powder into a solution. However, recent studies have also demonstrated as TiO_2 photoactivity can be significantly enhanced when used in the nanoparticle form (Han and Bai 2009). At large scale, the application of TiO_2 nanoparticles has been limited by the necessity of filtration of the catalyst after the treatment. This particular disadvantage, which results in a high cost, can be overcome by immobilizing TiO_2 nanoparticles on various substrates (Ma et al. 2001; Rao et al. 2003). Moreover, the highly effectiveness of TiO_2 in the nonselective degradation of organic contaminants has been largely demonstrated. However, conventional TiO_2 requires ultraviolet (UV) radiation ($\lambda < 385$ nm for anatase phase and <410 nm for rutile phase) to overcome its wide band gap energy ($\sim$3.2 and 3.0 eV

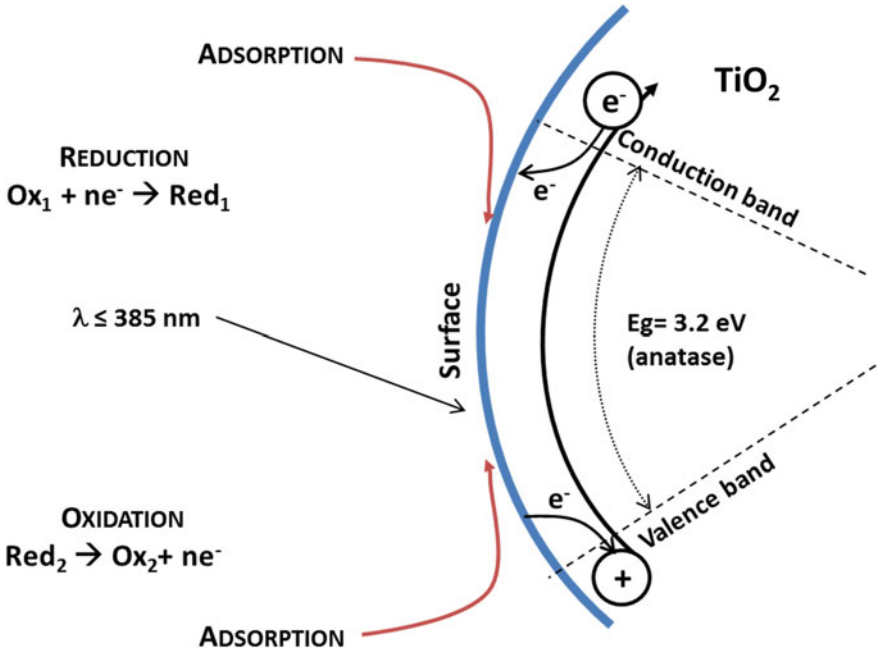

Fig. 3 General mechanism of photocatalytic process on TiO_2

giovanni.libralato@unina.it

for anatase and rutile phase respectively) for photocatalytic activation (Pelaez et al. 2009; Paul and Choudhury 2013). Thus, only photons with high energy as UV photons can start the process. It means that only an small fraction of solar radiation is useful for photocatalysis with TiO_2. In fact, only 5% of the incoming solar energy on the earth's surface is in the UV range (Kim et al. 2005). Photocatalytic efficiency of TiO_2 partially depends on the relative degree of branching of the reactive electron–hole pairs into interfacial charge-transfer reactions (Choi et al. 1994). Doping has been a good strategy to enhance the optical properties of the catalyst and reduce the band gap photocatalytic activation. By means of this approach, the possibility of solar light utilization for the treatment may be viable. Doping with transition metal ions, for example, can provide additional energy levels within the band gap of a semiconductor. Thus, electron transfer from one of these levels to the conduction band requires lower photon energy than in the situation of the undoped catalyst (Gupta and Tripathi 2011). TiO_2 has been doped with many different metals (Fe, Co, Ag) (Choi et al. 1994; Li and Li 2002; Lee et al. 2005) and nonmetal (N, F, C, S) (Pelaez et al. 2009; Choi et al. 2007a; Cong et al. 2007).

Zero valent iron (ZVI) is a reactive metal with standard redox potential ($E^0 = -0.44$ V). Since 1990s, ZVI has been also deeply studied demonstrating great suitability and efficiency in applications of environmental remediation and hazardous waste treatment. The removal mechanism of contaminants by ZVI considers the electrons transfer from ZVI to the contaminants which can be then transformed into non-toxic or less toxic species. Additionally, ZVI can degrade and oxidize a series of organic compounds in the presence of dissolved oxygen (DO) since ZVI transfers two electrons to O_2 to produce hydrogen peroxide (H_2O_2). Thus, the produced H_2O_2 can be reduced to water by another two-electron transfer from ZVI Finally, the combination of H_2O_2 and Fe^{2+} (naturally present in several waters) can produce hydroxyl radicals (·OH) available for supplementary oxidation of organic compounds (see reaction listed below) (Fu et al. 2014):

$$Fe^0 + O_2 + 2H^+ \rightarrow Fe^{2+} + H_2O_2$$
$$Fe^0 + H_2O_2 + 2H^+ \rightarrow Fe^{2+} + 2H_2O$$
$$Fe^{2+} + H_2O_2 \rightarrow Fe^{3+} + \cdot OH + OH^-$$

Moreover, among the qualities that have made ZVI popular are its non-toxicity, abundance, cheapness and easy production (Fu et al. 2014). Indeed, ZVI has been successfully used for the removal of a wide range of contaminants especially in the application of groundwater treatment (Joo et al. 2004). ZVI particles exhibit a core-shell structure (Fig. 4). The core mainly consists of zero-valent or metallic iron while the mixed valent oxide shell is formed as a result of oxidation of metallic iron (Li et al. 2006). The good reactivity of ZVI under ambient conditions serves as an excellent electron donor making this material particularly suitable in remediation applications (Stumm and Morgan 2012). Granular ZVI has started to be used in groundwater remediation in permeable reactive barrier (PRBs) systems (Gillham and O'Hannesin 1994; Gu et al. 1999).

giovanni.libralato@unina.it

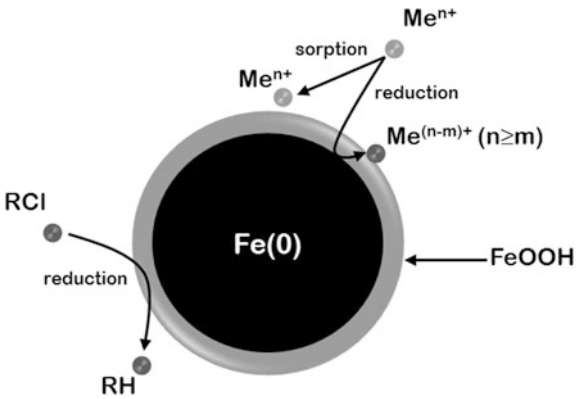

Fig. 4 The core-shell model of zero-valent nanoparticles (nZVI)

In these systems, a wide range of contaminants contained in the groundwater can be precipitated, adsorbed or transformed in contact with the ZVI surface when passing through the iron wall (Li et al. 2006). Nevertheless, the application of ZVI for persistent organic pollution into the subsurface environment have been limited especially because the particle size and the reactivity of conventional ZVI (Shih et al. 2011). A large amount of iron powder, in fact, is usually required even for a modest PRB structure (e.g., tons). Thus, cost associated with the construction of PRB for deeps aquifers remain too high for possible real applications (Li et al. 2006). Once again, nanoscale iron technology (nZVI) can be considered as an extension of the ZVI technology being the surface area of the nanoparticles (10–100 nm) 10 times larger than that of a microscale particle and being the reactivity also significantly enhanced (Tratnyek and Johnson 2006). Although nZVI particles have been already tested or used for field remediation, their use has been limited by the concerns related with toxicity and safety (UNEP 2007; US. EPA. 2008). However, the environmental applicability of nZVI can be easily extended when immobilizing iron nanoparticles in a support without losing its size and reactivity (Kim et al. 2010).

In Table 2 are summarized some examples of nanocatalyst application in water remediation.

2.3 Nanostructured and Reactive Membranes

Since conventional water treatment techniques as sedimentation, flocculation, coagulation, biological treatment, and activated carbon are not able to efficiently remove an wide range of contaminants, membranes processes are playing an important role in water purification (Theron et al. 2008). Water purification using water filtration technology has made great progresses due to developments in the field of nanomaterials. The origin of nanofiltration can be identified between the

giovanni.libralato@unina.it

Table 2 Examples of nanoparticles and nanomaterials as catalyst for water remediation

Nanocatalyst	Pollutant	Reference
TiO_2 nanoparticles	Textile Diazo Dye, Naphthol Blue Black	Nasr et al. (1996)
	Phenols	Andersson et al. (2002)
Doped TiO_2 nanoparticles		
– ZnO-doped TiO_2	Azo Dye	Ismail and Mazyck (2008)
– N-F-codoped TiO_2	Microcystin-LR	Pelaez et al. (2009)
– Nitrogen (N)-doped TiO_2	Methylene blue	Burda et al. (2003)
	Azo Dye	Liu et al. (2005)
– Fe(III)-doped TiO_2	Phenol	Nahar et al. (2006)
Carbon-Nanotube-TiO_2 composite	Organic, inorganic and biological agents	Woan et al. (2009)
Supported TiO_2 nanoparticles		
– Silica-supported TiO_2	Aromatics compounds	López-Muñoz et al. (2005)
	Fulvic acid	Fu et al. (2006)
– TiO_2 nanoparticles on graphene sheets	Chromium (VI)	Zhang et al. (2012)
nZVI	Chlorinated Methanes	Lien and Zhang (1999)
	Hexachlorobenzene	Shih et al. (2011)
– Green tea synthesized nZVI (GT-nZVI)	Bromothymol blue	Hoag et al. (2009)
Supported n-ZVI		
– NaY zeolite-supported nZVI	Potassium acid phthalate (KHP)	Wang et al. (2010)
– Polystyrene resins supported nZVI	Nitrate	Jiang et al. (2011)
– Activated carbon	Arsenic	Zhu et al. (2009)
Doped nZVI		
– Pd-nZVI	Trichloroethene	Yan et al. (2010)

1970s and 1980s when "loose RO" membranes were developed as intermediate units between ultrafiltration and reverse osmosis (Eriksson 1988; Sutherland 2008). It has been calculated that the investment cost for a nanofiltration plant is about the same as for a brackish water reverse osmosis plant, but the energy saving can be considerable by using nanofiltration instead of reverse osmosis (Eriksson 1988). In Table 3 are summarized the membrane's properties for the different membrane processes.

Nanofiltration is essentially a liquid phase process and very similar to reverse osmosis. When liquid is forced to pass through the membrane, some inorganic and organic solvents may be rejected and effectively separated. This happens by diffusion through the membrane with a pressure that is generally lower than in the

giovanni.libralato@unina.it

Table 3 Membranes processes

Membrane type	Pore size (nm)	Pressure (bar)
Reverse osmosis	<0.6	30–70
Nanofiltration	0.6–5	10–40
Ultrafiltration	5–50	0.5–10
Microfiltration	50–500	0.5–2

reverse osmosis but much higher than in the case of ultrafiltration. Then, with the development of thin film composite membranes, the unique ability to separate and fractionate ionic and low molecular weight species was strongly improved. Nanofiltration, was then confirmed as a recognized process. It appears obvious, then that the membranes play a fundamental role in the performance of the treatment and its applicability (Sutherland 2008). The great progresses made in the field of membrane synthesis and production has led to the spread of membrane processes for several uses.

The wide range of applications of nanofiltration makes these materials very attractive in ground water remediation, surface remediation, water potable treatment, and desalination. The possibility of removing cations, natural organic matter, biological contaminants, organic pollutants, nitrates and arsenic as application in drinking water industry has been already reviewed (Van der Bruggen and Vandecasteele 2003). The most commonly used membrane processes for water and wastewater treatment include microfiltration (MF), ultrafiltration (UF) and nanofiltration (NF) (Peltier et al. 2003; Van der Bruggen and Vandecasteele 2003; Qin et al. 2007). For desalination and water reclamation we more often refer to nanofiltration and reverse osmosis (RO) (Van der Bruggen and Vandecasteele 2002; Mohsen et al. 2003; Walha et al. 2007).

Differently from the meaning of nanofiltration, in which the term nano is referred to the size of the particles that are rejected by the membranes, in nanotechnology we would also consider "nanostructures membranes" (NSM) all those membranes with engineered nano-sized structures. In nanostructured membranes (NSM), either carbon nanotubes or nanocapillary arrays provide the basis for nanofiltration. They can be used to reject suspended particles, bacteria, macromolecules, viruses, colloids, organic compounds, and multivalent ions. Another type of nanotechnology membranes that could be really effective in water depuration is represented by nanoreactive membranes, where functionalized nanoparticles are able to decompose some pollutants and aid the filtration process.

Among the **nanostructured membranes**, carbon nanotubes (CNTs) have been proposed as a separation technology (Miller et al. 2001). CNTs can be in fact used to form membranes with ordered structure (Holt et al. 2006; Su and Guo 2011) showing high water permeability. The excellent CNTs properties, combined with their exceptional thermal and mechanical stability may in the future make them really competitive with ceramic and polymer materials in water separation. At the moment, however, their preparation must be improved (Theron et al. 2008). Several studies have been carried out in order to find the most efficient fabrication settings.

giovanni.libralato@unina.it

For example, in 2008, Corry indicated CNTs used in reverse osmosis were an efficient means of water desalination. He suggested that very large flows can be expected when using as membranes. A membrane comprising nanotubes could be expected to obtain 95% desalination with a flow rate of over 1500 times of existing membranes. Thus, though CNTs are able to well reject ions, they still conduct water at higher rates. Comprising less than 1 pore in 100 over the size of 10 Å in diameter, the efficiency could be increased 5–1000 times. The limitations are connected to the necessity of make these membranes strong enough to withstand the hydrostatic pressures applied to them (Corry 2008). The complications related with the preparation of these membranes are evident.

Other of nanostructured membranes are also possible. It is the case of **nanostructured thermotropic liquid-crystal (LC) materials** that can be synthetized (often in situ) by photopolymerization of a LC monomer (Henmi et al. 2012). Nanostructured LCs can form aligned and self-organized pathways for permeation on nanometer scale (Kato 2002; Sakai et al. 2006; Gin et al. 2006; Zhou et al. 2007a; Kato 2010; Ichikawa et al. 2011). They are on the good way to represent valid candidates for the construction of new water treatment membranes with ordered nanostructures. For instance, Henmi et al. used a nanostructured ion conductor material for the formation of a cubic (Cub_{bi}) liquid-crystal nanostructure with 3D-interconnected ionic channel network that could have great potential as ion-separator (Henmi et al. 2012). In this study, the salt rejection performance of the membrane was examined under an applied pressure of 0.75 MPa and a concentration of inorganic salts in the aqueous solution between 500 and 1500 ppm. The rejection of NaCl and $MgCl_2$ by the Cub_{bi} membrane was above 60%. Additional studies on the possibilities of combining the lyotropic LC (LLC) assembled nanostructured with heterogeneous catalysis and selective separation have been also carried out. In fact, it has been demonstrated that, by making polymerizable analogues of LLC mesogens, it is possible to stabilize the various LLC assemblies with retention of phase microstructure via photo-initiated radical crosslinking (Gin et al. 2006).

Although membrane filtration is a proven technology, membrane fouling keeps being one of the major drawbacks of the process. Therefore, that represents an important limiting factor to the wide use of membranes. Thus, functionalized membranes, that often show a good resistance to biofouling, can represent a good strategy to overcome this limitation. Accordingly, several reactive and functionalized membranes have also been developed for use in water filtration processes. Progress has been made in the last few years by combining different materials. Additional improvements are still expected considering the enormous advantages obtained by combining the properties of the various materials by producing interaction among the components. These membranes are often the result of conventional CNTs modification in order to make possible the enhancement of their properties and reach better efficiency in water remediation. An example is represented by nanosilver and multi-walled carbon nanotubes thin-film nanocomposite

giovanni.libralato@unina.it

(n-TFN) membrane (Kim et al. 2012). In this case, the presence of silver ions at different oxidation states (Ag^0, Ag^+, Ag^{2+}) can largely enhance membrane anti-biofouling properties, but are often ineffective in improving membrane permeability and rejection ratio. More frequently, researcher have combined membranes and metal oxide nanoparticles (mainly TiO_2) in order to increase the novelty of membrane materials, permeability, fouling resistance and permeate quality as well. In fact, combining the effects of chemical oxidation with the advantages of nanoparticle-based membranes it is even possible to mitigate the effect of fouling providing the membrane of a built-in oxidative functionality. The permeate quality would be additionally increased due to the decomposition of organic compounds on the catalytic membrane surface. Another example of combining nanofiltration with TiO_2 is represented by TiO_2 nanowire membrane. Zhang et al. (2008a), in fact, showed that by employing nanowires of 20–100 nm in diameter and variable length in the range of several micrometers to ten micrometers, it was possible to of almost the 100 and 94% of humic acid and total organic carbon removal. The photocatalytic activity exhibited by the TiO_2 nanowires was similar to that of TiO_2 powder P25 and, as expected, an excellent anti-fouling ability (Zhang et al. 2008a).

Finally, other examples of nanostructured membranes and nanoreactive membranes are summarized in Table 4.

2.4 *Bioactive Nanoparticles*

Nanotechnology is also offering a valid contribution in the field of water disinfection. The necessity of reducing the risk of waterborne infection is a topic of current concern. It is estimated that infectious disease cause almost 40% of the 50 million total annual deaths worldwide (Leonard et al. 2003). Generally, drinking water disinfection is carried out by means of chlorine, which also provides residual protection for some period of time against re-growth of bacteria and pathogens (Szewzyk et al. 2000). The undesirable taste and odors of the treated water by chlorine (Suffet 1995), together with the possibility to generate toxic by-products of disinfection negate in many ways the benefits (Rook 1974; Gopal et al. 2007). Therefore, nanotechnology may present a reasonable alternative for development of new chlorine-free biocodes. Among the most promising antimicrobial nanomaterials are metallic and metal-oxide nanoparticles, especially silver, and titanium dioxide catalysts for photocatalytic disinfections.

Several studies have been published on the application of silver (Ag) ions and silver compounds as biocides due to their strong toxicity to a wide range of microorganism (Spadaro et al. 1974; Zhao and Stevens 1998). Nevertheless, experiments carried out on nitrifying bacteria showed that the inhibition effect was stronger when using Ag-NP than when using dissolved Ag^+ or AgCl colloids (Choi et al. 2008). It was suggested that Ag-NP penetrate the bacterial membrane of

giovanni.libralato@unina.it

Table 4 Examples of nanostructured membranes and nanoreactive membranes for water remediation

Membranes	Function	Reference
Nanostructured membranes		
– CNTs	Ions rejection/desalination	Cohen-Tanugi and Grossman (2012), Corry (2008)
– MWCNTs thin-films nanocomposite membrane (*n*-TFN)	Ions rejection/desalination	Kim et al. (2012)
– Liquid-crystal nanostructured membranes	Ions rejection/desalination	Zhou et al. (2007a)
Nanoreactive membranes		
– TiO_2 nanoparticles self-assembled aromatic polyamide thin-film-composite (TFC) membrane	Bacteria inactivation	Kim et al. (2003)
	Biological toxins	(Choi et al. 2007b)
– TiO_2 nanowire membrane	Humic acid and TOC removal	Zhang et al. (2008a)
– Porous PVDF-ZrO_2 composite membranes	Separation	Bottino et al. (2002)
– Silver-nanoparticles/bacterial cellulose composites (AgNP-BC)	Antimicrobial activity	Wu et al. (2014)
– Bioactive Electrospun Silver Nanoparticles-Containing Polyurethane Nanofibers	Antimicrobial activity	Chen and Chiang (2010)
– Membrane modified with a PAA/PAH/Au colloid film	4-nitrophenol reduction	Dotzauer et al. (2006)
– Platinum nanoparticles/polyamidoamine (PAMAM) dendrimers incorporated in LbL films in conjunction with nickel tetrasulfonated phthalocyanine (PAMAM-Pt/NiTsPc LbL film)	electrocatalytic activity toward dopamine and hydrogen peroxide molecules	Siqueira et al. (2007)
– Zero-valent Fe laden cellulose acetate membrane	Trichloroethylene (TCE) removal	Wu et al. (2005)
– Polymer-impregnated ceramica lumina and silicon-carbon filters	Trihalogen methanes, PAHs, pesticide	Allabashi et al. (2007)

Escherichia coli (Sondi and Salopek-Sondi 2004) and other gram-negative bacteria (Morones et al. 2005). Additionally, studies carried out on Gram-positive bacteria demonstrated as the bactericidal properties of silver nanoparticles are dependent of their size and the shape. In 2005, in fact, Morones et al., tested the bactericidal properties of silver nanoparticles with dimension in a range of 1–100 nm determining that the only nanoparticles that present a direct interaction with the bacteria have a diameter in the range 1–10 nm (Morones et al. 2005). Pal et al., instead,

giovanni.libralato@unina.it

Table 5 Examples of stabilized and immobilized bioactive nanoparticles for water disinfection

Nanoparticle	Pollutant	Reference
Bactericidal paper impregnated with silver nanoparticles	Fecal contamination indicator	Dankovich and Gray (2011)
Stabilized Ag nanoparticles in presence of Daxad 19	*E. coli*	Sondi and Salopek-Sondi (2004)
Ultrafine cellulose acetate fibers with silver nanoparticles	Several *Gram-positive* and *Gram-negative* bacteria	Son et al. (2004)
Copper monodispersed nanoparticles into sepiolite	*E. coli* and *S. aureus*	Esteban-Cubillo et al. (2006)
Titanium dioxide coated multi-wall carbon nanotubes	*Bacillus cereus spores*	Krishna et al. (2005)
Titanium Dioxide	*E. coli*	Ireland et al. (1993)

studied the interaction of Gram-negative bacteria with silver nanoparticles of different shapes. They found that the bactericidal effect of these nanoparticles is strongly dependent on their shape. More so, truncated triangular silver nanoplates, with a {111} lattice plane as the basal plane, displayed the strongest biocidal action, compared with spherical and rod-shaped nanoparticles and with Ag^+ (in the form of $AgNO_3$) (Pal et al. 2007).

The stabilization and immobilization of bioactive nanoparticles in different matrixes has been also investigated. For example, Dankovich and Gray (2011) studied the deactivation of pathogenic bacteria by percolation through a paper sheet containing silver nanoparticles. The use of silver nanoparticle shows the intention to inactivate the bacteria and not to achieve their removal through filtration. The AgNP sheets exhibited antibacterial properties toward suspensions of *Escherichia coli* and *Enterococcus faecalis*, with log reduction values in the effluent of over log 6 and log 3, respectively. The silver loss from the AgNP sheets was minimal, with values under 0.1 ppm (the current US EPA and WHO limit for silver in drinking water) (Dankovich and Gray 2011). Other examples of stabilized and immobilized bioactive nanoparticles are listed in Table 5.

3 Synthesis and Characterization

The wide range of nanomaterials implies the possibility of having an extended selection of strategies for nanoparticles synthesis, shown by the methods suggested to synthesize the classes of nanoparticles mentioned above. Before going through some example of synthesis methods specific for these classes, it can be useful to simplify and consider the existent approaches as classified by Tiwari et al. (2008):

giovanni.libralato@unina.it

- **Self assembly**: this method considers the possibility to induce self-assembly of molecules to form nanostructure by manipulating physical and chemical conditions (pH, temperature, concentration, etc.).
- **Layer by layer deposition**: in this case, nanostructured membranes can be fabricated by layering the essay materials followed by eventual calcination in furnace.
- **Preparation of functional nanoparticles by thermal plasmas**: this approach contemplates the possibility of preparing functional nanoparticles (of silicide and boride) by induction in thermal plasmas. The mixed powders of the materials are injected into the plasma and then evaporated and reacted with boron. The vapor is quickly cooled after the plasma flame.
- **Gas phase synthesis and sol-gel processing**: these techniques represent two of the most common strategies for nanoparticles synthesis. Nanoparticles with consistent crystal structure, surface derivatization, and a high degree of mono-dispersity have been processed by both these techniques.
- **Crystallization**: crystal nanoparticles are synthesized in the presence of solution containing different amount of amino acids (material of composition).
- **Biogenic strategy**: this strategy contemplates the possibility of using self-assembled organic materials as templates or scaffolding for inorganic components.
- **Microbial synthesis**: living cells can be used to produce nanoparticles. As example, silver nanoparticles have been extracellularly produced by fungi and bacterial species (Bhainsa and D'Souza 2006; Bhattacharya and Gupta 2008).
- **Biomass reactions**: gold nanorods or other shaped nanoparticles have been produced by incubation of dead oat stems with an acidic aqueous solution of gold ions.
- **Other strategies**: sonochemical processes, cavitation, microemulsion are examples of other techniques useful in nanoparticles synthesis.

In Table 6 some example of nanoparticles synthesis are listed.

As already discussed in this chapter, the fundamental of nanotechnology is connected to the unique properties of materials when in the nanometer scale. However, as it is always complicated to reduce the dimension of a material to the nanoscale, characterizing these nano sized materials is even more complicated. Thus, research efforts are not only focused on the synthesis of new nanomaterials but are also dedicated to the discovery of new sophisticated nano characterization techniques to allow a proper monitoring of the properties and especially the dimension of materials in the nano range (Bhattacharyya and Ali 2008).

Different methods are available for characterizing nanomaterials. In first approximations, the techniques used to analyze the properties of these are the same used for the analysis of classical pollutants (Weinberg et al. 2011). On the basis of the probe used for to characterize the nanoparticles, the major techniques used can be classified as follows: (Hornyak et al. 2008):

giovanni.libralato@unina.it

Table 6 Examples of nanoparticles synthesis

Method of synthesis	Nanoparticle	Specification	Reference
Co-precipitation method	Magnetite nanoparticles	Dissolution of 1.5 g of $FeCl_2{\cdot}4H_2O$ and 3.0 g of $FeCl_3$ in 100 mL of deionized water under nitrogen gas flow (T = 0–90 °C). Addition of NH_4OH and coating agents to form the coated magnetite nanoparticles later dried in a vacuum at 80 °C for 24 h	Petcharoen and Sirivat (2012)
Self-reacting microemulsion method	Nanosized hydrous manganese dioxide	Addition of 32.4 mL of 0.1 mol L^{-1} $KMnO_4$ to AOT/iso-octane solution (prepared by adding 13.32 g of surfactant Aerosol-OT (AOT) to 300 mL of iso-octane). Dispersion of this solution by ultrasound for 30 min to prepare a dark brown precipitate later washed with distilled water and ethanol, and dried at 80 °C for 12 h	Xu et al. (2008)
Sol–gel and hydrothermal methods	Nickel ferrite nanoparticles	Preparation of aqueous solution after mixing of nickel nitrate (0.4 M) and ferric nitrate (0.8 M) solution with 70% aqueous solution of glycolic acid. Slow addition of 25% ammonia solution while stirring until the obtaining a transparent green solution (pH 7.5). Evaporation of the solution at 90 °C to form the sol gel. Then heating at 70 °C during 3 h and calcination at 700 °C during 10 h	Srivastava et al. (2009)
Pulse sonoelectrochemical methods	Silver nanoparticles	Mixing of 0.6 (for spherical nanoparticles), 2, 4, 20 (for nanorod structure) g/L $AgNO_3$ with nitrilotriacetate (NTA), in an aqueous solution under a N_2 atmosphere. The electrolyte volume was 50 mL. Deposition carried out typically in 25 min for a 20 g/L sample. Precipitate was centrifuged, washed with distilled water and ethanol, and dried under vacuum	Zhu et al. (2000)
Aerosol-assisted self-assembly method	Mesostructured spherical nanoparticles	TEOS [$Si(OCH_2CH_3)_4$], ethanol, water and dilute HCl were refluxed at 60 °C for 90 min. The sol was diluted with ethanol (1:2), then by addition of water and dilute HCl. Surfactants were added. The final reactant mole ratios (TEOS:EtOH:H_2O:HCl:surfactant) were 1:(0–22):(5–67):0.004:(0.006–0.23)	Lu et al. (1999)
Microbial synthesis	Silver nanoparticles	Atmospheric bacteria were grown on nutrient agar substrate containing 3.5 mM $AgNO_3$ under aerobic conditions at 30 °C. The colony was sub-cultured into 50 mL of nutrient broth containing 3.5 mM $AgNO_3$. The broth was inoculated with a loopful of bacteria and incubated for a period of 7 days in darkness at room temperature. The bacteria were then harvested by centrifugation (10,000 rpm) at room temperature	Pugazhenthiran et al. (2009)
One-pot synthesis and layer-by-layer assembly	Ag@TiO_2 core-shell nanoparticles	Addition of 20 mL of sonicated solution (TOB and acetylacetone in ethanol in a concentration of 5.75 mM each) to 5 mL of a fresh daily solution (3.8 mM $AgNO_3$ and 0.8 M H_2O in DMF). Heating of the mixed solution at a reflux temperature during 90 min. Dilution of the formed stable dispersion of DMF/ethanol with water for a period of 1 week (acidic pH) to 1 day (basic pH). Layer-by-layer deposition with a polyelectrolyte to form thin films of the core-shell nanoparticles	Pastoriza-Santos et al. (2000)

giovanni.libralato@unina.it

- Optical (Imaging) Probe Characterization Techniques;
- Electron Probe Characterization Techniques;
- Scanning Probe Characterization Techniques;
- Photon (Spectroscopic) Probe Characterization Techniques;
- Ion-Particle Probe Characterization Techniques;
- Thermodynamic Characterization Techniques.

The primary probe in **optical methods** is the visible light of wavelength within the 400 to the 800 nm range. The main problem of these techniques is related to their limited resolution to a few hundred microns. Optical characterization methods are primarily used for imaging. **Electron probe characterization** techniques use high-energy electron beams. These techniques are useful for imaging, chemical analysis and determination of materials structures. **Scanning probe characterization** methods are characterized by a finely sharped probe tip and a system that enables the tip to scan. The resolution achievable with these techniques is on the order of atoms. Among the techniques of this class we find the light scattering methods which are particular suitable for the measurement of nanoparticles in liquid media. Electron and scanning probe microscopy are preferred respect optical methods for characterization (size, shape, texture, structure, morphology and elemental composition) (Weinberg et al. 2011; Lens et al. 2013). In particular, electron microscopy is particularly suitable for elements with high electron density (Tiede et al. 2009). Scanning probe microscopy techniques are mainly used for broader categories of materials and generate high resolution and three dimensional images (Peters et al. 2011). Also **spectroscopic characterization** methods use UV-visible light as probe for the nanomaterial analysis. In this case, the techniques are based on the absorption or emission (fluorescence) of the photons. **Ion particle characterization** techniques are based on the analysis of the ionized components coming from the broken parent nanoparticles. Finally, **thermodynamic characterization** methods involve probes which are not a photon or an electron but a thermodynamic parameter such as temperature or pressure (Hornyak et al. 2008).

Nanoparticles are also known to be involved in instability phenomena. They can, in fact, be really reactive depending on the composition of the media. Furthermore they can aggregate, change their initial shape, etc. Also their properties can change during manipulation and storage. For this reason, it is generally extremely important to pre-quantification methods such as extraction, separation and fractionation methods (López-Serrano et al. 2014). In Table 7 the most used characterization, quantifications and separations techniques for nanomaterials have been summarized.

giovanni.libralato@unina.it

Table 7 Nanoparticles characterization, quantifications and separations techniques

Type of technique	Characterization technique	Information provided
Optical (Imaging) Probe Characterization Techniques	Confocal laser-scanning microscopy (CLSM)	Morphology
	Scanning near-field optical microscopy (SNOM)	Rastered images
	Dynamic light scattering (DLS)	Particle size (hydrodynamic diameter), zeta potential (nanoparticle's stability)
	Electrophoretic light scattering (ELS)	Zeta potential
	Brewster angle microscopy (BAM)	Gas-liquid interface images
Electron Probe Characterization Techniques	Scanning electron microscopy (SEM)	Rastered images, topology and morphology
	Electron probe microanalysis (EPMA)	Particle size and local chemical information
	Transmission electron microscopy (TEM)	Images, particle size and shape
	High-resolution transmission electron microscopy (HRTEM)	Chemical structure, images of the crystallographic structure
	Scanning transmission electron microscopy (STEM)	Elemental composition and electronic structure
	Low-energy electron diffraction (LEED)	Surface and adsorbate bonding
	Electron energy loss spectroscopy (EELS)	Inelastic electron interactions
	Auger electron spectroscopy (AES)	Chemistry of the surface
Scanning Probe Characterization Techniques	Atomic force microscopy (AFM) or Scanning-force microscopy (SFM)	Topology and surface structure (roughness measure)
	Chemical force microscopy (CFM)	Structural morphology
	Magnetic force microscopy (MFM)	Magnetic materials composition
	Scanning tunneling microscopy (STM)	Topology and surface structure
	Atomic probe microscopy (APM)	Three-dimensional images
	Field ion microscopy (FIM)	Chemical profiles
	Atomic probe tomography (APT)	Atoms locations
Photon (Spectroscopic) Probe Characterization Techniques	Ultraviolet photoemission spectroscopy (UPS)	Molecular orbital energies in the valence region
	UV-visible spectroscopy (UVVS)	Chemical composition
	Atomic absorption spectroscopy (AAS)	Chemical composition
	Inductively coupled plasma spectroscopy (ICP)	Elemental composition
	Fluorescence spectroscopy (FS)	Elemental composition
	Localized surface Plasmon resonance (LSPR)	Plasmonic properties

(continued)

giovanni.libralato@unina.it

Table 7 (continued)

Type of technique	Characterization technique	Information provided
Ion-Particle Probe Characterization Techniques	Rutherford back scattering (RBS)	Quantitative-qualitative elemental composition
	Small angle neutron scattering (SANS)	Surface characterization
	Nuclear reaction analysis (NRA)	Depth profile of solid thin films
	Raman spectroscopy (RS)	Particle size, shape and chemical composition
	X-ray diffraction (XRD)	Crystal structure
	Energy dispersive X-ray scattering (EDX)	Elemental composition
	Small angle X-ray scattering (SAXS)	Particle size (1-100 nm)
	Cathodoluminescence (CLS)	Characteristic emission
	Nuclear magnetic resonance spectroscopy (NMR)	Physical and chemical properties
Thermodynamic Characterization Techniques	Thermal gravimetric analysis (TGA)	Mass reduction under temperature exposition
	Differential thermal analysis (DTA)	Nanoparticle stability: difference in temperature between the sample and the reference when they are both put under thermal cycles
	Differential scanning calorimetry (DSC)	Nanoparticle stability: energy required to keep the sample at the same temperature than a reference sample when it undergoes a phase transition
	Brunauer-Emmett-Teller method (BET)	Surface area
	Sears method (Sears)	Colloid size, specific surface area
Others characterization's techniques	Nanoparticle tracking analysis (NTA)	Particle size (30-1000 nm)
	Turbidimetry	Particle concentration
	Resonant mass measurement (RMM)	Particle size
	Hyperspectral imaging	Spatial distribution and spectral characterization
Separation techniques	Field flow fractionation (FFF)	Separation on the basis of the size
	Hydrophobic interaction chromatography (HIC)	Separation by promoting hydrophobic effects
	Capillary electrophoresis (CE)	Separation on the basis of the size and the shape
	Isopycnic centrifugation	Separation on the basis of the size and the density

giovanni.libralato@unina.it

4 Environmental Impacts

Due to the rapid growth of the nanotechnology industry in the last years, it is reasonable to suppose that the emission of these applications can generate several sources of nanomaterials release in the environment. During the production or synthesis, for example, industrial waste can be produced which will be sent to landfill or used as production by-product. The release can occur during the movements of the materials due to leakages or during the manufacturing process as air emissions or release in water.

Obviously, depending on the application, the release of nanomaterials in the environment is strictly connected with their function, as in the case of water remediation, soil remediation, etc. Thus, reclaimed water that passed through nanomaterial-based processes could be the source of the nanoparticles releasing into surface water from such practices as spreading sewage sludge on the soil. This agriculture practice could result in soil contamination.

The concern of human exposure to nanoparticles and the absence of specific technologies for nanoparticles removal represent a controvertible theme for discussion. Some authors assert that there is no evidence to support possible nanoparticle contamination in water remediation that cannot be handled (Wiesner et al. 2006). Wiesner et al. (2006), in fact, suggest that nanoparticles are not as mobile as expected since their relatively large diffusivity would enable them to produce frequent contacts with the surface of porous materials such groundwater aquifers or sand filters used in potable water treatment (Wiesner et al. 2006). In spite of that, several authors commented on the potential adverse effects of nanomaterials on human health (Nel et al. 2006; Maynard 2007; Oberdörster et al. 2009; Simate et al. 2012; Sharifi et al. 2012) and the environment (Biswas and Wu 2005; Moore 2006; Aschberger et al. 2011).

Since it is possible that during the production and the use, the waste containing nanoparticles can reach the environment, the possibility for humans to enter in contact with nanoparticles represents a reality. Two ways of exposure are possible, external and internal. The first one is basically related to the bioavailability of nanoparticles in the surrounding environment. The second one is connected to metabolism and the transfer to organs and tissues of the nanoparticles taken in by the organism (López-Serrano et al. 2014).

When nanoparticles are present in air, the primary route of human exposure is by inhalation. Presence of fine particles PM10 and PM2.5 (particles with diameter below 10 and 2.5 μm respectively) are currently regulated on the basis of the "New air quality directive" (Directive 2008/50/EC). The limits are fixed to 50 $\mu g/m^3$ (exposure time of 24 h) and 40 $\mu g/m^3$ (exposure time of 1 year) for particles PM10 while it is fixed to 25 $\mu g/m^3$ (exposure time of 1 year) for PM2.5. Regulated fine (PM2.5) particle mass has been in fact demonstrated to be associated with increased symptoms and deaths from cardiovascular and respiratory causes (Seaton et al. 1995; Liao et al. 1999; Samet et al. 2000). Results for such effects due to ultrafine particles (less than 100 nm in diameter) are also emerging in a few studies

giovanni.libralato@unina.it

(Pekkanen et al. 1997; Ibald-Mulli et al. 2002; de Hartog et al. 2003). In the end, nanomaterials are clearly a unique class of materials characterized by novel and unique physicochemical properties. Nevertheless, there is concern about the impact to biological systems even though extended and detailed information on the hazards and risk that these materials impose are not well defined. Despite the increased number of nanomaterials-based publications over the years, the majority of publications are focused on the synthesis and development of novel nanomaterials and less than one percent have focused on their biological or toxicological impact. The potential hazard is directly related to toxicological effect in humans and environment (Nel et al. 2006). While the toxicity of many bulk materials is well understood, it is not known at what concentration or size the nanoscopic materials can begin to exhibit new toxicological effects due to their dimensions. Actually, there is a considerable gap between the available data on the nanomaterials production and toxicity evaluations. Moreover, despite the variety of different nanoparticles and nanomaterials, the toxicological effects of only limited ranges of nanomaterials have been investigated (Theron et al. 2008). Several studies have been focused on the toxicological effects of carbon nanotubes and metal oxide exposure. Regarding metal oxide nanoparticles (e.g., TiO_2, ZnO and Fe_2O_3) several studies have shown they can enter the human body and exhibit some toxicity such as inflammatory response, cytotoxicity response and cell membrane leakage (Tran et al. 2000; Jeng and Swanson 2006; Brunner et al. 2006).

Lam et al. (2004) and Warheit et al. (2004) reported the first peer-reviewed comparative toxicological assessment of nanotubes and quartz nanoparticles. The exposure during 7 and 90 days of mice to nanotubes showed dose-dependent lung lesions (Lam et al. 2004) while quartz nanomaterials exposure produced pulmonary inflammation and lung cellular proliferation and pathology (Warheit et al. 2004).

In Table 8 the toxicity effects of nanomaterials suggested after in vivo and in vitro studies are shown. The in vitro methods are ideal in nanotoxicology research because they can produce reproducible results rapidly and inexpensively without the use of animals. Simple in vitro methods that produce specific and quantitative measurements of toxicity are extremely valuable for initially evaluating the expected biocompatibility of new nanoparticles (Sharifi et al. 2012).

In summarizing, several studies demonstrated nanomaterials' carcinogenicity and or toxicity. However, it is still not completely clear if the toxicity effect is mainly a function of the concentration and chemical composition of the nanomaterial or if it is more correctly attributable to the small dimension of the particles. Hussian et al. (2005) performed in vitro toxicity test on BRL 3A rat liver cells of several types of metal-oxide nanoparticles (TiO_2, Fe_3O_4 and MoO_3) showing the relation between the toxicity effects and the concentration and chemical composition of the nanoparticles (Hussain et al. 2005). On the other side, the WHO International Agency for Research on Cancer (2004) clearly defined as harmless the TiO_2 itself and showed the increased hazard through inhalation when in the ultrafine size. IARC, then, classifies Titanium dioxide dust as an IARC Group 2B, that is possibly carcinogenic to humans (IARC 2010).

giovanni.libralato@unina.it

Depending on the environment in which we are considering the presence of nanomaterials, the fate can also change by interaction with the characteristic properties of the environment itself. As intrinsic nanomaterial properties (size, shape, distribution, surface area and charge, catalytic activity, etc.) can influence in the fate of nanomaterials, the properties of the natural water system can influence as well (ion composition, ionic strength, natural and/or dissolver organic matter (Lin et al. 2010; Weinberg et al. 2011). Processes and activities like aggregation, diffusion, sedimentation, degradation, photoreaction and transformation can modify the physical and chemical properties of the nanoparticles and then their fate in water (Baalousha et al. 2011). Human exposure to nanoparticles is strictly related to their fate and transport in the environment. Thus, the fate of metal oxide nanoparticles in water depends of their surface properties, size and the possibility to interact with other substances present into the water (Zhang et al. 2008b). Nanoparticles have been found to be present as aggregate in water and could not be dispersed as primary particles. In particular, studies have demonstrated that nanomaterials are very unstable in water because of their propensity to form agglomerate (Ju-Nam and Lead 2008). Determining whether they can be dispersed as primary nanoparticles is a key step in understanding their behavior in water. If aggregate, in fact, their behavior would be different from the primary nanoparticles (Zhang et al. 2008b).

The great release of these materials into the environment led to the necessity of adequate water treatment processes in order to make sure drinking water is free of possible harmful nanoparticles. Processes as coagulation, flocculation, sedimentation and filtration represent the key treatment technologies for drinking water production (Zhang et al. 2008b; Lens et al. 2013). Destabilization of the nanoparticle can be obtained through coagulation, then agglomeration by means of the flocculation process. In this way the agglomerated nanoparticles larger dimension can be easily removed by sedimentation. Advanced membrane filtration could ensure the removal of the smallest agglomerate or even discrete nanoparticles.

In wastewater treatment, the removal of nanoparticles can be achieved through adsorption, flocculation, aggregation and deposition, and biodegradation (e.g., activated sludge, MBR, etc.). In this environment, a possible problem could be represented by the presence of surfactants in wastewater which could functionalize the nanoparticles, stabilizing them and preventing their aggregation. Moreover, natural organic matter present into the wastewater may lead also to some changes in the properties of the nanomaterials (Lens et al. 2013).

After these considerations, it appears clear, even if the treatment plants can adequately remove nanomaterials, the necessity of synthesizing harmless nanoparticles is a challenge in which the scientific community has to invest its efforts. Moreover finding toxicity techniques for the evaluation of the toxic effects of these materials is fundamental as well.

giovanni.libralato@unina.it

Table 8 Examples of toxicity effects of nanomaterials of in vivo and in vitro assays

Nanomaterial	Assay	Effects	Reference
CNTs	In vivo on mice 0.1–0.5 mg by intratracheal instillation	5 of 9 mice died after exposure to 0.5 mg of the product	Lam et al. (2004)
Long (>20 μm) MWCNTs	In vivo on mice Intraperitoneal injection of 50 μg into the peritoneal cavity	Asbestos-like, length-dependent, pathogenic behaviour (in the short term)	Poland et al. (2008)
ZnO NPs	In vitro in RAW 264.7 murine macrophages (1–100 μg/mL)	Decreased cell viability, an elevated intracellular ROS level and higher cellular uptake observed at 100 μg/mL doses	Hong et al. (2013)
	In vivo on male ICR mice 1–100 μg/mL by using g.i. and i.p. administration routes	Increment in body weight, decrease in organ weight and mild to severe pathological inflammation depending on their different administration routes	
SWCNT	In vitro exposure of human epidermal keratinocytes (HaCaT) (0.06–0.24 mg/mL)	Accelerated oxidative stress and ultrastructural and morphological changes in cultured skin cells	Shvedova et al. (2003)
SWCNT	In vitro exposure of human embryo kidney cells (HEK293) (0.78–200 mg/mL)	Inhibition of cell proliferation, decrease cell adhesive ability	Cui et al. (2005)
SWNT, MWNT10, C_{60}	In vitro on alveolar macrophage (AM) 0–260 μg/cm^2 of SWNT and C_{60}; 0–22.60 μg/cm^2 of MWNT10	Cytotoxicity increase, reduction of the phagocytic ability exhibited in different measure for the material tested	Jia et al. (2005)
MWNT	In vitro exposure of HEKs (0.1–0.4 mg/mL)	Localization of MWCNT within the cell and irritation response	Monteiro-Riviere et al. (2005)
MWCNT (intact or ground)	In vivo on rats 0.5–5 mg by intratracheal instillation	Collagen-rich granulomas and surrounding alveolitis (under exposure of intact MWCNT); inflammatory and fibrotic responses (under exposure of ground MWCNT)	Muller et al. (2005)
Nanoscale TiO_2 (rods or dots)	In vivo on rats 1–5 mg by intratracheal instillation	Transient inflammatory and cell injury effects	Warheit et al. (2006)
TiO_2 nanoparticles anatase-sized (10–20 nm) and rulie-sized (200 nm)	In vitro exposure of human bronchial epithelias cells (BEAS 2B) (10 mg/mL)	DNA damage, liquid peroxidation and micronuclei formation (anatase form exposure) Less toxicity exhibited by rutile form	Gurr et al. (2005)
TiO_2 nanoparticles (anatase and rutile sized)	In vitro exposure to human lung epithelial cell (A549) (3–30 mg/mL)	Decreased cell viability	Sayes et al. (2006)

giovanni.libralato@unina.it

5 Conclusions

The scientific community is currently involved in the development of innovative new technologies and materials for water remediation focused on the provision of safe potable water. It is generally recognized that nanotechnology and its application may play an important role in resolving issues relating to water scarcity and water quality. The scientific community is diligently dedicated to searching new methods of synthesis to produce nanomaterials whose properties could be effective and safe for application in water treatment. The great potential of nanomaterials is obviously due to the large surface areas, the small dimension, great adsorption capacity, catalytic activity and sometimes microbial effectiveness. But a lot is still unknown about these materials. While much attention has been focused on the development and potential benefits of nanomaterials in water treatment processes, concerns have been raised regarding their potential human and environmental toxicity. The strong shape dependence, the instability and the possible transformation after aggregation and utilization of nanomaterials still raise controversy on their suitability in water remediation. To this effect, improvements in the field of nanomaterials characterization are also necessary. If almost everything is already known for bulk materials, the equivalent materials at the nano scale are still under investigation. It is of fundamental importance to fill this lack of knowledge with adequate studies on the safety of these materials in parallel with the new development of strategies for synthesis and application.

References

Albuquerque Júnior EC, Méndez MOA, Coutinho A dos R, Franco TT (2008) Removal of cyanobacteria toxins from drinking water by adsorption on activated carbon fibers. Mater Res 11:371–380. doi:10.1590/S1516-14392008000300023

Allabashi R, Arkas M, Hörmann G, Tsiourvas D (2007) Removal of some organic pollutants in water employing ceramic membranes impregnated with cross-linked silylated dendritic and cyclodextrin polymers. Water Res 41:476–486. doi:10.1016/j.watres.2006.10.011

Andersson M, Österlund L, Ljungström S, Palmqvist A (2002) Preparation of nanosize anatase and rutile TiO_2 by hydrothermal treatment of microemulsions and their activity for photocatalytic wet oxidation of phenol. J Phys Chem B 106:10674–10679. doi:10.1021/jp025715y

Aschberger K, Micheletti C, Sokull-Klüttgen B, Christensen FM (2011) Analysis of currently available data for characterising the risk of engineered nanomaterials to the environment and human health–lessons learned from four case studies. Environ Int 37:1143–1156. doi:10.1016/j.envint.2011.02.005

Baalousha M, Lead J, Ju-Nam Y (2011) Natural colloids and manufactured nanoparticles in aquatic and terrestrial systems. Treatise Water Sci 81:89–129

Bagheri S, Muhd Julkapli N, Bee Abd Hamid S (2014) Titanium dioxide as a catalyst support in heterogeneous catalysis. Sci World J 2014:727496. doi:10.1155/2014/727496

Baughman RH, Zakhidov AA, de Heer WA (2002) Carbon nanotubes—the route toward applications. Science 297:787–792. doi:10.1126/science.1060928

giovanni.libralato@unina.it

Bhainsa KC, D'Souza SF (2006) Extracellular biosynthesis of silver nanoparticles using the fungus *Aspergillus fumigatus*. Colloids Surf B Biointerfaces 47:160–164. doi:10.1016/j.colsurfb.2005.11.026

Bhattacharya D, Gupta RK (2008) Nanotechnology and potential of microorganisms

Bhattacharyya A, Ali SW (2008) Characterization techniques for nanotechnology applications in textiles. Indian J Fibre Text Res 33:304–317

Bina B, Pourzamani H, Rashidi A, Amin MM (2012) Ethylbenzene removal by carbon nanotubes from aqueous solution. J Environ Public Health 2012:817187. doi:10.1155/2012/817187

Biswas P, Wu C-Y (2005) Nanoparticles and the environment. J Air Waste Manage Assoc 55:708–746. doi:10.1080/10473289.2005.10464656

Boparai HK, Joseph M, O'Carroll DM (2011) Kinetics and thermodynamics of cadmium ion removal by adsorption onto nano zerovalent iron particles. J Hazard Mater 186:458–465. doi:10.1016/j.jhazmat.2010.11.029

Bottino A, Capannelli G, Comite A (2002) Preparation and characterization of novel porous PVDF-ZrO_2 composite membranes. Desalination 146:35–40. doi:10.1016/S0011-9164(02)00469-1

Breck DW (1974) Zeolite molecular sieves: structure

Brunner TJ, Wick P, Manser P et al (2006) In vitro cytotoxicity of oxide nanoparticles: comparison to asbestos, silica, and the effect of particle solubility. Environ Sci Technol 40:4374–4381. doi:10.1021/es052069i

Burda C, Lou Y, Chen X et al (2003) Enhanced nitrogen doping in TiO_2 nanoparticles. Nano Lett 3:1049–1051. doi:10.1021/nl034332o

Chen J-P, Chiang Y (2010) Bioactive electrospun silver nanoparticles-containing polyurethane nanofibers as wound dressings. J Nanosci Nanotechnol 10:7560–7564. doi:10.1166/jnn.2010.2829

Chen H, He J (2008) Facile synthesis of monodisperse manganese oxide nanostructures and their application in water treatment. J Phys Chem C 112:17540–17545. doi:10.1021/jp806160g

Chen X, Feng X, Liu J et al (1999) Mercury separation and immobilization using self-assembled monolayers on mesoporous supports (SAMMS). Sep Sci Technol 34:1121–1132. doi:10.1080/01496399908951084

Chen X, Lam KF, Yeung KL (2011) Selective removal of chromium from different aqueous systems using magnetic MCM-41 nanosorbents. Chem Eng J 172:728–734. doi:10.1016/j.cej.2011.06.042

Choi W, Termin A, Hoffmann MR (1994) The role of metal ion dopants in quantum-sized TiO_2: correlation between photoreactivity and charge carrier recombination dynamics. J Phys Chem 98:13669–13679. doi:10.1021/j100102a038

Choi H, Antoniou MG, Pelaez M et al (2007a) Mesoporous nitrogen-doped TiO_2 for the photocatalytic destruction of the cyanobacterial toxin microcystin-LR under visible light irradiation. Environ Sci Technol 41:7530–7535. doi:10.1021/es0709122

Choi H, Stathatos E, Dionysiou DD (2007b) Photocatalytic TiO_2 films and membranes for the development of efficient wastewater treatment and reuse systems. Desalination 202:199–206. doi:10.1016/j.desal.2005.12.055

Choi O, Deng KK, Kim N-J et al (2008) The inhibitory effects of silver nanoparticles, silver ions, and silver chloride colloids on microbial growth. Water Res 42:3066–3074. doi:10.1016/j.watres.2008.02.021

Chouyyok W, Wiacek RJ, Pattamakomsan K et al (2010) Phosphate removal by anion binding on functionalized nanoporous sorbents. Environ Sci Technol 44:3073–3078. doi:10.1021/es100787m

Cohen-Tanugi D, Grossman JC (2012) Water desalination across nanoporous graphene. Nano Lett 12:3602–3608. doi:10.1021/nl3012853

Cong Y, Zhang J, Chen F, Anpo M (2007) Synthesis and characterization of nitrogen-doped TiO_2 nanophotocatalyst with high visible light activity. J Phys Chem C 111:6976–6982. doi:10.1021/jp0685030

giovanni.libralato@unina.it

Corry B (2008) Designing carbon nanotube membranes for efficient water desalination. J Phys Chem B 112:1427–1434. doi:10.1021/jp709845u

Cravillon J, Münzer S, Lohmeier S-J et al (2009) Rapid room-temperature synthesis and characterization of nanocrystals of a prototypical zeolitic imidazolate framework

Cui D, Tian F, Ozkan CS et al (2005) Effect of single wall carbon nanotubes on human HEK293 cells. Toxicol Lett 155:73–85. doi:10.1016/j.toxlet.2004.08.015

Dankovich TA, Gray DG (2011) Bactericidal paper impregnated with silver nanoparticles for point-of-use water treatment. Environ Sci Technol 45:1992–1998. doi:10.1021/es103302t

de Hartog JJ, Hoek G, Peters A et al (2003) Effects of fine and ultrafine particles on cardiorespiratory symptoms in elderly subjects with coronary heart disease: the ULTRA study. Am J Epidemiol 157:613–623

David M. Dotzauer, Jinhua Dai, Lei Sun A, Bruening ML (2006) Catalytic membranes prepared using layer-by-layer adsorption of polyelectrolyte/metal nanoparticle films in porous supports

Eriksson P (1988) Nanofiltration extends the range of membrane filtration. Environ Prog 7:58–62. doi:10.1002/ep.3300070116

Esteban-Cubillo A, Pecharromán C, Aguilar E et al (2006) Antibacterial activity of copper monodispersed nanoparticles into sepiolite. J Mater Sci 41:5208–5212. doi:10.1007/s10853-006-0432-x

Feng X (1997) Functionalized monolayers on ordered mesoporous supports. Science 276 (80–):923–926. doi:10.1126/science.276.5314.923

Feng X, Liu J, Fryxell GE (1997) Self-assembled mercaptan on mesoporous silica (SAMMS) technology of mercury removal and stabilization. Richland, WA

Feynman RP (1960) There's plenty of room at the bottom. Eng Sci 23:22–36

Fryxell GE, Mattigod SV, Lin Y et al (2007) Design and synthesis of self-assembled monolayers on mesoporous supports (SAMMS): the importance of ligand posture in functional nanomaterials. J Mater Chem 17:2863. doi:10.1039/b702422c

Fu J, Ji M, Wang Z et al (2006) A new submerged membrane photocatalysis reactor (SMPR) for fulvic acid removal using a nano-structured photocatalyst. J Hazard Mater 131:238–242. doi:10.1016/j.jhazmat.2005.09.039

Fu F, Dionysiou DD, Liu H (2014) The use of zero-valent iron for groundwater remediation and wastewater treatment: a review. J Hazard Mater 267:194–205. doi:10.1016/j.jhazmat.2013.12.062

Giasuddin ABM, Kanel SR, Choi H (2007) Adsorption of humic acid onto nanoscale zerovalent iron and its effect on arsenic removal. Environ Sci Technol 41:2022–2027. doi:10.1021/es0616534

Gillham RW, O'Hannesin SF (1994) Enhanced degradation of halogenated aliphatics by zero-valent iron. Ground Water 32:958–967. doi:10.1111/j.1745-6584.1994.tb00935.x

Gin DL, Lu X, Nemade PR et al (2006) Recent advances in the design of polymerizable lyotropic liquid-crystal assemblies for heterogeneous catalysis and selective separations. Adv Funct Mater 16:865–878. doi:10.1002/adfm.200500280

Gopal K, Tripathy SS, Bersillon JL, Dubey SP (2007) Chlorination byproducts, their toxicodynamics and removal from drinking water. J Hazard Mater 140:1–6. doi:10.1016/j.jhazmat.2006.10.063

K. Goyal A, S. Johal E, Rath G (2011) Nanotechnology for water treatment. Curr Nanosci 7:640–654. doi:10.2174/157341311796196772

Gu B, Phelps TJ, Liang L et al (1999) Biogeochemical dynamics in zero-valent iron columns: implications for permeable reactive barriers. Environ Sci Technol 33:2170–2177. doi:10.1021/es981077e

Gupta SM, Tripathi M (2011) A review of TiO_2 nanoparticles. Chinese Sci Bull 56:1639–1657. doi:10.1007/s11434-011-4476-1

Gurr J-R, Wang ASS, Chen C-H, Jan K-Y (2005) Ultrafine titanium dioxide particles in the absence of photoactivation can induce oxidative damage to human bronchial epithelial cells. Toxicology 213:66–73. doi:10.1016/j.tox.2005.05.007

giovanni.libralato@unina.it

Han H, Bai R (2009) Buoyant photocatalyst with greatly enhanced visible-light activity prepared through a low temperature hydrothermal method. Ind Eng Chem Res 48:2891–2898. doi:10.1021/ie801362a

Henmi M, Nakatsuji K, Ichikawa T et al (2012) Self-organized liquid-crystalline nanostructured membranes for water treatment: selective permeation of ions. Adv Mater 24:2238–2241. doi:10.1002/adma.201200108

Hoag GE, Collins JB, Holcomb JL et al (2009) Degradation of bromothymol blue by "greener" nano-scale zero-valent iron synthesized using tea polyphenols. J Mater Chem 19:8671. doi:10.1039/b909148c

Holt JK, Park HG, Wang Y et al (2006) Fast mass transport through sub-2-nanometer carbon nanotubes. Science 312:1034–1037. doi:10.1126/science.1126298

Hong T-K, Tripathy N, Son H-J et al (2013) A comprehensive in vitro and in vivo study of ZnO nanoparticles toxicity. J Mater Chem B 1:2985. doi:10.1039/c3tb20251h

Hornyak GL, Dutta J, Tibbals HF, Rao A (2008) Introduction to nanoscience. CRC Press, Boca Raton

Hu J, Chen G, Lo IMC (2005) Removal and recovery of Cr(VI) from wastewater by maghemite nanoparticles. Water Res 39:4528–4536. doi:10.1016/j.watres.2005.05.051

Hu J, Tong Z, Hu Z et al (2012) Adsorption of roxarsone from aqueous solution by multi-walled carbon nanotubes. J Colloid Interface Sci 377:355–361. doi:10.1016/j.jcis.2012.03.064

Hussain SM, Hess KL, Gearhart JM et al (2005) In vitro toxicity of nanoparticles in BRL 3A rat liver cells. Toxicol In Vitro 19:975–983. doi:10.1016/j.tiv.2005.06.034

Hyung H, Kim J-H (2008) Natural organic matter (NOM) adsorption to multi-walled carbon nanotubes: effect of NOM characteristics and water quality parameters. Environ Sci Technol 42:4416–4421. doi:10.1021/es702916h

IARC (2010) IARC monographs on the evaluation of carcinogenic risks to humans, vol 93, Carbon Black, Titanium Dioxide, and Talc. IARC Press, Lyon

Ibald-Mulli A, Wichmann H-E, Kreyling W, Peters A (2002) Epidemiological evidence on health effects of ultrafine particles. J Aerosol Med 15:189–201. doi:10.1089/089426802320282310

Ichikawa T, Yoshio M, Hamasaki A et al (2011) 3D interconnected ionic nano-channels formed in polymer films: self-organization and polymerization of thermotropic bicontinuous cubic liquid crystals. J Am Chem Soc 133:2163–2169. doi:10.1021/ja106707z

Iijima S (1991) Helical microtubules of graphitic carbon. Nature 354:56–58

Ireland JC, Klostermann P, Rice EW, Clark RM (1993) Inactivation of *Escherichia coli* by titanium dioxide photocatalytic oxidation. Appl Environ Microbiol 59:1668–1670

Ismail AA, Mazyck DW (2008) Impact of heat treatment and composition of ZnO–TiO_2 nanoparticles for photocatalytic oxidation of an Azo dye. Ind Eng Chem Res 47:1483–1487. doi:10.1021/ie071255p

Jeng HA, Swanson J (2006) Toxicity of metal oxide nanoparticles in mammalian cells. J Environ Sci Health A Tox Hazard Subst Environ Eng 41:2699–2711. doi:10.1080/10934520600966177

Jia G, Wang H, Yan L et al (2005) Cytotoxicity of carbon nanomaterials: single-wall nanotube, multi-wall nanotube, and fullerene. Environ Sci Technol 39:1378–1383. doi:10.1021/es048729l

Jiang Z, Lv L, Zhang W et al (2011) Nitrate reduction using nanosized zero-valent iron supported by polystyrene resins: role of surface functional groups. Water Res 45:2191–2198. doi:10.1016/j.watres.2011.01.005

Joo SH, Feitz AJ, Waite TD (2004) Oxidative degradation of the carbothioate herbicide, molinate, using nanoscale zero-valent iron. Environ Sci Technol 38:2242–2247. doi:10.1021/es035157g

Ju-Nam Y, Lead JR (2008) Manufactured nanoparticles: an overview of their chemistry, interactions and potential environmental implications. Sci Total Environ 400:396–414. doi:10.1016/j.scitotenv.2008.06.042

Kanel SR, Manning B, Charlet L, Choi H (2005) Removal of arsenic(III) from groundwater by nanoscale zero-valent iron. Environ Sci Technol 39:1291–1298. doi:10.1021/es048991u

Kato T (2002) Self-assembly of phase-segregated liquid crystal structures. Science 295:2414–2418. doi:10.1126/science.1070967

giovanni.libralato@unina.it

Kato T (2010) From nanostructured liquid crystals to polymer-based electrolytes. Angew Chem Int Ed Engl 49:7847–7848. doi:10.1002/anie.201000707

Kelly SD, Kemner KM, Fryxell GE et al (2001) X-ray-absorption fine-structure spectroscopy study of the interactions between contaminant tetrahedral anions and self-assembled monolayers on mesoporous supports. J Phys Chem B 105:6337–6346. doi:10.1021/jp0045890

Kim SH, Kwak S-Y, Sohn B-H, Park TH (2003) Design of TiO_2 nanoparticle self-assembled aromatic polyamide thin-film-composite (TFC) membrane as an approach to solve biofouling problem. J Memb Sci 211:157–165. doi:10.1016/S0376-7388(02)00418-0

Kim S, Hwang S-J, Choi W (2005) Visible light active platinum-ion-doped TiO_2 photocatalyst. J Phys Chem B 109:24260–24267. doi:10.1021/jp055278y

Kim H, Hong H-J, Jung J et al (2010) Degradation of trichloroethylene (TCE) by nanoscale zero-valent iron (nZVI) immobilized in alginate bead. J Hazard Mater 176:1038–1043. doi:10.1016/j.jhazmat.2009.11.145

Kim E-S, Hwang G, Gamal El-Din M, Liu Y (2012) Development of nanosilver and multi-walled carbon nanotubes thin-film nanocomposite membrane for enhanced water treatment. J Memb Sci 394–395:37–48. doi:10.1016/j.memsci.2011.11.041

Krishna V, Pumprueg S, Lee S-H et al (2005) Photocatalytic disinfection with titanium dioxide coated multi-wall carbon nanotubes. Process Saf Environ Prot 83:393–397. doi:10.1205/psep.04387

Lam C-W, James JT, McCluskey R, Hunter RL (2004) Pulmonary toxicity of single-wall carbon nanotubes in mice 7 and 90 days after intratracheal instillation. Toxicol Sci 77:126–134. doi:10.1093/toxsci/kfg243

Landau MV, Vradman L, Valtchev V et al (2003) Hydrocracking of heavy vacuum gas oil with a Pt/H-beta-Al_2O_3 catalyst: effect of zeolite crystal size in the nanoscale range. Ind Eng Chem Res 42:2773–2782. doi:10.1021/ie020899o

Lee MS, Hong S-S, Mohseni M (2005) Synthesis of photocatalytic nanosized TiO_2–Ag particles with sol–gel method using reduction agent. J Mol Catal A: Chem 242:135–140. doi:10.1016/j.molcata.2005.07.038

Lens P, Virkutyte J, Jegatheesan V et al (2013) Nanotechnology for water and wastewater treatment. IWA Publishing

Leonard P, Hearty S, Brennan J et al (2003) Advances in biosensors for detection of pathogens in food and water. Enzyme Microb Technol 32:3–13. doi:10.1016/S0141-0229(02)00232-6

Li FB, Li XZ (2002) The enhancement of photodegradation efficiency using Pt–TiO_2 catalyst. Chemosphere 48:1103–1111. doi:10.1016/S0045-6535(02)00201-1

Li X, Elliott DW, Zhang W (2006) Zero-valent iron nanoparticles for abatement of environmental pollutants: materials and engineering aspects. Crit Rev Solid State Mater Sci 31:111–122. doi:10.1080/10408430601057611

Liao D, Creason J, Shy C et al (1999) Daily variation of particulate air pollution and poor cardiac autonomic control in the elderly. Environ Health Perspect 107:521–525

Lien H-L, Zhang W (1999) Transformation of chlorinated methanes by nanoscale iron particles. J Environ Eng 125:1042–1047. doi:10.1061/(ASCE)0733-9372(1999)125:11(1042)

Lin Y, Fryxell GE, Wu H, Engelhard M (2001) Selective sorption of cesium using self-assembled monolayers on mesoporous supports. Environ Sci Technol 35:3962–3966. doi:10.1021/es010710k

Lin D, Tian X, Wu F, Xing B (2010) Fate and transport of engineered nanomaterials in the environment. J Environ Qual 39:1896. doi:10.2134/jeq2009.0423

Ling X, Li J, Zhu W et al (2012) Synthesis of nanoscale zero-valent iron/ordered mesoporous carbon for adsorption and synergistic reduction of nitrobenzene. Chemosphere 87:655–660. doi:10.1016/j.chemosphere.2012.02.002

Liu Z, Zhang F-S (2010) Nano-zerovalent iron contained porous carbons developed from waste biomass for the adsorption and dechlorination of PCBs. Bioresour Technol 101:2562–2564. doi:10.1016/j.biortech.2009.11.074

giovanni.libralato@unina.it

Liu J, Fryxell GE, Mattigod SV et al (1998) Self-assembled monolayers on mesoporous support (SAMMS) technology for contaminant removal and stabilization. Richland, WA

Liu Y, Chen X, Li J, Burda C (2005) Photocatalytic degradation of azo dyes by nitrogen-doped TiO_2 nanocatalysts. Chemosphere 61:11–18. doi:10.1016/j.chemosphere.2005.03.069

Liu J, Zhao Z, Jiang G (2008) Coating Fe_3O_4 magnetic nanoparticles with humic acid for high efficient removal of heavy metals in water. Environ Sci Technol 42:6949–6954. doi:10.1021/es800924c

López-Muñoz M-J, van Grieken R, Aguado J, Marugán J (2005) Role of the support on the activity of silica-supported TiO_2 photocatalysts: structure of the TiO_2/SBA-15 photocatalysts. Catal Today 101:307–314. doi:10.1016/j.cattod.2005.03.017

López-Serrano A, Olivas RM, Landaluze JS, Cámara C (2014) Nanoparticles: a global vision. Characterization, separation, and quantification methods. Potential environmental and health impact. Anal Methods 6:38–56. doi:10.1039/C3AY40517F

Lu C, Liu C (2006) Removal of nickel(II) from aqueous solution by carbon nanotubes. J Chem Technol Biotechnol 81:1932–1940. doi:10.1002/jctb.1626

Lu Y, Fan H, Stump A et al (1999) Aerosol-assisted self-assembly of mesostructured spherical nanoparticles. Nature 398:223–226. doi:10.1038/18410

Lu C, Chung Y-L, Chang K-F (2005) Adsorption of trihalomethanes from water with carbon nanotubes. Water Res 39:1183–1189. doi:10.1016/j.watres.2004.12.033

Ma Y, Qiu J, Cao Y et al (2001) Photocatalytic activity of TiO_2 films grown on different substrates. Chemosphere 44:1087–1092. doi:10.1016/S0045-6535(00)00360-X

Majewski PJ (2007) Removal of organic matter in water by functionalised self-assembled monolayers on silica. Sep Purif Technol 57:283–288. doi:10.1016/j.seppur.2007.04.008

Maynard AD (2007) Nanotechnology: the next big thing, or much ado about nothing? Ann Occup Hyg 51:1–12. doi:10.1093/annhyg/mel071

Miller SA, Young VY, Martin CR (2001) Electroosmotic flow in template-prepared carbon nanotube membranes. J Am Chem Soc 123:12335–12342. doi:10.1021/ja011926p

Mohsen MS, Jaber JO, Afonso MD (2003) Desalination of brackish water by nanofiltration and reverse osmosis. Desalination 157:167. doi:10.1016/S0011-9164(03)00397-7

Monteiro-Riviere NA, Nemanich RJ, Inman AO et al (2005) Multi-walled carbon nanotube interactions with human epidermal keratinocytes. Toxicol Lett 155:377–384. doi:10.1016/j.toxlet.2004.11.004

Moore MN (2006) Do nanoparticles present ecotoxicological risks for the health of the aquatic environment? Environ Int 32:967–976. doi:10.1016/j.envint.2006.06.014

Morones JR, Elechiguerra JL, Camacho A et al (2005) The bactericidal effect of silver nanoparticles. Nanotechnology 16:2346–2353. doi:10.1088/0957-4484/16/10/059

Mukhopadhyay S (2011) Nanoscale multifunctional materials: science and applications. Wiley, New York

Muller J, Huaux F, Moreau N et al (2005) Respiratory toxicity of multi-wall carbon nanotubes. Toxicol Appl Pharmacol 207:221–231. doi:10.1016/j.taap.2005.01.008

Nahar MS, Hasegawa K, Kagaya S (2006) Photocatalytic degradation of phenol by visible light-responsive iron-doped TiO_2 and spontaneous sedimentation of the TiO_2 particles. Chemosphere 65:1976–1982. doi:10.1016/j.chemosphere.2006.07.002

Nasr C, Vinodgopal K, Fisher L et al (1996) Environmental photochemistry on semiconductor surfaces. Visible light induced degradation of a textile diazo dye, naphthol blue black, on TiO_2 nanoparticles. J Phys Chem 100:8436–8442. doi:10.1021/jp953556v

Nel A, Xia T, Mädler L, Li N (2006) Toxic potential of materials at the nanolevel. Science 311:622–627. doi:10.1126/science.1114397

Nune SK, Thallapally PK, Dohnalkova A et al (2010) Synthesis and properties of nano zeolitic imidazolate frameworks. Chem Commun (Camb) 46:4878–4880. doi:10.1039/c002088e

Oberdörster G, Stone V, Donaldson K (2009) Toxicology of nanoparticles: a historical perspective

Pal S, Tak YK, Song JM (2007) Does the antibacterial activity of silver nanoparticles depend on the shape of the nanoparticle? A study of the Gram-negative bacterium *Escherichia coli*. Appl Environ Microbiol 73:1712–1720. doi:10.1128/AEM.02218-06

giovanni.libralato@unina.it

Pastoriza-Santos I, Koktysh DS, Mamedov AA et al (2000) One-pot synthesis of Ag@TiO_2 core-shell nanoparticles and their layer-by-layer assembly. Langmuir 16:2731–2735. doi:10.1021/la991212g

Paul S, Choudhury A (2013) Investigation of the optical property and photocatalytic activity of mixed phase nanocrystalline titania. Appl Nanosci 4:839–847. doi:10.1007/s13204-013-0264-3

Pekkanen J, Timonen KL, Ruuskanen J et al (1997) Effects of ultrafine and fine particles in urban air on peak expiratory flow among children with asthmatic symptoms. Environ Res 74:24–33. doi:10.1006/enrs.1997.3750

Pelaez M, de la Cruz AA, Stathatos E et al (2009) Visible light-activated N-F-codoped TiO_2 nanoparticles for the photocatalytic degradation of microcystin-LR in water. Catal Today 144:19–25. doi:10.1016/j.cattod.2008.12.022

Peltier S, Cotte M, Gatel D et al (2003) Nanofiltration: improvements of water quality in a large distribution system. Water Sci Technol water supply 3:193–200

Petcharoen K, Sirivat A (2012) Synthesis and characterization of magnetite nanoparticles via the chemical co-precipitation method. Mater Sci Eng, B 177:421–427. doi:10.1016/j.mseb.2012.01.003

Peters R, ten Dam G, Bouwmeester H et al (2011) Identification and characterization of organic nanoparticles in food. TrAC Trends Anal Chem 30:100–112. doi:10.1016/j.trac.2010.10.004

Poland CA, Duffin R, Kinloch I et al (2008) Carbon nanotubes introduced into the abdominal cavity of mice show asbestos-like pathogenicity in a pilot study. Nat Nanotechnol 3:423–428. doi:10.1038/nnano.2008.111

Popov V (2004) Carbon nanotubes: properties and application. Mater Sci Eng R Reports 43:61–102. doi:10.1016/j.mser.2003.10.001

Pugazhenthiran N, Anandan S, Kathiravan G et al (2009) Microbial synthesis of silver nanoparticles by Bacillus sp. J Nanoparticle Res 11:1811–1815

Qin J-J, Oo MH, Kekre KA (2007) Nanofiltration for recovering wastewater from a specific dyeing facility. Sep Purif Technol 56:199–203. doi:10.1016/j.seppur.2007.02.002

Rao KVS, Rachel A, Subrahmanyam M, Boule P (2003) Immobilization of TiO_2 on pumice stone for the photocatalytic degradation of dyes and dye industry pollutants. Appl Catal B Environ 46:77–85. doi:10.1016/S0926-3373(03)00199-1

Rao G, Lu C, Su F (2007) Sorption of divalent metal ions from aqueous solution by carbon nanotubes: a review. Sep Purif Technol 58:224–231. doi:10.1016/j.seppur.2006.12.006

Rook JJ (1974) Formation of haloforms during chlorination of natural waters. Water Treat Exam 23:234–243

Sakai N, Kamikawa Y, Nishii M et al (2006) Dendritic folate rosettes as ion channels in lipid bilayers. J Am Chem Soc 128:2218–2219. doi:10.1021/ja058157k

Samet JM, Dominici F, Curriero FC et al (2000) Fine particulate air pollution and mortality in 20 US cities, 1987–1994. N Engl J Med 343:1742–1749

Savage N, Diallo MS (2005) Nanomaterials and water purification: opportunities and challenges. J Nanoparticle Res 7:331–342. doi:10.1007/s11051-005-7523-5

Sayes CM, Wahi R, Kurian PA et al (2006) Correlating nanoscale titania structure with toxicity: a cytotoxicity and inflammatory response study with human dermal fibroblasts and human lung epithelial cells. Toxicol Sci 92:174–185. doi:10.1093/toxsci/kfj197

Seaton A, Godden D, MacNee W, Donaldson K (1995) Particulate air pollution and acute health effects. Lancet 345:176–178. doi:10.1016/S0140-6736(95)90173-6

Sharifi S, Behzadi S, Laurent S et al (2012) Toxicity of nanomaterials. Chem Soc Rev 41:2323–2343. doi:10.1039/C1CS15188F

Shih Y, Hsu C, Su Y (2011) Reduction of hexachlorobenzene by nanoscale zero-valent iron: kinetics, pH effect, and degradation mechanism. Sep Purif Technol 76:268–274. doi:10.1016/j.seppur.2010.10.015

Shvedova AA, Castranova V, Kisin ER et al (2003) Exposure to carbon nanotube material: assessment of nanotube cytotoxicity using human keratinocyte cells. J Toxicol Environ Health A 66:1909–1926. doi:10.1080/713853956

giovanni.libralato@unina.it

Simate GS, Iyuke SE, Ndlovu S et al (2012) Human health effects of residual carbon nanotubes and traditional water treatment chemicals in drinking water. Environ Int 39:38–49. doi:10.1016/j.envint.2011.09.006

Singh T, Singhal R (2013) Reuse of a waste adsorbent poly(AAc/AM/SH)-Cu superabsorbent hydrogel, for the potential phosphate ion removal from waste water: matrix effects, adsorption kinetics, and thermodynamic studies. J Appl Polym Sci 129:3126–3139. doi:10.1002/app.39018

Siqueira JR, Crespilho FN, Zucolotto V, Oliveira ON (2007) Bifunctional electroactive nanostructured membranes. Electrochem Commun 9:2676–2680. doi:10.1016/j.elecom.2007.08.009

Son WK, Youk JH, Lee TS, Park WH (2004) Preparation of antimicrobial ultrafine cellulose acetate fibers with silver nanoparticles. Macromol Rapid Commun 25:1632–1637. doi:10.1002/marc.200400323

Sondi I, Salopek-Sondi B (2004) Silver nanoparticles as antimicrobial agent: a case study on *E. coli* as a model for Gram-negative bacteria. J Colloid Interface Sci 275:177–182. doi:10.1016/j.jcis.2004.02.012

Song W, Justice RE, Jones CA et al (2004) Synthesis, characterization, and adsorption properties of nanocrystalline ZSM-5. Langmuir 20:8301–8306. doi:10.1021/la049516c

Song W, Li G, Grassian VH, Larsen SC (2005) Development of Improved materials for environmental applications: nanocrystalline NaY zeolites. Environ Sci Technol 39:1214–1220. doi:10.1021/es049194z

Sousa FL, Daniel-da-Silva AL, Silva NJO, Trindade T (2015) Bionanocomposites for magnetic removal of water pollutants. In: Thakur VK, Thakur MK (eds) Eco-friendly polymer nanocomposites SE—9. Springer India, pp 279–310

Spadaro JA, Berger TJ, Barranco SD et al (1974) antibacterial effects of silver electrodes with weak direct current. Antimicrob Agents Chemother 6:637–642. doi:10.1128/AAC.6.5.637

Srivastava M, Chaubey S, Ojha AK (2009) Investigation on size dependent structural and magnetic behavior of nickel ferrite nanoparticles prepared by sol–gel and hydrothermal methods. Mater Chem Phys 118:174–180. doi:10.1016/j.matchemphys.2009.07.023

Stumm W, Morgan JJ (2012) Aquatic chemistry: chemical equilibria and rates in natural waters

Su J, Guo H (2011) Control of unidirectional transport of single-file water molecules through carbon nanotubes in an electric field. ACS Nano 5:351–359. doi:10.1021/nn1014616

Su F, Lu C (2007) Adsorption kinetics, thermodynamics and desorption of natural dissolved organic matter by multiwalled carbon nanotubes. J Environ Sci Health A Tox Hazard Subst Environ Eng 42:1543–1552. doi:10.1080/10934520701513381

Suffet IH (1995) Advances in taste-and-odor treatment and control

Sutherland K (2008) Developments in filtration: what is nanofiltration? Filtr Sep 45:32–35. doi:10.1016/S0015-1882(08)70298-2

Szewzyk U, Szewzyk R, Manz W, Schleifer KH (2000) Microbiological safety of drinking water. Annu Rev Microbiol 54:81–127. doi:10.1146/annurev.micro.54.1.81

Theron J, Walker JA, Cloete TE (2008) Nanotechnology and water treatment: applications and emerging opportunities

Tiede K, Hassellöv M, Breitbarth E et al (2009) Considerations for environmental fate and ecotoxicity testing to support environmental risk assessments for engineered nanoparticles. J Chromatogr A 1216:503–509. doi:10.1016/j.chroma.2008.09.008

Tiwari DK, Behari J, Sen P (2008) Application of nanoparticles in waste water treatment. World Appl Sci J 3:417–433

Tran CL, Buchanan D, Cullen RT et al (2000) Inhalation of poorly soluble particles. II. Influence of particle surface area on inflammation and clearance. Inhal Toxicol 12:1113–1126

Tratnyek PG, Johnson RL (2006) Nanotechnologies for environmental cleanup. Nano Today 1:44–48. doi:10.1016/S1748-0132(06)70048-2

UNEP (2007) GEO year book 2007—an overview of our changing environment. Nairobi, Kenya

US. EPA. (2008) Nanotechnology for Site Remediation Fact Sheet. Solid waste and emergency response

giovanni.libralato@unina.it

Van der Bruggen B, Vandecasteele C (2002) Distillation vs. membrane filtration: overview of process evolutions in seawater desalination. Desalination 143:207–218. doi:10.1016/S0011-9164(02)00259-X

Van der Bruggen B, Vandecasteele C (2003) Removal of pollutants from surface water and groundwater by nanofiltration: overview of possible applications in the drinking water industry. Environ Pollut 122:435–445. doi:10.1016/S0269-7491(02)00308-1

Walha K, Ben Amar R, Firdaous L et al (2007) Brackish groundwater treatment by nanofiltration, reverse osmosis and electrodialysis in Tunisia: performance and cost comparison. Desalination 207:95–106. doi:10.1016/j.desal.2006.03.583

Wang P, Lo IMC (2009) Synthesis of mesoporous magnetic gamma-Fe_2O_3 and its application to Cr(VI) removal from contaminated water. Water Res 43:3727–3734. doi:10.1016/j.watres.2009.05.041

Wang W, Zhou M, Mao Q et al (2010) Novel NaY zeolite-supported nanoscale zero-valent iron as an efficient heterogeneous Fenton catalyst. Catal Commun 11:937–941. doi:10.1016/j.catcom.2010.04.004

Warheit DB, Laurence BR, Reed KL et al (2004) Comparative pulmonary toxicity assessment of single-wall carbon nanotubes in rats. Toxicol Sci 77:117–125. doi:10.1093/toxsci/kfg228

Warheit DB, Webb TR, Sayes CM et al (2006) Pulmonary instillation studies with nanoscale TiO_2 rods and dots in rats: toxicity is not dependent upon particle size and surface area. Toxicol Sci 91:227–236. doi:10.1093/toxsci/kfj140

Weinberg H, Galyean A, Leopold M (2011) Evaluating engineered nanoparticles in natural waters. TrAC Trends Anal Chem 30:72–83. doi:10.1016/j.trac.2010.09.006

White BR, Stackhouse BT, Holcombe JA (2009) Magnetic gamma-Fe(2)O(3) nanoparticles coated with poly-l-cysteine for chelation of As(III), Cu(II), Cd(II), Ni(II), Pb(II) and Zn(II). J Hazard Mater 161:848–853. doi:10.1016/j.jhazmat.2008.04.105

Wiesner MR, Lowry GV, Alvarez P et al (2006) Assessing the risks of manufactured nanomaterials. Environ Sci Technol 40:4336–4345

Woan K, Pyrgiotakis G, Sigmund W (2009) Photocatalytic carbon-nanotube-TiO_2 composites. Adv Mater 21:2233–2239. doi:10.1002/adma.200802738

World Health Organization (WHO) (2004) Meeting the MDG drinking water and sanitation target : a mid-term assessment of progress/WHO/UNICEF Joint Monitoring Programme

Wu L, Shamsuzzoha M, Ritchie SMC (2005) Preparation of cellulose acetate supported zero-valent iron nanoparticles for the dechlorination of trichloroethylene in water. J Nanoparticle Res 7:469–476. doi:10.1007/s11051-005-4271-5

Wu J, Zheng Y, Song W et al (2014) In situ synthesis of silver-nanoparticles/bacterial cellulose composites for slow-released antimicrobial wound dressing. Carbohydr Polym 102:762–771. doi:10.1016/j.carbpol.2013.10.093

Xu C, Li B, Du H et al (2008) Electrochemical properties of nanosized hydrous manganese dioxide synthesized by a self-reacting microemulsion method. J Power Sources 180:664–670. doi:10.1016/j.jpowsour.2008.02.029

Yan H, Gong A, He H et al (2006) Adsorption of microcystins by carbon nanotubes. Chemosphere 62:142–148. doi:10.1016/j.chemosphere.2005.03.075

Yan W, Herzing AA, Li X et al (2010) Structural evolution of Pd-doped nanoscale zero-valent iron (nZVI) in aqueous media and implications for particle aging and reactivity. Environ Sci Technol 44:4288–4294. doi:10.1021/es100051q

Yantasee W, Warner CL, Sangvanich T et al (2007) Removal of heavy metals from aqueous systems with thiol functionalized superparamagnetic nanoparticles. Environ Sci Technol 41:5114–5119. doi:10.1021/es0705238

Zhang X, Du AJ, Lee P et al (2008a) TiO_2 nanowire membrane for concurrent filtration and photocatalytic oxidation of humic acid in water. J Memb Sci 313:44–51. doi:10.1016/j.memsci.2007.12.045

Zhang Y, Chen Y, Westerhoff P et al (2008b) Stability of commercial metal oxide nanoparticles in water. Water Res 42:2204–2212. doi:10.1016/j.watres.2007.11.036

giovanni.libralato@unina.it

Zhang K, Kemp KC, Chandra V (2012) Homogeneous anchoring of TiO_2 nanoparticles on graphene sheets for waste water treatment. Mater Lett 81:127–130. doi:10.1016/j.matlet.2012.05.002

Zhao G, Stevens SE (1998) Multiple parameters for the comprehensive evaluation of the susceptibility of *Escherichia coli* to the silver ion. Biometals 11:27–32. doi:10.1023/A:1009253223055

Zhou M, Nemade PR, Lu X et al (2007a) New type of membrane material for water desalination based on a cross-linked bicontinuous cubic lyotropic liquid crystal assembly. J Am Chem Soc 129:9574–9575. doi:10.1021/ja073067w

Zhou Q, Xiao J, Wang W (2007b) Comparison of multiwalled carbon nanotubes and a conventional absorbent on the enrichment of sulfonylurea herbicides in water samples. Anal Sci 23:189–192. doi:10.2116/analsci.23.189

Zhu J, Liu S, Palchik O et al (2000) Shape-controlled synthesis of silver nanoparticles by pulse sonoelectrochemical methods. Langmuir 16:6396–6399. doi:10.1021/la991507u

Zhu H, Jia Y, Wu X, Wang H (2009) Removal of arsenic from water by supported nano zero-valent iron on activated carbon. J Hazard Mater 172:1591–1596. doi:10.1016/j.jhazmat.2009.08.031

giovanni.libralato@unina.it

The Use of Al and Fe Nanoparticles for the Treatment of Micropollutants

Idil Arslan-Alaton and Tugba Olmez-Hanci

Abstract Increasing attention has been paid to the presence of micropollutants in water and wastewater due to their widespread application and incomplete removal during conventional treatment. Micropollutants may induce harmful impacts on human health as well as aquatic and terrestrial ecosystems at concentrations in the μg/L-ng/L range due to their persistence, bioaccumulation potential and toxicity. Until now, different strategies have been developed to alleviate the problem of micropollutants in the environment. Meanwhile, several types of Advanced Oxidation Processes (AOPs) have also been developed and applied for the effective, destructive treatment of problematic pollutants. AOPs involve the intermediacy of reactive oxygen species such as hydroxyl ($HO^{\cdot}$) and sulfate ($SO_4^{\cdot-}$) radicals. More recently, alternative, innovative AOPs using nanoscale materials have been explored. Zero-valent metals including zero-valent iron (ZVI) and zero-valent aluminum (ZVAl) have received increasing research interest due to their ease of use, high activity, availability and remarkable treatment performance. Their large surface area and the high number of active redox sites render nZVI and nZVAl good candidates for water and wastewater treatment. In this chapter, the application of ZVI- and ZVAl-mediated treatment systems for the degradation of organic and inorganic micropollutants has been presented and reviewed.

Keyword Hydrogen peroxide and persulfate activation · Hydroxyl radical · Micropollutants · Nanoparticles · Sulfate radical · Toxicity · Zero-valent aluminum · Zero-valent iron

List of Abbreviations and Symbols

4-CP	4-chlorophenol
AC	Activated carbon
ACTM	Acetaminophen

I. Arslan-Alaton (✉) · T. Olmez-Hanci
Department of Environmental Engineering, School of Civil Engineering,
Istanbul Technical University, Istanbul, Turkey
e-mail: arslanid@itu.edu.tr

© Springer International Publishing AG 2017

G. Lofrano et al. (eds.), *Nanotechnologies for Environmental Remediation*,
DOI 10.1007/978-3-319-53162-5_3

giovanni.libralato@unina.it

ADMI	American Dye Manufacturer's Institute
ANT	Anthracene
AO7	Acid orange 7
AOPs	Advanced oxidation processes
APEOs	Alkylphenol polyethoxylates
ATSDR	Agency for Toxic Substances and Diseases Registry
BaP	Benzo[a]pyrene
BOD_5	5 day biochemical oxygen demand
BPA	Bisphenol A
BTZ	Bentazon
CAP	Chloramphenicol
CMC	Carboxymethyl cellulose
COD	Chemical oxygen demand
DBP	Dibutyl phthalate
DCA	Dichloroacetate
DCP	2,4-dichlorophenol
DNT	2,4-dinitrotoluene
DO	Dissolved oxygen
DR23	Direct red 23
DW	Distilled water
EDC	Endocrine disrupting compounds
EDS	Energy dispersive X-ray spectroscopy
EDTA	Ethylene diamine tetra acetic acid
GC-ICP-MS	Gas chromatography coupled to inductively coupled plasma mass spectrometry
GC-MS	Gas chromatography-mass spectroscopy
HA	Humic acid
$HO^{\cdot}$	Hydroxyl radical
$HO_2^{\cdot}$	Hydroperoxyl radical
HP	Hydrogen peroxide
HPLC	High performance liquid chromatography
ICM	X-ray contrast media
ICP	Inductively coupled plasma
IOPA	Iopamidol
LC-MS	Liquid chromatography-mass spectroscopy
MTBE	Methyl tert-butyl ether
NACs	Nitroaromatic compounds
NGs	Nanographenes
nZVAl	Nanoscale zero-valent aluminum
nZVI	Nanoscale zero-valent iron
$O_2^{\cdot-}$	Superoxide radical
OG	Orange G (also: AO7)
OTCs	Organotin compounds
OxA	Oxalic acid

giovanni.libralato@unina.it

PAA	Porous anodic alumina
PAEs	Phthalic acid esters
PAHs	Polycyclic aromatic hydrocarbons
PCA	P-chloroaniline
PHE	Phenanthrene
PMS	Peroxymonosulfate
POM	Polyoxometalate
PPCPs	Pharmaceuticals and personal care products
PRBs	Permeable reactive barriers
PS	Persulfate
PVA	Polyvinyl alcohol
PYR	Pyrene
RGO	Reduced graphite oxide
RGY	Remazol golden yellow
ROS	Reactive oxygen species
RSM	Response surface methodology
SD	Sulfadiazine
SDS	Sodium n-dodecyl sulfate
SEM	Scanning electron microscope
SHE	Standard hydrogen electrode
$SO_4^{\cdot-}$	Sulfate radical
Sono-FL	Sonochemical Fenton-like treatment
T	Temperature
TAME	Tert-amyl methyl ether
TBA	Tert-butyl alcohol
TBT	Tributyltin
TEM	Transmission electron microscopy
TMeT	Trimethyltin
TOC	Total organic carbon
TP	Tap water
TX-45	Triton™ X-45
US EPA	United States Environmental Protection Agency
US	Ultrasound
UV	Ultraviolet
VOCs	Volatile organic compounds
WHO	World Health Organization
WW	Wastewater
XPS	X-ray photoelectron spectroscopy
XRD	X-ray diffraction
ZVAl	Zero-valent aluminum
ZVI	Zero-valent iron

giovanni.libralato@unina.it

1 Introduction

In recent years, the use of zero-valent metals such as ZVI and ZVAl for the treatment of organic contaminants and heavy metals in surface water, groundwater and wastewater has received considerable attention and encouraging results have been reported (Han et al. 2016; Bokare and Choi 2014). The major contaminants that have been treated by ZVI and ZVAl materials are industrial dyes, pharmaceuticals, explosives, pesticides, heavy metals, surfactants, arsenic, hexavalent chromium and heavy metals. The use of these nanoparticles offers several advantages including high abundance (for example Al is the third most ubiquitous element on earth and the most abundant metallic element) and relatively low commercial cost. ZVI and ZVAl-mediated treatment systems exhibit high oxidative capacity owing to their high redox potential and the enhanced aqueous solubility of ionic Fe and Al species. Consequently, the use of ZVI and ZVAl offers very promising alternatives for the degradation of micropollutants. In the forthcoming sections, general principles, advantages , application ranges and shortcomings/limits of these emerging treatment systems are presented and evaluated.

2 Treatment with Zero-Valent Iron

2.1 Basic Principles and Reaction Mechanism

Among the variety of AOPs available, in particular Fenton and Photo-Fenton Processes have gained more attention due to their superior reaction kinetics and treatment efficiencies (Safarzadeh-Amiri et al. 1996; Nadtochenko and Kiwi 1998; Arslan-Alaton and Teksoy 2007). Iron-based AOPs are kinetically and economically more attractive than other AOPs, thus extensive research on reaction pathways and critical process parameters has already been reported in scientific papers. More recently, heterogeneous Fenton systems such as ferrate [Fe (IV)] and ZVI applications have been developed to overcome some limitations of Fenton processes (Zhou and Jiang 2015; Li et al. 2014a). Although several Fenton and Fenton-like treatment systems involving Fe ions and hydrogen peroxide (HP), ZVI, ultra violet (UV)-, near-UV or even visible light have been developed, their common feature is the thermal (dark) Fenton reaction as given below;

$$Fe^{2+} + H_2O_2 \rightarrow Fe^{3+} + HO^{\cdot} + OH^- \quad 63\ M^{-1}s^{-1} \tag{1}$$

$$Fe^{3+} H_2O_2 \rightarrow Fe^{2+} + HO_2^{\cdot} + H^+ \quad 2.0 \times 10^{-3}\ M^{-1}s^{-1} \tag{2}$$

$$Fe^{2+} + HO_2^{\cdot}/O_2^{\cdot -} \rightarrow Fe^{3+} + H_2O_2 \quad 1.2 \times 10^6\ M^{-1}s^{-1} \tag{3}$$

The rate of $HO^{\cdot}$ formation in the above reactions depends on the solution pH that should be in the range of 2–5. Solution pH affects the steady-state concentration of

giovanni.libralato@unina.it

Fe^{2+} complexes in the reaction solution (Tang and Tassos 1997; Walling and Goosen 1973). The Fe^{2+} concentration is typically low because all regenerated Fe^{2+} is directly consumed by HP in the dark Fenton process to produce new $HO^{\cdot}$. Moreover, it has been demonstrated that the involvement of $Fe^{4+}_{(aq)}$ ions as reactive intermediates of the Fenton reaction cannot be ruled out [Fe^{3+}/Fe^{4+} = 1.4 eV vs. standard hydrogen electrode (SHE) at pH 7.0 and 1.8 eV vs. SHE at pH 10.0]. $HO^{\cdot}$ generally reacts with organic compounds by addition to double bonds possessing a sufficient electron density, hydrogen abstraction from alkyl or hydroxyl groups, or alternatively by electron transfer to the pollutant (Walling et al. 1974). In contrast, the reaction of a metal cation (Fe^{4+}) with aliphatic or aromatic organics proceeds exclusively by an electron transfer mechanism since other addition and abstraction reactions are not possible (Bossman et al. 1998). Besides, product identification, selectivity and pulse radiolysis studies confirmed that in particular Photo-Fenton reactions involve the intermediacy of $HO^{\cdot}$ (Pignatello et al. 1999) besides more selective species including ferrate (Fe^{4+}).

Although iron-based AOPs have successfully being applied for the treatment of micropollutants found in water and wastewater samples, serious shortcomings have so far hindered their full-scale application and commercialization as a treatment technology due to factors such as (i) pH dependency; (ii) pH re-adjustment requirements; (iii) solid waste production in the form of ferric hydroxide precipitate. This means that after treatment with the Fenton's reagent, the effluent pH has to be re-adjusted to neutral values prior to discharge or biological treatment in order to prevent biomass inhibition and enhance Fe removal by its precipitation. Hence alternatives to the homogenous treatment systems such as the use of ZVI, iron oxides (Fe_xO_y) and oxyhydroxides (FeOOH), iron-loaded zeolites and supported Fe have been explored (Zha et al. 2014; He et al. 2014; Gonzalez-Olmos et al. 2012). For example, Fe(III) oxides absorb light of suitable (near-UV) energy to promote the generation of electron-hole pairs that initiate redox reactions. In this way, adsorbed pollutants undergo hole and free radical oxidation in the reaction medium similar to semiconductor-mediated heterogeneous photocatalysis (Li et al. 2014b; Grčić et al. 2012). In these treatment systems, hole oxidation can be important considering that the bandgaps of Fe(III)-oxides range between 2.02 and 2.12 eV. These heterogeneous reactions are initiated by a surface complex formed between the oxidant (HP) and the Fe(III) oxide surface (metal centers). The Fe(III) oxide surface is immobilized in the crystal lattice and octahedrally coordinated by O_2 and OH^{-}. Upon excitation/activation, the Fe(III)OOH coordination bond is broken to produce active Fe(IV) = O species and $HO^{\cdot}$, whereas Fe(IV) = O is very unstable and immediately reacts with H_2O forming another $HO^{\cdot}$ (Li et al. 2014b).

More recently, alternatives to Fe(III) oxides have been explored and an immense scientific literature (Fu et al. 2014; Mueller et al. 2012; Kharisov et al. 2012; Crane and Scott 2012) in the treatment applications of ZVI and nanoscale ZVI (nZVI) accumulated. ZVI offers several advantages since it is very reactive having a reduction potential of −0.44 V vs. SHE, relatively non-toxic, abundant, cheap, easy to produce and handle (Fu et al. 2014; Greenlee et al. 2012; Grieger et al. 2010). ZVI may degrade organic compounds in the presence of dissolved oxygen (DO) by transferring two

giovanni.libralato@unina.it

electrons to produce HP. Then, HP can be reduced to water by another two electron transfer from ZVI. Moreover, ZVI corrosion releases Fe^{2+} ions from the particle surface to the reaction bulk, such that HP and Fe^{2+} can produce $HO^{\cdot}$ by the Fenton reaction (Bremner et al. 2006; Bergendahl and Thies 2004). Undoubtedly, an acidic pH environment is preferred to enhance Fe solubility in the solution bulk and corrosion of the ZVI surface (Fu et al. 2014; Zhao et al. 2010). The basic reactions involved in the ZVI/H^+/air-O_2 treatment system are given below;

$$Fe^0 + O_2 + 2H^+ \rightarrow Fe^{2+} + H_2O_2 \quad (4)$$

$$Fe^0 + H_2O_2 + 2H^+ \rightarrow Fe^{2+} + 2H_2O \quad (5)$$

$$Fe^{2+} + H_2O_2 \rightarrow Fe^{3+} + HO^{\cdot} + OH^- \quad (6)$$

Advantages and disadvantages of using ZVI for the treatment of micropollutants can be listed as follows; its high surface area (up to 100 m^2/g) and reactivity enabling prompt corrosion reactions; its low stability due to formation/accumulation of oxides and hydroxides inhibiting surface-driven redox reactions; ease of aggregation hindering long-term applicability; difficulties encountered in the separation of nZVI particles from the treated solution; low (acidic) pH requirements to enhance Fe solubility and Fenton/Fenton-like reactions (Kusic et al. 2011; Zhao et al. 2010; Diao and Yao 2009), respectively. In order to overcome these technical limitations, nZVI has also been supported on solid and porous materials such as carbon, resin, bentonite, kaolinite and zeolites (Salam et al. 2015; Wang et al. 2014a). In this way oxidation, reduction and adsorption capacities could be improved. Other methods to enhance the reactivity and stability of ZVI are; (i) doping with transition metals such as Pd, Cu, Ni or Pt, to enhance reduction rates by serving as hydrogen catalysts or reactive electron donors; (ii) preparing bimetallic materials (Fe/M = M:Ag, Pd, Ni) to accelerate the reaction rates; (iii) slowing down the deposition of corrosion products and reduce the formation of toxic intermediates on the particle surface (Trujillo-Reyes 2014; O'Carroll et al. 2013). Considering the applicability of ZVI/nZVI technology, some full-scale examples are ZVI-based permeable reactive barriers (PRBs) for the in situ remediation of groundwater and more than 200 ZVI-based PRBs have been installed at contaminated sites since the first field demonstration in 1995. In 2002, the United States Environmental Protection Agency (US EPA) designated the ZVI-PRB a standard remediation technology (Fu et al. 2014).

The reaction mechanism and processes undergoing during treatment of aqueous pollutants with nZVI particles has been outlined below (Wu et al. 2014);

(i) An iron oxide-Feo(OH)-layer immediately forms on nZVI being responsible for the core-shell structure in the nanoparticles.
(ii) The core is composed of metallic iron and acts as an electron donor source, promoting reduction of compounds.
(iii) The nZVI shell enables sorption, surface complexation and electron transport from and to the core (Wu et al. 2014; Li et al. 2014a). The shell layer

giovanni.libralato@unina.it

composition depends on the reaction medium and synthesis method. It is extremely reactive due to its amorphous structure, the presence of defective sites and the small size of nZVI. Due to their dual structure, nZVI can present characteristics of metallic and oxide iron, acting as both a reductant and an adsorbent (Li et al. 2014a).

Persulfate ($S_2O_8^{2-}$, PS) has drawn increasing attention as an alternative oxidant to HP in the abatement of organic contaminants in the last decade since it offers several advantages such as high aqueous solubility, high stability at room temperature, relatively low cost and benign end products such as sulfate, which is only biotoxic at substantial concentrations (Rodriguez et al. 2014). PS salts readily dissociate in water to persulfate anions that are strong and relatively stable oxidants (Zhao et al. 2010). However, PS treatment is generally associated with the production of sulfate radicals, i.e. $SO_4^{\cdot-}$ (2.6–2.8 V vs. SHE) which are very strong and reactive oxidizing agents. More recently, the Fenton-like reaction which is based on the activation of PS to generate $SO_4^{\cdot-}$ has exhibited a great potential in the oxidative treatment of refractory contaminants. $SO_4^{\cdot-}$ can be generated in different ways; from the activation of persulfate by UV, heat, microwave and transition metals such as Fe, Cu, Co, or Mn. However, ZVI activation is a relatively cost-effective, efficient and friendly technology compared with the other activation methods and thus has received considerable attention in the persulfate-driven oxidation of contaminants (Xiong et al. 2014; Kusic et al. 2011). ZVI activation not only serves as a slow-releasing source of Fe^{2+} but also provides a different, heterogeneous type of PS activation involving direct electron transfer from ZVI or surface-bound Fe^{2+}.

The mechanism of heterogeneous ZVI treatment in the presence of PS involves direct electron transfer from the ZVI or surface-bound Fe^{2+} to PS, continuing with a homogenous Fenton-like redox reaction that involves $SO_4^{\cdot-}$ production in the reaction bulk (Xu and Li 2010);

$$Fe^0 + S_2O_8^{2-} \rightarrow Fe^{2+} + 2SO_4^{2-} \tag{7}$$

$$Fe^{2+} + S_2O_8^{2-} \rightarrow Fe^{3+} + SO_4^{2-} + SO_4^{\cdot-} \quad k = 27\ M^{-1}s^{-1} \tag{8}$$

These reactions are analogous to the HP activation reactions in the presence of ZVI that were shown in Eqs. (5) and (6).

Parallel to the above reactions, $SO_4^{\cdot-}$ scavenging is also expected and may become significant when PS is provided in excessive amounts (overdosed). Under these circumstances, $SO_4^{\cdot-}$ are simultaneously consumed by Fe^{2+} and PS (Oh et al. 2010) as shown below;

$SO_4^{\cdot-}$ scavenging by Fe^{2+}:

$$Fe^{2+} + SO_4^{\cdot-} \rightarrow Fe^{3+} + SO_4^{2-} \quad k = 3 \times 10^8 M^{-1}s^{-1} \tag{9}$$

giovanni.libralato@unina.it

$SO_4^{\cdot-}$ scavenging by PS:

$$S_2O_8^{2-} + SO_4^{\cdot-} \rightarrow S_2O_8^{\cdot-} + SO_4^{2-} \quad k = 6.1 \times 10^5\,M^{-1}s^{-1} \qquad (10)$$

Therefore, it is important to optimize the oxidant (PS) concentration in the reaction solution to hinder unwanted side reactions and inhibition.

2.2 ZVI Applications for the Treatment of Industrial Micropollutants

Several applications exist for the treatment of industrial micropollutants in the scientific literature. Major applications are; groundwater remediation (removal of chlorinated volatile organic compounds (VOCs), pesticides, antibiotics, nitroaromatics, arsenic, nitrate and heavy metals) and industrial wastewater treatment (polychlorinated biphenyls, polybrominated diphenyl ethers, dyes, phenols, chlorinated phenols, heavy metals and metalloids). It is important to mention that in particular PS activation with ZVI has been frequently reported as an effective and hence promising treatment process. Thus in the forthcoming review section studies have been focused on the removal of micropollutants with ZVI activated PS.

2.2.1 Hexavalent Chromium

Due to its severe toxicity, the Agency for Toxic Substances and Diseases Registry (ATSDR) classifies Cr(VI) as the top 16th hazardous substance (ATSDR 2000). The World Health Organization (WHO) requires 50 μg/L of Cr(VI) in drinking water (WHO 1993). The treatment of Cr(VI)-bearing wastewater has stimulated a worldwide research interest. In a study conducted by Sun et al. (2015), ZVI nanorods modified with chitosan in porous anodic alumina (PAA) were prepared as an adsorbent medium. Adsorption of trace Cr(VI) was tested as a function of solution pH value, initial Cr(VI) concentration and adsorption time. The results showed that PAA could limit the size, disperse ZVI nanorods and protect them from corrosion/oxidation. In the adsorption process it was found that both PAA and chitosan can supply bridges between ZVI nanorods and Cr(VI) through surface electrostatic attraction. The optimum adsorption capacity obtained from the Langmuir model was 118.76 mg/g and in accordance with the experimental adsorption conducted at pH 5. X-ray photoelectron spectroscopy (XPS) revealed that Cr(VI) was reduced to Cr(III) on the adsorbent surface. The adsorption behavior of Cr(VI) could be described with the Langmuir and pseudo-second-order kinetic models which implied that the adsorption process was chemisorption. The Gibbs Free energy change indicated that the process of Cr(VI) onto adsorbent was

giovanni.libralato@unina.it

spontaneous. Besides, the aluminum sheets could be regenerated and anodized to produce PAA.

Although ZVI and nZVI treatment systems are effective in Cr(VI) reduction, there are still some parameters influencing the Cr(VI) reduction kinetics by ZVI which include the iron surface characteristics (presence of oxides, surface morphology) of the metals, the pH value, temperature of the bulk phase and existence of humic acid (HA) that all play important roles in electron transfer and adsorption processes. In view of these arguments, it may be expected that HA could also influence the Cr(VI) removal process by ZVI. In groundwater, ZVI and nZVI walls frequently undergo long period of HA adsorption and precipitation. Therefore, it is important to evaluate the role of HA in the ZVI reduction mechanism and system performance. For example, Wang et al. (2011) found that HA exerts an inhibitory effect on Cr(VI) removal by ZVI nanoparticles and Cr(VI) removal efficiencies decreased from 71.6, 58.4, 57.8 to 38.5% with increasing HA concentrations of 0, 5, 10, 20 and 40 mg/L, respectively. A dual effect of HA on Cr(VI) reduction by ZVI nanoparticles was observed; HA adsorbed on the surface of ZVI nanoparticles and occupied the active surface sites, leading to the decrease in Cr(VI) reduction rates.

2.2.2 Arsenic

Long-term exposure to drinking water containing arsenic (As) stimulates occurrences of skin, lung, bladder and kidney cancers and may even result in premature death (Bates et al. 1992). Therefore, the WHO and some countries (such as the US and China) lowered their guideline for drinking water quality from 50 to 10 μg/L for As (WHO 1993). As in water primarily derives from natural (dissolution and wreathing of arsenic minerals, biological activities) and anthropogenic (industrial waste, mining, agricultural, etc.) sources. As forms in water are inorganic and organic and the inorganic forms are more toxic than the organic counterparts. Additionally, As(III) is more toxic and difficult to be removed from water than As (V). On the other hand, nZVI has a high adsorption capacity for As(III) and As(V), but its application is limited in practical use due to its small particle size and aggregation effect (Zhu et al. 2009). Wang et al. (2014a) have used reduced graphite oxide (RGO) as a support due to its high surface area and stability. In order to utilize the advantage of nZVI and RGO as well as to avoid the shortcomings of using nZVI, nZVI was loaded onto RGO and its adsorption capacity for As(III) and As(V) was comparatively evaluated. Langmuir adsorption isotherms were established in batch experiments as 35.83 mg/g and 29.04 mg/g for As(III) and As(V), respectively. Adsorption kinetics fitted the pseudo-second-order model. The residual, total As concentration was found to meet the standard of WHO after the samples were treated with 0.4 g/L by nZVI-RGO when the initial concentration of As(III) and As(V) were below 8 and 3 mg/L, respectively. The residual concentration dropped to non-detectable values when the initial concentration of As(III) was 1 mg/L.

giovanni.libralato@unina.it

2.2.3 Heavy Metals

Heavy metals are one of the groups of contaminants which can be effectively removed by nZVI. However, the underlying mechanisms are quite complex. The aim of a study conducted by Calderon and Fullana (2015) was to determine the effect of nZVI aging in heavy metal remediation of water. The heavy metals Zn, Cd, Ni, Cu and Cr, which are typical elements found in ground and wastewater, were used as model pollutants. Results show a high removal capacity by nZVI in the first 2 h of reaction. However, after extended reaction times (t = 21 d), some of the metal ions, mainly Cd and Ni, which had already been adsorbed in the nZVI, were delivered back to the water. Cd and Ni showed maximum delivery rates (>60–65%). The start of the delivery time depended on the concentration of nZVI and was observed later when applying lower nZVI concentrations. Transmission electron microscopy (TEM) images demonstrated that no re-dissolution of Cr was observed in any circumstance, because it was the only element being incorporated into the nanoparticles core. Heavy metal (Zn, Cd, Ni, Cu) release from nZVI was speculatively due to nanoparticles oxidation caused by aging, which produced a nZVI surface crystallization.

2.2.4 Nitrate

Accumulation of high levels of nitrate in the aquatic environment is contributing to DO depletion, which might kill fish and create a harmful environment for human beings (Rabalais et al. 2002). Nitrates possess a high risk to human health and have been categorized in the US EPA's Drinking Water Contaminant List with a maximum contaminant level of 10 mg/L as nitrate-nitrogen (Scavia and Donnelly 2007). Nitrate is considered to be relatively nontoxic to the human body, but of main concern is its reduction to nitrite by denitrifying bacteria in the upper gastrointestinal tract, which may cause many diseases such as blue baby syndrome and even cancer (Rabalais and Turner 2001). Nitrites transform hemoglobin to methemoglobin by oxidation of ferrous iron (Fe^{2+}) in hemoglobin to ferric form (Fe^{3+}), preventing or reducing the ability of blood to transport oxygen, which might cause cyanosis and anoxemia (NRC 1995). In order to remove nitrate efficiently from water, ZVI nanoparticles (ZVINPs) were synthesized and then supported on high surface area nanographenes (NGs) to prepare a stable ZVINP/NG nanocomposite (Salam et al. 2015). X-ray Diffraction (XRD) measurements showed the stabilization of the ZVINPs upon their support on NGs, which ultimately enhanced their activity. The ZVINP/NG nanocomposite was used for the catalytic reduction of nitrate ions in model solution and the results showed the dependency of the removal process on the ZVINPs to NGs ratio in the nanocomposite, time of removal and solution pH. The effect of power ultrasound (US) was also explored. Obtained findings indicated that US could significantly decrease the treatment time required by the nanocomposite. The mechanism of nitrate reduction by the ZVINP/NG nanocomposite was studied and the results showed the conversion of nitrate to

giovanni.libralato@unina.it

nitrite and/or ammonia, and then to nitrogen gas. Nitrate removal involved three main steps; namely adsorption of nitrate onto the ZVINP surface; reduction and finally desorption into the solution bulk. There are two possible mechanisms proposed for nitrate reduction using ZVINPs, either the (i) direct transfer of electrons from metallic iron to the reaction bulk, or (ii) indirect electron transfer by hydrogen atoms yielding corrosion. An acidic pH was found to be favorable for nitrate reduction using ZVINPs because of enhanced dissolution of Fe(II)/(III) oxides and other protective layers which is a critical step in the efficiency and hence regeneration of ZVI for nitrate and nitrite reduction. In contrast, a basic medium transforms Fe(II) into ferrous hydroxide that is thermodynamically unstable and may be further oxidized to magnetite. The accumulation of magnetite on the ZVI surface slows down the redox reactions when the pH exceeds values to 6–7. With ZVINPs alone (without the support), nitrate removals reached 56% and 63% after 24 and 40 h treatment, respectively. When the nanocomposite (NG as the supporting material) was used, nitrate removal reached 68% after 24 h and 69% after 40 h due to the enhanced dispersion of ZVINPs hence improving the reduction reaction between ZVINPs and nitrate ions. In this work nitrite ions were detected with a very low concentration in the first stage of the reaction and then disappeared completely due to concomitant ammonium formation.

2.2.5 Organotin Compounds

Organotin compounds (OTCs) are highly toxic even in the ng/L concentration range. Due to their widespread use in industrial and agricultural applications they are present as global pollutants in the environment (Council Directive 1999). International conventions on the control of harmful anti-fouling systems on ships indicate their presence in the marine and terrestrial environment (Craig et al. 2003). For example, trimethyltin (TMeT) is neurotoxic and mainly occurs in landfill leachates (de Carvalho et al. 2010). In the landfill environment, tin is undergoing chemical and biological transformation. In this way, tin species can be modified by alkylation resulting in the formation of new organotin compounds (de Carvalho et al. 2010). Degradation of OTCs in landfill leachate is usually incomplete. Peeters et al. (2015) examined the adsorption and degradation of tributyltin (TBT) and TMeT found in landfill leachate with different Fe nanoparticles, namely Fe^0 (nZVI), FeO and Fe_3O_4 at varying reaction conditions. Leachate samples were treated at pH 8, pH 8 with Fe nanoparticles dispersed with tetramethyl ammonium hydroxide (TMAH) or by mixing, under aerated conditions for 7 days. The pH of the landfill leachate was also adjusted to pH 3 with citric acid prior to treatment with Fe nanoparticles. Size distribution of TBT and TMeT between the nanoparticles was determined by sequential filtration and their concentrations in the size fractions were measured by gas chromatography coupled to inductively coupled plasma mass spectrometry (GC-ICP-MS). TBT or TMeT were present in fractions with particle sizes of 42.5 or 2.5 nm, respectively. At pH 8, adsorption was the dominant removal mechanism whereas at pH 3 the Fenton redox reaction became more

giovanni.libralato@unina.it

active. TBT was mainly removed (96%) when nZVI was dispersed into landfill leachate by mixing firstly at pH 8 followed by treatment of the aqueous phase at pH 3. TMeT was less effectively (about 40%) removed by this treatment system.

2.2.6 Pesticides

Bentazon (3-(1-methylethyl)-1H-2,1,3-benzothiadiazin-4(3H)-one-2,2-dioxide; BTZ, molecular weight: 240 g/mol) is a post-emergence herbicide that has been widely used for selective control of broadleaf sedges and weeds in beans, rice, corn, peanuts and mint (Pourata et al. 2009). BTZ is toxic to human beings through oral ingestion or dermal absorption and can also cause eye irritation (Pourata et al. 2009). BTZ is biochemically resistant in nature and has a long half-life. In order to eliminate the negative impacts of BTZ on environment and public health, different treatment technologies have been studied to remove it from effluents including AOPs (Salman et al. 2011). More recently, Wei et al. (2016) studied ZVI activation of PS for BTZ removal. The $SO_4^{\cdot-}$ produced from the system was principally responsible for effective BTZ degradation. Key factors affecting the treatment performance were tested; including BTZ, PS and ZVI concentration, initial solution pH, temperature and common ions in water. Under the optimal ZVI (4.477 mM) and PS (0.262 mM) concentrations, a concentration of 0.021 mM BTZ was totally removed at an initial pH 6–7. Common ions exhibited different effects on BTZ removal. Al^{3+}, Cl^- and NO_3^- improved the treatment rates; NH_4^+, Ca^{2+} and Mg^{2+} did not influence the BTZ removal, whereas Mn^{2+}, Cu^{2+}, CO_3^{2-}, HCO_3^-, PO_4^{3-}, HPO_4^{2-} and $H_2PO_4^-$ inhibited the BTZ degradation. Most of BTZ could not be mineralized; instead, BTZ was degraded into three major degradation products including 2,1,3-benzothiadiazin-4(3H)-one-2,2-dioxide ($C_7H_6N_2O_3S$), 2-aminobenzoic acid (anthranilic acid; $C_7H_7NO_2$) and 2-amino-2-sulfobenzoic acid ($C_7H_7NO_5S$).

2.2.7 Polyaromatic Hydrocompounds (PAHs)

Polycyclic aromatic hydrocarbons (PAHs) are among the most widespread organic contaminants found in soils, natural waters and wastewater (Puglisi et al. 2007). The release of PAH into the environment can involve natural phenomenal (e.g. volcanic eruptions, forest fires) or anthropogenic activities (incomplete combustion of fuel, coal, wood, etc.). Due to their hydrophobic nature and low solubility in the aqueous phase, these species tend to be sorb on solid particulates, especially on the soil organic fractions (Rivas 2006). Knowing their potentially mutagenic or carcinogenic effects on human and animal health and their tendency to accumulate in the environment, their removal is considered as a priority task. Peluffo et al. (2016), applied activated PS for the remediation of a soil contaminated with the PAHs anthracene (ANT), phenanthrene (PHE), pyrene (PYR) and benzo[a]pyrene (BaP). PS activation was performed with ferric and ferrous sulfate salts (1–5 mM) as well as ZVI nanoparticles. Moreover, in order to improve the oxidation rate of

giovanni.libralato@unina.it

contaminants, the addition of sodium n-dodecyl sulfate (SDS) as an anionic surfactant was tested. Additionally, the role of HA acting as a reducing agent on PAHs conversion was examined. Removal efficiencies near 100% were achieved for ANT and BaP under all studied experimental conditions. Remarkable differences in removal efficiencies were observed for the reaction conditions in case of PHE and PYR. The highest conversions of PHE (80%) and PYR (near 100%) were achieved when nZVI was used as the PS activator. Similar results were obtained when activation was carried out either with ferric and ferrous iron salts. This could be explained by the presence of quinone-type compounds such as 9,10-anthraquinone, that can promote the reduction of Fe(III) to Fe(II), permitting more sulfate radical generation by the Fenton's reaction. However, the addition of HA did not produce an improvement of the process while surfactant addition slightly increased PAHs' removal. Besides, a kinetic model was developed describing PS consumption and contaminants removal using first-order kinetic models.

2.2.8 Pharmaceuticals (Antibiotics)

Contamination by pharmaceuticals and personal care products (PPCPs) in surface- and ground water are emerging as a potential, serious threat to the ecosystem and human health. PPCPs, especially antibiotics, are reported to act as an inhibitor of multi-xenobiotic resistance, which creates adverse effects on aquatic organisms (Kolpin et al. 2002). Due to antimicrobial effects, their high molecular weight and complex structure, antibiotics and other drugs usually cannot be removed effectively by conventional wastewater treatment methods (Underwood et al. 2011; Knapp et al. 2008). In the past decades, sulfonamides have been worldwide used due to their broad antimicrobial spectrum. The widespread overuse of sulfonamides, especially in the industry of livestock feeding has contaminated surface and underground water at many sites around the world and might allow antimicrobial agents to alter the microbial community structure yielding to global antibiotic resistance among microbial communities. This phenomenon poses serious human health problems and environmental risks through the food chain enrichment and water contamination. Consequently, a great deal of efforts is being made to eliminate this class of substances in surface water or wastewater.

Effective decomposition of the antibiotic sulfadiazine (SD) in a ZVI-catalyzed sonochemical Fenton-like treatment system (Sono-FL) was demonstrated by Zhou et al. (2016). Response surface methodology (RSM) was employed as an experimental design tool to optimize the proposed treatment process. Optimum conditions were established as pH 7.0, 0.94 mM ZVI, 1.90 mM PS and 20 W US to achieve the highest SD degradation efficiency of 90%. The effects of wastewater matrix (five inorganic anions and two chelating agents) on SD degradation were also examined. It was found that the SD removal was inhibited by SO_4^{2-}, NO_3^-, HCO_3^-/CO_3^{2-} and $H_2PO_4^-$ to different extents. Cl^- would lead to an enhancement at low concentrations (5 mM), but an inhibition was evident at high concentration (100 mM). Cl^- addition resulted in the formation of chlorinated organic

giovanni.libralato@unina.it

intermediates besides other SD decomposition products. Appropriate dosages of oxalic acid (OxA) or ethylene diamine tetraacetic acid (EDTA) enhanced SD degradation in the Sono-FL system, while excessive chelating agents acted as competitors. Inorganic ions and organic additives acted as $SO_4^{\cdot-}$ and $HO^{\cdot}$ scavengers beyond a critical concentration. OxA and EDTA not only acted as complexing agents to dissolve the released Fe ions from ZVI, but also provided additional oxidants such as HP and $[Fe(IV)O]^{2+}$ through electron transfer reactions of the iron-ligands species.

In another related work, Zou et al. (2014) developed a novel US-enhanced heterogeneous ZVI/PS (ZVI/PS/US) oxidation system for the treatment of the antibiotic SD. It was demonstrated that the ZVI/PS/US treatment system could achieve a significant synergy in the degradation of SD, as compared to its single treatment combinations (PS/US, ZVI/US, ZVI/PS). The first-order removal rate constant for SD was found in the range of $3.4 \pm 0.20\ h^{-1}$. Initial pH, ratio of $[Fe^0]$:[PS], US power and reaction temperature were further studied as process variables. SD could be effectively degraded with a relatively low PS concentration at a broad pH range of 3–7. Simultaneous evolution of soluble Fe ions and PS consumption were evaluated in three comparative systems (ZVI/US, ZVI/PS and ZVI/PS/US) during the reaction. The role of US was specifically examined; it enhanced the heterogeneous iron corrosion reactions and accelerated the bulk free radical chain/redox reactions. It could be demonstrated that the main reactive oxygen species (ROS) was $SO_4^{\cdot-}$, attacking of the amine group in the benzene ring and cleaving the C–N bonds in the heterocyclic ring. Another degradation pathway was proposed to be the direct cleavage of the S–N bond in the SD structure.

Chloramphenicol, (CAP), is a broad-spectrum antibiotic with excellent antibacterial properties, isolated from *Streptomyces venezuelae* in 1947. Inhibiting protein synthesis in microorganisms, CAP is effective against gram-positive and gram-negative cocci and bacilli, which makes it a popular choice to treat human and animal diseases (Lovett 1996). Various side effects of CAP, however, were established, e.g., fatal bone marrow depression and aplastic anemia. It has been reported that CAP concentrations in municipal sewage, river water and sediments were up to 47.4 μg/L, 19.0 μg/L and 1138 g/kg, respectively (Liu et al. 2009). Up to present, only a few studies on CAP removal from water or wastewater are available (Liu et al. 2009). CAP removal from aqueous solution with nanoscale-ZVI particles was systematically investigated by Xia et al. (2014) using batch experiments. The effects of the key parameters including nZVI concentration, initial pH and aeration on CAP removal were ascertained. CAP removal efficiency was found to be enhanced with increasing nZVI concentration and decreasing initial pH. Due to the Fenton reaction of the nZVI catalyzed by air-oxygen, higher CAP removal efficiency was observed in air than in nitrogen environment. At a nZVI concentration of 1.06 g/L, an initial pH of 6.8 and the presence of air, 100 mg/L CAP was completely removed within 5 min. The Raman analyses of nZVI particles before and after the process indicated that CAP was adsorbed and reduced on the surface of nZVI particles. The XPS analyses along with the inductively coupled plasma (ICP) results further confirmed that ZVI was oxidized during the treatment

giovanni.libralato@unina.it

process. From the liquid chromatography-mass spectroscopy (LC-MS) and gas chromatography-mass spectroscopy (GC-MS) results of the CAP reduction products, dechlorination followed by nitro group reduction was proposed to be the potential reduction routine of CAP by nZVI.

2.2.9 Chlorinated Organics

Chlorinated organics are very common water pollutants. They are used as intermediates for the production of synthetic organic chemicals and polymers like polyurethanes, rubber additives, dyes, pharmaceuticals, cosmetic products, pesticides and herbicides (Latorre et al. 1984). Because of their widespread applications and use, these toxic and/or recalcitrant compounds are considered as important environmental pollutants in industrial wastewaters and are subject to legislative control by the US EPA and EU countries (Boon et al. 2002). In a study of Hussain et al. (2012), the degradation of p-chloroaniline (PCA) by PS-activated ZVI was investigated through batch experiments. Effects of pH, temperature, and concentrations of ZVI and PS on PCA degradation were examined. The degradation of PCA increased with increasing ZVI due to increased activation of PS to produce sulfate radicals. PCA degradation was higher under acidic pH conditions (pH 2.0 and 4.0) compared to alkaline conditions. Complete degradation of PCA was obtained in 12 min by ZVI-activated PS at pH 4.0. An increase in the reaction temperature from 15 to 50 °C significantly enhanced the PCA degradation. Aniline, n-(4-chlorophenyl)-p-phenylene di-imine, 1-(4-Chlorophenyl)-3-phenylurea and 5-chloro-2-(4-chlorophenyl diazenyl) phenol were identified as the major intermediates of PCA oxidation by PS. Chlorophenols are characterized by their high toxicity and weak biodegradability; hence they constitute a toxic group of contaminants being harmful to organisms and human health at low concentrations (Cheng et al. 2007). Apart from their noxious effects, chlorophenols impart taste and odor to water and create substantial oxygen demand in receiving waters. In particular, 2,4-dichlorophenol (DCP) is a persistent contaminant frequently found in agricultural sites, water disinfected by chlorination as well as pulp and paper mill effluents. The main method for removing DCP has been either adsorption onto activated carbon (AC) or oxidative destruction via wet air oxidation, however both methods of treatment have their disadvantages and economic limitations (Rodriguez et al. 2012). Li et al. (2015) used various Fe-based materials such as Fe^{2+}, nZVI, and nano-Fe_3O_4 (nFe_3O_4) were used as heterogeneous catalysts to remove DCP. DCP removal increased from 6 to 12% with Fe^{2+}, nZVI and nFe_3O_4 to 6–38%, respectively. These data indicate that nZVI can potentially generate sulfate radicals in the presence of PS. UV, Scanning Electron Microscopy (SEM), Energy Dispersive X-ray Spectroscopy (EDS) and XRD demonstrated that changes on the surface of nZVI occurred owing to Fe^{2+} leaching and corrosion. It was further observed that DCP degradation increased when nZVI and PS concentrations

giovanni.libralato@unina.it

increased. However, it decreased when the initial pH and DCP concentration were elevated. More than 98% of DCP degradation was achieved within 180 min under optimum conditions, but less than 40% of COD was removed. The degradation of DCP exhibited an activation energy of 91.5 kJ/mol.

2.2.10 Nitroaromatics

Nitroaromatic compounds (NACs) can be reductively transformed by ZVI (Oh et al. 2002a, b). However, in the presence of PS, the degradation of NACs with PS and nZVI is much more complex and involves the intermediacy of $SO_4^{\cdot-}$, and hence reduction plus advanced oxidation reactions as well (Oh et al. 2003). It has been proposed that the electron-withdrawing nitro functional group hinders the oxidative attack by $SO_4^{\cdot-}$ (Oh et al. 2003). Hence, it is likely that reduction of NACs might facilitate the oxidative degradation of NACs and their reduction products. In a related work, the reduction by ZVI and oxidation by PS activated with ZVI have proven to destroy extremely recalcitrant organic compounds such as chlorinated solvents and NACs. Oh et al. (2010) examined the oxidation of 2,4-dinitrotoluene (DNT) by persulfate PS activated with ZVI through a series of batch experiments. The mechanism for ZVI activation was investigated by comparing the results with Fe^{2+}/PS oxidation. The effects of the molar PS:Fe ratio and pre-reduction with ZVI on DNT oxidation were also examined. DNT was stable in the presence of PS and transformed only when ZVI was added. Most DNT was degraded oxidatively by ZVI activated PS, whereas direct reduction of DNT by ZVI played a minor role in its overall degradation. The rate of DNT degradation increased with increasing ZVI concentration mainly due to the enhanced activation of PS by ZVI and Fe^{2+} by a Fenton-like oxidation system. In contrast to the ZVI/PS treatment system, where complete oxidation DNT was achieved, only around 20% DNT was degraded and the reaction slowed down rapidly when an equimolar concentration of Fe^{2+} was used instead of ZVI. Results indicated that ZVI was more effective than Fe^{2+} as an activating agent and potentially more suitable for environmental applications since it allows the slow and efficient release of Fe ions from the ZVI surface via corrosion. The reduction products of DNT were more rapidly oxidized by PS than DNT, suggesting that converting the nitro groups of NACs to amino groups prior to oxidation can greatly enhance their oxidation as evidence before in the case of azo dye treatment via reduction + chemical oxidation processes.

2.2.11 Textile (Azo) Dyes

Azo dyes, which contain one or more nitrogen to nitrogen double bonds (–N=N–) have been widely used in industries such as textiles, foodstuffs and leather. Textile azo dyes account for approximately 70% of all dyes in the market (Arslan-Alaton 2003). From the environmental point of view, azo dyes form a large group of

giovanni.libralato@unina.it

industrial pollutants that pose a serious threat to human beings because of their non-biodegradability, toxicity and the potential carcinogenic nature of their anoxic metabolites (Arslan-Alaton 2003; Arslan-Alaton et al. 2002). Hence, the fate and treatability of textile azo dyes and their metabolites has been attracting a widespread attention all over the world. For instance, Weng et al. (2015) investigated the decolorization of an azo dye, C.I. Direct Red 23 (DR23), by PS activated with ZVI aggregates (ZVI/PS). US and heat were used as enhancement tools in the ZVI/PS treatment system. Neither US-activated PS nor thermally activated PS was effective in oxidizing DR23. However, color removal was significantly enhanced by ZVI/PS combined with US (ZVI/PS/US) or heat (ZVI/PS/55 °C). Approximately 95% decolorization of 0.0001 M DR23 was achieved within 15 min in the ZVI/PS/US treatment system at an initial pH of 6.0, PS of 0.005 M, ZVI of 0.5 g/L and US irradiation of 106 W/cm^2 (60 kHz). Complete decolorization was achieved within 10 min in the ZVI/PS/55 °C treatment process. The rate of decolorization doubled when US was introduced in the ZVI/PS treatment system at different initial azo dye concentrations. The dependence of dye and true color (American Dye Manufacturer's Institute; ADMI color) depletion on PS concentration was also examined. DR23 was completely degraded and partially but quickly mineralized as could be traced by following the total organic carbon (TOC) parameter. In particular, increasing the temperature enhanced DR23 decolorization. The Arrhenius activation energy for the ZVI/PS combination was estimated to be 8.98 kcal/mol. Thus, both ZVI/PS/US and heated (thermally activated) ZVI/PS treatment systems were found to be practically feasible for the effective degradation of the direct azo dye.

In another related study, the decolorization of a fiber reactive monoazo dye, namely Remazol Golden Yellow (RGY; Reactive Orange 107), by PS oxidation activated with ZVI aggregate was investigated (Weng and Tao 2016). RGY decolorization was not effective in US-activated, heat-activated and base-activated PS oxidation; however significant color removal was achieved by applying the ZVI/PS combination. Decolorization was strongly influenced by pH, ZVI and PS concentration as well as temperature. Under optimum conditions which were established as pH 6.0, PS 0.005 M and ZVI 0.5 g/L 98% color removal of 100 mg/L RGY solution was obtained within 20 min treatment. The activation energy of the ZVI/PS system was only 0.479 kJ/mol, suggesting that the temperature dependence of RGY decolorization was minor. The presence of inorganic salts in the RGY solution had an adverse effect on decolorization. The inhibitory effect of various inorganic salts on decolorization followed the decreasing sequence of $Na_2HPO_4 \gg NaHCO_3 \gg NaClO_4 > NaCl > NaNO_3 > NaClO_4 >$ no salt addition. The ZVI aggregate was reusable and satisfactory decolorization was achieved with the repeated use of ZVI for five times. The ZVI/PS process provides an effective technology for effective RGY decolorization.

PS was also employed by Rodriguez et al. (2014) for the same monoazo dye (Reactive Orange 107; OG). PS was activated with ZVI to produce $SO_4^{\cdot-}$. Identification of oxidation intermediates was also carried in this study keeping the initial dye concentration 11.6 mM, with 153 mM of PS and 20 mM of ZVI at 20 °C. Phenol, benzoquinone, aniline, as well as phenolic and naphthalene type

giovanni.libralato@unina.it

compounds were identified by GC-MS and high performance liquid chromatography (HPLC) and an oxidation pathway was proposed for the oxidation of OG with iron activated PS. The effect of Fe oxidation states (0, II or III) in the oxidation of 0.1 mM OG was also studied in a 0.5 L capacity batch reactor at 20 °C. The initial Fe and PS concentrations employed were both 1 mM. Complete pollutant removal was achieved within the first 30 min when Fe II or III were employed as the activators. When ZVI was employed (particle diameter size 0.74 mm) the limiting step in $SO_4^{\cdot-}$ generation was the surface reaction between ZVI and color removal was retarded as compared with Fe(II) and Fe(III) ions. An increase in PS concentration to 6 mM for 0.2 mM OG resulted in complete color and toxicity removals together with 75% TOC abatement.

In another study, the removal of the textile azo dye Acid Orange 7 (AO7) by ZVI activated PS in the presence of US was performed (Wang et al. 2014b). The effects of PS concentration, ZVI addition, US power and initial pH on the decolorization rate of AO7 were investigated. The results showed that the decolorization rate increased with an increase in PS concentration from 0.1 to 0.5 g/L, an increase in ZVI from 0.1 to 0.5 g/L and an increase in US from 40 to 60 W. However, further increase in these parameter values did not further enhance the dye removal rates. The ZVI/PS/US process combination was capable of decolorizing the azo dye AO7 at an optimal pH of 5.8. The highest decolorization efficiency of 96.4% was achieved within 20 min with a PS concentration of 0.3 g/L, ZVI concentration of 0.5 g/L, an initial pH value of 5.8 and an US power of 60 W. The TOC removal efficiency reached 64% when the reaction time was extended to 60 min.

2.2.12 Polyvinyl Alcohol (PVA)

Polyvinyl alcohol (PVA) is commonly used in the textile industry as a sizing agent and in the pharmaceutical industry as an ophthalmic lubricant. PVA is also used in adhesives, paper-coating, emulsion paints, and detergent-based industries (Giroto et al. 2006). It has been shown that PVA is a biorecalcitrant chemical and it is difficult to convert PVA-laden wastewaters to innocuous end products like carbon dioxide and water, which is detrimental to the ecosystem and can lead to accumulation in the human body through the food chain (Tokiwa et al. 2001). PVA can also cause additional environmental problems due to its potential to mobilize heavy metals from sediments in water streams and lakes (Giroto et al. 2006). Unfortunately, conventional biological (e.g. activated sludge) treatment systems do not efficiently degrade PVA because the PVA degrading capacity of most microbial species is very specific and limited (Schonberger et al. 1997). Oh et al. (2009) reported that after 48 days of incubation, mixed cultures acclimated to a PVA solution showed only a 40% mineralization of PVA to the end products CO_2 and H_2O. In the present study, the oxidation of PVA by PS activated with heat, Fe^{2+} and Fe^0 (ZVI) was investigated via batch experiments. It was hypothesized that elevated temperature and the addition of Fe^{2+} or ZVI together with PS activates PS. Increasing the temperature from 20 to 60 or 80 °C accelerated the oxidation rate of

giovanni.libralato@unina.it

PVA, which achieved complete oxidation in 30 and 10 min, respectively. At 20 °C, the addition of Fe^{2+} or ZVI to the PS-H_2O/acid system significantly enhanced the oxidation of PVA. The optimal PS: Fe^{2+} or ZVI molar ratio was found to be 1:1. Complete oxidation of PVA was obtained with ZVI-activated PS after 120 min. Synergistic activation of persulfate by heat and Fe^{2+} or ZVI also enhanced the oxidation of PVA in the PS/water/acid system. By employing GC-MS analysis, an oxidation product of PVA was identified; namely vinyl acetic acid/acetate ($C_4H_6O_2$), which is readily biodegradable. Experimental results indicated that the oxidative treatment of PVA by activated PS is a viable option for the pretreatment of PVA-laden wastewater to improve its biodegradability.

2.2.13 Phthalates

Phthalic acid esters (PAEs) have received increasing attention in recent years due to their wide use as plasticizers and additives in cosmetics production (Ghisari et al. 2009). As a consequence, these toxic, recalcitrant and potentially endocrine disrupting compounds (EDCs) are ubiquitous in environments, causing a lot of harm to aquatic organisms and human health through food chain transmission and bioamplification (Wu et al. 2013a). Dibutyl phthalate (DBP) is one of the most frequently used PAE and suspected to be an EDC. DBP may have effects on the development of reproductive toxicity, mutagenesis and carcinogenesis (Lyche et al. 2009). DBP tends to be chemically and photolytically stable; its hydrolysis and volatilization occurs very slowly in the natural environment (Wu et al. 2013a; Xu and Li 2008). Therefore, both the US EPA and China National Environmental Monitoring Center have classified DBP as a priority pollutant. Li et al. (2014a) conducted batch tests to investigate the effect of initial pH on the degradation of DBP, the formation and evolution of iron corrosion products, and the role of iron oxides on the further degradation of DBP in ZVI-PS treatment system. Their study indicated that the half-lives for the oxidation of DBP by PS activated with ZVI were 30–176 min at pH 3.0–11.0, respectively. The constituents and the morphology of the iron corrosion coating along different initial pH and over reaction time were investigated with Raman spectroscopy, XPS and SEM. According to these measurements, magnetite (Fe_3O_4), wustite (FeO), hematite (a-Fe_2O_3) and goethite (alpha-FeOOH) were identified as the corrosion products on the ZVI surface. In alkaline and neutral solutions, the inner layer of iron oxides was mainly composed of alpha-Fe_2O_3 with some alpha-FeOOH, while the outer layer mostly consisted of Fe_3O_4 and alpha-FeOOH. Oppositely, the iron oxides formation in acidic solution mainly consisted of Fe_3O_4, alpha-FeOOH and a small amount of alpha-Fe_2O_3 and FeO in the inner layer, whereas the outer layer was mostly composed of alpha-Fe_2O_3 and to a lesser extent alpha-FeOOH. These iron corrosion coatings exhibited an inhibitory effect on the degradation of DBP, which may be due to that the iron oxides hindered the electron transfer from the ZVI core to the solid-liquid interface.

giovanni.libralato@unina.it

2.2.14 Bisphenol A (BPA)

Endocrine disruptors are linked to increasing cases of breast cancer, infertility, low sperm counts, genital deformities, obesity, early puberty and diabetes, as well as alarming mutations in wildlife (Flint et al. 2012). They are also suspicious of causing behavioral and learning problems in children which coincides with their intensive, global use (Flint et al. 2012). Among them, Bisphenol A (2,2-bis (4-hydroxyphenyl)propane; BPA) is a synthetic estrogen used to harden polycarbonate plastics and epoxy resins (O'Connor and Chapin 2003). BPA is fabricated into thousands of products made of hard, clear polycarbonate plastics and tough epoxy resins, including safety equipment, eyeglasses, computer and cell phone casings, water and beverage bottles. BPA is also consumed as a resin in dental fillings, as coatings on cans, as powder paints and as additives in thermal paper. BPA have also been detected in old landfill leachate (Rezg et al. 2014). Studies have demonstrated that BPA can affect growth, reproduction and development in aquatic organisms (O'Connor and Chapin 2003). Besides, evidence of endocrine-related effects in fish, aquatic invertebrates, amphibians and reptiles has been reported at relevant exposure levels being much lower than those required for acute toxicity (Flint et al. 2012). These low concentrations render their effective removal by conventional biological, physical and chemical methods difficult and costly. In the present study, the use of a commercial, air-stable, nZVI was examined for the treatment of 20 mg/L, aqueous BPA solutions (Girit et al. 2015). The influence of pH (3, 5, 7), addition of hydrogen peroxide (HP) and persulfate (PS) as oxidants (0.0, 1.25 and 2.5 mM) as well as temperature (25 and 50 °C) was studied for BPA treatment with 1 g/L ZVI. ZVI coupled with HP and PS provided effective treatment systems, which was based on rapid, ZVI-mediated decomposition of the above mentioned oxidants resulting in complete BPA as well as significant TOC (88%) removals in particular when PS was employed as the oxidant. Increasing the PS concentration and reaction temperature dramatically enhanced PS decomposition and BPA removal rates, whereas HP was not very effective in TOC removal at elevated temperatures. According to the bioassays conducted with *Vibrio fischeri* and *Pseudokirchneriella subcapitata*, the acute toxicity of aqueous BPA fluctuated first but decreased appreciably at the end of ZVI/PS treatment.

2.2.15 Octyl Phenol Polyethoxylate (Triton™ X-45)

Alkylphenol polyethoxylates (APEOs) are industrial compounds belonging to the class of nonionic surfactants that are designed to have both hydrophilic and hydrophobic properties (Ying 2006). Among them, octylphenol polyethoxylates have been widely used in cleaning products, paints, ink dispersants, textile preparation and leather processing, manufacture of pulp and paper, metalworking, cosmetics and personal care products (Ying et al. 2002). It has been reported that APEOs' aerobic/anaerobic transformation products (alkylphenols such as nonylphenol and octylphenol) are much more inhibitory and estrogenic than the

giovanni.libralato@unina.it

original surfactants (Routledge and Sumter 1996). Despite the above-mentioned concerns APEOs appear in several industrial applications where they cannot be replaced by alternative chemicals due to technical and economic reasons (Arslan-Alaton and Olmez-Hanci 2012). Consequently, the presence of these nonionic surfactants and their metabolites have been reported in water bodies, sediments and sludge associated with the continuing discharges from industrial and sewage treatment plants (Staples et al. 2001). Considering the above mentioned problems related with the presence of APEOs in water and wastewaters, 20 mg/L aqueous Triton™ X-45 (TX-45) a commercially important octylphenol polyethoxylate, was subjected to PS oxidation activated with ZVI nanoparticles (Temiz et al. 2016). After optimization of the ZVI/PS treatment combination (1 g/L ZVI; 2.5 mM PS at pH 5) in terms of pH (3–9), ZVI (0.5–5 g/L) and PS (0.5–5.0 mM) concentrations, TX-45 could be efficiently (>90%) degraded within short treatment periods (<60 min) accompanied with appreciable (>40%) TOC removals. The degree of PS consumption and Fe release were also followed during the experiments and a positive correlation existed between enhanced TX-45 removals and ZVI-activated PS consumption rates accompanied with a parallel Fe release. Acute toxicity tests were conducted within the scope of this study to examine the toxicological safety of ZVI/PS oxidation system. Acute toxicity profiles decreased significantly from an original value of 66% relative inhibition to 21% and from 16% relative inhibition to non-toxic values according to *V. fischeri* and *P. subcapitata* bioassays, respectively. The photobacterium *V. fischeri* appeared to be more sensitive to TX-45 and its degradation products than the microalgae *P. subcapitata*. The above case studies are comparatively summarized in Table 1.

2.3 Deactivation, Aggregation, Toxicity and Other Implications

Recent work related with the use of nZVI for environmental remediation has indicated that their application presents some serious limitations regarding their rapid oxidation (corrosion) and aggregation in the media (Trujillo-Reyes et al. 2014). Related work also demonstrated the kinetically attractive and high contaminant removal capacity of nZVI within the first hours of the reaction. However, after extended reaction times, the nZVI surface typically gets covered with Fe oxides and hydroxides, thus hindering effective degradation of the target pollutants (Wu et al. 2014). Moreover, water or wastewater constituents also start to competitively adsorb onto nZVI that may hinder further redox reactions of the original, targeted pollutant (Sun et al. 2015).

Aging of nZVI may also induce desorption of contaminants and degradation products which are then released back to the effluent. Recently, it could be shown that the water content enhances nZVI corrosion resulting in the rapid formation of ordered crystalline structures (Calderon and Fullana 2015). This aging effect is

giovanni.libralato@unina.it

giovanni.libralato@unina.it

Table 1 Application of ZVI for the treatment of micropollutants

Micropollutant	Process Type	Reaction conditions	Main results	Reference
2,4-dinitrotoluene (DNT)	ZVI/PS	DNT = 50 mg/L; ZVI = 0.2–10 g/L; PS = 250 mg/L; pH = 3	• DNT was stable in the presence of PS and only removed by ZVI activation • Complete DNT removal occurred with ZVI/PS • The reduction products of DNT (nitroaromatics) were more rapidly oxidized by PS than DNT	Oh et al. (2010)
Acid orange 7 (AO7)	ZVI/PS ZVI/PS/US	AO7 = 30 mg/L; ZVI = 0.1–1.0 g/L; PS = 0.1–1.0 g/L; pH = 3–9; V = 250 mL; US = 40–90 W; t = 20 min; T = 20 °C	• Highest performance was obtained with PS/US/ZVI • Color removal increased with increasing PS concentration (0.1–0.5 g/L), an increase in ZVI from 0.1 to 0.5 g/L and an increase in US power from 40 to 60 W • Optimal pH was 5.8 • Highest color removal (96.4%) was achieved in 20 min with 0.3 g/L PS, 0.5 g/L ZVI, 60 W US at pH 5.8	Wang et al. (2014b)
Bentazon (BTZ)	ZVI ZVI/PS	BTZ = 0.0125–0.0291 mM; ZVI = 0, 0.895, 2.686, 4.477, 6.267 mM; PS = 0, 0.262–1.050 mM; pH = 3–11; t = 0–90 min; T = 25–55 °C	• Under optimized ZVI (4.477 mM) and PS (0.262 mM) concentrations, 0.021 mM BTZ was totally removed at pH $\leq$ 7 • Al^{3+}, Cl^{-} and NO_3^{-} improved BTZ removal • NH_4^{+}, Ca^{2+} and Mg^{2+} did not significantly influence BTZ removal • Mn^{2+}, Cu^{2+}, CO_3^{2-}, HCO_3^{-}, PO_4^{3-}, HPO_4^{2-} and $H_2PO_4^{-}$ inhibited BTZ removal • Most BTZ was not mineralized but degraded into three main degradation products ($C_7H_6N_2O_3S$, $C_7H_7NO_2$ and $C_7H_7NO_5S$)	Wei et al. (2016)

(continued)

Table 1 (continued)

Micropollutant	Process Type	Reaction conditions	Main results	Reference
Bisphenol A (BPA)	ZVI/HP ZVI/PS	BPA = 20 mg/L; ZVI = 1 g/L; PS = 0, 1.25, 2.5 mM; pH = 3, 5, 7; V = 500 mL; 150 rpm; t = 120 min; T = 25, 50 °C	• Complete BPA and 88% TOC removals were achieved for ZVI/PS (PS = 2.5 mM, pH = 5) • Increasing PS and T dramatically enhanced PS decomposition and BPA removal rates • HP was not effective in TOC removal and at elevated T • According to the bioassays conducted with *V. fischeri* and *P. subcapitata*, acute toxicity first increased but decreased appreciably at the end of ZVI/PS treatment	Girit et al. (2015)
Chloramphenicol (CAP)	ZVI (*home-made*)	CAP = 100–110 mg/L;ZVI = 0.53, 1.06, 2.12 and 4.23 g/L; pH_0 = 2.8, 4.8, 6.8, 8.8 and 10.8; V = 40 mL; 150 rpm; presence of air/nitrogen gas	• Increasing the nZVI concentration and decreasing the pH enhanced CAP removal • The treatment process showed higher CAP removal in the presence of air-oxygen • In the presence of air, CAP removal was complete in 5 min for ZVI = 1.06 g/L, pH = 6.8 • Raman analysis confirmed that CAP was adsorbed and reduced on nZVI • XPS and ICP results confirmed that nZVI was oxidized after the process • LC-MS and GC-MS analyses indicated that CAP was reduced • Dechlorination followed by nitro group reduction was proposed	Xia et al. (2014)
Cr(VI)	ZVI fillings (*home-made*)	Cr(VI) = 20 mg/L; ZVI = 0.3–10 g/L; pH_0 = 6, V = 500–100 mL; 400 rpm; t = 0–180 min; T = 25 °C; HA = 0–40 mg/L	• Cr(VI) removal occurred via adsorption and reduction • HA inhibited Cr(VI) removal • Cr(VI) removal efficiencies decreased from 71.6, 58.4, 57.8 to 38.5% with increasing HA concentrations (0, 5, 10, 20–40 mg/L, respectively) • The inhibitory effect of HA could be eliminated with starch (0.5 g/L)	Wang et al. (2011)

(continued)

giovanni.libralato@unina.it

Table 1 (continued)

Micropollutant	Process Type	Reaction conditions	Main results	Reference
Direct red 23 (DR23)	ZVI/PS ZVI/PS/US ZVI/PS/base ZVI/PS/heat	DR23 = 2×10^{-5} M; ZVI = 0.5 g/L; PS = 0–5×10^{-3} M; 106 W/cm^2 (at 60 kHz); t = 0–30 min; T = 4–55 °C	• 95% decolorization of 0.0001 M DR23 was achieved in 15 min with PS/ZVI/US at pH 6.0, 0.005 M PS, 0.5 g/L ZVI and 106 W/cm^2 US • Complete decolorization was achieved in 10 min with ZVI/PS at 55 °C • The activation energy for ZVI/PS was found as 8.98 kcal/mol	Weng and Tsai (2016)
Direct red 80 (DR80)	ZVI/PS ZVI/PS/US ZVI/PS/US ZVI/US	DR80 = 25 mg/L; ZVI = 0.1–1.0 g/L; PS = 5×10^{-4}–10^{-2} M; pH_0 = 6.0–12.0; US = 120 W/L; t = 0–30 min; T = 16–55 °C	• 95% decolorization was achieved in 5 min with ZVI/PS at pH 6.0, 0.005 M PS and 0.5 g/L ZVI at 55 °C • The activation energy was obtained as 0.636 kJ/mol • GC-MS intermediates were naphthalene, naphthalene-2-sulfonic acid azobenzene, benzene, 1,2-benzenedicarboxylic acid, phthalic anhydride, formic acid acetic acid and oxalic acid	Weng et al. (2015)
Polyvinyl alcohol (PVA)	ZVI/PS Fe(II)/PS PS/heat	PVA = 50 mg/L; PS = 250 mg/L; PS:ZVI = 1:0.2–1:2 (molar ratio); V = 500 mL; 50 rpm; t = 120 min; T = 20, 40, 60,80 °C	• Increasing T from 20 to 60 or 80 °C accelerated PVA degradation which was complete in 30 and 10 min, respectively • At 20 °C addition of Fe(II) or ZVI dramatically enhanced PVA oxidation with PS • The optimum PS:Fe(0) molar ratio was 1:1 • Complete oxidation of PVA was obtained with ZVI/PS in 2 h • Only vinyl acetic acid was identified as the oxidation product, which is readily biodegradable	Oh et al. (2009)

(continued)

giovanni.libralato@unina.it

Table 1 (continued)

Micropollutant	Process Type	Reaction conditions	Main results	Reference
Reactive orange 107 (RO107)	ZVI/PS	RO107 = 0.1–0.2 mM (+11.6 mM for intermediate analyses); Fe = 20 mM; PS = 153 mM; V = 0.5 L; t = 250 min; T = 20 °C	• Complete removal was achieved in 30 min with Fe(II) • Activation of PS by Fe(III) also allowed complete OG removal • A longer reaction time was required with ZVI • Increasing the oxidant and activator concentrations decreased the final TOC and *P. phosphoreum* toxicity • Intermediates were mainly phenol and benzoquinone, but also aniline, phenolic compounds and naphthalene type compounds with quinone groups	Rodriguez et al. (2014)
Reactive orange 107 (RO107)	ZVI/PS ZVI/PS/US ZVI/PS/base PS/heat	RO107 = 25–100 mg/L ZVI = 0–1 g/L; PS = 2×10^{-4}–0.01 M; V = 0.5 L; pH_0 = 4–10; US = 120 W/L; ClO_4^-, Cl^-, NO_3^-, SO_4^{2-}, HCO_3^-, HPO_4^{2-} = 0–0.005 M; t = 20 min; T = 15–60 °C	• Optimum decolorization (98%) conditions for 100 mg/L RO107 removal were pH = 6.0, PS = 0.005 M, ZVI = 0.5 g/L, t = 20 min • The activation energy of the ZVI/PS treatment system was 0.479 kJ/mol • Inorganic salts inhibited decolorization rates • Satisfactory decolorization could be achieved with repeated use of ZVI for five times	Weng and Tao (2016)
Soil contaminated with the polycyclic aromatic hydrocarbons (PAHs) anthracene (ANT), phenanthrene (PHE), pyrene (PYR), benzo [a]pyrene (BaP)	ZVI/PS Fe(II)/PS Fe(III)/PS	ANT = 97 ± 6 mg/kg; PHE = 89 ± 2 mg/kg; PYR = 93 ± 1 mg/kg; BaP = 102 ± 1 mg/kg PS = 200 mM; t = 40 d;HA = 2000 mg/kg; SDS = 2.2 g/L (HA or SDS added 24 d before PS)	• Highest conversions of PHE (80%) and PYR (near 100%) were achieved when PS was activated with nZVI • Similar results were obtained with Fe(II) and Fe(III) • Addition of HA did not improve the process, while SDS addition slightly increased PAHs removal	Peluffo et al. (2016)

(continued)

giovanni.libralato@unina.it

Table 1 (continued)

Micropollutant	Process Type	Reaction conditions	Main results	Reference
Sulfadiazine (SD)	ZVI/US	SD = 20 mg/L; ZVI = 0.1–2.5 mM; PS = 0.1–2.5 mM; pH = 3, 5, 7, 9; V = 400 mL; 100 rpm; US = 20–140 W; T = 20 °C; ClO_4^-, Cl^-, NO_3^-, SO_4^{2-}, HCO_3^-, PO_4^{2-} = 0, 5, 100 mM	• Optimum conditions were pH = 7.0, ZVI = 0.94 mM, PS = 1.90 mM, US = 20 W established by experimental design-RSM, resulting in 97.39% SD removal • SD removal was inhibited by ClO_4^-, Cl^-, NO_3^-, SO_4^{2-}, HCO_3^-, HPO_4^2 to different extents • Addition of oxalic acid or EDTA could benefit SD degradation, while excessive chelating agents acted as competitive polluters	Zou et al. (2014)
Tributyltin (TBT) and trimethyltin (TMeT) in leachate	ZVI FeO Fe_3O_4	TBT, TMeT = 1000 ng/L (as Sn); pH_0 = 3, 8; t = 7d	• At pH 8 adsorption of TBT prevailed • At pH 3 (adjusted with citric acid) the Fenton reaction provoked TBT degradation • In leachate spiked with TBT and TMeT, TBT was effectively removed (96%) when nZVI was dispersed into leachate by mixing (pH 8 + pH 3 with citric acid) • With the same procedure, only 40% TMeT was removed from leachate • When tetra methyl ammonium hydroxide was used for nZVI dispersion, methylation of soluble nontoxic ionic tin species was provoked transforming them into highly toxic methyltin compounds	Peeters et al. (2015)
Triton™ X-45 (TX-45)	ZVI/HP ZVI/PS	TX-45 = 20 mg/L; ZVI = 1 g/L; PS = 0, 1.25, 2.5 mM; pH = 3, 5, 7, 9; V = 500 mL;150 rpm; t = 120 min; T = 25, 50 °C	• TX-45 could be efficiently (>90%) degraded within <60 min accompanied with >40% TOC removals • A positive correlation existed between enhanced TX-45 removals and PS consumption rates with a parallel Fe(II) release • Acute toxicity profiles decreased from an original value of 66–21 and 16% to non-toxic values according to *V. fischeri* and *P. subcapitata* bioassays, respectively • *V. fischeri* appeared to be more sensitive to TX-45 and its degradation products than *P. subcapitata*	Temiz et al. (2016)

giovanni.libralato@unina.it

more pronounced at elevated (less acidic) pH and compounds including lepidocrocite, magnetite, goethite and maghemite were found on the aged nZVI surface. Additionally, the reactivity of nZVI towards DO and water molecules produce Fe (III) oxides on the nZVI outer shell surface, hence leading to the entire loss of its reducing capacity (Calderon and Fullana 2015).

A serious limitation of nZVI in-and ex situ applicability for water remediation is its inherent tendency for aggregation. For example, to prevent particle aggregation during transportation through soil or underground aquifers, nZVI particles were often suspended in dispersing reagents or surface-modified with hydrophobic, air-stable chemicals (polymeric materials such as carboxymethyl cellulose-CMC, or polyacrylate dispersants) to enhance their mobility (Trujillo-Reyes et al. 2014). It should be pointed out here that the use of air stabilizers or other additives in order to modify the physicochemical properties of nZVI may cause undesired effects in the aquatic environment including toxicity, bioaccumulation as well as other ecotoxicological risks associated with the use of additional chemicals. Although nZVI often ages to stable Fe(III) oxides and eventually precipitates to the bottom of aquifers, the above-described surface modification of particles may change their bioavailability to aquatic organisms (Wu et al. 2014). Elucidating the fate and ecotoxicological risk of various forms of nZVI (before and after its application) in the aquatic environment is urgently needed before these are widely used as remediation materials.

As aforementioned, nZVI-mediated treatment is increasingly being used for the treatment of water or wastewater; however, the fate and ecotoxicological effects of nZVI in the treated effluent is still a relatively untouched area. Nano-iron metal and nano-iron oxides are among the most widely used engineered and naturally occurring nanostructures, and the increasing incidence of biological exposure to these nanostructures has raised concerns about their toxicity (Wu et al. 2014). ROS-induced oxidative stress is one of the most widely accepted toxic mechanisms and considerable efforts have recently been made to investigate the ROS-related activities of iron-based nanomaterials (Chen et al. 2013). The ROS levels in animal blood have been recognized to rise under certain physiological conditions including breeding, hypertension and inflammation. Within cells, ROS are continuously produced as by-products of electron transportation in the mitochondria and may also appear in other cellular locations after escaping the effective antioxidant defense. Therefore, in order to understand the biological effects of iron-based nanostructures like nZVI, it is important to characterize their ROS-related activities under specific bio-microenvironmental conditions including physiological pH and buffers, reducing agents and other organic substances (Wu et al. 2014).

Some bioassays indicated a potential ecotoxicological impact of nZVI on the aquatic environment. Differential toxic effects of CMC-stabilized-nZVI, nFe_3O_4 and Fe(II) ions at environmentally relevant exposure in early life stages of medaka fish was examined (Chen et al. 2013). The CMC-nZVI solution was more toxic to the medaka embryos than free Fe(II) and Fe(III) oxide in terms of acute mortality and sub-lethal developmental toxicity. The toxic effect of CMC-nZVI was

giovanni.libralato@unina.it

attributed to a combination of hypoxia, Fe(II) toxicity and ROS-mediated oxidative damage/stress. It could be demonstrated that CMC-nZVI induced substantially higher toxic effects including high bioaccumulation, developmental toxicity and oxidative stress in vivo than the other Fe forms. Specific physicochemical properties of nZVI such as surface modification and large surface area could lead to changes in chemical reactivity and particle aggregation rate which in turn might influence its bioavailability and/or uptake causing increased toxicity and bioaccumulation.

El-Temsah and Joner (2013) evaluated the degradation organo-chlorine insecticides from two types of soil with nZVI. After treatment, bioassays were conducted in soil and the aqueous phase of slurries using *Folsomia candida* and *Heterocypris incongruens*. After a 7-day treatment period, negative effects such as increased mortality and poor reproduction were found in both organisms in the presence of nZVI.

Wu et al. (2013b) reported that at a concentration of 200 mg/L, nZVI affected the bacterial community in activated sludge used for tertiary (nutrient) treatment. These negative effects on the mixed biocultures were associated with an increase in ROS.

Otero-Gonzalez (2013) assessed the toxicity of nZVI and Fe(III) oxide to the eukaryotic cell model microorganism *Saccharomyces cerevisiae* (yeast cells) besides other nanomaterials being used as environmental remediation catalysts. According to their study, nZVI exhibited low toxicity (44% inhibition at a concentration of 1000 mg/L) in the oxygen uptake test and a negligible effect on the cell membrane integrity. No toxic effect was observed for Fe(III) oxide. The effect of nZVI aggregation on its toxicity was also evaluated after modification with a non-toxic dispersant. The dispersant increased the stability and decreased the aggregation of the nanomaterials, thus affecting the interaction between the microorganism and the nanomaterial. IC_{20} value for nZVI increased from 625 mg/L to non-detectable values (IC_{20} > 1000 mg/L) for plain and modified materials.

As aforementioned, treatability studies with nZVI particles have demonstrated that redox reactions involving nZVI are very effective due to their high surface area. However, nZVI tend to agglomerate in water through direct interparticle interactions that will affect their ultimate removal capacity. Some researchers found that electrostatic repulsion, steric hindrance, and CMC can prevent their aggregation by enhancing their mobility and enabling their stable dispersion in the reaction medium. Currently, several researchers have studied the synthesis and application of nanostructured composites including nZVI, metal oxides and nanoscale bimetallic systems supported onto inorganic porous materials to enhance their dispersibility, stability as well as adsorptive and redox properties (Cabello et al. 2016). Some important examples are kaolinite-nZVI and zeolite-nZVI, bentonite-nZVI, rectorite-nZVI, organo-smectite-nZVI. magnetic nZVI supported onto n-benzyl-O-carboxymethyl chitosan (Trujillo-Reyes et al. 2014). These supported composites performed very well in the removal of micropollutants and could be re-used for several cycles. Furthermore, it has also been shown that adsorbent-supported nZVI showed better performance in the removal of contaminants compared to individual materials.

giovanni.libralato@unina.it

Most of the studies involving supported nZVI have been conducted in the form of batch experiments and under controlled reaction conditions meaning that experiments with actual contaminated waters are essentially lacking. Working with real effluent and conducting battery tests/bioassays to assess ecotoxicological impacts are proposed as future research subjects in the field of remediation with nZVI.

3 Treatment with Zero-Valent Aluminum

3.1 Basic Principles and Reaction Mechanism

Each AOP used in water and wastewater treatments has its own advantages and disadvantages with respect to simplicity, efficacy, ease of use and cost. Hence continuous improvements in treatment processes are always in demand. More recently, besides ZVI, ZVAl-based treatment systems were investigated to eliminate organic as well as inorganic pollutants found in water and wastewater. The use of ZVAl for micropollutant and heavy metal removals has some inherent advantages such as high natural abundance since Al is the most abundant metal in earth's crust as well as low weight (Bokare and Choi 2014). Compared to ZVI ($Fe^{2+} + 2e^- \rightarrow Fe^0$; $E^0 = -0.44$ V vs. SHE), ZVAl possesses a substantially lower standard reduction potential ($Al^{3+} + 3e^- \rightarrow Al^0$; $E^0 = -1.67$ V vs. SHE), resulting in a far greater thermodynamic driving force for electron exchange reactions. As ZVI, ZVAl has been studied for the reductive degradation of chlorinated organics through Al corrosion (Lien and Zhang 2002; Lien 2005; Chen et al. 2008) and reductive precipitation of some metals (Fu et al. 2015; Han et al. 2016). However, these processes where ZVAl acts as an electron donor are generally time-consuming and rather incomplete in terms of mineralization (Lien et al. 2010). Like the more well-known and studied ZVI, ZVAl may activate molecular oxygen in air to produce ROS, including HP, superoxide radical ($O_2^{\cdot-}$) and $HO^{\cdot}$. The ZVAl/H^+/air-O_2 system involves two major processes; the (i) corrosive dissolution of Al^{3+} and simultaneous reduction of O_2 to hydroperoxyl radical ($HO_2^{\cdot}$) leading to the formation of HP; (ii) the generation of $HO^{\cdot}$ by an electron transfer mechanism from ZVAl to molecular oxygen producing HP;

$$Al^0 \rightarrow Al^{3+} + 3e^- \tag{11}$$

$$O_2 + H^+ + e^- \rightarrow HO_2^{\cdot} \tag{12}$$

$$2HO_2^{\cdot} \rightarrow H_2O_2 + O_2 \tag{13}$$

$$Al^0 + 3H_2O_2 \rightarrow Al^{3+} + 3HO^{\cdot} + 3OH^- \tag{14}$$

The degradation of micropollutants by the ZVAl/H^+/air-O_2 treatment system is a relatively slow and inefficient process (Joo et al. 2005; Zhao et al. 2010; Temiz

giovanni.libralato@unina.it

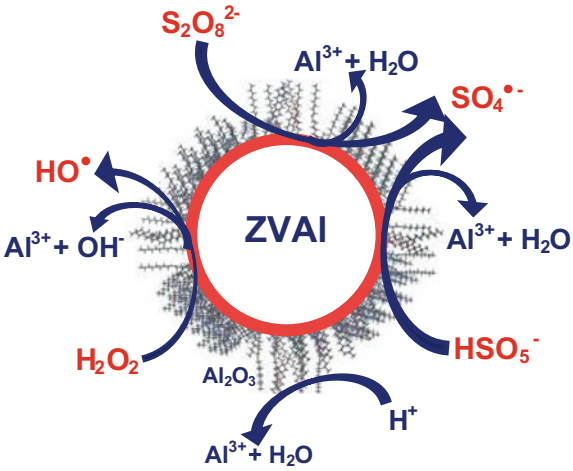

Fig. 1 Schematic of the reactions involved in the removal of aqueous micropollutants with ZVAl nanoparticles in the presence of the oxidants HP, PS and/or PMS

et al. 2016). Depending on the surface properties of ZVAl as well as the pH of the reaction solution, an induction period (lag phase) is typically observed for the removal of pollutants by the ZVAl/H^+/air-O_2 treatment system. Hence, external addition of oxidants such as HP, PS or peroxymonosulfate (PMS) is expected to enhance pollutant removal rates and efficiencies (Cai et al. 2015; Cheng et al. 2015; Arslan-Alaton et al., 2017a, b). On the other hand, activation of the above mentioned oxidants with ZVAl has rarely been investigated. The mechanism of enhanced $HO^{\cdot}$ and $SO_4^{\cdot -}$ formation in the presence of the HP, PS and PMS starts with the direct electron transfer from the Al^0 surface to the oxidants HP, PS and PMS under acidic pH values (pH < 4);

The ZVAl/HP treatment system;

$$Al^0 + 3H_2O_2 \rightarrow Al^{3+} + 3HO^{\cdot} + 3OH^- \quad (15)$$

The ZVAl/PS treatment system;

$$2Al^0 + S_2O_8{}^{2-} + 6H^+ + 1.5O_2 \rightarrow 2Al^{3+} + 2SO_4{}^{\cdot -} + 3H_2O \quad (16)$$

The ZVAl/PMS treatment system;

$$Al^0 + 3HSO_5^- + 3H^+ \rightarrow Al^{3+} + 3SO_4{}^{\cdot -} + 3H_2O \quad (17)$$

The formation of $HO^{\cdot}$ and $SO_4^{\cdot -}$ during ZVAl-mediated heterogeneous treatment in the presence of externally added oxidants is illustrated in Fig. 1.

giovanni.libralato@unina.it

3.2 Factors Affecting Treatment Performance

Studies conducted with ZVAl-mediated oxidation processes revealed that the $HO^{\cdot}$ and $SO_4^{\cdot-}$ production rate and yield is a strong function of the (i) initial reaction pH; (ii) initial ZVAl concentration and (iii) presence of an activator or inhibitor. Many studies indicated that particularly the initial reaction pH plays a pivotal role in the degradation of organic pollutants and heavy metal removals using the ZVAl/oxidant treatment system. The formation of free radicals through an electron transfer reaction from ZVAl to HP, PS and PMS (Eqs. 15–17) are highly favored under acidic conditions (pH < 4). On the other hand, it has also been shown that the presence of an oxide layer on the ZVAl surface is a major factor decreasing the reactivity and service life of ZVAl (Lin et al. 2009; Wu et al. 2014; Han et al. 2016). Hence, ZVAl-induced redox reactions can only be initiated after dissolution of this outer oxide layer. However, this layer cannot be easily removed at neutral to near-neutral pH values thus limiting the application of ZVAl treatment systems to acidic pH conditions (Bokare and Choi 2009). Some pretreatment methods were used to remove the oxide layer from ZVAl. For instance, acid washing was found to be an effective means for surface cleaning (Lai and Lo 2008; Bokare and Choi 2009; Zhang et al. 2012; Cheng et al. 2015; Han et al. 2016).

As can be followed from the reaction Eqs. (12), (14)–(17), ZVAl corrosion is accompanied by an increase in the solution pH leading to $Al(OH)_3$ formation (Cheng et al. 2015; Lien et al. 2010; Bokare and Choi 2009). The accumulation of Al(III) oxides and hydroxides on the ZVAl surface may hinder/retard $HO^{\cdot}$ and/or $SO_4^{\cdot-}$ generation, restraining the organic matter removal due to "surface passivation" (Bokare and Choi 2009). However, it has been evidenced that as long as the solution pH remains below 4 during the reaction, Al dissolution and hence oxidation reactions will continue (Bokare and Choi 2009).

A series of in-depth investigations regarding the effect of initial ZVAl concentration revealed that the degradation rate of contaminants increased with the increase of the ZVAl concentration because more reactive sites were available for electron transfer from the ZVAl surface to the in situ formed HP or externally added oxidants (Bokare and Choi 2009; Cai et al. 2015; Cheng et al. 2015; Arslan-Alaton et al., 2017a, b). However, a higher ZVAl concentration might not lead to a further improvement in treatment efficiencies mainly because both dissolution of the oxide layer and corrosion of Al will lead to H^+ depletion and hence inhibit the treatment process.

As mentioned earlier, the addition of the oxidants HP, PS or PMS might enhance the charge transfer and free radical formation reactions on the ZVAl surface (Cheng et al. 2015; Wang et al. 2014c; Wu et al. 2013c; Temiz et al. 2016; Arslan-Alaton et al., 2017a, b). In theory, the increase in oxidant concentration can be beneficial to the treatment system up to certain level, where further increase (the use of excessive oxidant concentrations) will have negative influence by lowering the free radical ($HO^{\cdot}$ and $SO_4^{\cdot-}$) concentrations available throughout unwanted side reactions (Buxton et al. 1988; Fernandez et al. 2004; Criquet and Vel Leitner 2009).

giovanni.libralato@unina.it

The respective scavenging reactions for HP, PS and PMS are given in Eqs. (18), (10) and (19), respectively (Buxton et al. 1988; Fernandez et al. 2004; Criquet and Vel Leitner 2009);

$$H_2O_2 + HO^{\cdot} \rightarrow HO_2^{\cdot} + H_2O \quad k = 1.2\text{–}4.5 \times 10^7\ M^{-1}s^{-1} \tag{18}$$

$$HSO_5^- + HO^{\cdot} \text{ or } SO_4^{\cdot -} \rightarrow SO_5^{\cdot -} + OH^- \text{ or } SO_4^{2-} + H^+ \quad k = 1.0 \times 10^5\ M^{-1}s^{-1} \tag{19}$$

External Fe^{2+}, Fe^{3+} or ZVI addition might also improve the efficiency of the ZVAl-mediated treatment systems. The dominant pathway of free radical formation in the ZVAl/H^+/air-O_2 system fortified with Fe^{2+}, Fe^{3+} or ZVI is largely replaced by a more efficient way of initiating Fenton and/or Fenton-like reactions that is thought to be more effective than ZVAl-mediated treatment. HA, a main component of dissolved organic matter found in natural water and wastewater, is another factor that may influence the oxidative efficiency of ZVAl-mediated treatment systems. HA exhibits dual roles in Fenton and Fenton-like reactions (Kang and Choi 2009; Lindsey and Tarr 2000); namely as an inhibiting and enhancing agent. HA affects charge transfer reactions of oxidants to form $HO^{\cdot}$ and/or $SO_4^{\cdot -}$. Additionally, HA may compete for reactive sites and ROS (free radicals) during treatment of pollutants by ZVAl (Liu et al. 2011; Wu et al. 2010).

3.3 *ZVAl Applications for the Treatment of Industrial Micropollutants*

Recent studies have demonstrated that ZVAl is an effective reagent for the remediation of groundwater and wastewater contaminated by various micropollutants including Cr(VI), heavy metals, arsenic, oxygenates, phenol and phenolic compounds, perchlorate, endocrine disrupting pollutants, pharmaceuticals and textile dyes. There is a growing interest the ZVAl/oxidant treatment system as is reflected in the increasing number of publications. Although descriptive experimental features of the articles reviewed in this section have already been specified below, a comparative list has also been provided in Table 2.

3.3.1 Hexavalent Chromium and Other Metals

In a recent study, Fe/Al bimetallic particles were used for the removal of Cr(VI) from wastewater (Fu et al. 2015). In this study Fe/Al bimetals with different Fe contents were synthesized and characterized before and after reaction with Cr(VI)

giovanni.libralato@unina.it

Table 2 Application of ZVAl for the treatment of micropollutants

Micropollutant	Process type	Reaction conditions	Main results	Reference
2,4-dichlorophenol (2,4-DCP)	ZVAl/H^+/air-O_2	2,4-DCP = 20 mg/L; ZVAl = 0–30 g/L; pH = 2–4; DO = 8.25 mg/L; V = 12 mL; 35 rpm; t = 10 h; T = 25 °C; HA = 5–50 mg/L	• More than 90% of 2,4-DCP was removed in 10 h at pH 2.5 containing 10 g/L ZVAl and 8.25 mg/L DO • Five primary intermediates were identified (4-chlorocatechol, 2-chlorohydroquinone, 2-chloro-1,4-benzoquinone, 4,6-dichlororesorcinol and 3,5-dichlorocatechol) • The presence of HA, higher DO levels and lower pH facilitated ROS formation and 2,4-DCP degradation	Lin et al. (2013)
4-chlorophenol (4-CP)	ZVAl/H^+/air-O_2	4-CP = 0.1 mM; ZVAl = 1–5 g/L; pH = 2–13; V = 50 mL; t = 600 min	• Near-complete (>95%) 4-CP degradation was achieved in 10 h • With increasing ZVAl concentration to 5 g/L, the time required for complete degradation was reduced to 5 h • At pH < 5, the oxidation of 4-CP decreased with increasing pH	Bokare and Choi (2009)
Acetaminophen (ACTM)	ZVAl/H^+/air-O_2	ACTM = 2 mg/L; ZVAl = 0–2 g/L; pH = 1.5, 2.5 and 3.5; V = 100 mL; 200 rpm; t = 16 h; T = 25 °C; Fe^{2+}= 0, 10 and 100 µM; Fe^{3+}= 0, 10 and 100 µM; Fe^0 = 0–0.2 g/L	• In acidic solutions (pH < 3.5), ZVAl displayed an excellent capacity to remove ACTM • More than 99% of ACTM was eliminated in 16 h at pH 1.5 with 2 g/L ZVAl and 2 mg/L ACTM at 25 ± 1 °C • Higher T and lower pH facilitated ACTM removal • The addition of ZVI, Fe^{2+} and Fe^{3+} accelerated the reaction • The primary intermediates were identified as hydroquinone, formate, acetate and nitrate	Zhang et al. (2012)

(continued)

giovanni.libralato@unina.it

Table 2 (continued)

Micropollutant	Process type	Reaction conditions	Main results	Reference
Acid orange 7 (AO7)	US ZVAl/air-O_2 US-ZVAl/air-O_2	AO7 = 5–40 mg/L; ZVAl = 0–6 g/L; pH = 2.5–7.5; US = 100–500 W; V = 50 mL; t = 30 min; T = 20–25 °C	• The degradation of AO7 by the ZVAl/air system was enhanced with US • The decolorization rate increased with increasing power density and ZVAl concentrations, but decreased with increasing pH and AO7 concentration •>96% of AO7 removal was achieved in 30 min under optimum conditions (AO7 = 20 mg/L, ZVAl = 2 g/L, pH = 2.5, US = 20 kHz/300 W)	Wang et al. (2014c)
Actual oilfield produced water	Fe/Cu/C and Fe/Al/C inner micro-electrolysis systems	COD = 435 mg/L; Fe/Al/C = 20 g/L; pH = 2–9; V = 500 mL; t = 180 min; T = 25 °C	• The optimum conditions were Fe = 13.3 g/L, AC = 6.7 g/L, Cu = 2.0 g/L or Al = 1.0 g/L, t = 120 min, pH = 4.0 • COD removal efficiencies were 39.3, 49.7 and 52.6% for Fe/C, Fe/Cu/C and Fe/Al/C treatment, respectively • BOD_5 to COD were raised from 0.18 to 0.35; speaking for an enhanced biodegradability	Zhang (2015)
Arsenic	ZVAl/O_2 ZVAl/O_2/POM ZVAl/O_2/Fe(II)	As(III) = 85 μM; ZVAl = 4 g/L; Fe^{2+}= 0.1 mM; POM ($HNa_2PW_{12}O_{40}$) = 0.1 mM; pH = 1–2; V = 250 mL; t = 0–400 min	• As(III) could not be oxidized by ZVAl in 150 min at pH 1 due to the presence of an oxide layer on ZVAl • 85 mM As(III) could be completely oxidized upon Fe(II) or POM addition due to initiation of the Fenton reaction or enhancement of HP production on ZVAl	Wu et al. (2013c)

(continued)

giovanni.libralato@unina.it

Table 2 (continued)

Micropollutant	Process type	Reaction conditions	Main results	Reference
Bisphenol A (BPA)	ZVAl/air-O_2	BPA = 2 mg/L; ZVAl = 0–4 g/L; pH = 1–3.5; V = 100 mL; 130 rpm; t = 12 h; T = 25 ± 1 °C; HA = 1–50 mg/L; Fe^{2+}= 1, 10 μM	• More than 75% of BPA was removed in 12 h at pH 1.5 with 4.0 g/L ZVAl and 2.0 mg/L BPA at 25 ± 1 °C • BPA removal was enhanced at higher ZVAl concentrations • Higher temperature and lower initial pH enhanced BPA removal • The addition of Fe^{2+} accelerated BPA removal • The primary products were identified as mono-hydroxylated BPA, hydroquinone, 2-(4-hydroxyphenyl) propane and 4-isopropenylphenol	Liu et al. (2011)
Cr(IV)	Fe/Al bimetallic particles	Cr(IV) = 20 mg/L; Fe/Al = 6 g/L; pH = 3–11; t = 90 min	• Bimetal with 0.75 g Fe/g Al exhibited high removal efficiency for Cr(VI) • Fe/Al bimetal could completely remove Cr(VI) from wastewater in 20 min • No Fe ions were released when bulk pH values were between 3.0 and 11.0 • The released Al^{3+} ions at acidic and neutral conditions were <0.2 mg/L • The bimetal could be used 4 times without losing activity at pH 3.0	Fu et al. (2015)

(continued)

giovanni.libralato@unina.it

giovanni.libralato@unina.it

Table 2 (continued)

Micropollutant	Process type	Reaction conditions	Main results	Reference
Heavy metal wastewater containing Cr(VI), Cd^{2+}, Ni^{2+}, Cu^{2+}, and Zn^{2+}	The mixture of acid-washed ZVI and ZVAl as reactive medium in PRBs.	Cr(VI), Cd^{2+}, Ni^{2+}, Cu^{2+}, Zn^{2+}= 20.0 mg/L; Acid washed gZVI/gZVAl mixture = 40/80, 60/60, 80/40; pH = 3.0, 5.4 and 7.0; flow rate = 1.0 mL/min; t = 0–700 h	• Acid-washed ZVI and ZVAl were more effective for heavy metal removal than ZVI and ZVAl • Cr(VI), Cd^{2+}, Ni^{2+}, Cu^{2+}, and Zn^{2+} were removed at 99.5% in 300 h using acid-washed 80 g/40 g ZVI/ZVAl in PRBs • The performance of PRBs improved with increasing pH • Cr(VI) and Cu^{2+} were more easily removed than Zn^{2+}, Ni^{2+} and Cd^{2+}	Han et al. (2016)
Iopamidol (IOPA)	ZVAl/HP ZVAl/PS	IOPA = 2 mg/L; ZVA = 1 g/L; PS and HP = 0.25 and 0.50 mM; pH = 3; V = 500 mL; 150 rpm; t = 120 min, T = 25 °C	• ZVA/PS (0.5 mM) treatment was more effective than ZVA/HP (0.25 mM) resulting in 95% IOPA removal after 120 min • After 120 min treatment IOPA removals decreased from 95% (PS/ZVA) and 41% (HP/ZVA) to 29% (PS/ZVA) and 13% (HP/ZVA) in distilled (pure) and surface water, respectively • Acute toxicity results exhibited a fluctuating trend depending on the sensitivity of the test organism (*V. fischeri* and *P. subcapitata*) and water matrix • A genotoxic activity test indicated that the original and treated IOPA solutions were not geno- but cytotoxic	Arslan-Alaton et al. (2017a)

(continued)

Table 2 (continued)

Micropollutant	Process type	Reaction conditions	Main results	Reference
Methyl tert-butyl ether (MTBE)	Bifunctional Al/O_2	MTBE = 1.4–14.2 mg/L; Bifunctional Al = 1 g/L; pH = 3.9–4.6; V = 150 mL; 50 rpm; t = 25 h; T = 22 °C	• ≈90% of MTBE was degraded by bifunctional Al in 24 h • Reaction products were acetone, methyl acetate, tert-butyl alcohol, and tert-butyl formate • XPS analysis indicated the formation of sulfate on the surface of bifunctional ZVAl • MTBE degradation rates increased by a factor of 2 as the surface sulfate concentrations increased from 233 to 641 μmol/m^2	Lien and Wilkin (2002)
Methyl tert-butyl ether (MTBE) and tert-amyl methyl ether (TAME)	Bifunctional Al/O_2	Bifunctional Al = 20 g/L; pH = 3.9–4.6; V = 150 mL; 50 rpm; t = 0–100 h; T = 22 °C	• Al created favorable reducing conditions while sulfur-containing species generated by the sulfation of ZVAl at the metal surface were considered as active sites • MTBE and TAME underwent parallel reactions where oxidation occurred on both sides of the ether linkage • The oxidation of MTBE produced primarily tert-butyl alcohol, tert-butyl formate, methyl acetate, and acetone while tert-amyl alcohol, tert-amyl formate, methyl acetate, methyl ethyl ketone and acetone were the reaction intermediates of TAME	Lien and Zhang (2002)
Orange G (OG)	ZVAl/US	OG = 10–80 mg/L; ZVAl = 0.5–2.5 g/L; HP = 0–100 mM; pH = 2–4; US = 0–900 W; V = 250 mL; t = 180 min; T = 25 °C	• The decolorization rate decreased with increasing pH values (2.0–4.0) and initial OG concentrations (10–80 mg/L) and increased with increasing US power (500–900 W) • In the range of 0.5–2.5 g/L, the optimum ZVAl was 2 g/L	Cai et al. (2015)

(continued)

giovanni.libralato@unina.it

Table 2 (continued)

Micropollutant	Process type	Reaction conditions	Main results	Reference
			• The decolorization rate was enhanced by 10–100 mM HP addition • Degradation products were aniline and 1-amino-2-naphthol-6,8-disulfonate	
Perchlorate	Acid-washed ZVAl/H^+/air-O_2	Perchlorate = 10 mg/L; ZVAl = 5–50 g/L; pH = 2–10; V = 100 mL; 180 rpm; T = 24 ± 1 °C	• 90–95% perchlorate was removed in 24 h with 35 g/L ZVAl at 4.5 ± 0.2 • Adsorption was involved in perchlorate removal	Lien et al. (2010)
Phenol	Acid-washed ZVAl/H^+/air-O_2	Phenol = 20 mg/L; ZVAl = 0–6 g/L; HP = 0–8 mM; pH = 1.5–4.5; V = 500 mL; 120 rpm; t = 3 h; T = 25 °C, HA = 0–50 mg/L	• Acid-washed ZVAl exhibited a greater capacity to remove phenol than ZVAl • With 4.0 mM HP phenol concentrations decreased from 20 to 0.3 mg/L by 6.0 g/L acid-washed ZVAl in 3 h at pH 2.7 • Addition of HP into the acid-washed ZVAl/H^+/air-O_2 system facilitated the reaction • Addition of HA inhibited the reaction	Cheng et al. (2015)
Triton™ X-45 (TX-45)	ZVAl/HP ZVAl/PS	TX-45 = 2 mg/L; ZVA = 1 g/L; PS and HP = 0.25 and 0.50 mM; pH = 3; V = 500 mL; 150 rpm; t = 120 min, T = 25 °C	• Limited TX-45 removals were obtained in the absence of nZVAl (HP, PS and PMS treatments) and oxidants (nZVAl/H^+/air-O_2 treatment) • Activation of HP, PS and PMS with nZVAl enhanced TX-45 degradation • The combined treatment system was highly affected by the characteristics of the water and wastewater • The inhibitory effect of TX-45 depended on the water/wastewater matrix and the sensitivity of the test organism • Original and nZVAl/PS-treated TX-45 did not exhibit cytotoxic or genotoxic effects	Arslan-Alaton et al. (2017b)

giovanni.libralato@unina.it

in order to elucidate the structure of Fe/Al and the reaction mechanism. Characterization of Fe/Al bimetallic particles showed that the core of the bimetal was Al, and the fine Fe particles were planted on the surface of Al. The introduction of fine Fe significantly increased the surface area and inhibited the corrosion products accumulating on the surface active sites of Al. So Fe/Al bimetallic particles with higher surface area have more active reaction sites for Cr(VI). The experimental findings demonstrated that under acidic and neutral conditions, the Fe/Al bimetal completely removed Cr(VI) from wastewater in 20 min. Even at pH 11.0, the achieved Cr(VI) removal efficiency was 93.5%. The Cr(VI) removal mechanism was described by considering three aspects. Firstly, numerous galvanic cells could form on the Fe/Al bimetallic particles. Through oxidation, the electrons from ZVAl were transferred to the solution through ZVI. Cr(VI) ions accepted electrons and get reduced to Cr(III). Therefore, planting Fe on the surface of Al improved the performance of Al, accelerated the electron transfer, and thus facilitated Cr(VI) removal. From this point, ZVI in the bimetal plays a key role in transferring electrons and thus can be regarded as a catalyst. Secondly, ZVAl can directly reduce Cr(VI) (as shown in Eq. 20). Thirdly, ZVI can also reduce Cr(VI) (see Eq. 21). XPS analysis indicated the removed Cr(VI) was immobilized via the formation of Cr(III) hydroxide and Cr(III)–Fe(III) hydroxide/oxyhydroxide on the surface of Fe/Al bimetal.

$$2Al^0 + 2HCrO_4^- + 14H^+ \rightarrow 2Al^{3+} + 2Cr^{3+} + 8H_2O \quad (20)$$

$$2Fe^0 + 2HCrO_4^- + 14H^+ \rightarrow 2Fe^{3+} + 2Cr^{3+} + 8H_2O \quad (21)$$

Han et al. (2016) studied the mixture of acid-washed ZVI and ZVAl as reactive media in PRBs to treat heavy metal wastewater containing Cr(VI), Cd^{2+}, Ni^{2+}, Cu^{2+} and Zn^{2+}. The performance of the column filled with an acid-washed ZVI + ZVAl mixture performed better than the column filled with single ZVI or ZVAl. At an initial of pH 5.4 and a flow rate of 1.0 mL/min, 99.5% Cr(VI), Cd^{2+}, Ni^{2+}, Cu^{2+}, and Zn^{2+} removal occurred in wastewater containing 20 mg/L of each heavy metal. Cr(VI) and Cu^{2+} were found to be easy to remove than Zn^{2+}, Ni^{2+} and Cd^{2+}, because the redox potential of chromium (Cr^{6+}/Cr^{3+}) and copper (Cu^{2+}/Cu) was +1.36 V and +0.34 V, respectively and hence greater than that of zinc (−0.76 V; Zn^{2+}/Zn), cadmium (−0.40 V; Cd^{2+}/Cd) and nickel (−0.24 V; Ni^{2+}/Ni). Consequently, all of the five heavy metals could be reduced with ZVAl (Eqs. 20 and 22). According to the redox potentials, Cr(VI) and Cu^{2+} were also easily reduced by ZVI (Eqs. 21 and 23), but Ni^{2+} and Cd^{2+} reduction by ZVI is hard and Zn^{2+} cannot be reduced by ZVI. The below given equations show the corresponding reactions with the heavy metals with M representing Ni, Cu, Zn and Cd;

$$2Al^0 + 3M^{2+} \rightarrow 2Al^{3+} + 3M \quad (22)$$

giovanni.libralato@unina.it

$$Fe^0 + Cu^{2+} \rightarrow Fe^{2+} + Cu \quad (23)$$

It was found that the above given heavy metal ions were removed through four mechanisms; firstly, the reduction of heavy metals ions by ZVI/ZVAl where ZVAl could reduce all of the five heavy metal ions, while ZVI could only reduce Cr(VI) and Cu^{2+}. Secondly, these metal ions could be removed by adsorption onto ZVI/ZVAl. Thirdly, the heavy metal ions were precipitated in the form of their hydroxides. The Fe–Al couple was effective in the reductive removal of heavy metal ions, where Al acted as the electron donor and Fe could transfer electrons to heavy metal ions.

3.3.2 Arsenic

Wu et al. (2013c) explored the potential applications of ZVAl or Al wastes such as Al beverage cans for the oxidation of As(III) to As(V) in an acidic solution under aerobic conditions. Results of the ZVAl/O_2 treatment experiments showed that As (III) could not be oxidized by ZVAl within 150 min at pH 1. Upon dissolutions of a small portion of the oxide layers on the surfaces of ZVAl in an acidic solution, DO was capable of interacting with ZVAl sites, leading to HP production. In other words, the oxide layer on the ZVAl did not inhibit HP production, but became a complete obstacle to As(III) oxidation. Under the same experimental conditions, As (III) was completely oxidized in 10 min after being added into acid-treated ZVAl. This observation demonstrated that in an aerobic environment, treatment systems with clean (unpassivated) ZVAl surfaces exhibited a higher oxidative capability. In the same study, As(III) oxidation on ZVAl catalyzed by polyoxometalate (POM) or Fe(II) in the presence of DO was also investigated. 85 μM As(III) could be completely oxidized with the addition of Fe(II) or POM with the formed Fenton reagents or enhancement of HP production, respectively, both on the ZVAl surfaces. Because Fe(II) and POM were more stable at low pH and rapidly scavenged the produced HP on the aerated ZVAl surface, $HO^{\cdot}$ production was more efficient. Under these conditions As(III) was rapidly oxidized with ZVAl/O_2 in the presence of Fe(III) and POM. With the addition of Fe(II), a Fenton reaction was created to accelerate As(III) oxidation; nonetheless, enhancement of the oxide layer removal and HP production facilitated As(III) oxidation in the presence of POM. Following the oxidative conversion of As(III) to As(V) in the ZVAl/Fe/O_2 system, As(V) was removed by the newly formed hydrous Al/Fe precipitates by increasing the solution pH to 6. Nonetheless, the As(V) removal was incomplete in the ZVAl/POM/O_2 system because the hydrolyzed products of POM, inhibited As(V) removal due to the competitive adsorption of the oxyanion on Al precipitates. In order to evaluate the potential applications of disposed Al metals and alloys for the conversion of As (III) to As(V) and its ultimate removal, an Al-based beverage can was selected as the model material. With the addition of 0.1 mM Fe(II), 85 mM As(III) was oxidized to As(V) within 20 min in the presence of the Al beverage can. However,

giovanni.libralato@unina.it

it took approximately 130 min to convert the same amount of As(III) to As(V) in the absence of Fe(II).

3.3.3 Perchlorate

Lien et al. (2010) examined perchlorate removal using either acid-washed ZVAl or Al hydroxide in batch reactors under ambient temperature and pressure. The authors examined the characteristics of aluminum and its reactions in ZVAl/air systems to understand the influence of Al corrosion on perchlorate removal. Approximately 90–95% of perchlorate was removed within 24 h in the presence of 35 g/L ZVAl at acidic pH (4.5 ± 0.2). Although Al is a strong reductant, this study indicated no explicit evidence to support perchlorate reduction while it was found that an adsorption process is involved in the perchlorate removal. Al hydroxide, a product of the ZVAl corrosion, has been confirmed as the effective composition for the perchlorate adsorption. The adsorption mechanism was attributed to the ion-pair formation at the Al hydroxide surface.

3.3.4 Pharmaceuticals

Recently, the removal of aqueous acetaminophen [N-(4-hydroxyphenyl) ethanamide, ACTM] using the ZVAl/H^+/air-O_2 system was investigated (Zhang et al. 2012). ACTM, the active ingredient of various over-the-counter analgesic and antipyretic drugs such as Tylenol®, is commonly available alone or in combination with other medications in households. Because of the widespread use and the low removal efficiency in the traditional wastewater treatment, ACTM has become one of the most frequently detected pharmaceuticals in the aquatic environment, with concentrations ranging from several ng/L to dozens of μg/L (Lin and Tsai 2009; Santos et al. 2009; Rosal et al. 2010; Sim et al. 2010). In this study, the reaction efficacy, influencing factors and reaction mechanism was explored. The enhancement in ACTM removal by introducing different iron species (Fe^0, Fe^{2+} and Fe^{3+}) into the ZVAl/H^+/air-O_2 system was also examined. More than 99% of 2 mg/L aqueous ACTM was removed in 16 h at pH 1.5 and 25 ± 1 °C by the ZVAl/H^+/air-O_2 treatment system and higher ZVAl concentrations enhanced the removal. Higher temperatures and acidic conditions facilitated ACTM removal that was above 99% under optimized reaction conditions. In the pH range of 1.5–3.5, ACTM removal decreased with increasing initial pH. The addition of different iron species Fe^0, Fe^{2+} and Fe^{3+} into ZVAl/H +/air-O_2 system dramatically accelerated the reaction likely due to the enhancing transformation of HP to $HO^{\cdot}$ via Fenton's reaction. The primary intermediate hydroquinone and the anions formate, acetate

giovanni.libralato@unina.it

and nitrate were identified as the major intermediates of ACTM oxidation with ZVAl/H^+/air-O_2.

3.3.5 Oxygenates

Oxygenates such as methyl tert-butyl ether (MTBE) and tert-amyl methyl ether (TAME) have been used as gasoline additives to reduce the level of carbon monoxide and VOCs from the emissions of motor vehicles. Due to leaking underground storage tanks and pipelines, the contamination of groundwater with oxygenates has become a growing concern (Lien and Wilkin 2002). Groundwater contaminated with MTBE threatens public health because MTBE has been classified as a potential human carcinogen. In a study conducted by Lien and Zhang (2002) a novel bifunctional Al capable of utilizing dioxygen for the oxidation of oxygenates was reported. In this study, MTBE and TAME were used to evaluate the effectiveness of bifunctional Al for the degradation of gasoline oxygenates in the presence of dioxygen under the ambient temperature and pressure. Detailed product studies on the use of bifunctional Al in reactions with MTBE, TAME and their reaction intermediates were also conducted to investigate possible reaction pathways. The capability of utilizing dioxygen by bifunctional Al suggested a catalytic characteristic of the material. Results indicated that Al serves as a reductant while the sulfur-containing species generated by the sulfation of Al on the metal surface were considered as active sites. The transformation of MTBE and TAME both exhibited similar product patterns. MTBE and TAME underwent similar parallel reaction pathways where oxidation occurred on both sides of ether linkage. The oxidation of MTBE produced primarily tert-butyl alcohol, tert-butyl formate, methyl acetate, and acetone while tert-amyl alcohol, tert-amyl formate, methyl acetate, methyl ethyl ketone and acetone as degradation products.

In another study, MTBE was removed by using bifunctional Al to activate molecular O_2 through a reductive process (Lien and Wilkin 2002). The active species on the bifunctional Al surface were determined and the rate and extent of MTBE oxidation were studied. The initial rate of tert-butyl MTBE degradation exhibited pseudo-first-order behavior and the half-life of reaction was less than 6 h. Characterization of bifunctional Al indicated the formation of sulfate on its surface. The rate of MTBE degradation was found to be a function of the concentration of the surface sulfate. MTBE degradation rates increased by a factor of two as surface sulfate concentrations increased from 233 to 641 μmol/m^2. Primary degradation products were also determined in this study as formate, acetone and methyl acetate.

3.3.6 Chlorinated Organics

Bokare and Choi (2009) examined 4-chlorophenol (4-CP) as the model pollutant to explore the potential of ZVAl/H^+/air-O_2 treatment. Nearly complete (>95%) 4-CP degradation was achieved in 10 h under air-O_2 equilibrated conditions

giovanni.libralato@unina.it

(ZVAl = 1 g/L; 4-CP = 100 μM; initial pH = 2.5). With increasing the ZVAl concentration from 1 to 5 g/L the time required for complete degradation was reduced to 5 h. Under acidic pH conditions (pH < 5), the oxidation of 4-CP decreased with increasing initial pH and complete inhibition was observed at initial pH $\geq$ 4. Because the surface oxide layer was found to be extremely stable in the pH range of 4.0–9.0, complete passivation of the ZVAl surface hindered the generation of ROS and suppressed the oxidation of 4-CP. Experimental results indicated that the ZVAl-induced redox process is initiated only after dissolution of the oxide layer. The authors also compared the ZVAl/O_2 and ZVI/O_2 treatment systems for the degradation of 4-CP. Although ZVI/O_2 treatment did not exhibit an induction period, the reaction completely stopped in 3 h and achieved only partial 4-CP removal. A significant induction period (lag phase) was observed for this treatment method; however full degradation of 4-CP could be achieved. The difference in activities was explained by the stability of the reaction pH and the speciation of Fe^{3+}, Al^{3+} and their corresponding hydroxides. In the same work, the degradation of aqueous dichloroacetate (DCA), phenol and nitrobenzene was also investigated to further extend the advantage offered by ZVAl over ZVI (ZVAl = 1 g/L, substrate = 100 μM, initial pH = 2.5). The ZVI/O_2 treatment system exhibited negligible activity for DCA degradation (Lee et al. 2007) while ≈85% removal could be achieved in 10 h using ZVAl instead of ZVI. Successful degradation of phenol and nitrobenzene was obtained with ZVAl/O_2 treatment.

The oxidative removal of DCP with the Al/O_2/acid system focused on factors affecting treatment performance such as DO and HA as well as elucidation of the dominant reaction pathway (Lin et al. 2013). Furthermore, reaction intermediates were identified and oxidation pathways were proposed. More than 90% of DCP was removed in 10 h at pH 2.5 in the presence of 10 g/L Al and 8.25 mg/L O_2. The removal of DCP was demonstrated to be acid- and oxygen-driven and accompanied by the release of chloride ions. While the reduction of O_2 to HP by ZVAl was obtained only at pH < 4.0, the subsequent Al-mediated transformation of HP to $HO^{\cdot}$ was achieved at milder pHs (pH < 5.0). Higher concentrations of O_2 in the reaction solutions, lowering the pH and introducing HA facilitated DCP removal. HA displayed enhancing effects on the transformation of HP to $HO^{\cdot}$. Furthermore, 4-chlorocatechol, 2-chlorohydroquinone, 2-chloro-1,4-benzoquinone, 4,6-dichlororesorcinol and 3,5-dichlorocatechol were identified as major oxidation intermediates.

3.3.7 Textile (Azo) Dyes

Degradation of the textile azo dye AO7 by ZVAl combined with US was investigated by Wang et al. (2014c). Preliminary studies (ZVAl = 2 g/L; US power = 300 W; initial pH = 2.5; t = 30 min) were conducted with sole US, sole ZVAl/air and ZVAl/US/air treatment systems. No degradation was observed for AO7 by US only, although $HO^{\cdot}$ could be formed during H_2O sonolysis. The same result was obtained with ZVAl only, although $HO^{\cdot}$ was generated in the reaction

giovanni.libralato@unina.it

solution. The Al oxide and Al hydroxide layers formed on ZVAl inhibited the reaction and the concentration of $HO^{\cdot}$ remained low compared with that of the combined ZVAl/US/air treatment process. The process variables considered for the treatment combinations were initial AO7 and ZVAl concentrations, US power as well as initial reaction (solution) pH. The decolorization rate increased with increase of power density and concentration of ZVAl but decreased with increasing initial pH and AO7 concentration. More than 96% AO7 removal was achieved in 30 min under optimized reaction conditions (AO7 = 20 mg/L, ZVAl = 2 g/L, pH = 2.5, US = 300 W/20 kHz).

Cai et al. (2015) studied the decolorization of the textile azo dye Orange G (OG; Acid Orange 10, C.I. 16230) in aqueous solution by ZVAl/US. The effects of various operating parameters (initial pH, initial dye, HP and ZVAl concentration as well as US power) was investigated. The decolorization rate was enhanced when the aqueous OG was irradiated simultaneously with US and ZVAl/acid. The decolorization rate decreased with increasing initial pH (2–4) and OG concentration (10–80 mg/L) and was also enhanced with increasing US power (500–900 W). An optimum value was reached with 2.0 g/L ZVAl in the range of 0.5–2.5 g/L. The fast corrosion of ZVAl led to Al^{3+}, H_2, $Al(OH)_3$ and H^+ formation which affected the cavitation events as well as cavitation-induced $HO^{\cdot}$ and HP production. The decolorization rate enhanced significantly upon HP addition in the range of 10–100 mM. The decolorization of OG involved the cleavage of the azo bond as verified by qualifying the dye intermediates aniline and 1-amino-2-naphthol-6,8-disulfonate via LC-MS detection.

3.3.8 Phenol

Cheng et al. (2015) examined acid-washed ZVAl (AW-ZVAl) in the presence of HP to remove phenol. The specific surface area of AW-ZVAl was 1.5 times higher than without ZVAl pretreatment. The increase of the surface area was attributed to the removal of oxide layers from the surface of ZVAl and the dissolution of ZVAl under acidic pH conditions. Phenol removal increased with increasing AW-ZVAl concentration because more reactive sites were available for electron transfer from the ZVAl surface to HP. The optimum reaction pH was found to be 2.5–3.5. The effect of HP addition (0–8 mM) on phenol removals by AW-ZVAl was also examined Increasing the initially added HP concentration from 1 to 2 mM increased the phenol removal efficiency; however, further increase did not improve phenol degradation. The presence of HA inhibited phenol removal due to competition with phenol for $HO^{\cdot}$. After 3 h-treatment of aqueous phenol (20 mg/L) with 6 g/L ZVA in the presence of 4 mM HP at an initial pH of 2.7, only 30% TOC removal (mineralization) was observed, whereas phenol removal was complete for the same treatment period. In order to investigate the reuse possibility of AW-ZVAl, phenol removal was also examined with recycled AW-ZVAl. Results indicated that AW-ZVAl could be directly reused without any treatment and appeared to be consistently effective over a treatment of five cycles.

giovanni.libralato@unina.it

3.3.9 Bisphenol A (BPA)

Liu et al. (2011) investigated the oxidative degradation of BPA and its mechanism using ZVAl-acid system under air-O_2 equilibrated conditions. ZVAl concentration, initial pH, the presence of HA and addition of Fe^{2+} all influenced the degradation of BPA. The results indicated that BPA degradation rate increased with increasing ZVAl concentrations due to increased surface area and active sites of ZVAl. BPA removal obtained after 12 h was 75 and 25% at pH 1.5 and 2.5, respectively. When the initial reaction pH was increased to 3.5, almost no BPA removal was observed for the same treatment period. The addition of Fe^{2+} accelerated the formation of $HO^{\cdot}$ and the subsequent degradation of BPA. HA inhibited BPA removal which was explained by the competitive reaction of HA with BPA for $HO^{\cdot}$. BPA oxidation intermediates were detected as mono- hydroxylated BPA, hydroquinone, 2-(4-hydroxyphenyl)propane and 4-isopropenylphenol.

3.3.10 X-Ray Contrast Media (Iopamidol)

Among the pharmaceuticals being frequently encountered in the aquatic ecosystems, iodinated X-ray contrast media (ICM) are chemicals used to enhance the imaging of organs or blood vessels during diagnostic tests. Modern contrast agents are typically composed of water-soluble iodinated compounds and classified as ionic and non-ionic (Ternes and Hirsch 2000). Among the commercial, non-ionic ICM, iopamidol (IOPA) is the most frequently detected ICM with concentrations up to 2.7 μg/L in raw water, 15 μg/L in treated sewage, 2.4 μg/L in groundwater and 0.49 μg/L in rivers (Perez and Barcelo 2007; Kummerer et al. 1998; Kormos et al. 2010). Arslan-Alaton et al. (2017a) explored the activation of HP and PS with ZVAl (1 g/L) for the treatment of the IOPA at pH 3. IOPA (2.6 μM) degradation was followed in different water matrices (pure water, tap water, raw surface water and tertiary treated sewage effluent). Both oxidants could be activated with ZVAl resulting in a dramatic enhancement of IOPA degradation. The ZVAl/PS (0.5 mM) treatment was more effecting than ZVAl/HP (0.25 mM) oxidation resulting in 95% IOPA removal after 120 min. IOPA and dissolved organic carbon (DOC) abatements were inhibited when IOPA was treated in raw surface water water and wastewater. After 120 min treatment, IOPA removals decreased from 95% (PS/ZVAl) and 41% (HP/ZVAl) in pure to 29% (PS/ZVAl) and 13% (HP/ZVAl) in surface water, respectively. IOPA could not be removed with PS/ZVAl in treated sewage, although DOC removal was still substantial (28%). For the HP/ZVAl combination, 24% DOC accompanied with 20% IOPA removal was achieved after 120 min in the same wastewater sample. Changes in acute toxicity were followed during PS/ZVAl treatment of IOPA in pure and surface water. These results exhibited a fluctuating trend depending on the sensitivity of the test organism (*V. fischeri* and *P. subcapitata*) and water matrix. A genotoxic activity analysis was also conducted and the UmuChromo assay indicated that the original and treated IOPA solutions were not genotoxic but cytotoxic.

giovanni.libralato@unina.it

3.3.11 Octyl Phenol Polyethoxylate (Triton™ X-45)

Arslan-Alaton et al. (2017b) studied the treatment of aqueous Triton™ X-45 (TX-45) solutions by HP, PS and PMS as well as their combinations with nanoscale ZVAl-mediated heterogeneous treatment systems under acidic pH (=3). Treatment performances were evaluated in distilled water (DW), raw surface water (SW), tap water (TW) and domestic wastewater treatment plant effluent (WW). Limited TX-45 removals were obtained in the absence of nZVAl (HP, PS and PMS treatments) and oxidants (nZVAl/H^+/air-O_2 treatment). The activation of HP, PS and PMS with nZVAl enhanced TX-45 degradation dramatically due to the acceleration of $HO^{\cdot}$ and $SO_4^{\cdot-}$ generation. The nZVAl/oxidant system was affected by the characteristics of the water/wastewater samples. In DW, TX-45 removal efficiencies decreased in the following order; nZVAl/PMS ≈ nZVAl/PS > nZVAl/HP, whereas the order was nZVAl/PMS > nZVAl/HP > nZVAl/PS in SW and WW. Bioassays conducted with the original and nZVAl/PS treated TX-45 in DW and SW indicated that the inhibitory effect of TX-45 differed according to the water/wastewater matrix and depended on the sensitivity of the test organism. Both the original and nZVAl/PS- treated TX-45 did not exhibit any cytotoxic or genotoxic effects.

3.3.12 Oilfield Produced Water

Zhang (2015) investigated the treatment of real oilfield produced water with Fe/Cu/C and Fe/Al/C inner micro-electrolysis (ME) systems in order to evaluate the feasibility of this process for wastewater treatment. Effects of reaction time, pH, metal and AC concentrations as well as the Fe:C mass ratio on wastewater treatment efficiencies were studied. The optimum conditions were reaction time = 120 min, initial solution pH = 4.0, Fe = 13.3 g/L, AC = 6.7 g/L, Cu = 2.0 g/L, Al = 1.0 g/L. Under optimized conditions, the chemical oxygen demand (COD) removals were 39.3, 49.7 and 52.6% for the Fe/C, Fe/Cu/C and Fe/Al/C processes, respectively. Al had a higher stimulatory effect than Cu on the Fe/C ME treatment process. It could be concluded that the Al concentration should be minimized despite its promoting effect on Fe/C ME treatment, considering the ecotoxicity of Al ions. Furthermore, the biodegradability index expressed as the BOD_5/COD ratio was elevated from 0.18 to >0.35 (Fe:C mass ratio = 2:1; reaction time = 2 h; initial pH = 4.0; Fe/C = 20 g/L) speaking for promising results for a subsequent biological treatment process.

3.4 Final Remarks on ZVAl-Mediated Treatment Systems

The experimental work being reviewed in the above sections demonstrated the remarkable capacity of ZVAl-mediated treatment systems (ZVAl/H^+/air-O_2 and

giovanni.libralato@unina.it

ZVAl/oxidant combinations) in the degradation of aqueous micropollutants. However, the surface oxide/hydroxide layer of commercial ZVAl particles restricts the applications of ZVAl-mediated treatment systems to acidic conditions (pH < 4). The ZVAl-induced redox process is initiated only after dissolution of this oxide layer. Thus, an appropriate pretreatment step is required. Acid washing has been offered as an effective method to alleviate this problem. Considering the substantial toxicity of dissolved ZVAl to aquatic life, plant species and human beings its post-treatment needs to be thoroughly examined at effluent of ZVAl-mediated systems. Nevertheless, its concentration in the treated water/wastewater can be simply controlled by $Al(OH)_3$ precipitation, a practice that is widely used in the flocculation in water and wastewater treatment. Applications of ZVAl-mediated treatment to actual waters/wastewaters are rather rare. Most of the researches have been performed using synthetically prepared samples comprising single organic pollutants, without considering the other constituents of water/wastewater which might affect the treatment performance. In other words, individual and/or combinative synergistic effects of other pollutants on ZVAl performance have been disregarded in these studies. The number of studies reporting the effect of operating parameters on the degradation of organic pollutants by far outweighs those that investigate the toxicity evolution during ZVAl-mediated treatment systems. For the complete evaluation of ZVAl-mediated systems as water and wastewater treatment options, determination of effluent toxicity is fundamental and a prerequisite for comprehensive protection of the environment. Moreover, the variety of the matrices studied in the literature cannot also facilitate the understanding of the actual situation. For example, Arslan-Alaton et al. (2017a, b) demonstrated that the removal efficiencies of organic pollutants and aquatic toxicity patterns being observed during ZVAl-mediated treatment of micropollutants in distilled (pure) water and real water or wastewater matrices were quite different from each other. The inhibitory effects (toxic responses) being recorded before, during and after treatment of micropollutants also depend on the test organism used in the toxicity tests. Consequently, it is advisable to include battery bioassays in treatability work involving ZVAl. This information as well as detailed risk assessment will provide useful information on whether ZVAl oxidation would be applicable in real-scale and/or integrated with conventional treatment systems.

4 Conclusions and Recommendations

Speaking for nZVI, from the above experimental results and observations it may be concluded that most studies related with the application of nZVI for the removal of micropollutants were performed for short treatment periods, with single model contaminants dissolved and in pure water. However, it should be noted that these conditions are far away from real world applications and thus could lead to an overestimation of the nZVI capacity and treatment performance. Most of the above-reported treatability studies have been conducted as batch experiments and

giovanni.libralato@unina.it

under controlled reaction conditions. Experiments carried out with real contaminated water or wastewater are only few. In summary, more case studies are needed to fully elucidate the desorption, regeneration and reusability of nZVI after several cycles of application, its assessment using actual water samples, industrial effluent and contaminated soils, the ecotoxicological impacts of the release of metal ions from nZVI into the environment as well as the evaluation and analysis of associated handling costs, carbon footprint and life cycle. It was demonstrated that nZVI rapidly ages in water due to corrosion and interactions with dissolved oxygen, water constituents and the water itself. Corrosion changes the structure and chemical properties of nZVI depending on environmental and treatment (reaction) conditions. Moreover, the ecotoxiological risks associated with nZVI application should be further investigated to question its real application potential for micropollutant removal.

ZVAl-mediated treatment systems on the other hand have attracted increasing interest over the last 5–10 years. Although treatment systems involving ZVAl appeared to be feasible for micropollutants removal, the presence and formation of a surface oxide layer limits its application under neutral to near-neutral pH conditions. Considering that Al is highly toxic to aquatic life, plant/soil species and human beings, its post-treatment and disposal need to be thoroughly examined before practical applications. The use of ZVAl together with ZVI as a medium in PRBs might be a viable and cost-effective technology for in situ remediation of groundwater. The use of ZVAl also offers an efficient alternative for ex situ oxidation processes owing to its exceptional reduction potential. The review indicated that there is an urgent need for detailed, comprehensive research on the combination of ZVAl with other advanced treatment technologies. It should be considered that bimetallic systems where ZVAl is used together with other zero-valent metals might achieve higher activity for the removal of various contaminants as compared with ZVAl only.

References

Arslan-Alaton I (2003) The effect of pre-ozonation on the biocompatibility of reactive dye hydrolysates. Chemosphere 51:825–833

Arslan-Alaton I, Olmez-Hanci T (2012) Advanced oxidation of endocrine disrupting compounds: review on alkyl phenols and bisphenol A. In: Lofrano G (ed) Green technologies for wastewater treatment-energy recovery and emerging compounds removal. Springer, Heidelberg, pp 59–90

Arslan-Alaton I, Teksoy S (2007) Acid dyebath effluent pretreatment using Fenton's reagent: process optimization, reaction kinetics and effects on acute toxicity. Dyes Pigm 73:31–39

Arslan-Alaton I, Akmehmet Balcioglu I, Bahnemann DW (2002) Advanced oxidation of a reactive dyebath effluent: comparison of O_3, H_2O_2/UV-C and TiO_2/UV-A processes. Water Res 36:1143–1154

giovanni.libralato@unina.it

Arslan-Alaton I, Olmez-Hancı T, Korkmaz G, Sahin C (2017a) Removal of iopamidol, an iodinated X-ray contrast media, by zero-valent aluminum-activated H_2O_2 and $S_2O_8^{2-}$ oxidation. Chem Eng J (in press)

Arslan-Alaton I, Olmez-Hanci T, Khoei S, Fakhri H (2017b) Oxidative degradation of triton X-45 using zero valent aluminum in the presence of hydrogen peroxide, persulfate and peroxymonosulfate. Catal Today 280:199–207

ATSDR, Agency for Toxic Substances Disease Registry (2000) Toxicological profile for chromium. Atlanta, Georgia

Bates MN, Smith AH, Hopenhayn-Rich C (1992) Arsenic ingestion and internal cancers: a review. Am J Epidemiol 135:273–299

Bergendahl JA, Thies TP (2004) Fenton's oxidation of MTBE with zero-valent iron. Water Res 38:327–334

Bokare AD, Choi W (2009) Zero-valent aluminum for oxidative degradation of aqueous organic pollutants. Environ Sci Technol 43:7130–7135

Bokare AD, Choi W (2014) Review of iron-free Fenton-like systems for activating H_2O_2 in advanced oxidation processes. J Hazard Mater 275:121–135

Boon N, de Gelder L, Lievens H, Siciliano SD, Top EM, Verstraete W (2002) Bioaugmenting bioreactors for the continuous removal of 3-chloroaniline by a slow release. Environ Sci Technol 36:4698–4704

Bossmann SH, Oliveros E, Göb S, Siegwart S, Dahlen EP, Payawan LM Jr, Matthias S, Wömer M, Braun AM (1998) New evidence against hydroxyl radicals as reactive intermediates in the thermal and photochemically enhanced Fenton reactions. J Phys Chem A 102:5542–5550

Bremner DH, Burgess AE, Houllemare D, Namkung K-C (2006) Phenol degradation by using hydroxyl radicals generated from zero-valence iron and hydrogen peroxide. Appl Catal B 63:15–19

Buxton GV, Greenstock CL, Helman WP, Ross AB (1988) Critical review of rate constants for reactions of hydrated electrons, hydrogen-atoms and hydroxyl radicals (˙OH/˙O−) in aqueous solution. J Phys Chem Ref Data 17:513–886

Cabello G, Gromboni MF, Pereira EC, Marken F (2016) In situ microwave-enhanced electrochemical reactions at stainless steel: nano-iron for aqueous pollutant degradation. Electrochem Commun 62:48–51

Cai MQ, Wei XQ, Song ZJ, Jin MC (2015) Decolorization of azo dye Orange G by aluminum powder enhanced by ultrasonic irradiation. Ultrason Sonochem 22:167–173

Calderon B, Fullana A (2015) Heavy metal release due to aging effect during zero valent iron nanoparticles remediation. Water Res 83:1–9

Chen L-H, Huang C-C, Lien H-L (2008) Bimetallic iron–aluminum particles for dechlorination of carbon tetrachloride. Chemosphere 73:692–697

Chen P-J, Wu W-L, Wu KC-W (2013) The zerovalent iron nanoparticle causes higher developmental toxicity than its oxidation products in early life stages of medaka fish. Water Res 47:3899–3909

Cheng R, Wang JL, Zhang WX (2007) Comparison of reductive dechlorination of p-chlorophenol using Fe^0 and nanosized Fe^0. J Hazard Mater 144:334–339

Cheng Z, Fu F, Pang Y, Tang B, Lu J (2015) Removal of phenol by acid-washed zero-valent aluminium in the presence of H_2O_2. Chem Eng J 260:284–290

Council Directive 1999/31/EC (1999) Council directive 1999/31/EC of 26 April 1999 on the landfill of waste. Official J Eur Commun OJ L182:1–19

Craig PJ, Eng G, Jenkins RO (2003) Occurrence and pathways of organometallic compounds in the environment-general considerations. In: Craig PJ (ed) Organometallic compounds in the environment. Wiley, Chichester, pp 1–55

Crane RA, Scott TB (2012) Nanoscale zero-valent iron: future prospects for an emerging water treatment technology. J Hazard Mater 211–212:112–125

Criquet J, Vel Leitner NK (2009) Degradation of acetic acid with sulphate radical generated by persulfate ions photolysis. Chemosphere 77:194–200

giovanni.libralato@unina.it

De Carvalho Oliveira C, Santelli RE (2010) Occurrence and chemical speciation analysis of organotin compounds in the environment: a review. Talanta 82:9–24

Diao M, Yao M (2009) Use of zero-valent iron nanoparticles in inactivating microbes. Water Res 43:5243–5251

El-Temsah YS, Joner EJ (2013) Effects of nano-sized zero-valent iron (nZVI) on DDT degradation in soil and its toxicity to collembola and ostracods. Chemosphere 92:131–137

Fernandez J, Maruthamuthu P, Renken A, Kiwi J (2004) Bleaching and photobleaching of orange II within seconds by the oxone/Co^{2+} reagent in Fenton-like processes. Appl Catal B Environ 49:207–215

Flint S, Markle T, Thompson S, Wallace E (2012) Bisphenol A exposure, effects, and policy: a wildlife perspective. J Environ Manag 104:19–34

Fu F, Dionysiou DD, Liu H (2014) The use of zero-valent iron for groundwater remediation and wastewater treatment: a review. J Hazard Mater 267:194–205

Fu F, Cheng Z, Dionysiou DD, Tang B (2015) Fe/Al bimetallic particles for the fast and highly efficient removal of Cr(VI) over a wide pH range: performance and mechanism. J Hazard Mater 298:261–269

Ghisari M, Bonefeld-Jorgensen EC (2009) Effects of plasticizers and their mixtures on estrogen receptor and thyroid hormone functions. Toxicol Lett 189:67–77

Girit B, Dursun D, Olmez-Hanci T, Arslan-Alaton I (2015) Treatment of aqueous bisphenol A using nano-sized zero-valent iron in the presence of hydrogen peroxide and persulfate oxidants. Water Sci Technol 71:1859–1868

Giroto JA, Guardani R, Teixeira ACSC, Nascimento CAO (2006) Study on the photo-Fenton degradation of polyvinyl alcohol in aqueous solution. Chem Eng Process 45:523–532

Gonzalez-Olmos R, Martin MJ, Georgi A, Kopinke F-D, Oller I, Malato S (2012) Fe-zeolites as heterogeneous catalysts in solar Fenton-like reactions at neutral pH. Appl Catal B Environ 125:51–58

Grčić I, Papić S, Žižek K, Koprivanac N (2012) Zero-valent iron (ZVI) Fenton oxidation of reactive dye wastewater under UV-C and solar irradiation. Chem Eng J 195–196:77–90

Greenlee L, Torrey JD, Amaro RL, Shaw JM (2012) Kinetics of zero valent iron nanoparticle oxidation in oxygenated water. Environ Sci Technol 46:12913–12920

Grieger KD, Fjordbøge A, Hartmann NB, Eriksson E, Bjerg PL, Baun A (2010) Environmental benefits and risks of zero-valent iron nanoparticles (n-ZVI) for in-situ remediation: risk mitigation or trade-off? J Contam Hydrol 118:165–183

Han W, Fu F, Cheng Z, Tang B, Wu S (2016) Studies on the optimum conditions using acid-washed zero-valent iron/aluminum mixtures in permeable reactive barriers for the removal of different heavy metal ions from wastewater. J Hazard Mater 302:437–446

He J, Yang X, Men B, Bi Z, Pu Y, Wang D (2014) Heterogeneous Fenton oxidation of catechol and 4-chlorocatechol catalyzed by nano-Fe_3O_4: role of the interface. Chem Eng J 258:433–441

Hussain I, Zhang Y, Huang S, Dua X (2012) Degradation of p-chloroaniline by persulfate activated with zero-valent iron. Chem Eng J 203:269–276

Joo SH, Feitz AJ, Sedlak DL, Waite TD (2005) Quantification of the oxidizing capacity of nanoparticulate zero-valent iron. Environ Sci Technol 39:1263–1268

Kang SH, Choi W (2009) Oxidative degradation of organic compounds using zero-valent iron in the presence of natural organic matter serving as an electron shuttle. Environ Sci Technol 43:878–883

Kharisov BI, Dias HVR, Kharissova OV, Jiménez-Pérez VM, Pérez BO, Flores BM (2012) Iron-containing nanomaterials: synthesis, properties, and environmental applications. RSC Adv 2:9325–9358

Knapp CW, Engemann CA, Hanson ML, Keen PL, Hall KJ, Graham DW (2008) Indirect evidence of transposon-mediated selection of antibiotic resistance genes in aquatic systems at low-level oxytetracycline exposures. Environ Sci Technol 42:5348–5353

Kolpin DW, Furlong ET, Meyer MT, Thurman EM, Zaugg SD, Barber LB, Buxton HT (2002) Pharmaceuticals, hormones, and other organic wastewater contaminants in US streams, 1999–2000: a national reconnaissance. Environ Sci Technol 36:1202–1211

giovanni.libralato@unina.it

Kormos JL, Schulz M, Kohler H-PE, Ternes TA (2010) Biotransformation of selected iodinated X-ray contrast media and characterization of microbial transformation pathways. Environ Sci Technol 44:4998–5007

Kummerer K, Erbe T, Gartiser S, Brinker L (1998) AOX emissions from hospitals into municipal waste water. Chemosphere 36:2437–2445

Kusic H, Peternel I, Koprivanac N, Loncaric Bozic A (2011) Iron-activated persulfate oxidation of an azo dye in model wastewater: influence of iron activator type on process optimization. J Environ Eng 137:454–463

Lai KCK, Lo IMC (2008) Removal of chromium (VI) by acid-washed zero-valent iron under various groundwater geochemistry conditions. Environ Sci Technol 42:1238–1244

Latorre J, Reineke W, Knackmuss HJ (1984) Microbial metabolism of chloroanilines: enhanced evolution by natural genetic exchange. Arch Microbiol 140:159–165

Lee J, Kim J, Choi W (2007) Oxidation on zero-valent iron promoted by polyoxometalate as an electron shuttle. Environ Sci Technol 41:3335–3340

Li H, Wan J, Ma Y, Huang M, Wang Y, Chen Y (2014a) New insights into the role of zero-valent iron surface oxidation layers in persulfate oxidation of dibutyl phthalate solutions. Chem Eng J 250:137–147

Li W, Wang Y, Irini A (2014b) Effect of pH and H_2O_2 dosage on catechol oxidation in nano-Fe_3O_4 catalyzing UV–Fenton and identification of reactive oxygen species. Chem Eng J 244:1–8

Li R, Jin X, Megharaj M, Naidu R, Chen Z (2015) Heterogeneous Fenton oxidation of 2,4-dichlorophenol using iron-based nanoparticles and persulfate system. Chem Eng J 264:587–594

Lien HL (2005) Transformation of chlorinated methanes by zero-valent aluminum coupled with Pd/Al_2O_3. Environ Technol 26:663–672

Lien HL, Wilkin R (2002) Reductive activation of dioxygen for degradation of methyl tert-butyl ether by bifunctional aluminum. Environ Sci Technol 36:4436–4440

Lien HL, Zhang W (2002) Novel bifunctional aluminum for oxidation of MTBE and TAME. J Environ Eng 128:791–798

Lien HL, Yu CC, Lee YC (2010) Perchlorate removal by acidified zero-valent aluminum and aluminum hydroxide. Chemosphere 80:888–893

Lin AYC, Tsai YT (2009) Occurrence of pharmaceuticals in Taiwan's surface waters: impact of waste streams from hospitals and pharmaceutical production facilities. Sci Total Environ 407:3793–3802

Lin CJ, Wang SL, Huang PM, Tzou YM, Liu JC, Chen CC, Chen JH, Lin C (2009) Chromate reduction by zero-valent Al metal as catalyzed by polyoxometalate. Water Res 43:5015–5022

Lin K, Cai J, Sun J, Xue X (2013) Removal of 2,4-dichlorophenol by aluminium/O_2/acid system. J Chem Technol Biotechnol 88:2181–2187

Lindsey ME, Tarr MA (2000) Inhibition of hydroxyl radical reaction with aromatics by dissolved natural organic matter. Environ Sci Technol 34:444–449

Liu H, Zhang G, Liu C-Q, Li L, Xiang M (2009) The occurrence of chloramphenicol and tetracyclines in municipal sewage and the Nanming River, Guiyang City, China. J Environ Monit 11:1199–1205

Liu W, Zhang H, Cao B, Lin K, Gan J (2011) Oxidative removal of bisphenol A using zero valent aluminum-acid system. Water Res 45:1872–1878

Lovett PS (1996) Translation attenuation regulation of chloramphenicol resistance in bacteria—a review. Gene 179:157–162

Lyche JL, Gutleb AC, Bergman Å, Eriksen GS, Murk AJ, Ropstad E, Saunders M, Skaare JU (2009) Reproductive and developmental toxicity of phthalates. J Toxicol Environ Health Part B Critical Rev 12:225–249

Mueller NC, Braun J, Bruns J, Cerník M, Rissing P, Rickerby D, Nowack B (2012) Application of nanoscale zero valent iron (nZVI) for groundwater remediation in Europe. Environ Sci Pollut Res 19:550–558

giovanni.libralato@unina.it

Nadtochenko VA, Kiwi J (1998) Photolysis of $FeOH^{2+}$ and $FeCl_2^+$ in aqueous solution. Photodissociation kinetics and quantum yields. Inorg Chem 37:5233–5238

National Research Council (NRC) (1995) Nitrate and nitrite in drinking water. National Academic Press, Washington, DC

O'Carroll D, Sleep B, Krol M, Boparai H, Kocur C (2013) Nanoscale zero valent iron and bimetallic particles for contaminated site remediation. Adv Water Resour 51:104–122

O'Connor JC, Chapin RE (2003) Critical evaluation of observed adverse effects of endocrine active substances on reproduction and development, the immune system, and the nervous system. Pure Appl Chem 75:2099–2123

Oh SY, Cha DK, Chiu PC (2002a) Graphite-mediated reduction of 2,4-dinitrotoluene with elemental iron. Environ Sci Technol 36:2178–2184

Oh SY, Cha DK, Kim BJ, Chiu PC (2002b) Effect of adsorption to elemental iron on the transformation of 2,4,6-trinitrotoluene and hexahydro-1,3,5-trinitro-1,3,5-triazine in solution. Environ Toxicol Chem 21:1384–1389

Oh SY, Chiu PC, Kim BJ, Cha DK (2003) Enhancing Fenton oxidation of TNT and RDX through pretreatment with zero-valent iron. Water Res 37:4275–4283

Oh SY, Kim HW, Park JM, Park HS, Yoon C (2009) Oxidation of polyvinyl alcohol by persulfate activated with heat, Fe^{2+}, and zero-valent iron. J Hazard Mater 168:346–351

Oh SY, Kang SG, Chiu PC (2010) Degradation of 2,4-dinitrotoluene by persulfate activated with zero-valent iron. Sci Total Environ 408:3464–3468

Otero-González L, García-Saucedo C, Field JA, Sierra-Álvarez R (2013) Toxicity of TiO_2, ZrO_2, Fe^0, Fe_2O_3, and Mn_2O_3 nanoparticles to the yeast, *Saccharomyces cerevisiae*. Chemosphere 93:1201–1206

Peeters K, Lespes G, Milačič R, Ščančar J (2015) Adsorption and degradation processes of tributyltin and trimethyl tin in landfill leachates treated with iron nanoparticles. Environ Res 142:511–552

Peluffo M, Pardo F, Santos A, Romero A (2016) Use of different kinds of persulfate activation with iron for the remediation of a PAH-contaminated soil. Sci Total Environ 563-564:649–656

Perez S, Barcelo D (2007) Fate and occurrence of X-ray contrast media in the environment. Anal Bioanal Chem 387:1235–1246

Pignatello JJ, Liu D, Huston P (1999) Evidence for an additional oxidant in the photoassisted Fenton reaction. Environ Sci Technol 33:1832–1839

Pourata R, Khataee AR, Aber S, Daneshvar N (2009) Removal of the herbicide Bentazon from contaminated water in the presence of synthesized nanocrystalline TiO_2 powders under irradiation of UV-C light. Desalination 249:301–307

Puglisi E, Cappa F, Fragoulis G, Trevisan M, Del Re AAM (2007) Bioavailability and degradation of phenanthrene in compost amended soils. Chemosphere 67:548–556

Rabalais NN, Turner RE (2001) Hypoxia in the northern Gulf of Mexico: coastal hypoxia: consequences for living resources and ecosystems, coastal and estuarine studies 58. American Geophysical Union, Washington, DC

Rabalais NN, Turner RE, Scavia D (2002) Beyond science into policy: Gulf of Mexico hypoxia and the Mississippi River. Bioscience 52:129–142

Rezg R, El-Faza S, Gharbi N, Mornagui B (2014) Bisphenol A and human chronic diseases: current evidences, possible mechanisms, and future perspectives. Environ Int 64:83–90

Rivas FJ (2006) Polycyclic aromatic hydrocarbons sorbed on soils: a short review of chemical oxidation based treatments. J Hazard Mater 138:234–251

Rodriguez S, Santos A, Romero A, Vicente F (2012) Kinetic of oxidation and mineralization of priority and emerging pollutants by activated persulfate. Chem Eng J 213:225–234

Rodriguez S, Vasquez L, Costa D, Romero A, Santos A (2014) Oxidation of Orange G by persulfate activated by Fe(II), Fe(III) and zero valent iron (ZVI). Chemosphere 101:86–92

Rosal R, Rodríguez A, Perdigón-Melóon JA, Petre A, García-Calvo E, Gómez MJ, Agüera A, Fernández-Alba AR (2010) Occurrence of emerging pollutants in urban wastewater and their removal through biological treatment followed by ozonation. Water Res 44:578–588

giovanni.libralato@unina.it

Routledge EJ, Sumpter JP (1996) Estrogenic activity of surfactants and some of their degradation products assessed using a recombinant yeast screen. Environ Toxicol Chem 15:241–248
Safarzadeh-Amiri A, Bolton JR, Cater SR (1996) The use of iron in advanced oxidation processes. J Adv Oxid Technol 1:18–26
Salam MA, Fageeh O, Al-Thabaiti SA, Obaid AY (2015) Removal of nitrate ions from aqueous solution using zero-valent iron nanoparticles supported on high surface area nanographenes. J Mol Liq 212:708–715
Salman JM, Njoku VO, Hameed BH (2011) Bentazon and carbofuran adsorption onto date seed activated carbon: kinetics and equilibrium. Chem Eng J 173:361–368
Santos JL, Aparicio I, Callejón M, Alonso E (2009) Occurrence of pharmaceutically active compounds during 1-year period in wastewaters from four wastewater treatment plants in Seville (Spain). J Hazard Mater 164:1509–1516
Scavia D, Donnelly KA (2007) Reassessing hypoxia forecasts for the Gulf of Mexico. Environ Sci Technol 41:8111–8117
Schonberger H, Baumann A, Keller W (1997) Study of microbial degradation of polyvinyl alcohol (PVA) in wastewater treatment plants. Am Dyestuff Rep 86:9–18
Sim WJ, Lee JW, Oh JE (2010) Occurrence and fate of pharmaceuticals in wastewater treatment plants and rivers in Korea. Environ Pollut 158:1938–1947
Staples CA, Naylor CG, Williams JB, Gledhill WE (2001) Ultimate biodegradation of alkylphenol ethoxylate surfactants and their biodegradation intermediates. Environ Toxicol Chem 20:2450–2455
Sun L, Yuan Z, Gong W, Zhang L, Xu Z, Su G, Han D (2015) The mechanism study of trace Cr (VI) removal from water using Fe^0 nanorods modified with chitosan in porous anodic alumina. Appl Surf Sci 328:606–613
Tang W, Tassos S (1997) Oxidation kinetics and mechanisms of trihalomethanes by Fenton's reagent. Water Res 31:1117–1125
Temiz K, Olmez-Hanci T, Arslan-Alaton I (2016) Zero-valent iron-activated persulfate oxidation of a commercial alkyl phenol polyethoxylate. Environ Technol 29:1–11
Ternes TA, Hirsch R (2000) Occurrence and behavior of W-ray contrast media in sewage facilities and the aquatic environment. Environ Sci Technol 34:2741–2748
Tokiwa Y, Kawabata G, Jarerat A (2001) A modified method for isolating poly (vinyl alcohol)—degrading bacteria and study of their degradation patterns. Biotechnol Lett 23:1937–1941
Trujillo-Reyes J, Peralta-Vide JR, Gardea-Torresdey JL (2014) Supported and unsupported nanomaterials for water and soil remediation: are they a useful solution for worldwide pollution? J Hazard Mater 280:487–503
Underwood JC, Harvey RW, Metge DW, Repert DA, Baumgartner LK, Smith RL, Roane TM, Barber LB (2011) Effects of the antimicrobial sulfamethoxazole on groundwater bacterial enrichment. Environ Sci Technol 45:3096–3101
Walling C, Goosen A (1973) Mechanism of the ferric ion catalyzed decomposition of hydrogen peroxide. Effect of organic substrates. J Am Chem Soc 95:2987–2991
Walling C, El-Taliawi GM, Johnson RA (1974) Fenton's reagent. IV. Structure and reactivity relations in the reactions of hydroxyl radicals and the redox reactions of radicals. J Am Chem Soc 96:133–139
Wang Q, Cissoko N, Zhou M, Xu X (2011) Effects and mechanism of humic acid on chromium (VI) removal by zero-valent iron (Fe^0) nanoparticles. Phys Chem Earth 36:442–446
Wang A, Guo W, Hao F, Yue X, Leng Y (2014a) Degradation of Acid Orange 7 in aqueous solution by zero-valent aluminum under ultrasonic irradiation. Ultrason Sonochem 21:572–575
Wang C, Luo H, Zhang Z, Wu Y, Zhang J, Chen S (2014b) Removal of As(III) and As(V) from aqueous solutions using nanoscale zero valent iron-reduced graphite oxide modified composites. J Hazard Mater 268:124–131
Wang X, Wang L, Li J, Qiu J, Cai C, Zhang H (2014c) Degradation of Acid Orange 7 by persulfate activated with zero valent iron in the presence of ultrasonic irradiation. Sep Purif Technol 122:41–46

giovanni.libralato@unina.it

Wei X, Gao N, Li C, Deng Y, Zhou S, Li L (2016) Zero-valent iron (ZVI) activation of persulfate (PS) for oxidation of bentazon in water. Chem Eng J 285:660–670

Weng C-H, Tao H (2016) Highly efficient persulfate oxidation process activated with Fe^0 aggregate for decolorization of reactive azo dye Remazol Golden Yellow. Arabian J Chem. doi:10.1016/j.arabjc.2015.05.012

Weng C-H, Tsai K-L (2016) Ultrasound and heat enhanced persulfate oxidation activated with Fe^0 aggregate for the decolorization of C.I. Direct Red 23. Ultrason Sonochem 29:11–18

Weng C-H, Ding F, Lin Y-T, Liu N (2015) Effective decolorization of polyazo direct dye Sirius Red F3B using persulfate activated with Fe^0 aggregate. Sep Purif Technol 147:147–155

WHO (World Health Organization) (1993) Guidelines for drinking-water quality, vol 1-recommendations, 2nd edn. Geneva

Wu YY, Zhou SQ, Qin FH, Zheng K, Ye XY (2010) Modeling the oxidation kinetics of Fenton's process on the degradation of humic acid. J Hazard Mater 179:533–539

Wu CC, Hus LC, Chiang PN, Liu JC, Kuan WH, Chen CC, Hwang CE (2013a) Oxidative removal of arsenite by Fe(II)- and polyoxometalate (POM)-amended zero-valent aluminum (ZVAl) under oxic conditions. Water Res 47:2583–2591

Wu Q, Liu H, Ye LS, Li P, Wang Y-H (2013b) Biodegradation of Di-n-butyl phthalate esters by *Bacillus* sp. SASHJ under simulated shallow aquifer condition. Int Biodeter Biodegr 76:102–107

Wu D, Shen Y, Ding A, Mahmood Q, Liu S, Tu Q (2013c) Effects of nanoscale zero-valent iron particles on biological nitrogen and phosphorus removal and microorganisms in activated sludge. J Hazard Mater 262:649–655

Wu H, Yin JJ, Wamer WG, Zeng M, Lo YM (2014) Reactive oxygen species-related activities of nano-iron metal and nano-iron oxides. J Food Drug Anal 22:86–94

Xia S, Gu Z, Zhang Z, Zhang J, Hermanowicz SW (2014) Removal of chloramphenicol from aqueous solution by nanoscale zero-valent iron particles. Chem Eng J 257:98–104

Xiong X, Sun B, Zhang J, Gao N, Shen J, Li J, Guan X (2014) Activating persulfate by Fe^0 coupling with weak magnetic field: performance and mechanism. Water Res 62:53–62

Xu X-R, Li X-Y (2008) Adsorption behaviour of dibutyl phthalate on marine sediments. Mar Pollut Bull 57:403–408

Xu X-R, Li X-Z (2010) Degradation of azo dye Orange G in aqueous solutions by persulfate with ferrous ion. Sep Purif Technol 72:105–111

Ying GG (2006) Fate, behavior and effects of surfactants and their degradation products in the environment. Environ Int 32:417–431

Ying GG, William B, Kookana R (2002) Environmental fate of alkylphenols and alkylphenol ethoxylates—a review. Environ Int 28:215–226

Zha S, Cheng Y, Gao Y, Chen Z, Megharaj M, Naidu R (2014) Nanoscale zero-valent iron as a catalyst for heterogeneous Fenton oxidation of amoxicillin. Chem Eng J 255:141–148

Zhang Q (2015) Treatment of oilfield produced water using Fe/C micro-electrolysis assisted by zero-valent copper and zero-valent aluminium. Environ Technol 36:515–520

Zhang H, Cao B, Liu W, Lin K, Feng J (2012) Oxidative removal of acetaminophen using zero valent aluminum-acid system: efficacy, influencing factors, and reaction mechanism. J Environ Sci 24:314–319

Zhao J, Zhang Y, Quan X, Chen S (2010) Enhanced oxidation of 4-chlorophenol using sulfate radicals generated from zero-valent iron and peroxydisulfate at ambient temperature. Sep Purif Technol 71:302–307

Zhou Z, Jiang J-Q (2015) Treatment of selected pharmaceuticals by ferrate (VI): performance, kinetic studies and identification of oxidation products. J Pharmaceut Biomed 106:37–45

Zhou T, Zou X, Mao J, Wu X (2016) Decomposition of sulfadiazine in a sonochemical Fe^0-catalyzed persulfate system: parameters optimizing and interferences of wastewater matrix. Appl Catal B Environ 185:31–41

Zhu H, Jia Y, Wu X, Wang H (2009) Removal of arsenic from water by supported nano zero-valent iron on activated carbon. J Hazard Mater 172:1591–1596

Zou X, Zhou T, Mao J, Wu X (2014) Synergistic degradation of antibiotic sulfadiazine in a heterogeneous ultrasound-enhanced Fe^0/persulfate Fenton-like system. Chem Eng J 257:36–44

giovanni.libralato@unina.it

Environmental Nanoremediation and Electron Microscopies

Elisabetta Carata, Elisa Panzarini and Luciana Dini

Abstract Cleaning up the environment from various sources of pollution is a commitment to not only preserve ecological health but also human health. Pollution in the environment can be remediated using a range of techniques including nanotechnologies. Environmental remediation techniques use various approach to remove or degrade environmental pollution in soils, waters, groundwater, and air. There are two different strategies to apply the nanotechnologies to environmental remediation: ex situ techniques that consist in the removing pollutant from sites and then treating; in situ techniques that make up of cleaning up directly in the polluted site. Both strategies are highly efficient but it's necessary to know the nanomaterials used to nanoremediate the environment, so the electron microscopy offers an important tool to characterize and quantify NMs in environmental; evaluate NMs transformation in the environment and consequences for bioavailability and toxicity; analysis uptake and internal distribution of NMs in model animals. Research addressing these key topics will reduce the uncertainty in ecological risk assessment and support the sustainable development of nanotechnology.

Keywords Environmental remediation · Electron microscopy · Nanomaterials

1 Introduction

Environmental implications of nanotechnology, defined as the possible effects on the environment due to use of nanotechnology equipment and materials, possess a double face presenting benefits and hazards. Nanotechnology innovations can improve environment safety through cleaning up of existing pollution, amelioration of manufacturing methods to reduce the generation of new pollution, and making alternative energy sources more cost effective, but nanotech materials, if released into the environment, can generate the pollution.

E. Carata · E. Panzarini · L. Dini (✉)
Di.S.Te.B.A, University of Salento, 73100 Lecce, Italy
e-mail: luciana.dini@unisalento.it

© Springer International Publishing AG 2017

G. Lofrano et al. (eds.), *Nanotechnologies for Environmental Remediation*,
DOI 10.1007/978-3-319-53162-5_4

giovanni.libralato@unina.it

Rising prices for raw materials and energy, coupled with the increasing environmental awareness of consumers, are responsible for a large number of "nanoproducts" on the market that promise certain advantages for environment and climate protection. In fact, nanomaterials exhibit special physical and chemical properties that make them interesting for novel, environmentally friendly products. For examples, nanomaterials increased life time for resistance against mechanical stress or weathering, for reducing cleaning of soil- and water-resistant coatings, for improving the energy efficiency of buildings, for reducing weight and save energy during transport by their addition to materials. In the chemical industry, nanomaterials special catalytic properties to boost energy and resource efficiency, can also replace environmentally problematic chemicals in certain fields of application. This, in turn, raised high hopes in nanotechnology optimized products and processes for many strategic production as energy and for storage. Many of these products/processes are currently in the development phase and are destined to contribute significantly to climate protection and solve energy concerns in the future. The emphasis that is often placed on the sustainable potential of nanotechnology, nonetheless, reflects unsubstantiated expectations. Determining the real effects of a product on the environment—both positive and negative—requires to examine the entire life cycle from production to disposal (Klaine et al. 2008; Sharma et al. 2015).

Maintaining and restoring the quality of air, water and soil is one of the great challenge of our time but the descriptions of environmental benefits fail to consider the amount of resources and energy consumed in producing this. Most countries face serious environmental problems, such as the availability of drinking water, the treatment of waste and wastewater, air pollution and soil and groundwater contamination. In many cases conventional remediation, including the degradation, sequestration, or other related approaches that result in reduced risks to human and environmental receptors posed by chemical and radiological contaminants, and treatment technologies have shown only limited effectiveness in reducing the level of pollutants, especially in soil and water. The benefits, which arise from the application of nanomaterials for remediation, would be more rapid and cost-effective clean-up of wastes.

Cost-effective remediation techniques pose a major challenge in the development of adequate remediation methods that protect the environment. Substances of significant concern in remediation of soils, sediment, and groundwater include heavy metals (e.g., mercury, lead, cadmium) and organic compounds (e.g., benzene, chlorinated solvents, creosote, and toluene). Specific control and design of materials at the molecular level may in part increased affinity, capacity, and selectivity for pollutants. Nanotechnology promises a potential revolution in approach to remediation. (Mueller and Nowack 2010). It is important that nanoparticles can display totally new characteristics due to their high surface to volume ratio and small size (Hochella and Madden 2005) rendering them significantly more reactive than larger particles (Rickerby and Morrison 2007); thus these properties can be exploited in environmental remediation.

giovanni.libralato@unina.it

However, it should be taken in mind that the remedy itself (i.e. nanomaterial) can cause pollution as well. If synthesis, stability, and toxicity of engineered metal nanoparticles (ENPs) have been extensively studied during the past two decades, few attention has been paid to the formation, fate, and ecological effects of ENPs and, most important of naturally-occurring nanoparticles (NNPs). Numerous studies have been conducted on the fate and behaviour of ENPs and NNPs released into the environment, especially with the aim of examining their effects on humans and the ecosystems. Recent investigations have established that significant accumulation of nanoparticles (NPs) occurs in aquatic biofilms. These studies point to the emerging roles of biofilms for influencing partitioning and possibly transformations of NPs in both natural and engineered systems. Bacteria are essential components of all natural and many engineered systems. The most active fractions of bacteria are now recognized to occur as biofilms, where cells are attached and surrounded by a secreted matrix of "sticky" extracellular polymeric substances. Since attached biofilms are efficient "sponges" for NPs, efforts to elucidate the fundamental mechanisms guiding interactions between NPs and biofilms have just begun (Ikuma et al. 2015; Battin et al. 2009; Ferry et al. 2009; Nevius et al. 2012; Kroll et al. 2014; Flemming and Wingender 2010; Nevius et al. 2012). The biofilms play an important role by influencing environmental partitioning of NPs within natural systems, therefore are efficient in a wide range of systems such as wastewater treatment (Wuertz et al. 2000; Hu et al. 2005; Hawari and Mulligan 2006), drinking-water filtration (Lehtola et al. 2004; Berry et al. 2006), and marine and freshwater systems (Schlekat et al. 1998; Decho 2000; Battin et al. 2009).

The interaction between biofilm and nanoparticles can be illustrate in three different phases: transport of NPs near to biofilm, NPs attachment to the biofilm surface and migration into the biofilm (Fig. 1). At each of these steps, the interactions are a complex interplay of a myriad of factors including, but not limited to, NPs characteristics, physicochemical and biological makeup of the biofilm matrix, and environmental parameters such as water chemistry, flow, and temperature (El Abed et al. 2012). The NPs characteristics have been reported to impact their interactions with biofilm-coated surfaces at all three steps of the interactions. NPs transport through the water column has been studied extensively (Lecoanet and Wiesner 2004; Jaisi et al. 2008; Phenrat et al. 2009). Surface modification of NPs, through ligand capping during synthesis or post-synthesis passive sorption of organic molecules, plays a critical role in NP–biofilm interactions (Ikuma et al. 2014). In fact, pure and single-component NPs are rare or non-existent in the environment. ENPs are typically functionalized by specific organic ligands for a variety of target applications. When these capped NPs are being used or released in various environments, they are often subjected to further modifications in an uncontrollable manner by passive sorption of different organic molecules. The biofilm is involved not only in the mechanism of trapping the environmental NPs but also in degradation of environmental pollution. In fact, natural biofilms play a critical role in the biogeochemical cycling of elements which can lead to NPs formation. For example, microbes precipitate metals in the form of NPs as a detoxification mechanism. Reith et al. (2006, 2010) have shown that gold

giovanni.libralato@unina.it

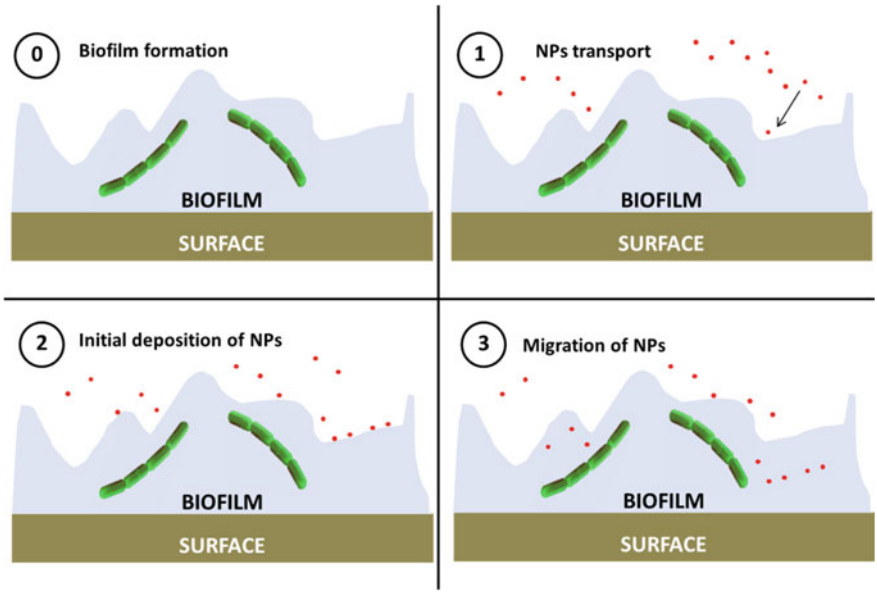

Fig. 1 The three steps involved in NP–biofilm interactions: *1* transport of NPs to the vicinity of the biofilm, *2* initial deposition of NPs onto the biofilm surface, and *3* migration of NPs into deeper areas of the biofilm. NPs may also interact directly with cell surfaces within the biofilm matrix

dissolution and re-precipitation of nanoparticulate gold is directly coupled with biofilms on gold grain surfaces. Biofilms dominated by sulphate reducing bacteria were found to be responsible for the formation of zinc sulphide NPs (Labrenz et al. 2000; Labrenz and Banfield 2004).

2 Nano-Materials and Environmental Applications

Pollution results from resource production and consumption, which in their current state are very wasteful and most wastes cannot be reintegrated into the environment effectively or cheaply. Nanotechnology offers many advantages in this field by improving existing environmental technologies and/or creating new technology. In this context, nanotechnology has three main capabilities that can be applied in the fields of environment, including the clean-up (TiO_2, nZVI, dendrimers), (remediation) and purification (nanoparticulate photocatalysts, nanoclays) the detection of contaminants (sensing and detection), and the pollution prevention (Yunus et al. 2012) (Fig. 2).

giovanni.libralato@unina.it

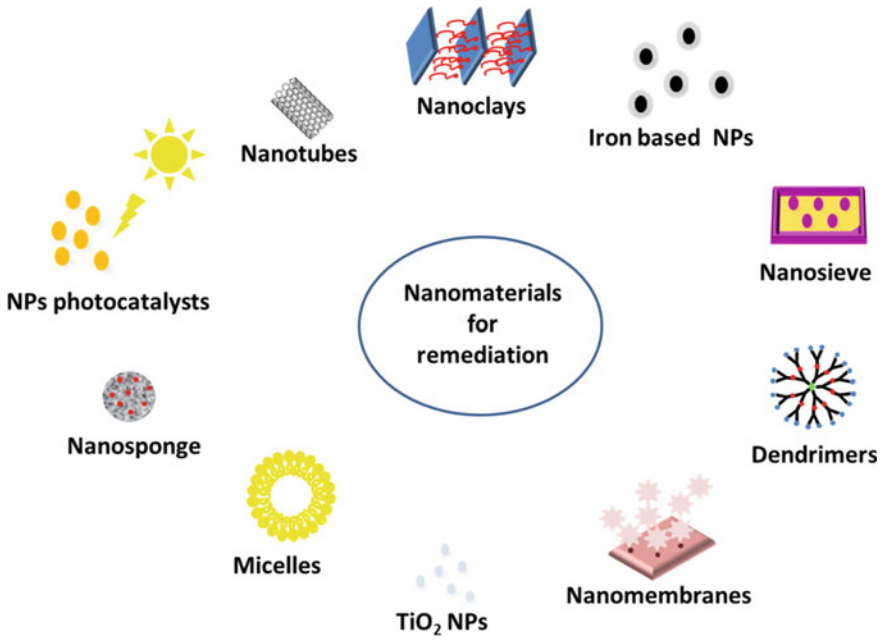

Fig. 2 Graphic representation of different nanomaterials used in nanoremediation

2.1 Titanium Dioxide (TiO_2) Based Nanoparticles

Nanoparticles that are activated by light, such as the large band-gap semiconductors titanium dioxide (TiO_2) and zinc oxide (ZnO), are frequently studied for their ability to remove organic contaminants from various media. These nanoparticles have the advantages to be readily available, inexpensive, and present low toxicity. Titanium dioxide (TiO_2) is one of the popular materials used in various applications because of its semiconducting, photocatalytic, energy converting, electronic and gas sensing properties. Titanium dioxide crystals are present in three different polymorphs in nature that, in the order of their abundance, are Rutile, Anatase and Brookite. Many researchers are focused on TiO_2 nanoparticle and its application as a photocatalyst in water treatment. The semiconducting property of TiO_2 is necessary for the removal of different organic pollutants through excitation of TiO_2 semiconductor with a light energy greater than its band gap, which could generate electron hole pairs. These may be exploited in different reduction processes at the semiconductor/solution interface (Farrè et al. 2011; Mansoori et al. 2008). The photocatalytic properties of TiO_2 nanoparticles have an extensive application in remediation of wastewater, produced from industries such as paint, textile, plastic, tannery and paper, containing anionic and cationic dyes released into the environment which are mostly non-degradable in natural condition. For example Rezaei and Salam (2016) have synthesized an anatase–graphene-nanocomposite by an

giovanni.libralato@unina.it

eco-friendly method. Their results indicated that anatase and TiO_2 graphene oxide are able to remove dye cations from aqueous solution according to the first order kinetics while in the TiO_2 reduced graphene oxide system, the dye degradation is controlled by second order kinetics, resulting in an increase in methylene blue degradation from 80 to 94% over 40 min (Razei and Salam 2016). TiO_2 photocatalysts revealed its potential, also, for rapid degradation of recalcitrant compounds, such as malachite green dye a model pollutant, in wastewater using visible light (Narayana et al. 2011).

The photocatalytic degradation of Marine Remazol RGB 150% gran, Ultra Red Remazol gran, two textile commercial azo dyes, mediated by Degussa P25, a TiO_2 based nanomaterials which consists of 75% anatase and 25% rutile was successfully achieved by Saggioro et al. (2011). Their results indicated that the photocatalytic degradation of two dyes in water with powdered TiO_2 depended on the concentration of dye, amount of photocatalyst used, UV-irradiation time, solution pH and concentration of added hydrogen peroxide.

2.2 Iron Based Nanoparticles

The iron based nanoparticles are very high flexible for both in situ and ex situ remediation. For example, nanoparticles are easily deployed in ex situ slurry reactors for the treatment of contaminated soils, sediments, and solid wastes. Alternatively, they can be anchored onto a solid matrix such as carbon, zeolite, or membrane for enhanced treatment of water, wastewater, or gaseous process streams. Direct subsurface injection of nanoscale iron particles, whether under gravity-feed or pressurized conditions, has been shown to effectively degrade chlorinated organics such as trichloroethylene to environmentally benign compounds. The use of zero-valent iron (ZVI or Fe^0) for in situ remedial treatment has been expanded to include all different kinds of contaminants. Zero-valent iron removes aqueous contaminants by reductive dechlorination, in the case of chlorinated solvents, or by reducing to an insoluble from, in the case of aqueous metal ions. Fine ZVI materials can be subdivided into different categories based on particle size, composition of the particles (metallic, bimetallic), surface modifications and the solution medium or carrier material (supported, emulsion, etc.). In this manner, there are *Micro-scale zero-valent iron (mZVI)* [(bi)metallic particles with a diameter greater than 1 μm] and *Nano-scale zero-valent iron (nZVI)* [(bi)metallic particles with a diameter smaller than 100 nm].The larger specific surface area and the higher zero-valent iron content of nZVI are responsible for a higher degradation rate of $VOCl_3$ (dechlorination) than that observed for reactive nano-scale iron product (RNIP) (Fu et al. 2014). However, the outer magnetite shell of RNIP slow down reaction with water (H_2 formation), that results in a longer life of such particles (Liu et al. 2005). The limited stability and mobility of pure nZVI provides the *impetus* for the development of modified nZVI. Finally, there is a growing variety of nano-scale bimetallic particles defined *Modified nZVI* which, in addition

giovanni.libralato@unina.it

to zero-valent iron or another metal, contain a second metallic material. Here, one metal (e.g., Fe and Zn) is mainly the electron donor, and the other (e.g., Pd, Pt, Ni) is the catalyst of the reaction. Such nanoscale bimetallic particles are also sometimes called catalysed nZVI particles. Catalysed nZVI particles allow much higher reaction rates but their life is limited. Examples of such materials are: Fe/Pd, Fe/Ag, Fe/Ni, Fe/Co, Fe/Cu, Zn/Pd (Zhang et al. 2003) Ag/Pd, Au/Pd (Nutt et al. 2005). Fe/Pd particles cause high reaction rates in comparison with pure nZVI. In addition, Pd has a high selectivity for the C–Cl bond. However, research by Huang et al. (2009) shows that Ni is a cheaper alternative for the expensive Pd. Fe/Ni particles can achieve the complete degradation of perchloroethene (PCE) to ethane. Another type of iron nanoparticles are the 'Supported' nano-scale particles with a hydrophilic carrier consisting of polymers, e.g. poly(acrylic acid), (Ponder et al. 2001; Schrick et al. 2002). The anionic carrier material is supposed to prevent the aggregation and sedimentation of the particles, resulting in the increase of inject ability, mobility and spread. Finally, another type of iron nanoparticles includes Emulsified nZVI particles (EZVI) that has been specifically developed for the treatment of free phases of chlorinated solvents (DNAPLs, Dense Non-Aqueous Phase Liquids) (Quinn et al. 2005). Plant oils and all kinds of surfactants can be used to prepare this emulsion. More specifically, this is a surfactant-stabilised biodegradable emulsion, diameter of about 40 μm and specific gravity of about 1.1 kg/l, which forms drops with an oil-water membrane around the nZVI or mZVI particles in water drops (Quinn et al. 2005). As the emulsion also nZVI behaves as a DNAPL, it will move through the soil in the same way as the DNAPL to be remediated, thus allowing for maximum contact (Mansoori et al. 2008). The use of in situ abiotic reduction using zero-valent iron (ZVI) has been shown to be a successful alternative to groundwater extraction for chlorinated solvent sites. ZVI has been used for in situ remediation by placing large quantities of granular metal directly in the flowpath of contaminated groundwater to act as a permeable reactive barrier (PRB) (Bennett et al. 2010).

2.3 Nanoparticulate Photocatalysts and Catalysts

Catalysis involves the modification of a chemical reaction rate, mostly speeding up or accelerating the reaction rate by a substance called catalyst that is not consumed throughout the reaction. Usually, the catalyst participates in the reaction by interacting with one or more of the reactants and, at the end of process, it is regenerated without any changes. There are two main kinds of catalysts, homogeneous and heterogeneous. The homogeneous type is dispersed in the same phase as the reactants, that ordinarily is a gas or a liquid solution. Heterogeneous catalyst is in a different phase from the reactants and is separated by a phase boundary. Heterogeneous catalytic reactions typically take place on the surface of a solid support, e.g., silica or alumina. These solid materials have very high surface areas that usually arise from their impregnation with acids or coating with catalytically

giovanni.libralato@unina.it

active material, e.g. platinum-coated surfaces. Catalysts usually have two principal roles in nanotechnology areas: (1) in macro quantities, they can be involved in some processes for the preparation of a variety of other nanostructures like quantum dots and nanotubes; (2) some nanostructures themselves can serve as catalysts for certain chemical reactions. The chemical activity of a conventional heterogeneous catalyst is proportional to its overall specific surface area per unit volume, which is customarily reported in the unit of m^2/g, with typical values for commercial catalysts in the range of 100–400 m^2/g. There are different procedures to enhance the surface area of the catalyst, which result in voids or empty spaces within the material. It is quite common for these materials to have pores with diameters in the nanometer range (Mansoori et al. 2008). An interestingly application of photocatalysis is the use of Pd/Al_2O_3 for remediation of methane, in particular the adsorption states, photodissociation, and photodesorption of methane on Pd clusters of various sizes on a thin epitaxial Al_2O_3 film show very pronounced size effects and remarkable differences to the behaviour on Pd(111) single-crystal surfaces. These results strongly suggest that metal clusters of different sizes and shapes provide a unique way for controlling both photochemical and thermal reactions of hydrocarbons at metal surfaces (Watanabe et al. 1999). Another application of these nanomaterials is the treatment of water. Reactivity of TiO_2 nanofibers, nanofiber composites (Au/TiO2), and P25 nanoparticles was explored toward a suite of organic micropollutants, N,N-diethyl-m-toluamide (DEET), atrazine, carbamazepine, and sulfamethoxazole, which are known to be recalcitrant to traditional treatment processes. To explore the influence of water quality on performance, particularly matrixes representative of water treatment systems, the reactivity of optimal nanofibers toward DEET was explored by Nalbandian et al. (2015) in water samples collected from the University of Iowa Water Treatment Plant (UIWTP). The UIWTP treats a surface water source (the Iowa River) with a process train of coagulation/flocculation, sedimentation, softening, chlorination, and filtration. Samples were collected after filtration (simulating photocatalytic treatment as a final polishing step for drinking water) and after sedimentation (simulating photocatalytic treatment applications in dirtier matrixes) (Nalbandian et al. 2015).

2.4 Nanoclays

Clays are layered minerals with space in between the layers where they can adsorb positive and negative ions and water molecules. Clays undergo also exchange interactions of adsorbed ions with the outside. Although clays are very useful for many applications, they have one main disadvantage, i.e. the lack of permanent porosity. To overcome this, researchers have been looking for a way to prop and support the clay layers with molecular pillars. Most of the clays can swell and thus increase the space in between their layers to accommodate the adsorbed water and ionic species. These clays were employed in the pillaring process. As stated previously, ultra-fine TiO_2 powders have large specific surface areas, but due to their easy agglomeration, an

giovanni.libralato@unina.it

adverse effect on their catalytic performance has been observed (Ding et al. 1999; Mansoori et al. 2008). The clays are a non-polluting and can be used also as a de-polluting agent, like in water and wastewater treatment, or as a pollution control agent, in waste liners and storage (Yuan et al. 2013). The nanoclays are good adsorbents of ionic or polar compounds but not of non-ionic or hydrophobic organic compounds, for example are employed to remove from water and groundwater the Diclofenac, a non-steroidal anti-inflammatory drug used in human medical care as analgesic, antiarthritic and antirheumatic compound; concerning pollutants classification, it is considered among the emerging contaminants which are chemicals recently discovered in natural streams as a result of human and industrial activities (Grassi et al. 2012). Other examples of drug adsorption are the use of bentonite to remove amoxicillina (Putra et al. 2009), montmorillonite to remove trimethoprim (Bekçi et al. 2006) and natural zeolite to remove enrofloxacin (Ötker et al. 2005).

2.5 Nanotubes

The discovery of fullerenes and carbon nanotubes has opened a new chapter in carbon chemistry. Superconducting and magnetic fullerides, atoms trapped inside the fullerene cage, chemically bonded fullerene complexes, and nanometer-scale helical carbon nanotubes are some very interestingly type of carbon based materials. The creation of the hollow carbon buck minster fullerene molecule as well as methods to produce and purify bulk quantities of it has triggered an explosive growth of research in the field. Carbon nanotubes, in particular, hold tremendous potential for applications because of their unique properties, such as high thermal and electrical conductivities, high strength, high stiffness, and special adsorption properties. Carbon nanotubes have cylindrical pores and adsorbent molecules interact with their carbon atoms on the surrounding walls. This interaction between molecules and solid surface depends on the pore size and geometry. When a molecule is placed in between two flat surfaces, i.e., in a slit-shaped pore, it interacts with both surfaces, and the potentials on the two surfaces overlap. The extent of the overlap depends on the pore size. However, for cylindrical and spherical pores, the potentials are greater because more surface atoms interact with the adsorbed molecule. In addition, carbon nanotubes are highly graphitic (much more than the activated carbons) (Mansoori et al. 2008). Hence, the carbon nanotubes can adsorb molecules much stronger than activated carbons, which have slit-shaped or wedge-shaped pores. Carbon nanotubes (CNTs) show adsorption capability and high adsorption efficiency for removal of heavy metals (Pyrzyńska and Bystrzejewski 2010). The application of carbon nanotubes for the removal of chromium (VI) from wastewater is one of the pioneer studies which have been done in environmental field (Nassereldeen et al. 2009; Muataz et al. 2009). Naghizadeh, indeed, has demonstrated that the carbon nanotubes can be considered as a promising adsorbent for the removal of arsenic from large volume of aqueous solutions (Naghizadeh et al. 2012).

giovanni.libralato@unina.it

2.6 Dendrimers and Nanosponges

Another example of environmental treatment and remediation-related application of nanomaterials includes dendritic nanoscale chelating agents for polymer-supported ultrafiltration (PSUF). Dendrimers are highly branched polymers with controlled composition and an architecture that consists of nanoscale features. In other words, dendrimers or cascade molecules have branching construction similar to a tree, in which one trunk forms several large branches; each forming smaller branches. The roots of the tree also have the same branching mode of growth. This kind of architecture characterized by fractal geometry in which dimensions are not just integers such as 2 or 3, but also fractions. These nanostructures can be designed to encapsulate metal ions and zero-valent metals, enabling them to dissolve in suitable media or bind to appropriate surfaces. Modification of any compound in these branched polymeric structures give variety of means for controlling critical macromolecular parameters such as internal and external rigidity, hydrophilicity and hydrophobicity, degrees of void, excluded volumes, and response to stimuli such as changes in solvent polarity and temperature (Mansoori et al. 2008). Because heavy metals cannot be destroyed or degraded and moreover, mineralisation (degradation) is a very slow process under natural conditions. Immobilisation and concentration of metals onto suitable sorbents seem to be a viable option for their removal from water and wastewater. The polyamidoamine (PAMAM) is a dendrimer that has a strong binding affinity for toxic heavy-metal ions in aqueous solutions. In particular the polyamidoamine dendrimers terminated with primary amine as a new class of chelating agents, which were able to bind Cu(II) ions (Diallo et al. 1999). Later on, Rether and Schuster (2003), used PAMAM dendrimers modified with *N*-benzoylthiourea for selective and recovery of heavy metals such as Co^{2+}, Cu^{2+}, Hg^{2+}, Ni^{2+}, Pb^{2+} and Zn^{2+} from wastewater. Zhang et al. (2015) have proposed a graphene oxide/polyamidoamines dendrimers (GO/PAMAMs) composites, synthesized via modifying GO with 2.0 G PAMAM for the adsorption of acid Bordeaux B (ABB), a common antibacterial agent (Zhang et al. 2015).

2.7 Micelles

Micelles are self-assembled surfactant materials in a bulk solution. Surfactants or "Surface active agents" are usually organic compounds that are amphipathic, by containing both hydrophobic (tails) and hydrophilic groups (heads). Therefore, they are typically soluble in both organic solvents and water. There are hundreds of compounds that can be used as surfactants and are usually classified by their ionic behaviour in solutions: anionic, cationic, non-ionic or amphoteric (zwitterionic). Each surfactant class has its own specific properties. A surfactant can be classified by the presence of formally charged groups in its head. There are no charge groups in a head of non-ionic surfactant. The head of an ionic surfactant carries a net

giovanni.libralato@unina.it

charge: if negative the surfactant is called anionic; if the charge is positive, it is called cationic. If a surfactant contains a head with two oppositely charged groups, it is termed zwitterionic. The concentration at which surfactants begin to self-assemble and form micelles is known as Critical Micelle Concentration or CMC. When micelles appear in the water, their tails form a core that is like an oil droplet, and their (ionic) heads form an outer shell that maintains favourable contact with water. The self-assembled surfactant is referred to as "reverse micelle" when surfactants assemble in the oil. In this case, the heads are in the core and the tails have favourable contact with oil. Surfactant-enhanced remediation techniques have shown significant potential in their application for the removal of polycyclic aromatic hydrocarbon (PAHs) pollutants in the soil. Increasing surfactant concentration in the solution has shown higher effectiveness in the extraction of NAPLs (non-aqueous phase liquids) and PAHs. At high concentrations, surfactant solutions improve the formation of pollutant emulsions that are hard to extract from the sample (Mansoori et al. 2008).

2.8 Nanomembrane and Nanosieve

A membrane is a semi-permeable and selective barrier between two phases (retentive and permeate) through which only selected chemical species may diffuse. Membrane filtration is frequently employed for the separation of dissolved solutes in a fluid or the separation of a gas mixture. Historically, membrane technology has had wide application in wastewater treatment and desalination via reverse osmosis. In this method, a pressure difference across a membrane is employed to overcome the osmotic pressure gradient. The smaller water molecules are literally pushed through the membrane while the large solute species are retained behind. This technology was used for the extraction of phenols, removal of heavy metal cations such as zinc, cadmium, chromium, copper, lead, palladium and mercury from wastewater and also for removal of alkali metal cations such as Na^+, K^+, Li^+ and Cs^+, radioactive fission products, such as Cs-137, Sr-90, Ce-139 and Eu-152 and anions, such as chlorides, sulphate, phosphate and chromate (Mansoori et al. 2008).

3 The Study of Nanomaterials Applied to the Environmental Remediation: The Role of Electron Microscopy Techniques

The nanomaterials in the environment and their potential hazardous (nanopollution) and/or beneficial (nanoremediation) properties are not yet fully understood. Ideally, for application in nanoremediation, nanomaterials are expected to feature several key properties, including high reactivity for the removal of contaminants, high

giovanni.libralato@unina.it

mobility in porous media (e.g., aquifers, soil), high reactive longevity after injection and low toxicity to the biota in the surrounding environment (Crane 2012; Grieger et al. 2015). These properties are the main drivers in designing the nanomaterials for remediation, but in practice it is very impossible to achieve all these properties simultaneously. In addition, in regard to nanowaste management, current research questions mostly focus on the fate of nanomaterials in various waste streams, and in some cases on perturbing effects of nanomaterials on waste treatment process. Concentration, elemental composition, particle size, size distribution, shape and morphology are often determined before more distinct material features, such as particle crystallinity or surface properties. In general, for nanowaste management it is necessary the monitoring of the specific parameters, reported below (Part et al. 2015):

Particle number concentration and mass concentration: this information it is important for the toxicity and in order to value the presence of this species as stemming or ions

The elemental composition: the fate and the behaviour of nanomaterials depend on the chemical element that are used for core, shell or coating.

Particle size and particle distribution are important for characterization, and for define the uptake and toxicity mechanisms.

The *shape* influence the uptake, transport and toxicity, but it's also important in order to define the aggregation capacity.

Surface properties as *charge, functionality and surface area* determine the toxicity, aggregation and the bioavailability.

Several analytical methods, grouped in microscopy electron (EM) techniques and light scattering techniques, are available to measure the particle properties. The first group includes Transmission Electron Microscopy (TEM), Scanning Electron Microscopy (SEM) and Scanning Probe Microscopy (SPM). The other one includes Dynamic Light Scattering (DLS) and Small Angle X-ray Scattering (SAXS). Many recent studies have emphasised the importance of using a multi-method approach, where the role of EM is pivotal. In the Fig. 3 are reported different EM techniques and their field of application regarding nanomaterials properties.

Microscopy techniques provide the most direct methods to characterize NMs by enabling direct visualization of size, shape and state of aggregation. Optical microscopes, whose diffraction is $\lambda/2NA$ (where λ is wavelength and NA is numerical aperture of lens which is usually 1.0), do not offer adequate spatial resolution thus they do not are able to distinctively identify two objects that are separated from few hundreds of nanometers. The electrons present a unique method of imaging at the nanoscale. If the electron can be accelerated using high voltage, energy beam is produced with a wavelength much shorter than that of light used in the optical microscope. Therefore, electron microscopes can be used to image nanoscale in great detail. These microscopes can routinely achieve magnifications in the order of 1 million and can differentiate objects that are located as close as 0.1 nm.

The role of EM in characterization of nanomaterials is already reported by us (Dini et al. 2015; Prasad et al. 2015); in this paper the distinctive technical features

giovanni.libralato@unina.it

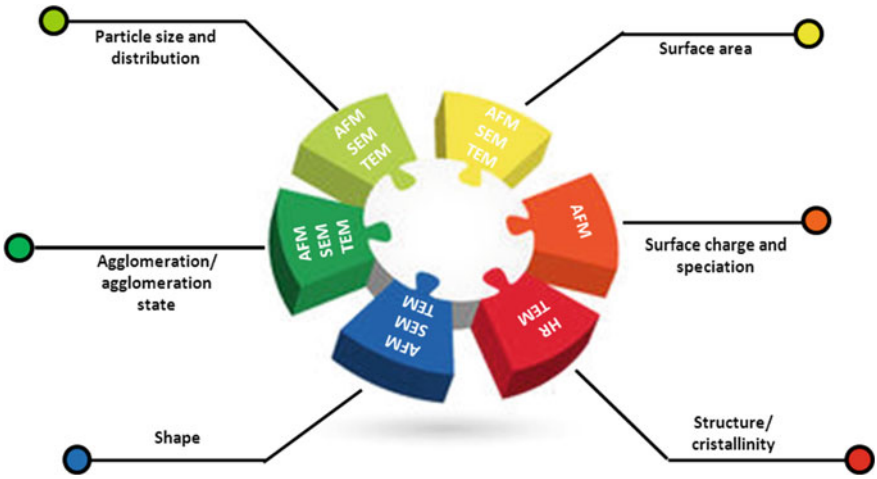

Fig. 3 Schematic representation of the tools used to analysed the nanoparticles parameters

of different electron microscopes are reported. Here we focus on the use of EM in characterizing nanomaterials involved in nanoremediation.

TEM. Transmission Electron Microscopy (TEM) is an essential characterization tool for directly imaging nanomaterials to obtain quantitative measures of particle and grain size, size distribution, and morphology. TEM can image particles beyond the diffraction limit of optical microscope and provide direct visual information about crystallinity and lattice spacing. Flawless imaging of nanoparticles using TEM depends on the contrast of the sample that strictly depends on the sample thickness (the amount of material that the electron beam must pass through) and the sample material (heavier atoms scatter more electrons and therefore have a smaller electron mean free path than lighter atoms). Thus, the samples are prepared by drying nanoparticles on a copper grid coated with a thin layer of carbon, so materials (e.g., metal nanoparticles, oxides, polymeric nanoparticles, carbon nanotubes, quantum dots, and magnetic nanoparticles) with electron densities that are significantly higher than amorphous carbon are easily imaged. So, to obtain high-quality images, with the greatest amount of contrast between the particles and the surroundings, it is necessary: thoroughly clean samples and concentrate samples.

As already known, particle size and size distribution of NMs is very important and requires monodispersion of nanoparticles solution. For particles that are bound together, the necking between particles is examined to determine if the particles were potentially individual in solution or whether the particles are sintered together. If potentially individual, the diameter of each particle is used as the measurement for the size statistics. If sintered or irregularly shaped, the particle diameter is measured at a fixed angle for all particles in the image. An alternative method of analyzing sintered or non-spherical particles is to use image analysis software to determine the cross-sectional area of the particles and convert the area to an equivalent spherical diameter.

giovanni.libralato@unina.it

Particularly in imaging nanomaterials involved in environmental remediation, the aggregation state is a key factor that depends on deposition of samples onto grid. A number of factors influence the deposition of samples onto a TEM grid, including (i) the solvent evaporation dynamics and the wetting behaviour of the solvent, (ii) electrostatic or sterical stabilization of the particles, (iii) the diffusion of the particles through the solvent during the drying process, and (iv) sample concentration. In order to reduce agglomeration on the grid to improve imaging, it is necessary to use specially functionalized grids and sample deposition techniques. For some samples, repeated cycles of sample deposition and drying on a TEM grid can increase the density of sample on the grid, however this may also lead to a loss of image quality due to an increase in the amount of organic or inorganic impurities that are also deposited from the sample. Because the properties of nanoparticles are crucial to their performance and/or the performance of products containing nanoparticles, it is very important to have a fundamental understanding of the deformation mechanisms occurring in nanoparticles, including the type and density of crystal defects participating in these deformation processes. In fact, crystal defects such as surface steps, can affect the catalytic and thermal properties of individual nanoparticles, whereas dislocations and twins can affect the mechanical properties, radiation resistance and energy release exhibited by individual nanoparticles. For example, the crystalline structure and morphology of the molybdenum disulfide and graphitic carbon nitride (MoS_2–g–C_3N_4) nanocomposites were characterized by transmission electron microcopy (TEM), high-resolution TEM (HRTEM). The TEM images display the MoS_2 nanosheet structure. By analysing the HRTEM image it was found that MoS_2 had a layered structure with a interlayer space of 0.645 nm, which could be assigned to the (002) plane. TEM analysis clearly shows that MoS_2 nanoparticles are well dispersed and wrapped by the layered g–C_3N_4, which causes the overlap of crystalline lattice. From the HRTEM images of 1.5 wt%MoS_2–g–C_3N_4 composites, it is possible to clearly observe the interface of hetero-structure (Wen et al. 2016).

Due to their low cost, highly reactive surface sites and high in situ reactivity, the most widely studied nanoparticles for environmental remediation are nanoscale zero-valent iron (nZVI) (Wang et al. 1997; Elliott et al. 2001; Zhang et al. 2003). Due to its ability to directly image nanoscale materials, TEM is a powerful tool to study nZVI. TEM measures the hard particle limits defined by the iron components. On the other hand, inorganic surface layer can also be examined, and this may be very useful to examine core-shell structures of nZVI such as oxide minerals or Pd used for enhancing stability or catalytic reactivity of nZVI in the environment. Other modes of TEM can be applied in studying of nZVI. Dark-field imaging allows to discriminate individual particles within nZVI agglomerates linked by oxide layers (Yan et al. 2010a, 2012) or internal grain structures of nZVI (Nurmi et al. 2005). By using X-ray energy dispersive spectroscopy (XEDS) semi-quantitative information about the elemental composition of nZVI can be achieved; also, STEM-XEDS assess the spatial distribution of bimetallic nZVI, their reactions mechanism and effectiveness in remediation at nanoscopic level (Yan et al. 2010a, b).

giovanni.libralato@unina.it

In general, sample preparation is one of the challenging aspects of TEM analysis and in the case of nZVI this is very pivotal due to the high reactivity of nZVI with oxygen under normal atmospheric conditions. Moreover, magnetic properties of nZVI complicate this. There is need to prepare sample in anaerobic chambers or vacuum desiccators to avoid contact with oxygen rich atmospheres and to immobilise nZVI onto carbon-coated grids with a functionalised polymer (e.g., poly-L-lysine).

SEM. The scanning electron microscope (SEM) allows to analyse various signals upon the interaction of the electron beam with the sample. The processing of these signals produce a wide range of information not only morphological, but also compositional and structural concerning related at the sample. SEM can provide information of shape and size of particles three dimensional information on surfaces features and texture, crystalline and amorphous structures, and elemental composition. The shape and the size of that volume depends on the characteristics of the incident beam and the composition of the sample and, in many cases, are more extensive in the diameter of the beam thus causing the resolution limit. SEM has been used in examining nZVI in terms of aggregation state, surface morphology (Kanel et al. 2005, 2006) and spatial distribution of nZVI on solid substrates (Üzüm et al. 2009; Wu et al. 2013; Bezbaruah et al. 2009). XEDS may be coupled to SEM analysis to achieve qualitative element/composition identification. The limit of SEM technique correlates with the oxide layer thickness, thus SEM requires a thick oxide layer on ZVI microparticles (Chekli et al. 2000).

ESEM. Electron and atomic force microscopy (EM and AFM) have proven to be powerful tools for the imaging and characterisation of nanoparticles. The conventional application of nanomaterials for environmental samples, e.g. nanoparticles in natural waters, is, however, still a challenge (Tiede et al. 2009). For example, in scanning and transmission electron microscopy (SEM, TEM), due to the vacuum conditions in the sample chamber, sample preparation such as coating, drying, staining, freezing and embedding is essential and therefore only perturbed samples can be imaged. This can lead to imaging artefacts. Environmental SEM (ESEM) is a possibility to overcome the vacuum conditions in the SEM sample chamber and allows imaging of hydrated samples (Bogner et al. 2005). ESEM provides spatial resolutions of 10 nm or less. Compared to SEM, ESEM produces different, perhaps complementary, information for biological specimens (Doucet et al. 2005). Cell structures are visible with SEM, but external polymers around cells are more apparent in ESEM (Callow et al. 2003; Doucet et al. 2005; Douglas and Douglas 2001). The balance of gas flows into and out of the ESEM sample chamber determines its pressure. The multiple apertures are situated below the objective lens and separate the sample chamber from the column. This feature allows the column to remain at high vacuum while the specimen chamber may sustain pressures as high as 50 Torr. The temperature and humidity of the sample can also be manually controlled to provide a suitable environment for maintaining the biological samples in their natural state. The relative humidity in an ESEM specimen chamber can be controlled (Stokes and Donald 2000), so ESEM is particularly useful for hydrated materials (Stokes and Donald 2000; Stokes 2001). A gaseous secondary electron

giovanni.libralato@unina.it

detector (GSED) exploits the gas in the specimen chamber for signal amplification. BSED operation produces positive ions that have the added benefit of limiting charging of non-conductive specimens (Stokes and Donald 2000).

The study of biofilm needs the use of ESEM in wet or partially hydrated states in order to analysis the sample without the formation of damages and changes in specimen morphology. This gave the possibility to the visualization of biofilm surfaces in their natural wet anaerobic state (Darkin et al. 2001). Recently, Schwartz et al. (2009) used ESEM imaging to obtain information about the bacterial composition, matrix composition, and spatial biofilm structures of natural biofilms grown on filter materials at waterworks. It does not require prior fixing and staining of the biofilm, minimizes biofilm dehydration and thus preserves native morphologies including surface structures (Walker et al. 2001) and native morphologies of bacteria and biofilms (e.g., Priester et al. 2007) and it is able to achieve high magnifications, comparable with SEM. Shrinkage is prevented and artefact formation is reduced.

SPM. Scanning Probe Microscopy (SPM), including atomic force microscopy (AFM), scanning tunnelling microscopy (STM) scanning near-field optical microscopy (SNOM or NSOM), is a technique that utilises a sharp tip (the probe) to scan over the surface of a sample. The application of SPM in nanomaterials exploited in nanoremediation involves the use of AFM in characterization of particle height, morphology, aggregation state and distribution of nZVI (Kiruba et al. 2012; Lin et al. 2008; Qiu et al. 2016). Since AFM analysis can be conducted under a wide range of controlled conditions, such as vacuum, liquid or moist conditions, etc., it is possible to minimize sample damage and oxidation representing a very advantageous tool in nZVI characterization.

STM can be used in the presence of conductive samples in imaging the topography at atomic resolution by exploiting the tunnelling current generated an electrically biased sharp tip and the sample surface. Qiu and coworkers used STM to study the change in surface profiles after reaction in aqueous solution of iron surface with Cr(III) and Se(IV) causing the smoothed out of roughness (protrusions) on the surface (Qiu et al. 2016).

4 Conclusions

Cleaning up the environment from various sources of pollution is imperative not only to protect the ecological health but also for the general public health. Unfortunately, many environment resources such as groundwater are precious one and are continuously threatened by various natural and human-made contaminants. Recent study demonstrated the presence of millions polluted sites in Europe, of which approximately 350,000 sites constitute a potential risk to humans or to the environment. Environmental remediation use various methods to remove and/or break-down contaminants in polluted soils, surface waters, groundwater, as well as in sediments. In recent years, the use of ENMs have gained increased amounts of

giovanni.libralato@unina.it

attention as potential remediation techniques, often cited as an attractive, cost-effective alternative to conventional approaches. To date, it is estimated that there are between 45 and 70 sites around the world that have used nanoremediation techniques either at pilot or full study scales (Karn et al. 2009; Bardos et al. 2014; PEN 2015). ENMs are also being developed for other environmentally-related activities, such as the use of absorbent nanowires for oil spills, anti-fouling, nanomaterials for desalination processes using reverse osmosis, as well as photocatalytic nanomaterials that can be used for disinfection or decontamination of drinking waters. At the same time, however, there are a number of concerns with the use of engineered nanomaterials for remediation. For instance, nanoremediation is largely untested, particularly at field scale. This raises questions on not only the real-world efficacy at large-scale field sites polluted with different kinds of contaminates but also in terms of the behaviour of these nanomaterials in different types of environments which vary in temperature, hydrogeology, and sub-surface conditions like pH and soil porosity. In order to answer at these questions it's necessary known the physician-chemical properties of nanomaterials, such as particle size, surface chemistry and bulk composition. For this purpose to ensure efficient remediation, it is crucial to accurately assess and understand the implications of these properties before deploying these materials into contaminated environments. Many analytical techniques are now available to determine these parameters, such as electron microscopy and light scattering for determination of particle size, size distribution and aggregate state, and X-ray techniques for the characterisation of surface chemistry and bulk composition.

References

Bardos P, Bone B, Daly P, Elliott D, Jones S, Lowry G, Merly C (2014) A risk/benefit appraisal for the application of nano-scale zero valent iron (nZVI) for the remediation of contaminated sites. WP9 NanoRem

Battin TJ, VonDerKammer F, Weilhartner A, Ottofuelling S, Hofmann T (2009) Nanostructured TiO_2: transport behaviour and effects on aquatic microbial communities under environmental conditions. Environ Sci Technol 43:8098–8104. doi:10.1021/es9017046

Bekçi Z, Seki Y, Yurdakoç MK (2006) Equilibrium studies for trimethoprim adsorption on montmorillonite KSF. J Hazard Mater B133:233–242

Bennett P, He F, Zhao D, Aiken B, Feldman L (2010) In situ testing of metallic iron nanoparticle mobility and reactivity in a shallow granular aquifer. J Contam Hydrol 116:35–46

Berry D, Xi C, Raskin L (2006) Microbial ecology of drinking water distribution systems. Curr Opin Biotechnol 17:297–302. doi:10.1016/j.copbio. 7 May 2006

Bezbaruah AN, Krajangpan S, Chisholm BJ, Khan E, Bermudez JJE (2009) Entrapment of iron nanoparticles in calcium alginate beads for groundwater remediation applications. J Hazard Mater 166:1339–1343

Bogner A, Thollet G, Basset D, Jouneau PH, Gauthier C (2005) Wet STEM: a new development in environmental SEM for imaging nano-objects included in a liquid phase. Ultramicroscopy 104 (3–4):290–301

giovanni.libralato@unina.it

Callow JA, Osborne MP, Callow ME, Baker F, Donald AM (2003) Use of environmental scanning electron microscopy to image the spore adhesive of the marine alga Enteromorpha in its natural hydrated state. Colloids Surf B Biointerfaces 27(4):315–321

Chekli L, Bayatsarmadi B, Sekine R, Sarkar B, Shen AM, Scheckel KG, Skinner W, Naidu R, Shon Lombi HK, Donner E (2000) Analytical characterisation of nanoscale zero-valent iron: a methodological review. Langmuir 16:2230–2236

Crane RA, Scott TB (2012) Nanoscale zero-valent iron: future prospects for an emerging water treatment technology. J Hazard Mater 211–212:112–125

Daniel SCGK, Vinothini G, Subramanian N, Nehru K, Sivakumar M (2012) Biosynthesis of Cu, ZVI, and Ag nanoparticles using Dodonaea viscosa extract for antibacterial activity against human pathogens. J Nanopart Res 15:1–10

Darkin MG, Gilpin C, Williams JB, Sangha CM (2001) Direct wet surface imaging of an anaerobic biofilm by environmental scanning electron microscopy: application to landfill clay liner barriers. Scanning 23(5):346–350

Decho AW (2000) Exopolymer-mediated microdomains as a structuring agent for microbial activities. In: Riding R (ed) Microbial sediments. Springer, Berlin, pp 9–15

Diallo MS, Balogh L, Shafagati A, Johnson JH, Goddard WAI, Tomalia DA (1999) Poly (amidoamine) dendrimers: a new class of high capacity chelating agents for Cu(II) ions. Environ Sci Technol 33(1999):820–824

Ding Z, Zhu HY, Lu GQ et al (1999) Photocatalytic properties of titania pillared clays by different drying methods. J Colloid Inter Sci 209:193–199

Dini L, Panzarini E, Mariano S, Passeri D, Reggente M, Rossi M, Vergallo C (2015) Microscopies at the nanoscale for nano-scale drug delivery systems. Curr Drug Targets 16(13):1512–1530

Doucet FJ, Lead JR, Maguire L, Achterberg EP, Millward GE (2005) Visualisation of natural aquatic colloids and particles—a comparison of conventional high vacuum and environmental scanning electron microscopy. J Environ Monit 7(2):115–121

Douglas S, Douglas DD (2001) Structural and geomicrobiological characteristics of a microbial community from a cold sulfide spring. Geomicrobiol J 18(4):401–422

El Abed S, Ibnsouda SK, Latrache H, Hamadi F (2012) Scanning electron microscopy (SEM) and environmental SEM: suitable tools for study of adhesion stage and biofilm formation

Elliott DW, Zhang WX (2001) Field assessment of nanoscale bimetallic particles for groundwater treatment. Environ Sci Technol 35(24):4922–4926

Farré M, Sanchís J, Barcelo D (2011) Analysis and assessment of the occurrence, the fate and the behavior of nanomaterials in the environment. Trends Anal Chem 30(3)

Ferry JL, Craig P, Hexel C, Sisco P, Frey R, Pennington PL et al (2009) Transfer of gold nanoparticles from the water column to the estuarine food web. Nat Nanotechnol 4:441–444. doi:10.1038/nnano.2009.157

Flemming H-C, Wingender J (2010) The biofilm matrix. Nat Rev Microbiol 8:623–633. doi:10.1038/nrmicro2415

Fu F, Dionysiou DD, Liu H (2014) The use of zero-valent iron for groundwater remediation and wastewater treatment: a review. J Hazard Mater 267:194–205

Grassi M, Kaikioglu G, Belgiorno V, Lofrano G (2012) Removal of emerging contaminants from water and wastewater by adsorption process. In: Green chemistry for sustainability

Grieger KD, Hjorth R, Rice J, Kumar N, Bang J (2015) Nano-remediation: tiny particles cleaning up big environmental problems. Blog entry for IUCN

Hawari AH, Mulligan CN (2006) Biosorption of lead(II), cadmium(II), copper(II) and nickel(II) by anaerobic granular biomass. Bioresour Technol 97:692–700. doi:10.1016/j.biortech.2005.03.033

Hochella MF Jr, Madden AS (2005) Earth's nano-compartment for toxic metals. Elements 1:199–203

Hu Z, Hidalgo G, Houston PL, Hay AG, Shuler ML, Abruna HD et al (2005) Determination of spatial distributions of zinc and active biomass in microbial biofilms by two-photon laser scanning microscopy. Appl Environ Microbiol 71:4014–4021. doi:10.1128/AEM.71.7.4014-4021.2005

giovanni.libralato@unina.it

Huang YY, Liu F, Li HD (2009) Degradation of tetrachloromethane and tetrachloroethene by Ni/Fe bimetallic nanoparticles. J Phys Conf Ser 188:012014

Ikuma K, Madden AS, Decho AW, Lau BLT (2014) Deposition of nanoparticles onto polysaccharide-coated surfaces: implications for nanoparticle–biofilm interactions. Environ Sci Nano 1:117–122. doi:10.1039/c3en00075c

Ikuma K, Decho AW, Lau BLT (2015) When nanoparticles meet biofilms—interactions guiding the environmental fate and accumulation of nanoparticles. Front Microbiol 6. doi:10.3389/fmicb.2015.00591

Jaisi DP, Saleh NB, Blake RE, Elimelech M (2008) Transport of single-walled carbon nanotubes in porous media: filtration mechanisms and reversibility. Environ Sci Technol 42:8317–8323. doi:10.1021/es801641v

Kanel SR, Manning B, Charlet L, Choi H (2005) Removal of arsenic(III) from groundwater by nanoscale zero-valent iron. Environ Sci Technol 39(5):1291–1298

Kanel SR, Greneche JM, Choi H (2006) Arsenic(V) removal from groundwater using nano scale zero-valent iron as a colloidal reactive barrier material. Environ Sci Technol 40(6):2045–2050

Karn B, Kuiken T, Otto M (2009) Nanotechnology and in situ remediation: a review of the benefits and potential risks. Environ Health Perspect 117(12):1813–1831

Klaine SJ, Alvarez PJJ, Batley GE, Fernandes TF, Handy RD, Lion DY, Mahendra S, McLaughlin MJ, Lead JR (2008) Nanomaterials in the environment: behaviour, fate, bioavailability, and effects. Environ Toxicol Chem 27(9):1825–1851

Kroll A, Behra R, Kaegi R, Sigg L (2014) Extracellular polymeric substances (EPS) of fresh water biofilms stabilize and modify CeO_2 and Ag nanoparticles. PLoS One 9:e110709. doi:10.1371/journal.pone.0110709

Labrenz M, Banfield JF (2004) Sulfate-reducing bacteria-dominated biofilms that precipitate ZnS in a subsurface circumneutral-pH mine drainage system. Microb Ecol 47:205–217. doi:10.1007/s00248-003-1025-8

Labrenz M, Druschel GK, Thomsen-Ebert T, Gilbert B, Welch SA, Kemner KM et al (2000) Formation of sphalerite (ZnS)deposits in natural biofilms of sulfate-reducing bacteria. Science 290:1744–1747. doi:10.1126/science.290.5497.1744

Lecoanet HF, Wiesner MR (2004) Velocity effects on fullerene and oxide nanoparticle deposition in porous media. Environ Sci Technol 38:4377–4382. doi:10.1021/es035354f

Lehtola MJ, Miettinen IT, Keinanen MM, Kekki TK, Laine O, Hirvonen A et al (2004) Microbiology, chemistry and biofilm development in a pilot drinking water distribution system with copper and plastic pipes. Water Res 38:3769–3779. doi:10.1016/j.watres.2004.06.024

Lin Y-T, Weng C-H, Chen F-Y (2008) Effective removal of AB24 dye by nano/micro-size zero-valent iron. Sep Purif Technol 64:26–30

Liu YQ, Majetich SA, Tilton RD, Sholl DS, Lowry GV (2005) TCE dechlorination rates, pathways and efficiency of nanoscale iron particles with different properties. Environ Sci Technol 39(1338):1345

Mansoori GA, Bastami TR, Ahmadpour A, Eshaghi Z (2008) Environmental application of nanotechnology In: Annual review of nano research (Chapter 2), vol 2

Muataz AA, Fettouhi M, Al-Mammum A, Yahya N (2009) Lead removal by using carbon nanotubes. Int J Nanopart 2:329–338

Mueller NC, Nowack B (2010) Nanoparticles for remediation: solving big problems with little particles, Elements 6:395–400. doi:10.2113/gselements.6.6.395 (1811-5209/10/0006-0395$2.50)

Naghizadeh A, Yari AR, Tashauoei HR, Mahdavi M, Derakhshani E, Rahimi R, Bahmani P (2012) Carbon nanotubes technology for removal of arsenic from water. Arch Hyg Sci 1(1):6–11

Nalbandian MJ, Greenstein KE, Shuai D, Zhang M, Choa Y, Parkin GF, Myung NV, Cwiertny DM (2015) Synthesis of photoactive TiO_2 nanofibers and Au/TiO_2 nanofiber composites: structure and reactivity optimization for water treatment applications. Environ Sci Technol 49:1654–1663. doi:10.1021/es502963t

giovanni.libralato@unina.it

Narayana RL, Matheswaran M, Abd Aziz A, Saravanan P (2011) Photocatalytic decolourization of basic green dye by pure and Fe, Co doped TiO_2 under daylight illumination. Desalination 269 (2011):249–253

Nassereldeen AK, Muataz AA, Abdullah A, Mohamed ES, Alam MD, Yahya N (2009) Kinetic adsorption of application of carbon nanotubes for Pb(II) removal from aqueous solution. J Environ Sci 21:539–544

Nevius BA, Chen YP, Ferry JL, Decho AW (2012) Surface-functionalization effects on uptake of fluorescent polystyrene nanoparticles by model biofilms. Ecotoxicology 21:2205–2213. doi:10.1007/s10646-012-0975-3

Nurmi JT, Tratnyek PG, Sarathy V, Baer DR, Amonette JE, Pecher K, Wang C, Linehan JC, Matson DW, Penn RL, Driessen MD (2005) Characterization and properties of metallic iron nanoparticles: spectroscopy, electrochemistry, and kinetics. Environ Sci Technol 39(5):1221–1230

Nutt MO, Hughes JB, Wong MS (2005) Designing Pd-on-Au bimetallic nanoparticle catalysts for trichloroethene hydrodechlorination. Environ Sci Technol 39:1346–1353

Ötker HM, Akmehmet-Balcioğlu I (2005) Adsorption and degradation of enrofloxacin, a veterinary antibiotic on natural zeolite. J Hazard Mater 122:251–258

Part F, Zecha G, Cuson T, Sinner E-K, Huber-Humer M (2015) Current limitations and challenge in nanowaste detection, characterisation and monitoring. Waste Manag 43:407–420

PEN (2015) The project on emerging nanotechnologies. In: Nanoremediation map. Available: http://www.nanotechproject.org/inventories/remediation_map/

Phenrat T, Kim HJ, Fagerlund F, Illagasekare T, Tilton RD, Lowry GV (2009) Particle size distribution, concentration, and magnetic attraction affect transport of polymer-modified FeO nanoparticles in sand columns. Environ Sci Technol 43:5079–5085. doi:10.1021/es900171v

Ponder SMD, Darab JG, Mallouk TE (2001) Remediation of Cr(VI) and Pb(II) aqueous solutions using supported, nanoscale zerovalent iron. Environ Sci Technol 34(12):2564–2569

Prasad A, Leada JR, Baalousha M (2015) An electron microscopy based method for the detection and quantification of nanomaterial number concentration in environmentally relevant media. Sci Total Environ 537:479–486

Priester JH, Horst AM, Van De Werfhorst LC, Saleta JL, Mertes LAK, Holden PA (2007) Enhanced visualization of microbial biofilms by staining and environmental scanning electron microscopy. J Microbiol Methods 68(2):577–587

Putra EK, Pranowo R, Sunarso J, Indraswati N, Ismadji S (2009) Performance of activated carbon and bentonite for adsorption of amoxicillin from wastewater: mechanisms, isotherms and kinetics. Water Res 43:2419–2430

Pyrzyńska K, Bystrzejewski M (2010) Comparative study of heavy metal ions sorption onto activated carbon, carbon nanotubes, and carbon-encapsulated magnetic nanoparticles. Colloids Surf A Physicochem Eng Aspects 362(1–3):102–109

Qiu SR, Lai HF, Roberson MJ, Hunt ML, Amrhein C, Giancarlo LC, Flynn GW, Yarmoff JA (2016) Removal of contaminants from aqueous solution by reaction with iron surfaces. Anal Chim Acta 903:13–35. doi:10.1016/j.aca.2015.10.040 Epub 2015 Nov 6

Quinn J, Clausen C, Brooks K, Coon C, O'Hara S, Krug T, Major D, Yoon WS, Gavaskar A, Holdsworth T (2005) Field demonstration of DNAPL dehalogenation using emulsified zerovalent iron. Environ Sci Technol (39)

Reith F, Rogers SL, Mcphail DC, Webb D (2006) Biomineralization of gold: biofilms on bacterioform gold. Science 313:233–236. doi:10.1126/science.1125878 (Res 5:323–332)

Reith F, Fairbrother L, Nolze G, Wilhelmi O, Clode PL, Gregg A et al (2010) Nanoparticle factories: biofilms hold the key to gold dispersion and nugget formation. Geology 38:843–846. doi:10.1130/G31052.1

Rether A, Schuster M (2003) Selective separation and recovery of heavy metal ions using water-soluble *N*-benzoylthiourea modified PAMAM polymers. React Funct Polym 57 (2003):13–21

giovanni.libralato@unina.it

Rezaei M, Salem S (2016) Photocatalytic activity enhancement of anatase–graphene nanocomposite for methylene removal: degradation and kinetics Spectrochim Acta Part A Mol Biomol Spectrosc 167:41–49. 5 Oct 2016

Rickerby D, Morrison M (2007) Report from the workshop on nanotechnologies for environmental remediation, JRC Ispra. Available at www.nanowerk.com/nanotechnology/reports/reportpdf/report101.pdf

Saggioro EM, Oliveira AS, Pavesi T, Maia CG, Ferreira LFV, Moreira JC (2011) Use of titanium dioxide photocatalysis on the remediation of model textile wastewaters containing azo dyes. Molecules 16: 10370–10386. doi:10.3390/molecules161210370

Schlekat CE, Decho AW, Chandler GT (1998) Sorption of cadmium to bacterial extracellular polymeric sediment coatings under estuarine conditions. Environ Toxicol Chem 17:1867–1874. doi:10.1002/etc.5620170930

Schrick B, Blough JL, Jones AD, Mallouk TE (2002) Hydrodechlorination of trichloroethylene to hydrocarbons using bimetallic nickel-iron nanoparticles. Chem Mater 14(12):5140–5147

Schwartz T, Jungfer C, Heißler S, Friedrich F, Faubel W, Obst U (2009) Combined use of molecular biology taxonomy, Raman spectrometry, and ESEM imaging to study natural biofilms grown on filter materials at waterworks. Chemosphere 77(2):249–257

Sharma VK, Filip J, Zboril R, Varma RS (2015) Natural inorganic nanoparticles formation, fate, and toxicity in the environment. Chem Soc Rev 44:8410–8423

Stokes DJ (2001) Characterization if soft condensed matter and delicate materials using environmental scanning electron microscopy (ESEM). Adv Eng Mater 3(3):126–130

Stokes DJ, Donald AM (2000) In situ mechanical testing of dry and hydrated breadcrumb in the environmental scanning electron microscope (ESEM). J Mater Sci 35(3):599–607

Tiede K, Tear SP, David H, Boxall AB (2009) Imaging of engineered nanoparticles and their aggregates under fully liquid conditions in environmental matrices. Water Res 43(13):3335–3343. doi:10.1016/j.watres.2009.04.045

Üzüm C, Shahwan T, Eroğlu AE, Hallam KR, Scott TB, Lieberwirth I (2009) Synthesis and characterization of kaolinite-supported zero-valent iron nanoparticles and their application for the removal of aqueous Cu2+ and Co2+ ions. Appl Clay Sci 43:172–181

Walker JT, Verran J, Boyd RD, Percival S (2001) Microscopy methods to investigate structure of potable water biofilms. Methods Enzymol 337(2001):243–255

Wang C-B, Zhang W (1997) Synthesizing nanoscale iron particles for rapid and complete dechlorination of TCE and PCBs. Environ Sci Technol 31(7):2154–2156

Watanabe K, Matsumoto Y, Kampling M, Al-Shamery K, Freund HJ (1999) Photochemistry of methane on Pd/Al_2O_3 model catalysts: control of photochemistry on transition metal surfaces. Angew Chem Int Ed 38(15)

Wen MQ, Xiong T, Zang ZG, Wei W, Tang XT, Dong F (2016) Synthesis of MoS_2/g-C_3N_4 nanocomposites with enhanced visible-light photocatalytic activity for the removal of nitric oxide (NO). Opt Express 24(10):10205–10212. doi:10.1364/OE.24.010205

Wu X, Yang Q, Xu D, Zhong Y, Luo K, Li X, Chen H, Zeng G (2013) Simultaneous adsorption/reduction of bromate by nanoscale zerovalent iron supported on modified activated carbon. Ind Eng Chem Res 52:12574–12581

Wuertz S, Muller E, Spaeth R, Pfleiderer P, Flemming H-C (2000) Detection of heavy metals in bacterial biofilms and microbial flocs with the fluorescent complexing agent Newport Green. J Ind Microbiol Biotechnol 24:116–123. doi:10.1038/sj.jim.2900784

Yan W, Herzing AA, Kiely CJ, Zhang WX (2010a) Nanoscale zero-valent iron (nZVI): aspects of the core-shell structure and reactions with inorganic species in water. J Contam Hydrol 118(3–4):96–104

Yan W, Herzing AA, Li XQ, Kiely CJ, Zhang WX (2010b) Structural evolution of Pd-doped nanoscale zero-valent iron (nZVI) in aqueous media and implications for particle aging and reactivity. Environ Sci Technol 44(11):4288–4294

Yan W, Vasic R, Frenkel AI, Koel BE (2012) Intraparticle reduction of arsenite (As(III)) by nanoscale zerovalent iron (nZVI) investigated with in situ x-ray absorption spectroscopy. Environ Sci Technol 46(13):7018–7026

giovanni.libralato@unina.it

Yuan GD, Theng BKG, Churchman GJ, Gates WP (2013) Clays and clay minerals for pollution control. In: Developments in clay science (Chapter 5), vol 5A. p 587

Yunus IS, Harwin, Kurniawan A, Adityawarman D, Indarto A (2012) Nanotechnologies in water and air pollution treatment. Environ Technol Rev 1(1):136–148

Zhang WX (2003) Nanoscale iron particles for environmental remediation: an overview. J Nanopart Res 5:323–332

Zhang F, He S, Zhang C, Peng Z (2015) Adsorption kinetics and thermodynamics of acid Bordeaux B from aqueous solution by graphene oxide/PAMAMs. Water Sci Technol 72 (7):1217–1225. doi:10.2166/wst.2015.328

giovanni.libralato@unina.it

Adsorption and Desorption Properties of Carbon Nanomaterials, the Potential for Water Treatments and Associated Risks

Marinella Farré, Josep Sanchís and Damià Barceló

Abstract The water technologies based on the physicochemical adsorption are methods extensively used because are fast, efficient, and cost effective. In this regard, the adsorption capabilities of carbonaceous materials have been widely exploited. From the activated carbon, fullerenes, carbon nanotubes (CNTs) to the latest graphene-based materials are highly efficient for contaminant removal from aqueous solution because of their large specific surface area, porosity, and reactivity, in particular, in the case of carbon nanomaterials (CNMs). In this chapter, the adsorption properties and mechanisms of CNMs are revised. The recent developments for contaminants removal from aqueous systems are provided, the most relevant works discussed, and the development tendency of adsorbents are analysed in detail. However the potential of CNMs as emerging environmental contaminants should be as well deemed. Therefore, the methods to minimize the impact of the use of these new materials in waters technology are account and, the studies on the environmental occurrence, fate and behaviour of CNMs as emerging contaminants will be presented. To conclude, the potential associated risks of CNMs as environmental contaminants is considered, with particular attention to their influence on the toxicity modulation of co-contaminants in the same compartments.

Keywords Adsorption · Water treatments · Carbon nanomaterials · Fullerenes · CNTs · MWCNTs · SWCNTs · Graphene · Toxicity · Trojan-Horse effects

M. Farré (✉) · J. Sanchís · D. Barceló
Institute of Environmental Assessment and Water Research (IDAEA-CSIC),
C/Jordi Girona, 18-26 Barcelona, Catalonia, Spain
e-mail: mfuqam@cid.csic.es

D. Barceló
Catalan Institute of Water Research (ICRA),
C/Emili Grahit, 101 Girona, Catalonia, Spain

© Springer International Publishing AG 2017

G. Lofrano et al. (eds.), *Nanotechnologies for Environmental Remediation*,
DOI 10.1007/978-3-319-53162-5_5

giovanni.libralato@unina.it

1 Introduction

The different molecular configurations that pure carbon can take are known as carbon allotropes. During the last decades, several new carbon allotropes at the nano-scale have been discovered and are under the classification of carbon nanomaterials (CNMs).

CNMs present different dimensionalities including zero-dimensional (0-D) systems, such as fullerenes, nanohorns, nanodiamonds and nanotoroids among others, one-dimensional (1D) systems such as single- and multiwalled carbon nanotubes, and nanoribbons. Two-dimensional (2D) structures such as Haeckelites, graphene and graphene-like structures as super-graphene. Three-dimensional (3D) systems such as Schwarzite-like structures. Several of these NMs have been created by nanotechnology, but some others are also of natural origin and may have been in the environment for millions of years. For example, fullerenes have been detected in geological deposits from the Cretaceous-Tertiary boundary (Becker et al. 1994), and CNTs were found in ice cores dated as being about 10,000 years old (Murr et al. 2004a). Also, natural processes such as volcanoes or forest fires can also produce pristine fullerenes and CNTs. On the other hand, these species have also been found to be incidentally produced by industrial combustion processes, and engines (Pérez et al. 2009a).

Since the discovery of C_{60} fullerene by Kroto et al. (1985), due to their unique mechanical, chemical and physical properties, CNMs have attracted interest in many fields of application such as new materials, sorbents, energy storage, sensors, drug delivery, field-emission devices, microelectronics and wastewater treatment technologies.

Fullerenes are molecules composed entirely of carbon, which take the form of a hollow sphere or ellipsoid. Fullerenes exhibit positive Gaussian curvature due to the presence of pentagonal carbon rings. In general, carbon nanostructures with non-hexagonal rings modifies the Gaussian curvature of the structure, creating unexpected properties exactly where the defects are located. For example, by enhancing their adsorption properties.

During the 1990s gave rise to the synthesis of cylindrical fullerene derivatives, the carbon nanotubes (CNTs), which can be single walled (SWCNTs) or multi-walled (MWCNTs) with concentric cylinders up to 5–40 nm in diameter. MWCNTs are composed of concentric cylindrical shells coaxially arranged around a central hollow area with spacing between the layers, while SWCNTs are made of a single cylinder sheet held together by van der Waals bonds (Balasubramanian and Burghard 2005). Currently, the syntheses for their mass production are the electric arc discharge (Journet et al. 1997), laser ablation (Guo et al. 1995) and chemical vapour decomposition (CVD) (Dai et al. 1996). These structures have excellent thermal and electrical conductivities. Because of their inherent hydrophobicity, a lot of research has been devoted to modifying the surface properties of CNTs to improve the stability of their aqueous suspensions. The main current uses of these materials are in microelectronics, catalysis, battery and fuel cell electrodes,

giovanni.libralato@unina.it

super-capacitors, conductive coatings, water-purification systems, plastics, orthopaedic implants, adhesives, and keeps gaining interest looking for other new applications.

Nanodiamonds constitute another group of CNMs that present active surface and a diamond-like hardness has wear resistance to corrosion. They can be produced with angstrom finishes of polished surfaces that can be very useful for some applications and excellent optical properties (Mochalin et al. 2012). Carbon-based nano-diamonds are soluble in water and have excellent biocompatibility, and they have been used as light beacons for chemotherapy (Sotoma et al. 2015). While nanodiamonds are produced by compression of graphite, by compression of fullerene nanoroads are produced showing to be the hardest and least compressible known material. Besides, nanoroads are wide band gap semiconductors that exhibit a high negative electron affinity, chemical inertness, high Young's modulus, and room-temperature thermal conductivity (Yu et al. 2014). These materials have been the starting point for different nano-composite materials with applications in photocatalysis (Li et al. 2012a).

Graphene is one of the newest CNMs. It is composed of a single atomic layer of carbon atoms bound in a hexagonal network. Since its first isolation in 2004, it has grabbed the attention of the research community, since graphene is approximately 200 times stronger than structural steel and highly conductive, making it ideal for high-speed electronics and photonics. Therefore, it is a candidate to replace semiconductor chips. Graphene transistors can potentially run at faster speeds and cope with higher temperatures.

CNMs exhibit different electronic properties according to their configuration. For example, SWCNTs could show character either metallic or a semiconductor depending, on the way they are rolled up (Dresselhaus et al. 1992). In particular, nanotubes with armchair chirality have metallic properties, whereas zigzag tubes present semiconductor behaviour. By unzipping a carbon nanotube, or graphene can be redistributed exhibiting semiconductor or metallic properties.

The chemical activity of CNMs can be correlated to their morphology, thus with their Gaussian curvature and carbon bond hybridization (sp, sp^2, or sp^3). In this context, there are novel carbon nanostructures that exhibit different types of Gaussian curvature displaying a particular chemical activity. A selective surface modification will directly correlate with changes in their chemical, electrical, and magnetic properties. The addition of doping atoms, the generation of defects, or functionalization, results in the modification of CNMs changing their ability of interact with the surrounding environment dramatically. Doping is a technique to tune the electronic and chemical properties of CNMs (Leary and Westwood 2011; Pinzón et al. 2012). Defect generation such as the introduction of non-hexagonal carbon rings constitutes another approach to alter these properties. Also, the chemical functionalization of the surface of CNMs with carboxylic and amine groups, polymers and biomolecules is another manner to enhance adsorption or to change the electronic properties.

One of the main general characteristics of CNMs is their absorption capability due to their high specific surface area. For this reason, these materials have great

giovanni.libralato@unina.it

potential for more efficient, and faster decontamination processes for both organic and inorganic pollutants. However, in spite of the promising results obtained using technologies based on CNMs their potential environmental impact should also be considered. Nowadays the emissions of CNMs to the environment have not been well established yet, and also their occurrence, fate, behaviour and toxicity are not well understood. Therefore, CNMs constituted an emerging risk that should be assessed to assure their sustainable development and use.

In this chapter, the primary mechanisms of adsorption of CNMs will be reviewed as well as their potential use in advanced wastewater treatments. In contrast with their occurrence and sources in the environment. The potential risks associated to CNMs in the environment will be considered, with particular emphasis on their potential ability to modulate the toxicity of co-contaminants present in the same environmental compartment.

2 Adsorption Capability of Carbon Nanomaterials and Removal of Contaminants

The interactions between organic and inorganic compounds with CNMs can be classified on:

- Chemisorption: Strong interactions that involve the formation of covalent bonds
- Adsorption: Non-covalent attachments that involve weak interactions such as hydrogen bonds, electrostatic, hydrophobic, and π-interactions, and the endohedral filling of their empty inner cavities

In the following sections, the mechanisms of adsorption on CNMs will be presented. First, the studies on the adsorption capabilities of gas and vapours on solid materials will be discussed. These studies that were pioneers in the field established the underlying mechanisms that ruling these interactions. Second, the CNMs adsorption capabilities for organic and inorganic compounds in solutions will be reviewed considering their potential applications in wastewater treatments.

2.1 Gas and Vapour Adsorption Capabilities of Carbon Nanomaterials

During the 90s started the mass production of fullerenes using different approaches. The first studies on the adsorption capabilities of fullerene considered the gas adsorption on solid forms considering their porosity. Ismail and Rodgers (1992) studied the gas adsorption of various batches of fullerene C_{60}. It was observed that depending on sample preparation and purification, and different adsorption capabilities were exhibited. These was related to the presence of point defects that can

giovanni.libralato@unina.it

be formed by desolvation, and that can lead to the formation of different mesopores, and a different distribution of mesopores/micropores in the crystalline structure.

Later, most of the studies of the adsorption of organic gases and vapours on fullerenes were carried out using inverse gas chromatography (IGC). This technique consists of the use of gas columns refilled with the material to be studied, in this case, fullerenes. Using this technique Abraham et al. (2004) determined the gas-solid partition coefficients for different gases and vapours on a mixture of C_{60}/C_{70} fullerenes. The results were analysed using the solvation equation, which linearly relates the partition constant of solutes with the fullerenes with different solvation parameters (dipolarity-polarizability, π-interactions and the ability of hydrogen bonds formation). Fullerenes were weakly polarizable, and their behaviour was found to be more similar to alkenes rather than polyaromatic molecules.

In another study, Davydov et al. (2000) used the same technique to study the thermodynamic properties (the adsorption heats and the equilibrium constants) that ruled the adsorption of different organic compounds on C_{60} crystals in comparison to on graphitized carbon black. The adsorption potential of the surface of fullerenes was lower than the surface of graphitized carbon black because the dispersive interactions were weaker in the case of fullerenes. Therefore, the adsorption equilibrium constants for alkanes and aromatic compounds were also lower in the case of fullerenes. While, aliphatic and aromatic alcohols and electron-donor compounds as amines, ketones and nitriles can be more efficiently adsorbed on fullerenes surface. In summary, the fullerenes molecules presents electron-donor and electron-acceptor properties in agreement with Abraham et al. (2004). Also in the same line Papirer et al. (1999), proved that the dispersive component of the surface energy of C_{60} fullerene is lower in compare with graphite or black carbon.

Chao and Shih (1998) using the oscillation of a piezoelectric crystal during adsorption/desorption processes studied the selectivity of C_{60} for organic compounds. For polar organic compounds, it was shown the following sequence: carboxylic acids > aldehydes > amines > alcohols > ketones. In general, the mechanism of adsorption for polar molecules was explained by physical adsorption except amines and dithiols, which were chemisorbed. Regarding non-polar compounds, the alkynes presented chemisorption too and were strongly adsorbed on the fullerenes than the alkanes and alkenes.

Folman and co-workers presented a series of adsorption studies (Fastow et al. 1992, 1993; Folman et al. 1997; Lubezky et al. 1993, 1996, 1998) of several gases on C_{60} fullerene. In these studies, using infrared (IR) spectroscopy, the preferred sites of adsorption were elucidated and indicated a stronger interaction of some gases as CO, CO_2, N_2O and NO with C_{60} fullerene than with other carbon allotropes.

The interest of hydrogen as a fuel has increased during the last decades. The gas adsorption capabilities of fullerenes have also been exploited for gas storage for hydrogen (Pupysheva et al. 2008). In particular during the recent years using hetero-fullerenes, decorated fullerenes and doped fullerenes (Sun et al. 2005, 2006; Thornton et al. 2009; Yu et al. 2015a; Chandrakumar and Ghosh 2008; El-Barbary 2016; Er et al. 2015; Ozturk et al. 2016).

giovanni.libralato@unina.it

Besides fullerenes, also CNTs, both SWCNTs and multi MWCNTs, can efficiently adsorb gases such as NH_3, NO, NO_2, H_2, SF_6, and Cl_2. In fact, this property has been used in multiple gas-sensor applications (Balasubramanian and Burghard 2005; Baughman et al. 2002; Lawal 2016; Meyyappan 2016; Naghadeh et al. 2016; Yang et al. 2010a). Most of the recent developments take the profit of chemically functionalized CNTs (Aroutiounian 2015; Dhall et al. 2013; Karakuscu et al. 2015; Mu et al. 2014), or/and incorporating CNTs into polymers (Badhulika et al. 2014; Lai et al. 2014). A promising application of CNTs is also the adsorption of hydrogen. Dillon et al. (1997) showed that a gas can condense to high density inside SWNTs. In this work, it was proved that hydrogen can condense inside the SWNTs under conditions that do not induce this in the mesoporous of activated carbon. The hydrogen uptake in CNTs suggested the potential of SWCNTs as a hydrogen-storage material for fuel-cell electric vehicles. In addition, Liu et al. (1999), evidenced the high storage capacity of these materials. They found a hydrogen storage capacity of 4.2 weight percentage, or a hydrogen to carbon atom ratio of 0.52, at room temperature under a modestly high pressure (about 10 MPa) for a SWNT sample of about 500-mg weight that was soaked in hydrochloric acid and then heat-treated in the vacuum. Moreover, 78.3% of the adsorbed hydrogen was efficiently released under ambient pressure at room temperature. In general, it has been proved that hydrogen molecules weakly bind on sp^2-bonded carbon materials by interactions type van der Waals thus can be desorbed at very low temperatures. Materials that are exhibiting positive Gaussian curvatures, such as fullerenes and CNT, present higher hydrogen binding affinity than flat structures as graphene. However, it has been shown that the structural defects and chemical doping enhance the binding energy (Bénard and Chahine 2007; Cabria et al. 2005; Chen et al. 1999; Mananghaya 2015; Prabhakaran and Deschamps 2015; Yang 2000). In addition, the nonpolar character of hydrogen drive dipole–dipole induced interactions, as the London dispersion forces (Pumera 2011) with graphene-based systems. A large number of theoretical studies have been performed, and it has been shown that the spatial distribution of hydrogen adsorbed on graphene is delocalized. The molecular hydrogen exhibits free lateral movement, and just there is a slight attractive force of 1.2 kJ/mol in an H_2–graphene system at room temperature (Patchkovskii et al. 2005). The free energy of physisorption corresponds to the equilibrium constant of 1.6, therefore, a very low adsorption capacity. However, the use of sandwich structures can increase the hydrogen binding.

Hydrogen spillover is the process where molecular hydrogen is dissociated onto a metal catalyst and hydrogen atoms are transferred onto another surface, typically with a lower hydrogen content. This can be observed when Pt and Pd have been used as metal catalysts when graphene acts as support. Singh et al. (2009), theoretically demonstrated that this process is a thermodynamic and kinetic favourable process, while it is unfavourable to occur on pristine graphene.

Also Kwon (2010) has investigated the atomic hydrogen adsorption on the graphene surface. He found that the calculated binding energy displays a broad range of values depending on the binding sites and that an individual configuration exhibits the binding curve showing a hysteresis in the transition between an

giovanni.libralato@unina.it

intermediate bond and a chemical bond. However, when another free hydrogen atom exists nearby, the bound hydrogen atom can be desorbed easily to form molecular hydrogen. In fact, there is an enormous interest in the use of graphene for energy storage. However, the properties of graphene strongly depends on the method of fabrication employed.

2.2 *Sorption of Contaminants in Aqueous Solution by Carbon Nanomaterials*

Due to their versatility and simplicity, carbonaceous materials are effective for separation process and water decontamination applications. Porous carbon favours adsorption of contaminants from the liquid phase, and they have been extensively studied and employed to adsorb and remove contaminants in solution.

For example, activated carbon has been shown to be an excellent method for the removal of certain organic compounds from aquatic media. In general, its efficiency depends on its porosity, the surface chemistry, non-electrostatic interactions, such as π–π dispersion, hydrophobic or donor–acceptor interactions between the surface carbonyl groups (electron donors) and the aromatic rings acting as electron acceptors.

In the case of CNMs, they present enhanced capabilities in comparison with other carbon adsorbents such as activated carbon typically used for wastewater treatments. For this reason, during the last years, their applications have been studied for more efficient and faster decontamination processes.

Key features of CNMs are their high specific surface, which is transduced in higher adsorption rates. This superior efficiency enables their use to develop more compacted equipment, which can be useful for decentralized applications and point-of-use systems. And, in addition, these CNMs are cost efficient regarding materials production. In the following section, recent applications of CNMs for the adsorption of pollutants from aquatic systems are reviewed.

2.2.1 Carbon Nanotubes

Due to their tubular structures and large length/diameter ratio as well as their chemical, electronic and mechanical properties CNTs present excellent adsorption capabilities and are the best-studied CNMs for contaminants removal.

In aqueous media, adsorption on CNT follows a ***heterogeneous adsorption behaviour*** (Pan and Xing 2008) because cannot be described using a single coefficient models, such as Freundlich (Pyrzynska et al. 2007; Su and Lu 2007), Langmuir (Su and Lu 2007), BET (Hilding et al. 2001), and Polanyi-Manes (Yan et al. 2008). The presence of structural defects, functionalization groups, and groove regions between CNT bundles produce high-energy adsorption sites.

giovanni.libralato@unina.it

Besides, CNTs present the phenomena of surface condensation that occur when organic compounds are adsorbed on their surfaces by multiple layers (Sekar et al. 2004). The first couple of layers interacts with the surface of CNTs, while molecules beyond the first two layers interact with each other. Therefore, there is a distribution of the energy. Organic compounds will be priority adsorbed at high-energy sites first and then spread to places with lower energy. For these reasons heterogeneous adsorption is one of the main features of adsorption on CNTs (Pan and Xing 2008). Another important characteristic is the ***hysteresis***, the potential to establish strong interaction based on non-covalent forces as π–π-interactions, van de Waals and electrostatic forces and hydrophobic interactions with organic molecules containing aromatic rings. These interactions distort adsorption/desorption mechanisms (Pan and Xing 2008). In addition, ***multiple mechanisms can operate simultaneously*** in response to the changes of environmental conditions, thus, the relative contribution of an individual mechanism to the overall adsorption is of major importance to predict organic chemical adsorption on CNTs (Pan and Xing 2008).

Besides adsorption of CNTs are affected by the properties of CNTs including:

- Physical properties
- Morphology
- Functionalization

Also, it should be mentioned that CNTs possess high-adsorption sites that can modify the surface chemistry of CNTs can be modified on demand. However, due to their hydrophobicity, CNTs have to be stabilized in aqueous suspension to avoid aggregation that reduces their active surface.

Furthermore, CNTs exhibit antimicrobial properties because can cause oxidative stress and destroy the cell membranes. During the last years, different applications have been reported. In Table 1, a summary of recent applications of CNTs as adsorbents for removal of contaminants from water is presented.

CNTs have been investigated as adsorbents to remove organic compounds from wastewater. De Martino et al. (2012) studied the sorption capacity of the herbicide 4-chloro-2-methylphenoxyacetic acid, also known as MCPA, on a type of SWCNT and three MWCNTs with average outer diameters of 15, 30 and 50 nm. The most efficient sorbent was the SWCNT. The herbicide was bound to the CNTs by a combination of electron donor-acceptor interactions and hydrogen bonds. The experiments of cyclic sorption showed that the pesticide was totally removed by two sorption cycles on the SWCNT and MWCNT15. Finally, desorption studies in ethanol showed a potential re-use of the SWCNT. In another study, Ji et al. (2010), explored the adsorption of monoaromatic compounds (phenol and nitrobenzene) and pharmaceuticals on CNTs activated with KOH etching. In this study, it was shown that the specific surface area increased from 410.7 to 652.8 m^2/g for SWNT and from 157.3 to 422.6 m^2/g for MWNT by the activation of KOH. Moreover, the number of pores was increased, and thus, the adsorption capability for the removal of selected compounds was enhanced 2–3 times on SWNT and 3–8 times on

giovanni.libralato@unina.it

Table 1 Summary of recent applications of CNMs for the removal of contaminants from aqueous media

Compounds removed	Specific adsorbent material	Observations	Ref.
Carbon nanotubes			
Antibiotic: sulfamethazine	Carbonaceous nanocomposite made from carboxyl functionalized MWCNT	This new composite was obtained by dip-coating straw biomass in carboxyl functionalized MWCNT solution and then pyrolysed at 300 and 600 °C in the absence of air	Zhang et al. (2016)
Antibiotics: oxytetracycline (OXY) and ciprofloxacin (CIP)	SWCNT and different MWCNTs	The Brouers-Sotolongo equation was the best fitting isotherm model. The highest removal capacities were registered using SWCNTS for both antibiotics (724 mg/g for CIP and 554 mg/g for OXY)	Ncibi and Sillanpää (2015)
Dye: rhodamine B	MWCNTs-cobalt ferrite nanocomposites	The results showed that the pseudo-second order model best described the data as reflected in the lowest value for the sum of squared residuals. Among the various adsorption isotherms tested, the Langmuir isotherm provided the best fit. The adsorption capacity was lowest in $CoFe_2O_4$ (5.165 mg/g) and highest with MWCNT-COOH (42.68 mg/g)	Oyetade et al. (2015)
Dye: Sudan	Magnetic MWCNTs synthesized by hydrothermal synthesis of Fe_3O_4 NPs onto CNTs	The adsorption kinetic was well fitted by the pseudo second-order kinetic model. The adsorption isotherm data could be well described by the Freundlich equations	Sun et al. (2015)
Metal ions: Bi(III)	MWCNTs	The adsorption kinetic was well fitted by the pseudo second-order kinetic model, whereas, the adsorption mechanism occurs in two consecutive steps	Al-Saidi et al. (2016)
Metal ions: Cd(II)	CNT-PAC composite	The surface properties of CNT-PAC were modified by oxidative functionalization using two different methods: sonication with $KMnO_4$ and	Al Saadi (2016)

(continued)

giovanni.libralato@unina.it

Table 1 (continued)

Compounds removed	Specific adsorbent material	Observations	Ref.
		refluxing with HNO_3 at 140 °C. $KMnO_4$-treated CNT-PAC exhibited the highest sorption capacity for cadmium uptake which increased from 4.77 mg/g (untreated CNT-PAC) to 11.16 mg/g; resulting in Cd^{2+} removal efficiency from 38.87 to 98.35%	
Metal ions: Cr(VI)	ACF/CNT (activated carbon fiber/carbon nanotube) composites	The adsorption capacity gradually reduced with increment of adsorbent dose The adsorption kinetic was well fitted by the pseudo second-order kinetic model. The adsorption isotherm data could be well described by the Freundlich equations	Wang et al. (2016b)
Metal ions: Cu(II)	4′-(4-hydroxyphenyl)-2,2′:6′,2″-terpyridine (HO-Phttpy) onto the surface of multiwalled **carbonnanotubes** (MWCNTs) to obtain nitrogen-functionalized MWCNTs (MWCNT-ttpy)	Maximum adsorption capacity: q_e = 31.65 mg/g	Oyetade et al. (2016)
Metal ions: Pb(II) and Cu(II)	MWCNT entrapped into polymer matrix by poly(vinyl alcohol) (PVA)-boric acid crosslinking. Thus, a novel macroporous composite adsorbent (PVA/CNTs)	The results from the sequential adsorption–desorption cycles showed that PVA/CNTs beads exhibited good desorption and reusability	Jing and Li (2016)
Organic chemicals: sulfamethoxazole, ofloxacin, norfloxacin, bisphenol A (BPA) and phenanthrene (PHE)	Fluorinated MWCNTs	The enhanced adsorption may be attributed the pores generated on the coated PTFE and the dispersed MWCNT aggregates due to the increased electrostatic repulsion after fluorination. The rearrangement of the bundles or diffusion of the adsorbates in inner pores were the likely reason for the strong	Li et al. (2016)

(continued)

giovanni.libralato@unina.it

Table 1 (continued)

Compounds removed	Specific adsorbent material	Observations	Ref.
		desorption hysteresis. The butterfly structure of bisphenol A resulted in its high sorption and strong desorption hysteresis	
Pharmaceuticals: carbamazepine, diclofenac sodium and tetracycline	Porous granular CNTs	The maximum adsorption capacity was 369.5 μmol/g for carbamazepine, 284.2 μmol/g for tetracycline and 203.1 μmol/g for diclofenac	Shan et al. (2016)
Pharmaceuticals: diclofenac and naproxen	MWCNTs	Wastewater treatment by H_2O_2 or UV	Czech and Oleszczuk (2016)
Surfactants: anionic surfactant, sodium dodecyl benzene sulphonate (SDBS)	MWCNTs	The adsorption kinetic was well fitted by the pseudo second-order kinetic model. The adsorption isotherm data could be well described by the Freundlich equations	Mortazavi and Farmany (2016)
Surfactants: non-ionic (TX-100), cationic (CTAB) and anionic (SDBS) surfactants	MWCNTs	MWCNTs showed promising removal capacities with 359, 312 and 156 mg/g for TX-100, SDBS and CTAB, respectively	Ncibi et al. (2015)
TEX: toluene (T), ethyl benzene (E), and xylene (X)	Functionalized magnetic MWCNTs nano-composite (APCNT-KOH)	Maximum adsorption capacity ($q_{m,toluene}$ = 63.34 mg/g, $q_{m,ethylbenzene}$ = 249.44 mg/g, $q_{m,m\text{-}xylene}$ = 227.05 mg/g, $q_{m,o\text{-}xylene}$ = 138.04 mg/g, $q_{m,p\text{-}xylene}$ = 105.59 mg/g)	Yu et al. (2016)
Veterinary drug: Nitrofurazone	MWCNTs	Maximum adsorption capacity at 283 K were close to 50.8 mg/g	Wu and Xiong (2016)
Graphene			
Antibiotics and pharmaceuticals	Activated graphene (G-KOH)	The adsorption kinetic was represented by a pseudo-second-order model and a Langmuir isotherm model showed a better fit	Yu et al. (2015b)
Chlorophenols	Graphene oxide composite	Adsorption equilibrium was achieved within 10 min, presented efficient separation from water under an external magnetic field, and was easily regenerated using dilute	Yan et al. (2016)

(continued)

giovanni.libralato@unina.it

Table 1 (continued)

Compounds removed	Specific adsorbent material	Observations	Ref.
		NaOH aqueous solution after reaching saturated adsorption	
Dye: acridine orange	Magnetic calcium silicate graphene oxide composite adsorbent (MGSi)	The adsorption kinetic was well fitted by the pseudo second-order kinetic model. The adsorption isotherm data could be well described by the Freundlich equations	Wang et al. (2016b)
Dye: anionic orange IV	Graphene oxide (GO) and activated graphene oxide (GO_{KOH})	Adsorption capacity was 606.1 mg/g for orange IV The adsorption process was endothermic following the pseudo-second-order kinetics and the Langmuir isotherm models	Guo et al. (2016)
Dye: methylene blue	Graphene oxide flakes functionalized with 3-amino-1-propane sulfonic acid (denoted as GO_{SULF}) as a powder or incorporated into an ionomer membrane such as Nafion	Dye photo-catalytic degradation and removal	Scalese et al. (2016)
Ions: Se(IV), Se(VI)	Functionalized water-dispersible magnetic nanoparticle-graphene oxide (MGO) composites	MGO (dosage 1 g/L) shows removal percentage of >99.9% for Se(IV) and ~80% for Se (VI) from water (pH 6–7) within 10 s	Fu et al. (2014)
Metal ions: Cu(II)	Magnetic polyaniline/graphene oxide (MPANI/GO) composites	The MPANI/GO composites were effective materials for the removal of Cu(II) from large volumes of aqueous solutions and could be separated by using magnetic separation method in the practical applications	Liu et al. (2016b)
PAHs: phenanthrene	Surfactant mediated exfoliation of multilayer graphene	The findings on exfoliation of graphene sheets and related adsorption properties highlight not only their potential applications as efficient adsorbent but also its possible environmental risk	Zhao et al. (2014)

(continued)

giovanni.libralato@unina.it

Table 1 (continued)

Compounds removed	Specific adsorbent material	Observations	Ref.
Plasticiser: bisphenol A	Reduced graphene oxide nanosheets decorated with tunable magnetic NPs	The results indicate that the adsorption process is fitted to Langmuir model and the composites with lower density of MNPs represent better adsorption ability. In addition, its kinetics follows pseudo-second-order rate equation. The adsorbents could be recovered by magnetic separation and desorption of BPA	Zhang et al. (2014)
Radioactive metal ions: Uranium(VI)	Amino functionalized magnetic graphene oxide composite (AMGO)	The AMGO can be easily recovered from the solution with the magnetic separation within one minute. The kinetic data were following the pseudo-second-order equation. The Langmuir model fitted the sorption isotherm data The maximum sorption capacity of the AMGO for U (VI) was 141.2 mg/g	Chen et al. (2016)

MWNT. The activated CNTs showed improved adsorption reversibility for the selected compounds. Sotelo et al. (2012), compared the use of activated carbon, MWCNTs and carbon nanofibers for the adsorption from water solutions the pharmaceuticals atenolol, caffeine, diclofenac, and isoproturon, and an endocrine disruptor. The experiments were carried out in ultrapure water and effluents of a municipal wastewater treatment plant. The adsorption capacities were studied in the temperature range of 25–65 °C and pH range from 3 to 9. Temperature presented a low influence on CNTs adsorption, while for different compounds optimal the optimal pH was found. To correlate the experimental data six different isotherm models including Langmuir, Freundlich, Sips, Redlich-Peterson, Toth and an extended Langmuir model, were tested. The results obtained showed the following order of the best-fitted adsorption isotherm models: Freundlich isotherm ≈ Langmuir isotherm > Toth isotherm > Redlich-Peterson isotherm, for caffeine, diclofenac and isoproturon. In spite of higher adsorption capacity is showed in most of the studies for CNTs, recently, the adsorption of ibuprofen and tetracycline onto a commercial granular activated carbon, MWCNTs, and two types of activated carbons were investigated. And, the highest adsorption capacities were obtained for activated carbons. These results were linked to the textural and surface chemical properties of the adsorbents (Álvarez-Torrellas et al. 2016).

giovanni.libralato@unina.it

In addition to the adsorption capability of contaminants by CNTs from the aquatic media have been also used to remove contaminants from soils. For example, Taha and Mobasser (2015), have explored the adsorption of two groups of persistent organic pollutants (POPs), the dichlorodiphenyltrichloroethane (DDT) and polychlorinated biphenyls (PCBs) on three nanomaterials including MWCNT, nano-clay and nano-Alumina. The results of this study indicated that MWCNTs was a better adsorbent material compared to the other for both contaminants in this work.

Another relevant group of applications is the use of CNTs for removal of micro pollutants as metals. In Table 1, different recent applications of CNTs for the removal of metal ions in aqueous media are reported.

CNTs can be used not only as adsorbents but also as supports for adsorption materials. Recent different review articles have compiled these applications (Chawla et al. 2015; Gupta et al. 2016; Ihsanullah et al. 2016; Stafiej and Pyrzynska 2007; Fu and Wang 2011). As well different thermodynamics and kinetics studies have been carried out. For example, the adsorption thermodynamics and kinetics of removal of Pb^{2+} on CNTs were studied by Li et al. (2005). The adsorption data was well fit to the Freundlich isotherm. It was found that the adsorption capacity linearly increased with temperature. The adsorption data followed the pseudo-second-order rate model. In another study Li et al. (2003) studied the individual and competitive adsorption of Pb^{2+}, Cu^{2+} and Cd^{2+} by nitric acid treated MWCNTs. The maximum sorption capacities calculated by applying the Langmuir equation to single ion adsorption isotherms were 97.08, 24.49 and 10.86 mg/g for Pb^{2+}, Cu^{2+} and Cd^{2+}, respectively, at an equilibrium concentration of 10 mg/l. The competitive adsorption studies showed that the affinity order of three metal ions adsorbed by these MWCNTs was $Pb^{2+} > Cu^{2+} > Cd^{2+}$. The Langmuir adsorption model was representative for the experimental data of Pb^{2+} and Cu^{2+}, but it does not fit with the Cd^{2+} adsorption data. Wang et al. (2005), studied the adsorption of the radionuclide 243Am(III) to MWCNTs. In this case, it was reported that the sorption was strongly dependent on pH and weakly dependent on the ionic strength. MWCNTs were shown very efficient to adsorb 243Am(III) by forming very stable complexes. Chemisorption and chemo-complexation were the main mechanisms of 243Am(III) of adsorption.

The influence of different functions has also been explored for the removal of metal ions. For example, Oyetade et al. (2016) studied nitrogen functionalised CNTs as a novel adsorbent for the removal of Cu(II) ions from aqueous solution. In this study, it was investigated the introduction of 4′-(4-hydroxyphenyl)-2,2′:6′,2″-terpyridine onto the surface of MWCNTs to obtain nitrogen-functionalized derivatives. The experiments were conducted at pH 5 and the equilibrium was reached in 360 min. The adsorption process fitted with a pseudo-second order model. Among the isotherms tested isotherms, Langmuir provided the best fit to the data at the equilibrium. Thermodynamic studies revealed that the adsorption process was spontaneous and endothermic. In addition, good desorption efficiency

giovanni.libralato@unina.it

from the nitrogen functionalized MWCNTs, indicating its possible regeneration and the recovery of the Cu^{2+}. In another recent study, MWCNT were entrapped into the polymer matrix by poly(vinyl alcohol) (PVA)-boric acid crosslinking. The resultant macro-porous composite adsorbent (PVA/MWCNTs) was used to remove heavy metal ions. The results from the sequential adsorption–desorption cycles showed that PVA/MWCNTs beads exhibited good desorption and reusability (Jing and Li 2016).

Another relevant feature of CNTs is their antibacterial activity. The first study in regards to the antibacterial activity of SWCNTs was presented by Kang et al. (2007) In this work, it was demonstrated that SWCNTs could cause severe membrane damages. In another study, the same group reported that the size of CNTs was an important factor affecting the antibacterial activity. Also, the superior activity of SWCNTs in compared with MWCNTs was also demonstrated. According to the authors finding SWCNTs could penetrate into the cell wall better than MWCNTs due to their smaller nanotube diameter (Kang et al. 2008). On the contrary, Yang et al. (2010b) studied the effect of SWCNTs length on the antimicrobial activity and in this case the longer SWCNTs showed a stronger antimicrobial activity due to their improved aggregation with bacterial cells (Yang et al. 2010b). In another study, Dong et al. (2012) investigated the antibacterial properties of SWCNTs against *Salmonella enteric*, *Escherichia coli*, and *Enterococcus faecium* dispersed in different surfactant solutions including sodium holate, sodium dodecyl benzenesulfonate, and sodium dodecyl sulphate. SWCNTs exhibited antibacterial activity against both *S. enteric* and *E. coli*, which was improved with the increase of CNTs concentrations.

During the recent years, a plethora of studies has informed about different CNT derivatives for antibacterial applications using metal NPs combinations and membrane composites (Chen et al. 2015a; Hao et al. 2015; Shahriary et al. 2015; Sharma et al. 2015; Shi et al. 2016; Lee et al. 2016; Liu et al. 2016a). Many of them exploiting the advantages of the combined effect of silver NPs and CNTs (Shahriary et al. 2015; Chang et al. 2016; Karumuri et al. 2016; Sedaghat 2015; Dosunmu et al. 2015).

2.2.2 Fullerenes

C_{60}-fullerene (Buckminster fullerene) is the most investigated fullerene. However, nowadays, an important number of different functionalization and modification are possible. The mechanisms of adsorption of organic contaminants by fullerenes have been investigated and compared with other carbonaceous materials such as activated carbon and carbon soot for their application in the removal of organic contaminants and micro-pollutants from wastewaters. In these cases, the adsorption capability on fullerenes has been mainly attributed to their high active area and the dispersive forces. In general, similar mechanisms ruled the adsorption on fullerene and graphitized carbon black, but metal oxides like silica could enhance the adsorption capacity (Yang et al. 2009). Yang et al. (2009), confirmed that the

giovanni.libralato@unina.it

dispersion state of fullerenes is affecting by several orders of magnitude the adsorption of naphthalene. On the other hand, it was found that the desorption of naphthalene from C_{60} fullerene into aqueous solutions exhibit strong hysteresis.

Recently, the density functional method has been employed to compare the adsorption ability of simple and doped fullerenes with different heteroatoms (Al, B, Si, N, P, and S) (Amiraslanzadeh 2016). A variety of sulphurs (H_2S, SO_2, and thiophene) were selected to study their interactions with fullerenes. The calculated adsorption energies showed that all sulphurs have exothermic interaction with all fullerenes. Besides, it was revealed that the heteroatoms doping is bearing extra electrons, the energy gap is reduced, and this decrease is more than the expected by heteroatoms doping by with electron defect. In general, better adsorption of SO_2 by fullerenes was obtained, and among all fullerenes, aluminium-doped fullerenes, and then boron-doped fullerenes and nitrogen-doped fullerenes were the best adsorbents for these sulphurs.

The use of fullerenes-extracted soot, the by-product of fullerene synthesis, has not much been employed. However, Nakagawa et al. (2014) presented an interesting application of a derivative of this composite material as an adsorbent of hexavalent chromium in water. In this case, the fullerenes-extracted soot was reacting with ethylenediamine to introduce amino groups. Then the composite was used as an adsorbent of hexavalent chromium [Cr(VI)] for removing Cr(VI) from aqueous solutions. The primary results of this study have indicated that the adsorption of Cr(VI) was highly dependent on pH, and the optimal adsorption was obtained at pH 3.0. The data of Cr(VI) adsorption by fullerenes-extracted soot modified with ethylenediamine fit the Langmuir isotherm equation. And, the adsorption capacity was 93 mg/g.

In recent years, several works have shown that nano filtration and reverse osmosis are capable of removing trace organic compounds from wastewater. During the past years, fullerene-containing polymers have been incorporated into membrane technology because it has been shown that polymer membranes modified with CNMs can substantially improve their original properties. Moreover, some polymeric membranes based on hydrophobic polymers such as poly (2,6-dimethyl-1,4-phenylene oxide) (PPO) modified by CNMs as fullerene C_{60} can improve the removal and adsorptive behaviours of trace contaminants such as estrogens. Jin et al. (2007) studied the ability to adsorb and remove the natural hormone estrone from wastewater using asymmetric membranes based on PPO modified by fullerene C_{60}. The result of this study showed excellent results with a percentage of removal higher tan 96% using different PPO membranes modified with various percentages of fullerene PPO; 2%wtC_{60}-PPO; 10%wtC_{60}-PPO. However, the results of the long-term filtrations experiments revealed that the membrane modified with a 10% of fullerene was more stable along the time.

The adsorption capabilities of fullerenes have also been exploited for water disinfection. Lyon and Alvarez (2008), Lyon et al. (2008) proposed that water suspensions of C_{60} fullerene exert ROS-independent oxidative stress in bacteria (protein oxidation, in the cell membrane, and cellular respiration disruption) by direct contact between fullerenes and the bacterial cell. This mechanism differs

giovanni.libralato@unina.it

from antibacterial mechanisms previously reported that involves ROS generation. Fullerenes showed antimicrobial activity against different bacteria, such as *E. coli*, *Salmonella* and *Streptococcus* spp. (Tegos et al. 2005). The antibacterial effect can be explained by the inhibition of energy metabolism (Bellucci 2009). The hydrophobic character of fullerenes surface facilitates the interaction with cell membranes (Lyon and Alvarez 2008; Lyon et al. 2008). This fact has been considered in different antimicrobials applications (Yang et al. 2014). In addition the possibility to functionalized fullerenes has opened a new window to obtain different classes of fullerenes (positively charged, neutral, and negatively charged) with different antibacterial properties. Cationic derivatives have presented the maximum antibacterial effect on *E. coli* and *Shewanella oneidensis* (Nakamura and Mashino 2009). This fact could be as a result of the interactions between the negatively charged bacteria with cationic fullerenes (Nakamura and Mashino 2009). Also, the antibacterial properties of two water-soluble derivatives of the fullerene obtained by the addition of protonated amines and deprotonated carboxylic groups have been studied. The results confirmed previous results and positively charged derivative bounded to the *E. coli* cells (Deryabin et al. 2014).

2.2.3 Graphene

Graphene is a two-dimensional NM and a single-atom layer of graphite that attracts the research interests because of its unique structure and exceptional properties. In particular, graphene-based materials offer a broad range of potentialities for wastewater decontamination and environmental remediation.

The graphene-based materials are deemed currently as “star materials” for the high-efficient removal of organic and inorganic pollutants from aqueous solution (Wang et al. 2013). In Table 1 the adsorption and the application in water treatment technologies of graphene-based materials for organic and inorganic contaminants removal are summarized.

Graphene-based composites have been applied to remove various organic contaminants, aromatic compounds (Li et al. 2012b; Kim et al. 2015; Wu et al. 2013a; Yang et al. 2015; Zhang et al. 2013), such as dyes (Li et al. 2011; Guo et al. 2016; Scalese et al. 2016), bisphenol A (Xu et al. 2012; Zhang et al. 2014), phenols (Li et al. 2012c, d) and antibiotics (Gao et al. 2012; Tang et al. 2013). Primary driving interactions are similar to those involved in CNTs surfaces, and as well different mechanisms may have simultaneous influences, such as electrostatic interactions, van der Waals type interactions, π-π bonds, anion-cation interaction and hydrogen bonds. According to the different adsorbates, different types of adsorption mechanisms will be predominant. For example, Ramesha et al. (2011) indicated that anionic and cationic dyes could be efficiently adsorbed by graphene and graphene oxide because of the high surface area and the negative surface charge. The interactions between the charged dyes and graphene are electrostatic, van der Waals type interactions or both depending on the system.

giovanni.libralato@unina.it

Three-dimensional (3D) graphene oxide sponge (GO sponge) has been shown to be excellent for contaminants removal. Also graphene/GO-composites improve the adsorptive performance of graphene by solving some limitations of this material in adsorption processes such as easy folding and aggregation. Therefore, a high number of applications have been developed. For example, methylene blue and methyl violet can be adsorbed on the GO sponge. This process involved in endothermic chemical adsorption through π-π bonds and anion–cation interactions with an activation energy of 50 and 71 kJ/mol (Liu et al. 2012a).

In another work, methylene blue was removed by adsorption (Liu et al. 2012b) using a composite of 3D graphene with $Mg(OH)_2$ composite ($Mg(OH)_2$–rGO), which presents high surface area and pore volume. In addition, this composite can be reused without almost no loss of adsorption after washing with ethanol. In a recent study, graphene oxide flakes functionalized with 3-amino-1-propanesulfonic acid (GOSULF) incorporated into an ionomer membrane as Nafion were proposed for water purification. The adsorption of and the posterior photo catalytic degradation on the GOSULF membrane (Nafion-GOSULF) of an anionic dye, methyl orange, were studied (Scalese et al. 2016). In another recent study, Wang et al., synthesized 3D flower-like TiO_2 microsphere decorated graphene composite (FT/GN) based on the hydrothermal reduction of graphene oxide and formation of TiO_2 microsphere in the presence of poly(vinyl pyrrolidine) (PVP). The TiO_2 microsphere/graphene composite was used for removal of organic dye from water.

Good results have also been obtained for other organic pollutants such as antibiotics as tetracycline on GO. In this case, adsorption was conducted via π-π interaction and cation-π bonding (Gao et al. 2012). A graphene-like composite was presented by Chao et al. (2014). A graphene-like layered hexagonal boron nitride was prepared for the adsorption of the fluoroquinolone antibiotic gatifloxacin from aqueous solution. Excellent adsorption characteristics were shown with a removal rate of 90%. This material has presented good fitting with Langmuir isotherm model and a maximum adsorption capacity of 88.5 mg/g. In another approach, Yu et al. (2015b) prepared and tested an alkali-activated graphene adsorbents for ciprofloxacin removal. Also, in this case, experimental results showed a better fit with the Langmuir isotherm model and a high adsorption capacity of 195 mg/g.

On the other hand, hybridized carbon materials composed by graphene and CNTs (Sui et al. 2012) has also been used for metal and contaminants removal. For example in desalinization processes.

In addition to organic pollutants removal, different applications of graphene-like composites have been reported for the adsorption of inorganic contaminants.

However, the adsorption of inorganic contaminants as heavy metals by graphene-like composites is mainly due to physical adsorption, electrostatic attraction and chemical interaction between the ions and the surface functional groups of those materials. In spite of that, an excellent performance has been shown by some of these materials. For example, few-layered graphene oxide (FGO) was prepared by the modified Hummers, to be used as an adsorbent of metal ions from

giovanni.libralato@unina.it

aqueous solutions (Zhao et al. 2011a, b, 2012). According to the Langmuir model, the maximum adsorption capacities of Pb(II), Cd(II), Co(II), and U(VI) on graphene oxide calculated from the Langmuir model were 1850, 106.3, 68.2, and 97.5 mg/g, respectively. The surface complexation occurs through Lewis acid–base interaction between metal ions and oxygen—containing functional groups of FGO, resulting in excellent yields regarding heavy metals adsorption. In another example, Zhu et al. (2012) have synthesized magnetic graphene composites decorated with core @ double-shell nanoparticles (MGNCs) via a thermo-decomposition process for chromium removal. Excellent efficiency in fast removal of Cr(VI) (5 min) was obtained. In a similar manner, other magnetic graphene/GO-based composites have been developed for the removal of uranium (Chen et al. 2016), Cu(II) (Chen et al. 2015b; Liu et al. 2016b) and Cr(VI) (Wang et al. 2015).

Due to the fast and easy-operation, magnetisable separation using graphene-based materials can overcome many limitations for the large-scale industrial application in wastewater treatments such as filtration, centrifugation, or gravitational separation. Therefore, during the last years, these composites have also been exploited for the separation of organic pollutants such as glyphosate (Yamaguchi et al. 2016), chlorophenols (Yan et al. 2016), p-nitrophenol (Liu et al. 2016c) and dyes (Jiang et al. 2016; Wang et al. 2016a).

As in the case of fullerenes and CNTs, the antibacterial properties of graphene have also been considered. In general, graphene oxide nanosheets that could be dispersed in water are employed. Graphene oxide produced by chemical modification of the graphene with suspended hydroxyl, epoxyl, and carboxyl groups. The proposed mechanism of antimicrobial activity is the physical interaction with the cell membrane, followed by the formation of cell-graphene oxide aggregates and the induction the cell membrane disruption. For example, Azimi et al. (2014) proved the antimicrobial activity of functionalised graphene oxides: graphene oxide-chlorophyllin and graphene oxide-chlorophyllin-Zn against *E. coli*. The mechanism of action proposed was the *E. coli* membrane damage. Furthermore, metal toxicity played a major role in the antibacterial activity.

During the recent years, the advantages of nanocomposites composed of graphene and metal NPs as silver NPs, has been reported. For example, high antibacterial activity against both gram negative and positive bacteria using SWCNTs-Ag and graphene oxide-Ag nanocomposites have been shown. However, the activity of SWCNTs-Ag was superior, probably due to a superior dispersion of Ag NPs into the SWCNTs (Yun et al. 2013).

Ag-carbon nanocomplexes also showed efficient inhibitory activity against different pathogens such as *Burkholderia cepacia* and multidrug-resistant *Acinetobacter baumannii* (Leid et al. 2012).

giovanni.libralato@unina.it

3 Retention and Reuse of Carbon Nanomaterials Used in Water Treatments

The retention and reuse of CNMs are fundamental to consider during the technological design regarding both risks associated with CNMs emissions and device costs. In general, applying separation processes or immobilizing the NMs in the system by mean of membranes, etc. solve these potential issues.

Among the different separation system, the use of membranes filtrations has been proposed. However, the suspended matter of wastewater can be also retained by the membrane and significantly reduce the reaction efficiency. Thus raw water pretreatment is usually required to reduce the turbidity and the matrix effect of wastewater.

Some of the current research is designed to facilitate the collection of NMs after the treatment. E.g. Wang et al. design and synthesized carbon nanotube ponytails (CNTPs) by integrating CNTs into micrometer-sized colloidal particles, which greatly improves the effectiveness of post-treatment separation using gravitational sedimentation, magnetic attraction, and membrane filtration.

NMs also can be immobilized on various platforms such as resins and membranes to avoid further separation. In this regard, the use of 3D graphene sponges is also very convenient to use the adsorption capacity of this material or also use this material as support of other nanoparticles (NPs) or NMs. But, it should be mentioned that current immobilization techniques usually result in significant loss of the treatment efficiency.

Another important option is the use of magnetic NPs-nanocomposites, low-field magnetic separation is a possible energy-efficient option.

However, little is known about the release of NMs in general, and CNMS in particular, from nanotechnology enabled devices. However, the potential release is expected to be largely dependent on the type of NM involved, the immobilization technique or the separation method. In addition, the release of metal ions from NMs should also be considered with special attention.

The detection of released nanomaterials is a major technical hurdle for risk assessment and it still remains challenging. Nowadays, a few number of analytical methods are able to detect CNMs in the environment. Therefore, this fact cannot be properly assessed. In the next sections, this issues will be discussed in detail.

4 Occurrence, Fate, Behaviour and Toxicity of Carbon Nanomaterials in the Environment

CNMs are emitted into the environment because of natural, incidental and nanotechnological sources.

- CNMs of natural origin can be produced by combustion and other highly energetic processes such as volcanic eruptions (Jehlička et al. 2003; Buseck and Adachi 2008) and wildfires. Combustion processes produce large amounts of

giovanni.libralato@unina.it

CNMs: mainly amorphous carbon NPs, MWCNT (Murr et al. 2004b; Murr and Soto 2005) and fullerenes (Goel et al. 2002). Carbon nanotubes aggregates dating about 10,000 years old were found in a Greenland ice core (Esquivel and Murr 2004).

- Also, human activity unintentionally contributes to the emission of CNMs, being the main source in the environment (Wigginton et al. 2007). Indoor and outdoor air particulates contain complex mixtures of metal NPs and MWCNT aggregates, mainly related to traffic activity (Murr et al. 2006), which are transported through the atmosphere and undergo deposition to surface soils and water bodies.
- Finally, engineered NMs are *manufactured materials, containing particles, in an unbound state or as an aggregate or as an agglomerate and where, for 50% or more of the particles in the number size distribution, one or more external dimensions is in the size range 1–100 nm* (Commission 2013). Nanotechnology development and the synthesis of novel engineered NMs opens the door for their introduction into the environment (Hendren et al. 2011; Gottschalk and Nowack 2011) with ecological risks which are still to be understood. For this reason, NMs are considered as emerging pollutants. Although NMs from nanotechnology sources are emitted in lower amounts in comparison with those produced in combustion processes, it should be highlighted that the wide range of different materials that can be produced nowadays by nanotechnology, all of them exhibiting different properties and enhanced reactivity poses an additional risk.

Once released into the environment, NMs are distributed, especially in water and porous media (Wiesner et al. 2006). NMs mobility depends not only on the primary characteristics of NMs, but also on environmental conditions (pH, ionic strength, natural organic matter), which determine the course of the processes of aggregation and adsorption. In addition, once in the environment primary NMs can be transformed, changing their mobility and toxicity. During the last decade, a great effort has been made on environmental nanotoxicology (also known as nanoecotoxicology) research. Nevertheless, limited information is currently available, in many cases, due to the lack of quantitative analytical methods for their determination in complex environmental samples. The lack of quantitative analytical methods for the determination of CNTs and other CNMs is one of the principal issues to perform realistic environmental risk assessment studies. To date, few analytical methods have been developed for the quantitation of CNMs in the environment, and almost all of them were devoted to fullerenes. In Table 2, a summary of analytical methods for the determination of fullerenes in the environment is presented. Most of these methods have been considered in different review articles (Pérez et al. 2009b; Isaacson et al. 2007). Very briefly, these methods are based on a separation step, generally by liquid-liquid extraction (LLE) (Chen et al. 2008; Xiao et al. 2011; Kolkman et al. 2013), solid-phase extraction (SPE) (Chen et al. 2008; Xiao et al. 2011; Kolkman et al. 2013), or by filtration followed by ultrasonic assisted extraction (UAE) with toluene (Farré Ml et al 2010; Sanchís et al. 2013). After the extraction the analysis is usually performed by liquid chromatography coupled to mass spectrometry (LC-MS).

giovanni.libralato@unina.it

Table 2 Summary of analytical methods for the determination of fullerenes in environmental samples

Ref.	CNMs	Extractio method	Analytical column	Ionization source (ionization mode)/ Detection	Matrix
Farré Ml et al (2010), Sanchís et al. (2013)	C_{60}, C_{70} & NMFP	UAE	C18	ESI(-)-MS/MS	WW
Wang et al. (2010a)	C_{60}, C_{70}	LLE	Buckyprep	LC-UV	–
Sanchís et al. (2012)	C_{60}, C_{70} and Func.	UAE	C18	ESI(-)-MS/MS	Air part
Chen et al. (2008)	Aggr.	UA-DLLME		APPI(-)-MS/MS	WW
Núñez et al. (2012)	Pristine fullerenes	UAE	C18	APPI(-)-HRMS	Freshwater
Sanchís et al. (2015)	C_{60}, C_{70} and Func.	UAE	C18	ESI(-)-MS/MS	Soil
Kolkman et al. (2013)	C_{60}, C_{70} & Func.	SPE C18	Buckyprep	ESI(-)-HRMS	Freshwater

4.1 Occurrence of Carbon Nanomaterials in the Environment

During the last years, several publications have presented the analysis of fullerenes in the environment (Farré et al. 2010; Sanchís et al. 2012, 2013; Núñez et al. 2012; Carboni et al. 2014). However, for other types of carbon NMs, such as CNT, due to their variable lengths and structures, similar approaches are not feasible. Therefore, for some CNMs as CNTs their fate, environmental behaviour and potential risk can only be estimated using models.

Nonetheless, other difficulties that should be overcome are the lack of standardised approaches to characterise the toxicological behaviour of CNMs: among them, (1) the potential presence of impurities in the standards, (2) the methods to conveniently prepare test suspension, and (3) the most adequate toxicity tests procedures. For example, CNMs suspension preparations can change surface properties of CNMs or change their aggregation states with, in both cases, an impact on the final toxicity. Moreover, toxicity tests designed for the toxicity evaluation of bulk materials are not suitable enough to assess the toxicity of CNMs regarding end-points and experimental design to avoid artefacts.

In Table 3, different works reporting the quantification of CNMs in environmental samples are reported.

giovanni.libralato@unina.it

Table 3 Works reporting the quantification of fullerenes by MS and HPLC-MS

Ref.	Analysis	Separation	Detection	MLOD
Water samples				
Chen et al. (2008)	C_{60} in tap and SW	Nova-Pak C18 (150 × 3.9 mm) with tol: ACN (55:45)	Source: APCI MS: QqQ Acq. SIM	C_{60} (SW): 0.3 µg/L
Isaacson et al. (2007)	C_{60} in ultrapure water	Cosmosil Buckyprep (150 × 4.0 mm) with tol: MeOH (95:05)	Source: APPI MS: QqQ Acq. SIM	Not detailed
Farré Ml et al. (2010)	C_{60}, C_{70} and [60]NMFP in SW and WW	Purospher Sta RP-18 (12.5 × 2.0, 5 µm) with tol: MeOH (55:45)	Source: APCI MS: QqLiT Acq.pSRM	C_{60} (SW): 2 ng/L C_{70} (SW): 5 ng/L [60]NMFP (SW): 12 ng/L C_{60} (WW): 5 ng/L C_{70} (WW): 8 ng/L [60]NMFP (WW): 20 ng/L
Wang et al. (2010a)	C_{60} in WW	Cosmosil Buckyprep (250 × 4.6 mm, 5 µm) with toluene	Source: APCI MS: QqQ Acq.: SIM	C_{60} (WW): 4–11 µg/L
Núñez et al. (2012)	C_{60}, C_{70}, C_{76}, C_{78}, C_{84} in SW	Hypersil GOLD C18 column (150 × 2.1 mm, 1.9 µm particle size, 175 Å)	Source: Heated ESI and APPI MS: QqQ Acq. SIM	C_{60} (SW): 0.01 ng/L C_{70} (SW): 0.01 ng/L C_{76} (SW): 4.6 ng/L C_{78} (SW): 0.75 ng/L C_{84} (SW): 5.0 ng/L
Astefanei et al. (2015)	C_{60}, C_{70}, C_{76}, C_{78}, C_{84} and three engineered fullerenes in SW	Hypersil GOLD C18 column (150 × 2.1 mm, 1.9 µm particle size, 175 Å)	Source: heated ESI, APCI and APPI MS: QqQ Acq. SRM and SIM	C_{60} (SW): 2.3 pg/L C_{70} (SW): 3.4 pg/L C_{76} (SW): 1.2 ng/L C_{78} (SW): 600 pg/L C_{84} (SW): 1.6 ng/L [60]PCBM (SW): 1.4 pg/L [60]PCBB (SW): 1.9 pg/L

(continued)

giovanni.libralato@unina.it

Table 3 (continued)

Ref.	Analysis	Separation	Detection	MLOD
				[60]NMFP (SW): 0.4 pg/L
Soil and sediment samples				
Carboni et al. (2016)	C_{60}, C_{70}	Biphenyl-coated stationary LC phase	Source: ion booster electro spray ionization (IB-ESI) MS: QTOF Acq. SRM and SIM	C_{60} (soils): 84 pg/Kg C_{70} (soils): 168 pg/Kg
Sanchís et al. (2015)	C_{60}, C_{70} [60]NMFP [60]CPTAE [60]PCBM [60]ThPCBM [70]PCBM	Cosmosil Buckyprep (250 × 4.6 mm, 5 µm) with toluene	Source: APPI MS: Q-OrbitrapMS Acq. SRM and SIM	C_{60}: 0.12 pg/g C_{70}: 0.072 pg/g [60]NMFP: 0.083 pg/g [60]CPTAE: 1.3 pg/g [60]PCBM: 0.062 pg/g [60]ThPCBM: 0.15 pg/g [70]PCBM: 0.52 pg/g
Carboni et al. (2014)	C_{60}, C_{70}	Cosmosil Buckyprep (250 × 4.6 mm, 5 µm) with toluene/methanol	UV detection	C_{60} (soils): 3 ng/g C_{70} (soils): 10 ng/g
Atmosphere				
	C_{60}, C_{70} [60]NMFP [60]CPTAE [60]PCBM [60]ThPCBM [70]PCBM	Hypersil GOLD C18 column (150 × 2.1 mm, 1.9 µm particle size, 175 Å)	Source: Heated ESI and APPI MS: QqQ Acq. SIM	5.4–20.1 pg/m^3

Acq. Acquisition mode; *MLOD* method limit of detection; *pSRM* pseudo selected, reaction monitoring; *QqLiT* hybrid quadrupole-linear ion trap; *QqQ* triple quadrupole; *SIM* selected ion monitoring; *SRM* selected reaction monitoring; *SW* surface water; *WW* wastewater

giovanni.libralato@unina.it

4.2 Fate and Behaviour of Carbon Nanomaterials

4.2.1 In the Aquatic Environment

CNMs are virtually insoluble in water [e.g., the estimated solubility for C_{60} fullerene was 1.3×10^{-11} ng/mL (Heymann 1996) with a log K_{ow} of 6.67 (Jafvert and Kulkarni 2008)]. Therefore, fullerenes suspensions in the aquatic environment are likely to bind sediments and particulate matter (Li et al. 2008a), as was observed in wastewater effluents (Farré et al. 2010). Also, fullerenes tend to aggregate each other, forming polar clusters with negative surface charges (Duncan et al. 2007), which polarise the unpaired electrons of immediate water molecules stabilising colloidal suspensions up to the 100 mg/L (Fortner et al. 2005).

The behaviour (agglomeration, growth, and deposition) of CNMs aggregates in aqueous suspension follows the Derjaguin-Landau-Verwey-Overbeek (DLVO) model (Verwey et al. 1999; Derjaguin et al. 1987; Xing et al. 2010; Chang and Bouchard 2013), which is based on equilibria between two interactions: the electrostatic and the van der Waals forces. According to DLVO, the surface of NPs is surrounded by a double layer of ions, which confers an electrical charge to the particle. Electrostatic repulsion among NPs is equilibrated by attractive van der Waals forces. The aggregation of individual NPs leads to larger aggregates that, eventually, may flocculate.

The standard DLVO model, although approximate, is still a basic approach for explaining the qualitative behaviour of CNMs suspensions in different ionic strength and pH conditions:

- **Influence of ionic strength**: An increase in the ionic strength leads to a reduction in the energy barrier between colloids due to compression of the electric double layer. In this situation, the attractive van der Waals interactions dominates, and this leads to the formation of larger aggregates with lower Zeta potential. Subsequently, more NPs are expected to flocculate when the ionic strength increases (Brant et al. 2005; Jiang et al. 2009).
- **Influence of pH**: At low pH, aggregates present a positive surface charge and, conversely, at high pH, a negative surface charge. The isoelectric point is the neutral pH at with a particle has zero net surface charge. When medium pH is far more acidic or basic than the characteristic isoelectric point, NPs tend to be smaller and tend to present higher Zeta potential values. On the contrary, at intermediate pHs, close to the isoelectric point, van der Waals interaction are predominant leading to further aggregation and favouring sedimentation.

Most works that study the distribution and aggregation behaviour of CNMs in the aquatic environment were undertaken using C_{60} fullerene as model carbon NP. These aggregates of C_{60}, dispersed in water, are often called nC_{60}. Nevertheless, some works based on other CNMs have also been carried out; e.g., Brant et al. (2007) studied the aggregation behaviour of C_{70} and other functionalized fullerenes. In this work, a lesser tendency of aggregation, forming bigger and

giovanni.libralato@unina.it

less stable aggregates was reported for C_{70}, and phenyl-C_{61}-butyric acid methyl ester ([60]PCBM)-fullerene was stabilised after 33 days, reaching mean hydrodynamic values of 1082 ± 16 nm. Hou and Jafvert (2008) through different experiments performed using either, lamp and sunlight, showed that irradiation in the presence of oxygen oxidises nC_{60} aggregates. Lee et al. (2009) identified the transformation products of nC_{60} irradiated with monochromatic ultraviolet (UV) light at 254 nm, finding that epoxides and ethers can be formed.

The presence of organic matter, sunlight and the presence of surfactant are other factors that modify the stability of fullerene suspensions. Under relevant environmentally conditions, (1) pseudo-first order oxygenation, (2) hydroxylation reactions and (3) partial mineralisation have been proved for nC_{60} under long-term irradiation (Hwang and Li 2010). In the case of CNTs, the irradiation in environmental conditions leads (1) to carboxylation processes and (2) to the reaction with ROS species (singlet oxygen and hydroxyl radicals) (Qu et al. 2013). A statistically significant increase in carbonyl and hydroxyl functional groups was observed (Qu et al. 2013). Oxidative biodegradation has also been reported (Russier et al. 2010).

4.2.2 In Soils

The expected sources of CNMs in soils are dry and wet atmospheric deposition processes and the use of WWTP sludge for agriculture purposes (Navarro et al. 2013). Once in soils, the sorption to clay in conjunction with the effect of electrostatic repulsion of cations steers the aggregates mobility (Li et al. 2008a; Sedlmair et al. 2013).

Wang et al. studied the transport and retention of nC_{60} aggregates in water-saturated soil columns. In all of their experiments, the aggregates were not detected in column effluents, demonstrating the high affinity and retention of nC_{60} aggregates in soil. Moreover, the addition of humic acids increased the transport of fullerenes (Wang et al. 2010b). In another work, Li et al. (2008b), studied the retention of fullerenes in quartz sands columns and the maximum retention capacities were calculated. The retention capacity ranged from 0.44 to 13.99 μg/g, depending on the flow. More recently, Zhang et al. also observed a dependency between the soil retention capacity and the nC_{60} flow in a Lula soil, while such variation was not seen in Ottawa sand. This effect was attributed to the fact that Lula soil grains were smaller, more irregular, roughly shaped and heterogeneous (Zhang et al. 2012). Cationic species also modified the mobility of fullerene aggregates: with Ca^{2+} ions, the deposition increased more than with Na^{+} ions.

The stability of fullerenes in superficial soils might be relatively short due to the oxidation processes catalysed by UV light (Chibante and Heymann 1993). Nevertheless, the retention in a reductive environment (e.g., sulphur-rich environments) can satisfactorily explain the long-term durability of fullerenes as reported before (Buseck 2002).

giovanni.libralato@unina.it

In the case of SWCNTs, the presence of mesoporous and organic matter might significantly increase their mobility. Additionally, Khan et al. (2013), observed that SWCNT exhibited a certain degree of mobility through a municipal solid waste, including paper, metal (aluminium cans), food surrogates, plastic (beads) and glass (beads). Consequently, potential pollution of landfill soils may occur. Because CNTs are likely to be oxidised in environmental conditions (Qu et al. 2013), it is also important to evaluate the mobility of oxidised nanotubes. The mobility of oxidised MWCNTs (OMWCNTs) aggregates through glass bead columns was assessed (Yang et al. 2013). The results of this study showed that in agreement with the DLVO theory, ionic strength, pH and the organic material content were found to be the main factors driving the OMWCNTs aggregates' mobility and properties.

In the case of graphene, since their main applications are in microelectronics, their life-cycle assessment indicates that most of it may end in landfills. However, the mobility of graphene flakes in soils has not been assessed. Recently, it has been hypothesised that graphene in soils may be physically modified, and it will leach (Arvidsson et al. 2013). But, since the solubility of graphene sheets and nano-flakes in water is virtually zero, graphene is likely to float and accumulate in the water-air interface, similarly than oil spills.

4.2.3 In the Atmosphere

The fate and behaviour of CNMs in the atmosphere have not been assessed yet. Nevertheless, it can be hypothesised that once emitted to the atmosphere, e.g. by combustion sources, carbon-based NMs, such as fullerenes will be associated to atmospheric particulate first to be finally deposited. It is well known that UV radiation and ozone can oxidise C_{60} (Lee et al. 2009; Chibante and Heymann 1993). Hence, radical degradation processes of fullerenes in the atmosphere are likely to play a role. Until now, other CNMs have been much less studied.

4.3 Toxicity of Carbon-Based NMs

The central mechanisms associated with carbon-based NMs toxicity are oxidative stress, the membrane disruption and DNA damages.

C_{60} fullerene has been used as model fullerene in most ecotoxicity studies. In this case, oxidative stress from ROS species has been commonly associated with lipid peroxidation (Sayes et al. 2005). However, the origin of ROS species is under debate. ROS species may be produced by NMs or by cells when they interact with fullerenes (Lyon et al. 2006). On membrane disruption, Fang et al. observed changes in the membrane lipid composition after exposure. An increase was detected in the levels of iso- and ante iso-branched fatty acids and monounsaturated fatty acids that can enhance membrane permeability (Fang et al. 2007). Fullerenes have also been related to interferences in the DNA repairing mechanisms (Dinesh et al. 2012).

giovanni.libralato@unina.it

In the case of CNTs, they can also pass through cell membranes (Kang et al. 2007) producing the generation of ROS species and, consequently, oxidative stress (Manna et al. 2005; Murray et al. 2009). Physical disruption of the cell membranes (Kang et al. 2007) has also been observed. Also, some authors have reported their accumulation in tissues (Yang et al. 2008). All these effects are dependent on CNTs characteristics such as length (Magrez et al. 2006), aggregates size (Magrez et al. 2006), the presence of functional groups (Liu et al. 2008; Sayes et al. 2006; Klaper et al. 2010), structural imperfections (Muller et al. 2008) and the presence of impurities, in particular, metals impurities (Shvedova et al. 2005). Due to the high variety of CNTs and the types of differences highly influencing their final toxicity, it is difficult to compare the results from different studies, particularly, when substantially different CNT have been tested (Magrez et al. 2006).

During the last decade a high amount of research has been undertaken to assess the toxicity of NMs, in general, and those based on carbon, in particular. However, different inconsistencies have been encountered. The first is that toxicity tests for raw materials evaluation are not suitable to test NMs, e.g., in the case of the aquatic toxicity tests for carbon-based NMs, controversy arises from water suspension preparation methods. The main approaches reported for the preparation of fullerene suspensions are:

- **The long-term stirring method**: Aggregates are round-shaped and large (often in the micron-scale). It is a time-consuming approach, and the resulting suspensions are unstable.
- **The solvent transfer method** (Oberdörster 2004): fullerenes are first suspended in an organic solvent (commonly, tetrahydrofurane or toluene). A particular volume of this organic suspension is transferred to ultrapure water, and the organic solvent is evaporated by heating or rotary evaporation. Aggregates remain in water suspensions. The aggregates produced by this method are smaller than by long-term stirring, but residues of solvent are present (Fortner et al. 2005).
- **The ultrasound-assisted method** (Lovern and Klaper 2006): this method involves no organic solvent. Fullerene-aggregates present sharp edges and are smaller than by prolonged stirring. This is the most straightforward approach to obtaining fullerene suspensions at lab-scale but is far from reproducing real environmental conditions.

The toxicity tests were dependent on the methods used to prepare the suspensions. In this sense, suspensions prepared by solvent transfer methods and by ultrasounds presented higher toxicity than those by long-term stirring. Thus, long-term stirring is the currently accepted approach, because it is more ecologically representative.

giovanni.libralato@unina.it

4.3.1 Toxicity Tests Based on Aquatic Organisms

The effects of C_{60} aggregates in freshwater invertebrate such as the *D. magna* have been extensively studied. Their adsorption to the digestive tract has been reported (Tao et al. 2011; Tervonen et al. 2011). It should be remarked that depending on the preparation process differences in toxicity results were obtained. E.g. Lovern et al. measured the toxic effects of fullerene aggregates prepared either by sonication or by solvent-transfer method (Lovern and Klaper 2006). LC_{50} of the suspension obtained by the solvent transfer method was 460 µg/L while those obtained by ultrasounds presented lower toxicity values, with LC_{50} concentrations of 7.9 mg/L.

Different studies have shown that SWCNT presented antimicrobial activity due to their action on the bacterial cell membrane (Kang et al. 2007). Nevertheless, some bacteria such as *Cupriavidus metallidurans* were shown to be resistant to MWCNT aggregates, probably because of their particular efflux systems which make them able of to be detoxification (Simon-Deckers et al. 2009).

Several studies have assessed the potential toxicity of CNTs to *D. magna*. E.g. Zhu et al. determined EC_{50} concentrations of 1.306 and 8.723 mg/L for SWCNT and MWCNT respectively. Suspensions were prepared by "vigorous shaking" (Zhu et al. 2009) and the bioaccumulation of purified and ultra-sonicated suspensions of SWCNT was studied (Petersen et al. 2009a). SWCNTs were adsorbed on the digestive tract with low depuration rates of 50–85%. On the other hand, low acute toxicity and some sub-lethal effects have been observed in tests carried out using fish as test species. E.g. in an experiment performed by Smith et al., rainbow trout were exposed to 0.5 mg/L of SWCNT dispersed with ultrasounds and sodium dodecyl sulphate during 10 days. Abnormal respiration rates were observed. In addition, an increase of fish aggressive behaviours was ascertained. This change on the fish aggressiveness led to the stop of the experiment on the day no. 10 because of ethical reasons (mortality was caused by the attack of fish each other). This experiment also revealed that after exposure several physiological abnormalities were produced in fish. In addition, control experiments with sodium dodecyl sulphate were carried out in order to discard the toxic effects of this substance (Smith et al. 2007).

A small number of studies have been carried to date to assess the potential toxicity of graphene in aquatic organisms. Among them, the antimicrobial activity of graphene oxide to *E. coli* was reported (Akhavan and Ghaderi 2012). In contrast, experiments performed with *Amphibalanus amphitrite nauplii* exposed to single layers of graphene oxide showed very low toxicity with no-adverse observed effects level (NOAEL) of 500 mg/L (Mesarič et al. 2013). In another work the exposure of the nematode *Caenorhabditis elegans* to graphene oxide showed ROS production with the subsequent oxidative stress (Wu et al. 2013b). In another study, the toxicity of pristine graphene monolayer flakes and graphene nanopowder grade C1 was investigated (Pretti et al. 2014). In general, the toxicity was inversely proportional to the particle size, as expected. The bioluminescence inhibition of the marine bacteria *Vibrio fischeri* showed EC_{50} values ranging from 1.75 to 1.95 mg/L in

giovanni.libralato@unina.it

5, 15 and 30 min incubation times. The growth inhibition of *Dunaliella tertiolecta* showed EC_{50} values between 1.14 and 2.25 mg/L. As can be seen in all these experiments, effective concentrations were much higher than those expected in the environment. However, chronic exposures have not been properly evaluated. In a more recent study (Sohn et al. 2015), the acute toxicity of SWCNTs was assessed towards freshwater organisms including the microalgae (*Raphidocelis subcapitata* and *Chlorella vulgaris*), a micro-crustacean (*D. magna*), and a fish (*Oryzias latipes*). The test was carried out according to the OECD test guidelines (201, 202, and 203). The results revealed that SWCNTs inhibited the growth of the algae *R. subcapitata* and *C. vulgaris* representing "acute category 3" in the Globally Harmonized System (GHS) of classification and labelling of chemicals. While the acute toxicity test with *O. latipes* and *D. magna* did not show any effects up to a concentration of 100.00 mg/L SWCNTs, indicating no hazard category in the GHS classification. In conclusion, SWCNTs were found to induce acute ecotoxicity in freshwater microalgae.

4.3.2 Toxicity Tests Based on Sediment and Soil Organisms

In Table 4 a summary of carbon-based NM toxicity tests is presented. As can be seen, in an experiment presented by Pakarinen et al. (2011) no acute or sub-lethal effects were observed when *Lumbriculus variegatus* was exposed to a suspension of 60 mg/kg_{dw} of fullerene aggregates prepared by long-term stirring. In another study, Johansen et al. (2008) studied soil microbial communities exposed to fullerenes during 14 days. In this experiment, no changes regarding the total respiration, the biomass, the number and diversity of bacteria and the total number and diversity of protozoans were observed. Only small variations in the genetic diversity of the microbiota were found. On the other hand, it was shown that soil invertebrates are affected in a dose-dependent way, at population, and at individual levels. While the adult of earthworms (*Lumbricus rubellus*) did not exhibit significant mortality, when they were exposed to 15.4 and 154 mg/kg of C_{60} fullerene their cocoon production and juvenile growth rate was significantly decreased, and juvenile mortality was as well significant (Van der Ploeg et al. 2011).

It has been reported that the benthic populations are affected at high concentrations by the presence of CNTs. For example, the biodiversity of a benthic community exposed during 15 months to concentrations up to 2 mg/kg of MWCNT was statistically affected (Velzeboer et al. 2013). The antimicrobial activity of CNTs was also observed in soil communities but only at extremely high concentrations. The soil microbial activity was mitigated at 5000 mg/kg of MWCNT (Chung et al. 2011).

In summary, one challenge in the ecotoxicity assessment of CNMs is the lack of analytical techniques able to assess their presence in the environment. Nowadays, only the particular case of fullerenes has been solved but nor for carbon nanotubes neither structures based on graphene have been developed quantitative approaches for real samples and concentrations. E.g., radioactively labelled-CNTs have to be

giovanni.libralato@unina.it

Table 4 Summary of relevant studies reporting thetoxicity of fullerenes and CNTs to benthic and soil organisms

Ref.	NMs	Organism	Matrix	Effects
Pakarinen et al. (2011)	C_{60}	*Lumbriculus variegatus*	Sediment	– No effects up to 60 mg/kg_{dw}
Chung et al. (2011)	C_{60}	Total microbial community	Soil	– No effects in total respiration
Pakarinen et al. (2011)	C_{60}	Total microbial community	Soil	– No effects in total respiration and biomass – Changes in biodiversity
Johansen et al. (2008), Tong et al. 2007)	C_{60}	*Lumbricus rubellus*	Soil	– No adult mortality at 154 mg/kg – Alteration in gene expression – Gut and muscles damage – Juvenile mortality – Decreased cocoon production – Decreased juvenile growth rate
Van der Ploeg et al. (2011)	SWCNT	*Amphiascus tenuiremis*	Sediment	– Significant mortality – Reduced development success – Reduced fertility
Velzeboer et al. (2013)	MWCNT	Total microbial community	Soil	– Decrease in respiration at 500 and 5000 mg/kg
Van Der Ploeg et al. (2013)	DWCNT	*Eisenia veneta*	Soil	– No effects in growth and mortality up to 495 mg/kg – Cocoon production altered

used in laboratory studies (Guo et al. 2013), but additional work is needed to develop reliable analytical procedures for non-labelled.

Therefore, is tough to establish real scenarios of exposure. Moreover, CNMs are composed primarily of carbon presenting different shapes directly linked with their properties. However, many techniques (e.g., dynamic light scattering) utilize equations and assumptions based on spheres. Thus, making measurements of carbon nanomaterial concentrations is challenging and prone to artifacts (Edgington et al. 2014).

On the other hand, the lack of stability of CNMs suspensions in aqueous media also complicates their toxicity assessment.

In the absence of stabilizing agents, carbon NMs often agglomerate and settle out of solution in aqueous test media typically used in nano-ecotoxicity experiments. However, the use of these dispersive agents or other methods can distort the

giovanni.libralato@unina.it

shape and size of aggregates, and they are ecologically irrelevant. Therefore, some agreements in this sense should be considered by the research community, and the test must be adapted as much as possible to those reproducing real scenarios of exposure.

Also, critical information for understanding the reliability of test methods, such as test method precision, robustness, reproducibility, and variability within and among laboratories, are rarely published for nano-ecotoxicity studies in general. For example, very few interlaboratory studies have been conducted so far (Petersen et al. 2014).

Another important aspect is the form in which CNMs are released into the environment from nanotechnological applications and consumer products. Therefore, ecotoxicological testing of pure CNMs standards may overestimate or underestimate their potential risks.

Finally, very few studies have been conducted assessing the interaction of CNMs with other co-contaminants in the same environment. How adsorption capabilities can influence in the bioavailability of co-contaminants and how hysteresis can play a significant role in their transport and in the modulation of their toxicity should be properly studied using complex mixtures of CNMs and organic toxicants contaminants. These phenomena are known as Trojan-Horse effect and it will be considered in the next section.

5 Trojan-Horse Effects

Thanks to their adsorption/desorption properties CNMs can stabilize, transport and desorb other toxicants. CNMs can change the bioavailability, and or certain properties of co-contaminants, producing the modulation of their toxicity. This effect known as Trojan-horse effect is influenced by the composition of the mixtures, their relative concentrations and different environmental conditions such as the pH.

In fact, this capacity is explored in various applications, e.g., in nano-medicine that studied the use of CNMs as drug carriers for chemotherapy or the use of reusable CNMs for contaminants removal in advanced wastewater treatments.

However, in the environment these effects in complex mixtures have not well understood yet, enhancing the uncertainty of the risk associated with NMs. During the recent years, some studies started to study synergisms/antagonisms between organic contaminants and CNMs. E.g. Baun et al. (2008) observed changes in the acute toxicity of atrazine, methyl parathion, pentachlorophenol and phenanthrene to *D. magna* in the presence of nC_{60}-aggregates. Also, Hg^{2+} bioavailability to zebra fish was enhanced in the presence of fullerene aggregates. The joint effects induced by fullerene C_{60} and As(III) in zebra fish hepatocytes. Hepatocytes of zebra fish *Danio rerio* were exposed to As(III) (2.5 or 100 μM), fullerene C_{60} or As + fullerene C_{60} for 4 h. The main results showed that cells co-exposed to fullerene C_{60} had a significantly higher accumulation of As(III), showing a

giovanni.libralato@unina.it

Trojan-horse effect, which did not result in higher cell toxicity. Instead, co-exposure of As(III) with fullerene C_{60} showed to reduce cellular injury (Azevedo Costa et al. 2012). In another study, Park et al. (2011) studied the association between aqueous C_{60} aggregates and 17α-ethinyl estradiol (EE2). The results measuring the vitellogenin gene expression in zebra fish showed that bioavailability of EE2 was reduced with increasing concentration of C_{60} fullerene aggregates, and bioavailability of EE2 decreased further after aging 28 days with C_{60} fullerene aggregates. Reduction in EE2 bioavailability was correlated with computed surface area of C_{60} fullerene aggregates, and reduced bioavailability of EE2 upon aging was consistent with absorption of EE2 within C_{60} fullerene aggregates. Results indicate that C_{60} fullerene aggregates can reduce the bioavailability of some substances and influence environmental fate and transport of associated substances.

The Trojan–horse effects between other CNMs and organic contaminants have also been evaluated. Recently, Sanchís et al. (2016) studied the toxicity of three CNMs (fullerene-soot, MWCNTs, and graphene) by two standardized toxicity bioassays: the immobilization of the invertebrate *D. magna* and the bioluminescence inhibition of *V. fischeri*. In addition, synergistic and antagonistic effects of binary mixtures composed of fullerene soot and organic co-contaminants as malathion, glyphosate, diuron, triclosan, and nonylphenol were assessed. The isobologram method was used to evaluate the concentrations producing an effect, in comparison to those effects expected by a simple additive approach. In this study, antagonism was the predominant effect. However, synergism was also observed as in the case of *D. magna* exposed to mixtures of malathion and fullerene soot. *D. magna* was shown to be the most sensitive assay when CNMs were present. The vector function of NMs aggregates and the unexpected release inside living organisms was proven for malathion.

The interaction between CNTs and polycyclic aromatic hydrocarbons (PAHs) and other hydrophobic compounds may drive to changes in the global toxicity of nonpolar pollutants (Farré et al. 2009). For example, diuron toxicity in Chlorella vulgaris was enhanced in the presence of MWCNTs (Schwab et al. 2013). In other studies, phenanthrene bioavailability to *Oryzias latipes* was increased by MWCNT (Su et al. 2013), and the pyrene bioaccumulation in earthworms was decreased by MWCNT and SWCNT (Petersen et al. 2009b). Outside of aqueous media, different toxicity behaviour was observed when plants exposed to pesticides in soils were contaminated with various concentrations of fullerenes and CNTs (De La Torre-Roche et al. 2013). Lerman et al. (2013) evaluated the interaction between SWCNTs, carbamazepine, bisphenol A, phenanthrene and dissolved organic matter (DOM). The hydrophobic neutral fraction of the DOM exhibited the strongest reductive effect on carbamazepine adsorption. In contrast, the hydrophobic acid fraction decreased the adsorption of carbamazepine mainly via direct competition. When DOM and bisphenol A were co-introduced, the adsorption of carbamazepine was significantly reduced. This study suggests that the chemical nature of DOM can significantly affect the sorptive behaviour of polar organic pollutants with CNTs when all are introduced in the same system.

giovanni.libralato@unina.it

Finally, it should be noted that much less work has been performed to assess the influence of other CNMs such as graphene on the toxicity of other co-contaminants. The influence of graphene nanoplatelets as a vector for aromatic environmental pollutants were assessed (Lammel et al. 2015). In this study, the increase of cellular uptake and associated risk in vitro hepatoma cell line PLHC-1 of the topminnow fish (Poeciliopsis lucida) was studied. It was observed that pre- and co-exposure of cells to graphene oxide and carboxyl graphene nanoplatelets had a potentiating effect increasing the effective concentration of aryl hydrocarbon receptor (AhR) by facilitating their passive diffusion into the cells. Thus, it damage the cells' plasma membrane and/or by transporting them over the plasma membrane via a Trojan horse-like mechanism.

Considering the different studies, it can be summarized that most of the CNMs induce adsorption of organic and inorganic co-contaminants. Initially, the adsorption stabilizes and transports the co-contaminants but also reduce their bioavailability. However, hysteresis can facilitate the desorption by environmental facilitating bioavailability and enhancing toxicity. Other factors influencing on this process are the relative polarity of the adsorbates, their concentrations and the presence of other co-contaminants in competition.

6 Barriers and Research Needs

Although nanotechnology is promising for advanced water and wastewater treatment processes, their readiness for commercialization varies widely. While some of these processes are already on the market, others require a significant investment in research before to pass at full-scale applications. The main current challenges include technical hurdles, cost-effectiveness, and the evaluation of their potential environmental and human risk.

There are five significant research gaps for full-scale applications of nanotechnology in water/wastewater treatment.

- First, test the technologies under real conditions of water and wastewaters.
- Second, the study of the potential impact of these technologies in the environment is required. However, to do this, is necessary to develop quantitative and qualitative reliable analytical methods to characterize and measure their emissions. Besides, reliable ecotoxicity test properly designed and standardized continues being necessary. NMs possess unique challenges for risk assessment and management, as they are small particles instead of molecules or ions for which risk evaluation framework and protocols are already in place.
- Third, the long-term efficiency of these materials should also be determined. Most of the studies at laboratory scale to date have been conducted for relatively short periods of time.

giovanni.libralato@unina.it

- Fourth, despite the superior performance, the adoption of innovative technologies strongly depends on the cost-effectiveness and currently most of the NMs for water and wastewater treatment are costly. However, the potential of reuse of CNMs can be an advantage in this sense.
- Finally, the compatibility between novel nanotechnologies and current water and wastewater treatments and infrastructure also needs to be addressed. Therefore, for short-term implementation, it is important, the design these new technologies considering minimal changes to the existing infrastructures.

7 Conclusions

Nowadays, the main challenges faced by novel technologies for water and wastewater treatments based on nanotechnology are safety issues, measurement methods, lack of standardization, lack of regulation, sometimes the high cost of materials production, technical hurdles, and difficult implementation, but many of them are perhaps only temporary. To overcome these barriers, the collaboration between research, industry and regulatory bodies is essential.

The development of nanotechnology but avoiding unintended consequences can provide the efficient treatments currently necessary to face water scarcity, environmental pollution and to protect the environment and human health. CNMs, thanks to their unique adsorption capabilities, can be key materials in these developments. However, some gaps of information about their potential risks, in particular, toxicity and Trojan-Horse effects, should be previously assessed and the standard procedures for their application should be established.

Acknowledgements This work has been funded by the Spanish Ministry of Science and Innovation through the projects Nano-Transfer (ERA-NET SIINN PCIN-2015-182-CO2-01) and Integra-Coast (CGL2014-56530-C4-1-R).

References

Abraham JK et al (2004) A compact wireless gas sensor using a carbon nanotube/PMMA thin film chemiresistor. Smart Mater Struct 13(5):1045–1049

Akhavan O, Ghaderi E (2012) *Escherichia coli* bacteria reduce graphene oxide to bactericidal graphene in a self-limiting manner. Carbon 50(5):1853–1860

AlSaadi MA et al (2016) Removal of cadmium from water by CNT-PAC composite: effect of functionalization. Nano 11(1)

Al-Saidi HM et al (2016) Multi-walled carbon nanotubes as an adsorbent material for the solid phase extraction of bismuth from aqueous media: kinetic and thermodynamic studies and analytical applications. J Mol Liq 216:693–698

Álvarez-Torrellas S et al (2016) Comparative adsorption performance of ibuprofen and tetracycline from aqueous solution by carbonaceous materials. Chem Eng J 283:936–947

giovanni.libralato@unina.it

Amiraslanzadeh S (2016) The effect of doping different heteroatoms on the interaction and adsorption abilities of fullerene. Heteroat Chem 27(1):23–31
Aroutiounian VM (2015) Gas sensors based on functionalized carbon nanotubes. Front Struct Civil Eng 9(4):333–354
Arvidsson R, Molander S, Sandén BA (2013) Review of potential environmental and health risks of the nanomaterial graphene. Hum Ecol Risk Assess Int J 19(4):873–887
Astefanei A, Núñez O, Galceran MT (2015) Characterisation and determination of fullerenes: a critical review. Anal Chim Acta 882:1–21
Azevedo Costa CL et al (2012) In vitro evaluation of co-exposure of arsenium and an organic nanomaterial (fullerene, C 60) in zebrafish hepatocytes. Comp Biochem Physiol C Toxicol Pharmacol 155(2):206–212
Azimi S et al (2014) Synthesis, characterization and antibacterial activity of chlorophyllin functionalized graphene oxide nanostructures. Sci Adv Mat 6(4):771–781
Badhulika S, Myung NV, Mulchandani A (2014) Conducting polymer coated single-walled carbon nanotube gas sensors for the detection of volatile organic compounds. Talanta 123:109–114
Balasubramanian K, Burghard M (2005) Chemically functionalized carbon nanotubes. Small 1 (2):180–192
Baughman RH, Zakhidov AA, De Heer WA (2002) Carbon nanotubes—the route toward applications. Science 297(5582):787–792
Baun A et al (2008) Toxicity and bioaccumulation of xenobiotic organic compounds in the presence of aqueous suspensions of aggregates of nano-C60. Aquat Toxicol 86(3):379–387
Becker L et al (1994) Fullerenes in the 1.85-billion-year-old Sudbury impact structure. Science 265(5172):642–645
Bellucci S (2009) Nanoparticles and nanodevices in biological applications
Bénard P, Chahine R (2007) Storage of hydrogen by physisorption on carbon and nanostructured materials. Scripta Mater 56(10):803–808
Brant J, Lecoanet H, Wiesner M (2005) Aggregation and deposition characteristics of fullerene nanoparticles in aqueous systems. J Nanopart Res 7(4–5):545–553
Brant JA et al (2007) Fullerol cluster formation in aqueous solutions: implications for environmental release. J Colloid Interface Sci 314(1):281–288
Buseck PR (2002) Geological fullerenes: review and analysis. Earth Planet Sci Lett 203(3–4):781–792
Buseck PR, Adachi K (2008) Nanoparticles in the atmosphere. Elements 4(6):389–394
Cabria I, López MJ, Alonso JA (2005) Enhancement of hydrogen physisorption on graphene and carbon nanotubes by Li doping. J Chem Phys 123(20)
Carboni A et al (2014) An analytical method for determination of fullerenes and functionalized fullerenes in soils with high performance liquid chromatography and UV detection. Anal Chim Acta 807:159–165
Carboni A et al (2016) A method for the determination of fullerenes in soil and sediment matrices using ultra-high performance liquid chromatography coupled with heated electrospray quadrupole time of flight mass spectrometry. J Chromatogr A 1433:123–130
Chandrakumar KRS, Ghosh SK (2008) Alkali-metal-induced enhancement of hydrogen adsorption in C60 fullerene: an ab initio study. Nano Lett 8(1):13–19
Chang X, Bouchard DC (2013) Multiwalled carbon nanotube deposition on model environmental surfaces. Environ Sci Technol 47(18):10372–10380
Chang YN et al (2016) Antimicrobial behavior comparison and antimicrobial mechanism of silver coated carbon nanocomposites. Process Saf Environ Prot 102:596–605
Chao YC, Shih JS (1998) Adsorption study of organic molecules on fullerene with piezoelectric crystal detection system. Anal Chim Acta 374(1):39–46
Chao Y et al (2014) Development of novel graphene-like layered hexagonal boron nitride for adsorptive removal of antibiotic gatifloxacin from aqueous solution. Green Chem Lett Rev 7 (4):330–336

giovanni.libralato@unina.it

Chawla J, Kumar R, Kaur I (2015) Carbon nanotubes and graphenes as adsorbents for adsorption of lead ions from water: a review. J Water Supply Res Technol AQUA 64(6):641–659
Chen P et al (1999) High H_2 uptake by alkali-doped carbon nanotubes under ambient pressure and moderate temperatures. Science 285(5424):91–93
Chen Z, Westerhoff P, Herckes P (2008) Quantification of C60 fullerene concentrations in water. Environ Toxicol Chem 27(9):1852–1859
Chen S, Liu D, Wang H (2015a) Preparation of modified multiwalled carbon nanotubes/chitosan composites and their antifouling properties. Huagong Xuebao/CIESC J 66(11):4689–4695
Chen JH et al (2015b) Highly effective removal of Cu(II) by triethylenetetramine-magnetic reduced graphene oxide composite. Appl Surf Sci 356:355–363
Chen L et al (2016) One-step fabrication of amino functionalized magnetic graphene oxide composite for Uranium(VI) removal. J Colloid Interface Sci 472:99–107
Chibante LPF, Heymann D (1993) On the geochemistry of fullerenes: stability of C60 in ambient air and the role of ozone. Geochim Cosmochim Acta 57(8):1879–1881
Chung H et al (2011) The effect of multi-walled carbon nanotubes on soil microbial activity. Ecotoxicol Environ Saf 74(4):569–575
Commission E (2013) Commission Delegated Regulation (EU) No 1363/2013
Czech B, Oleszczuk P (2016) Sorption of diclofenac and naproxen onto MWCNT in model wastewater treated by H_2O_2 and/or UV. Chemosphere 149:272–278
Dai H et al (1996) Single-wall nanotubes produced by metal-catalyzed disproportionation of carbon monoxide. Chem Phys Lett 260(3–4):471–475
Davydov VY et al (2000) Thermodynamic characteristics of adsorption of organic compounds on molecular crystals of C60 fullerene. Zh Fiz Khim 74(4):712–717
De La Torre-Roche R et al (2013) multiwalled carbon nanotubes and C60 fullerenes differentially impact the accumulation of weathered pesticides in four agricultural plants. Environ Sci Technol 47(21):12539–12547
De Martino A et al (2012) Removal of 4-chloro-2-methylphenoxyacetic acid from water by sorption on carbon nanotubes and metal oxide nanoparticles. RSC Adv 2(13):5693–5700
Derjaguin BV, Churaev NV, Muller VM (1987) Wetting films. In: Surface forces. Springer, pp 327–367
Deryabin DG et al (2014) The activity of [60]fullerene derivatives bearing amine and carboxylic solubilizing groups against *Escherichia coli*: a comparative study. J Nanomat 2014
Dhall S, Jaggi N, Nathawat R (2013) Functionalized multiwalled carbon nanotubes based hydrogen gas sensor. Sens Actuators, A 201:321–327
Dillon AC et al (1997) Storage of hydrogen in single-walled carbon nanotubes. Nature 386 (6623):377–379
Dinesh R et al (2012) Engineered nanoparticles in the soil and their potential implications to microbial activity. Geoderma 173:19–27
Dong L, Henderson A, Field C (2012) Antimicrobial activity of single-walled carbon nanotubes suspended in different surfactants. J Nanotechnol
Dosunmu E et al (2015) Silver-coated carbon nanotubes downregulate the expression of Pseudomonas aeruginosa virulence genes: a potential mechanism for their antimicrobial effect. Int J Nanomed 10:5025–5034
Dresselhaus MS, Dresselhaus G, Saito R (1992) Carbon fibers based on C60 and their symmetry. Phys Rev B 45(11):6234–6242
Duncan LK, Jinschek JR, Vikesland PJ (2007) C60 colloid formation in aqueous systems: effects of preparation method on size, structure, and surface charge. Environ Sci Technol 42(1):173–178
Edgington AJ et al (2014) Microscopic investigation of single-wall carbon nanotube uptake by *Daphnia magna*. Nanotoxicology 8(SUPPL 1):2–10
El-Barbary AA (2016) Potential energy of H_2 inside the C_{116} fullerene dimerization: an atomic analysis. J Mol Struct 1112:9–13
Er S, De Wijs GA, Brocks G (2015) Improved hydrogen storage in Ca-decorated boron heterofullerenes: a theoretical study. J Mat Chem A 3(15):7710–7714

giovanni.libralato@unina.it

Esquivel EV, Murr LE (2004) A TEM analysis of nanoparticulates in a Polar ice core. Mater Charact 52(1):15–25
Fang J et al (2007) Effect of a fullerene water suspension on bacterial phospholipids and membrane phase behavior. Environ Sci Technol 41(7):2636–2642
Farré M et al (2009) Ecotoxicity and analysis of nanomaterials in the aquatic environment. Anal Bioanal Chem 393(1):81–95
Farré Ml et al (2010) First determination of C60 and C70 fullerenes and *N*-methylfulleropyrrolidine C60 on the suspended material of wastewater effluents by liquid chromatography hybrid quadrupole linear ion trap tandem mass spectrometry. J Hydrol 383:44–51
Fastow M et al (1992) IR spectra of CO and NO adsorbed on C60. J Phys Chem 96(15):6126–6128
Fastow M, Kozirovski Y, Folman M (1993) IR spectra of CO_2 and N_2O adsorbed on C60 and other carbon allotropes—a comparative study. J Electron Spectrosc Relat Phenom 64–65 (C):843–848
Folman M, Fastow M, Kozirovski Y (1997) Surface heterogeneity of C60 as studied by infrared spectroscopy of adsorbed CO and adsorption potential calculations. Langmuir 13(5):1118–1122
Fortner JD et al (2005) C60 in water: nanocrystal formation and microbial response. Environ Sci Technol 39(11):4307–4316
Fu F, Wang Q (2011) Removal of heavy metal ions from wastewaters: a review. J Environ Manage 92(3):407–418
Fu Y et al (2014) Water-dispersible magnetic nanoparticle-graphene oxide composites for selenium removal. Carbon 77:710–721
Gao Y et al (2012) Adsorption and removal of tetracycline antibiotics from aqueous solution by graphene oxide. J Colloid Interface Sci 368(1):540–546
Goel A et al (2002) Combustion synthesis of fullerenes and fullerenic nanostructures. Carbon 40 (2):177–182
Gottschalk F, Nowack B (2011) The release of engineered nanomaterials to the environment. J Environ Monit 13(5):1145–1155
Guo T et al (1995) Catalytic growth of single-walled nanotubes by laser vaporization. Chem Phys Lett 243(1–2):49–54
Guo X et al (2013) Biological uptake and depuration of radio-labeled graphene by *Daphnia magna*. Environ Sci Technol 47(21):12524–12531
Guo Y et al (2016) Removal of anionic azo dye from water with activated graphene oxide: kinetic, equilibrium and thermodynamic modeling. RSC Adv 6(46):39762–39773
Gupta VK et al (2016) Study on the removal of heavy metal ions from industry waste by carbon nanotubes: effect of the surface modification: a review. Crit Rev Env Sci Technol 46(2):93–118
Hao X et al (2015) Metal ion-coordinated carboxymethylated chitosan grafted carbon nanotubes with enhanced antibacterial properties. RSC Adv 6(1):39–43
Hendren CO et al (2011) Estimating production data for five engineered nanomaterials as a basis for exposure assessment. Environ Sci Technol 45(7):2562–2569
Heymann D (1996) Solubility of fullerenes C60 and C70 in seven normal alcohols and their deduced solubility in water. Fullerene Sci Technol 4(3):509–515
Hilding J et al (2001) Sorption of butane on carbon multiwall nanotubes at room temperature. Langmuir 17(24):7540–7544
Hou W-C, Jafvert CT (2008) Photochemical transformation of aqueous C60 clusters in sunlight. Environ Sci Technol 43(2):362–367
Hwang YS, Li Q (2010) Characterizing photochemical transformation of aqueous nC60 under environmentally relevant conditions. Environ Sci Technol 44(8):3008–3013
Ihsanullah et al (2016) Heavy metal removal from aqueous solution by advanced carbon nanotubes: critical review of adsorption applications. Sep Purif Technol 157:141–161
Isaacson CW et al (2007) Quantification of fullerenes by LC/ESI-MS and its application to in vivo toxicity assays. Anal Chem 79(23):9091–9097

giovanni.libralato@unina.it

Ismail IMK, Rodgers SL (1992) Comparisons between fullerene and forms of well-known carbons. Carbon 30(2):229–239
Jafvert CT, Kulkarni PP (2008) Buckminsterfullerene's (C60) octanol-water partition coefficient (Kow) and aqueous solubility. Environ Sci Technol 42(16):5945–5950
Jehlička J et al (2003) Evidence for fullerenes in solid bitumen from pillow lavas of Proterozoic age from Mítov (Bohemian Massif, Czech Republic). Geochim Cosmochim Acta 67(8):1495–1506
Ji L et al (2010) Adsorption of monoaromatic compounds and pharmaceutical antibiotics on carbon nanotubes activated by KOH etching. Environ Sci Technol 44(16):6429–6436
Jiang J, Oberdörster G, Biswas P (2009) Characterization of size, surface charge, and agglomeration state of nanoparticle dispersions for toxicological studies. J Nanopart Res 11 (1):77–89
Jiang Y et al (2016) Magnetic chitosan-graphene oxide composite for anti-microbial and dye removal applications. Int J Biol Macromol 82:702–710
Jin X et al (2007) Estrogenic compounds removal by fullerene-containing membranes. Desalination 214(1–3):83–90
Jing L, Li X (2016) Facile synthesis of PVA/CNTs for enhanced adsorption of Pb^{2+} and Cu^{2+} in single and binary system. Desalin Water Treat 1–14
Johansen A et al (2008) Effects of C60 fullerene nanoparticles on soil bacteria and protozoans. Environ Toxicol Chem 27(9):1895–1903
Journet C et al (1997) Large-scale production of single-walled carbon nanotubes by the electric-arc technique. Nature 388(6644):756–758
Kang S et al (2007) Single-walled carbon nanotubes exhibit strong antimicrobial activity. Langmuir 23(17):8670–8673
Kang S et al (2008) Antibacterial effects of carbon nanotubes: size does matter! Langmuir 24 (13):6409–6413
Karakuscu A et al (2015) SiOCN functionalized carbon nanotube gas sensors for elevated temperature applications. J Am Ceram Soc 98(4):1142–1149
Karumuri AK et al (2016) Silver nanoparticles supported on carbon nanotube carpets: influence of surface functionalization. Nanotechnology 27(14)
Khan IA et al (2013) Single-walled carbon nanotube transport in representative municipal solid waste landfill conditions. Environ Sci Technol 47(15):8425–8433
Kim HH et al (2015) Clean transfer of wafer-scale graphene via liquid phase removal of polycyclic aromatic hydrocarbons. ACS Nano 9(5):4726–4733
Klaper R et al (2010) Functionalization impacts the effects of carbon nanotubes on the immune system of rainbow trout, Oncorhynchus mykiss. Aquat Toxicol 100(2):211–217
Kolkman A et al (2013) Analysis of (functionalized) fullerenes in water samples by liquid chromatography coupled to high-resolution mass spectrometry. Anal Chem 85(12):5867–5874
Kroto HW et al (1985) C60: Buckminsterfullerene. Nature 318(6042):162–163
Kwon YK (2010) Hydrogen adsorption on sp^2-bonded carbon structures: ab-initio study. J Korean Phys Soc 57(4):778–786
Lai YT, Kuo JC, Yang YJ (2014) A novel gas sensor using polymer-dispersed liquid crystal doped with carbon nanotubes. Sens Actuators, A 215:83–88
Lammel T, Boisseaux P, Navas JM (2015) Potentiating effect of graphene nanomaterials on aromatic environmental pollutant-induced cytochrome P450 1A expression in the topminnow fish hepatoma cell line PLHC-1. Environ Toxicol 30(10):1192–1204
Lawal AT (2016) Synthesis and utilization of carbon nanotubes for fabrication of electrochemical biosensors. Mater Res Bull 73:308–350
Leary R, Westwood A (2011) Carbonaceous nanomaterials for the enhancement of TiO_2 photocatalysis. Carbon 49(3):741–772
Lee J et al (2009) Transformation of aggregated C60 in the aqueous phase by UV irradiation. Environ Sci Technol 43(13):4878–4883

giovanni.libralato@unina.it

Lee KJ, Cha E, Park HD (2016) High antibiofouling property of vertically aligned carbon nanotube membranes at a low cross-flow velocity operation in different bacterial solutions. Desalin Water Treat 1–11

Leid JG et al (2012) In vitro antimicrobial studies of silver carbene complexes: activity of free and nanoparticle carbene formulations against clinical isolates of pathogenic bacteria. J Antimicrob Chemother 67(1):138–148

Lerman I et al (2013) Adsorption of carbamazepine by carbon nanotubes: effects of DOM introduction and competition with phenanthrene and bisphenol A. Environ Pollut 182:169–176

Li YH et al (2003) Competitive adsorption of Pb^{2+}, Cu^{2+} and Cd^{2+} ions from aqueous solutions by multiwalled carbon nanotubes. Carbon 41(14):2787–2792

Li YH et al (2005) Adsorption thermodynamic, kinetic and desorption studies of Pb^{2+} on carbon nanotubes. Water Res 39(4):605–609

Li D et al (2008a) Effect of soil sorption and aquatic natural organic matter on the antibacterial activity of a fullerene water suspension. Environ Toxicol Chem 27(9):1888–1894

Li Y et al (2008b) Investigation of the transport and deposition of fullerene (C60) nanoparticles in quartz sands under varying flow conditions. Environ Sci Technol 42(19):7174–7180

Li N et al (2011) Preparation of magnetic $CoFe_2O_4$-functionalized graphene sheets via a facile hydrothermal method and their adsorption properties. J Solid State Chem 184(4):953–958

Li Y et al (2012a) One-dimensional metal oxide nanotubes, nanowires, nanoribbons, and nanorods: synthesis, characterizations, properties and applications. Crit Rev Solid State Mater Sci 37(1):1–74

Li S et al (2012b) Fabrication of magnetic Ni nanoparticles functionalized water-soluble graphene sheets nanocomposites as sorbent for aromatic compounds removal. J Hazard Mater 229–230:42–47

Li J, Liu CY, Liu Y (2012c) Au/graphene hydrogel: synthesis, characterization and its use for catalytic reduction of 4-nitrophenol. J Mater Chem 22(17):8426–8430

Li Y et al (2012d) Equilibrium, kinetic and thermodynamic studies on the adsorption of phenol onto graphene. Mater Res Bull 47(8):1898–1904

Li H et al (2016) Adsorption mechanism of different organic chemicals on fluorinated carbon nanotubes. Chemosphere 154:258–265

Liu C et al (1999) Hydrogen storage in single-walled carbon nanotubes at room temperature. Science 286(5442):1127–1129

Liu Z et al (2008) Circulation and long-term fate of functionalized, biocompatible single-walled carbon nanotubes in mice probed by Raman spectroscopy. Proc Natl Acad Sci 105(5):1410–1415

Liu F et al (2012a) Three-dimensional graphene oxide nanostructure for fast and efficient water-soluble dye removal. ACS Appl Mat Interfaces 4(2):922–927

Liu T et al (2012b) Adsorption of methylene blue from aqueous solution by graphene. Colloids Surf, B 90(1):197–203

Liu YZ et al (2016a) Antibacterial properties of multi-walled carbon nanotubes decorated with silver nanoparticles. Curr Nanosci 12(4):411–415

Liu Y et al (2016b) Synthesis of magnetic polyaniline/graphene oxide composites and their application in the efficient removal of Cu(II) from aqueous solutions. J Env Chem Eng 4 (1):825–834

Liu F et al (2016c) Magnetic porous silica-graphene oxide hybrid composite as a potential adsorbent for aqueous removal of p-nitrophenol. Colloids Surf, A 490:207–214

Lovern S, Klaper R (2006) *Daphnia magna* mortality when exposed to titanium dioxide and fullerene (C_{60}) nanoparticles. Environ Toxicol Chem 25(4):1132–1137

Lubezky A, Kozirovski Y, Folman M (1993) Induced IR spectra of N_2 and O_2 adsorbed on evaporated films of ionic crystals. J Phys Chem 97(5):1050–1054

Lubezky A, Chechelnitsky L, Folman M (1996) IR spectra of CH_4, CD_4, C_2H_4, C_2H_2, CH_3OH and CH_3OD adsorbed on C60 films. J Chem Soc Faraday Trans 92(12):2269–2274

Lubezky A, Kozirovski Y, Folman M (1998) IR spectral shifts and adsorption potentials of CO and N_2 adsorbed on LiF and LiCl. J Electron Spectrosc Relat Phenom 95(1):37–44

giovanni.libralato@unina.it

Lyon DY, Alvarez PJJ (2008) Fullerene water suspension (nC60) exerts antibacterial effects via ROS-independent protein oxidation. Environ Sci Technol 42(21):8127–8132
Lyon DY et al (2006) Antibacterial activity of fullerene water suspensions: effects of preparation method and particle size. Environ Sci Technol 40(14):4360–4366
Lyon DY et al (2008) Antibacterial activity of fullerene water suspensions (nC60) is not due to ROS-mediated damage. Nano Lett 8(5):1539–1543
Magrez A et al (2006) Cellular toxicity of carbon-based nanomaterials. Nano Lett 6(6):1121–1125
Mananghaya M (2015) Hydrogen adsorption of novel N-doped carbon nanotubes functionalized with Scandium. Int J Hydrogen Energy 40(30):9352–9358
Manna SK et al (2005) Single-walled carbon nanotube induces oxidative stress and activates nuclear transcription factor-kB in human keratinocytes. Nano Lett 5(9):1676–1684
Mesarič T et al (2013) Effects of nano carbon black and single-layer graphene oxide on settlement, survival and swimming behaviour of *Amphibalanus amphitrite* larvae. Chem Ecol 29(7):643–652
Meyyappan M (2016) Carbon nanotube-based chemical sensors. Small 12(16):2118–2129
Mochalin VN et al (2012) The properties and applications of nanodiamonds. Nat Nanotechnol 7 (1):11–23
Mortazavi SS, Farmany A (2016) High adsorption capacity of MWCNTs for removal of anionic surfactant SDBS from aqueous solutions. J Water Supply: Res Technol AQUA 65(1):37–42
Mu H et al (2014) Fabrication and characterization of amino group functionalized multiwall carbon nanotubes (MWCNT) formaldehyde gas sensors. IEEE Sens J 14(7):2362–2368
Muller J et al (2008) Structural defects play a major role in the acute lung toxicity of multiwall carbon nanotubes: toxicological aspects. Chem Res Toxicol 21(9):1698–1705
Murr LE, Soto KF (2005) A TEM study of soot, carbon nanotubes, and related fullerene nanopolyhedra in common fuel-gas combustion sources. Mater Charact 55(1):50–65
Murr LE et al (2004a) Chemistry and nanoparticulate compositions of a 10,000 year-old ice core melt water. Water Res 38(19):4282–4296
Murr LE et al (2004b) Carbon nanotubes, nanocrystal forms, and complex nanoparticle aggregates in common fuel-gas combustion sources and the ambient air. J Nanopart Res 6(2):241–251
Murr L et al (2006) Combustion-generated nanoparticulates in the El Paso, TX, USA/Juarez, Mexico Metroplex: their comparative characterization and potential for adverse health effects. Int J Env Res Public Health 3(1):48–66
Murray AR et al (2009) Oxidative stress and inflammatory response in dermal toxicity of single-walled carbon nanotubes. Toxicology 257(3):161–171
Naghadeh SB et al (2016) Functionalized MWCNTs effects on dramatic enhancement of MWCNTs/SnO_2 nanocomposite gas sensing properties at low temperatures. Sens Actuators, B Chem 223:252–260
Nakagawa T, Kokubo K, Moriwaki H (2014) Application of fullerenes-extracted soot modified with ethylenediamine as a novel adsorbent of hexavalent chromium in water. J Env Chem Eng 2(2):1191–1198
Nakamura S, Mashino T (2009) Biological activities of water-soluble fullerene derivatives. J Phys Conf Ser 159
Navarro DA et al (2013) Behaviour of fullerenes (C60) in the terrestrial environment: potential release from biosolids-amended soils. J Hazard Mater 262:496–503
Ncibi MC, Sillanpää M (2015) Optimized removal of antibiotic drugs from aqueous solutions using single, double and multi-walled carbon nanotubes. J Hazard Mater 298:102–110
Ncibi MC, Gaspard S, Sillanpää M (2015) As-synthesized multi-walled carbon nanotubes for the removal of ionic and non-ionic surfactants. J Hazard Mater 286:195–203
Núñez O et al (2012) Atmospheric pressure photoionization mass spectrometry of fullerenes. Anal Chem 84(12):5316–5326
Oberdörster E (2004) Manufactured nanomaterials (fullerenes, C60) induce oxidative stress in the brain of juvenile largemouth bass. Environ Health Perspect 112(10):1058
Oyetade OA et al (2015) Effectiveness of carbon nanotube-cobalt ferrite nanocomposites for the adsorption of rhodamine B from aqueous solutions. RSC Adv 5(29):22724–22739

giovanni.libralato@unina.it

Oyetade OA et al (2016) Nitrogen-functionalised carbon nanotubes as a novel adsorbent for the removal of Cu(ii) from aqueous solution. RSC Adv 6(4):2731–2745
Ozturk Z, Baykasoglu C, Kirca M (2016) Sandwiched graphene-fullerene composite: a novel 3-D nanostructured material for hydrogen storage. Int J Hydrogen Energy 41(15):6403–6411
Pakarinen K et al (2011) Adverse effects of fullerenes (nC60) spiked to sediments on *Lumbriculus variegatus* (Oligochaeta). Environ Pollut 159(12):3750–3756
Pan B, Xing B (2008) Adsorption mechanisms of organic chemicals on carbon nanotubes. Environ Sci Technol 42(24):9005–9013
Papirer E et al (1999) Comparison of the surface properties of graphite, carbon black and fullerene samples, measured by inverse gas chromatography. Carbon 37(8):1265–1274
Park JW et al (2011) The association between nC 60 and 17α-ethinylestradiol (EE2) decreases EE2 bioavailability in zebrafish and alters nanoaggregate characteristics. Nanotoxicology 5 (3):406–416
Patchkovskii S et al (2005) Graphene nanostructures as tunable storage media for molecular hydrogen. Proc Natl Acad Sci USA 102(30):10439–10444
Pérez S, Farré Ml, Barceló D (2009a) Analysis, behavior and ecotoxicity of carbon-based nanomaterials in the aquatic environment. TrAC Trends Anal Chem 28(6):820–832
Pérez S, Farré MI, Barceló D (2009b) Analysis, behavior and ecotoxicity of carbon-based nanomaterials in the aquatic environment. TrAC. Trends Anal Chem 28(6):820–832
Petersen EJ et al (2009a) Biological uptake and depuration of carbon nanotubes by *Daphnia magna*. Environ Sci Technol 43(8):2969–2975
Petersen EJ et al (2009b) Influence of carbon nanotubes on pyrene bioaccumulation from contaminated soils by earthworms. Environ Sci Technol 43(11):4181–4187
Petersen EJ et al (2014) Methods to assess the impact of UV irradiation on the surface chemistry and structure of multiwall carbon nanotube epoxy nanocomposites. Carbon 69:194–205
Pinzón JR, Villalta-Cerdas A, Echegoyen L (2012) Fullerenes, carbon nanotubes, and graphene for molecular electronics. In: Topics in current chemistry, pp 127–174
Prabhakaran PK, Deschamps J (2015) Room temperature hydrogen uptake in single walled carbon nanotubes incorporated MIL-101 doped with lithium: effect of lithium doping. J Porous Mater 22(6):1635–1642
Pretti C et al (2014) Ecotoxicity of pristine graphene to marine organisms. Ecotoxicol Environ Saf 101:138–145
Pumera M (2011) Graphene-based nanomaterials for energy storage. Energy Environ Sci 4 (3):668–674
Pupysheva OV, Farajian AA, Yakobson BI (2008) Fullerene nanocage capacity for hydrogen storage. Nano Lett 8(3):767–774
Pyrzynska K, Stafiej A, Biesaga M (2007) Sorption behavior of acidic herbicides on carbon nanotubes. Microchim Acta 159(3–4):293–298
Qu X, Alvarez PJJ, Li Q (2013) Photochemical transformation of carboxylated multi-walled carbon nanotubes: role of reactive oxygen species. Environ Sci Technol 47(24):14080–14088
Ramesha GK et al (2011) Graphene and graphene oxide as effective adsorbents toward anionic and cationic dyes. J Colloid Interface Sci 361(1):270–277
Russier J et al (2010) Oxidative biodegradation of single-and multi-walled carbon nanotubes. Nanoscale 3(3):893–896
Sanchís J et al (2012) Occurrence of aerosol-bound fullerenes in the mediterranean sea atmosphere. Environ Sci Technol 46(3):1335–1343
Sanchís J et al (2013) Quantitative trace analysis of fullerenes in river sediment from Spain and soils from Saudi Arabia. Anal Bioanal Chem 405(18):5915–5923
Sanchís J et al (2015) Liquid chromatography-atmospheric pressure photoionization-Orbitrap analysis of fullerene aggregates on surface soils and river sediments from Santa Catarina (Brazil). Sci Total Environ 505:172–179
Sanchís J et al (2016) New insights on the influence of organic co-contaminants on the aquatic toxicology of carbon nanomaterials. Environ Sci Technol 50(2):961–969

giovanni.libralato@unina.it

Sayes CM et al (2005) Nano-C_{60} cytotoxicity is due to lipid peroxidation. Biomaterials 26 (36):7587–7595
Sayes CM et al (2006) Functionalization density dependence of single-walled carbon nanotubes cytotoxicity in vitro. Toxicol Lett 161(2):135–142
Scalese S et al (2016) Cationic and anionic azo-dye removal from water by sulfonated graphene oxide nanosheets in Nafion membranes. New J Chem 40(4):3654–3663
Schwab F et al (2013) Diuron sorbed to carbon nanotubes exhibits enhanced toxicity to *Chlorella vulgaris*. Environ Sci Technol 47(13):7012–7019
Scott-Fordsmand JJ et al (2008) The toxicity testing of double-walled nanotubes-contaminated food to *Eisenia veneta* earthworms. Ecotoxicol Environ Saf 71(3):616–619
Sedaghat S (2015) Anchoring of silver nanoparticles onto functionalized multiwall-carbon nanotube and evaluation of antibacterial effects. Fullerenes, Nanotubes, Carbon Nanostruct 23 (6):483–487
Sedlmair J et al (2013) Interaction between carbon nanotubes and soil colloids studied with X-ray spectromicroscopy. Chem Geol 329:32–41
Sekar M, Sakthi V, Rengaraj S (2004) Kinetics and equilibrium adsorption study of lead(II) onto activated carbon prepared from coconut shell. J Colloid Interface Sci 279(2):307–313
Shahriary L et al (2015) One-step synthesis of Ag-reduced graphene oxide-multiwalled carbon nanotubes for enhanced antibacterial activities. New J Chem 39(6):4583–4590
Shan D et al (2016) Preparation of regenerable granular carbon nanotubes by a simple heating-filtration method for efficient removal of typical pharmaceuticals. Chem Eng J 294:353–361
Sharma M, Madras G, Bose S (2015) Unique nanoporous antibacterial membranes derived through crystallization induced phase separation in PVDF/PMMA blends. J Mat Chem A 3(11):5991–6003
Shi H et al (2016) Effect of polyethylene glycol on the antibacterial properties of polyurethane/carbon nanotube electrospun nanofibers. RSC Adv 6(23):19238–19244
Shvedova AA et al (2005) Unusual inflammatory and fibrogenic pulmonary responses to single-walled carbon nanotubes in mice. Am J Physiol-Lung Cell Mol Physiol 289(5):L698–L708
Simon-Deckers A et al (2009) Size-, composition- and shape-dependent toxicological impact of metal oxide nanoparticles and carbon nanotubes toward bacteria. Environ Sci Technol 43 (21):8423–8429
Singh AK, Ribas MA, Yakobson BI (2009) H-spillover through the catalyst saturation: an ab initio thermodynamics study. ACS Nano 3(7):1657–1662
Smith CJ, Shaw BJ, Handy RD (2007) Toxicity of single walled carbon nanotubes to rainbow trout, (Oncorhynchus mykiss): respiratory toxicity, organ pathologies, and other physiological effects. Aquat Toxicol 82(2):94–109
Sohn EK et al (2015) Acute toxicity comparison of single-walled carbon nanotubes in various freshwater organisms. BioMed Res Int 2015
Sotelo JL et al (2012) Adsorption of pharmaceutical compounds and an endocrine disruptor from aqueous solutions by carbon materials. J Env Sci Health—Part B Pesticides, Food Contam, Agric Wastes 47(7):640–652
Sotoma S et al (2015) Comprehensive and quantitative analysis for controlling the physical/chemical states and particle properties of nanodiamonds for biological applications. RSC Adv 5(18):13818–13827
Stafiej A, Pyrzynska K (2007) Adsorption of heavy metal ions with carbon nanotubes. Sep Purif Technol 58(1):49–52
Su F, Lu C (2007) Adsorption kinetics, thermodynamics and desorption of natural dissolved organic matter by multiwalled carbon nanotubes. J Environ Sci Health—Part A Toxic/Hazard Subst Environ Eng 42(11):1543–1552
Su Y et al (2013) Risks of single-walled carbon nanotubes acting as contaminants-carriers: potential release of phenanthrene in Japanese Medaka (Oryzias latipes). Environ Sci Technol 47(9):4704–4710

giovanni.libralato@unina.it

Sui Z et al (2012) Green synthesis of carbon nanotube-graphene hybrid aerogels and their use as versatile agents for water purification. J Mater Chem 22(18):8767–8771
Sun Q et al (2005) Clustering of Ti on a C60 surface and its effect on hydrogen storage. J Am Chem Soc 127(42):14582–14583
Sun Q et al (2006) First-principles study of hydrogen storage on Li12C60. J Am Chem Soc 128 (30):9741–9745
Sun X et al (2015) Removal of sudan dyes from aqueous solution by magnetic carbon nanotubes: equilibrium, kinetic and thermodynamic studies. J Ind Eng Chem 22:373377
Taha MR, Mobasser S (2015) Adsorption of DDT and PCB by nanomaterials from residual soil. PLoS ONE 10(12)
Tang Y et al (2013) Synthesis of reduced graphene oxide/magnetite composites and investigation of their adsorption performance of fluoroquinolone antibiotics. Colloids Surf, A 424:74–80
Tao X et al (2011) Effects of stable aqueous fullerene nanocrystal (nC60) on *Daphnia magna*: evaluation of hop frequency and accumulations under different conditions. J Env Sci 23 (2):322–329
Tegos GP et al (2005) Cationic fullerenes are effective and selective antimicrobial photosensitizers. Chem Biol 12(10):1127–1135
Tervonen K et al (2011) Analysis of fullerene-C_{60} and kinetic measurements for its accumulation and depuration in *Daphnia magna*. Environ Toxicol Chem 29(5):1072–1078
Thornton AW et al (2009) Metal-organic frameworks impregnated with magnesium-decorated fullerenes for methane and hydrogen storage. J Am Chem Soc 131(30):10662–10669
Tong Z et al (2007) Impact of fullerene (C60) on a soil microbial community. Environ Sci Technol 41(8):2985–2991
Van der Ploeg MJC et al (2011) Effects of C_{60} nanoparticle exposure on earthworms (*Lumbricus rubellus*) and implications for population dynamics. Environ Pollut 159(1):198–203
Van der Ploeg MJC et al (2013) C60 exposure induced tissue damage and gene expression alterations in the earthworm *Lumbricus rubellus*. Nanotoxicology 7(4):432–440
Velzeboer I, Peeters ETHM, Koelmans AA (2013) Multiwalled carbon nanotubes at environmentally relevant concentrations affect the composition of benthic communities. Environ Sci Technol 47(13):7475–7482
Verwey EJW, Overbeek JTG, Overbeek JTG (1999) Theory of the stability of lyophobic colloids. Courier Dover Publications
Wang X et al (2005) Sorption of 243Am(III) to multiwall carbon nanotubes. Environ Sci Technol 39(8):2856–2860
Wang C, Shang C, Westerhoff P (2010a) Quantification of fullerene aggregate nC60 in wastewater by high-performance liquid chromatography with UV-vis spectroscopic and mass spectrometric detection. Chemosphere 80(3):334–339
Wang Y et al (2010b) Transport and retention of fullerene nanoparticles in natural soils. J Environ Qual 39(6):1925–1933 (All rights reserved. No part of this periodical may be reproduced or transmitted in any form or by any means, electronic or mechanical, including photocopying, recording, or any information storage and retrieval system, without permission in writing from the publisher)
Wang S et al (2013) Adsorptive remediation of environmental pollutants using novel graphene-based nanomaterials. Chem Eng J 226:336–347
Wang H et al (2015) Facile synthesis of polypyrrole decorated reduced graphene oxide-Fe_3O_4 magnetic composites and its application for the Cr(VI) removal. Chem Eng J 262:597–606
Wang H, Chen Y, Wei Y (2016a) A novel magnetic calcium silicate/graphene oxide composite material for selective adsorption of acridine orange from aqueous solutions. RSC Adv 6 (41):34770–34781
Wang LP et al (2016b) Adsorption behavior of ACF/CNT composites for Cr(VI) from aqueous solution. In: Material science and environmental engineering—proceedings of the 3rd annual 2015 international conference on material science and environmental engineering, ICMSEE 2015

giovanni.libralato@unina.it

Wiesner MR et al (2006) Assessing the risks of manufactured nanomaterials. Environ Sci Technol 40(14):4336–4345
Wigginton NS, Haus KL, Hochella MF Jr (2007) Aquatic environmental nanoparticles. J Environ Monit 9(12):1306–1316
Wu Y-Y, Xiong Z-H (2016) Multi-walled carbon nanotubes and powder-activated carbon adsorbents for the removal of nitrofurazone from aqueous solution. J Dispersion Sci Technol 37(5):613–624
Wu HX et al (2013a) In situ growth of monodispersed Fe_3O_4 nanoparticles on graphene for the removal of heavy metals and aromatic compounds. Water Sci Technol 68(11):2351–2358
Wu Q et al (2013b) Contributions of altered permeability of intestinal barrier and defecation behavior to toxicity formation from graphene oxide in nematode *Caenorhabditis elegans*. Nanoscale 5(20):9934–9943
Xiao Y, Chae S-R, Wiesner MR (2011) Quantification of fullerene (C60) in aqueous samples and use of C70 as surrogate standard. Chem Eng J 170(2–3):555–561
Xing B, Xu J, Huang PM (2010) Environmental and colloidal behavior of engineered nanoparticles. In: Molecular environmental soil science at the interfaces in the Earth's critical zone. Springer, Berlin, Heidelberg, pp 246–248
Xu J, Wang L, Zhu Y (2012) Decontamination of bisphenol A from aqueous solution by graphene adsorption. Langmuir 28(22):8418–8425
Yamaguchi U, Bergamasco NR, Hamoudi S (2016) Magnetic $MnFe_2O_4$-graphene hybrid composite for efficient removal of glyphosate from water. Chem Eng J 295:391–402
Yan XM et al (2008) Adsorption and desorption of atrazine on carbon nanotubes. J Colloid Interface Sci 321(1):30–38
Yan H et al (2016) Efficient removal of chlorophenols from water with a magnetic reduced graphene oxide composite. Sci China Chem 59(3):350–359
Yang RT (2000) Hydrogen storage by alkali-doped carbon nanotubes-revisited. Carbon 38 (4):623–626
Yang S-T et al (2008) Long-term accumulation and low toxicity of single-walled carbon nanotubes in intravenously exposed mice. Toxicol Lett 181(3):182–189
Yang DH et al (2009) Fullerene nanohybrid metal oxide ultrathin films. Curr Appl Phys 9(2 SUPPL)
Yang W et al (2010a) Carbon nanomaterials in biosensors: should you use nanotubes or graphene. Angewandte Chemie—Int Ed 49(12):2114–2138
Yang C et al (2010b) Antimicrobial activity of single-walled carbon nanotubes: length effect. Langmuir 26(20):16013–16019
Yang J et al (2013) Transport of oxidized multi-walled carbon nanotubes through silica based porous media: influences of aquatic chemistry, surface chemistry, and natural organic matter. Environ Sci Technol 47(24):14034–14043
Yang X et al (2014) Fullerene-biomolecule conjugates and their biomedicinal applications. Int J Nanomed 9(1):77–92
Yang K, Chen B, Zhu L (2015) Graphene-coated materials using silica particles as a framework for highly efficient removal of aromatic pollutants in water. Sci Rep 5
Yu Y, Wu L, Zhi J (2014) Diamond nanowires: fabrication, structure, properties, and applications. Angewandte Chemie—Int Ed 53(52):14326–14351
Yu JG et al (2015a) Graphene nanosheets as novel adsorbents in adsorption, preconcentration and removal of gases, organic compounds and metal ions. Sci Total Environ 502:70–79
Yu F, Ma J, Bi D (2015b) Enhanced adsorptive removal of selected pharmaceutical antibiotics from aqueous solution by activated graphene. Environ Sci Pollut Res 22(6):4715–4724
Yu F et al (2016) Magnetic iron oxide nanoparticles functionalized multi-walled carbon nanotubes for toluene, ethylbenzene and xylene removal from aqueous solution. Chemosphere 146:162–172
Yun H et al (2013) Antibacterial activity of CNT-Ag and GO-Ag nanocomposites against gram-negative and gram-positive bacteria. Bull Korean Chem Soc 34(11):3261–3264

giovanni.libralato@unina.it

Zhang L et al (2012) Transport of fullerene nanoparticles (nC60) in saturated sand and sandy soil: controlling factors and modeling. Environ Sci Technol 46(13):7230–7238
Zhang C et al (2013) Adsorption of polycyclic aromatic hydrocarbons (fluoranthene and anthracenemethanol) by functional graphene oxide and removal by pH and temperature-sensitive coagulation. ACS Appl Mat Interfaces 5(11):4783–4790
Zhang Y et al (2014) Recyclable removal of bisphenol A from aqueous solution by reduced graphene oxide-magnetic nanoparticles: adsorption and desorption. J Colloid Interface Sci 421:85–92
Zhang C et al (2016) Efficacy of carbonaceous nanocomposites for sorbing ionizable antibiotic sulfamethazine from aqueous solution. Water Res 95:103–112
Zhao G et al (2011a) Few-layered graphene oxide nanosheets as superior sorbents for heavy metal ion pollution management. Environ Sci Technol 45(24):10454–10462
Zhao G et al (2011b) Removal of Pb(ii) ions from aqueous solutions on few-layered graphene oxide nanosheets. Dalton Trans 40(41):10945–10952
Zhao G et al (2012) Preconcentration of U(vi) ions on few-layered graphene oxide nanosheets from aqueous solutions. Dalton Trans 41(20):6182–6188
Zhao J et al (2014) Adsorption of phenanthrene on multilayer graphene as affected by surfactant and exfoliation. Environ Sci Technol 48(1):331–339
Zhu X et al (2009) Acute toxicities of six manufactured nanomaterial suspensions to *Daphnia magna*. J Nanopart Res 11(1):67–75
Zhu J et al (2012) One-pot synthesis of magnetic graphene nanocomposites decorated with core@double-shell nanoparticles for fast chromium removal. Environ Sci Technol 46(2):977–985

giovanni.libralato@unina.it

Nanomaterials for Adsorption and Heterogeneous Reaction in Water Decontamination

Chun Zhao, Yuanyuan Liu, Yongjun Sun, Jiangya Ma, Yunhua Zhu, Zhihua Sun, Zhaoyang Wang, Lei Ding, Guang Yang, Junfeng Li, Liqiang Zhou, Jun Wang, Guocheng Zhu, Peng Zhang, Huifang Wu and Huaili Zheng

Abstract In recent decades, nanomaterials have been intensively studied for water decontamination, especially for contaminants of emerging concern. Details are provided on a series of engineered nanomaterials for water decontamination by the mechanisms of adsorption, heterogeneous oxidation, and reduction. The degradation, mineralization, and detoxification of various organic contaminants and removal of several inorganic pollutants in aqueous environment by nanomaterials, evaluation of the feasibility of applying nanotechnologies in water industry are also discussed.

C. Zhao (✉) · Y. Liu · H. Zheng
Key Laboratory of the Three Gorges Reservoir Region's Eco-Environment, Ministry of Education, Chongqing University, Chongqing 400045 People's Republic of China
e-mail: pureson@163.com; pureson@cqu.edu.cn

Y. Liu
e-mail: Liuyuanyuan@cqu.edu.cn

C. Zhao · Y. Liu · H. Zheng
National Centre for International Research of Low-Carbon and Green Buildings, Chongqing University, Chongqing 400045, People's Republic of China

Y. Sun · H. Wu
College of Urban Construction, Nanjing Tech University, Nanjing 211800, People's Republic of China

J. Ma · Y. Zhu · L. Ding
School of Civil Engineering and Architecture, Anhui University of Technology, 59 Hudong Road, Maanshan 243002, People's Republic of China

C. Zhao · Z. Sun · Z. Wang · G. Yang · J. Li
College of Water and Architectural Engineering, Shihezi University, Shihezi 832000, People's Republic of China

G. Zhu · P. Zhang
Chongqing Institute of Green and Intelligent Technology, Chinese Academy of Sciences, Chongqing 400714, People's Republic of China

© Springer International Publishing AG 2017

G. Lofrano et al. (eds.), *Nanotechnologies for Environmental Remediation*,
DOI 10.1007/978-3-319-53162-5_6

giovanni.libralato@unina.it

Keywords Nanomaterials · Adsorption · Heterogeneous oxidation · Heterogeneous reduction · Carbon nanotubes · Graphene · Magnetic nano-adsorbents · Titanium dioxide · Zinc oxide · Iron-based nanomaterials · Nano zerovalent iron · Metallic nanomaterials · FeS nanoparticles · Nanocomposites · Alloy nanomaterials · Inorganic pollutants · Organic pollutants · Heavy metal ion · Dye

1 Introduction

As known, water is one of the world's irreplaceable resources, connecting several socio-ecological, economic and geophysical systems at multiple scales, while less than 1% of the global supply of water is available and reliable for human consumption (Bogardi et al. 2012; Grey et al. 2002). For many years, removing natural organic matter (NOM) and microbial contaminants (bacteria, viruses, and protozoa) are the main target for drinking water treatment by traditional processes, like coagulation, sedimentation, filtration, and disinfection. However, due to the rapid industrialization and urbanization, emerging hazardous inorganic and organic contaminants in groundwater, surface water and reservoir have become a principal concern to the environment and the public health (Kar et al. 2016; Revitt and Ellis 2016). Many conventional wastewater treatments do not effectively remove emerging contaminants to meet increasingly stringent water quality standards.

In recent decades, engineered nanomaterials (ENMs), including carbon nanomaterials, metal and metal oxide engineered nanomaterials, magnetic-core composite nanoparticles, chitosan and chitosan-based nanocomposites, have been intensively investigated for environmental remediation, especially for water decontamination. Nanomaterials, also referred to as nanoparticle, nanofiber, and nanowire, are materials that fall within the size range of 1–100 nm at least in one dimension. When materials enter the nanometer scale, surface and interface effect, quantum size effect, small size effect, and macroscopic quantum tunnel effect occur (Losurdo et al. 2009). These nanometer effects make it have stronger adsorption and/or heterogeneous reaction properties for most water pollutants compared to the corresponding bulk material. The relative sizes of nanomaterials and common water contaminants are illustrated at Fig. 1. Therefore, nanotechnologies have great potential in advancing water and wastewater treatment to improve treatment efficiency as well as to augment water supply through safe use of unconventional water sources (Qu et al. 2013). Recently,

L. Zhou
Chongqing Solid Waste Management Center,
Chongqing 401147, People's Republic of China

J. Wang
Chongqing Research Academy of Environmental Sciences,
Chongqing 401147, People's Republic of China

giovanni.libralato@unina.it

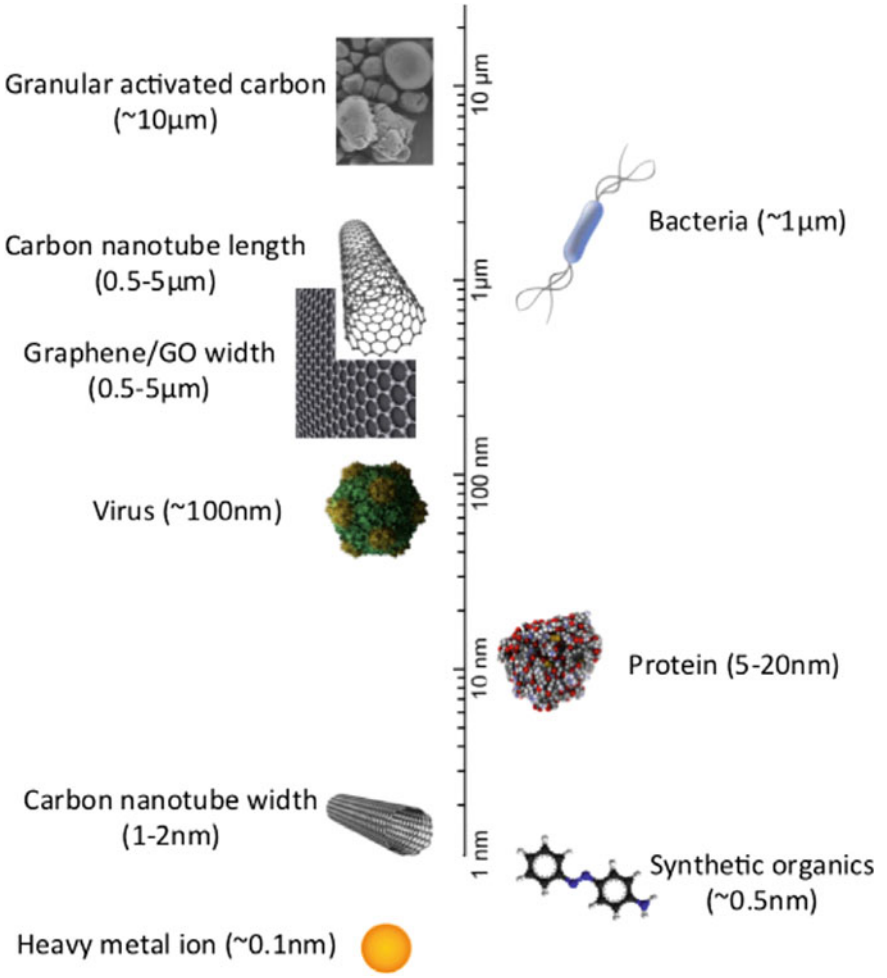

Fig. 1 The relative sizes of nanomaterials and common water contaminants (Smith and Rodrigues 2015)

nanomaterials were applied to water treatment to act as effective adsorbents (Daer et al. 2015; Smith and Rodrigues 2015; Tofighy and Mohammadi 2011), filters (Brady-Estevez et al. 2008; Liu et al. 2015), disinfectants (Smith and Rodrigues 2015; Liu et al. 2015; Baker 2001; Li et al. 2008; Wahab et al. 2014; Bogdanovic et al. 2015), and reactive agents (Stefaniuk et al. 2016; Liu et al. 2016; Nemecek et al. 2015; Gong et al. 2012). Some of these technologies were proved to remove the contaminations from water much more cost-effective than traditional water and wastewater treatment materials and/or methods due to their nanometer size, large surface area and high reactivity. In this chapter, we discuss in detail some significant studies and the

giovanni.libralato@unina.it

application of ENMs for the water treatment of removing organic and inorganic pollutants in recent years.

2 Nanomaterials for Adsorption in Water Decontamination

Adsorbents formed as nanometer-sized particles are currently in the stage of fast development. Many applications of nanomaterials in water decontamination depend on the excellent adsorption properties of nanomaterials, which are drawing widespread attention. Thus, we provide the latest development of nanomaterials for adsorption of various pollutants in water. In this section, a series of nanometer sized adsorbents, including carbon nanotubes, graphene, metal nano-adsorbents, metal oxide nano-adsorbents, and magnetic nano-adsorbents, are introduced with their performance of water purification.

2.1 Carbon Nanotubes

Carbon nanotubes (CNTs), which have layered hollow structures, are seamless, nanometer tubular in shape, and composed of curled grapheme. The tubular structure further assembles to form single-walled carbon nanotubes (SWCNTs) and multi-walled carbon nanotubes (MWCNTs) in van der Waals force. CNTs have porous and hollow structures with large surface area and light mass density. In addition, CNTs have strong interaction with pollutant molecules (Chen et al. 2009; Machado et al. 2011; Li et al. 2011). Therefore, CNTs have been widely used to remove various toxic and harmful pollutants in aqueous solution as illustrated at Table 1.

1. **Adsorption of inorganic pollutants**

The adsorption process is generally applied to control and limit the effect of inorganic species on human health and environment. Heavy metals are considered as one of inorganic pollutants. Lu and Liu (2006) studied the sorption characteristics of nickel(II) from aqueous solution using SWCNTs and MWCNTs as sorbents. The removal rate of Ni(II) by SWCNTs and MWCNTs were about 68.36 and 54.94%, respectively, which were much higher than that of granular active carbon (GAC). Lu and Chiu (2006) used NaClO to modify CNTs and investigated the adsorption of Zn^{2+} in aqueous solution. They found that the adsorption effect of CNTs was better than that of activated carbon (AC). The removal rates of Zn^{2+} by SWCNTs and MWCNTs were 87.32 and 65.36%, respectively. Li et al. (2003) studied the individual and competitive adsorption capacities of Pb^{2+}, Cu^{2+}, and Cd^{2+} by nitric acid-treated MWCNTs. They demonstrated that the adsorption capacity of CNTs was significantly improved by acid treatment. The removal rate of Pb(II) by acidified MWCNTs in 6 h was about 85%, which was fivefold greater

giovanni.libralato@unina.it

Table 1 Contaminants adsorbed by carbon nanotubes in aqueous solution

Adsorption material	Absorbent	Adsorbate	Concentration (mg/L)	Maximum adsorption capacity and removal rate	References
Heavy metal ion	MWCNTs	Pb^{2+}	10	97.08 mg/g, 97.08%	Li et al. (2003)
		Cu^{2+}	10	24.49 mg/g, 24.49%	Li et al. (2003)
		Cd^{2+}	10	10.86 mg/g, 10.86%	Li et al. (2003)
		Zn^{2+}	10–80	32.68 mg/g, 65.36%	Lu and Chiu (2006)
	SWCNTs	Zn^{2+}	10–80	43.66 mg/g, 87.32%	Lu and Chiu (2006)
Inorganic nonmetal ions	CNTs	F^{-}	12	28.7 mg/g, 83.3%	(Li et al. 2001)
Organic compounds	CNTs	Carboxylic	20–200	0.161 mmol/g, 79.63%	Su et al. (2010)
		Lactonic	20–200	0.043 mmol/g, 50.09%	(Su et al. 2010)
		Phenolic	20–200	0.016 mmol/g, 42.39%	Su et al. (2010)
	CNTs	Trihalomethanes (THMs)	2000	2.72 mg/g, 80%	Lu et al. (2005)

than that of AC. Peng et al. (2005) prepared a novel adsorbent, ceria supported on CNTs (CeO_2-CNTs), for the removal of arsenate from water. The adsorption capacity of CeO_2-CNTs was significantly enhanced by Ca^{2+} and Mg^{2+} with the removal rate of As(V) at 94%, which suggested that it was a promising adsorbent for drinking water purification.

2. **Adsorption of organic pollutants**

CNTs also have a strong adsorption capacity for a large number of organic pollutants, such as nitroaromatics (Chen et al. 2007), amino-substituted aromatics (Chen et al. 2008), sulfonamide antibiotics (Ji et al. 2009), tetracycline (Ji et al. 2009), oxytetracycline, carbamazepine (Oleszczuk et al. 2009), nonionic aromatic compounds (Chen et al. 2008), and phenolic compounds (Lin and Xing 2008). Studies showed that the adsorptions of organic pollutants with CNTs were greatly enhanced by the mechanism of hydrophobic interaction (Pan and Xing 2008), π-π conjugated effect (Chen et al. 2008), pi-pi electron-donor-acceptor (EDA) interaction (Yang and Xing 2010), and n-pi EDA interaction (Fagan et al. 2004). Gotovac et al. (2007) demonstrated that the adsorption of polyaromatic hydrocarbons on carbon nanotubes was enhanced by the oxidation of the carbon

giovanni.libralato@unina.it

nanotube surface due to the strengthened π-π conjugated effect between carbon nanotubes and polyaromatic hydrocarbons. Lu et al. (2005) used CNTs for the adsorption of trihalomethanes (THMs) from water. The results showed that CNTs had better adsorption properties of THMs than powdered activated carbon (PAC), and the adsorbed amounts of THMs by CNTs and PAC were 2.41 and 0.063 mg/g, respectively. Brady-Estévez et al. (2010) found that the repulsive force between virus and SWNT can be decreased by increasing the ionic strength up to 100 times, and the removal rate of virus by SWNT was about 83% in aqueous solution.

2.2 *Graphene*

Graphene is a two-dimensional honeycomb lattice structure consisting of six membered rings of carbon, which thickness is only 0.335 nm. According to reports, the theoretical surface area of graphene is about 2600 m^2/g; its elastic modulus is 35 GPa; and its electrical conductivity is up to 7200 s/m at room temperature (Yuan et al. 2015). The removal of various of pollutants in aqueous solution by graphene-based nanomaterials is shown in Table 2.

1. **Adsorption of inorganic pollutants**

Many studies focused on the adsorption of heavy metal ions by graphene-based nanomaterials. Graphene has a good adsorption of heavy metal ions. Zhao et al. (2012) studied the effect of ion concentration, temperature, and pH on adsorption of the radioactive element U^{6+} by GO, and the removal rate was about 97.5%, which was much higher than that of other nanomaterials. They found that pH had a strong influence on the adsorption of U^{6+} by GO, whereas ionic strength had almost no effect on adsorption.

Another study investigates the adsorption capacity of GO on different metal ions. Zhao et al. (2011) prepared layered GO nanosheets and studied the adsorption of Cd^{2+} and Co^{2+} in aqueous solution. The effects of pH, ionic strength, and humic acid on adsorption were investigated. The results showed that the pH value had a strong influence on the adsorption of GO, and the effect of ionic strength on adsorption was ignorable. At pH 6, the removal rates of Cd(II) and Co(II) by GO were 50 and 25%, respectively. Stiko et al. (2013) studied the adsorption of different metal ions by GO. The competitive adsorption was in the following order: $Pb^{2+} > Cu^{2+} > Cd^{2+} > Zn^{2+}$. The maximum adsorption capacities of Cu^{2+}, Zn^{2+}, Cd^{2+}, and Pb^{2+} at pH 5 by GO were achieved at 294, 345, 530, and 1119 mg/g, respectively. Besides, the tendency of agglomeration and precipitation was observed for GC-Me(II) after the adsorption, showing an open path to remove heavy metal ions from aqueous solution.

2. **Adsorption of organic pollutants**

Graphene is one of the most promising absorbents for organic pollutants control in aqueous environment (Yu et al. 2014). Yang et al. (2011) studied the adsorption

giovanni.libralato@unina.it

Table 2 Adsorption of pollutants by graphene-based nanomaterials in aqueous solution

Adsorption material	Absorbent	Adsorbate	Concentration (mg/L)	Maximum adsorption capacity and removal rate	References
Dyes	Graphene oxide	Methylene blue	250	714, 99%	Dursun and Kalayci (2005)
	Graphene	Cationic red X-GRL	20–140	317, 95%	Li et al. (2011)
	Graphene oxide	Methyl violet	100	467, 98.8%	Liu et al. (2012)
	Carbon nanotube-graphene hybrid aerogels	Rhodamine B (RhB)	100–4000	150.2, 78%	Sui et al. (2012)
		Magenta	100–4000	180.8, 80%	Sui et al. (2012)
		Acid fuchsin	100–4000	35.8, 80%	Sui et al. (2012)
Organic compounds	Graphene	Phenol	50	28.26, 85%	Li et al. (2012)
	Graphene	Bisphenol A (BPA)	10	182, 90%	Xu et al. (2012)
	Graphite oxide	Humic acid (HA)	30	190, 88%	Hartono et al. (2009)
Heavy metal ion	Graphene nanosheets	Pb^{2+}	40	35, 95%	Huang et al. (2011)
	Graphite oxide	Zn^{2+}	10–100	246, 91.6%	Wang et al. (2013)
	Graphene oxide nanosheets	U^{6+}	100	299, 80%	Li et al. (2012)
	Graphite oxide	Au^{3+}	60	108.34, 95.4%	Liu et al. (2013)
		Pd^{2+}	60	80.78, 94.64%	Liu et al. (2013)
		Pt^{4+}	60	71.38, 99.37%	Liu et al. (2013)

of MB by GO in water. The adsorption capacity was as high as 714 mg/g. Liu et al. (2012) tested graphene on the adsorption capacity of MB. The maximum adsorption capacity reached 153.85 mg/g, and the removal rate was higher than 99%. Sun et al. (2012) enhanced the absorbing capability of GO by using sodium hydrosulfite as reductant. Under identical conditions, GO without redox modification showed a

giovanni.libralato@unina.it

maximum acridine orange adsorption capacity of 1.4 g/g, while GO with redox modification showed a maximum acridine orange adsorption capacity of 3.3 g/g.

2.3 Metal and Metal Oxide Nano-adsorbents

At the nanoscale, some basic properties of metals, such as melting point, magnetic, color, electrical properties, optical properties, mechanical properties, and chemical properties, would greatly differ from that of bulk materials. The surface of the nanometal, especially at the edges and corners, had high activity for adsorption or catalyzation. Cu, Pd, Pt, Ag, Au, Co, and Ni were commonly metal elements used as nanomaterials for adsorption. GNR Tripathi and Clements (2003) demonstrated that silver nanoparticles had a good adsorption of 2-mercaptopyrimidine in aqueous solution. Jang et al. (2004) showed that the adsorption of 4-biphenylmethanethiolate onto gold nanoparticles became more effective with increasing mean diameters of particle size from 6 to 97 nm. Sumesh et al. (2011) found that water-soluble silver nanoparticles supported on alumina were an efficient system for mercuric ions removal from water. The removal rate of Hg^{2+} was about 80% in 24 h with the maximum adsorption capacity at 0.8 g Hg^{2+} per g of silver.

In addition, nanosized metal oxides (NMOs), including nanosized ferric oxides, manganese oxides, aluminum oxides, titanium oxides, magnesium oxides, nano zinc oxide, nano zirconium oxide, and cerium oxides (Peterson et al. 2010; Zhang et al. 2010; Huang et al. 2009; Sheela et al. 2012), are also widely used as adsorbent materials. Recent studies suggested that respectable NMOs exhibited very favorable sorption of heavy metals and organic pollutants, resulting in deep removal of these toxic contaminants in water. The application of NMOs adsorbents for water treatment is shown in Table 3.

2.4 Magnetic Nano-adsorbents

Magnetic nano-adsorbents, including inorganic magnetic nano-adsorbents and organic magnetic nano-adsorbents, have the potential advantages of efficient recycling, little environmental pollution, and low-cost for removing toxic organic compounds and/or heavy metal ions from water. It can be easily separated from water immediately through applied magnetic field.

1. **Inorganic magnetic nano-adsorbents**

Inorganic magnetic nanoparticles were a combination of inorganic materials and magnetic nanoparticles through physical or chemical method. The inorganic magnetic nano-adsorbents have large specific surface area with good adsorption

giovanni.libralato@unina.it

Table 3 Application of metal oxide nano-adsorbents for water decontamination

Nano metal oxide adsorbents	Pollutants	Concentration (mg/L)	Maximum adsorbing capacity and removal rate	References
Nano MgO	Azo dye pollutants	50–600	Congo red (471–588 mg/g, 99%), Methyl orange (similar to 370 mg/g, 99%), Sudan III (similar to 180 mg/g, 99%)	Li et al. (2012)
Nano ZrO_2	As(III, V)	100	Initial concentration 30 ppb, As(III) (60%), As (V) (removal rate 50%)	Cui et al. (2013)
Nano Fe_3O_4	Ni(II), Cu (II), Cd(II), Cr(VI)	100	the adsorptionrate of Cu^{2+}, Cr^{6+}, Cd^{2+} and Ni^{2+} was 99.8, 97.6, 84.75 and 88.5%, respectively	Shen et al. (2009)
Nano SiO_2	Humic acids	1000	700 mg/L, 70%	(Liang et al. 2011)
Nano-TiO_2	Zn, Cd	50	15.3 mg/g Zn, 86.2%; 7.9 mg/g Cd, 85.7%	Liang et al. (2004)
Anatase nanoparticles	Lead, Copper, Arsenic	20	31.25 mg/g for lead, 97.41%; 23.74 mg/g for copper, 62.57%; and 16.98 mg/g for arsenic, 49.29%	Kocabas-Atakli and Yurum (2013)
nano-Al_2O_3	Thallium	10	3.15 mg/L, 31.5%	Zhang et al. (2008)
Nano NiO	Cd(II), Pb (II)	100–600	90.3 mg/L Cd (II), 90.3%; 151 mg/L Pb (II), 75.6%	Sheela and Nayaka (2012)
Nano-SiO_2	Cd^{2+}, Ni^{2+}, Pb^{2+}	100	40.73 mg/g Cd^{2+}, 90%; 31.29 mg/gNi^{2+}, 85%; 96.79 mg/g Pb^{2+}, 88%	Najafi et al. (2012)
Nano-TiO_2	Hg(II)	50	39.48 mg/g, 96%	Ghasemi et al. (2012)
Nano-SnO_2	Pb^{2+}	20	6.7 mg/g, 95	Ma et al. (2010)
Nano-TiO_2	Pb, Cd, Cu, Ni, Zn	100	42.3 μmol/g Pb, 99%; 63.6 μmol/g Cd, 99%; 61.7 μmol/g Ni, 71%	Engates and Shipley (2011)
Nano-γ-Fe_2O_3	As(V)	10–110	50 mg/g, 92%	Tuutij Rvi et al. (2009)
Nano-α-Fe_2O_3	As(III), As (V)	200	achieved about 90% As(III) removal and more than 80% of As(V)	Tang et al. (2011)
Nano CuO	Pb(II)	100–300	115 mg/g, 99%	Farghali et al. (2013)
Nano Fe_3O_4@C	Methyl blue	10–175	117 mg/g, 96.3%	Wu et al. (2014)

(continued)

giovanni.libralato@unina.it

Table 3 (continued)

Nano metal oxide adsorbents	Pollutants	Concentration (mg/L)	Maximum adsorbing capacity and removal rate	References
Goethite nano particulate	As(V)	100	72.4 mg/g, 94%	Ghosh et al. (2012)
Nano-CeO_2	Arsenic(V)	40	18.15 mg/g, 98.15%	Feng et al. (2012)
Malachite nanoparticles	Chromate, arsenate ions	500	82.2 mg/g chromate, 75%; 57.1 mg/g arsenate, 66%	Saikia et al. (2011)
Nano-ZrO_2	As(III) and As(V)	10–150	83.2 mg/g As(III), 94%; 32.5 mg/g As(V), 92%	Cui et al. (2012)

Table 4 Heavy metals adsorbed by Fe_3O_4 magnetic nanoparticles modified with inorganic materials

Adsorbent	Heavy metals	Concentration (mg/L)	Adsorption capacity/ (mg g^{-1}) and removal rate	References
Magnetic activated carbon	Cu^{2+}	60	37.96, 92.6%	Mikelsaar et al. (2012)
Magnetic MWCNYs	Cd^{2+}, Cu^{2+}, Zn^{2+}	20	19.93Cd^{2+}, 90%; 19.57Cu^{2+}, 90%	Kritis et al. (2016)
Graphene—carbon nanotubes-MNPs	As^{5+}	100	6.5, 90%	Vadahanambi et al. (2013)
Magnetic graphene	Cr^{6+}	1	1.03, 99%	Zhu et al. (2012)
Fe_3O_4@SiO_2 magnetic core-shell structure	U^{6+}	20–200	52, 98%	Fan et al. (2012)
Fe_3O_4@MnO_2 magnetic core-shell structure	Cd^{2+} Cu^{2+}, Pb^{2+}, Zn^{2+}	10–50	Cd^{2+}: 53.2, 80%	Kim et al. (2013)
Double metal oxide modified magnetic nanoparticles (Mag–Fe–Mn)	As^{3+}	100	47.76, 98%	Shan and Tong (2013)

capacity of metal ions. Besides, the adsorption capacity and selectivity of the inorganic nano-adsorbents can be greatly improved by surface modification with functional groups (e.g., –SH, –COOH, and $–NH_2$). Currently, activated carbon, CNTs, graphene, silica gel, and metal oxide have been combined with magnetic nanoparticles for the treatment of heavy metals in water, as shown in Table 4.

giovanni.libralato@unina.it

2. Organic magnetic nano-adsorbents

Organic magnetic nano-adsorbents are a combination of polymer and inorganic magnetic particles. The introduction of the polymer inhibits the accumulation of the magnetic particles, reduces the toxicity, and increases particle surface effect (Kalia et al. 2014). Polymer has two categories: the first type is natural polymers, including chitosan, gelatin, cellulose, and starch (Tataru et al. 2011); the second type is synthetic polymers, including polystyrene, polyacrylic acid, polyamide, polyaniline, and their copolymer (Cui et al. 2010).

Natural polymer materials were ubiquitous in nature with low prices and biodegradability characteristics. Chitosan is one of the most investigated natural polymer, and the removal of heavy metals by magnetic chitosan nanomaterials is shown in Table 5.

Although natural polymer composite magnetic adsorbents could effectively improve the adsorption and removal rate of heavy metal ions in water, their adsorption capacity and selectivity are not good enough for application. Therefore, synthetic polymers have been investigated for the improvement. The synthetic polymers are easier to transfer functional groups on crosslinking to form selective adsorption with high capacity. Ozay et al. (2009) prepared an aqueous gel with 2-acrylamide and 2-methyl-1-propane sulfonic acid, and wrapped it with magnetic iron particles. The synthetic magnetic polymer composite adsorbent could remove toxic heavy metal ions, including Cd^{2+}, Pb^{2+}, Cu^{2+}, and Cr^{3+}, from water efficiently. Hao et al. (2010) prepared magnetic nanoparticles modified with amino (MNP-NH_2). The maximum adsorption capacity of Cu^{2+} reached 25.77 mg/g, and the removal rate of Cu^{2+} by MNP-NH_2 was 98% from polluted river and tap water, showing a good selectivity for target pollutant in a complicated matrix.

Table 5 Heavy metals adsorbed by magnetic chitosan nanomaterials

Adsorbent	Heavy metals	Concentration (mg/L)	Adsorption capacity/(mg g^{-1}) and removal rate	References
Magnetic chitosan nano-materials	Cr^{6+}	180	55.8, 90%	Thinh et al. (2013)
	Cu^{2+}	100–120	35.5, 96%	Chang et al. (2014)
	Hg^{2+}	15	2.8, 71.6%	Lee et al. (2014)
	Pb^{2+}, Cu^{2+}, Zn^{2+}	25–250	6.9 (Pb^{2+}), 72.1%; 4.5 (Cu^{2+}), 66.7%; 28.8 (Zn^{2+}), 43.9%	Yin and Talapin (2013)
	Pb^{2+}	10	10, 96%	Hua et al. (2012)

giovanni.libralato@unina.it

3 Nanomaterials for Heterogeneous Oxidation in Water Decontamination

Some nanomaterials are acknowledged to have a potent catalytic oxidation property and are widely used in water pollution control as one of the advanced oxidation processes (Park et al. 2016). TiO_2 nanoparticals, Fe_3O_4 nanoparticals, ZnO nanoparticals and the other nanomaterials are drawn extensive attention by researchers in various countries. These advanced and sophisticated nanomaterials were synthesized in different approaches for photocatalytic oxidation, Fenton or Fenton-like oxidation, sonocatalytic oxidation, and electrochemical oxidation in water treatment (Koutahzadeh et al. 2016). Therefore, breakthroughs of these new materials research are expected to bring rapid development in engineering application for water environment protection.

3.1 TiO_2 Nanoparticles

Titanium dioxide (TiO_2) nanoparticles is an excellent photocatalyst for refractory organics degradation in aqueous solution under UV light irradiation (Chen et al. 2015). When TiO_2 was irradiated by UV light, electrons leap onto the conduction band forming conduction band electrons (e^-) and leaving holes (h^+). The electrical potential of the holes is at least 3.0 eV, which is much higher than that of common oxidants (Staniszewska et al. 2015). As a result, the hydroxyl group (OH^-) or H_2O absorbed on the surface of TiO_2 nanoparticles can be oxidized into hydroxyl radicals (·OH) with high activity. Meanwhile, the produced conduction band electrons can also react with O_2 and generate superoxide free radicals, such as $\cdot O_2^-$ and $\cdot HO_2$. These active free radicals play a positive role in oxidation of most organic compounds and a few inorganic compounds into CO_2, H_2O, and small inorganic molecules (SIM). The photocatalytic oxidation mechanism of TiO_2 nanoparticles in the degradation of refractory organics (R) is presented in Eqs. (1)–(8) (Deng et al. 2016) and (Fig. 2).

$$TiO_2\ \text{nanoparticals} + h\gamma \rightarrow TiO_2(e^-, h^+) \tag{1}$$

$$e^- + h^+ \rightarrow \text{heat} \tag{2}$$

$$h^+ + OH^- \rightarrow \cdot OH \tag{3}$$

$$e^- + O_2 \rightarrow \cdot O_2^- \tag{4}$$

$$\cdot O_2^- + H^+ \rightarrow HO_2 \tag{5}$$

giovanni.libralato@unina.it

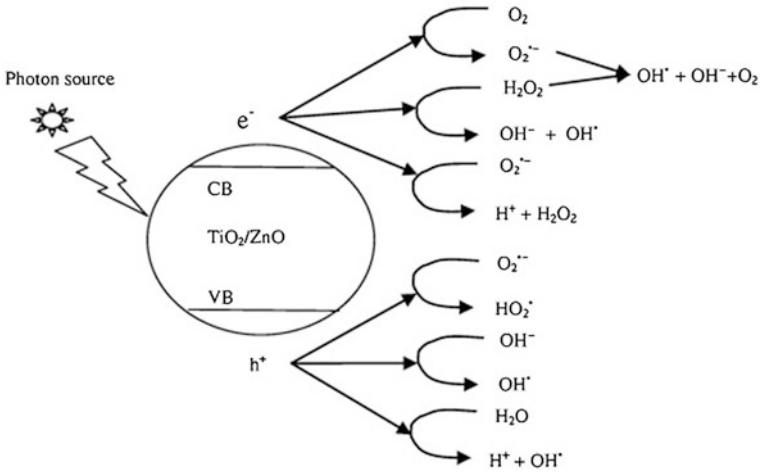

Fig. 2 Mechanisms for ROS generation by TiO_2/ZnO under illumination (Hossain et al. 2014). h^+_{vb} = Valence band hole; e^-_{cb} = Conduction band electron; $O_2^{\cdot -}$ = Superoxide radical; ·OH = Hydroxyl radical

$$2HO_2\cdot \rightarrow O_2 + H_2O_2 \tag{6}$$

$$H_2O_2 + {}^{\cdot}O_2^- \rightarrow \cdot OH + OH^- + O_2 \tag{7}$$

$$R + {}^{\cdot}OH \left(\text{or } {}^{\cdot}O_2^-\right) \rightarrow CO_2 + H_2O + SIM \tag{8}$$

Besides, the favorable photochemical stability, high reactivity, and non-toxic property of TiO_2 nanoparticles in chemical reaction are also the main advantages for its application in water treatment. In 1976, dechloridation of polychlorinated biphenyl was firstly realized by TiO_2 turbid liquid under irradiation of near ultraviolet, initiating the development of photocatalytic oxidation technologies based on TiO_2 nanoparticles (Jo and Tayade 2016). Over the past several decades, a series of functional nanomaterials based on nano-TiO_2 have been extensively studied in water treatment for the removal of various pollutants. Mahmoodi and Arami (2009) employed an immobilized TiO_2 nanoparticals photocatalytic oxidation reactor for the degradation of textile dye, Acid Blue 25 (AB 25), in wastewater. The results showed that more than 90% of AB 25 with an initial concentration of 50 mg/L was successfully removed after 85 min. Moreover, it was suggested that this nanomaterial could be also effective in oxidation of other acid anthraquinone dyes which have similar chemical structures with AB 25, such as AB 41, 53 and 230. Nanocrystalline TiO_2 can be prepared through the hydrolysis of titanium tetraisopropoxide. Tayade et al. (2007) found that a better degradation of acetophenone, nitrobenzene, methylene blue and malachite green was realized by anatase phase TiO_2 compared with rutile phase, which was attributed to appropriate band-gap, rich hydroxyl groups and porous surface. Zhao et al. (2010) also reported the

giovanni.libralato@unina.it

detoxification of oxytetracycline (OTC), a broad-spectrum antibiotic, by zeolite particles loaded with nano-TiO_2 under UV irradiation. The composite photocatalysts demonstrated a better anti-interference capability of radical scavengers and humic acid than nano-TiO_2 (Zhao et al. 2014). Additionally, the photo-oxidation of TiO_2 for the degradation of organic pesticide, such as herbicide, insecticides and fungicides, has also attracted widespread interest (Ma et al. 2014).

However, the UV light only holds 4–5% of whole solar spectrum energy on earth while visible light accounts for about 45%. In order to utilize the visible light spectrum, many improvements and exploration for the modification of TiO_2 into a form known as visible light-active TiO_2 were conducted, including narrowing the bandgap of TiO_2 and introducing a localized mid gap energy states in TiO_2 by doping with a series of metal or nometal elements (Shokri et al. 2016). Li et al. (2015) studied photocatalysis oxidation property of CdS/TiO_2 nanofibers with size of 50–100 nm for the degradation of organic dyes under visible irradiation. The results indicated that 96% of eosin red, 91% of Congo red, and 86% of methylene blue were decolored by CdS/TiO_2 in 60, 120 and 170 min, respectively. The modification of Cu-doped TiO_2 nanoparticles was prepared by Yang et al. (2015) for treating methyl orange at an initial concentration of 20 mg/L under UV-Vis irradiation. An obvious enhancement in degrading performance was observed by 0.5–1.5% of Cu doped TiO_2 nanoparticles compared with undoped TiO_2. Besides, Cu-doped TiO_2 nanoparticles were also proved to be effective in decreasing the recombination probability of photoinduced electron-hole pair. Moreover, ThanhThuy et al. (2013) synthesized a novel sensitized TiO_2 nanopaticles for the removal of pentachlorophenol in aqueous solution. In their research, ZnSe nanoparticles with a bandgap of 2.7 eV was doped onto the surface of 100 nm TiO_2 nanotube array films. The removal ratio of pentachlorophenol was achieved at 99% by ZnSe/TiO_2 nanoparticles while only 64% was removed by non-sensitized TiO_2. Additionally, nitrogen and fluorine co-doped TiO_2 was prepared for decomposing oxytetracycline under visible light. The experimental results demonstrated that nitrogen and fluorine combined with TiO_2 exhibited an excellent photocatalytic activity under visible light irradiation (Zhao et al. 2013).

3.2 ZnO Nanoparticals

Nano-ZnO, as a semiconductor nanomaterial, is also considered to be a potential photocatalyst due to its promising photocatalytic activity, non-toxic and inexpensive character. Consequently, nano-ZnO has been immensely investigated for the degradation of organic pollutants in wastewater (Akhavan 2011). Oskoei et al. (2015) tested the degradation of humic acid (HA) in aqueous solution by nano-ZnO under UV irradiation. According to experimental results, almost 98.95% of HA was removed by 0.5 g/L nano-ZnO within 0.5 h under acidic environment. Raizada et al. (2014) prepared the ZnO-activated carbon (AC) and ZnO-brick grain particle (BGP) nanocomposites using co-precipitation method for photocatalytic

giovanni.libralato@unina.it

degradation of dye. Nano-ZnO was found to be highly dispersed on the surface of AC or BGP. The obtained results demonstrated that nano-ZnO/AC exhibited a higher adsorption and oxidation performance than that of nano-ZnO/BGP. Besides, both of these two nanocomposites were easily separated and reused through sedimentation. ·HO and $\cdot O_2^-$ were considered to be the most critical active groups in this photocatalytic reaction. Moreover, Li et al. (2014) prepared a ZnO/rectorite nanocomposite for the photocatalytic degradation of MB under solar light irradiation. More than 99% of MB at an initial concentration of 15 mg/L was removed by 0.9 g/L ZnO/rectorite in 120 min. No obvious decrease in degradation rate was detected within five times of consecutive experimental runs, showing a relatively stable of ZnO/rectorite nanocomposite under solar light irradiation and an ideal reusability of the catalyst for future industrial application (Fig. 3).

However, ZnO photocatalysts show a poor performance under solar light due to the wide band gap. To overcome the barrier, many strategies have been applied to active ZnO nanostructured photocatalysts under visible light, including surface modification via organic compound sensitization, coupling with a narrow band gap semiconductor, and metal and/or nonmetal doping (Samadi et al. 2016). Sun et al. (2013) studied the degradation of methyl orange dye by N-doped ZnO nanoparticles under simulated solar light. Kuriakose et al. (2014) synthesized Co-doped ZnO nanorods and nanodisks for the degradation of MB under sunlight irradiation. The results demonstrated an enhanced photocatalytic activity than pure ZnO due to the combined effects of larger surface area and better charge separation efficiency.

In addition, based on modified ZnO nanoparticals, other catalytic oxidation systems were also reported. Soltani et al. (2016) immobilized nano-ZnO on the surface of biosilica as a composite catalyst for a textile dye wastewater treatment by sonocatalytic reaction. The results showed that the decolorizations of methylene blue (MB) by sonocatalytic ZnO-biosilica nanoparticals and nano-ZnO were 77.8 and 53.6%, respectively. The addition of persulfate ion ($S_2O_8^{2-}$) in the system can enhance the color removal to 99.4% due to the generation of sulfate radicals.

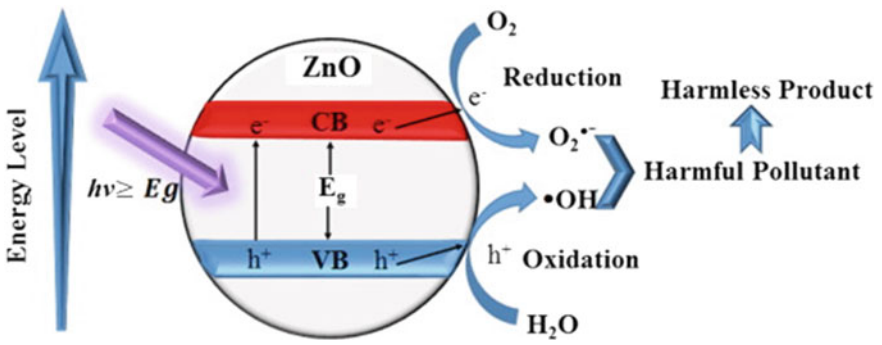

Fig. 3 Schematic illustration of the formation of charge carriers (e^- and h^+) and photocatalytic degradation of pollutant on the ZnO nanostructured surface (Samadi et al. 2016)

giovanni.libralato@unina.it

Forouzani et al. (2015) investigated the catalytic activity of Cu-doped nano ZnO (nano-CuZnO) with H_2O_2 at ambient temperatures without light irradiation. The results indicated that almost 99% of benzyl alcohol was degraded with nano-CuZnO in 180 min, while only 70% of benzyl alcohol was decomposed with pure nano-ZnO after 5 h.

3.3 Fe_3O_4 Nanoparticals and Iron-Based Nanomaterials

Fe_3O_4 with inverse spinel structure is recognized as a common magnetic material, and nanometer sized Fe_3O_4 has drawn extensive attention by various researchers due to its unique super paramagnetic and catalytic nature (Wu et al. 2012). In recent years, nano-Fe_3O_4 was widely used in heterogeneous Fenton oxidation of various organic pollutants in water, which has a higher catalytic activity compared with non-nanometer sized iron-based materials. There are two valences of Fe in nano-Fe_3O_4 (Fe^{+2} and Fe^{3+}) (Zeng et al. 2010). Both Fe^{2+} and Fe^{3+} can play an important role in the Fenton reaction. Hydroxyl radicals can be formed and released in Fenton process through the Haber-Weiss mechanism, which is exhibited in Eqs. (9)–(10) (Pariti et al. 2014).

$$Fe^{2+} + H_2O_2 \rightarrow Fe^{3+} + OH^- + \cdot OH \quad k_1 = 76\ M^{-1}\ s^{-1} \tag{9}$$

$$Fe^{3+} + H_2O_2 \rightarrow Fe^{2+} + H^+ + HO_2\cdot \quad 0.001 \leq k_2 \leq 0.01\ M^{-1}\ s^{-1} \tag{10}$$

Generally, two different approaches can be employed to prepare nano-Fe_3O_4. One is mixing of Fe^{2+} with Fe^{3+} before precipitation (Mohammadi and Kassaee 2013), while the other is partial reduction of Fe^{3+} in specific environment (Yu et al. 2011). After obtaining the nano-Fe_3O_4, appropriate catalytic oxidation system was also established for the degradation of organic pollutants in water. Li et al. (2014) investigated heterogeneous UV-Fenton of nano-Fe_3O_4 with particle size of 50–100 nm in catechol oxidation. The results revealed that pH and H_2O_2 dosage were significant factors in the process. The pH at 7.0 was optimal for achieving 93% of COD removal rate. Catechol oxidation was found to be more effective with higher H_2O_2 dosage, although it is not helpful for the enhancement of H_2O_2 utilization. HO· was the initial free radicals produced in UV-Fenton reaction, resulting the forming of secondary oxidants O_2^1 and $O_2^{-\cdot}$. Similar heterogeneous Fenton oxidation was studied by He et al. (2014), 57.84 m^2/g quasi-spherical nano-Fe_3O_4 was used for the oxidation of 4-chlorocatechol and catechol. The results showed that both of the two pollutants were effectively decomposed and mineralized with H_2O_2. The generated active groups in reaction were ·HO and $HO_2^-/O_2^{-\cdot}$, which further promoted the production of oxygen-centered radicals or carbon-centered radicals for target pollutants degradation. Besides, the heterogeneous electro-Fenton oxidation of catechol catalyzed by nano-Fe_3O_4 was investigated (Hou et al. 2015). Under the optimal

giovanni.libralato@unina.it

conditions, catechol (110 mg/L) was almost completely degraded in 120 min with nano-Fe_3O_4 at 1.0 g/L, current density at 10 mA/cm^2, and pH at 3.0.

Moreover, the effect of additive on catalytic oxidation by nano-Fe_3O_4 was also studied. Sun et al. (2014) investigated the effect of nitrilotriacetic acid (NTA) on the degradation of carbamazepine by nano-Fe_3O_4/H_2O_2 system. With the introduction of NTA (0.5–1.0 mM), the degradation of carbamazepine was obviously improved even at a lower dosage of nano Fe_3O_4 and H_2O_2. Enhanced heterogeneous catalytic oxidation reaction on nano-Fe_3O_4 nanopaticle surface and homogeneous Fenton-like reaction in aqueous solution by Fe-NTA complexes were considered to be the dominant mechanism in this process. Yang et al. (2016) analyzed the effect of phosphate on oxidation of 1,2-dihydroxybenzene based on nano-Fe_3O_4 catalytic system. The result indicated the removal efficiency decreased with the increase of phosphate. The proposed mechanism was that the phosphate has an intensive reaction with the surface sites of nano-Fe_3O_4, and the absorbed 1, 2-dihydroxybenzene could be displaced by phosphate from the surface of nano-Fe_3O_4 at acidic and neutral environment.

Except for nano-Fe_3O_4 mentioned above, some other iron-based nanomaterials for water treatment were also proposed by researchers. Sheydaei et al. (2014) synthesized a novel nanomaterial by immobilizing γ-FeOOH nanoparticles on the surface of granular activated carbon (GAC) through precipitation approach, and then used for textile wastewater treatment by photo Fenton-like process. The experimental results showed that the decolorization ability of γ-FeOOH-GAC/H_2O_2/UV process was more effective than the others. Fe^{2+} and Fe^{3+} sourced from γ-FeOOH played an important role in the generation of hydroxyl radical.

Nano zero-valent iron was also successfully applied in sono-Fenton process for the degradation of organics from palm oil mill effluent by Taha and Ibrahim (2014). It was found that nano zero-valent iron presented a better performance than $FeSO_4$ as a ferrous iron (Fe^{2+}) source during the reaction. As a result, 80% of COD in diluted palm oil mill effluent was removed after 120 min. Actually, free radical was sourced from Fe^{2+}, and the reaction mechanism of Fe^0 to Fe^{2+} were illustrated in Eqs. (11)–(13). Kurian and Nair (2014) synthesized nano nickel-zinc ferrite catalysts through sol-gel auto combustion method for the degradation of 4-chlorophenol by Catalytic Wet Peroxide Oxidation in aqueous solution. The nickel-zinc ferrite catalyst was tested to be effective and reusable for target compound degradation, and the reaction process was proved to be heterogeneous catalytic reaction due to no significant iron leaching.

$$Fe^0 \rightarrow Fe^{2+} + 2e^- \tag{11}$$

$$Fe^0 + H_2O \rightarrow Fe^{2+} + H_2 + 2OH^- \tag{12}$$

$$2Fe^0 + 4H^+ + O_2 \rightarrow 2Fe^{2+} + 2H_2O \tag{13}$$

giovanni.libralato@unina.it

4 Nanomaterials for Heterogeneous Reduction in Water Decontamination

A number of studies have elaborated and classified the nanomaterials for water treatment based on their functions in unit operation processes (Daer et al. 2015; Smith and Rodrigues 2015; Li et al. 2008; Ravi and Vadukumpully 2016; Ong et al. 2016; Qu et al. 2013; Chong et al. 2010). For instance, nanoscale zero-valent iron (nZVI) generally removes the pollutants from wastewater via heterogeneous reduction (Di Palma et al. 2015). The reagent loses electron to be transferred to oxidant and reach the equilibrium in the process of reduction reaction. Plenty of studies with respect to nanomaterials for heterogeneous reduction have primarily focused on metal-based nanomaterials or their modified materials (Stefaniuk et al. 2016; Qu et al. 2013; Strongin 2004; Carpenter et al. 2015; Adeleye et al. 2016; Prasse and Ternes 2010; Gong et al. 2016; Botes and Cloete 2010). nZVI has been most-commonly applied for water treatment and environmental remediation (Stefaniuk et al. 2016; Di Palma et al. 2015), while the majority of other remediation and water treatment studies with nanomaterials remain at a bench or pilot scale proof of concept stage (Qu et al. 2013).

Herein, we provide an overview of nanomaterials for heterogeneous reduction in water decontamination. In this review, nanomaterials for heterogeneous reduction are divided into four classes: metallic nanomaterials, alloy nanomaterials, compound nanomaterials and composite nanomaterials. In addition, we introduce the removal of pollutants of every nanomaterial from each category.

4.1 Metallic Nanomaterials

Metallic nanomaterials have singular and unique structures compared with coarse crystal materials, including Fe, Co, Ni, Cu, Zn, Ag, etc. Recently, nanoscale metallic materials have been synthesized and applied in various fields (Zhang et al. 2014; Vivero-Escoto and Huang 2011). However, among these Metallic nanomaterials, only zero-valent iron (ZVI) nanoparticles are predominately applied to remove/immobilize contaminations in wastewater by heterogeneous reduction either in laboratory research or in field remediation (Stefaniuk et al. 2016; Adeleye et al. 2016). Since nZVI nanoparticles were initially and effectively applied to in situ remediation of groundwater (Gillham and Ohannesin 1994), nZVI as a reducing agent of removal of contaminations in groundwater, has generally become a very attractive research topic. The effectiveness of nZVI in the elimination of various contaminants has been demonstrated successfully on the laboratory scale (Mueller and Nowack 2010), and some studies also show that nZVI has been taken into pilot-scale and field-scale application of a contaminated site (Stefaniuk et al. 2016; Adeleye et al. 2016; Su et al. 2012; Li et al. 2014a, b; Mueller et al. 2012; Yirsaw et al. 2015). Currently, nZVI has been very effective for the transformation

giovanni.libralato@unina.it

and detoxification of a wide variety of environmental contaminants including organics such as chlorinated organic pollutants (Mueller et al. 2012; Wang and Zhang 1997; Liu and Lowry 2006; Shih et al. 2011; Cheng et al. 2007), organic dyes (Fan et al. 2009), and other organic contaminants (Joo et al. 2005; Shih and Tai 2010; Thompson et al. 2010; Choe et al. 2001; Scott et al. 2011), and inorganic anions (Kanel et al. 2006; Blowes et al. 1997; Chen et al. 2008; Xi et al. 2010).

1. **Chlorinated Organics removal**

Chlorinated pollutants and several chloro pesticides are less degradable under aerobic conditions. Wang and Zhang reported that the concentration of trichloroethylene (TCE) after reduced by nZVI at ambient temperature of 22 °C reached as low as below the detection limit at the initial concentration of 20 mg/L and the dosage of 2 g/100 mL (Wang and Zhang 1997). Another study presented the first reported miscible-displacement experiments to study the fate and transport of chlorinated solvents flowing through zero-valent metal. The simultaneous TCE and ethylene breakthrough curves were described with an equilibrium sorption/degradation model and a two-site partial nonequilibrium sorption model with degradation and production to indicate that sorption is an important process to be considered when TCE flows through zero-valent metal systems (Casey et al. 2000).

The mechanism of dechlorination was initially identified as reductive reaction due to the existence of Fe^0, Fe^{2+} and H_2 (Matheson and Tratnyek 1994). Deng added the complex agent to the reaction system to identify that Fe^{2+} rarely participated in the reductive reaction (Deng et al. 1999). Recently, it has come to light that chlorinated organic compounds are adsorbed to nZVI and forms a complex to weaken the covalent bonding of C–Cl with the formation of the complex to achieve the final dechlorination as seen in Eqs. (11) and (14) (Mueller et al. 2012; Liu et al. 2005). A number of researches also show that nZVI has a favorable ability to remove other organic compounds such as chlorinated ethenes (Dries et al. 2005; Song and Carraway 2005, 2008; Lien and Zhang 1999), tetrachloroethylene (PCE) (Klimkova et al. 2008), polychlorinated biphenyls (PCBs) (Lowry and Johnson 2004; Zhang 2003) and halogenated aliphatics (Stefaniuk et al. 2016; Qu et al. 2013; Strongin 2004; Adeleye et al. 2016; Gillham and Ohannesin 1994; Yirsaw et al. 2015; Zhang 2003).

$$\mathrm{R-Cl} + \mathrm{n}e^- + m\mathrm{H}^- \rightarrow products + 3\mathrm{Cl}^- \tag{14}$$

2. **Organic dyes removal**

Azo dyes make water treatment more difficult through the conventional methods because of the fact that they are intended to be produced to resist the breakdown of long-term exposure to sunlight, water, and other atrocious conditions. Much attention has been paid on the treatment of azo dyes by nZVI as an environmental friendly and effective reducing agent in recent years (Fan et al. 2009; Nam and Tratnyek 2000; Perey et al. 2002; Hou et al. 2007; Shu et al. 2007; Lin et al. 2008;

giovanni.libralato@unina.it

He et al. 2012; Cao et al. 1999; Deng et al. 2000). Fan et al. (2009) reported that within a 10 min reaction, the degradation efficiency was found to be above 85% at an nZVI dosage of 0.5 g/L, when the initial concentration of methyl orange was fixed at 100 mg/L. Lin et al. (2008) conducted the batch experiments to indicate that the degradation efficiency increases with the increase of ZVI concentration and temperature, and that the reaction follows pseudo-first order kinetics, the reaction rate of which is highly pH-dependent. The mechanism is shown in Eqs. (15)–(16), where D^{2-} represents the deprotonated AB24 ion, >FeOH is the hydroxyl groups of the ferric hydroxides coated on the surface of ZVI particles. The rapid decolorization of azo, anthraquinone and triphenylmethane dyes in aqueous solution by ZVI was compared to show that the degradation followed the first-order kinetic well and ZVI was a universal and efficient reductant for rapid decolorization of these three dyes (He et al. 2012).

$$D^{2-} + \mathrm{Fe}^0 \rightarrow \mathrm{Fe}^{2+} + D^{4-} \quad \text{at} \quad \mathrm{pH} < 6 \tag{15}$$

$$D^{2-} + > \mathrm{FeOH} \rightarrow \mathrm{FeOHD}^- \quad \text{at} \quad \mathrm{pH} > 6 \tag{16}$$

3. Other organic contaminants removal

There are some organic materials on the contaminated site that can be degraded by nZVI (Lim et al. 2007; Fang et al. 2011). Chloroacetanilide herbicide were completely removed by 4 g/L nZVI from pesticide wastewater with an initial concentration of 40 mg/L, with the rate constant, 38.5×10^{-5} L/(h m^2), outclassing 3.8–7.7 $\times$ 10^{-5} L/(h m^2) of micro iron powder (Thompson et al. 2010). Zhang found that the degradation efficiency of 2,4,6-trinitrotoluene was as high as 99% with 3 h reaction with an nZVI dosage of 5 g/L, at an initial concentration of 80 mg/L (Zhang et al. 2010). Similar to chlorinated organics, brominated organic compounds may be removed from the contaminated sites by nZVI with the similar pathway of degradation (Shih and Tai 2010; Fang et al. 2011).

4. Inorganics removal

Zero-valent nanoparticles have been extensively assessed as a reactive medium to remove/immobilize inorganic contaminants such as metals, radionuclides, oxyanions from groundwater, surface water and wastewater (Daer et al. 2015; Stefaniuk et al. 2016; Adeleye et al. 2016; Li et al. 2014; Mueller et al. 2012; Yirsaw et al. 2015; Chen et al. 2008; Zhang 2003; Riba et al. 2008; Crane and Scott 2012).

Recently, the release of heavy metals into groundwater, surface water and river has raised serious human and ecological health concerns due to their carcinogenic nature. Heavy metals are non-biodegraded and some have been identified as priority pollutants (Fu and Wang 2011). nZVI has come into people's horizons to reduce a variety of heavy metals because of high efficiency within short reaction time. Xi et al. conducted Pb^{2+} removal tests to measure the reaction rate by nZVI. When the pH value was fixed at 4.0 and the initial concentration at 500 mg/L, the efficiency

giovanni.libralato@unina.it

was found to be 99.9% after 15 min of contact time with iron nanoparticles (Xi et al. 2010). At the pH value of 5.0, the degradation reaction of $Cr_2O_7^{2-}$ by nZVI followed pseudo first order kinetics and reached equilibrium within 5 h with an above 99% removal of Cr(VI) as shown in Eq. (17) (Liu et al. 2010).

$$2Fe^0 + Cr_2O_7^{2-} + 14H^+ \rightarrow 2Fe^{3+} + 2Cr^{3+} + 7H_2O \quad (17)$$

Reinsch et al. (2010) found the properties of nZVI were transformed with long-term exposure to inorganic anions and indicated that the reduction reaction took place between iron nanoparticles and inorganic anions during the remediation of groundwater. Wang affirmed the reactivity of the spherical nZVI with a larger surface area via denitrification of nitrate. The optimization of factors controlling the reduction of nitrate was discussed (Wang et al. 2006). Some studies also showed nZVI was also applied to remove/immobilize radionuclides (Riba et al. 2008; Dickinson and Scott 2010; Crane et al. 2011; Klimkova et al. 2011; Ponder et al. 2001). Dickinson and Scott came to the conclusion that uranium in aqueous solution was removed by nZVI to 1.5% of the initial concentration within 1 h regardless of oxic or anoxic situation and remained stable on the surface of the ZVI partilces for 48 h (Dickinson and Scott 2010).

4.2 Alloy Nanomaterials

Fu et al. (2014) and Mueller et al. (2012) have verified that nZVI has some weaknesses such as a lack of stability, difficult separation from the medium being purified, rapid passivation of the material, and limited mobility of the particles because of the formation of agglomerates in enhancing the effectiveness in the removal of contaminants. Thus, nZVI has been recently modified through different methods, one of which is the admixtures of nobler metals (Pd, Pt, Ag, Ni, Cu, etc.) to alloy nanomaterials mainly applied to remove the organic materials (Lim et al. 2007; Zhang et al. 1998; Alonso et al. 2002; Elliott and Zhang 2001; Tee et al. 2009; Bokare et al. 2008; Chen et al. 2014; Huang et al. 2013; Wu and Ritchie 2008; Xu and Zhang 2000). The alloy nanomaterials are a diverse category of nanoscale substances that are composed of one, two, or, less commonly, three metals (Crane and Scott 2012). Bimetallic nanomaterials for contaminant remediation have frequently been used in the experimental stage including Pd/Fe (Wang and Zhang 1997; Zhang et al. 1998; Tee et al. 2009; Huang et al. 2013; Wu and Ritchie 2008; Lien and Zhang 2005, 2007; Wei et al. 2006; Shih et al. 2016; Guasp and Wei 2003; Xu et al. 2004; Nagpal et al. 2010; Smuleac et al. 2011), Ni/Fe (Lim et al. 2007; Zhang et al. 1998, 2007; Tee et al. 2005, 2009; Bokare et al. 2008; Barnes et al. 2010; Lee and Doong 2014; Schrick et al. 2002; Xu et al. 2009, 2012; Cheng et al. 2010), Ag/Fe (Xu and Zhang 2000), Pd/Zn (Zhang et al. 1998), etc. They are produced with the desired amounts of noble metals applied on the surface of reductive nanomaterials by chemical methods.

giovanni.libralato@unina.it

Currently, it is reported that bimetallic nanomaterials have been taken into bench-scale experiments to degrade a wide variety of common organic materials (Lim et al. 2007; Zhang et al. 1998; Xu and Zhang 2000; Lien and Zhang 2007; Wei et al. 2006; Guasp and Wei 2003; Nagpal et al. 2010; Schrick et al. 2002; Tee et al. 2005; Cheng et al. 2010). For example, Fe^0 nanoparticles were coated with a thin layer of palladium to produce nano Pd/Fe. The modified material was applied into reduction of PCE and TCE, and the efficiency was simultaneously compared with that of ZVI nanoparticles and iron powder. The results indicated that the reduction rate of Pd/Fe nanoparticles was significantly higher than that of Fe^0 nanoparticles and iron powder (Wang and Zhang 1997).

The reductive reaction between organics and alloy nonamaterials is related to the parameter such as the concentration of modified material, dosage of additive, size and specials of noble metal, the type of organics, etc. Nagpal and Bokare conducted the batch experiments to investigate the effect of Fe-Pd mass concentration on the lindane degradation efficiency, indicating that the efficiency increased with increasing concentrations and 5 mg/L of lindane was completely dechlorinated within 5 min at a catalyst loading of 0.5 g/L (Nagpal et al. 2010). Four different sizes of nickel were applied on the surface of nZVI to produce Ni/Fe nanomaterials to dechlorinate pentachlorophenol and an evidently more efficient dechlorination was obtained with the decrease of nano-Ni particle size (Cheng et al. 2010). The increases in the dosage of Pd/Fe nanoparticles and temperature enhanced degradation rates and efficiency, and the removal mechanism included oxidation and reduction adsorption (Guasp and Wei 2003).

Lindane (5 mg/L) was completely decomposed by nano Pd/Fe within 10 min and the degradation reaction followed first-order kinetics (Nagpal et al. 2010). Carbon tetrabromide (CTB), bromoform (BF) and dibromomethane (DBM) were completely removed by nano-scale Ni/Fe particles in 2, 2, 3.5 h respectively, and investigated for their first-order kinetics reductive degradation pathways (Lim et al. 2007). During the reductions of chlorinated organic contaminants such as TCE or PCE, hydrogen was observed to be the predominant driver for degradation, by breaking C–Cl bonds and swapping itself for chlorine (Schrick et al. 2002) and the rate of TCE reduction has been recorded as significantly limited by monometallic nZVI (Barnes et al. 2010; Schrick et al. 2002).

4.3 Compound Nanomaterials (FeS)

Compared to elemental nanomaterials, compound nanomaterials have also shown great potential for remediation of contaminated groundwater. Nonetheless, the study for reductive removal of pollutants by compound nanomaterials was rarely reported other than FeS nanoparticles. Iron sulfide (FeS) or mackinawite is an important reductant providing a supply of Fe(II) and S(-II) species, both of which can act as electron donors.

giovanni.libralato@unina.it

1. **Organics removal**

FeS nanoparticles have been exhibited to be rather effective for reductive transformation and detoxification of chlorinated organic compounds (COCs), such as Trichloroethylene (TCE), Tetrachloroethylene (PCE). Through the reaction COCs could be partially or completely dechlorinated to ethane and chloride (Amir and Lee 2012). Besides, COCs are often found with inorganic contaminants such as heavy metals. Co-present metals may impact the dechlorination rates considerably. For instance, Amir and Lee (2012) suggested that Co(III) showed a significant role in electron transfer mediation for reductive dechlorination of PCE by nanomackinawite (nFeS). At pH 8.3, PCE was fully degraded in nFeS-Co(III) suspension in 120 h. The dechlorination kinetic rate constant in the nFeS-Co(III) suspension ($0.188 \pm 0.003\ h^{-1}$) was 145 times greater than that in nFeS suspension.

2. **Inorganics removal**

In addition to organic contaminants, FeS nanoparticles can also availably reduce inorganic pollutants, such as Cr(VI), Se(IV) and U(VI).

FeS particles may provide a source of Fe(II) and S(-II) species, both of which may facilitate chromate reduction (Patterson et al. 1997). Liu et al. (2016) examined optimized process parameters of FeS nanoparticles, and it showed that the 0.05 wt % CMC stabilized FeS had a higher Cr(VI) removal capacity of 683 mg/g FeS at initial Cr(VI) concentration of 50 mg/L at pH 5.6, and up to 92.48% Cr(VI) was removed within 15 min.

The radioactive isotope 79Se is a fission product, which has caused great interest due to its long half life. The Selenium solubility is largely controlled by Se oxidation state. In the tetravalent and hexavalent oxidation states, Se prevails as mobile aqueous oxyanions, while Se(0) and Se(-II) form solids with low solubility (Scheinost et al. 2008). However, reductant such as FeS may effectively affect the environmental fate and transport of Se. Scheinost and Charlet (2008) found that selenite was rapidly reduced to insoluble Se(0) and FeSe within one day by nanoparticulate mackinawite.

Typical radionuclide uranium (U) is a redox-active actinide element, and redox conditions may strongly affect the reactivity and mobility of U. Hence, Some U remediation approaches focus on converting highly water soluble and more toxic U (VI) to immobile U(IV) (Bi et al. 2013; Bi and Hayes 2014). Hyun et al. (2012) studied the ability of nanocrystalline mackinawite to reduce uranium (VI) in an O_2 and CO_2 free model system, and the aqueous U(VI) was removed almost completely over the wide pH range between 5 and 11 at the initial U(VI) concentration of 5×10^{-5} M following the Eqs. (18)–(21).

$$UO_2^{2+} + \equiv FeS \Leftrightarrow \equiv S^{2-} - UO_2^{2+} + Fe^{2+} \tag{18}$$

$$S^{2-} - UO_2^{2+} \Leftrightarrow S^0(s) - UO_2(s) \tag{19}$$

giovanni.libralato@unina.it

$$FeS(s) + H_2O \Leftrightarrow Fe^{2+} + HS^- + OH^- \quad (20)$$

$$UO_2^{2+} + HS^- \Leftrightarrow UO_2(s) - S^0(s) + H^+ \quad (21)$$

4.4 Composite Nanomaterials

Composite nanomaterials contain two or more types of functionalities, show unique physical and chemical properties, and lead to markedly enhanced performance. It is known that ZVI nanoparticles have been primitively applied into the remediation of groundwater since the year of 1994 (Gillham and Ohannesin 1994). The reductive nanomaterials have been most extensively studied with different kinds of nanomaterials derived such as metallic and alloy nanomaterials. However, due to the frangibility to oxidation of the metallics and the difficult contact with the hydrophilic organics, some researchers have modified these substances to composite nanomaterials for heterogeneous reduction in water decontamination (Qu et al. 2013; Fu and Wang 2011). Recently, some studies show that the different characteristic reductive species are generated through deposition on the supporter and encapsulated nZVI in matrices composed of activated carbon, biochar, graphene, carbon nanotubes or polymer membranes (Stefaniuk et al. 2016; Crane and Scott 2012). Besides, there are other nanomaterials for heterogeneous reduction to be less-commonly focused, including nano Fe_3O_4/Fe, Fe/FeS nanoparticles, nanoscale TiO_2/Fe^0, et al. Due to the difficult separation of nZVI from the purified matrix in the course of remediation, such materials as silica (Tang et al. 2006; Li et al. 2011), activated carbon (Hoch et al. 2008; Zhang et al. 2010; Zhu et al. 2009; Chen et al. 2014), biochar (Yan et al. 2015; Zhou et al. 2014), graphene (Liu et al. 2014), polymer membranes (Tesh and Scott 2014; Horzum et al. 2013; Parshetti and Doong 2009; Ma et al. 2015), polymer nanofibers (Bhaumik et al. 2014, 2015a, b), calcium alginate (Bezbaruah et al. 2009, 2011, 2013; Ravikumar et al. 2016), chitosan (Liu et al. 2010) or gum Arabic (Long and Ramsburg 2011), could support and immobilize nZVI to improve its physicochemical properties to remove contaminations better by fixing nZVI on their surface or trapping inside their pores (Tesh and Scott 2014; Yan et al. 2013).

There are other modified materials with the potential to reduce the inorganic or organics. For instance, Lv et al. (2012) synthesized Fe/Fe_3O_4 nanocomposites by adding Fe_3O_4 nanoparticles (nFe_3O_4) into the reaction solution during the preparation of ZVI. nFe_3O_4 could make ZVI attach to its surface and then form a stable Fe/Fe_3O_4 system. Kim et al. (2011) developed a new one-pot method to prepare Fe/FeS core-shell nanoparticles using dithionite at room temperature. Huang et al. (2007) and Pan et al. (2012) obtained nZVI particles and TiO_2 sample by dropping $FeCl_3$ to $NaBH_4$ solution through chemical coprecipitization–peptization method, respectively. And then the composites were produced by submerging in a 1% neutral TiO_2 sol–gel to coat a thin layer of TiO_2 on the Fe^0 surface.

giovanni.libralato@unina.it

Different types of composite nanomaterials have been extensively assessed as a reactive medium to remove/immobilize organic and inorganic compounds from contaminated sites as below.

1. **Organics removal**

There are many nano-composites used for the degradation of a common and highly important pollutant, trichloroethylene (TCE) (Smuleac et al. 2011; Yan et al. 2015; Parshetti and Doong 2009). For instance, biochar supported nZVI composite was synthesized to enhance the TCE removal in aqueous solutions. The batch experiment indicated that the degradation efficiency of TCE was 99.4% in the presence of nZVI/biochar and persulfate within 5 min, significantly higher than 56.6% in nZVI and persulfate system under the same conditions, which provides the evident that the nano-composite has great potential in the degradation of toxic organic pollutants (Yan et al. 2015). Kim et al. (2011) used TCE as a model compound to examine the efficiency of Fe/FeS for the removal of pollutants in the aqueous solutions. The Fe/FeS nanoparticles exhibited a high reactivity toward TCE removal, and within less than 2 h, complete reduction was achieved by 2 g/L Fe/FeS at the initial TCE concentration of 0.11 mM. Besides, the Fe/FeS shows a much higher reactivity toward contaminants than the pure Fe nanoparticles, mainly because the deposition of FeS on the Fe surface can facilitate conduction of electrons from ZVI core to adsorbed TCE, thereby resulting in the remarkable rate enhancement of TCE reduction.

A template-free method was used to prepare composite nanofibers of poly-aniline/Fe^0 for the reductive degradation and removal of Congo red from aqueous solutions, which showed that a complete degradation of 50 mg/L Congo red arrived after 5 min with a minimum dosage (1 g/L), and the Congo red degradation rate followed a pseudo-first-order kinetic model of reaction (Bhaumik et al. 2015).

Huang et al. (2007) applied the TiO_2/Fe^0 nano-composite with UV irradiation to the degradation of azo dye (Acid Black-24) from a simulated wastewater, with a much higher reactivity with 40% reduction in less than 1.0 h than microscale and nanoscale Fe^0 and TiO_2 particles.

2. **Inorganics removal**

Li et al. (2011) showed that the removal of Cr(VI) from groundwater with nZVI deposited on silica dust, was 22.5% more effective in metal removal compared to the use of non-modified nZVI.

The mutual promoting effects of Fe/Fe_3O_4 system could be speculated as the following two aspects: (1) The electron transfer reaction between nZVI and nFe_3O_4 could be facilitated and then reduced Fe^{3+} on the surface of Fe_3O_4 to regenerate surface Fe^{2+}, the active species for Cr(VI) removal; (2) the electron transfer on the interface of metal oxide prevented superficial oxidation and passivation of nZVI particles guaranteeing the continuous reaction exhibited in Eqs. (22)–(25). Based on the above two aspects, the removal efficiency of Cr(VI) by Fe/Fe_3O_4

giovanni.libralato@unina.it

nano-composites is highly improved. It is reported that 96.4% Cr(VI) could be removed by these novel nano-composites within 2 h at pH of 8.0 and initial Cr concentration of 20 mg/L, compared with 48.8% by bare nFe_3O_4 and 18.8% by bare nZVI (Lv et al. 2012).

$$2HCrO_4^- + 3Fe^0 + 14H^+ \rightarrow 3Fe^{2+} + 2Cr^{3+} + 8H_2O \quad (22)$$

$$2CrO_4^{2-} + 3Fe^0 + 16H^+ \rightarrow 3Fe^{2+} + 2Cr^{3+} + 8H_2O \quad (23)$$

$$HCrO_4^- + 3Fe^{2+}_{solution}/Fe^{2+}_{surf} + 7H^+ \rightarrow 3Fe^{3+}_{solution}/Fe^{3+}_{surf} + Cr^{3+} + 4H_2O \quad (24)$$

$$2CrO_4^{2-} + 3Fe^{2+}_{solution}/Fe^{2+}_{surf} + 8H^+ \rightarrow 3Fe^{3+}_{solution}/Fe^{3+}_{surf} + Cr^{3+} + 4H_2O \quad (25)$$

Nano-composites could be related to denitrification as well. Bezbaruah et al. (2009) conducted batch nitrate degradation experiments by iron nanoparticles in calcium alginate beads, indicating that 50–73% nitrate-N removal was achieved over a 2 h period. Pan et al. (2012) compared the efficiencies of nitrate removal from aqueous solution by TiO_2, nZVI and TiO_2/Fe^0 nano-composite (NTFC) in the prepared system under UV illumination. The results proved that only NTFC achieved satisfactory transformation of nitrate to N_2, which provided a new promising method for water treatment.

5 Conclusion

On the basis of the above discussion, ENMs have great potential for the treatment of inorganic and organic contaminated water. On one aspect, some of the ENMs can be alternatives for some steps of the ordinary water treatment process due to higher cost-efficiency; on the other aspect, ENMs can play as a complementary process for the ordinary water treatment plants in the case of emergency control and removal of low levels of contaminants. Besides, the effectiveness and cost of ENMs can be further improved with the development of synthesis and modification methods for industrial-scale production. However, we should notice that most ENMs are still studied in the laboratory scale. Some ENMs for the removal of inorganics and/or organics contaminants in water are still under investigation. The results of laboratory experiments do not always reflect the natural conditions of contaminated sites, so some of pilot tests are necessary. Moreover, during water treatment, the release of applied ENMs may occur. The implications of ENMs to human and the environment should be fully considered before its application at large scale. Therefore, more work is needed in order to have a completed assessment for the practical application of ENMs for water decontamination.

giovanni.libralato@unina.it

References

Adeleye AS et al (2016) Engineered nanomaterials for water treatment and remediation: costs, benefits, and applicability. Chem Eng J 286:640–662

Akhavan O (2011) Photocatalytic reduction of graphene oxides hybridized by ZnO nanoparticles in ethanol. Carbon 49(1):11–18

Alonso F, Beletskaya IP, Yus M (2002) Metal-mediated reductive hydrodehalogenation of organic halides. Chem Rev 102(11):4009–4091

Amir A, Lee W (2012) Enhanced reductive dechlorination of tetrachloroethene during reduction of cobalamin (III) by nano-mackinawite. J Hazard Mater 235–236:359–366

Baker JR (2001) Nanomaterial antimicrobial agents. Abstr Pap Am Chem Soc 221:616–617

Barnes RJ et al (2010) Inhibition of biological TCE and sulphate reduction in the presence of iron nanoparticles. Chemosphere 80(5):554–562

Bezbaruah AN et al (2009) Entrapment of iron nanoparticles in calcium alginate beads for groundwater remediation applications. J Hazard Mater 166(2–3):1339–1343

Bezbaruah AN et al (2011) Encapsulation of iron nanoparticles in alginate biopolymer for trichloroethylene remediation. J Nanopart Res 13(12):6673–6681

Bezbaruah AN et al (2013) Ca-alginate-entrapped nanoscale iron: arsenic treatability and mechanism studies. J Nanopart Res 16(1):2175

Bhaumik M et al (2014) Composite nanofibers prepared from metallic iron nanoparticles and polyaniline: high performance for water treatment applications. J Colloid Interface Sci 425: 75–82

Bhaumik M et al (2015a) Polyaniline/Fe-0 composite nanofibers: an excellent adsorbent for the removal of arsenic from aqueous solutions. Chem Eng J 271:135–146

Bhaumik M, McCrindle RI, Maity A (2015b) Enhanced adsorptive degradation of Congo red in aqueous solutions using polyaniline/Fe^0 composite nanofibers. Chem Eng J 260:716–729

Bi Y, Hayes KF (2014) Nano-FeS inhibits UO_2 reoxidation under varied oxic conditions. Environ Sci Technol 48(1):632–640

Bi Y et al (2013) Oxidative dissolution of UO_2 in a simulated groundwater containing synthetic nanocrystalline mackinawite. Geochim Cosmochim Acta 102:175–190

Blowes DW, Ptacek CJ, Jambor JL (1997) In-situ remediation of Cr(VI)-contaminated groundwater using permeable reactive walls: laboratory studies. Environ Sci Technol 31 (12):3348–3357

Bogardi JJ et al (2012) Water security for a planet under pressure: interconnected challenges of a changing world call for sustainable solutions. Curr Opin Environ Sustain 4(1):35–43

Bogdanovic U et al (2015) Nanomaterial with high antimicrobial efficacy-copper/polyaniline nanocomposite. ACS Appl Mater Interfaces 7(3):1955–1966

Bokare AD et al (2008) Iron-nickel bimetallic nanoparticles for reductive degradation of azo dye Orange G in aqueous solution. Appl Catal B Environ 79(3):270–278

Botes M, Cloete TE (2010) The potential of nanofibers and nanobiocides in water purification. Crit Rev Microbiol 36(1):68–81

Brady-Estevez AS, Seoktae K, Elimelech M (2008) A single-walled-carbon-nanotube filter for removal of viral and bacterial pathogens. Small 4(4):481–484

Brady-Estévez AS et al (2010) Impact of solution chemistry on viral removal by a single-walled carbon nanotube filter. Water Res 44(13):3773–3780

Cao JS et al (1999) Reducing degradation of azo dye by zero-valent iron in aqueous solution. Chemosphere 38(3):565–571

Carpenter AW, de Lannoy CF, Wiesner MR (2015) Cellulose nanomaterials in water treatment technologies. Environ Sci Technol 49(9):5277–5287

Casey FXM, Ong SK, Horton R (2000) Degradation and transformation of trichloroethylene in miscible displacement experiments through zerovalent metals. Environ Sci Technol 34 (23):5023–5029

giovanni.libralato@unina.it

Chang RM, Kauffman RJ, Kwon Y (2014) Understanding the paradigm shift to computational social science in the presence of big data. Decis Support Syst 63:67–80
Chen W, Duan L, Zhu D (2007) Adsorption of polar and nonpolar organic chemicals to carbon nanotubes. Environ Sci Technol 41(24):8295–8300
Chen W et al (2008a) Adsorption of hydroxyl- and amino-substituted aromatics to carbon manotubes. Environ Sci Technol 42(18):6862–6868
Chen J, Chen W, Zhu D (2008b) Adsorption of nonionic aromatic compounds to single-walled carbon nanotubes: effects of aqueous solution chemistry. Environ Sci Technol 42(19): 7225–7230
Chen SY, Chen WH, Shih CJ (2008c) Heavy metal removal from wastewater using zero-valent iron nanoparticles. Water Sci Technol 58(10):1947–1954
Chen CL, Wang XK, Nagatsu M (2009) Europium adsorption on multiwall carbon nanotube/iron oxide magnetic composite in the presence of polyacrylic acid. Environ Sci Technol 43 (7):2362–2367
Chen SS et al (2014a) Dechlorination of tetrachloroethylene in water using stabilized nanoscale iron and palladized iron particles. Desalination Water Treat 52(4–6):702–711
Chen WF et al (2014b) Dechlorination of hexachlorobenzene by nano zero-valent iron/activated carbon composite: iron loading, kinetics and pathway. RSC Adv 4(87):46689–46696
Chen Q, Xin Y, Zhu X (2015) Au-Pd nanoparticles-decorated TiO_2 nanobelts for photocatalytic degradation of antibiotic levofloxacin in aqueous solution. Electrochim Acta 186:34–42
Cheng R, Wang JL, Zhang WX (2007) Comparison of reductive dechlorination of p-chlorophenol using Fe-0 and nanosized Fe-0. J Hazard Mater 144(1–2):334–339
Cheng R et al (2010) Dechlorination of pentachlorophenol using nanoscale Fe/Ni particles: role of nano-Ni and its size effect. J Hazard Mater 180(1–3):79–85
Choe S et al (2001) Rapid reductive destruction of hazardous organic compounds by nanoscale Fe-0. Chemosphere 42(4):367–372
Chong MN et al (2010) Recent developments in photocatalytic water treatment technology: a review. Water Res 44(10):2997–3027
Crane RA, Scott TB (2012) Nanoscale zero-valent iron: future prospects for an emerging water treatment technology. J Hazard Mater 211–212:112–125
Crane RA et al (2011) Magnetite and zero-valent iron nanoparticles for the remediation of uranium contaminated environmental water. Water Res 45(9):2931–2942
Cui XJ et al (2010) Molecular characteristics and functional analysis of full-length hepatitis B virus quasispecies from a patient with chronic hepatitis B virus infection. Virus Res 150(1–2):43–48
Cui H et al (2012) Strong adsorption of arsenic species by amorphous zirconium oxide nanoparticles. J Ind Eng Chem 18:1418–1427
Cui H et al (2013) Exceptional arsenic (III, V) removal performance of highly porous, nanostructured ZrO_2 spheres for fixed bed reactors and the full-scale system modeling. Water Res 47(16):6258–6268
Daer S et al (2015) Recent applications of nanomaterials in water desalination: a critical review and future opportunities. Desalination 367:37–48
Deng BL, Burris DR, Campbell TJ (1999) Reduction of vinyl chloride in metallic iron-water systems. Environ Sci Technol 33(15):2651–2656
Deng N et al (2000) Discoloration of aqueous reactive dye solutions in the UV/Fe-0 system. Water Res 34(8):2408–2411
Deng L et al (2016) SnS_2/TiO_2 nanocomposites with enhanced visible light-driven photoreduction of aqueous Cr(VI). Ceram Int 42(3):3808–3815
Di Palma L, Gueye MT, Petrucci E (2015) Hexavalent chromium reduction in contaminated soil: a comparison between ferrous sulphate and nanoscale zero-valent iron. J Hazard Mater 281: 70–76
Dickinson M, Scott TB (2010) The application of zero-valent iron nanoparticles for the remediation of a uranium-contaminated waste effluent. J Hazard Mater 178(1–3):171–179
Dries J et al (2005) Combined removal of chlorinated ethenes and heavy metals by zerovalent iron in batch and continuous flow column systems. Environ Sci Technol 39(21):8460–8465

giovanni.libralato@unina.it

Dursun AY, Kalayci CS (2005) Equilibrium, kinetic and thermodynamic studies on the adsorption of phenol onto chitin. J Hazard Mater 123(1–3):151–157
Elliott DW, Zhang WX (2001) Field assessment of nanoscale bimetallic particles for groundwater treatment. Abstr Pap Am Chem Soc 35(24):4922–4926
Engates KE, Shipley HJ (2011) Adsorption of Pb, Cd, Cu, Zn, and Ni to titanium dioxide nanoparticles: effect of particle size, solid concentration, and exhaustion. Environ Sci Pollut Res 18(3):386–395
Fagan SB et al (2004) 1,2-dichlorobenzene interacting with carbon nanotubes. Nano Lett 4 (7):1285–1288
Fan J et al (2009) Rapid decolorization of azo dye methyl orange in aqueous solution by nanoscale zerovalent iron particles. J Hazard Mater 166(2–3):904–910
Fan FL et al (2012) Rapid removal of uranium from aqueous solutions using magnetic Fe_3O_4@SiO_2 composite particles. J Environ Radioact 106:40–46
Fang ZQ et al (2011a) Effective removal of antibiotic metronidazole from water by nanoscale zero-valent iron particles. Desalination 268(1–3):60–67
Fang ZQ et al (2011b) Degradation of the polybrominated diphenyl ethers by nanoscale zero-valent metallic particles prepared from steel pickling waste liquor. Desalination 267 (1):34–41
Farghali AA et al (2013) Adsorption of Pb(II) ions from aqueous solutions using copper oxide nanostructures. Beni-Suef Univ J Basic Appl Sci 2(2):61–71
Feng Q et al (2012) Adsorption and desorption characteristics of arsenic onto ceria nanoparticles. Nanoscale Res Lett 7(84):1–8
Forouzani M et al (2015) Comparative study of oxidation of benzyl alcohol: influence of Cu-doped metal cation on nano ZnO catalytic activity. Chem Eng J 275:220–226
Fu FL, Wang Q (2011) Removal of heavy metal ions from wastewaters: a review. J Environ Manage 92(3):407–418
Fu FL, Dionysiou DD, Liu H (2014) The use of zero-valent iron for groundwater remediation and wastewater treatment: a review. J Hazard Mater 267:194–205
Ghasemi Z et al (2012) Thermodynamic and kinetic studies for the adsorption of Hg(II) by nano-TiO_2 from aqueous solution. Adv Powder Technol 23(2):148–156
Ghosh MK et al (2012) Arsenic adsorption on goethite nanoparticles produced through hydrazine sulfate assisted synthesis method. Korean J Chem Eng 29(1):95–102
Gillham RW, Ohannesin SF (1994) Enhanced degradation of halogenated aliphatics by zero-valent iron. Ground Water 32(6):958–967
Gong Y et al (2012) Immobilization of mercury in field soil and sediment using carboxymethyl cellulose stabilized iron sulfide nanoparticles. Nanotechnology 23(29)
Gong Y, Tang J, Zhao D (2016) Application of iron sulfide particles for groundwater and soil remediation: a review. Water Res 89:309–320
Gotovac S et al (2007) Adsorption of polyaromatic hydrocarbons on single wall carbon nanotubes of different functionalities and diameters. J Colloid Interface Sci 314(1):18–24
Grey D et al (2002) Water security in one blue planet: twenty-first century policy challenges for science. Philos Trans R Soc A Math Phys Eng Sci 2013:371
Guasp E, Wei R (2003) Dehalogenation of trihalomethanes in drinking water on Pd-Fe bimetallic surface. J Chem Technol Biotechnol 78(6):654–658
Hao YM, Man C, Hu ZB (2010) Effective removal of Cu(II) ions from aqueous solution by amino-functionalized magnetic nanoparticles. J Hazard Mater 184(1–3):392–399
Hartono T et al (2009) Layer structured graphite oxide as a novel adsorbent for humic acid removal from aqueous solution. J Colloid Interface Sci 333(1):114–119
He Y et al (2012) The comparative study on the rapid decolorization of azo, anthraquinone and triphenylmethane dyes by zero-valent iron. Chem Eng J 179:8–18
He J et al (2014) Heterogeneous Fenton oxidation of catechol and 4-chlorocatechol catalyzed by nano-Fe_3O_4: role of the interface. Chem Eng J 258:433–441
Hoch LB et al (2008) Carbothermal synthesis of carbon-supported nanoscale zero-valent iron particles for the remediation of hexavalent chromium. Environ Sci Technol 42(7):2600–2605

giovanni.libralato@unina.it

Horzum N et al (2013) Chitosan fiber-supported zero-valent iron nanoparticles as a novel sorbent for sequestration of inorganic arsenic. RSC Adv 3(21):7828–7837
Hossain F et al (2014) Antimicrobial nanomaterials as water disinfectant: applications, limitations and future perspectives. Sci Total Environ 466:1047–1059
Hou MF et al (2007) The effect of substituent groups on the reductive degradation of azo dyes by zerovalent iron. J Hazard Mater 145(1–2):305–314
Hou B et al (2015) Heterogeneous electro-Fenton oxidation of catechol catalyzed by nano-Fe_3O_4: kinetics with the Fermi's equation. J Taiwan Inst Chem Eng 3(4):1–11
Hua M et al (2012) Heavy metal removal from water/wastewater by nanosized metal oxides: a review. J Hazard Mater 211–212:317–331
Huang C et al (2007) Characteristic of an innovative TiO_2/Fe^0 composite for treatment of azo dye. Sep Purif Technol 58(1):152–158
Huang L et al (2009) Preparation of cuprous oxides with different sizes and their behaviors of adsorption, visible-light driven photocatalysis and photocorrosion. Solid State Sci 11(1): 129–138
Huang Z et al (2011) Adsorption of Lead(II) ions from aqueous solution on low-temperature exfoliated graphene nanosheets. Langmuir 27(12):7558–7562
Huang Q et al (2013) Reductive dechlorination of tetrachlorobisphenol A by Pd/Fe bimetallic catalysts. J Hazard Mater 262:634–641
Hyun SP et al (2012) Uranium(VI) reduction by iron(II) monosulfide mackinawite. Environ Sci Technol 46(6):3369–3376
Jang SM et al (2004) Adsorption of 4-biphenylmethanethiolate on different-sized gold nanoparticle surfaces. Langmuir 20(5):1922–1927
Ji L et al (2009a) Adsorption of sulfonamide antibiotics to multiwalled carbon nanotubes. Langmuir 25(19):11608–11613
Ji L et al (2009b) Mechanisms for strong adsorption of tetracycline to carbon nanotubes: a comparative study using activated carbon and graphite as adsorbents. Environ Sci Technol 43 (7):2322–2327
Jo WK, Tayade RJ (2016) Facile photocatalytic reactor development using nano-TiO_2 immobilized mosquito net and energy efficient UVLED for industrial dyes effluent treatment. J Environ Chem Eng 4(1):319–327
Joo SH et al (2005) Quantification of the oxidizing capacity of nanoparticulate zero-valent iron. Environ Sci Technol 39(5):1263–1268
Kalia S et al (2014) Magnetic polymer nanocomposites for environmental and biomedical applications. Colloid Polym Sci 292(9):2025–2052
Kanel SR, Greneche JM, Choi H (2006) Arsenic(V) removal from groundwater using nano scale zero-valent iron as a colloidal reactive barrier material. Environ Sci Technol 40(6):2045–2050
Kar S et al (2016) Classification of river water pollution using Hyperion data. J Hydrol 537: 221–233
Kim E et al (2011) Facile synthesis and characterization of Fe/FeS nanoparticles for environmental applications. ACS Appl Mater Interfaces 3(5):1457–1462
Kim EJ et al (2013) Hierarchically structured manganese oxide-coated magnetic nanocomposites for the efficient removal of heavy metal ions from aqueous systems. ACS Appl Mater Interfaces 5(19):9628–9634
Klimkova S et al (2008) Application of nanoscale zero-valent iron for groundwater remediation: laboratory and pilot experiments. NANO 3(4):287–289
Klimkova S et al (2011) Zero-valent iron nanoparticles in treatment of acid mine water from in situ uranium leaching. Chemosphere 82(8):1178–1184
Kocabas-Atakli ZO, Yurum Y (2013) Synthesis and characterization of anatase nanoadsorbent and application in removal of lead, copper and arsenic from water. Chem Eng J 225:625–635
Koutahzadeh N, Esfahani MR, Arce PE (2016) Removal of acid black 1 from water by the pulsed corona discharge advanced oxidation method. J Water Process Eng 10:1–8
Kritis AA et al (2016) Latest aspects of aldosterone actions on the heart muscle. J Physiol Pharmacol 67(1):21–30

giovanni.libralato@unina.it

Kuriakose S, Satpati B, Mohapatra S (2014) Enhanced photocatalytic activity of Co doped ZnO nanodisks and nanorods prepared by a facile wet chemical method. Phys Chem Chem Phys 16 (25):12741–12749

Kurian M, Nair DS (2014) Heterogeneous Fenton behavior of nano nickel zinc ferrite catalysts in the degradation of 4-chlorophenol from water under neutral conditions. J Water Process Eng 8:37–49

Lee CC, Doong RA (2014) Enhanced dechlorination of tetrachloroethylene by polyethylene glycol-coated zerovalent silicon in the presence of nickel ions. Appl Catal B Environ 144: 182–188

Lee J, Kao H, Yang S (2014) Service innovation and smart analytics for industry 4.0 and big data environment. Procedia CIRP 16:3–8

Li YH et al (2001) Adsorption of fluoride from water by amorphous alumina supported on carbon nanotubes. Chem Phys Lett 350(5–6):412–416

Li YH et al (2003a) Competitive adsorption of Pb^{2+}, Cu^{2+} and Cd^{2+} ions from aqueous solutions by multiwalled carbon nanotubes. Carbon 41(14):2787–2792

Li YH et al (2003b) Adsorption of fluoride from water by aligned carbon nanotubes. Mater Res Bull 38(3):469–476

Li Q et al (2008) Antimicrobial nanomaterials for water disinfection and microbial control: potential applications and implications. Water Res 42(18):4591–4602

Li J et al (2011a) Effect of surfactants on Pb(II) adsorption from aqueous solutions using oxidized multiwall carbon nanotubes. Chem Eng J 166(2):551–558

Li YH et al (2011b) Adsorption of cationic red X-GRL from aqueous solutions by graphene: equilibrium, kinetics and thermodynamics study. Chem Biochem Eng Q 25(4):483–491

Li YC, Li TL, Jin ZH (2011c) Stabilization of Fe-0 nanoparticles with silica fume for enhanced transport and remediation of hexavalent chromium in water and soil. J Environ Sci 23(7): 1211–1218

Li Y et al (2012a) Equilibrium, kinetic and thermodynamic studies on the adsorption of phenol onto graphene. Mater Res Bull 47(8):1898–1904

Li Z et al (2012b) Uranium(VI) adsorption on graphene oxide nanosheets from aqueous solutions. Chem Eng J 210:539–546

Li X et al (2012c) Pore size and surface area control of MgO nanostructures using a surfactant-templated hydrothermal process: high adsorption capability to azo dyes. Colloids Surf A Physicochem Eng Aspects 408:79–86

Li S et al (2014a) Effective photocatalytic decolorization of methylene blue utilizing ZnO/rectorite nanocomposite under simulated solar irradiation. J Alloy Compd 616(31):227–234

Li W, Wang Y, Irini A (2014b) Effect of pH and H_2O_2 dosage on catechol oxidation in nano-Fe_3O_4 catalyzing UV—Fenton and identification of reactive oxygen species. Chem Eng J 244:1–8

Li SL et al (2014c) Zero-valent iron nanoparticles (nZVI) for the treatment of smelting wastewater: a pilot-scale demonstration. Chem Eng J 254:115–123

Li SL et al (2014d) Nanoscale zero-valent iron (nZVI) for the treatment of concentrated Cu(II) wastewater: a field demonstration. Environ Sci Process Impacts 16(3):524–533

Li X et al (2015) The synthesis of CdS/TiO_2 hetero-nanofibers with enhanced visible photocatalytic activity. J Colloid Interface Sci 452:89–97

Liang P, Shi TQ, Li J (2004) Nanometer-size titanium dioxide separation/preconcentration and FAAS determination of trace Zn and Cd in water sample. Int J Environ Anal Chem 84(4): 315–321

Liang L, Luo L, Zhang S (2011) Adsorption and desorption of humic and fulvic acids on SiO_2 particles at nano- and micro-scales. Colloids Surf A Physicochem Eng Aspects 384(1–3): 126–130

Lien HL, Zhang WX (1999) Transformation of chlorinated methanes by nanoscale iron particles. J Environ Eng ASCE 125(11):1042–1047

Lien HL, Zhang WX (2005) Hydrodechlorination of chlorinated ethanes by nanoscale Pd/Fe bimetallic particles. J Environ Eng ASCE 131(1):4–10

giovanni.libralato@unina.it

Lien HL, Zhang WX (2007) Nanoscale Pd/Fe bimetallic particles: catalytic effects of palladium on hydrodechlorination. Appl Catal B Environ 77(1–2):110–116
Lim TT, Feng J, Zhu BW (2007) Kinetic and mechanistic examinations of reductive transformation pathways of brominated methanes with nano-scale Fe and Ni/Fe particles. Water Res 41(4):875–883
Lin D, Xing B (2008) Adsorption of phenolic compounds by carbon nanotubes: role of aromaticity and substitution of hydroxyl groups. Environ Sci Technol 42(19):7254–7259
Lin YT, Weng CH, Chen FY (2008) Effective removal of AB24 dye by nano/micro-size zero-valent iron. Sep Purif Technol 64(1):26–30
Liu YQ, Lowry GV (2006) Effect of particle age (Fe-o content) and solution pH on NZVI reactivity: H-2 evolution and TCE dechlorination. Environ Sci Technol 40(19):6085–6090
Liu YQ et al (2005) TCE dechlorination rates, pathways, and efficiency of nanoscale iron particles with different properties. Environ Sci Technol 39(5):1338–1345
Liu TY et al (2010a) Effects of physicochemical factors on Cr(VI) removal from leachate by zero-valent iron and alpha-Fe_2O_3 nanoparticles. Water Sci Technol 61(11):2759–2767
Liu TY et al (2010b) Entrapment of nanoscale zero-valent iron in chitosan beads for hexavalent chromium removal from wastewater. J Hazard Mater 184(1–3):724–730
Liu F et al (2012a) Three-dimensional graphene oxide nanostructure for fast and efficient water-soluble dye removal. ACS Appl Mater Interfaces 4(2):922–927
Liu T et al (2012b) Adsorption of methylene blue from aqueous solution by graphene. Colloids Surf B Biointerfaces 90:197–203
Liu L et al (2013) Adsorption of Au(III), Pd(II), and Pt(IV) from aqueous solution onto graphene oxide. J Chem Eng Data 58(2):209–216
Liu FL et al (2014) Graphene-supported nanoscale zero-valent iron: removal of phosphorus from aqueous solution and mechanistic study. J Environ Sci 26(8):1751–1762
Liu Y et al (2015) Degradation of the common aqueous antibiotic tetracycline using a carbon nanotube electrochemical filter. Environ Sci Technol 49(13):7974–7980
Liu Y et al (2016) Optimized synthesis of FeS nanoparticles with a high Cr(VI) removal capability. J Nanomater
Long T, Ramsburg CA (2011) Encapsulation of nZVI particles using a gum Arabic stabilized oil-in-water emulsion. J Hazard Mater 189(3):801–808
Losurdo M et al (2009) Spectroscopic ellipsometry and polarimetry for materials and systems analysis at the nanometer scale: state-of-the-art, potential, and perspectives. J Nanopart Res 11 (7):1521–1554
Lowry GV, Johnson KM (2004) Congener-specific dechlorination of dissolved PCBs by microscale and nanoscale zerovalent iron in a water/methanol solution. Environ Sci Technol 38 (19):5208–5216
Lu CY, Chiu HS (2006) Adsorption of zinc(II) from water with purified carbon nanotubes. Chem Eng Sci 61(4):1138–1145
Lu C, Liu C (2006) Removal of nickel(II) from aqueous solution by carbon nanotubes. J Chem Technol Biotechnol 81(12):1932–1940
Lu C, Chung Y, Chang K (2005) Adsorption of trihalomethanes from water with carbon nanotubes. Water Res 39(6):1183–1189
Lv X et al (2012) Highly active nanoscale zero-valent iron (nZVI)-Fe_3O_4 nanocomposites for the removal of chromium(VI) from aqueous solutions. J Colloid Interface Sci 369(1):460–469
Ma X et al (2010) A novel strategy to prepare ZnO/PbS heterostructured functional nanocomposite utilizing the surface adsorption property of ZnO nanosheets. Catal Today 158(3–4):459–463
Ma J et al (2014) Fabrication of Ag/TiO_2 nanotube array with enhanced photo-catalytic degradation of aqueous organic pollutant. Physica E Low-Dimens Syst Nanostruct 58:24–29
Ma BW et al (2015) Modification of ultrafiltration membrane with nanoscale zerovalent iron layers for humic acid fouling reduction. Water Res 71:140–149
Machado FM et al (2011) Adsorption of reactive red M-2BE dye from water solutions by multi-walled carbon nanotubes and activated carbon. J Hazard Mater 192(3):1122–1131

giovanni.libralato@unina.it

Mahmoodi NM, Arami M (2009) Degradation and toxicity reduction of textile wastewater using immobilized titania nanophotocatalysis. J Photochem Photobiol B 94(1):20–24
Matheson LJ, Tratnyek PG (1994) Reductive dehalogenation of chlorinated methanes by iron metal. Environ Sci Technol 28(12):2045–2053
Mikelsaar AV et al (2012) Epitope of titin A-band-specific monoclonal antibody Tit1 5 H1.1 is highly conserved in several Fn3 domains of the titin molecule. Centriole staining in human, mouse and zebrafish cells. Cell Div 7(1):1–10
Mohammadi R, Kassaee MZ (2013) Sulfochitosan encapsulated nano-Fe_3O_4 as an efficient and reusable magnetic catalyst for green synthesis of 2-amino-4H-chromen-4-yl phosphonates. J Mol Catal A Chem 380:152–158
Mueller NC, Nowack B (2010) Nanoparticles for remediation: solving big problems with little particles. Elements 6(6):395–400
Mueller NC et al (2012) Application of nanoscale zero valent iron (NZVI) for groundwater remediation in Europe. Environ Sci Pollut Res 19(2):550–558
Nagpal V et al (2010) Reductive dechlorination of gamma-hexachlorocyclohexane using Fe-Pd bimetallic nanoparticles. J Hazard Mater 175(1–3):680–687
Najafi M, Yousefi Y, Rafati AA (2012) Synthesis, characterization and adsorption studies of several heavy metal ions on amino-functionalized silica nano hollow sphere and silica gel. Sep Purif Technol 85:193–205
Nam S, Tratnyek PG (2000) Reduction of azo dyes with zero-valent iron. Water Res 34(6):1837–1845
Nemecek J et al (2015) Combined abiotic and biotic in-situ reduction of hexavalent chromium in groundwater using nZVI and whey: a remedial pilot test. J Hazard Mater 300:670–679
Oleszczuk P, Pan B, Xing B (2009) Adsorption and desorption of oxytetracycline and carbamazepine by multiwalled carbon nanotubes. Environ Sci Technol 43(24):9167–9173
Ong CS et al (2016) Nanomaterials for biofouling and scaling mitigation of thin film composite membrane: a review. Desalination
Oskoei V et al (2015) Removal of humic acid from aqueous solution using UV/ZnO nano-photocatalysis and adsorption. J Mol Liq 213:374–380
Ozay O et al (2009) Removal of toxic metal ions with magnetic hydrogels. Water Res 43 (17):4403–4411
Pan B, Xing B (2008) Adsorption mechanisms of organic chemicals on carbon nanotubes. Environ Sci Technol 42(24):9005–9013
Pan JR et al (2012) Reductive catalysis of novel TiO_2/Fe^0 composite under UV irradiation for nitrate removal from aqueous solution. Sep Purif Technol 84:52–55
Pariti A et al (2014) Superparamagnetic Au-Fe_3O_4 nanoparticles: one-pot synthesis, biofunctionalization and toxicity evaluation. Mater Res Express 1(3)
Park CM et al (2016) Environmental behavior of engineered nanomaterials in porous media: a review. J Hazard Mater 309:133–150
Parshetti GK, Doong RA (2009) Dechlorination of trichloroethylene by Ni/Fe nanoparticles immobilized in PEG/PVDF and PEG/nylon 66 membranes. Water Res 43(12):3086–3094
Patterson RR, Fendorf S, Fendorf M (1997) Reduction of hexavalent chromium by amorphous iron sulfide. Environ Sci Technol 31(7):2039–2044
Peng XJ et al (2005) Ceria nanoparticles supported on carbon nanotubes for the removal of arsenate from water. Mater Lett 59(4):399–403
Perey JR et al (2002) Zero-valent iron pretreatment for enhancing the biodegradability of azo dyes. Water Environ Res 74(3):221–225
Peterson JW et al (2010) Experimental determination of ampicillin adsorption to nanometer-size Al_2O_3 in water. Chemosphere 80(11):1268–1273
Ponder SM et al (2001) Surface chemistry and electrochemistry of supported zerovalent iron nanoparticles in the remediation of aqueous metal contaminants. Chem Mater 13(2):479–486
Prasse C, Ternes T (2010) Removal of organic and inorganic pollutants and pathogens from wastewater and drinking water using nanoparticles—a review, pp 55–79

giovanni.libralato@unina.it

Qu X et al (2013a) Nanotechnology for a safe and sustainable water supply: enabling integrated water treatment and reuse. Acc Chem Res 46(3):834–843
Qu X, Alvarez PJ, Li Q (2013b) Applications of nanotechnology in water and wastewater treatment. Water Res 47(12):3931–3946
Raizada P et al (2014) Solar photocatalytic activity of nano-ZnO supported on activated carbon or brick grain particles: role of adsorption in dye degradation. Appl Catal A 486(1–2):159–169
Ravi S, Vadukumpully S (2016) Sustainable carbon nanomaterials: recent advances and its applications in energy and environmental remediation. J Environ Chem Eng 4(1):835–856
Ravikumar KVG et al (2016) A comparative study with biologically and chemically synthesized nZVI: applications in Cr(VI) removal and ecotoxicity assessment using indigenous microorganisms from chromium-contaminated site. Environ Sci Pollut Res 23(3):2613–2627
Reinsch BC et al (2010) Chemical transformations during aging of zerovalent iron nanoparticles in the presence of common groundwater dissolved constituents. Environ Sci Technol 44(9):3455–3461
Revitt DM, Ellis JB (2016) Urban surface water pollution problems arising from misconnections. Sci Total Environ 551–552:163–174
Riba O et al (2008) Reaction mechanism of uranyl in the presence of zero-valent iron nanoparticles. Geochim Cosmochim Acta 72(16):4047–4057
Saikia J, Saha B, Das G (2011) Efficient removal of chromate and arsenate from individual and mixed system by malachite nanoparticles. J Hazard Mater 186(1):575–582
Samadi M et al (2016) Recent progress on doped ZnO nanostructures for visible-light photocatalysis. Thin Solid Films 605:2–19
Scheinost AC, Charlet L (2008) Selenite reduction by mackinawite, magnetite and siderite: XAS characterization of nanosized redox products. Environ Sci Technol 42(6):1984–1989
Scheinost AC et al (2008) X-ray absorption and photoelectron spectroscopy investigation of selenite reduction by FeII-bearing minerals. J Contam Hydrol 102(3–4):228–245
Schrick B et al (2002) Hydrodechlorination of trichloroethylene to hydrocarbons using bimetallic nickel-iron nanoparticles. Chem Mater 14(12):5140–5147
Scott TB et al (2011) Nano-scale metallic iron for the treatment of solutions containing multiple inorganic contaminants. J Hazard Mater 186(1):280–287
Shan C, Tong M (2013) Efficient removal of trace arsenite through oxidation and adsorption by magnetic nanoparticles modified with Fe-Mn binary oxide. Water Res 47(10):3411–3421
Sheela T, Nayaka YA (2012) Kinetics and thermodynamics of cadmium and lead ions adsorption on NiO nanoparticles. Chem Eng J 191:123–131
Sheela T et al (2012) Kinetics and thermodynamics studies on the adsorption of Zn(II), Cd(II) and Hg(II) from aqueous solution using zinc oxide nanoparticles. Powder Technol 217:163–170
Shen YF et al (2009) Preparation and application of magnetic Fe_3O_4 nanoparticles for wastewater purification. Sep Purif Technol 68(3):312–319
Sheydaei M, Aber S, Khataee A (2014) Preparation of a novel γ-FeOOH-GAC nano composite for decolorization of textile wastewater by photo Fenton-like process in a continuous reactor. J Mol Catal A Chem 392(11):229–234
Shih YH, Tai YT (2010) Reaction of decabrominated diphenyl ether by zerovalent iron nanoplarticles. Chemosphere 78(10):1200–1206
Shih YH, Hsu CY, Su YF (2011) Reduction of hexachlorobenzene by nanoscale zero-valent iron: kinetics, pH effect, and degradation mechanism. Sep Purif Technol 76(3):268–274
Shih YH et al (2016) Concurrent oxidation and reduction of pentachlorophenol by bimetallic zerovalent Pd/Fe nanoparticles in an oxic water. J Hazard Mater 301:416–423
Shokri A, Mahanpoor K, Soodbar D (2016) Evaluation of a modified TiO_2 (GO–B–TiO_2) photo catalyst for degradation of 4-nitrophenol in petrochemical wastewater by response surface methodology based on the central composite design. J Environ Chem Eng 4(1):585–598
Shu HY et al (2007) Reduction of an azo dye acid black 24 solution using synthesized nanoscale zerovalent iron particles. J Colloid Interface Sci 314(1):89–97
Sitko R et al (2013) Adsorption of divalent metal ions from aqueous solutions using graphene oxide. Dalton Trans 42(16):5682–5689

giovanni.libralato@unina.it

Smith SC, Rodrigues DF (2015) Carbon-based nanomaterials for removal of chemical and biological contaminants from water: a review of mechanisms and applications. Carbon 91:122–143

Smuleac V et al (2011) Green synthesis of Fe and Fe/Pd bimetallic nanoparticles in membranes for reductive degradation of chlorinated organics. J Membr Sci 379(1–2):131–137

Soltani RDC et al (2016) Ultrasonically induced ZnO—biosilica nanocomposite for degradation of a textile dye in aqueous phase. Ultrason Sonochem 28:69–78

Song H, Carraway ER (2005) Reduction of chlorinated ethanes by nanosized zero-valent iron: kinetics, pathways, and effects of reaction conditions. Environ Sci Technol 39(16):6237–6245

Song H, Carraway ER (2008) Catalytic hydrodechlorination of chlorinated ethenes by nanoscale zero-valent iron. Appl Catal B Environ 78(1–2):53–60

Staniszewska M, Graca B, Nehring I (2015) The fate of bisphenol A, 4-tert-octylphenol and 4-nonylphenol leached from plastic debris into marine water—experimental studies on biodegradation and sorption on suspended particulate matter and nano-TiO_2. Chemosphere 145:535–542

Stefaniuk M, Oleszczuk P, Ok YS (2016) Review on nano zerovalent iron (nZVI): from synthesis to environmental applications. Chem Eng J 287:618–632

Strongin D (2004) Environmental applications: treatment/remediation using nanotechnology: an overview, vol 890, pp 202–204

Su F, Lu C, Hu S (2010) Adsorption of benzene, toluene, ethylbenzene and p-xylene by NaOCl-oxidized carbon nanotubes. Colloids Surf A Physicochem Eng Aspects 353(1):83–91

Su CM et al (2012) A two and half-year-performance evaluation of a field test on treatment of source zone tetrachloroethene and its chlorinated daughter products using emulsified zero valent iron nanoparticles. Water Res 46(16):5071–5084

Sui Z et al (2012) Green synthesis of carbon nanotube-graphene hybrid aerogels and their use as versatile agents for water purification. J Mater Chem 22(18):8767–8771

Sumesh E, Bootharaju MS, Pradeep AT (2011) A practical silver nanoparticle-based adsorbent for the removal of Hg^{2+} from water. J Hazard Mater 189(1–2):450–457

Sun L, Yu H, Fugetsu B (2012) Graphene oxide adsorption enhanced by in situ reduction with sodium hydrosulfite to remove acridine orange from aqueous solution. J Hazard Mater 203:101–110

Sun SB et al (2013) Synthesis of N-doped ZnO nanoparticles with improved photocatalytical activity. Ceram Int 39(5):5197–5203

Sun SP et al (2014) Enhanced heterogeneous and homogeneous Fenton-like degradation of carbamazepine by nano-Fe_3O_4/H_2O_2 with nitrilotriacetic acid. Chem Eng J 244:44–49

Taha MR, Ibrahim AH (2014) Characterization of nano zero-valent iron (nZVI) and its application in sono-Fenton process to remove COD in palm oil mill effluent. J Environ Chem Eng 2(1):1–8

Tang NJ et al (2006) Highly stable carbon-coated Fe/SiO_2 composites: synthesis, structure and magnetic properties. Carbon 44(3):423–427

Tang W et al (2011) Arsenic(III, V) removal from aqueous solution by ultrafine α-Fe_2O_3 nanoparticles synthesized from solvent thermal method. J Hazard Mater 192(1):131–138

Tataru G, Popa M, Desbrieres J (2011) Magnetic microparticles based on natural polymers. Int J Pharm 404(1–2):83–93

Tayade RJ et al (2007) Photocatalytic degradation of dyes and organic contaminants in water using nanocrystalline anatase and rutile TiO_2. Sci Technol Adv Mater 8(6):455–462

Tee YH, Grulke E, Bhattacharyya D (2005) Role of Ni/Fe nanoparticle composition on the degradation of trichloroethylene from water. Ind Eng Chem Res 44(18):7062–7070

Tee YH, Bachas L, Bhattacharyya D (2009) Degradation of trichloroethylene and dichlorobiphenyls by iron-based bimetallic nanoparticles. J Phys Chem C 113(22):9454–9464

Tesh SJ, Scott TB (2014) Nano-composites for water remediation: a review. Adv Mater 26 (35):6056–6068

ThanhThuy TT, Feng H, Cai Q (2013) Photocatalytic degradation of pentachlorophenol on $ZnSe/TiO_2$ supported by photo-Fenton system. Chem Eng J 223:379–387

giovanni.libralato@unina.it

Thinh NN et al (2013) Magnetic chitosan nanoparticles for removal of Cr(VI) from aqueous solution. Mater Sci Eng C Mater Biol Appl 33(3):1214–1218
Thompson JM, Chisholm BJ, Bezbaruah AN (2010) Reductive dechlorination of chloroacetanilide herbicide (alachlor) using zero-valent iron nanoparticles. Environ Eng Sci 27(3):227–232
Tofighy MA, Mohammadi T (2011) Adsorption of divalent heavy metal ions from water using carbon nanotube sheets. J Hazard Mater 185(1):140–147
Tripathi G, Clements M (2003) Adsorption of 2-mercaptopyrimidine on silver nanoparticles in water. J Phys Chem B 107(40):11125–11132
Tuutij Rvi T et al (2009) As(V) adsorption on maghemite nanoparticles. J Hazard Mater 166(2–3):1415–1420
Vadahanambi S et al (2013) Arsenic removal from contaminated water using three-dimensional graphene-carbon nanotube-iron oxide nanostructures. Environ Sci Technol 47(18):10510–10517
Vivero-Escoto JL, Huang YT (2011) Inorganic-organic hybrid nanomaterials for therapeutic and diagnostic imaging applications. Int J Mol Sci 12(6):3888–3927
Wahab R et al (2014) Enhance antimicrobial activity of ZnO nanomaterial's (QDs and NPs) and their analytical applications. Physica E Low-Dimens Syst Nanostruct 62:111–117
Wang CB, Zhang WX (1997) Synthesizing nanoscale iron particles for rapid and complete dechlorination of TCE and PCBs. Environ Sci Technol 31(7):2154–2156
Wang W et al (2006) Preparation of spherical iron nanoclusters in ethanol-water solution for nitrate removal. Chemosphere 65(8):1396–1404
Wang H et al (2013) Adsorption characteristics and behaviors of graphene oxide for Zn(II) removal from aqueous solution. Appl Surf Sci 279:432–440
Wei JJ et al (2006) Catalytic hydrodechlorination of 2,4-dichlorophenol over nanoscale Pd/Fe: reaction pathway and some experimental parameters. Water Res 40(2):348–354
Wu LF, Ritchie SMC (2008) Enhanced dechlorination of trichloroethylene by membrane-supported Pd-coated iron nanoparticles. Environ Prog 27(2):218–224
Wu ZS et al (2012) 3D nitrogen-doped graphene aerogel-supported Fe_3O_4 nanoparticles as efficient electrocatalysts for the oxygen reduction reaction. J Am Chem Soc 134(22):9082–9085
Wu R et al (2014) Hydrothermal preparation of magnetic Fe_3O_4@C nanoparticles for dye adsorption. J Environ Chem Eng 2(2):907–913
Xi YF, Mallavarapu M, Naidu R (2010) Reduction and adsorption of Pb^{2+} in aqueous solution by nano-zero-valent iron-A SEM, TEM and XPS study. Mater Res Bull 45(10):1361–1367
Xu Y, Zhang WX (2000) Subcolloidal Fe/Ag particles for reductive dehalogenation of chlorinated benzenes. Ind Eng Chem Res 39(7):2238–2244
Xu XH et al (2004) Catalytic dechlorination of 2,4-dichlorophenol in water by nanoscale Pd/Fe bimetallic system. Chin J Catal 25(2):138–142
Xu XH et al (2009) Catalytic dechlorination of p-NCB in water by nanoscale Ni/Fe. Desalination 242(1–3):346–354
Xu J, Wang L, Zhu Y (2012a) Decontamination of bisphenol A from aqueous solution by graphene adsorption. Langmuir 28(22):8418–8425
Xu FY et al (2012b) Highly active and stable Ni-Fe bimetal prepared by ball milling for catalytic hydrodechlorination of 4-chlorophenol. Environ Sci Technol 46(8):4576–4582
Yan WL et al (2013) Iron nanoparticles for environmental clean-up: recent developments and future outlook. Environ Sci Process Impacts 15(1):63–77
Yan JC et al (2015) Biochar supported nanoscale zerovalent iron composite used as persulfate activator for removing trichloroethylene. Bioresour Technol 175:269–274
Yang K, Xing B (2010) Adsorption of organic compounds by carbon nanomaterials in aqueous phase: Polanyi theory and its application. Chem Rev 110(10):5989–6008
Yang S et al (2011) Removal of methylene blue from aqueous solution by graphene oxide. J Colloid Interface Sci 359(1):24–29
Yang XJ et al (2015) Preparation and photocatalytic performance of Cu-doped TiO_2 nanoparticles. Trans Nonferrous Met Soc China 25(2):504–509

giovanni.libralato@unina.it

Yang X et al (2016) Effect of phosphate on heterogeneous Fenton oxidation of catechol by nano-Fe_3O_4: inhibitor or stabilizer? J Environ Sci 39(1):69–76
Yin Y, Talapin D (2013) The chemistry of functional nanomaterials. Chem Soc Rev 42(7):2484–2487
Yirsaw BD et al (2015) Environmental application and ecological significance of nano-zero valent iron. J Environ Sci
Yu C et al (2011) Fe_3O_4 nano-whiskers by ultrasonic-aided reduction in concentrated NaOH solution. Particuology 9(1):86–90
Yu J et al (2014) Aqueous adsorption and removal of organic contaminants by carbon nanotubes. Sci Total Environ 482:241–251
Yuan W, Bi S, Cao M (2015) Formaldehyde molecule adsorbed on graphene: a first-principles study. Mater Rev 29(18):156–159
Zeng T et al (2010) Fe_3O_4 nanoparticles: a robust and magnetically recoverable catalyst for three-component coupling of aldehyde, alkyne and amine. Green Chem 12(12):570–573
Zhang WX (2003) Nanoscale iron particles for environmental remediation: an overview. J Nanopart Res 5(3–4):323–332
Zhang WX, Wang CB, Lien HL (1998) Treatment of chlorinated organic contaminants with nanoscale bimetallic particles. Catal Today 40(4):387–395
Zhang WH, Quan X, Zhang ZY (2007) Catalytic reductive dechlorination of p-chlorophenol in water using Ni/Fe nanoscale particles. J Environ Sci 19(3):362–366
Zhang L et al (2008) Studies on the capability and behavior of adsorption of thallium on nano-Al_2O_3. J Hazard Mater 157(2–3):352–357
Zhang L et al (2010a) Kinetic and thermodynamic studies of adsorption of gallium(III) on nano-TiO_2. Rare Met 29(1):16–20
Zhang X et al (2010b) Degradation of 2,4,6-trinitrotoluene (TNT) from explosive wastewater using nanoscale zero-valent iron. Chem Eng J 158(3):566–570
Zhang D et al (2010c) Carbon-stabilized iron nanoparticles for environmental remediation. Nanoscale 2(6):917–919
Zhang C, Yao Y, Chen SH (2014) Size-dependent surface energy density of typically fcc metallic nanomaterials. Comput Mater Sci 82:372–377
Zhao C et al (2010) Photodegradation of oxytetracycline in aqueous by 5A and 13X loaded with TiO_2 under UV irradiation. J Hazard Mater 176(1–3):884–892
Zhao G et al (2011) Few-layered graphene oxide nanosheets as superior sorbents for heavy metal ion pollution management. Environ Sci Technol 45(24):10454–10462
Zhao G et al (2012) Preconcentration of U(VI) ions on few-layered graphene oxide nanosheets from aqueous solutions. Dalton Trans 41(20):6182–6188
Zhao C et al (2013) Role of pH on photolytic and photocatalytic degradation of antibiotic oxytetracycline in aqueous solution under visible/solar light: kinetics and mechanism studies. Appl Catal B Environ 134:83–92
Zhao C et al (2014) Advantages of TiO_2/5A composite catalyst for photocatalytic degradation of antibiotic oxytetracycline in aqueous solution: comparison between TiO_2 and TiO_2/5A composite system. Chem Eng J 248:280–289
Zhou YM et al (2014) Biochar-supported zerovalent iron for removal of various contaminants from aqueous solutions. Bioresour Technol 152:538–542
Zhu HJ et al (2009) Removal of arsenic from water by supported nano zero-valent iron on activated carbon. J Hazard Mater 172(2–3):1591–1596
Zhu J et al (2012) One-pot synthesis of magnetic graphene nanocomposites decorated with core@double-shell nanoparticles for fast chromium removal. Environ Sci Technol 46(2): 977–985

giovanni.libralato@unina.it

Nano Based Photocatalytic Degradation of Pharmaceuticals

Giusy Lofrano, Giovanni Libralato, Sanjay K. Sharma and Maurizio Carotenuto

Abstract The removal of emerging contaminants from wastewater is urgently required and even more necessary for wastewater reuse. Since conventional WWTPs are not designed to treat water polluted with pharmaceuticals present at trace levels, the applied treatments are mostly ineffective in their removal. Therefore the use of more efficient processes for removing or improving the biodegradability of these compounds has become necessary. Among several advanced oxidation process, nano based photocatalytic processes represent a challenging alternative for pharmaceuticals removal due to its capacity to utilize the solar radiation as the light source, thus reducing significantly electric power required and therefore saving treatment costs and to operate without pH adjustment. This chapter is aimed at describing the state of the art in the heterogeneous photocatalytic degradation of pharmaceuticals using different nano particles (NPs).

Keywords Nanoparticles · Emerging contaminants · Catalysts · Nanomaterials

Abbreviations

Abbreviations	Pharmaceuticals
ACY	Acyclovir

G. Lofrano (✉) · M. Carotenuto
Department of Chemistry and Biology, University of Salerno,
via Giovanni Paolo II 132, 84084 Fisciano, Salerno, Italy
e-mail: glofrano@unisa.it

G. Libralato
Department of Environmental Sciences, Informatics and Statistics,
University Cà Foscari Venice, Via Torino 155, 30172 Venezia-Mestre, Italy

G. Libralato
Department of Biology, University of Naples Federico II, Complesso
Universitario di Monte S. Angelo, Via Cinthia ed. 7, 80126 Naples, Italy

S.K. Sharma
Green Chemistry and Sustainability Research Group, Department
of Chemistry, JECRC University, Jaipur 303905, India

© Springer International Publishing AG 2017

G. Lofrano et al. (eds.), *Nanotechnologies for Environmental Remediation*,
DOI 10.1007/978-3-319-53162-5_7

giovanni.libralato@unina.it

AMI	Amiloride
AMX	Amoxicillin
AMP	Ampicillin
ATL	Atenolol
B	Bendroflumethiazide
CBZ	Bendroflumethiazide
CAP	Chloramphenicol
CIP	Ciprofloxacin
CLX	Cloxacillin
CDN	Codeine
DCF	Diclofenac
ERY	Erythromycin
ERYA	Erythromycylamine
ETA	Ethacrynic acid
FLU	Flumequine
F	Furosemide
IBP	Ibuprofene
LEVO	Levofloxacin
LNC	Lincomycin
LZP	Lorazepam
MT	Metronidazole
MOX	Moxifloxacin
Naproxen	NPX
NOR	Norfloxacin
OFL	Ofloxacin
OXA	Oxacillin
PRC	Paracetamol
PZQ	Praziquantel
RIF	Rifampicin
SMT	Sulfanethazine
SMX	Sulfamethoxazole
TC	Tetracycline
TYL	Tylosine
VAN	Vancomycin

1 Introduction

The release of pharmaceuticals in water bodies has dealt a growing attention over the last years (Rizzo et al. 2009; Xekoukoulotakis et al. 2010; Van Doorslaer et al. 2015; Lofrano et al. 2014, 2016; Agarwal et al. 2017). They are mostly introduced in the sewage system through excretion of un-metabolized compounds after medical use or

giovanni.libralato@unina.it

inappropriate disposal and then conveyed into the wastewater treatment plants (WWTPs) (Teixeira et al. 2016). Pharmaceutical and pharmaceutical residues include antibiotics, anticonvulsants, antipsychotic, analgesics, beta-blocker, lipid regulators, and antihistamines ranging in the range of ng to mg per liter (Zuccato et al. 2005). Since conventional WWTPs are not designed to treat water polluted with pharmaceuticals present at trace levels, the applied treatments are mostly ineffective in their removal. As a consequence, they reach the aquatic system and can be detected in groundwater (Barnes et al. 2008), drinking water (Benotti et al. 2009), surface water (Hirsch et al. 1999; Batt et al. 2006; Yan et al. 2013; Yang et al. 2011), sediment (Zhou et al. 2011) and agricultural lands (Hu et al. 2010; Karci and Balcioglu 2009). Although, pharmaceuticals do not generally present acute toxic effects on aquatic organisms due to their low concentrations, concerns have been raised for chronic exposure due to their continuous and uncontrolled release into the environment acting as slightly persistent pollutants (Isidori et al. 2009; Lofrano et al. 2014). Among them, antibiotics represent one of the most urgent environmental problems, primarily due to the potential for the development of antimicrobial resistance among microorganisms (Akiyama and Savin 2010; Fuentefria et al. 2011).

The limitations of conventional WWTPs in removing these bio-recalcitrant molecules point toward the urgent need for improved WWTPs such as Advanced Oxidation Processes (AOPs), a special class of oxidation techniques characterized by production of $^{\cdot}OH$ radicals (Lofrano et al. 2016). Amongst several AOPs, heterogeneous photocatalysis has proven its potential in degrading pharmaceutic compounds from aqueous matrices (Zhang et al. 2010; Lofrano et al. 2014; Van Doorslaer et al. 2015) representing a promising alternative for their removal due to its capacity to utilize the solar radiation as the light source, thus reducing significantly electric power required and therefore saving treatment costs and to operate without pH adjustment.

The elimination of mother compounds does not necessarily result in toxicity removal, since the photocatalytic degradation can produce intermediate by-products, which can still exert adverse biological effects. Therefore, to evaluate the overall behaviour and efficiency of the process, it is worth to assess not only the removal of a specific compound, but also the whole ecotoxicity potential (Rizzo et al. 2009; Libralato et al. 2010, 2016; Carotenuto et al. 2014; Lofrano et al. 2014). So far, ecotoxicity data for AOPs treated solutions of pharmaceuticals are scarce or missing, making their environmental risk assessment difficult.

Because the use of AOPs may be a promising approach for pharmaceuticals wastewater treatment, a great attention is focused on the potential of many types of nanoparticles (NPs) for photocatalysis applications. Amongst all NPs, TiO_2 is the most employed photocatalyst because of its favourable (photo-)chemical properties and low toxicity (Libralato et al. 2013, 2014), and ZnO is considered one of the most promising alternative because of its unique characteristics, such as direct and wide band gap in the near-ultra violet (UV) spectral region, strong oxidation ability, good photocatalytic property, and a large free-exciton binding energy (Lee et al. 2016). Recently, CuO and Ga_2O_3 have been also tested as alternative to more conventional photocatalysts (El-Sayed et al. 2014).

giovanni.libralato@unina.it

This chapter is aimed at describing the state of the art in the heterogeneous photocatalytic degradation of pharmaceuticals using different NPs. Since it is nearly impossible to review comprehensively photocatalysis studies, we have tried to summarize an overview of some of the more fundamental aspects, which are in their own right extremely scientifically interesting and which also need to be better understood in order to make significant progress and development with applications.

2 Fundamentals of Heterogeneous Photocatalysis

In the heterogeneous photocatalytic process, UV is utilized as an energy source and certain NPs act as a semiconductor (SC) photo-catalyst. For UV irradiation, its corresponding electromagnetic spectrum can be classified as UV-A, UV-B and UV-C, according to its emitting wavelength. The UV-A range has its light wavelength spans from 315 to 400 nm (3.10–3.94 eV), while UV-B has wavelength range of 280–315 nm (3.94–4.43 eV) and the germicidal UV-C ranges from 100 to 280 nm (4.43–12.4 eV).

Illuminated SCs, by photons having an energy level that exceeds their band gap energy ($E > E_g$) excite electrons (e^-) from the valence band to the conduction band and holes (h^+) are produced in the valence band (reaction 1). The photo-generated valence band holes react with either water (H_2O) or hydroxyl ions (OH^-) adsorbed on the catalyst surface to generate hydroxyl radicals ($^{\cdot}OH$), which are strong oxidant (reactions 2 and 3). The photo-generated electrons in the conduction band may react with oxygen to form superoxide ions ($O_2^{\cdot-}$) (reaction 4). The superoxide ions can then react with water to produce hydrogen peroxide and hydroxyl ions (reaction 5). Cleavage of hydrogen peroxide by the conduction band electrons yields further hydroxyl radicals and hydroxyl ions (reaction 6).

$$SC + h\nu \rightarrow SC(e^- + h^+) \tag{1}$$

$$SC(h^+) + H_2O \rightarrow H^+ + OH^{\cdot} \tag{2}$$

$$SC(h^+) + OH^- \rightarrow OH^{\cdot} \tag{3}$$

$$SC(e^-) + O_2 \rightarrow O_2^- \tag{4}$$

$$O_2^- + H_2O + H^+ \rightarrow H_2O_2 + OH^- \tag{5}$$

$$H_2O_2 + e^- \rightarrow OH^{\cdot} + OH^- \tag{6}$$

The hydroxyl ions can then react with the valence band holes to form additional $^{\cdot}OH$. Degradation of organic substances can be achieved by their reaction with $^{\cdot}OH$ or direct attack from the valence band holes. Recombination of the photo-generated electrons and holes may occur and indeed it has been suggested that pre-adsorption

giovanni.libralato@unina.it

of substrate (organic substance) onto the photocatalyst is a prerequisite for highly efficient degradation (Elmolla and Chadhuri 2010).

3 Nano-TiO_2 Based Photocatalysis

Titania based catalysts have proven to be useful and efficient photocatalysts for the abatement of pharmaceuticals (Lofrano et al. 2014, 2016). During the photocatalytic degradation process, the efficiency of the system is related to some experimental variables that is mainly light irradiation intensity, catalyst and target compound concentrations, and pH. Typically, the rate of the photocatalytic degradation increases with the increase in light intensity and catalyst concentration up to a plateau value. Lofrano et al. (2016) reported that the degradation rate of 25 mg L^{-1} CAP increased when the concentration of TiO_2 increased up to 1.6 g TiO_2 L^{-1}. Beyond this value, the removal efficiency decreased (Fig. 1).

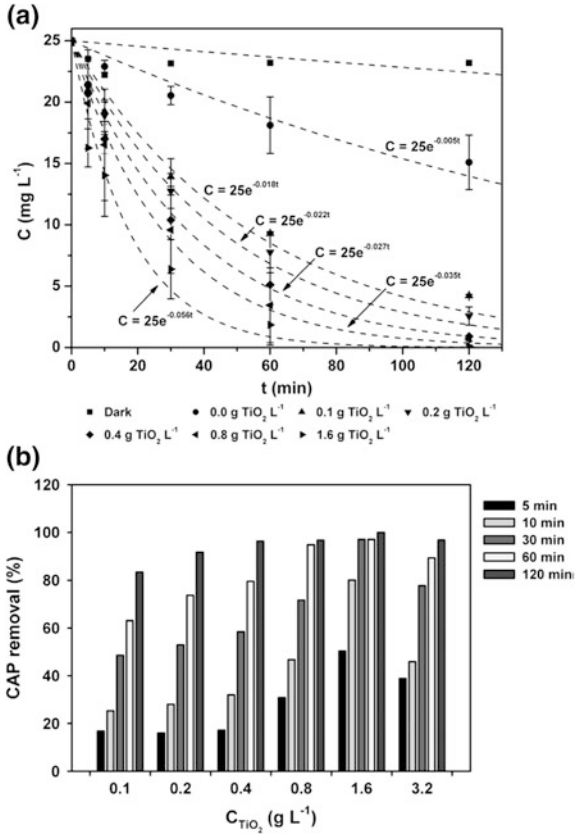

Fig. 1 Photocatalytic kinetic curves (**a**) and removal percentage (**b**) of CAP (25 mg L^{-1}) after 5, 10, 30, 60 and 120 min at 0.0, 0.1, 0.2, 0.4 and 1.6 g L^{-1} of TiO_2 at pH 5.5. Dark experiments at 1.6 g L^{-1} of TiO_2 (only Fig. 1a—no significant differences could be observed in dark experiments at various TiO_2 concentrations investigated); 3.2 g L^{-1} of TiO_2 kinetic curve was not reported due to a removal efficiency decrease (Fig. 1b) compared to 1.6 g L^{-1} of TiO_2 (Lofrano et al. 2016, with kind permission of Elsevier)

giovanni.libralato@unina.it

A similar trend was observed by Chatzitakis et al. (2008) during the photocatalytic degradation of 50 mg L^{-1} CAP. They raised TiO_2 concentration from 0.25 to 4 g L^{-1} observing a decrease in the initial reaction rate meaning that the photo-oxidation reached the saturation level. The optimum quantity depends on the nature of the organic compound and the photoreactor's geometry.

Regarding the pollutant concentration, it has been observed that the degradation rate does not increase linearly. Instead, at relatively high pollutant concentration, the slopes of the degradation curve decrease gradually (Giraldo-Aguirre et al. 2015). In Fig. 2, it is shown the treatment of 5, 10 and 20 mg L^{-1} DCF considering 250 mg/L of Degussa P25 TiO_2 as catalyst. Degradation decreased with increasing initial concentration, i.e. at 60 min corresponded to 99.5, 61 and 46% at 5, 10 and 20 mg L^{-1} DCF, respectively (Achilleos et al. 2010).

Generally the best degradation occurs at pH values at which the higher adsorption of the pollutant onto the catalyst surface occurs (Van Doorslaer et al. 2011). In some cases, the pollutant adsorption can also be detrimental. Consequently, to maximize the efficiency of the process an evaluation and optimization of the experimental parameters should be always carried out (Giraldo-Aguirre et al. 2015).

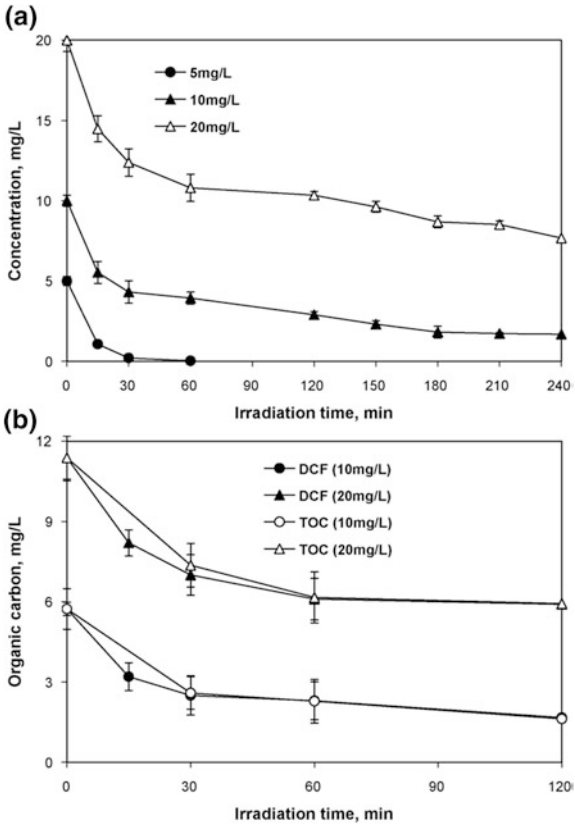

Fig. 2 Effect of initial DCF concentration (5, 10 and 20 mg L^{-1}) treated by 250 mg L^{-1} Degussa P25 TiO_2: **a** concentration–time profiles; **b** comparison between TOC and carbon contained in DCF (Achilleos et al. 2010, with kind permission from Elsevier)

giovanni.libralato@unina.it

Several researches are also studying the influence that the presence of coexistent organic compounds and inorganic salts has to TiO_2-based photocatalysts (Guillard et al. 2003; Lair et al. 2008). The general and unanimous criteria are the detrimental effects that adsorption of inorganic ions plays on heterogeneous photocatalysis by trapping photogenerated holes and scavenging OH. during photocatalytic processes (Carbajo et al. 2016). Giraldo-Aguirre et al. (2015) evaluated the photocatalytic degradation of OXA and interfering substances observing a slight inhibition related to excipients in commercial formulation or inorganic ions in minerals.

Depending on process conditions, the photocatalysis can achieve a complete mineralization of pollutants. Paola et al. (2006) reported that the use of UV/TiO_2 was able to achieve complete mineralization of 50 mg/L LNC antibiotic in 8 h. Abellán et al. (2007) reported 82% removal of 100 mg L^{-1} SMX by degradation and 23% total organic carbon (TOC) reduction by UV/TiO_2 in 6 h. Palominos et al. (2008) reported that the complete removal of FLU by TiO_2 photocatalysis (0.5 g TiO_2 L^{-1}) occurred after 30 min at pH 6.

4 Nano ZnO Based Photocatalysis

Daneshvar et al. (2004) reported that ZnO could be a suitable alternative to TiO_2 its photocatalytic capability is anticipated to be similar to that of TiO2. Moreover, ZnO is relatively cheaper compared to TiO_2 whereby the usage of TiO_2 are uneconomic for large scale water treatment operations. Since ZnO can absorb a larger fraction of the solar spectrum than TiO_2, it is considered more suitable for photocatalytic degradation assisted by sunlight (Sakthivel et al. 2003). The major drawbacks of ZnO are the wide band gap energy and photocorrosion. The light absorption of ZnO is limited in the visible light region which is due to its wide band energy. This results in fast recombination of photogenerated charges and thus caused low photocatalytic efficiency (Gomez-Solís et al. 2015).

ZnO has proven to be a potential photocatalyst to treat various type of organic pollutants such as phenols, fungicides, herbicides (Mijin et al. 2009), pharmaceuticals (Elmolla and Chaudhuri 2010; Palominos et al. 2009).

As in TiO_2 based phototacatalysis, ZnO concentration, pH and irradiation time strongly influence the process efficiency. Elmolla and Chaudhuri (2010) reported that the optimum operating conditions for complete degradation of AMX, AMP and CLX antibiotics in an aqueous solution containing 104, 105 and 103 mg L^{-1}, respectively were: 0.5 g ZnO L^{-1}, irradiation time 180 min and pH 11. The effect of pH on pharmaceuticals degradation can be explained by taking into consideration the properties of both the catalyst and antibiotics at different pHs. For ZnO, the zero point charge is 9.0 ± 0.3 and hence the ZnO surface is positively charged at $pH < 9$ and is negatively charged at $pH > 9$. Degradation of pharmaceuticals compounds typically increases with ZnO concentration presumably due to increase

giovanni.libralato@unina.it

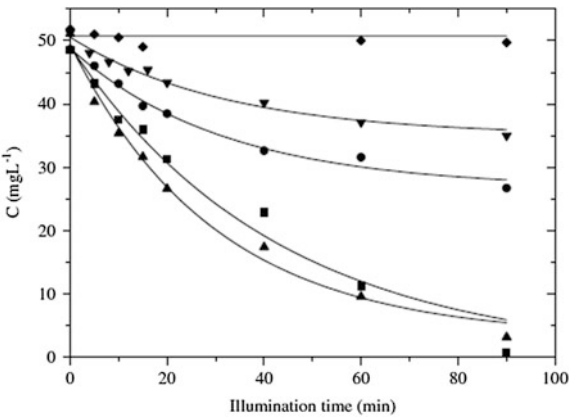

Fig. 3 Photodegradation of 50 mg L^{-1} CAP as a function of irradiation time in the presence of 1 g L^{-1} *Filled square* TiO_2-P25, *Filled circle* TiO_2 (A), *Filled up triangle* ZnO, *Filled down triangle* TiONa, *Filled diamond* without catalysts (from Chatzitakis et al. 2008, with kind permission of Elsevier)

of ·OH production. However, increasing ZnO concentration above such limits does not produce any significant improvement. This may be due to decreasing UV light penetration as a result of increasing turbidity and thus decreasing the photoactivated volume of the suspension (Daneshvar et al. 2004).

Few studies supported the assertion that ZnO is a better photocatalyst than TiO_2 (Chatzitakis et al. 2008) (Fig. 3). After 90 min of illumination, photocatalysis with 1 g L^{-1} of ZnO resulted to the approximately complete (90%) degradation of CAP 50 mg L^{-1} (Chatzitakis et al. 2008). Although ZnO is more efficient than TiO_2 in visible light photocatalytic degradation of some organic compounds in aqueous solution, it is not stable as TiO_2.

5 Nano CuO Based Photocatalysis

Copper(II) oxide has low cost and toxicity. As the photocatalytic mechanism suggests both photocatalyst and light source are necessary for the degradation reaction. Compared to TiO_2 and ZnO where an operative wavelength <400 nm is required, CuO photocatalysis is based on UV-C.

The effect of various concentrations of nano-CuO (0.05–0.3 g L^{-1}) can change the photocatalytic degradation rate of metronidazole (1 mg L^{-1}) as investigated by El Sayed et al. (2014). As previously reported for TiO_2 and ZnO, it could be observed that the initial removal rate increased with the increase in catalyst concentration up to a maximum after about 120 min and remaining almost constant thereafter. The optimum catalyst concentration for the degradation of metronidazole was set at 0.2 g L^{-1}.

giovanni.libralato@unina.it

6 Doped Catalysts

The recombination of photogenerated hole and electron is the major disadvantage in semiconductor photocatalysis. This recombination step lowers the quantum yield and causes energy wasting. Therefore, the recombination process should be inhibited to ensure efficient photocatalysis. Metal doping could counter the recombination problem by enhancing the charge separation between electrons and holes. In addition, the dopants may trap electrons, reducing the chances of electronehole recombination that deactivates the photocatalytic system (Lee et al. 2016).

By doping different NPs specifically constructed to be used as catalysts, it is possible to maximize the solar light utilization in AOPs. To date, several methods for achieving visible-light-driven photocatalysis or for increasing the lifetime of the photoproduced electron-holes pairs are widely investigated. It is known that pure TiO_2 exhibits relatively high activity only under ultraviolet (UV) light irradiation (E_g = 3.2 eV), leading to a low utilization of solar light. To improve the absorption ability of TiO_2 in the visible region, several strategies have been involved including the decrease of TiO_2 particle size and the doping of TiO_2 and several other commercially available nanocrystalline semiconductors (e.g. ZnO or CuO) with metal ions or non-metallic species (N, C, S, B, P, F, or I) (Song et al. 2008). The enhanced activity of TiO_2 towards visible light is also achieved by the doping with N, S or C application of the supports (Al_2O_3, SiO_2) and, mainly by the formation of the nanocomposites, with carbon nanotubes (CNT) (Czech and Buda 2015). However, metal-doped photocatalysts, which better exploit solar light, suffer from the problem of releasing metal pollutant species, sometimes extremely toxic metals, due to photocorrosion phenomena. On the other hand, the majority of photocatalytic action in non-metal doped photocatalysts illuminated by solar light is still generated by UV-C since the contribution from the visible part of the spectrum is small. Moreover, the stability and long-term efficacy of non-metal doped TiO_2 photocatalysts have not been tested.

Nitrogen doping via sol gel synthesis using diverse anion precursors (e.g. amines, nitrates, ammonium salts, ammonia and urea) (Pelaez et al. 2012) has been verified as a very efficient modification route of TiO_2 photocatalyst, activated in the visible spectrum via the formation of localized energy states within the band gap of TiO_2 or even oxygen deficiencies created during the reaction with the anion precursor (Moustakas et al. 2013). Three possible scenarios, including substitutional or interstitial N doping and defects formed due to disorder in the nanoparticle surface are sketched in Fig. 4a–c.

An alternative route for the visible light activation of TiO_2 has been recently put forward based on the calcination of TiO_2 in the presence of urea (Mitoraj and Kisch 2008). The resulting materials were shown to consist of TiO_2 core covered by a poly(tri-s-triazine) shell, in situ formed on the TiO_2 surface by the thermal decomposition of urea (Mitoraj and Kisch 2010) as sketched in Fig. 4d.

giovanni.libralato@unina.it

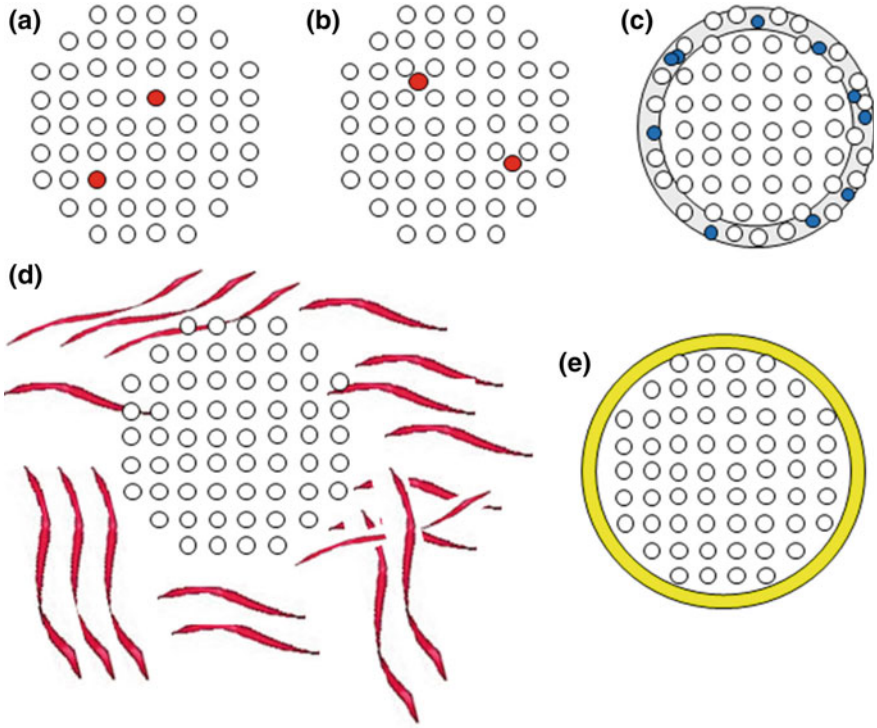

Fig. 4 Sketch of possible modification routes for TiO_2 to become visible light active: **a** substitutional N doping, **b** interstitial N doping, **c** defect formation by surface doping, **d** polymeric carbon-nitride/TiO_2 composite structure and **e** sensitization of the surface by carbonaceous species in the form of a surface capping layer (from Moustakas et al. 2013 with kind permission by Elsevier)

7 Suspended Catalysts or Thin Films?

The photocatalysts could be used in slurry or supported forms. Many researchers investigated immobilization of NPs, mainly TiO_2, on different support materials to improve the photocatalytic activity and make the separation of treated effluent more effective (Lu et al. 2011; Yap and Lim 2011; Vilar et al. 2013). The most important properties of a suitable support are as follows: chemical inertness, high specific surface area and transparency to UV radiation. Coating surfaces with nanoparticles has relatively low improvement on photocatalytic reaction because of the low particles dispersion and limited mass transfer between the pollutants molecules and the catalyst (Zhu et al. 2013; Hinojosa-Reyes et al. 2013). When the photocatalyst is dispersed as slurry inside the reactor, higher degradation rates are achieved due to high solid to liquid contact area but high axial flow rates are necessary to prevent the catalysts from settling. Furthermore the powders are not easy to precipitate and

giovanni.libralato@unina.it

Table 1 Nanoparticles used for photocalitic degradation of pharmaceuticals

Pharmaceutic. compounds	Catalysts				Modified Catalysts				References
	TiO_2	ZnO	CuO	TiO_2/ zeolite	N-TiO_2	C- TiO_2	Fe-SnO_2/ Co_3O_4	TiO_2/SiO_2	
AMX		■							Elmolla and Chaudhuri, (2010); Klauson et al., (2010)
				■					Kanakaraju et al., (2015)
AMP		■							Elmolla and Chaudhuri, (2010)
CAP		■							Chatzakis et al., (2008)
	■								Chatzakis et al., (2008); Zhang et al., (2010); Lofrano et al., (2016)
CIP	■								An e tal., (2010); Paul et al., (2010); Van Doorslaer et al., (2011)
CBZ								■	Czech et al., (2015)
CLX		■							Elmolla and Chaudhuri (2010)
DCF	■								Pérez-Estrada et al., (2005); Calza et al., (2006); Méndez-Arriaga et al., (2008); Rizzo et al., (2009); Achilleos et al., (2010); Martínez et al., (2011)
				■					Salaeh et al., (2016)
ERY	■								Xekoukoulotakis et al., (2010)
FLU	■								Palominos et al., (2008)
IBP	■								Choina et al., (2013)
LEVO	■								Nasuhoglu et al., (2012)
LNC	■								Paola et al., (2006)
MOX	■								Van Doorslaer et al., (2011); Van Doorslaer et al., (2015)
MT			■						El-Sayed et al., (2014)
							■		Agarwall et al., (2017)
NOR	■								Haque et al., (2007);
						■			Chen et al., (2012)
NPX	■								Kanakaraju et al., (2015) ; Jallouli et al., (2016), (http://www.sciencedirect.com/science/article/pii/S0304389415301722)
OXA	■								Giraldo-Aguirrea et al., (2015)
PRC	■								Yang et al., (2008)
SMX	■								Abellán et al. (2007)
SPY	■				■				Vaiano et al., (2015)
TC	■								Yahiat et al., (2011); Maroga Mboula et al., (2012)
TYL	■								Yahiat et al., (2011)
VAN	■								Lofrano et al., (2014)

recover from water, preventing their regeneration and reuse (Paschoalino et al. 2012). To overcome this problem, magnetically separable composite photocatalysts such as TiO_2/Fe_3O_4 and $TiO_2/SiO_2/Fe_3O_4$ have been prepared and applied to the degradation of pollutants (Hu et al. 2011) (Table 1).

giovanni.libralato@unina.it

8 Oxidation by Products

The assessment of contaminants disappearance is not enough to ensure the absence of residual products because the photocatalytic treatment may give rise to a variety of organic intermediates which can themselves be toxic, and in some cases, more persistent than the original substrate.

To identify by products formed by photocatalytic treatment is not an easy task, however fragmentation pathways studies are available for several pharmaceuticals as reported in Table 2. Photocatalysis would result in the mineralization of organic carbon and release of nitrogen and chlorides from the molecule. Photocatalytic transformation of the nitrogen moieties to N_2, NH_4^+, NO_2^- or NO_3^- depends on the initial oxidation state of nitrogen and on the structure of the organic.

The removal of 50 mg L^{-1} VAN solution yields maximum concentrations of 2.45 and 2.53 mg $N–NH_3$ L^{-1} after 120 min of photocatalytic oxidation using 0.1 and 0.2 g TiO_2 L^{-1}, respectively. When 0.2 g TiO_2 L^{-1} were applied up to 87% of the stoichiometric amount of chloride was reached within 120 min of irradiation, corresponding to 0.087 mmol L^{-1} (Lofrano et al. 2014). Nitrate formation was not observed throughout the photocatalytic oxidation process, probably due to

Table 2 Fragmentation pathway studies of photocatalytic treated pharmaceuticals

ACY	Li et al. (2016)
AMI	Giancotti et al. (2008)
AMX	Klauson et al. (2010)
ATL	Ji et al. (2013)
B	Giancotti et al. (2008)
CAP	Garcia-Segura et al. (2014), Gao et al. (2016)
CDN	Kuo et al. (2016)
CIP	An et al. (2010)
DCF	Calza et al. (2006), Martínez et al. (2011), Michael et al. (2014)
ERY	Gao et al. 2016
ERYA	
ETA	Giancotti et al. (2008)
F	Giancotti et al. (2008)
IBP	Choina et al. (2013), Michael et al. (2014)
LNC	Gao et al. (2016)
LZP	Sousa et al. (2013)
NPX	Kanakaraju et al. (2015a, b) (http://www.sciencedirect.com/science/article/pii/S0045653515007912)
OFL	Jimenez-Villarin et al. (2016)
PZQ	Čizmic et al. (2016)
RIF	Gao et al. (2016)
SMT	Fukahori and Fujiwara (2015)
TC	Gao et al. (2016)

giovanni.libralato@unina.it

insufficient irradiation time. Accordingly Elmolla and Chaudhuri (2010) did not detect nitrate ions during the first 6 h of photocatalytic oxidation of AMX, AMP and CLX. No evidence was found by Abellan et al. (2007) about the presence of the anions NO_2^- or NO_3^- within 10 h of photocatalytic treatment of 100 mg L^{-1} SMX solution.

9 Future Challenges

The removal of emerging contaminants from wastewater is urgently required and even more necessary for wastewater reuse. In order to meet this challenge, the future of nano catalysts is to be used in development of green technologies with high levels of removal efficiency of contaminants and energy saving to facilitate direct water reuse.

Knowing that photocatalytic processes are managed by different parameters: pH, irradiance/wavelength, catalyst loading, surface area, surface charge, concentration and nature of substrate/pollutant, reactor geometry, etc., many efforts have been faced by the scientific community trying to correlate catalysts properties with photocatalytic activity, and the resulting outcomes always pointed out a mixed balance between certain surface, electronic and structural properties that seemed to be playing important roles on the overall photocatalytic behaviour, where, simultaneously, a very significant dependence on the photoreactor geometry and the corresponding operational conditions appeared to be also taking place. Therefore, the photocatalytic activity of every catalyst is essentially specific and related to the chemical nature of pollutant.

Nanomaterials can be immobilized in the form of nanostructured thin films on different substrates in order to evaluate their potential applications in combined membrane-photocatalytic treatments.

In terms of integration of these nanostructured photocatalytic films on membrane, research is still in its beginning and much remains to be done. Judicious engineering of the semiconductor nanostructured materials may significantly enhance to the development of an green technology, energy saving and highly efficient for emerging contaminants removal.

References

Abellán MN, Bayarri B, Gimènez J, Costa J (2007) Photocatalytic degradation of sulfamethoxazole in aqueous suspension of TiO_2. Appl Catal B: Environ 74:233–241

Achilleos A, Hapeshi E, Xekoukoulotakis NP, Mantzavinos D, Fatta-Kassinos D (2010) Factors affecting diclofenac decomposition in water by UV-A/TiO2 photocatalysis. Chem Eng J 161 (1):53–59

giovanni.libralato@unina.it

Agarwal S, Tyagi I, Gupta VK, Sohrabi M, Mohammadi S, Golikand AN, Fakhri A (2017) Iron doped SnO2/Co3O4 nanocomposites synthesized by sol-gel and precipitation method for metronidazole antibiotic degradation. Mater Sci Eng, C 70:178–183

Akiyama T, Savin MC (2010) Populations of antibiotic-resistant coliform bacteria change rapidly in a wastewater effluent dominated stream. Sci Total Environ 408:6192–6201

An T, Yang H, Li G, Song W, Cooper WJ, Nie X (2010) Kinetics and mechanism of advanced oxidation processes (AOPs) in degradation of ciprofloxacin in water. Appl Catal B 94(3): 288–294

Barnes KK, Kolpin DW, Furlong ET, Zaugg SD, Meyer MT, Barber LB (2008) A national reconnaissance of pharmaceuticals and other organic wastewater contaminants in the United States—I) Groundwater. Sci Total Environ 402(2):192–200

Benotti MJ, Trenholm RA, Vanderford BJ, Holady JC, Stanford BD, Snyder SA (2009) Pharmaceuticals and endocrine disrupting compounds in U.S. Drink Water 43:547–603

Batt AL, Bruce IB, Aga DS (2006) Evaluating the vulnerability of surface waters to antibiotic contamination from varying wastewater treatment plant discharges. Environ pollut 142(2): 295–302

Hua-Lin Cai HL, Feng Wang F, Huan-De Li HD, Wen-Xing Peng WX, Rong-Hua Zhu RH, Deng Y, Jiang P, Yan M, Hu SM, Lei SY, Chen C (2014) Quantitative analysis of erythromycylamine in human plasma by liquid chromatography-tandem mass spectrometry and its application in a bioequivalence study of dirithromycin enteric-coated tablets with a special focus on the fragmentation pattern and carryover effect. J Chromatogr B 947–948: 156–163

Calza P, Sakkas VA, Medana C, Baiocchi C, Dimou A, Pelizzetti E, Albanis T (2006) Photocatalytic degradation study of diclofenac over aqueous TiO2 suspensions. Appl Catal B 67(3):197–205

Carbajo J, Jiménez M, Miralles S, Malato S, Faraldos M, Bahamonde A (2016) Study of application of titania catalysts on solar photocatalysis: influence of type of pollutants and water matrices. Chem Eng J 291:64–73

Carotenuto M, Lofrano G, Siciliano A, Aliberti F, Guida M (2014) TiO2 photocatalytic degradation of caffeine and ecotoxicological assessment of oxidation by-products. Global Nest Journal 16 (3):265–275

Chatzitakis A, Berberidou C, Paspaltsis I, Kyriakou G, Sklaviadis T, Poulios I (2008) Photocatalytic degradation and drug activity reduction of chloramphenicol. Water Res 42 (1):386–394

Čizmić M., Ljubas D, Ćurković L., Škorić I., Babić S. (2016) Kinetics and degradation pathways of photolytic and photocatalytic oxidation of the anthelmintic drug praziquantel. J Hazard Mater (in press). doi:10.1016/j.jhazmat.2016.04.065

Choina J, Kosslick H, Fischer C, Flechsig GU, Frunza L, Schulz A (2013) Photocatalytic decomposition of pharmaceutical ibuprofen pollutions in water over titania catalyst. Appl Catal B 129:589–598

Czech B, Buda W (2015) Photocatalytic treatment of pharmaceutical wastewater using new multiwall-carbon nanotubes/TiO2/SiO2 nanocomposites. Environ Res 137:176–184

Daneshvar N, Salari D, Khataee AR (2004) Photocatalytic degradation of azo dye acid red 14 in water on ZnO as an alternative catalyst to TiO2. J Photochem Photobiol A: Chem 162:317–322

Elmolla ES, Chaudhuri M (2010) Degradation of amoxicillin, ampicillin and cloxacillin antibiotics in aqueous solution by the UV/ZnO photocatalytic process. J Hazard Mater 173(1):445–449

El-Sayed GO, Dessouki HA, Jahin HS, Ibrahiem SS (2014) Photocatalytic degradation of metronidazole in aqueous solutions by copper oxide nanoparticles. J Basic Environ Sci 1: 102–110

Fuentefria DB, Ferreira AE, Corcao G (2011) Antibiotic-resistant *Pseudomonas aeruginosa* from hospital wastewater and superficial water: are they genetically related? J Environ Manage 92:250–255

Fukahori S, Fujiwara T (2015) Photocatalytic decomposition behavior and reaction pathway of sulfamethazine antibiotic using TiO_2. J Environ Manage 157:103–110

giovanni.libralato@unina.it

Gao B, Dong S, Liu J, Liu L, Feng Q, Tan N, Liu T, Bo L, Wang L (2016) Identification of intermediates and transformation pathways derived from photocatalytic degradation of five antibiotics on $ZnIn_2S_4$. Chem Eng J 304:826–840

Garcia-Segura S, Cavalcanti EB, Brillas E (2014) Mineralization of the antibiotic chloramphenicol by solar photoelectro-Fenton: From stirred tank reactor to solar pre-pilot plant. Appl Catal B 144:588–598

Giancotti V, Medana C, Aigotti M, Pazzi M, Baiocchi C (2008) LC–high-resolution multiple stage spectrometric analysis of diuretic compounds Unusual mass fragmentation pathways. J Pharm Biomed Anal 48:462–466

Giraldo-Aguirre AL, Erazo-Erazo ED, Flórez-Acosta OA, Serna-Galvis EA, Torres-Palma RA (2015) TiO_2 photocatalysis applied to the degradation and antimicrobial activity removal of oxacillin: Evaluation of matrix components, experimental parameters, degradation pathways and identification of organics by-products. J Photochem Photobiol, A 311:95–103

Gomez-Solís C, Ballesteros JC, Torres-Martínez LM, Juarez-Ramírez I, Torres LAD, Zarazua-Morin ME, Lee SW (2015). Rapid synthesis of ZnO nano-corncobs from Nital solution and its application in the photodegradation of methyl orange. J Photochem Photobiol A Chem 298:49–54

Guillard C, Lachheb H, Houas A, Ksibi M, Elaloui E, Herrmann JM (2003) Influence of chemical structure of dyes, of pH and of inorganic salts on their photocatalytic degradation by TiO_2 comparison of the efficiency of powder and supported TiO2. J Photochem Photobiol A: Chem 158:27–36

Haque MM, Muneer M (2007) Photodegradation of norfloxacin in aqueous suspensions of titanium dioxide. J Hazard Mater 145(1): 51–57

Hinojosa-Reyes M, Arriaga S, Diaz-Torres LA, Rodríguez-González V (2013) Gas-phase photocatalytic decomposition of ethylbenzene over perlite granules coated with indium doped TiO2. Chem Eng J 224:106–113. doi:10.1016/j.cej.2013.01.066

Hirsch R, Ternes T, Haberer K, Kratz KL (1999) Occurrence of antibiotics in the aquatic environment. Sci Total Environ 225(1):109–118

Hu X, Yang J, Zhang J (2011) Magnetic loading of TiO2/SiO2/Fe3O4 nanoparticles on electrode surface for photoelectrocatalytic degradation of diclofenac. J Hazard Mater 196:220–227

Hu X, Zhou Q, Luo Y (2010) Occurrence and source analysis of typical veterinary antibiotics in manure, soil, vegetables and groundwater from organic vegetable bases, northern China. Environ Pollut 158(9):2992–2998

Isidori M, Bellotta M, Cangiano M, Parrella A (2009) Estrogenic activity of pharmaceuticals in the aquatic environment. Environ Int 35:826–829

Ji Y, Zhou L, Ferronato C, Yang X, Salvador A, Zeng C, Chovelon JM (2013) Photocatalytic degradation of atenolol in aqueous titanium dioxide suspensions: kinetics, intermediates and degradation pathways. J Photochem Photobiol, A 254:35–44

Jimenez-Villarin J, Serra-Clusellas A, Martínez C, Conesa A, Garcia-Montaño J, Moyano E (2016) Liquid chromatography coupled to tandem and high resolution mass spectrometry for the characterisation of ofloxacin transformation products after titanium dioxide photocatalysis. J Chromatogr A 1443:201–210

Kanakaraju D, Kockler J, Motti CA, Glass BD, Oelgemöller M (2015a) Titanium dioxide/zeolite integrated photocatalytic adsorbents for the degradation of amoxicillin. Appl Catal B 166: 45–55

Kanakaraju D, Motti CA, Glass BD, Oelgemöller M (2015b) TiO2 photocatalysis of naproxen: effect of the water matrix, anions and diclofenac on degradation rates. Chemosphere 139: 579–588

Karcı A, Balcıoğlu IA (2009) Investigation of the tetracycline, sulfonamide, and fluoroquinolone antimicrobial compounds in animal manure and agricultural soils in Turkey. Sci Total Environ 407(16):4652–4664

Klauson D, Babkina J, Stepanova K, Krichevskaya M, Preis S (2010) Aqueous photocatalytic oxidation of amoxicillin. Catal Today 151(1):39–45

giovanni.libralato@unina.it

Kuo CS, Lin CF, Hong PKA (2016) Photocatalytic mineralization of codeine by UV-A/TiO2—kinetics, intermediates, and pathways. J Hazard Mater 301:137–144

Lair A, Ferronato C, Chovelon JM, Herrmann JM (2008) Naphthalene degradation in water by heterogeneous photocatalysis: an investigation of the influence of inorganic anions. J Photochem Photobiol A: Chem 193:193–203

Lee, KM, Lai CW, Ngai KS, Juan JC (2016) Recent developments of zinc oxide based photocatalyst in water treatment technology: a review. Water Res 88:428–448

Li G, Nie X, Gao Y, An T (2016) Can environmental pharmaceuticals be photocatalytically degraded and completely mineralized in water using g-C_3N_4/TiO_2 under visible light irradiation?—implications of persistent toxic intermediates. Appl Catal B 180:726–732

Libralato G, Annamaria VG, Francesco A (2010) How toxic is toxic? A proposal for wastewater toxicity hazard assessment. Ecotoxicol Environ Saf 73(7):1602–1611

Libralato G, Gentile E, Ghirardini AV (2016) Wastewater effects on Phaeodactylum tricornutum (Bohlin): setting up a classification system. Ecol. Ind 60:31–37

Libralato G, Minetto D, Totaro S, Mičetić I, Pigozzo A, Sabbioni E, Ghirardini AV (2013) Embryotoxicity of TiO_2 nanoparticles to Mytilus galloprovincialis (Lmk). Mar Environ Res 92:71–78

Libralato G (2014) The case of Artemia spp. in nanoecotoxicology. Mar Environ Res 101:38–43

Lofrano G, Carotenuto M, Senem Uyguner C, Vitagliano A, Siciliano A., Guida M (2014) An integrated chemical and ecotoxicological assessment for the photocatalytic degradation of vancomycin. Environ Tech 35(10):1234–1242

Lofrano G, Libralato G, Adinolfi R, Siciliano A., Iannece P, Guida M, Giugni M, Volpi Ghirardini A, Carotenuto M (2016) Photocatalytic degradation of the antibiotic chloramphenicol and effluent toxicity effects. Ecotox Environ Saf 123:65–71

Lu X, Jiang J, Sun K, Cui D (2011) Applied surface science characterization and photocatalytic activity of Zn2+–TiO2/AC composite photocatalyst. Appl Surf Sci 258:1656–1661. doi:10.1016/j.apsusc.2011.09.042

Martínez C, Fernández MI, Santaballa JA, Faria J (2011) Aqueous degradation of diclofenac by heterogeneous photocatalysis using nanostructured materials. Appl Catal B 107(1):110–118

Méndez-Arriaga F, Esplugas S, Giménez J (2008) Photocatalytic degradation of nonsteroidal anti-inflammatory drugs with TiO2 and simulated solar irradiation. Water Res 42:585–594

Mboula VM, Hequet V, Gru Y, Colin R, Andres Y (2012) Assessment of the efficiency of photocatalysis on tetracycline biodegradation. J Hazard Mater 209:355–364

Michael I, Achilleos A, Lambropoulou D, Osorio Torrens V, Pérez S, Petrović M, Barceló D, Fatta-Kassinos D (2014) Proposed transformation pathway and evolution profile of diclofenac and ibuprofen transformation products during (sono)photocatalysis. Appl Catal B 147:1015–1027

Mitoraj D, Kisch H (2008) the nature of nitrogen-modified titanium dioxide photocatalysts active in visible light. Angew Chem Int Ed 47(51):9975–9978

Mitoraj D, Kisch H (2010) On the mechanism of urea-induced titania modification. Chem A Eur J 16(1):261–269

Moustakas NG, Kontos AG, Likodimos V, Katsaros F, Boukos N, Tsoutsou D, Falaras P (2013) Inorganic–organic core–shell titania nanoparticles for efficient visible light activated photocatalysis. Appl Catal B 130:14–24

Nasuhoglu D, Rodayan A, Berk D, Yargeau V (2012) Removal of the antibiotic levofloxacin (LEVO) in water by ozonation and TiO2 photocatalysis. Chem Eng J 189:41–48

Paola AD, Addamo M, Augugliaro V, García-López E, Loddo V, Marcì G, Palmisano L (2006) Photodegradation of lincomycin in aqueous solution. Inter J Photoenergy 1–6(47418)

Palominos R, Freer J, Mondaca MA, Mansilla HD (2008) Evidence for hole participation during the photocatalytic oxidation of the antibiotic flumequine. J Photochem Photobiol Chem 193:139–145

Paschoalino FCS, Paschoalino MP, Jord E, de Figueiredo Jardim W (2012) Evaluation of TiO_2, ZnO, CuO and Ga_2 O_3 on the Photocatalytic Degradation of Phenol Using an Annular-Flow Photocatalytic Reactor

giovanni.libralato@unina.it

Paul T, Dodd MC, Strathmann TJ (2010) Photolytic and photocatalytic decomposition of aqueous ciprofloxacin: transformation products and residual antibacterial activity. Water Res 44 (10):3121–3132

Pelaez M, Nolan NT, Pillai SC, Seery MK, Falaras P, Kontos AG, Entezari MH (2012) A review on the visible light active titanium dioxide photocatalysts for environmental applications. Appl Catal B 125:331–349

Pérez-Estrada LA, Maldonado MI, Gernjak W, Agüera A, Fernández-Alba AR, Ballesteros MM, Malato S (2005) Decomposition of diclofenac by solar driven photocatalysis at pilot plant scale. Catal Today 101(3):219–226

Rizzo L, Meric S, Kassinos D, Guida M, Russo F, Belgiorno V (2009) Degradation of diclofenac by TiO2 photocatalysis: UV absorbance kinetics and process evaluation through a set of toxicity bioassays. Water Res 43(4):979–988

Xekoukoulotakis N, Xinidis N, Chroni M, Mantzavinos D, Venieri D, Hapeshi E, Fatta-Kassinos D (2010) UV-A/TiO2 photocatalytic decomposition of erythromycin in water: factors affecting mineralization and antibiotic activity. Catal Today 151:29–33

Sakthivel TS, Neppolian B, Shankar MV, Arabindoo B, Palanichamy M, Murugesan V (2003) Solar photocatalytic degradation of azo dye: comparison of photocatalytic efficiency of ZnO and TiO2. Sol Energy Mater Sol Cells 77

Salaeh S, Perisic DJ, Biosic M, Kusic H, Babic S, Stangar UL, Bozic AL (2016) Diclofenac removal by simulated solar assisted photocatalysis using TiO2-based zeolite catalyst; mechanisms, pathways and environmental aspects. Chem Eng J 304:289–302

Sousa MA, Lacina O, Hrádková P, Pulkrabová J, Vilar VJP, Gonçalves C, Boaventura RAR, Hajšlová J, Alpendurada MF (2013) Lorazepam photofate under photolysis and TiO_2-assisted photocatalysis: Identification and evolution profiles of by-products formed during phototreatment of a WWTP effluent. Water Res 47:5584–5593

Teixeira S, Gurke R, Eckert H, Kühn K, Fauler J, Cuniberti G (2016) Photocatalytic degradation of pharmaceuticals present in conventional treated wastewater by nanoparticle suspensions. J Environ Chem Eng 4(1):287–292

Vaiano V, Sacco O, Sannino D, Ciambelli P (2015) Photocatalytic removal of spiramycin from wastewater under visible light with N-doped TiO_2 photocatalysts. Chem Eng J 261:3–8

Vilar VJP, Boaventura RAR, Faria JL (2013) Photocatalytic activity of TiO_2-coated glass raschig rings on the degradation of phenolic derivatives under simulated solar light irradiation. Chem Eng J 224:32–38. doi:10.1016/j.cej.2012.11.027

Yap P-S, Lim T-T, Srinivasan M (2011) Nitrogen-doped TiO2/AC bi-functional composite prepared by two-stage calcination for enhanced synergistic removal of hydrophobic pollutant using solar irradiation. Catal Today 161:46–52. doi:10.1016/j.cattod.2010.09.024

Van Doorslaer X, Demeestere K, Heynderickx PM, Van Langenhove H, Dewulf J (2011) UV-A and UV-C induced photolytic and photocatalytic degradation of aqueous ciprofloxacin and moxifloxacin: reaction kinetics and role of adsorption. Appl Catal B: Environ 101:540–547

Van Doorslaer X, Haylamicheal ID, Dewulf J, Van Langenhove H, Janssen CR, Demeestere K (2015) Heterogeneous photocatalysis of moxifloxacin in water: chemical transformation and ecotoxicity. Chemosphere 119:S75–S80

Yahiat S, Fourcade F, Brosillon S, Amrane A (2011) Removal of antibiotics by an integrated process coupling photocatalysis and biological treatment–case of tetracycline and tylosin. Int Biodeterior Biodegradation 65(7):997–1003

Yan C, Yang Y, Zhou J, Liu M, Nie M, Shi H, Gu L (2013) Antibiotics in the surface water of the Yangtze Estuary: occurrence, distribution and risk assessment. Environ Pollut 175:22–29

Yang JF, Ying GG, Zhao JL, Tao R, Su HC, Liu YS (2011) Spatial and seasonal distribution of selected antibiotics in surface waters of the Pearl Rivers, China. J Environ Sci Health B 46(3): 272–280

Yang L, Liya EY, Ray MB (2008) Degradation of paracetamol in aqueous solutions by TiO2 photocatalysis. Water Res 42(13):3480–3488

giovanni.libralato@unina.it

Zhang J, Fu D, Xu Y, Liu C (2010) Optimization of parameters on photocatalytic degradation of chloramphenicol using TiO2 as photocatalyist by response surface methodology. J Environ Sci 22(8):1281–1289

Zhou LJ, Ying GG, Zhao JL, Yang JF, Wang L, Yang B, Liu S (2011) Trends in the occurrence of human and veterinary antibiotics in the sediments of the Yellow River, Hai River and Liao River in northern China. Environ Pollut 159(7):1877–1885

Zhu C, Wang X, Huang Q, Huang L, Xie J, Qing C et al (2013) Removal of gaseous carbon bisulfide using dielectric barrier discharge plasmas combined with TiO2 coated attapulgite catalyst. Chem Eng J 225:567–573. doi:10.1016/j.cej.2013.03.107

Zuccato E, Castiglioni S, Fanelli R (2005) Identification of the pharmaceuticals for human use contaminating the Italian aquatic environment. J Hazard Mater 122(3):205–209

giovanni.libralato@unina.it

Removal of Copper, Iron and Zinc from Soil Washing Effluents Containing Ethylenediaminedisuccinic Acid as Chelating Agent Through Sunlight Driven Nano-TiO_2-Based Photocatalytic Processes

Laura Clarizia, Marco Race, Luca Onotri, Ilaria Di Somma, Nunzio Fiorentino, Roberto Andreozzi and Raffaele Marotta

Abstract The aim of the present study is the application of integrated solar nano-TiO_2 based photocatalytic processes for the removal of copper, iron, zinc and (*S*,*S*)-ethylenediamine-*N*,*N*′-disuccinic acid (EDDS), used as chelating agent, from soil washing effluents produced by the remediation of samples of potentially polluted soils taken in the "Land of Fires" (Italy). Removal efficiencies of 93.5% (copper), 99.6% (iron), 99.4% (zinc), 97.2% (EDDS) and 80.7% (TOC) were reached through sunlight driven photocatalytic treatments carried out in parabolic trough collectors located in Naples (Italy). The removal degrees were achieved for an incident UVA solar energy per unit volume ($Q_{j,n}$) of 580 kJ L^{-1}, estimated by taking into account both the effective irradiated surface area of the photoreactor (9.79×10^{-2} m^2) and the local solar irradiances collected during the experiments. The combined nano-TiO_2-photocatalytic processes applied were shown to sufficiently decontaminate the soil washing effluents to permit the recycling in the soil washing treatment or discharging to public sewers. The study suggests that the two-step solar photocatalytic process investigated can be really adopted as a useful

L. Clarizia · R. Andreozzi · R. Marotta (✉)
Dipartimento di Ingegneria Chimica, dei Materiali e della Produzione Industriale, Università di Napoli Federico II, P.le V. Tecchio 80, 80125 Naples, Italy
e-mail: rmarotta@unina.it

M. Race
Dipartimento di Ingegneria Civile, Edile ed Ambientale, Università di Napoli Federico II, P.le V. Tecchio 80, 80125 Naples, Italy

L. Onotri · N. Fiorentino · R. Andreozzi · R. Marotta
Centro Interdipartimentale di Ricerca Ambiente, Università di Napoli Federico II, via Mezzocannone 16, 80136 Naples, Italy

I. Di Somma
Centro Nazionale delle Ricerche IRC-CNR, Istituto di Ricerche sulla Combustione, P.le V. Tecchio 80, 80125 Naples, Italy

© Springer International Publishing AG 2017

G. Lofrano et al. (eds.), *Nanotechnologies for Environmental Remediation*,
DOI 10.1007/978-3-319-53162-5_8

giovanni.libralato@unina.it

solution for the decontamination of soil washing streams from some heavy metals and chelating organic agents.

Keywords Solar nano-photocatalysis · Soil washing effluent · EDDS · Metal removal · Sacrificial nano-photocatalysis · "Land of Fires"

1 Introduction

The contamination of natural soils by heavy metals (HMs) is a worldwide concern due to the toxic effects that these elements could have on living organisms (Järup 2003). In order to face the problem, several remediation techniques, based on physical, chemical, and even biological processes, have been proposed (Mulligan et al. 2001). Among the chemical techniques for remediating soils polluted by toxic HMs, soil washing technique is one of the most promising "ex-situ" processes employing different extracting organic substances (Voglar and Lestan 2012). However, a large part of chelating agents are almost recalcitrant, once released into the environment. Consequently, soil washing processes based on the use of biodegradable synthetic chelants, such as (S,S)-N,N′-ethylenediamine disuccinic acid (EDDS), as replacement of persistent chelating agents have received great attention for the treatment of polluted soils (Dermont et al. 2008). The major drawback is the need of treating the soil washing effluents containing HMs extracted from soil and chelating agent. Consequently, exhausted soil washing wastewater cannot be directly discharged into the aquatic environment neither into sewer effluents. Moreover, the traditional technologies, such as adsorption, flocculation or precipitation, have been demonstrated to be ineffective for treating these soil washing effluents because the chelating agent does not favor the separation of the HMs from the liquid phase due to a high thermodynamic stability of the metal-chelant complexes (Vohra and Davis 2000; Hong et al. 1999).

Among the processes proposed for treating of soil washing solutions (Molinari et al. 2004; Pociecha and Lestan 2009; Englehardt et al. 2007; Liu et al. 2007), the solar driven photocatalytic systems can be adopted due to its simplicity and economicity (Bandala et al. 2008; Fabbri et al. 2008; Davezza et al. 2011). Previous studies, carried out on home-prepared solutions (Satyro et al. 2014a) and real soil washing effluents (Satyro et al. 2014b, 2016) using exclusively simulated solar radiation (lamps), demonstrated the possibility to removal toxic HMs, such as copper and zinc and EDDS, from the aqueous mixtures through different photocatalytic treatments and eventually to extend the treatment to sunlight driven processes. The present study proposes the use of nano-TiO_2 based direct solar photocatalytic processes combined for reducing the concentration level of copper, iron and zinc and chelating agent (EDDS) in real soil washing effluents to values acceptable for discharging in municipal sewers or for their reuse.

giovanni.libralato@unina.it

2 Materials and Methods

2.1 Materials

(*S*,*S*)-ethylenediamine-*N*,*N*′-disuccinic acid–trisodium salt solution (35% in H_2O), titanium(IV) nanoxide (pure crystalline anatase phase, average size 25–70 nm, 99.8% w/w) and perchloric acid (ACS reagent 70%) were purchased from Sigma–Aldrich and used as received. The soils were sampled from a site located in the countryside of Giugliano (Fig. 1), a city in the province of Naples (Italy), characterized by some of the highest levels of solar irradiation in Europe. In this area, so-called "Land of Fires", very toxic wastes have been disposed and burned for years (approximately since '70s). In order to understand the seriousness of the problem, it is important to consider that in some particular areas of this Land, a 300% excess, as compared to the data of the Campania region has been recorded in few years in diseases such as stomach, liver, bronchus, and bladder cancers as well as malformations and birth defects, which is compatible with the lack of remediation of the polluted sites and persistence of waste mismanagement to date (Triassi et al. 2015; Comba et al. 2006). This excess mortality has been also related to the presence of heavy metals (Albanese et al. 2008), mainly arising the emissions in the more urbanized areas.

Soil samples were manually collected from the top 20 cm over an area of about one square meter and then stored in hermetic containers. The samples were sieved and only the particles smaller than 2.0 mm were used in the tests and analytical determinations.

2.2 Methods

2.2.1 Soil Washing Procedure

Soil washing experiments were carried out in 2 L polyethylene bottles in triplicate. EDDS was used as the chelating agent. The tests were carried out at a natural pH

Fig. 1 The geographical area in which soils were sampled (geographic coordinates N40° 96′05″, E14°11′84″)

giovanni.libralato@unina.it

value of 7.5–7.9, fixing the liquid-to-solid ratio (L/S) to 10:1 and the EDDS washing solution initial concentration to 0.50 mM. The samples were stirred in a mechanical shaker (Edmund Bühler, Kombischüttler KL2) at 190 rpm for 96 h at ambient temperature. Blank tests (soil washing solutions without EDDS) were carried out using bi-distilled water.

2.2.2 Photocatalytic Procedure: Outdoor Experiments

The photocatalytic runs under direct sunlight were carried during the period June–July 2015 at University of Naples (Italy, local latitude 40°50′00″N, longitude 14°12′00″E) by using a flat plate collector with a multitubular reactor (PTC), supported by an aluminum structure (Fig. 2). The flat plate collector (9 dm^2) was made up of 8 parallel borosilicate glass tubes (internal diameter 4 mm, external diameter 7 mm, length 34.6 cm) connected by plastic junctions. The soil washing effluent to be treated was kept re-circulating at a rate of 80 L h^{-1}. Some runs were carried out varying the re-circulating rate (60 L h^{-1}). The solution recirculation between the refrigerated tank (1.5 L, 25 °C) and the collectors was carried out using a peristaltic pump (Watson Marlow 505S). The total volume of the reactor (V_t) is constituted by the irradiated PTC volume (V_{ir}) and the dead volume (recirculation tank and connecting tubes). The irradiated volume of PTC was 3.42×10^{-2} L. The total volume of the device ranged between 0.30 and 0.85 L. The flat plate collector surface was covered with aluminum foils. The average incident solar radiation was typically about 15 ± 10 W m^{-2} in the wavelength range 315–400 nm and 950 ± 150 W m^{-2} in the range 400–1100 nm. The amount of UVA solar energy received by the nth-sample ($Q_{j,n}$, kJ L^{-1}), per unit volume of solution, in the time interval Δt_n was calculated from the following equation:

$$Q_{j,n} = Q_{j,n-1} + \Delta t_n \cdot UV_{G,n} \cdot \left[\frac{A_{ir}}{V_t}\right] \quad (1)$$

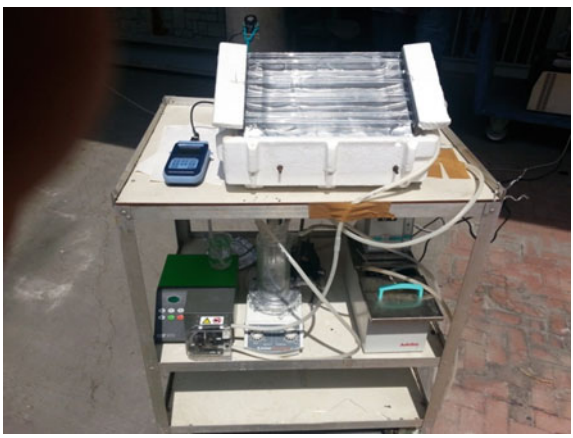

Fig. 2 Solar photoreactor adopted

giovanni.libralato@unina.it

where t_n is the experimental time corresponding to the nth-sample, V_t the total volume of the reactor, A_{ir} the illuminated surface area, and $UV_{G,n}$ the average solar ultraviolet radiation (300–400 nm) measured during the period Δt_n.

2.2.3 Photocatalytic Procedure: Indoor Experiments

Solar simulated photocatalytic runs were carried out in an annular batch glass reactor having an irradiated volume (V_{ir}) and an illuminated surface area (A_{ir}) equal to 0.28 L and 3.39 dm^2 respectively. The reactor was equipped with:

- a polychromatic sodium lamp (Helios Italquartz, model Na 15F) with a nominal power of 150 W and a wavelength range between 350 and 800 nm. The photon fluxes of the Na-lamp, measured by UVA radiometer (DELTA OHM, model HD2102.1), were 2.84 W m^{-2} (315–400 nm) and 2.02×10^3 W m^{-2} (400–800 nm). The emission spectrum of the Na-lamp is reported in Fig. 3a.
- a high pressure Hg lamp with a nominal power of 125 W mainly emitting in the wavelength range of 300–400 nm (Helios Italquartz). The photon flux of the Hg-lamp in the wavelength range 280–400 nm was 30.03 W m^{-2}. The emission spectrum of the mercury vapour lamp is shown in Fig. 3b.

2.2.4 Analytical Procedures

Metal concentrations were determined through Atomic Absorption Spectrometry (AAS), using Varian Model 55B SpectrAA (F-AAS) equipped with flame (acetylene/air) with a deuterium background correction, GBC Avanta AAS with graphite furnace (GF-AAS). Elemental analysis was performed using a Perkin-Elmer Series II 2400 CHNS/O Elementary Analyzer. The pH of the soil was measured according to EPA Method 9045C. Organic matter was evaluated using the Loss On Ignition (LOI) index (Shulte 1995).

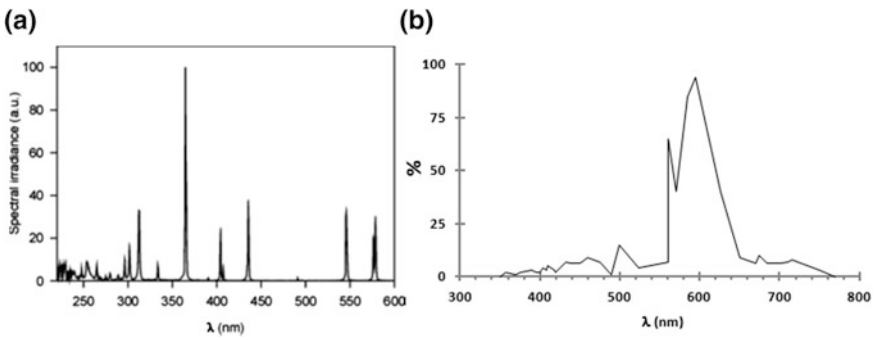

Fig. 3 Emission spectra of the mercury (**a**) and sodium (**b**) lamps

giovanni.libralato@unina.it

The EDDS analyses were performed through a modification of a colorimetric method previously reported (Vandevivere et al. 2001). After adjusting the pH at 2.0, the sample (3.3 mL) and a proper amount of the reagent solution, containing cupric sulphate (2 mM), were added to a volumetric flask (5.0 mL). Cu(II)-EDDS, a blue complex, is formed and its concentration was quantified through spectrophotometric analysis at 670 nm (ATI-Unicam UV/Vis spectrophotometer).

Total organic carbon analyses were performed by means of a TOC Shimadzu 5000A. COD analyses were carried out by using HACH kit (0–1500 ppm). The theoretical oxygen demand (ThOD) was calculated from the following equation:

$$C_{10}H_{13}N_2O_8^{3-} + \frac{25}{2}O_2 + H^+ \rightarrow 10CO_2 + 7H_2O + 2NO_3^- \qquad (r.1)$$

The oxalic acid concentration was measured by HPLC chromatography (Agilent 1100) equipped with Alltech OA-1000 Organic Acids column using a sulfuric acid aqueous solution (2 N) as mobile phase. The pH of the aqueous solutions was determined using an Orion 960 pH meter with a glass pH electrode. All measurements were carried out in triplicate and the average values were considered (standard deviation <5%).

3 Results and Discussion

The soil characteristics are reported in Table 1. The pH was close to neutrality (EPA 2003) and the LOI index is 7.19%. The metals concentrations were lower than both the Italian regulatory limits for soils and the mean values of metal concentration measured in natural soils, except for copper and zinc. Therefore, in the soil washing experiments, the aim was to remove Cu and Zn from the soil.

3.1 Soil Washing Effluents

The average analytical concentrations of Cd, Cr, Cu, Fe, Mn, Ni, Pb and Zn contained in the soil-washing effluents from the polluted soil sample after 96 h of contact time are reported in Fig. 4. The results indicate the presence in the effluents, containing EDDS as chelating agent, of copper, and zinc at concentration levels too high for their discharge in public sewers or in surface waters. Consequently, post-treatment processes were required to reduce copper and zinc concentration below the Italian regulatory limits (Cu: 0.4 mg L^{-1}, Zn: 1 mg L^{-1}) (D.Lgs.152/2006 2006) before releasing them into civil sewers. Moreover, it was detected a concentration for iron was quite close to the value of Italian regulatory limit (Fe: 4 mg L^{-1}) (D.Lgs.152/2006 2006).

giovanni.libralato@unina.it

Table 1 Comparison between the collected soil parameters and the Italian regulatory limits and mean values of metal concentrations in natural soils

		Soil	[a]Limits Italian legislation	[b]Mean values for soils
	LOI	7.19 ± 0.15		
	pH	7.1		
%	C	3.96 ± 0.21		
	H	2.47 ± 0.18		
	N	0.42 ± 0.09		
	S	0.43 ± 0.12		
ppm	Mg	$2.1 \times 10^4 \pm 1.0 \times 10^2$		
	Ca	$4.4 \times 10^5 \pm 8.2 \times 10^2$		
	Cu	$2.2 \times 10^2 \pm 39.2$	1.2×10^2	51
	Pb	24.37 ± 2.3	1.0×10^2	1.0×10^2
	Cr	33.17 ± 1.1	1.5×10^2	5.0×10^2
	Ni	8.27 ± 0.8	1.2×10^2	2.5×10^2
	Zn	$1.8 \times 10^2 \pm 11.8$	1.5×10^2	1.5×10^2
	Cd	0.40 ± 0.1	2.0	0.35
	Fe	$1.4 \times 10^4 \pm 3.2 \times 10^2$		2.8×10^5
	Mn	$5.1 \times 10^2 \pm 72.1$		1.5×10^3

[a]D.Lgs.152/2006 (2006)
[b]EPA Method 9045C

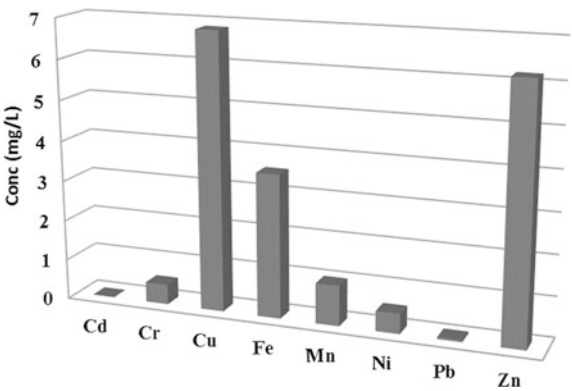

Fig. 4 Metals concentrations (mg L^{-1}) in the effluent after 96 h of soil washing process

3.2 Solar Photocatalytic Processes

On the basis of the findings previously reported (Satyro et al. 2014b), an optimal sequence of two separate photocatalytic processes (aerated nano-TiO_2-photocatalysis, as first step, and "sacrificial" nano-TiO_2-photocatalysis, as second stage) able to ensure the highest efficiency Cu, Zn, Fe and EDDS removal was chosen. For

giovanni.libralato@unina.it

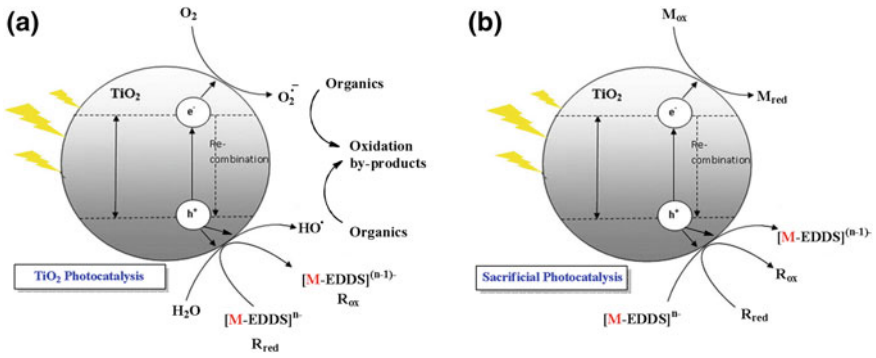

Fig. 5 Schemes for TiO_2 based photocatalysis (**a**) and TiO_2 sacrificial photocatalysis (**b**)

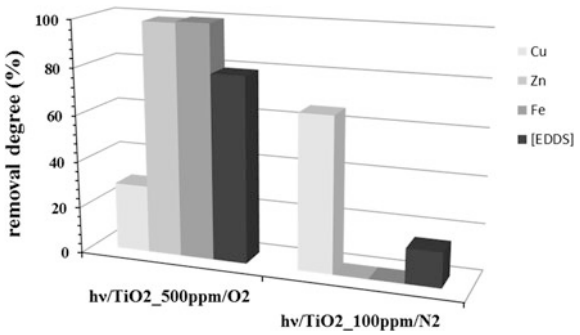

Fig. 6 Removal of metals and EDDS from soil washing effluents through two sequential TiO_2 photocatalytic steps by irradiation with natural sunlight source. $[EDDS]_o$ = 0.45 mM. (▫) Cu, (▫) Zn, (▫) Fe, (■) EDDS

sake of clarify, a general scheme for each step is reported in Fig. 5. It is clear that the main differences between the two scheme are:

(1) the absence of oxygen in the case of sacrificial photocatalysis (Fig. 5b). In fact, in deoxygenated solutions, the photogenerated electrons can react with certain dissolved metals ions by reduction reactions whereas positive holes oxidize a sacrificial agent, i.e. EDDS and its by-products;
(2) in the case of aerated photocatalysis (Fig. 5a), the generation of hydroxyl radicals with attack EDDS and other organic species.

The removal degrees of the chelating agent, copper, iron, zinc and EDDS in soil washing effluents under direct natural sunlight, using the photocatalytic treatment sequence, described above, are shown in Fig. 6.

Nano-TiO_2_500 ppm/O_2/hν (first step): t_r = 23 h; nano-TiO_2_100 ppm/N_2/hν (second step): t_r = 20 h

giovanni.libralato@unina.it

The first step allowed to reach high removals of the chelating agent due to the occurrence of reactions between EDDS and hydroxyl and/or hydroperoxyl radicals (r.5), formed by the photolysis of Fe(III)-EDDS and Fe(III)-L complexes (r.2–r.4), where L represents by-photoproducts (Wu et al. 2014):

$$\text{Fe(III)} - \text{EDDS/L} \xrightarrow{h\nu} \text{Fe(II)} + \text{R}^{\cdot} \tag{r.2}$$

$$\text{R}^{\cdot} \xrightarrow{\text{O}_2/\text{H}^+} \text{R}' + \text{HO}_2^{\cdot} \tag{r.3}$$

$$2\ \text{Fe(II)} + \text{HO}_2^{\cdot} + \text{H}_2\text{O} \rightarrow 2\text{Fe(III)} + \text{HO}^{\cdot} + 2\text{HO}^- \tag{r.4}$$

$$\text{EDDS} \xrightarrow{\text{HO}_2^{\cdot}/\text{HO}^{\cdot}} \text{by-products} \tag{r.5}$$

by reaction of oxygen with photogenerated TiO_2-electrons:

$$\text{O}_2 + 2\text{e}^- + 2\text{H}^+ \rightarrow \text{H}_2\text{O}_2 \tag{r.6}$$

$$\text{H}_2\text{O}_2 + 2\text{e}^- \rightarrow \text{HO}^{\cdot} + \text{HO}^- \tag{r.7}$$

and by reaction of water molecules with TiO_2 positive holes:

$$\text{H}_2\text{O} + \text{h}^+ \rightarrow \text{HO}^{\cdot} + \text{H}^+ \tag{r.8}$$

Acceptable values of iron and zinc removal were also gained due to the precipitation of these metals as insoluble hydroxides and their adsorption onto TiO_2 catalyst after EDDS degradation. On the other hand, the first photocatalytic step was almost ineffective in removing copper species probably due to the existence of soluble Cu-hydroxo-complexes, such as $Cu(OH)^+$, at the adopted pH (Cuppett et al. 2006).

During the second step (sacrificial photocatalysis), residual copper and EDDS were completely removed. Copper elimination during the second step is due to the reduction of cupric ions to zero-valent copper by photogenerated electrons:

$$\text{Cu(II)} + 2\text{e}^- \rightarrow \text{Cu} \downarrow \tag{r.9}$$

leading to a further EDDS destruction by the reaction with positive holes:

$$\text{EDDS} + \text{h}^+ \rightarrow \text{by-products} + \text{H}^+ \tag{r.10}$$

The results indicate that wastewaters can be successfully treated under "outdoor" conditions, once the photoreactor has been properly characterized. To collect valuable information for scaling-up the solar treatment plant, concentration data for the species removed should be plotted against the incident solar energy per unit of volume ($Q_{j,n}$, kJ L^{-1}), instead of the irradiation time (Curcó et al. 1996). However, it is important to know the value of the illuminated surface area of the photoreactor (A_{ir}). Due to the possibility of using many types of reflecting surfaces whose area

giovanni.libralato@unina.it

may be quite different, generally, it is necessary to directly measure this value. To this purpose, a method is proposed based on the concentration data collected during the oxidation of a standard species during some "indoor" and "outdoor" photocatalytic runs, which were carried out using the same oxalic acid aqueous solution on which nano-anatase titanium dioxide (at the same load) was suspended. Indoor experiments were performed in a batch recirculating lab-system, using two different radiating sources (Hg-lamp or Na-lamp).

Since both (i) the emitting powers of the lamps in the wavelengths range 280–400 nm (30.03 and 2.84 W m^{-2} for Hg- and Na-lamps, respectively) and (ii) the illuminated surface area (A_{ir} = 3.39 dm^2) of the "indoor" reactor are known, the results, shown in Fig. 7, of typical experiments carried out can be reported as a linear plot of oxalic acid concentration against $Q_{j,n}$ for different total volumes of the reactor, from which the values for the apparent reaction rate constant (k_{app}) were derived by the slope of each straight line.

The k_{app} constant is the product of some variables which can be identified in the following way. According to literature indications (De Lasa et al. 2005), the following material balance can be written for a batch photocatalytic reactor:

$$V_t \cdot \frac{dc}{dt} = -V_{ir} \cdot r \tag{2}$$

in which:

$$r = k \cdot \Phi \cdot \left[1 - e^{(-2.3 \cdot \mu \cdot l \cdot q)}\right] \cdot \frac{A_{ir}}{V_{ir}} \cdot UV_{G,n} \cdot f(c) \tag{3}$$

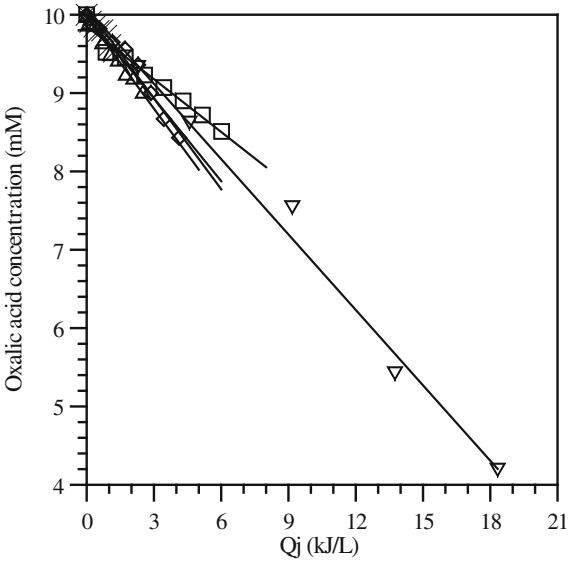

Fig. 7 Oxalic acid concentration versus accumulated energy for different UV-Vis artificial lamps at varying total volume of the reactor (V_t). [Oxalic acid]$_o$ = 10 mM, nano-TiO_2 initial load = 500 mg L^{-1}; pH = 2.0, T = 25 °C, V_{ir} = 0.28 L, recycle flow rate 80 L h^{-1}. Hg-lamp: V_t = 0.4 L (*downward triangle*); Na-lamp: V_t = 0.4 L (*white square*), V_t = 0.6 L (*white diamond*), V_t = 1.0 L (*upward triangle*), V_t = 2.0 L (*multiplication*)

giovanni.libralato@unina.it

where k, Φ, μ, l, q, and $f(c)$ are the kinetic constant, the photocatalyst quantum yield, the suspension extinction coefficient (sum of the absorption and scattering coefficients), the light pathway length of the reactor, the photocatalyst load, and a function of the organic species concentration, respectively.

According to literature indications (Rabek 1982), a zero-order dependence is reported for the photocatalytic degradation of oxalic acid for which $f(c) = k'$. Therefore, rearranging Eq. 2:

$$dc = -kk' \cdot \Phi \cdot \left[1 - e^{(-2.3 \cdot \mu \cdot l \cdot q)}\right] \cdot \frac{A_{ir}}{V_{ir}} \cdot UV_{G,n} \cdot \frac{V_{ir}}{V_t} \cdot dt \tag{4}$$

In finite terms:

$$\Delta c = -k'' \cdot \Phi \cdot \left[1 - e^{(-2.3 \cdot \mu \cdot l \cdot q)}\right] \cdot Q_{j,n} \tag{5}$$

with $kk' = k''$.

The oxalic acid concentration at different reaction times can be thus calculated as:

$$[Oxalic\ acid]_t = [Oxalic\ acid]_o - k_{app} \cdot Q_{j,n} \tag{6}$$

where:

$$k_{app} = k'' \cdot \Phi \cdot \left[1 - e^{(-2.3 \cdot \mu \cdot l \cdot q)}\right] \tag{7}$$

Following this approach, it is possible to calculate an average value (0.42 mmol kJ^{-1}) for the term $k'' \cdot \Phi$ reported in Eq. 7, dividing each k_{app} constant, estimated through the data reported in Fig. 7, by the $\left[1 - e^{(-2.3 \cdot \mu \cdot l \cdot q)}\right]$ factor. The mean value of this product ($\overline{k''\Phi}$) depends upon the type of titanium dioxide used, its load, and the organic species oxidized (oxalic acid). The value thus calculated for $\overline{k''\Phi}$ term can be used to predict the decrease in concentration of oxalic acid against $Q_{j,n}$ when one of the suspensions, previously used in "indoor" experiments, is sent to an "outdoor" solar photoreactor.

When a set of data for oxalic acid concentration is available from solar photocatalytic oxidation runs in a selected photoreactor, in which the illuminated and total volumes are known, it is possible to estimate the best value of the illuminated area (A_{ir}). To this aim, the value of energy received from the solution used in the calculation must correspond to that of $Q_{j,n}$ minimizing the differences between the experimental data and the straight line.

According to the procedure described above, an average value of 9.79×10^{-2} m^2 was thus estimated for the illuminated area of the solar photoreactor (PTC) using experimental data of oxalic acid consumption versus $Q_{j,n}$ with different V_t/V_{ir} volume ratios. This value was used to calculate the $Q_{j,n}$ values (1) required to achieve the desired removal percentage degrees of EDDS, copper, zinc,

giovanni.libralato@unina.it

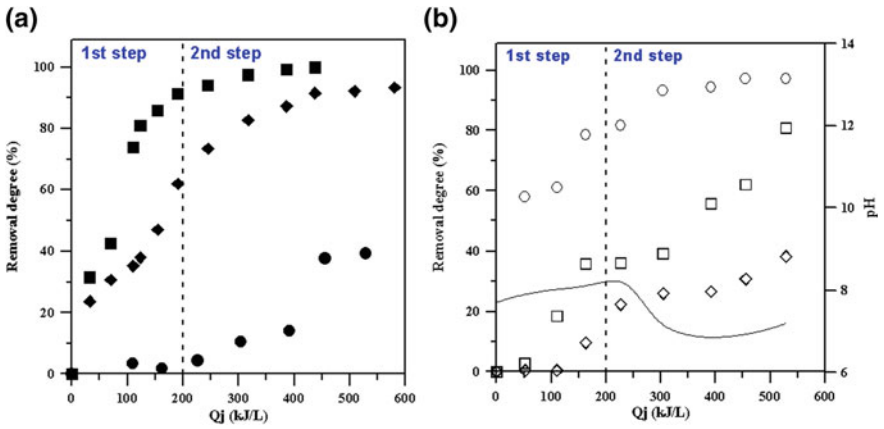

Fig. 8 Removal degrees of Zn (*black square*), Cu (*black diamond*), NO_3^- (*black circle*), EDDS (*white circle*), TOC (*white square*) and COD (*white diamond*) and pH (*continuous lines*) profiles during the two solar sequential photocatalytic treatments

nitrate, COD, and TOC for the soil washing effluents treated through the photocatalytic sequence TiO_2/O_2 and TiO_2/N_2 (Fig. 8a, b).

Removal efficiencies of 93.5% (copper), 99.4% (zinc) and 97.2% (EDDS) were achieved for $Q_{j,n}$ value of 580 kJ L^{-1}. Moreover, an iron removal of 99.6% was reached at the end of the first step (data not shown). It is noteworthy to observe that the TOC and COD removal degree functions show a double S-shape profile, reaching maximum values close to 80 and 40%, respectively. This "anomalous" result may be explained considering that EDDS oxidation occurs in several sequential reactions pathways, which differ from each other depending on whether the degradation step involves decarboxylation and oxygenation reactions or not.

However, the value of COD/ThOD ratio (0.76) calculated for a reference solution containing the sole EDDS at a known concentration, indicates that COD data are not strictly representative for the content of oxidizable organic carbon for different treated samples. This result, which is the consequence of an incomplete EDDS oxidation during COD determination runs, leading to uncorrect COD measurements, has been reported previously for EDTA, a structural isomer of EDDS (Anderson et al. 2007). It is remarkable to observe that during the second step it was also reached a 40% value of removal degree of nitrate, initially present in the soil washing effluent at 48 ppm. This result is of significant importance because it would suggest the use of combined sunlight driven photocatalytic reduction processes also for removing nitrates from aqueous effluents.

The decrease in pH from 7.70 to 6.85 (Fig. 8b) indicates the formation of carboxylic acids during the photodegradation of chemical intermediates, which are further mineralized thus resulting in a moderate pH increase (7.20) for more prolonged reaction times (Qj > 500 kJ L^{-1}).

giovanni.libralato@unina.it

4 Fixed Cost Estimation

From the data reported in Fig. 8a, it can been deducted that an incident solar energy per unit volume of 425 kJ L^{-1} is required to achieve a removal degree of 100 and 90% of zinc and copper, respectively. This result, under the adopted experimental conditions ($UV_{G,n}$ = 15 W m^{-2}), was reached within 30 h of treatment time indicated as "soil washing treatment cycle". Assuming that it is necessary to treat a volume of soil washing effluent equal to 10 m^3, a geometrical surface area of about 1630 m^2 can be inferred from Eq. 1, by taking into account an average scaling factor of 1.61. If an investment cost of 210 \$ m^{-2} for a flat plate collector is considered (Kalogirou 2003), a capital cost of about 345.000 \$ for the solar photoreactor is thus estimated. This value would be taken into account as a fixed cost for a minimum required lifetime of a solar collector of 10 years (Shanmuga Priya et al. 2008). Assuming a lifetime of ten years for the photoreactor, and seventy "soil washing treatment cycles" for year, a treatment cost estimation, consumable chemicals neglecting, was 493 \$/m^3 of soil treated. It is noteworthy to stress that the estimated cost is mainly affected by the photoreactor design, the solar irradiation conditions and the chemical composition of the aqueous effluents.

5 Conclusions

A sequence of two solar nano-TiO_2-photocatalytic processes was tested to remove copper, iron, zinc, and EDDS from real soil washing wastewater at neutral pH conditions.

The results collected from experimental runs demonstrate that iron and zinc are mainly removed by precipitation as insoluble hydroxides during the first step (oxygenated nano-TiO_2-based photocatalysis) whereas the second step (nano-TiO_2-sacrificial photocatalysis) is necessary to reduce cupric ions to zero-valent copper which precipitates from the solution.

Acknowledgements This study was carried out within the EU Project LIFE11 ENV/IT/000275 (ECOREMED).

References

Albanese S, De Luca ML, De Vivo B, Lima A, Rezzi G (2008) Relationships between heavy metal distribution and cancer mortality rates in the Campania region Italy. In: De Vivo B, Belkin HE, Lima A (eds) Environmental geochemistry: site characterization, data analysis and case histories. Elsevier, Amsterdam, pp 387–400

Anderson JE, Mueller SA, Kim BR (2007) Incomplete oxidation of ethylenediaminetetraacetic acid in chemical oxygen demand analysis. Water Environ Res 79:1043–1049

giovanni.libralato@unina.it

Bandala ER, Velasco Y, Torres LG (2008) Decontamination of soil washing wastewater using solar driven advanced oxidation processes. J Hazard Mater 160:402–407

Comba P, Bianchi F, Fazzo L, Martina L, Menegozzo M, Minichilli F, Mitis F, Musmeci L, Pizzuti R, Santoro M, Trinca S, Martuzzi M (2006) Cancer mortality in an area of Campania (Italy) characterized by multiple toxic dumping sites. Ann NY Acad Sci 1076:449–461

Cuppett JD, Duncan SE, Dietrich AM (2006) Evaluation of copper speciation and water quality factors that affect aqueous copper tasting response. Chem Senses 31:689–697

Curcó D, Malato S, Blanco J, Giménez J (1996) Photocatalysis and radiation absorption in a solar plant. Sol Energy Mater Sol Cells 44:199–217

Davezza M, Fabbri D, Bianco Prevot A, Pramauro E (2011) Removal of alkylphenols from polluted sites using surfactant-assisted soil washing and photocatalysis. Environ Sci Pollut Res 18:783–789

D.Lgs.152/2006 (2006) Norme in materia ambientale. Gazzetta Ufficiale 88, S.O. 96

De Lasa HI, Serrano B, Salaices M (2005) Photocatalytic reaction engineering. Springer, Berlin

Dermont G, Bergeron M, Mercier G, Richer-Laflèche M (2008) Soil washing for metal removal: a review of physical/chemical technologies and field applications. J Hazard Mater 152:1–31

Englehardt JD, Meeroff DE, Echegoyen L, Deng Y, Raymo FM, Shibata T (2007) Oxidation of aqueous EDTA and associated organics and coprecipitation of inorganics by ambient iron-mediated aeration. Environ Sci Technol 41:270–276

EPA Method 9045C (2003) Soil and waste pH. In: Test methods for evaluating solid waste, physical/chemical methods. EPA Publication SW-846, US Environmental Protection Agency

Fabbri D, Prevot AB, Zelano V, Ginepro M, Pramauro E (2008) Removal and degradation of aromatic compounds from a highly polluted site by coupling soil washing with photocatalysis. Chemosphere 71:59–65

Hong APK, Li C, Banerji SK, Regmi T (1999) Extraction, recovery, and biostability of EDTA for remediation of heavy metal-contaminated soil. Soil Sediment Contam 8:81–103

Järup L (2003) Hazards of heavy metal contamination. Br Med Bull 68:167–182

Kalogirou S (2003) The potential of solar industrial process heat applications. Appl Energy 76:337–361

Liu X, Yu G, Han W (2007) Granular activated carbon adsorption and microwave regeneration for the treatment of 2,4,5-trichlorobiphenyl in simulated soil-washing solution. J Hazard Mater 147:746–751

Molinari R, Gallo S, Argurio P (2004) Metal ions removal from wastewater or washing water from contaminated soil by ultrafiltration-complexation. Water Res 38:593–600

Mulligan CN, Yong RN, Gibbs BF (2001) Remediation technologies for metal-contaminated soils and groundwater: an evaluation. Eng Geol 60:193–207

Pociecha M, Lestan D (2009) EDTA leaching of Cu contaminated soil using electrochemical treatment of the washing solution. J Hazard Mater 165:533–539

Rabek JF (1982) Experimental methods in photochemistry and photophysics 2. Wiley, New York

Satyro S, Marotta R, Clarizia L, Di Somma I, Vitiello G, Dezotti M, Pinto G, Dantas RF, Andreozzi R (2014a) Removal of EDDS and copper from waters by TiO_2 photocatalysis under simulated UV-solar conditions. Chem Eng J 251:257–268

Satyro S, Race M, Marotta R, Dezotti M, Spasiano D, Mancini G, Fabbricino M (2014b) Simulated solar photocatalytic processes for the simultaneous removal of EDDS, Cu(II), Fe(III) and Zn(II) in synthetic and real contaminated soil washing solutions. J Environ Chem Eng 2:1969–1979

Satyro S, Race M, Di Natale F, Erto A, Guida M, Marotta R (2016) Simultaneous removal of heavy metals from field-polluted soils and treatment of soil washing effluents through combined adsorption and artificial sunlight-driven photocatalytic processes. Chem Eng J 283:1484–1493

Schulte EE (1995) Recommended soil organic matter tests. Recomm Soil Test Proced North East USA Northeast Reg Publ, 52–60

Shanmuga Priya S, Premalatha M, Anantharaman N (2008) Solar photocatalytic treatment of phenolic wastewater potential, challenges and opportunities. ARPN J Eng Appl Sci 3(6):36–41

giovanni.libralato@unina.it

Triassi M, Alfano R, Illario M, Nardone A, Caporale O, Montuori P (2015) Environmental pollution from illegal waste disposal and health effects: a review on the "Triangle of Death". Int J Environ Res Public Health 12:1216–1236

Vandevivere PC, Saveyn H, Verstraete W, Feijtel TCJ, Schowanek DR (2001) Biodegradation of metal-[S, S]-EDDS complexes. Environ Sci Technol 35:1765–1770

Voglar D, Lestan D (2012) Electrochemical treatment of spent solution after EDTA-based soil washing. Water Res 46:1999–2008

Vohra MS, Davis AP (2000) TiO_2-assisted photocatalysis of lead-EDTA. Water Res 34(3): 952–964

Wu Y, Brigante M, Dong W, De Sainte-Claire P, Mailhot G (2014) Toward a better understanding of Fe(III)–EDDS photochemistry: theoretical stability calculation and experimental investigation of 4-tert-butylphenol degradation. J Phys Chem A 118:396–403

giovanni.libralato@unina.it

Impact of Silver Nanoparticles on Wastewater Treatment

Jeanette Brown

Abstract Silver nanoparticles (AgNPs, nanosilver) are used as an excellent antimicrobial agent in many consumer products. These nanoparticles are often released during washing and eventually enter wastewater treatment plants. The objective of this study was to evaluate how silver nanoparticles would affect wastewater treatment systems for organic and nutrient removal. The results demonstrated that nitrifying bacteria are especiall susceptible to inhibition by silver nanoparticles. At a concentration of 0.4 mg/L total AG, a mixture of silver ions and AgNPs (50:50 mass ratio, average size 15-21 nm) inhibited nitrification by 11.5 percent. During a nanosilber shock loading event lasting for 12 hours, a peak concentration of 0.5 mg/L Ag in the activated sludge basin (more than 95% assocated with biomass) was detected, resulted in a prolonged period (>1 month) of nitrification inhibition reaching a maximum of 50%, as evidenced by accumulations of ammonia and nitrite in the wastewater effluetn. In batch anaerobic digestion studies, AgNPs at the concentration of 19 mg/L (19,000 ppb) started to reduce cumulative biogas production, although the inhibition could be due to the accompanied nitrate in the nanosilver suspension. Results from the aerobic and anaerobic treatment studies suggest that accumulation of silver in acivated sludge may have a detrimental effect on nitrification and nutrient removal, if the concentration reaches theshold levels. The suggested threshold concentration of total silver including nanosilver in wastewater influent is 0.1 mg/L.

Keywords Silver Nanoparticles · Wastewater · Toxicity · Nitrification · Anaerobic digestion

Principal Investigator: Zhiqiang Hu, University of Missouri, Columbia, MO

Used and edited with Permission from: Water Environment Research Foundation, Alexandria, VA

J. Brown (✉)
Manhattan College, Manhattan College Parkway, Riverdale, NY, USA
e-mail: Jeanette.brown@Manhattan.edu

© Springer International Publishing AG 2017

G. Lofrano et al. (eds.), *Nanotechnologies for Environmental Remediation*,
DOI 10.1007/978-3-319-53162-5_9

giovanni.libralato@unina.it

1 Introduction

Silver nanoparticles (AgNPs) are emerging as one of the commonly used nanomaterials. Although silver has been used as an antimicrobial agent for centuries, silver nanoparticles (AgNPs or nanosilver) are relatively new. These nanosized particles are known to exhibit antimicrobial/antiviral properties, superior catalytic activity and improved sensitivity of spectroscopy like surface enhanced Raman spectroscopy (SERS).

Silver in the form of nanoparticles can be more toxic than the bulk counterpart (Choi and Hu 2008; Navarro et al. 2008). This is partly because of the high surface/volume fraction so that a large proportion of silver atoms are in direct contact with the microbial surface. Nanoparticles are believed to generate reactive oxygen species (ROS) to inhibit microbial growth (Adams et al. 2006; Lin et al. 2006; Nel et al. 2006). An antimicrobial mechanism of free radical involvement near the Ag nanoparticle surface was presented recently based on electron spin resonance (ESR) measurements. The formation of free radicals may cause subsequent free radical induced membrane damage to the cells (Kim et al. 2007). Furthermore, toxicity is presumed to be size and shape dependent, because small sized nanoparticles (Kloepfer et al. 2005; Morones et al. 2005) can pass through cell membranes and accumulation of intracellular nanoparticles leading to detrimental effects on cell function. Hence, there are several major differences that could potentially result in a distinct hazard profile for nanosilver.

While AgNPs are an excellent antimicrobial agent for medical applications, the toxicity and the risk of nanosilver to the environment and public health remains to be evaluated adequately. The mechanism responsible for effects due to nanosilver exposure is unclear, although it is likely to involve bound forms of oxidized silver on the cell surface, uptake and release of high concentrations of silver ions within cellular compartments, and disruption of membranes through catalytic or physical processes. Although the mechanisms of nanosilver toxicity remain to be elucidated, silver nanoparticles have already a wide range of applications. As an antimicrobial agent, AgNPs are used for fiber coating, shoe odor control, new detergents, hydrogels and plastics to prevent bacterial and fungal growth. Nanoparticles released from various consumer products can be toxic to the benign microorganisms such as nitrifying bacteria in wastewater treatment plants (WWTPs) and the natural environment.

In a typical wastewater treatment process (Fig. 1), wastewater containing solids, organic matter, and nutrients (nitrogen and phosphorous) flows through a primary (1st) clarifier where approximately 50–70% of solids and 25–40% of organic matter measured as Chemical Oxygen Demand (COD) or Biochemical oxygen demand (BOD) is removed (Metcalf and Eddy 2013). The rest of solids (colloids) and organic matter are degraded in bioreactors, where a significant amount of nitrogen and/or phosphorous are removed depending on the processes being used. In some treatment facilities, the collected biomass/sludge from clarifiers is digested before final disposal. Unlike organic colloids (1 nm–1 μm) in wastewater (Levine et al. 1991; Stumm and Morgan 1996), silver nanoparticles are not biodegradable.

giovanni.libralato@unina.it

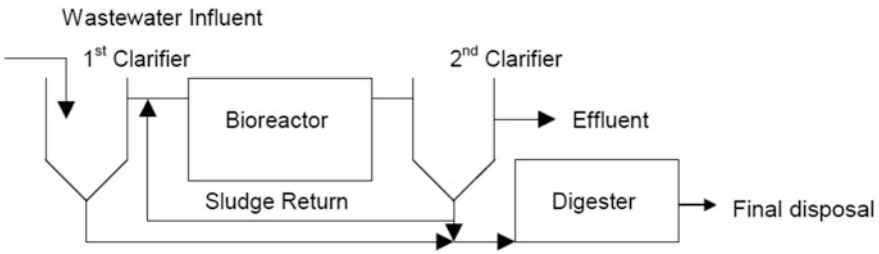

Fig. 1 A schematic of wastewater treatment process

Dissolved organic carbon in wastewater is efficiently removed in treatment process. Silver ions in wastewater are also removed efficiently (>94%) because of their strong complexation with many ligands such as chloride (K = 109.7), sulfide (K = 1049) (K is the stability constant or the overall formation constant to form silver-ligand complexes or precipitates) (Shafer et al. 1998; Wang 2003). Little is known about the fate and impact of silver nanoparticles in wastewater treatment systems. Do silver nanoparticles undergo partitioning and transformation in various wastewater treatment processes? How do they affect the metabolic activities of activated sludge during wastewater treatment? These are important questions that were evaluated to understand their impact on various wastewater and sludge treatment processes in Water Resource Recovery Facilities (WRRFs).

As nanosilver-based consumer products continue to rapidly grow, nanoparticles from various consumer products will likely enter sewers and WRRFs. However, the fate and adverse impact of AgNPs on wastewater treatment remain largely unknown. Therefore it is important to understand the impact of silver nanoparticles on activated sludge WWTP.

Silver nanoparticles are emerging as one of the fastest growing nanomaterials with wide applications; the wastewater community has recently raised concerns about nanosilver entering treatment facilities. If they are not well managed or disposed of appropriately, increasing numbers of nanosilver products would threaten wastewater operation because of the increased load of silver in wastewater since most facilities treatments are biologically base. Laboratory scale studies showed that 1 mg/L nanosilver inhibited microbial growth by approximately 80% (Choi et al. 2008). Furthermore, smaller sized AgNPs (<5 nm) appeared to be more toxic than any other forms of silver (Choi and Hu 2008). As nanotechnology enhanced products rapidly increase in the market, the risk that AgNPs will be released into sewage systems and eventually released to rivers, streams, and lakes in treatment plant effluent is therefore of concern.

Nanosilver in wastewater may be converted into Ag^+ ions (Benn and Westerhoff 2008), complexed with ligands, agglomerated, or still be present as nanoparticles. Silver nanoparticles likely accumulate in activated sludge (Benn and Westerhoff 2008). However, the biological fate and adverse impact of silver nanoparticles on wastewater treatment remained largely unknown.

giovanni.libralato@unina.it

Many treatment facilities are required to remove nitrogen and phosphorous. Because nutrient removal is important, the impact on biological nutrient removal was evaluated. Three different configurations were used for the study: Modified Ludzack-Ettinger (MLE), membrane bioreactors (MBR), and integrated fixed film activated sludge (IFAS).

Biological nitrogen removal involves two steps; nitrification and denitrification. Nitrification converts ammonia first to nitrite (Eq. 1) and then to nitrate (Eq. 2).

$$2NH_4^+ + 3O_2 \rightarrow 2NO_2^- + 4H^+ + 2H_2O \quad (1)$$

$$2NO_2^- + O_2 \rightarrow 2NO_3^- \quad (2)$$

There are two groups of autotrophic organisms responsible for these conversions. The first step (Eq. 1) is carried out by ammonia oxidizing bacteria (AOB) and the second step (Eq. 2) by nitrite oxidizing bacteria (NOB). These autotrophic organisms require aerobic conditions; typically dissolved oxygen (DO) concentrations of about 1.5–2.0 mg/L. They are slow growing organisms and sensitive to low temperatures, as temperature decreases so does their growth rate.

Denitrification is the biological conversion of nitrate to nitrogen gas (Eq. 3) which uses facultative heterotrophic organisms and requires an anoxic environment. The anoxic environment must have DO concentrations less than 0.3 mg/L and the presence of nitrate. Nitrification must occur in order for denitrification to occur. If a treatment plant cannot nitrify because of process constraints or influent characteristics, then it will be unable to remove nitrogen.

$$2NO_3^- + 10e^- + 12H^+ \rightarrow N_2 + 6H_2O \quad (3)$$

Earlier work by Hu et al. (2004) studied the degree of nitrification inhibition by silver nanoparticles found that nitrifying bacteria are especially susceptible to inhibition by silver nanoparticles and the accumulation of silver could have detrimental effects on wastewater treatment. The intrinsic slow growth of the autotrophic nitrifying bacteria and their high sensitivity to environmental perturbations often result in cell growth inhibition by toxic chemicals. Other work sought to determine size-dependent inhibition by Ag nanoparticles and evaluate the relationship between the inhibition and reactive oxygen species (ROS). The researchers observed that inhibition to nitrifying organisms correlated with the fraction of AgNPs <5 nm in the suspension. It appeared that these size nanoparticles could be more toxic to bacteria than any other fractions of nanoparticles or their counterpart bulk species. This research evaluated the role of sulfide and ligand strength in controlling nanosilver toxicity to nitrifying bacteria that are important in wastewater treatment. They found that sulfide appeared to be the only ligand to effectively reduce nanosilver toxicity.

giovanni.libralato@unina.it

2 Experimental Conditions

To evaluate the impact of silver nanoparticles on wastewater treatment and nitrogen removal, three lab-scale bioreactors were considered using MBR, IFAS, and MLE, respectively. These bioreactors presented similar configurations. Each bioreactor had three baffled chamber compartments: an influent basin followed by an aerobic basin, and further followed by an internal clarifier. The three reactors operated at the same hydraulic retention time (HRT = 1 day) and solids retention time (SRT = 20 days). Activated sludge from a treatment facility was inoculated into all reactors at the beginning of the operation. The feed synthetic wastewater was designed to represent domestic wastewater.

Microbial Growth and Inhibition Batch Test Aliquots of microbial cultures (60 mL) were collected from the bioreactor and the microbial growth rates were inferred from specific oxygen uptake rate measurements using a batch extant respirometric assay. Each test was done in triplicate. The biomass suspensions were amended with AgNPs at final total Ag concentrations of 0–6.9 mg/L. The biomass suspensions were aerated with pure oxygen gas before NH_4^+–N (10 mg N/L as NH_4NO_3) was added. A decrease in DO level in the respirometric vessel due to nitrification was measured by a DO probe (YSI model 5300A, Yellow Springs, OH) and continuously monitored at 4 Hz by an interfaced personal computer. The inhibition of nitrifying bacterial growth, or nitrification inhibition, was inferred from the difference between the measured specific oxygen uptake rate (SOUR control) in the absence and presence (SOUR sample) of Ag species, as reported earlier (Choi et al. 2009).

Shock Load Experiment of AgNPs in Activated Sludge Systems A shock loading event was simulated to determine the impact of an accidental release of nanosilver from industrial activities. To assess how activated sludge responds to exposure of a shock loading of silver nanoparticles in activated sludge systems, the freshly prepared silver nanoparticles were applied to the aeration basin of the MLE bioreactor. The shock load lasted for 12 h during which a prepared AgNP stock suspension at a concentration of $\sim$20 mg/L was separately and continuously added into the aeration basin at a constant flow rate. The concentration of prepared.

AgNPs and the flow rate were chosen so that a target of total silver concentration of 1 mg/L in the MLE bioreactor at the end of dose was negligible compared to the influent feed rate, based on the mass balance analysis and the flow rate containing AgNPs.

During and after shock loading of AgNPs the effluent samples of the MLE bioreactor were periodically collected for analysis. Before and after shock loading, aliquots of biomass were periodically taken from the aeration basin of the MLE bioreactor for the measurements of autotrophic and heterotrophic microbial activities inferred from the SOUR by the batch extant respirometric assay.

During and after the shock loading, aliquots (20 mL) of the mixed liquor samples were taken and biomass was separated. Total silver concentrations were determined in the biomass phase. The reactor effluent samples were periodically

giovanni.libralato@unina.it

taken to measure the total silver concentrations in aqueous phase. Both total and dissolved silver (ions and colloids) were determined in mixed liquor suspended solids (MLSS) and wastewater effluent.

TEM Analysis of AgNPs Treated Bacteria Transmission electron microscopy (TEM) was used to study bactericidal action of nanosilver to *E. coli* and nitrifiers.

Nitrifying Bacterial Community Analysis Terminal Restriction Fragment Length Polymorphism (T-RFLP) was used to analyze nitrifying bacterial community in the MLE bioreactor based on the known 16S rRNA genes of ammonia-oxidizing bacteria and nitrite oxidizing bacteria as described in a previous study (Siripong and Rittmann 2007).

Nanosilver Synthesis and Characterization The freshly prepared nanoparticle suspensions contained roughly 50/50 of Ag^{+} and AgNPs and almost complete AgNPs by adding NaBH4 at the concentrations of 0.14 and 0.7 mM, respectively. The nanosilver suspensions having an average particle size of 15–21 nm (via TEM analysis) were characterized as described earlier (Choi et al. 2009). The results from TEM were generally consistent with those by dynamic light scattering (DLS) showing peak particle sizes of 25–29 nm (Fig. 2).

3 Results

Bioreactor Performance COD was used instead of BOD throughout these studies as the measurement for organic compounds in the wastewater. During the start-up phase, COD was removed in all three reactors (MBR, MLE and IFAS). For all three bioreactors, the average influent COD was maintained at 327 ± 54 mg/L. After the start-up phase, the influent COD level was increased to a new target value of

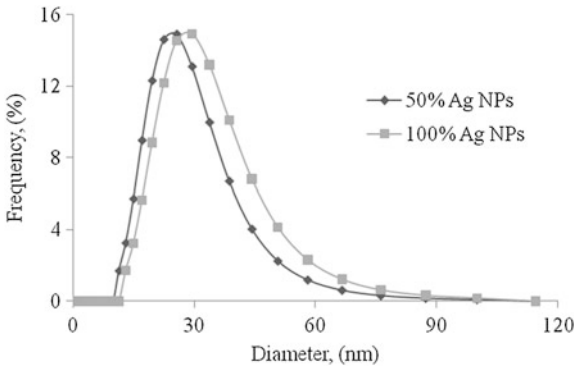

Fig. 2 Particle size analysis of the two types of nanosilver suspensions by dynamic light scattering. The freshly prepared nanoparticle suspensions contained roughly 50/50 of Ag+ and AgNPs (e.g., 50% AgNPs), and AgNPs (100% AgNPs, *filled square*). The average particle sizes were 29 and 25 nm for 100% AgNPs and 50% AgNPs, respectively

giovanni.libralato@unina.it

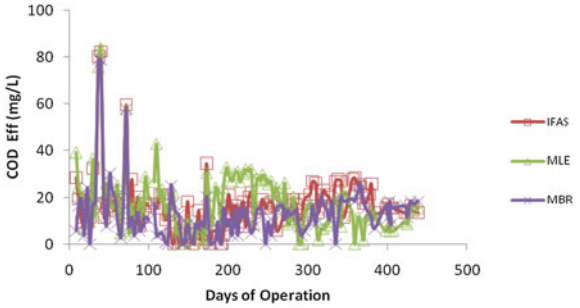

Fig. 3 Influent and effluent COD

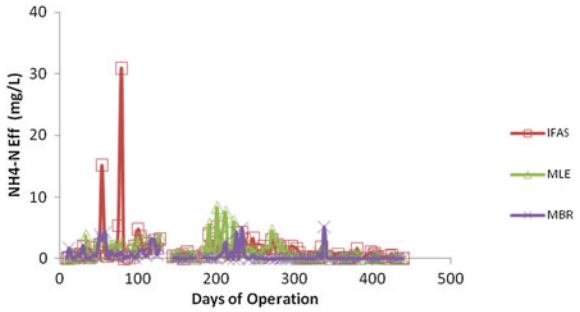

Fig. 4 Influent and effluent NH_4–N

500 mg/L from day 65 onwards. COD was still efficiently removed in all three reactors. For the three bioreactors, influent COD was maintained at an average of 523 ± 89 mg/L. The average effluent COD concentration of MBR was 10 ± 10 mg/L corresponding to a 98% COD removal rate. For the IFAS, the average effluent COD was 13 ± 12 mg/L, with an overall removal efficiency of 97%. In the MLE reactor, the average effluent COD was 15 ± 12 mg/L and the COD removal efficiency was 97% (Fig. 3).

The average effluent NH_4^+−N concentration was less than 1 mg/L and an average removal efficiency of 97% was achieved in the three systems Fig. 4. Most of influent ammonium concentration was converted to nitrate in the effluent, indicating efficient nitrification.

Effluent nitrate concentration was determined throughout the test period (Fig. 5). During the start-up phase, in the MLE reactor, the total nitrogen (TKN plus nitrate and nitrite) removal efficiency was 40%, indicating partial denitrification. This was likely due to the recirculation of the mixed liquor from the aeration basin to influent chamber of the MLE bioreactor. The MBR system also showed partial total nitrogen removal (30%) for the same reason.

For the IFAS system the total nitrogen removal efficiency was only 10%, possibly because no recirculation was provided in the IFAS.

During the period of study, no biofilm was formed on the plastic media and the mechanism of simultaneous nitrification and denitrification was unlikely established. From day 65 onwards, in the MLE reactor, the total nitrogen removal

giovanni.libralato@unina.it

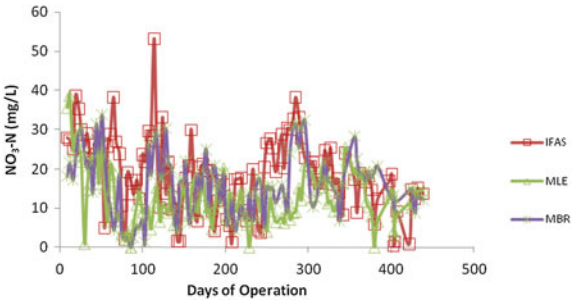

Fig. 5 Influent and effluent NO_3–N

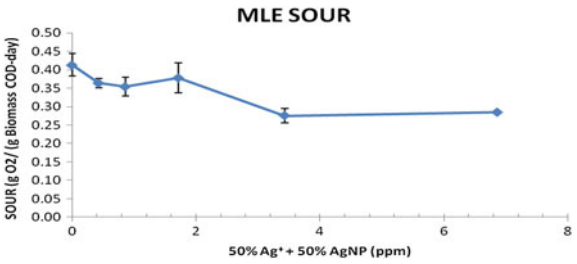

Fig. 6 Effect of AgNPs on bacterial growth rate inferred from specific oxygen uptake rate measurements. Biomass was taken from the MLE reactor with an average biomass concentration of 2258 Mg/L COD. *Error bars* represent one standard error of the mean (n = 4)

efficiency increased to 58, 57, and 24% for the MLE, MBR, and IFAS bioreactor, respectively.

Batch Nanosilver Inhibition Study The effect of silver nanoparticles on autotrophic microbial activities of biomass from the MLE reactor was quantified using an extant respirometric assay. The results showed the SOUR rates decreased with increasing AgNP concentration after the bacteria were exposed to a mixture of Ag^+ and AgNPs (50/50 in mass ratio) demonstrating that AgNPs inhibited autotrophic microbial activities at low silver concentrations (Fig. 6).

Nitrification was inhibited (11.5%) at the total silver concentration of 0.4 mg/L. However, the maximum inhibition was about 38% at 6.9 mg/L total Ag (Fig. 7). The inhibition by AgNPs did not follow a linear relationship with Ag concentration, likely due to the complexation of Ag^+ with anions such as Cl^- present in wastewater (Choi et al. 2009). The result is not unexpected because interaction of AgNPs with bacteria influences AgNP toxicity, which is mediated by Ag^+ (Navarro et al. 2008).

Shock loading of Nanosilver in MLE Reactor The total silver concentrations in mixed liquor of the aeration basin and in wastewater effluent were increased. At the end of AgNP shock loading, the total silver concentrations in MLSS and effluent reached the peak values of 0.75 and 0.046 mg Ag/L (close to detection limit), respectively (Fig. 7).

giovanni.libralato@unina.it

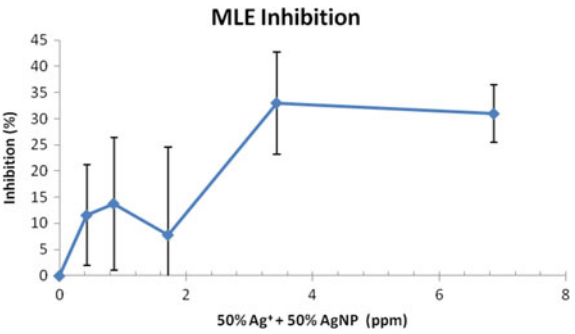

Fig. 7 Nitrification inhibition by AgNPs in the MLE system. Biomass was taken from the MLE reactor with an average biomass concentration of 2258 mg/L COD. *Error bars* represent one standard error of the mean

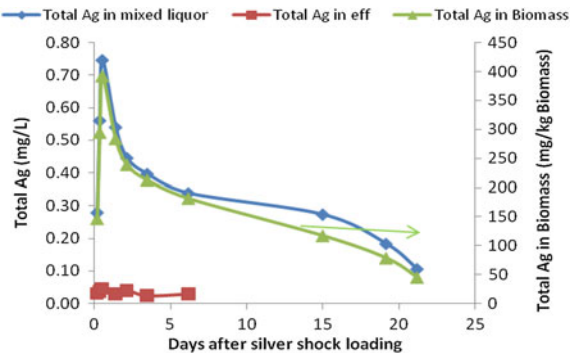

Fig. 8 Total silver concentrations in mixed liquor and wastewater effluent of the MLE reactor during and after 12-h nanosilver shock loading

The total silver concentration in wastewater effluent after passing 1000 MW cut-off membrane was the same as that in the effluent with no filtration, indicating that all AgNPs (initial average size = 15–21 nm) were likely retained by activated sludge in the MLE bioreactor. The results indicated that approximate 5% of the total silver dosed in the system existed as soluble forms in wastewater effluent, most likely in the form of silver ions that were released from the silver nanoparticles adsorbed to the biomass (Fig. 8).

After stopping the 12 h AgNP shock loading, the total silver concentration in the MLSS phase decreased exponentially, while the total silver concentrations in wastewater effluent remained relatively constant in the next 7 days, indicating a slow and continuous silver ion release from AgNP dissolution. About 22 days after shock loading, there was still some Ag accumulation (<0.1 mg/L) in the mixed liquor. It was predicted that after 25–30 days the silver nanoparticles in the biomass would be washed out in the continuous flow MLE system.

There was no significant difference between the COD concentrations in the effluent of MLE before and after nanosilver shock loading Fig. 9. This was confirmed by the heterotrophic microbial activity measurements before and after silver nanoparticles shock loading. The heterotrophic SOUR values before and after AgNPs shock loading were similar (Fig. 10). At the onset of nanosilver shock loading, the effluent ammonium concentration appeared to increase (Fig. 11) while

giovanni.libralato@unina.it

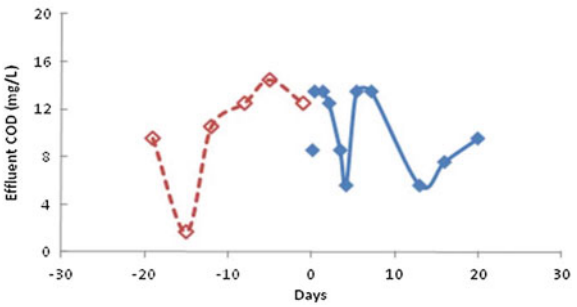

Fig. 9 Effluent COD concentration in MLE reactor before (*red*) and after (*blue*) nanosilver shock loading

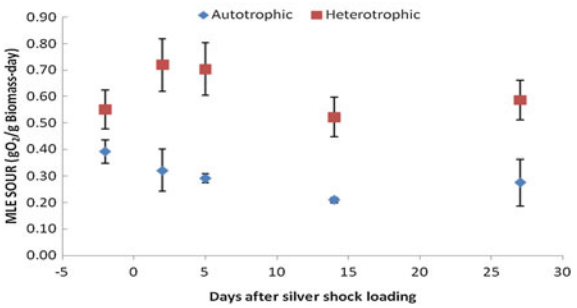

Fig. 10 Autotrophic (*blue*) and heterotrophic (*red*) activities inferred from SOUR measurements in the MLE reactor before and after nanosilver shock loading. *Error bars* represent one standard error of the mean (n = 4)

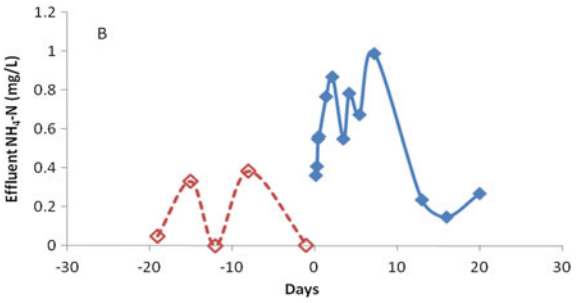

Fig. 11 Effluent ammonium concentration in the MLE reactor before (*red*) and after (*blue*) nanosilver shock loading

the nitrate concentration in the effluent was correspondingly decreased (Fig. 12). After 2 days, the effluent ammonium concentration reached the peak value and then decreased gradually. This trend indicated that a shock loading of silver nanoparticles inhibited nitrification, as it was also indicated from the slight accumulation of nitrite in wastewater effluent starting one day after the shock loading (Fig. 13). Results of the autotrophic microbial activities (Fig. 10) further confirmed that nitrification was inhibited after shock loading. After the shock loading, the autotrophic SOUR values appeared to decrease. The recovery of nitrification activity was slow, which took more than 25 days of silver shock loading after the majority of the silver nanoparticles in biomass were washed out.

giovanni.libralato@unina.it

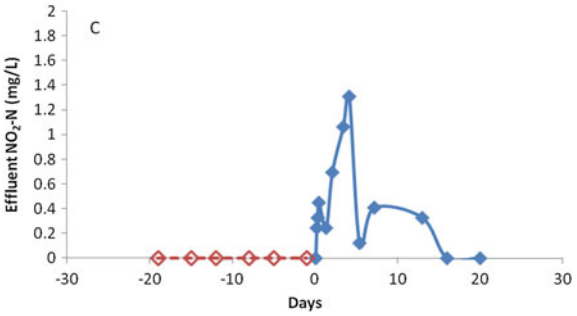

Fig. 12 Effluent nitrite concentration in the MLE reactor before (*red*) and after (*blue*) nanosilver shock loading

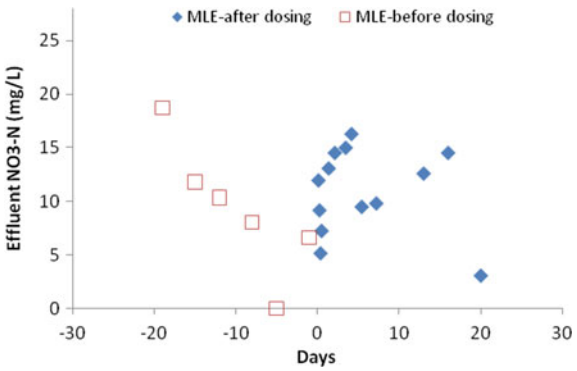

Fig. 13 Effluent nitrate concentration in the MLE reactor before and after nanosilver shock loading

T-RFLP analysis indicated the difference of nitrifying bacterial community structure in the MLE tanks before and after treatment with AgNPs. Before nanosilver shock loading, *Nitrosomonas* was the dominant genus of ammonia-oxidizing bacteria while *Nitrospira* and *Nitrobacter* species were dominant among nitrite-oxidizing bacterial populations in the MLE. In contrast, there was a substantial decrease in the AOB population after nanoparticle shock loading. *Nitrobacter* population was not detected and *Nitrospira* peak size reduced considerably after nanosilver treatment. Therefore, it appeared that the higher nitrifying activities might be correlated with more diversity of nitrifying bacterial populations in the MLE before silver nanoparticles shock loading. Introduction of silver nanoparticles resulted in an adverse effect on nitrifying bacterial population. The results of T-RFLP analysis showed that the decrease of population size in *Nitrosomonas,* non-detection of *Nitrobacter* species and population size reducing of *Nitrospira* could account for relative late recovery of NOB microbial activity as inferred from prolonged nitrite accumulation after shock loading of silver nanoparticles.

giovanni.libralato@unina.it

4 Conclusions

The bacterial responses to nanosilver exposure were evaluated in this study by monitoring the change of reactor effluent water quality, heterotrophic and autotrophic bacterial activities and nitrifying bacterial community structure.

- At a concentration of 0.4 mg/L total Ag, AgNPs presented in a mixture of Ag^+ and AgNPs (average size = 15–21 nm) inhibited nitrification by 11.5%.
- A 12 h period of AgNP shock loading to the MLE system resulted in the peak total silver concentration of 0.75 mg Ag/L in the MLE reactor. The continuous flow-through model indicated that the total silver including AgNPs in the activated sludge phase would be washed out after 25 days.
- After the nanosilver shock loading, nitrification was inhibited by about 50% and a slight accumulation of nitrite concentration in wastewater effluent was observed. There was no inhibition on heterotrophic activity or the removal of organic matter in the MLE activated sludge system.
- Nitrification inhibition after nanosilver shock loading was consistent with a shift or loss of nitrifying population in the MLE reactor. The ammonium-oxidizing bacteria had experienced the decrease of population size after 12 h nanosilver exposure, while for NOB, *Nitrobacter* was lost and *Nitrospira* experienced a similar decrease in population size.

References

Adams LK, Lyon DY, Alvarez PJJ (2006) Comparative eco-toxicity of nanoscale TiO_2, SiO2, and ZnO water suspensions. Water Res 40:3527–3532

Benn TM, Westerhoff P (2008) Nanoparticle silver released into water from commercially available sock fabrics. Environ Sci Technol 42:4133–4139

Choi OK, Hu ZQ (2008) Size dependent and reactive oxygen species related nanosilver toxicity to nitrifying bacteria. Environ Sci Technol 42:4583–4588

Choi OK, Deng K, Kim NJ, Ross L, Surampalli YR, Hu ZQ (2008) The inhibitory effects of silver nanoparticles, silver ions, and silver chloride colloids on microbial growth. Water Res 42:3066–3074

Choi OK, Clevenger TE, Deng BL, Ross L, Surampalli YR, Hu ZQ (2009) Role of sulfide and ligand strength in controlling nanosilver toxicity. Water Res 43:1879–1886

Hu Z (2010) Impact of silver nanoparticles on wastewater treatment. Water Environment Research Foundation

Hu Z, Chandran K, Grasso D, Smets BF (2004) Comparison of nitrification inhibition by metals in batch and continuous flow reactors. Water Res 38(18):3949–3959

Kim JS, Kuk E, Yu KN, Kim JH, Park SJ, Lee HJ, Kim SH, Park YK, Park YH, Hwang CY, Kim YK, Lee YS, Jeong DH, Cho MH (2007) Antimicrobial effects of silver nanoparticles. Nanomed-Nanotechnol Biol Med 3:95–101

Kloepfer JA, Mielke RE, Nadeau JL (2005) Uptake of CdSe and CdSe/ZnS quantum dots into bacteria via purine-dependent mechanisms. Appl Environ Microbiol 71:2548–2557

Levine AD, Tchobanoglous G, Asano T (1991) Size distributions of particulate contaminants in waste-water and their impact on treatability. Water Res 25:911–922

giovanni.libralato@unina.it

Lin WS, Huang YW, Zhou XD, Ma YF (2006) In vitro toxicity of silica nanoparticles in human lung cancer cells. Toxicol Appl Pharmacol 217:252–259

Metcalf E, Eddy HP (2013) Wastewater engineering treatment, disposal and reuse, 5th edn. McGraw-Hill, New York

Morones JR, Elechiguerra JL, Camacho A, Holt K, Kouri JB, Ramirez JT, Yacaman MJ (2005) The bactericidal effect of silver nanoparticles. Nanotechnology 16:2346–2353

Navarro E, Piccapietra F, Wagner B, Marconi F, Kaegi R, Odzak N, Sigg L, Behra R (2008) Toxicity of silver nanoparticles to *Chlamydomonas reinhardtii*. Environ Sci Technol 42:8959–8964

Nel A, Xia T, Madler L, Li N (2006) Toxic potential of materials at the nanolevel. Science 311:622–627

Shafer MM, Overdier JT, Armstong DE (1998) Removal, partitioning, and fate of silver and other metals in wastewater treatment plants and effluent-receiving streams. Environ Toxicol Chem 17:630–641

Siripong S, Rittmann BE (2007) Diversity study of nitrifying bacteria in full-scale municipal wastewater treatment plants. Water Res 41:1110–1120

Stumm W, Morgan JJ (1996) Aquatic chemistry: chemical equilibria and rates in natural waters, 3rd edn. Wiley, New York

Wang JM (2003) Interactions of silver with wastewater constituents. Water Res 37:4444–4452

giovanni.libralato@unina.it

Environmental Effects of nZVI for Land and Groundwater Remediation

G. Libralato, A. Costa Devoti, A. Volpi Ghirardini and D.A.L. Vignati

Abstract The development of nanostructured materials enable the upgrade of traditional treatment with macro- and micro-sized iron. Nano-zerovalent iron (nZVI) present interesting characteristics like high surface-area-to-volume ratio, levels of stepped surface, and surface energies. nZVI is typically made of 5-40 nm sized Fe^0/Fe-oxide particles and can rapidly transform many environmental contaminants into less harmful products (e.g. dehalogenation or metal reduction) being promising as an in situ remediation agent. We present the state-of-the-art of nZVI based treatment technologies considering their environmental and (eco-)toxicological implications.

Keywords Land remediation · nZVI · Dehalogenation · Reduction · Ecotoxicology

1 Main Characteristics and Applications of nZVI

Nanotechnology is one of the fastest growing sectors of the high-tech economy, with more than 800 consumer products using nanomaterials (NMs) with personal, commercial, medical, and military uses (http://www.nanotechproject.org/cpi/). The term nanoparticle (NP) is generally used to refer to a small particle with at least two

G. Libralato (✉)
Department of Biology, University of Naples Federico II,
Complesso Universitario di Monte S. Angelo, Via Cinthia ed. 7,
80126 Naples, Italy
e-mail: giovanni.libralato@unina.it

G. Libralato · A. Costa Devoti · A. Volpi Ghirardini
Department of Environmental Sciences, Informatics and Statistics,
University Ca' Foscari Venice, Via Torino, 155, 30172 Mestre-Venice, Italy

D.A.L. Vignati
LIEC UMR 7360, CNRS and Université de Lorraine,
8, rue du Général Delestraint, 57070 Metz, France

© Springer International Publishing AG 2017

G. Lofrano et al. (eds.), *Nanotechnologies for Environmental Remediation*,
DOI 10.1007/978-3-319-53162-5_10

giovanni.libralato@unina.it

dimensions <100 nm. The small size and large surface area per unit mass reveal characteristics that can be useful in hazardous waste site remediation and contaminant removal such as in the case of nano-zerovalent iron (nZVI). This type of material has a wide use in land and groundwater applications. The power of iron-based technologies in remediation activities is widely known due to the ability of this metal to act as a reductant (Elliott and Zhang 2001) or sorbent (Liu et al. 2014) for soil contaminants.

Over the past decade the development of nanostructured materials has led to the upgrade of traditional treatment with macro- and micro-sized iron (Kim et al. 2010). The introduction of nano-scale is explained from physical characteristics: nano-metals have high surface-area-to-volume ratio, high levels of stepped surface, and high surface energies. Particularly, nZVI can remove contaminants through reduction, oxidation, adsorption, precipitation or co-precipitation (Yang et al. 2013). Since the conventional micro-sized ZVI (mZVI) has low reactivity towards lightly chlorinated hydrocarbons, Wang and Zhang (1997) pioneered the application of nZVI for environmental remediation. Due to its unique properties, nZVI is able to effectively eliminate or neutralize certain recalcitrant pollutants that can be found in contaminated soils and groundwater. nZVI particles are typically 5–40 nm sized Fe^0/Fe-oxide particles and can rapidly transform many environmental contaminants into less harmful products being promising as an in situ remediation agent. Due to its small size and increased reactivity, nZVI has the potential to be more effective than mZVI that is already in use for contaminant remediation in soil and groundwater aquifers. However, little information is known about the environmental fate of nZVI once it has undergone biological and non-biological processes within a contaminated aquifer. For this reason, it is important to find out what are the possible impacts of these NMs once they enter the environment and how they could potentially affect human health or the ecosystem. Despite these concerns, nZVI technology and its application seem a very promising, efficient and cost-effective method for remediating contaminated soil and groundwater aquifer sites (Lee et al. 2014).

The scale of soil and groundwater contamination is enormous and its complexity seemingly intractable. In the US, more than 1500 sites have been put on the Superfund list (Zhang 2003), but less than one third of them have been cleaned up in the past decade. In Italy, 39 sites of national interest (in 2013) and other 12,943 local sites affected from low to extremely high levels of contamination are waiting for some kind of remediation (MinAMb 2015). Agricultural soil is decreasing both in terms of quantity and quality. The problem of water scarcity, which from a strictly economical point of view translates into higher costs for clean water and wastewater treatment (WWT) due to the higher technological effort necessary, is not solely restricted to developing countries in dry areas, but it is also of high concern for developed countries worldwide (e.g., in some states of the USA such as California, Arizona, New Mexico, or Australia, India and Europe). In the EU, 44% of freshwater abstraction is used for cooling in energy production, 24% for agriculture, 21% for public water supply, and 11% for industry, even though geographical differences exist in the destination use (Hussain et al. 2002).

giovanni.libralato@unina.it

The average cost for cleaning up a Superfund site has been reported to be more than 25 million dollars. According to USEPA, over 418,000 underground storage tank (UST) leakages had been confirmed as of September 30, 2001. While much work has been and continues to be done, there are still about 150,000 UST sites remaining to be cleaned up (Zhang 2003). The numbers of other contaminated sites such as abandoned mining sites, landfills, and industrial sites are just as staggering. If \$100/ton or \$100/m^3 (a commonly used yardstick by consultants) is needed to clean up the contaminated soil and/or water, the aggregated financial burden for site cleanup is truly colossal. Thus the problem of land as well as water contamination is extremely challenging.

ZVI iron has been used successfully in the past to remediate groundwater by construction of a permeable reactive barrier (PRB) intercepting and dechlorinating chlorinated hydrocarbons such as trichloroethylene (TCE) in groundwater plumes (Lee et al. 2014). Currently, ZVI (micro and macro-scale) is used in PRBs for contaminated sites' remediation. Commonly, a PRB contains granular iron as the reactive medium degrading chlorinated organics into potentially non-toxic dehalogenated organic compounds and inorganic chloride. In its simplest form, a PRB is a trench built across the flow path of a groundwater plume. The trench is filled with a suitable reactive or adsorptive medium capable of removing contamination from the groundwater and protecting down gradient water resources or receptors. Despite their minuscule status, nanoscale particles may hold the potential to cost-effectively address some of the challenges of site remediation (Masciangioli and Zhang 2003; Zhang 2003; Libralato et al. 2016). Two factors contribute to NPs' capabilities as an extremely versatile remediation tool. Microscale ZVI (granular ZVI) has been used as a treatment reagent for in situ groundwater remediation for many years, in particular within permeable reactive barriers (NATO 1998). nZVI is a type of iron NP that has been already injected in situ as a groundwater and aquifer treatment. Whilst the possibility of unique characteristics gives nZVI promise for beneficial applications, it is simultaneously a cause of concern, as there is a degree of uncertainty with regards to particle behavior, fate and toxicity. As produced, most nZVI tested falls into the 10–100 nm size range (Nurmi et al. 2005), although it tends to agglomerate to form larger particles.

In 2000, the first documented field trial of nZVI involved treatment of TCE in groundwater at a manufacturing site in Trenton (New Jersey, USA) (Elliott and Zhang 2001). Several commentators anticipated that nZVI technology would take off rapidly because of its perceived benefits such as rapid and complete contaminant degradation. In 2007, a European report forecast that the 2010 world market for environmental nanotechnologies would be around \$6 billion (Rickerby and Morrison 2007), but in practice, at present, this market has not been achieved. To date, the use of nZVI in remediation is largely a niche application for chlorinated solvents in aquifers, competing with more established techniques such as in situ bioremediation, chemical reduction and granular ZVI. Lee et al. (2014) reviewed 60 field applications worldwide. Bardos et al. (2015) identified about 70 projects around the world at pilot or full scale. Within the identified case studies, only 17 were in Europe (Czech Republic, Germany and Italy) focusing mainly on the

giovanni.libralato@unina.it

degradation of chlorinated solvents for plume (i.e. pathway interruption) management although pilot studies have also demonstrated successful treatment of benzene, toluene, ethylbenzene and xylene (BTEX), perchlorates, hexavalent chromium, diesel fuel, polychlorinated byphenyls (PCBs) and pesticides. O'Carroll et al. (2013) detailed the chemical processes involved in the treatment of chlorinated solvents and various metals by nZVI. Several approaches can be taken to NP deployment for contaminant remediation, including direct injection. The limited adoption of nZVI is linked to uncertainty over the balance of benefits versus risks from NP use in remediation. Additional factors that are likely to have hindered the development of nanoremediation market are its cost compared to other technologies and its social acceptance. The latter has been a particular impediment to the adoption of nZVI because of a heightened perception of risk of nanotechnology's use amongst the public and other stakeholders including landowners (Bardos et al. 2015). Process based remediation techniques seen as "new" within a particular jurisdiction have historically encountered significant market barriers and required verified field based performance data to gain widespread regulatory and market acceptance. It is not unusual for such evidence to be demanded by regulators and landowners for specific conditions encountered or perceived in their country. Given the heightened perception of potential risks from NPs in the environment, as well as the limited evidence base related to nZVI use in the field, particularly for its modified forms, it is likely that a higher burden of proof will be required by regulators prior to permitting of nZVI based in situ remediation techniques, compared with other in situ remediation techniques.

Although the establishment of nanoremediation market has been slow, there are a number of initiatives and development opportunities to expand its uptake. The use of nZVI instead of using micro/macro-scale Fe^0 materials could potentially eliminate the need for using PRBs and be more effective in both cost feasibility and contaminant remediation. Laboratory studies indicated that a wider range of chlorinated hydrocarbons may be dechlorinated using various nanoscale iron particles, including chlorinated methanes, ethanes, benzenes, and potentially, PCBs, some pesticides, heavy metals, and dyes (EPA 2007). Several factors play a role in determining a nanoscale iron product's reactivity, including particle size, reactive surface area, the presence or absence of hydrogenation catalysts (e.g., palladium), the method of manufacture, the morphology of the particle (porosity), its crystalline structure, impurities and coating, and whether or not particles have been exposed to acid washing (Dupont Chemicals 2007). nZVI can be distributed into the subsurface using a variety of carrying fluids; water, nitrogen gas, and vegetable oil being the most commonly used. Slurries of water and nZVI powder can be injected into the contaminated zone using nitrogen gas as a carrier. This helps the iron powder dispersal in the subsurface and creates contact between contaminants and iron. Alternatively, nZVI can be mixed with vegetable oil and water to create an emulsion, which is then injected into the contaminant zone (ESTCP 2006).

Bare nZVI is composed of a core, which consists primarily of zerovalent or metallic iron while the mixed valence (i.e., Fe(II) and Fe(III)) oxide shell is formed as a result of oxidation of the metallic iron. Iron typically exists in the environment

giovanni.libralato@unina.it

as iron(II)-and iron(III)-oxides, and as such, ZVI is a manufactured material. Thus far, applications of ZVI have focused primarily on the electron-donating properties of nZVI. Under ambient conditions, nZVI is fairly reactive in water and can serve as an excellent electron donor, which makes it a versatile remediation material (Stumm and Morgan 1996). According to the core-shell model, the mixed valence iron oxide shell is largely insoluble under neutral pH conditions and may protect the ZVI core from rapid oxidation. A report by Tratnyek and Johnson (2006) stated that the greater reactivity that is often ascribed to NPs can be the result of larger overall surface area, greater density of reactive sites on the particle surfaces, and/or higher intrinsic reactivity of the reactive surface sites. Together, these factors have produced three operationally distinct results for nZVI: (i) degradation of contaminants that do not react detectably with larger particles of similar material (e.g., PCBs); (ii) more rapid degradation of contaminants that already react at useful rates with larger particles (e.g., chlorinated ethylene); or (iii) more favorable products from contaminants that are rapidly degraded by larger materials, but that yield undesirable by-products (e.g., carbon tetrachloride) (Tratnyek and Johnson 2006). Elemental iron slowly oxidizes to ferrous iron and releases two electrons. These electrons begin to function in a variety of reactions that lead to the transformation of target contaminants as reported in Fig. 1. It is intended that toxic contaminants (e.g., TCE, trichloroethylene) would be reductively dechlorinated to an essentially non-toxic mixture of ethane, ethene, and acetylene. nZVI works best under anaerobic conditions, especially in the case of beta-elimination reactions. Decreased dissolved oxygen (DO) and oxidation-reduction potential levels (ORP) (≤ -400 mV) are ideal conditions to facilitate target contaminant degradation (USEPA 2005b). ORP depends on the transfer of electrons between chemical species and determines the reduction potential of an aqueous solution. Like pH, the reduction potential represents an intensity factor. Reduction potential measurement is useful as an analytical tool in monitoring changes in an aqueous system rather than determining their absolute value.

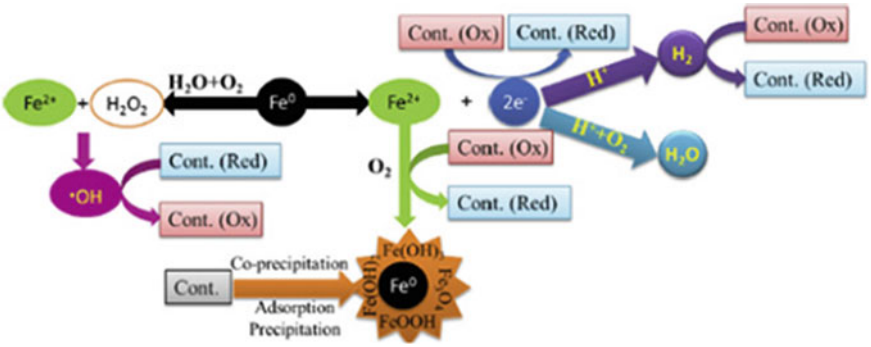

Fig. 1 Illustration of the major reactions occurring in the Fe^0/H_2O system and the mechanisms of contaminants removal. Reproduced from Guan et al. (2015)

giovanni.libralato@unina.it

With regard to the interaction between NPs and biota, it was observed that some NMs that enter animal tissues may be able to pass through cell membranes or cross the blood-brain barrier. This may be a beneficial characteristic for such uses as targeted drug delivery and other disease treatments, but could result in unintended impacts in other uses or applications. Inhaled NPs may become lodged in the lung or be translocated, and the high durability and reactivity of some NMs raise issues about their fate in the environment (Lockman et al. 2004). At present, not enough information exists to assess environmental exposure for most engineered NMs. This information is important because governments will need a sound scientific basis for reducing/limiting/avoiding unforeseen future impacts resulting from the introduction of NPs and NMs into the environment. A NMs risk assessment work sheet by the DuPont Chemical Company in 2007 stated that toxicity, human hazard, and environmental fate and effects data available from potential suppliers of nZVI are highly variable in both quality and completeness. It also stated that, in many cases, it is not clear from the information provided whether the Environmental Health and Safety (EHS) data are based on nZVI or on larger sized iron powder. Typical warnings include: (i) Skin irritation; (ii) Eye irritation; (iii) Harmful if inhaled—irritating to mucous membranes and upper respiratory tract; (iv) May be harmful if swallowed. Large doses will produce a laxative effect; (v) Toxicological properties have not been thoroughly investigated; (vi) Dissolved iron and manganese concentrations in groundwater may increase. nZVI that is released into the air in the form of particulate matter could cause the first three aforementioned effects (i–iii). Particulate matter triggers an acute inflammatory response in lungs, thus stimulating the secretion of cytokines, chemokines, reactive oxidation species (ROS), and transcription factors (Gwinn and Vallyathan 2006). Naturally occurring and engineered NPs can remain airborne over a long period because of the small size and light weight (Biswas and Wu 2005). Therefore, an increased likelihood that they will travel long distances, and interact with gases and other airborne particles is possible. When considering the fact that most NPs are suspended in some type of liquid, surfactant medium, or pumped directly into the soil and water for contaminated groundwater remediation purposes, this may not be an important factor. Several studies are currently available on nZVI (eco)toxicological effects (Bardos et al. 2015; Libralato et al. 2016), but just few studies took into consideration field concentrations and the effects on environmental matrices post-treatment.

Currently, the advantages of nZVI over mZVI for aqueous contaminants removal are as follows (Comba et al. 2011): (1) some aqueous contaminant species that have been proven unsuccessful for remediation using mZVI can be effectively removed using nZVI because of its large reactive surface area, (2) nZVI can be used for more rapid degradation of contaminants, (3) the formation of some undesirable by-products during remediation using mZVI can be avoided by using the more reactive nZVI, resulting from a more complete degradation of pollutants, and (4) injecting nZVI to the source of contamination is believed to be faster and more effective for groundwater treatment than either the pump-and-treat or PRB methods (USEPA 2005a).

giovanni.libralato@unina.it

Despite the potential for the use of manufactured NPs, there are still particular concerns that must be addressed in regard to the effectiveness, application and safety of this new technology. These issues include (i) the mobility of NPs under subsurface conditions; (ii) the kinetics and products of contaminant degradation by nZVI; (iii) whether the nZVI maintains its reactivity during the time period of treatment; (iv) human (occupational exposure) and environmental health (fate and effects of nZVI after the treatment).

1.1 Tools in Nanoremediation

Nanoremediation is supported by a growing number of nFe^0 based engineered NPs including bare nZVI, bimetallic NPs associated nFe with other elements and Fe NPs coated with various biopolimers. The first work about nZVI was published by Wang and Zhang (1997) reporting an efficient method of synthesizing nanoscale iron and palladized iron particles and evidences about their use for the elimination of TCE as reported in Fig. 2. The first pilot tests about the use of nZVI were conducted in the summer of 2000 in Trenton (USA) for the purification of groundwaters contaminated with TCE, tetrachloroethylene (PCE), vinyl chloride (VC), and chloroform. Approximately, 1.7 kg of modified Pd/nZVI was applied at an average concentration of 1.125 g/L. After four weeks of remediation a 96.5% reduction of chloroorganic contaminants was obtained (Elliott and Zhang 2001).

1.2 Environmental Behavior

The environmental behavior of NPs and NMs is controlled by their intrinsic physico-chemical properties, the specific modifications of native NPs to allow for

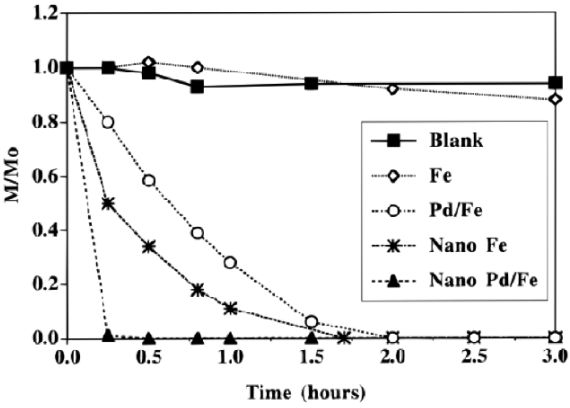

Fig. 2 Degradation kinetics of TCE using commercial Fe powders (Fe), Pd-modified commercial Fe powders (Pd/Fe), nanoscale Fe particles (nFe), and nanoscale Pd/Fe particles (nano Pd/Fe). Initial TCE concentration was 20 mg/L; metal to solution ratio was 2 g/100 mL. Reproduced from Whang and Zang (1997)

giovanni.libralato@unina.it

their desired uses and/or limit unwanted environmental impacts and their overall interactions with master environmental variables such as pH, ionic strength, redox conditions and composition of relevant environmental matrices (Park et al. 2016; Stefaniuk et al. 2016). The main use of nZVI being for the remediation of contaminated soils and groundwater (Lefevre et al. 2016), most research is currently devoted to understand their behavior in these two matrices. Indeed, contrary to the unwanted release of other NMs, nZVI is purposely introduced into the environment to react with contaminants. Understanding the reactions that nZVI will undergo under variable (realistic) scenarios is therefore necessary to maximize the efficiency of the intended remediation process while limiting uncontrolled long-distance transport and adverse effects to biota.

The complexity of real environmental settings and the specificity of contamination at various sites still prevent a unifying model of nZVI fate in the environment. However, available knowledge highlights some points of general validity that will serve to foster further responsible use of nZVI. NMs in the environment can undergo four main types of transformation (Lowry et al. 2012): chemical, physical, biological and transformations following interactions with macromolecules. These reactions control persistence, reactivity and bioavailability of NMs in the environments. It is noteworthy that some transformations (e.g., dissolution and release of toxic cations) will increase the environmental mobility and toxicity of metallic NMs, while other processes (e.g., adsorption onto natural organic matter) will have opposite effects. ZVI NPs are often specifically modified to increase their dispersion in the environment, limit their aggregation and slow down passivation in order to guarantee maximum efficiency for the intended remediation purposes at a specific site (Stefaniuk et al. 2016). However, the mechanism of contaminant removal by nZVI involves in itself the loss of the nano-character of nZVI (Peeters et al. 2016; Noubactep 2010). The commonly accepted mechanisms by which nZVI remove contaminants is via the oxidation of Fe(0) to Fe(II) with the concomitant reduction of the contaminant. Noubactep (2010) also points out the importance of adsorption processes following these initial steps by highlighting that Fe(II) is unstable under typical environmental conditions and tends to further oxidize to Fe(III) which then precipitates in the form of oxides or oxyhydroxides. As a consequence, the natural tendency of Fe(0) to oxidize to Fe(II), which is part of the cleaning action of nZVI, leads to the progressive loss of its nano-character. Apart from this behavior which is essentially linked to the intrinsic properties of nZVI (even in the presence of modifications), nZVI mobility can be further modified by specific environmental factors.

Dong et al. (2016) examined the effects of pH and fulvic acid concentration on the stability and reactivity of nZVI (synthesized using borohydride reduction) in a background electrolyte solution of 1 mM NaCl, which was considered as representative of groundwater conditions. An increase in pH from 5 to 7 units resulted in a faster sedimentation of nZVI, indicating enhanced aggregation. On the other hand, the sedimentation at pH 9 was similar to what was observed at pH 5. The effect of pH follows from the related changes in particle surface charge which varied from positive (pH = 5) to neutral (pH 7) and, eventually, negative (pH 9). The presence of particle charges augments the inter-particle repulsive forces, thus

giovanni.libralato@unina.it

increasing the stability of the nZVI suspension. However, aggregation was observed at all the examined pH values with about 80% of the nZVI particles having aggregated at pH 5 and 9 (almost 100% at pH 7) after 60 min from the preparation of the suspensions. Addition of increasing concentrations of fulvic acids slowed down the aggregation kinetics at pH 5 and 7, but not at pH 9. In any case, even in the presence of 10 mg/L of fulvic acids, about 70% of the particles had aggregated after 60 min at pH 7. An increase in ionic strength also seems to favor nZVI aggregation as documented by studies showing an increased retention of nZVI in laboratory experiments with packed sand columns (Raychoudhury et al. 2012; Lin et al. 2010). Liu et al (2016) also examined the behavior of freshly prepared nZVI under anoxic and oxic conditions over 72 h. Most importantly, nZVI remained stable over 72 h indicating that, in field situations, transport into anoxic zones may enhance the environmental persistence of nZVI. Considering that nZVI is most effective under anoxic conditions, joint studies on process efficiency, environmental behavior and interactions with biota in such conditions are granted.

The effect of the presence of humic acids (HA) in groundwater can vary depending on the type of surface modification of nZVI. Adsorption of HA to nZVI was shown to enhance the stability of nZVI coated with polycarylic acid (PAA), but to favor aggregation of nZVI modified with Tween-20 or starch (Dong and Lo 2013). However, as already pointed out for pH, the eventual trend of nZVI to aggregate remained visible in both presence and absence of HA. Thus, after an incubation time of 60 min, about 80% of PAA coated nZVI had aggregated in the absence of HA and about 60% in the presence of 20 mg/L HA. On the other hand, in similar experimental conditions, only 20% of the starch-coated nZVI aggregated in the presence of HA compared with the lack of significant aggregation in the absence of HA (Dong and Lo 2013). In the case of nZVI modified with carboxylmethyl cellulose (CMC), a HA concentration of 1 mg/L reduced aggregation by about 40%, but HA concentrations of 5 and 10 mg/L did not have any major effect on the NPs' stability (Jung et al. 2014). The interactions between HA and CMC-modified ZVI can be further modified by the presence of electrolytes with the actual effects depending on the specific combinations of HA and electrolyte concentrations (Jung et al. 2014).

Comparison of nZVI behavior in artificial versus real-world matrices suggests that nZVI has a strong tendency to aggregate (i.e., to become less mobile) in ultrapure water, forest spring water and landfill leachate, although the distribution of the aggregates and the kinetics of their formation can be somewhat variable (Peeters et al. 2016). The aggregation behavior of nZVI was not markedly changed by the addition of a dispersant (tetramethylammonium hydroxide—TMAH) although TMAH increased the stability of FeO NPs to a variable extent depending on the tested matrix (Peeters et al. 2016). The relative constancy of nZVI behavior is noteworthy considering the ranges of pH (5.5–8.0 units), conductivity (0.055–6800 $\mu S\ cm^{-1}$) and total organic content (<0.005–760 $mg\ L^{-1}$) covered by the three matrices. These observations are a promising for the definition of a general behavioral pattern of nZVI under realistic operation conditions. Park et al (2016) suggest two general patterns for the environmental mobility of engineered NMs in

giovanni.libralato@unina.it

porous media: a favorable pattern leading to NP immobilization and an unfavorable pattern conductive to increased mobility. Besides the master parameters examined above, Park et al. (2016) highlight that the final environmental behavior of nZVI will also be linked to the soil hydraulic properties and specific site characteristics. Considering that the most typical application of nZVI is injection into soils and/or groundwater, it is also important to understand how far the injected nZVI can travel after its reaction with the soil matrix under variable in situ conditions (Lefevre et al. 2016). The actual injection technology will determine the mobility of nZVI during the operational phase of the remediation, but it is desirable that the injected nZVI will remain immobile once delivered to the intended place of action. In the absence of unwanted environmental migration which may occur under anoxic conditions enhancing the stability of nZVI (Liu et al. 2016), nZVI will gradually transform into iron minerals that should remain immobile in the soil matrix (Zhao et al. 2016).

2 (Eco)Toxicology

2.1 Bacteria

Ecotoxicity can be caused by direct nZVI association with biological components, oxidative stress compounds generated by nZVI, and membrane permeability. Kim et al. (2010) studied the mechanism of *Escherichia coli* inactivation by nZVI by monitoring ROS. Using fluorescence assay [3′-(*p*-aminophenyl) fluorescein (APF) and 3′-(*p*-hydroxyphenyl) fluorescein (HPF) (Invitrogen)], they concluded that the bactericidal activities of nZVI under de-aerated conditions involved the generation of intracellular oxidants, such OH^- or Fe(IV) produced by the reaction with H_2O_2 or other reactive species, resulting in serious damage to cell membrane integrity and respiratory activity.

Liu et al. (2014) studied the influence of nZVI on nitrate removal by the coccoid *Paracoccus* sp. known for its NO_3^- reducing ability. They compared the nitrate removals using nZVI-free cells and nZVI-amended cells under both aerobic and anaerobic conditions. Under aerobic conditions, 66.9% of nitrate was removed by free cells while addition of nZVI (50 mg/L) into cells promoted nitrate removals with an efficiency of 85.2%. They associated this increase with the formation of H_2 produced by iron corrosion, which could be used as an electron source for free cells. However, as nZVI concentration increased, the removal efficiency decreased. This was due to the fact that the Fe^{2+} concentration increased with increased nZVI concentration, leading to increased Fe^{2+} toxicity to cells. Similar results were obtained under anaerobic conditions (Liu et al. 2014).

Yang et al. (2013) studied the potential negative impact of nZVI on anaerobic digestion methanogenesis resulting in its partial inhibition due to cell integrity disruption. The inhibition was coincident with the fast hydrogen production and accumulation due to nZVI dissolution under anaerobic conditions with a methane

giovanni.libralato@unina.it

reduction of >20%. Conversely, other authors (Kirschling et al. 2010; Xiu et al. 2010) found a stimulation of sulfate reducing bacteria (SRB) and methanogen growth in TCE contaminated aquifer materials. Marsalek et al. (2012) highlighted the presence of inhibitory effects of nZVI on the photosynthetic activity of cyanobacteria because of rapid coating of Fe and Fe(III) hydroxide onto their cells. As reported in Marsalek et al. (2012), a green-colored dispersion of untreated cyanobacteria at an ecologically relevant concentration of 250 μg/L of cyanobacteria was stable for 24 h, while an identical dispersion treated with nZVI (50 mg/L) after 24 h reaction appeared clear and free of live cyanobacteria. The decomposed biomass containing heavy Fe(III) hydroxide settled down and scanning electron microscopy (SEM) analysis of filtered and air-dried sediment indicated that the reaction product was not a nano-sized material (Marsalek et al. 2012).

2.2 Macrophytes and Soil Organisms

Macrophytes are essential components of our ecosystem, regulating the carbon and nitrogen cycles and constituting an important food source for humans and wildlife. Impact assessment of nZVI used for land remediation must then consider the potential effects on plants. Libralato et al. (2016) investigated the effects of nZVI on *Lepidium sativum, Sinapis alba* and *Sorghum saccharatum* up to concentrations used in field activities (50 g/L) and also compared the effects of nZVI with those of ionic- and micro-sized iron. Results reported no significant adverse effects even at 50 g/L of mZVI and nZVI, while some effects were evidenced for the ionic form. Biostimulation effects occurred at higher levels of nZVI. Microscopic analysis of *S. saccharatum* roots (Fig. 3) exposed to nZVI revealed the presence of black spots and coatings, but, apparently, no uptake by tissues (Libralato et al. 2016).

Similar results were highlighted by Ma et al. (2013) considering *Typha latifolia* and hybrid poplars. However, in contrast with Libralato et al. (2016), they reported a drastic reduction in *T. latifolia* weight and shoot height after four weeks of exposure to 1 g/L of nZVI (nominal concentration). El-Temsah et al. (2016) showed the effect of two differently synthesized types of nZVI on barley and flax. Adverse effects were observed on nZVI-B (produced by precipitation with borohydride) while stimulatory or no effects were detected on nZVI-T treated organisms (produced by gas phase reduction of iron oxides under H_2—NANOFER 25S, NANOIRON, Czech Republic), stating that the way a NM is synthetized can greatly influence its toxicity. Wang et al. (2016) assessed the effects of nZVI on rice up to 1 g/L. nZVI induced visible iron deficiency chlorosis and significant inhibition of seedlings growth. nZVI transferred to the rice seedlings caused the cortex tissue of root to be seriously damaged, inducing the inhibition of active Fe transported from the root to shoot.

Since nZVI is intended for use in soil, there is an evident need to evaluate the potential toxicity of Fe NPs on soil biota both to preserve soil ecosystem and prevent the elimination of organisms useful in contaminants' degradation. Among

giovanni.libralato@unina.it

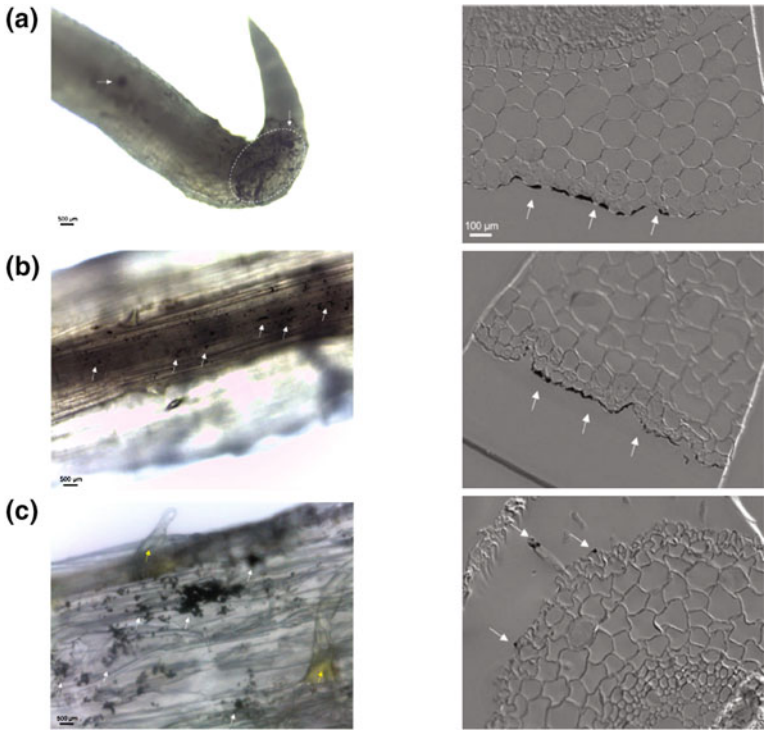

Fig. 3 On the *left* bright-field micrographs illustrating root apex of *S. saccharatum* treated with 992 mg/L of nZVI for 72 h at 25 °C. *White arrows* indicate nZVI aggregates, while *yellow* ones root hairs. On the *right* differential interference contrast images of unstained, transverse sections of leaf (**a**), shoot (**b**) and root (**c**) of *S. saccharatum* treated with the same concentration at the same condition. *White arrows* indicate the presence of nZVI deposits/agglomerates/precipitates. Reproduced from Libralato et al. (2016)

soil organisms, earthworms play a key role in terrestrial ecosystems by recycling organic matter and mineral nutrients and maintaining soil structure (Blouin et al. 2013). El-Temsah et al. (2016) verified an increase of earthworm mortality (*Eisenia fetida*) after 14 d exposure to the solid fraction of soil slurry from 15% of negative controls up to 33 and 22% in soil treated with nZVI-T and nZVI-B, respectively. After 28 d, corresponding values were 46, 33 and 67% mortality, respectively. For soils treated in columns, no significant increase in mortality was observed for treatments with nZVI compared to controls. Significant reduction in earthworm body weight was observed only for nZVI-B. Other treatments showed higher body weights compared to controls. Reproduction was completely inhibited in both column soil and slurry soil after treatment with nZVI-B. No reduction in production of juveniles or cocoon was observed with nZVI-T, except a 50% reduction of cocoons in column soil.

giovanni.libralato@unina.it

2.3 Human Cells

The behavior of NPs in complex systems like human body is quite unknown and a case-by-case basis survey is required (Gornati et al. 2016) considering also the results from Čábalová et al. (2015). They estimated the presence and quantity of micro- and nanosized particles and inter-individual differences in their distribution and composition in nasal mucosa obtained by mucotomy from patients with chronic hypertrophic rhinosinusitis (age 19–74, n = 6 including student and industrial worker). In all samples, NPs of different elemental composition were found with Fe being the most abundant element. Several studies indicated that ingested or inhaled NPs can cross biological barriers and migrate in small numbers to various organs and tissues (Lockman et al. 2004; Gornati et al. 2016) where they can potentially damage organ systems particularly sensitive to oxidative stress (OS). Gornati et al. (2016) carried out nZVI cytotoxicity and gene expression experiments on SKOV-3 (human ovarian carcinoma) and U87 (human glioblastoma) cells line investigating cell viability, cellular localization and uptake quantification by internalized metals. Results showed that nZVI are readily internalized by the cells (<5%) (Fig. 4). On gene expression, Fe NPs caused effects similar to their corresponding ions.

The small size and high-surface area of NPs, combined with their ability to generate reactive oxygen species (ROS) or release toxic metals at cell surfaces, may contribute to their final toxicity. To identify the mechanism through which nZVI can damage cells, Keenan et al. (2009) carried out a series of experiments considering nZVI in phosphate-buffered saline (PBS) solution exposed to oxygen in the presence and absence of human bronchial epithelial cells. Results evidenced a production of oxidants causing lung irritation. Ferrous iron (Fe^{2+}) is converted to ferric iron (Fe^{3+}) leading to oxidative damage over longer time periods. Further studies were carried out by Phenrat et al. (2008) about the effects of four ZVIs on rodent cells like cultured microglia (BV2) and neurons (N27) (Fig. 5) including fresh (bare) nZVI, oxidized nZVI ("aged") and two poly-aspartate surface-modified (SM) nZVI (SML, laboratory generated; MRNIP, commercially available product). They conducted this experiment to examine the possibility that nZVI or its by-products could produce OS-mediated neurotoxicity. Intracellular H_2O_2 generated from the oxidative burst was produced in response to both fresh nZVI and

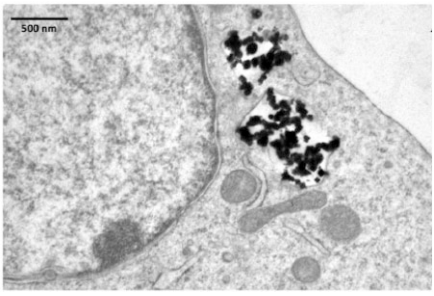

Fig. 4 Transmission electron microscopy picture of SKOV-3 cells exposed to nZVI NPs. Inside the cell, nZVI is localized inside vesicles but not in the cytoplasm or in nucleus and mitochondria. Reproduced from Gornati et al. (2016)

giovanni.libralato@unina.it

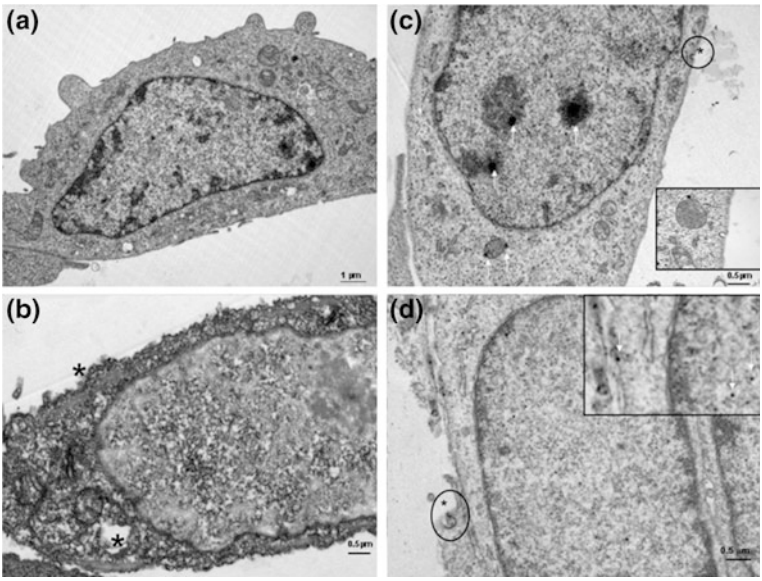

Fig. 5 Nuclear chromatin of control N27 neurons displayed a high contrast appearance and ultrastructurally normal cytoplasm (**a**). In contrast, the cytoplasm of N27 neurons exposed to fresh nZVI (1 ppm, 3 h) appeared darker and more condensed, and displayed a fibrillar material around the cell's internal membrane (*asterisks*) and a perinuclear distribution of floccular material (**b**). The cytoplasm of N27 neurons, treated with either laboratory-generated SML-nZVI (**c**) or MRNIP (**d**) (1 ppm, 3 h) appeared relatively normal ultrastructurally, although ZVI agglomerates (~ 200–500 nm) and single NPs were noted in the nuclei and cytoplasm in response to both treatments (**c** and **d**, insert). Invaginations of the neuron's cell membrane, suggestive of clathrin-lined endocytotic vesicles, were also noted in both SM-nZVI treated samples (**c** and **d**, *circles*, *asterisks*). Reproduced from Phenrat et al. (2008)

"aged" nZVI. Depolarization of the mitochondrial membrane, an index of apoptosis, occurred only in response to fresh nZVI. Ultrastructurally, nZVI produced a perinuclear floccular material and cytoplasmic granularity. Reductions of intracellular ATP affected the microglia in the following rank order: fresh nZVI > "aged" ZVI > SM ZVI NPs.

3 Outlook

This overview provided a basic knowledge about the discussion on hurdles for the commercialisation of nZVI, case study applicability, potential authority acceptance considering that the environmental marketplace is driven and constrained by regulations and laws, supporting funding for controlled pilot and field projects, clarifying the potentiality of using these new technologies because of their inherent risk and largely unknown effects. Only a few studies to date have investigated the

giovanni.libralato@unina.it

potential for nZVI to pose an environmental risk, including a very small number of toxicity and ecotoxicity researches of nZVI's potential to cause adverse effects in laboratory studies. This is to substitute one set of risks (i.e. site contamination) by another set of risks (potential risk from nZVI application) in terms of "risk–risk trade-off" illustrating the need to thoroughly analyze technology options before their full-scale introduction and commercialisation. In particular, such analyses should be performed at the early stages of development on the basis of the precautionary principle. In the perspective of life cycle impact analysis, factors such as persistence, bioaccumulation and toxicity, the Best Available Technology, and the use of zero-emission and zero-discharge approaches should be considered.

Given the expected benefits of using nZVI as an environmental remediation option and the largely unknown risks of its use, it is imperative that environmental engineers, scientists and decision makers are made fully aware of these benefits, risks, and uncertainties. Research needs also concern some of the challenges that traditional quantitative risk assessments face as a decision support tool under extreme conditions of uncertainty for ENMs and the need to better anticipate potential environmental risks of nZVI. These aspects are important given the early stage of use and development of nZVI, in which identified potential risks may still have the possibility to be mitigated or managed during the technology's maturing and development process while also aiming to reap the benefits of its use as an environmental remediation option.

Further assessment is surely required to fully understand nZVI environmental risk considering the fact that most studies are currently only laboratory based. Although some common patterns on nZVI environmental behaviour and interactions mechanisms with biota are emerging, site-specific conditions and organism-specific characteristics still remain important variables in real-world applications. Further guidance on how to comprehensively and transparently make decisions regarding nZVI use in relation to the potential risks for human and environmental health therefore remains a priority.

References

Bardos P, Bone B, Daly P, Elliott D, Jones S, Lowry G, Merly C (2015) A risk/benefit appraisal for the application of nano-scale zero valent Iron (nZVI) for the remediation of contaminated sites supporting MS3—NanoRem information for decision makers—initial version. Taking nanotechnological remediation processes from lab scale to end user applications for the restoration of a clean environment project Nr.: 309517 EU, 7th FP, NMP.2012.1.2 WP9: Dissemination, Dialogue with Stakeholders and Exploitation

Biswas P, Wu CY (2005) Nanoparticles and the environment. J Air Waste Manage Assoc 55 (6):708–746

Blouin M, Hodson ME, Delgado EA, Baker G, Brussaard L, Butt KR, Dai J, Dendooven L, Peres G, Tondoh JE, Cluzeau D, Brun J-J (2013) A review of earthworm impact on soil function and ecosystem services. Eur J Soil Sci 64(2):161–182

Čábalová L, Čabanová K, Bielniková H, Kukutschová J, Dvořáčková J, Dědková K, Zelenik K, Komínek P (2015) Micro-and nanosized particles in nasal mucosa: a pilot study. BioMed Res Int

giovanni.libralato@unina.it

Comba S, Di Molfetta A, Sethi, R (2011) A comparison between field applications of nano-, micro-, and millimetric zero-valent iron for the remediation of contaminated aquifers. Water Air Soil Pollut 215(1–4):595–607

Dong H, Lo IMC (2013) Influence of humic acid on the colloidal stability of surface-modified nano zero-valent iron. Water Res 47(1):419–427

Dong H, Ahmad K, Zeng G, Li Z, Chen G, He Q, Xie Y, Wu Y, Zhao F, Zeng Y (2016) Influence of fulvic acid on the colloidal stability and reactivity of nanoscale zero-valent iron. Environ Pollut 211:363–369

DuPont Chemicals (2007) Nanomaterial risk assessment worksheet: zero valent nano sized iron nanoparticles (nZVI) for environmental remediation

Elliott DW, Zhang WX (2001) Field assessment of nanoscale bimetallic particles for groundwater treatment. Environ Sci Technol 35(24):4922–4926

El-Temsah YS, Sevcu A, Bobcikova K, Cernik M, Joner EJ (2016) DDT degradation efficiency and ecotoxicological effects of two types of nano-sized zero-valent iron (nZVI) in water and soil. Chemosphere 144:2221–2228

EPA (2007) Nanotechnology white paper. EPA 100/B-07/001

ESTCP (2006) Protocol for enhanced in situ bioremediation using emulsified edible oil industrial environmental services

Gornati R, Pedretti E, Rossi F, Cappellini F, Zanella M, Olivato I, Sabbioni E, Bernardini G (2016) Zerovalent Fe, Co and Ni nanoparticle toxicity evaluated on SKOV-3 and U87 cell lines. J Appl Toxicol 36(3):385–393

Guan X, Sun Y, Qin H, Li J, Lo IM, He D, Dong H (2015) The limitations of applying zero-valent iron technology in contaminants sequestration and the corresponding countermeasures: the development in zero-valent iron technology in the last two decades (1994–2014). Water Res 75:224–248

Gwinn MR, Vallyathan V (2006) Nanoparticles: health effects: pros and cons. Environ Health Perspect 1818–1825

Hussain I, Raschid L, Hanjra MA, Marikar F, Van Der Hoek W (2002) Wastewater use in agriculture: review of impacts and methodological issues in valuing impacts: with an extended list of bibliographical references, vol 37, Iwmi

Jung B, O'Carroll D, Sleep B (2014) The influence of humic acid and clay content on the transport of polymer-coated iron nanoparticles through sand. Sci Total Environ 496:155–164

Keenan CR, Goth-Goldstein R, Lucas D, Sedlak DL (2009) Oxidative stress induced by zero-valent iron nanoparticles and Fe(II) in human bronchial epithelial cells. Environ Sci Technol 43(12):4555–4560

Kim JY, Park HJ, Lee C, Nelson KL, Sedlak DL, Yoon J (2010) Inactivation of *Escherichia coli* by nanoparticulate zerovalent iron and ferrous ion. Appl Environ Microbiol 76(22):7668–7670

Kirschling TL, Gregory KB, Minkley EG Jr, Lowry GV, Tilton RD (2010) Impact of nanoscale zerovalent iron on geochemistry and microbial populations in trichloroethylene contaminated aquifer materials. Environ Sci Technol 44(9):3474–3480

Lee CC, Lien HL, Wu SC, Doong RA, Chao CC (2014) Reduction of priority pollutants by nanoscale zerovalent iron in subsurface environments. Aquananotechnol Glob Prospects 63

Lefevre E, Bossa N, Wiesner MR, Gunsch CK (2016, in proof) A review of the environmental implications of in situ remediation by nanoscale zero valent iron (nZVI): behavior, transport and impacts on microbial communities. Sci Total Environ. doi:10.1016/j.scitotenv.2016.02.003

Libralato G, Costa Devoti A, Zanella M, Sabbioni E, Mičetić I, Manodori L, Pigozzo A, Manenti S, Groppi F, Ghirardini AV (2016) Phytotoxicity of ionic, micro-and nano-sized iron in three plant species. Ecotoxicol Environ Saf 123:81–88

Lin Y-H, Tseng H-H, Wey M-Y, Lin M-D (2010) Characteristics of two types of stabilized nano zero-valent iron and transport in porous media. Sci Total Environ 408(10):2260–2267

Liu Y, Li S, Chen Z, Megharaj M, Naidu R (2014) Influence of zero-valent iron nanoparticles on nitrate removal by Paracoccus sp. Chemosphere 108:426–432

giovanni.libralato@unina.it

Liu A, Liu J, Han J, Zhang W-X (2016, in proof) Evolution of nanoscale zero-valent iron (nZVI) in water: microscopic and spectroscopic evidence on the formation of nano- and micro-structured iron oxides. J Hazard Mater. doi:10.1016/j.jhazmat.2015.12.070

Lockman PR, Koziara JM, Mumper RJ, Allen DD (2004) Nanoparticle surface charges alter blood–brain barrier integrity and permeability. J Drug Target 12(9–10):635–641

Lowry GV, Espinasse BP, Badireddy AR, Richardson CJ, Reinsch BC, Bryant LD, Bone AJ, Deonarine A, Chae S, Therezien M, Colman BP, Hsu-Kim H, Bernhardt ES, Matson CW, Wiesner MR (2012) Long-term transformation and fate of manufactured Ag nanoparticles in a simulated large scale freshwater emergent wetland. Environ Sci Technol 46(13):7027–7036

Ma X, Gurung A, Deng Y (2013) Phytotoxicity and uptake of nanoscale zero-valent iron (nZVI) by two plant species. Sci Total Environ 443:844–849

Marsalek B, Jancula D, Marsalkova E, Mashlan M, Safarova K, Tucek J, Zboril R (2012) Multimodal action and selective toxicity of zerovalent iron nanoparticles against cyanobacteria. Environ Sci Technol 46(4):2316–2323

Masciangioli T, Zhang WX (2003) Peer reviewed: environmental technologies at the nanoscale. Environ Sci Technol 37(5):102A–108A

MinAmb (2015) Ministero dell'Ambiente e dela Tutela del Territorio e del Mare. http://www.minambiente.it/

NATO (1998) NATO/CCMS pilot study evaluation of demonstrated and emerging technologies for the treatment of contaminated land and groundwater (phase III)

Noubactep C (2010) The fundamental mechanism of aqueous contaminant removal by metallic iron. Water SA 36:663–670

Nurmi JT, Tratnyek PG, Sarathy V, Baer DR, Amonette JE, Pecher K, Wang C, Linehan JC, Matson DW, Penn RL, Driessen MD (2005) Characterization and properties of metallic iron nanoparticles: spectroscopy, electrochemistry, and kinetics. Environ Sci Technol 39(5):1221–1230

O'Carroll D, Sleep B, Krol M, Boparai H, Kocur C (2013) Nanoscale zero valent iron and bimetallic particles for contaminated site remediation. Adv Water Resour 51:104–122

Park CM, Chu KH, Heo J, Her N, Jang M, Son A, Yoon Y (2016) Environmental behavior of engineered nanomaterials in porous media: a review. J Hazard Mater 309:133–150

Peeters K, Lespes G, Zuliani T, Ščančar J, Milačič R (2016) The fate of iron nanoparticles in environmental waters treated with nanoscale zero-valent iron, FeONPs and Fe_3O_4NPs. Water Res 94:315–327

Phenrat T, Long TC, Lowry GV, Veronesi B (2008) Partial oxidation ("aging") and surface modification decrease the toxicity of nanosized zerovalent iron. Environ Sci Technol 43 (1):195–200

Raychoudhury T, Tufenkji N, Ghoshal S (2012) Aggregation and deposition kinetics of carboxymethyl cellulose-modified zero-valent iron nanoparticles in porous media. Water Res 46(6):1735–1744

Rickerby DG, Morrison M (2007) Report from the workshop on nanotechnologies for environmental remediation

Stefaniuk M, Oleszczuk P, Ok YS (2016) Review on nano zerovalent iron (nZVI): from synthesis to environmental applications. Chem Eng J 287:618–632

Stumm W, Morgan JJ (1996) Aquatic chemistry, chemical equilibria and rates in natural waters. Environmental Science and Technology Series

Tratnyek PG, Johnson RL (2006) Nanotechnologies for environmental cleanup. Nano Today 1 (2):44–48

USEPA (2005a) Nanoscale ZVI injection rapidly reduced source CVOCs in bedrock ground water

USEPA (2005b) Workshop on nanotechnology for site remediation U.S. Department of Commerce, Washington, DC, 20–21 Oct 2005

Wang CB, Zhang WX (1997) Synthesizing nanoscale iron particles for rapid and complete dechlorination of TCE and PCBs. Environ Sci Technol 31(7):2154–2156

giovanni.libralato@unina.it

Wang J, Fang Z, Cheng W, Yan X, Tsang PE, Zhao D (2016) Higher concentrations of nanoscale zero-valent iron (nZVI) in soil induced rice chlorosis due to inhibited active iron transportation. Environ Pollut 210:338–345

Xiu ZM, Jin ZH, Li TL, Mahendra S, Lowry GV, Alvarez PJ (2010) Effects of nano-scale zero-valent iron particles on a mixed culture dechlorinating trichloroethylene. Bioresour Technol 101(4):1141–1146

Yang Y, Guo J, Hu Z (2013) Impact of nano zero valent iron (NZVI) on methanogenic activity and population dynamics in anaerobic digestion. Water Res 47(17):6790–6800

Zhang WX (2003) Nanoscale iron particles for environmental remediation: an overview. J Nanopart Res 5(3–4):323–332

Zhao X, Liu W, Cai Z, Han B, Qian T, Zhao D (2016) An overview of preparation and applications of stabilized zero-valent iron nanoparticles for soil and groundwater remediation. Water Res 100:245–266

giovanni.libralato@unina.it

Use of Nanoparticles for Reduction of Odorant Production and Improvements in Dewaterability of Biosolids

Jeanette Brown

Abstract Odor production and dewaterability are two major issues of concern for many utilities during conditioning and beneficial use of biosolids. Several studies have been performed over the past decades to understand the factors influencing polymer-aided dewatering. In the last few years, much research has been performed to better understand the mechanisms of odor production from biosolids, and the factors that affect their production. However, no reliable methods have yet been developed to control these issues. This study proposes a new concept, using nanoparticle additives for improving dewatering and reducing odoers, based on an understanding of the mechanisms of dewatering and odorant production in biosolids. Nanoparticles (or nanomaterials) are novel materials with uniques physical and chemical properties. Ten different nanoparticles with varying chemistry and structures were developed and evaluated. Digested and return activated sludges from a number of treatment plants were tested using these nanoparticles for improvement in dewatering and reduction in odorant production. Results from these preliminary studies indicated that some of the nanoparticles were effective in improving dewatering and/or reducing odors. Depending upon the source of sludge, between 20% and 60% reduction in polymer dose was observed. This was accompanied by a 10–20% increase in cake solids. Further, 30% to over 70% reduction in the production of volatile organic sulfur compounds (odor causing compounds) was observed. Filtrate TSS as well as colloidal and soluble concentrations decreased by 50–75% using nanoparticles. While this study provide preliminary information on the role of nanoparticles for sludge dewatering and odor control, additional studies are required to understand the mechanisms and to

Principal Investigators: Ganesh Rajagopalan, Ph.D., Kennedy/Jenks Consultants.

Matthew J. Higgins, Ph.D., Bucknell University.

Used and edited with Permission from: Water Environment Research Foundation, Alexandria, VA

J. Brown (✉)
Manhattan College, Manhattan College Parkway, Riverdale, NY, USA
e-mail: Jeanette.brown@Manhattan.edu

© Springer International Publishing AG 2017

G. Lofrano et al. (eds.), *Nanotechnologies for Environmental Remediation*,
DOI 10.1007/978-3-319-53162-5_11

giovanni.libralato@unina.it

improve nanoparticles composition and configuration for cost effective biosolids treatment using nanoparticles.

Keywords Nanoparticles · Odor · Dewaterability · Biosolids

1 Introduction

Odor production and dewaterability are two major issues of concern for many wastewater treatment facilities especially associated with processing and beneficial reuse of biosolids. Recent surveys of wastewater operators have shown that odors are a top concern in their process operations (Adams et al. 2007; Dixon and Field 2004). In the last few years, much research has been performed to better understand the mechanisms of odor production from biosolids, and the factors that affect their production. However, no reliable methods have yet been developed to control these odors. This study proposed a new concept, using nanoparticle additives for reducing odors, based on a thorough understanding of the mechanisms of odorant production in biosolids. Additional benefits of this approach included improved dewaterability of biosolids, and lowering polymer dose and centrate BOD levels.

2 Biosolids and Odor Production

Odors produced by biosolids are primarily due to the production of volatile organic sulfur compounds (VOSCs) which include methyl mercaptan, dimethyl sulfide, and dimethyl disulfide, and odorous volatile aromatic compounds (OVACs) such as p-cresol, indole, skatole (Chen et al. 2006; Higgins et al. 2006a; Novak et al. 2006). Studies have shown that most of these odor causing compounds (OCCs) are produced through microbial degradation of bioavailable protein in biosolids (Higgins et al. 2006a, 2008; Chen et al. 2006).

A number of factors have been shown to affect bioavailable protein such as digestion processes, polymer dose and type, dewatering processes, and cake conveyance methods (Higgins et al. 2002, 2005, 2006a; Murthy et al. 2003; Novak et al. 2006). For example, compared to belt filter press dewatering, high solids centrifuges were shown to release more bioavailable protein which increased the production of OCCs. Similarly, higher polymer doses were associated with greater production of OCCs as observed through an odor panel study as well as a field trial (Higgins et al. 2005). The polymer acted to bind protein in solution and this protein was then sequestered in the cake, increasing the available protein pool for the production of odors. In fact, research has shown that the polymer demand for conditioning is proportional to the protein content remaining in solution after digestion (Higgins et al. 2006b).

giovanni.libralato@unina.it

The polymer demand is largely associated with coagulation of these small biopolymers that were not degraded during digestion. Interestingly, the protein that is bound by the polymer appears to be bioavailable in the cake and can lead to OCC production. Several approaches are available to reduce the production of OCCs which target the substrate for odorant production, mainly protein. These include improved digestion to enhance protein degradation, low shear dewatering to reduce the release of protein during dewatering, and binding of protein (e.g., to Fe/Al surfaces) to make it less bioavailable in the cake.

Research has shown that the addition of iron or alum during sludge conditioning can bind protein molecules and reduce their bioavailability (Dentel and Gossett 1982; Chen et al. 2007). In an ongoing study by the Water Environment Research Foundation (WERF) odor research team, the addition of alum reduced the production of OCCs by 50–100% during laboratory as well as field trials (Chen et al. 2007). Similar results were found by Higgins et al. (2002) using iron addition in a field trial with the Philadelphia Water Department biosolids. These studies supported the hypothesis that alum and iron bind protein in the cake, which in turn, reduced its bioavailability and subsequent odor production.

2.1 Nanoparticles and Biosolids

Despite a large number of studies performed on odor control and sludge dewatering, one major area that had not be systematically addressed is the role of submicron/nanoparticles. This includes (i) the fate of biogenic nanoscale suspended solids in the sludge, as well as (ii) the role of nanoscale dewatering aids to improve sludge conditioning. Evidence in the literature indicates that nanoparticles have significant potential to improve polymer binding and solids dewatering efficiency (Honig et al. 1993; Bernier and Begin 1994).

Nanoparticles are characterized by extremely small size (1–100 nm) and significantly high surface area compared to conventional micron-sized particles of the same chemical composition. At the nanoscale size, many materials have been demonstrated to be far more reactive than conventional materials. Also, in many cases the mechanisms of nanoscale material reactions are different than those of their micron-sized counterparts (Shelke 2007). Because of their unique properties, nanoscale materials have recently replaced their dissolved/micron-sized counterparts in several industrial/commercial products (WWICS 2006). Recently, nanoscale metal-oxide adsorbents (TiO_2, FeO, zerovalent iron) have been shown to adsorb (bind) dissolved organic/inorganic constituents more effectively than conventional adsorbents during water/wastewater treatment (Ganesh et al. 2007; Cao et al. 2005).

Furthermore, in the paper industry, nanoscale silica and metal oxide additives have been shown to improve retention and drainage characteristics of pulp and fiber materials. In a study by Lindstrom et al. (1989), compared to a polymer-only system that retained (bound) only 20% of fines, addition of nanoscale aluminum

giovanni.libralato@unina.it

hydroxide improved fines retention to over 80%. In a study that evaluated a variety of nanosilica additives for paper retention, the charge density, size, as well as sequence of addition impacted the efficiency of fiber retention (Andersson and Lindgren 1996). The optimum additive dosing decreased with increasing charge density (~1.8 mg/L of nanosilica for 80% retention at charge density of 0.59 meq/g compared to 4 mg/g dosing at a charge density of 0.27 meq/g). Furthermore, the retention capacity increased with decreasing particle size (3 nm silica retained 60% more fiber than 5.4 nm), although there appeared to be an optimum size below which the retention efficiency decreased. In general, tighter/porous floc formation (bridging), charge neutralization, and effective polymer binding are reported as the mechanisms involved with enhanced pulp retention and drainage using nanoparticles. Micro-sized silica are not effective in improving pulp retention and drainage. During biosolids treatment, the mechanisms of odorant molecules adsorption and biosolids dewaterability are comparable to the retention and drainage phenomenon, respectively, in pulp and paper industry. Some results showed that the addition of metal oxide nanoparticles to anaerobically digested biosolids during dewatering removed more than 90% of the sub-micron particles that were not removed by the cationic polymer alone (Fig. 1; Ganesh et al. 2009). Based on previous work, most of these particles are likely to have high protein content (Higgins et al. 2006b). Hence, it can be hypothesized that the smaller particle size of the nanoparticles are able to access binding sites on the biopolymer and reduce the bioavailability of the materials which are precursors to odor production. Furthermore, data from Ganesh et al. (2009), as well as Wang et al. (2007), showed that nanoparticles have the potential to reduce polymer demand, improve dewaterability, as well as lower the BOD/nutrient load in the return centrate. For example, during dewatering of a thickened waste activated sludge using metal oxide nanoparticles, the optimum polymer dose (i.e., the dose that produced the lowest CST) was reduced appreciably by addition of nanoparticles (Fig. 2).

These data indicated that, compared to a 'polymer-only' treatment, addition of nanoparticles (along with polymer dosing) had the potential to (1) reduce odorant

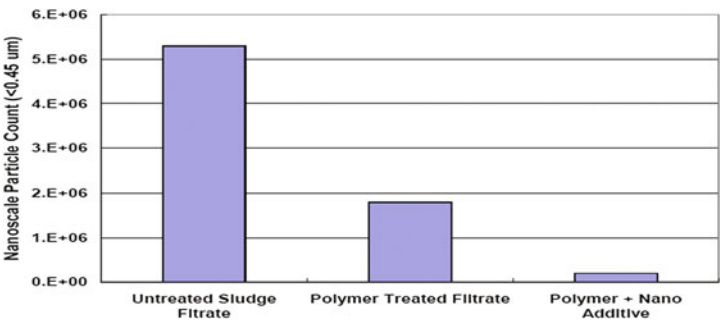

Fig. 1 Sub-micron particles in dewatered centrate after treatment using nanoparticle additive

giovanni.libralato@unina.it

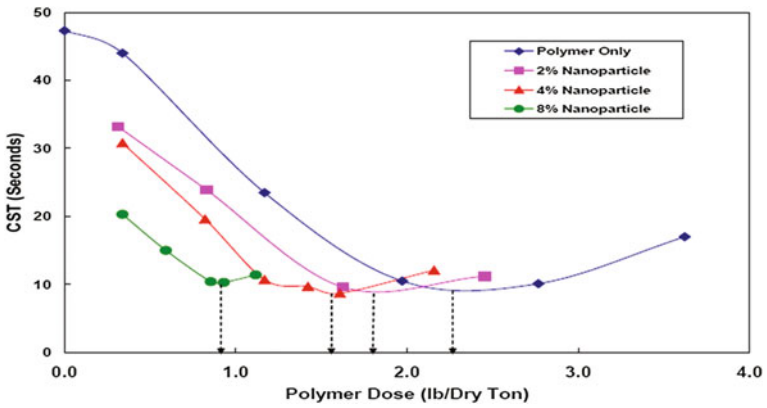

Fig. 2 Effect of metal oxide nanoparticles addition on the CST profile as function of polymer dose *arrows* indicate approximate optimum polymer dose

production by binding biogenic nanoparticles, and lowering polymer demand, and (2) improve biosolids dewaterability through better floc formation.

3 Research Overview

Laboratory-scale studies were performed using anaerobically digested sludge conditioned with cationic polymer to determine the effect of adding nanoscale materials during conditioning and dewatering on polymer demand, dewatering characteristics, centrate/filtrate quality and odorant production. These experiments examined the effect of:

1. nanoparticle characteristics
2. nanoparticle dosage
3. sequence of nanoparticle addition relative to polymer addition
4. dewatering device on the ability of nanoparticles to improve dewatering and reduce odorant production

During the experiments, dewaterability was evaluated by capillary suction time (CST) and specific resistance to filtration (SRF). The centrate/filtrate quality was characterized by:

1. Chemical Oxygen Demand (COD),
2. total nitrogen,
3. zeta potential,
4. nanoparticle count and size distribution, and
5. solids concentration.

In addition, the sludge cake was analyzed for odorant production during storage.

giovanni.libralato@unina.it

Initially, a screening study was conducted using about a dozen different combinations of nanoparticles, sizes, and configurations on the anaerobically digested sludge. Nanoparticles were synthesized using chemicals currently used in water/wastewater treatment or other environmentally benign materials. The additives were used in conjunction with cationic polymer.

The screening evaluated dewaterability using standard measures of CST, and odorant production through headspace gas chromatography (GC) of the cake samples. For the screening study, nanoparticles (2% DS) were added prior to the polymer and dewatered using a high solids centrifuge simulation process.

This study evaluated the factors and mechanisms that influence the role of nanoparticles during polymer aided dewatering and biosolids odor production. The research consisted of two steps: (1) performed screening studies, and (2) performed detailed evaluations. Nanoparticles with different morphologies were synthesized for this study by NEI Corporation (Somerset, NJ, USA). The size and morphology of particles play a significant role in sludge dewatering and odor control. For example, a treatment media composed of aggregated nanoparticles will likely interact differently with the sludge particles than a non-aggregated treatment media: whereas the latter will had higher accessible surface area (and hence have higher protein binding efficacy), the former showed better resistance to shear.

4 Initial Screening of Nanoparticles

Nanoparticles with different morphologies were synthesized for this study by NEI Corporation (Somerset, NJ). The size and morphology of particles play a significant role in sludge dewatering and odor control. For example, a treatment media composed of aggregated nanoparticles will likely interact differently with the sludge particles than a non-aggregated treatment media: whereas the latter will have higher accessible surface area (and hence have higher protein binding efficacy), the former could show better resistance to shear.

Screening tests were performed on a total of 10 different nanoparticles and over 90 different individual tests were completed with 10 nanoparticles. A summary of the characteristics of the different nanoparticles is provided in Table 1.

The results from the screening tests varied with the type of nanoparticle, polymer used, and the mixing shear. While several nanoparticles reduced the optimum polymer dose requirements, in general, NM-5, NM-6, NM-7, and NM-8 were more effective than others in reducing optimum polymer dose. NM-2 and NM-5 improved percent solids in the dewatered cake. NM-5, NM-6, and NM-7 were more effective than other nanoparticles tested in reducing odor production from biosolids. An example of this trend is shown in Fig. 3.

In this study, dewatered cake from an existing wastewater treatment plant (Selinsgrove, PA) was mixed with different nanoparticles and the odorant concentration was measured. Figure 3 shows the cumulative odor produced from the control and nanoparticles added samples after 9 days of incubation. NM-5, NM-6,

giovanni.libralato@unina.it

Table 1 Summary of nanoparticle characteristics

Nanoparticle name	Zeta-potential (mV)[a]	Primary particle size (nm)	Aggregate size[b] (nm)	Surface area (m^2/g)
NM-1	+31.3	60	406	14.5
NM-2	−20	10–13	313	156.2
NM-3	+36.8	30	N/A	264.3
NM-4	+46.8	30	72.6	32.1
NM-5	+43.6	N/A	706.0	N/A
NM-6	+	~1	~1	~1 nm
NM-7	+36.3	<100	184.1	16.1
NM-8	+41 8	<50	N/A	27.0
NM-9	+39.5	60	194.0	14.5
NM-10	+22.2	60–120	60–120	20.0

[a]Preliminary estimates

[b]The surface area numbers suggest that the primary particle size is significantly smaller than the aggregate (or secondary) size. For example, NM-2 has a primary particle size of approximately 10–13 nm, while the aggregate size is much larger, 313 nm

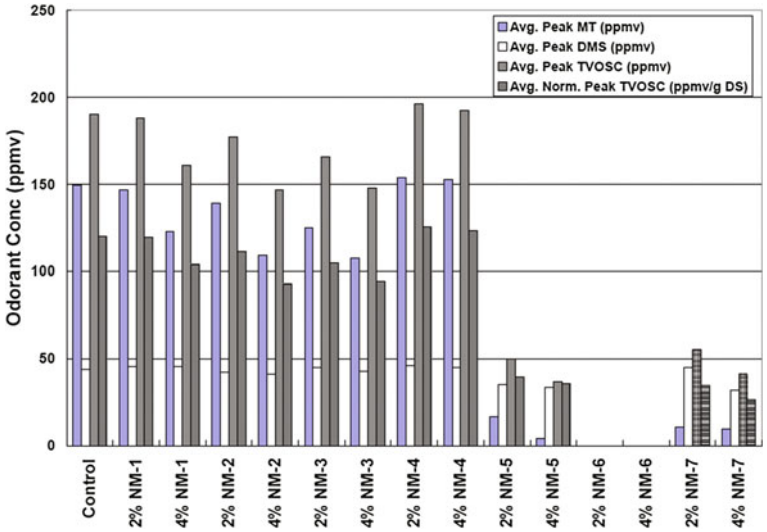

Fig. 3 Odorant production from dewatered selinsgrove cake mixed with nanoparticles

and NM-7 produced significantly lower levels of methandriol (MT), dimethyl sulfide (DMS), and total volatile organic sulfur compounds than control and other nanoparticles added samples. Based on these results, nanoparticles NM-5, NM-6, and NM-7 were selected for additional evaluations.

These three nanoparticles were all cationic, although their size does vary considerable. For example, NM-6 has an aggregate size of about 1 nm, while

giovanni.libralato@unina.it

NM-7 and NM-5 are much larger, 184 and 706, respectively. As a result, it was difficult to pinpoint the key characteristics that make the material effective. A key difference is also the atoms that make up the nanoparticles which could also impact their abilities to improve dewatering and reduce odors.

5 Dewatering Testing and Odor Impact

The goals of the additional dewatering tests were first to establish under what dewatering conditions the nanoparticles are effective, and also determine how they impact odors under these varying conditions. Three key parameters are of interest:

- Polymer type—effect of charge density
- Dewatering process—effect of shear
- Effect of sequence of addition

The effect of addition sequence has already been investigated in several other studies, and the optimum location for additives appears to be before the polymer addition. This gives the material time to interact with the particles which can then allow reduction in polymer dose through charge neutralization.

A series of experiments were performed with combinations of nanoparticles and polymers with varying characteristics. The hypothesis was that the nanoparticles may be more effective with certain polymer characteristics than others. For example, charge neutralization and polymer bridging have shown to be the two key mechanisms for conditioning sludge with polyelectrolytes. When using nanoparticles with cationic charge, they could play a role in the charge neutralization of the particles, and thereby reduce the polymer requirements for conditioning. This would be more evident with polymers of lower charge density. Therefore, use of a polymer with lower charge density could be used effectively in conjunction with a nanoparticle and achieve similar or improved dewatering characteristics. In addition, polymers with lower charge densities are less expensive than polymers with higher charge density, which could lead to additional savings. For example, going from a medium to a high charge density polymer of similar molecular weight could increase the cost by around $0.25 per kg of polymer.

A series of tests were performed to investigate the effect of polymer charge density and molecular weight on the conditioning and dewatering characteristics of RAS and digested sludge. Two sets of polymers were investigated, Series 1 with a medium to high charge density and Series 2, which had a low to high charge density. NM-6 was used as the model nanoparticle for these experiments at a constant dosage of 2%. The polymers evaluated and their characteristics are shown in Table 2.

Capillary Suction Time (CST), cake solids, and vacuum filtration were used to measure dewatering efficiency of various combinations of polymers and nanoparticles compared to a control without nanoparticles.

giovanni.libralato@unina.it

Table 2 Summary of polymer characteristics investigated

Polymer name	Charge density	Molecular weight	Form
Series 1 cationic polymers			
Praestol 536K	Medium	High	Dry granule
Praestol 650BC	Medium/high	High	Dry granule
Zetag 8818	High	High	Emulsion
Series 2 cationic polymers			
Betz 2682	Low—15%	High	Emulsion
Betz 2680	Medium—40%	High	Emulsion
Betz 2688	High—80%	High	Emulsion

In the case of a medium charge density polymer, Praestol 536k, with RAS and digested sludge, the effect of the NM-6 addition was much greater. As shown in Fig. 4, the optimum polymer dose is slightly lower with the nanoparticle, but also the CST is lower at the OPD, indicating better dewaterability with the nanoparticle. The cake solids from the vacuum filtration test also show better dewaterability with the nanoparticle, as shown in Fig. 5.

The 650BC polymer has a medium/high charge density and high molecular weight and is a commonly used polymer in the wastewater industry. The polymer dose—CST profiles for the RAS samples are shown in Fig. 7 for the control with polymer only and the nanoparticle/polymer combination.

As shown in Fig. 7, the NM-6 did not have a large effect on the polymer dose profile and did not reduce the polymer required for conditioning. Similarly, the cake solids profile is shown in Fig. 8, and no differences were measured with the NM-6 addition compared to the polymer only samples. The comparison of the effect of the cationic nanoparticle with a medium and medium/high charge density confirms the hypothesis that the nanoparticle should have more effect with a lower charge density polymer (Fig. 6).

The results with the digested sludge and polymer 650BC were better with the NM-6 addition. Figure 9 shows the CST profile for the samples. The addition of NM-6 achieved the breakpoint in the curve around 8 g/kg DS, while the polymer only sample reached that point around 11.5 g/kg. The cake solids were also slightly improved with the addition of the NM-6 to the sludge prior to the polymer addition as shown in Fig. 10.

The CIBA Zetag 8818 polymer is a high charge density and high molecular weight polymer. The polymer has a higher charge density than the 650BC polymer. The CST profile results for the conditioning and dewatering tests with the RAS are shown in Fig. 11. Similar to the 650BC polymer with the RAS, the NM addition did not have an effect on the polymer dose and CST. The cake solids profile also did not show any differences with the Zetag 8818 polymer and RAS sample as shown in Fig. 12.

For the digested sludge samples, the addition of the NM-6 had a slight effect on the CST polymer dose profile (Fig. 13), but was not as much as the 650BC or the 536K polymers which had lower charge densities. Similarly, the cake solids profile,

giovanni.libralato@unina.it

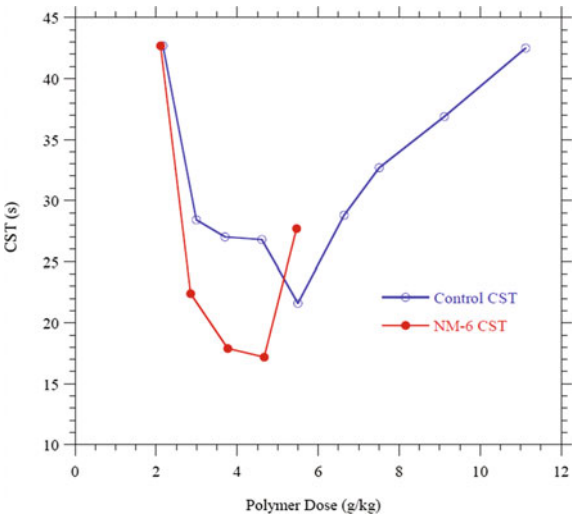

Fig. 4 Digested sludge CST as a function of 536K polymer dose with and without 2% NM-6 addition

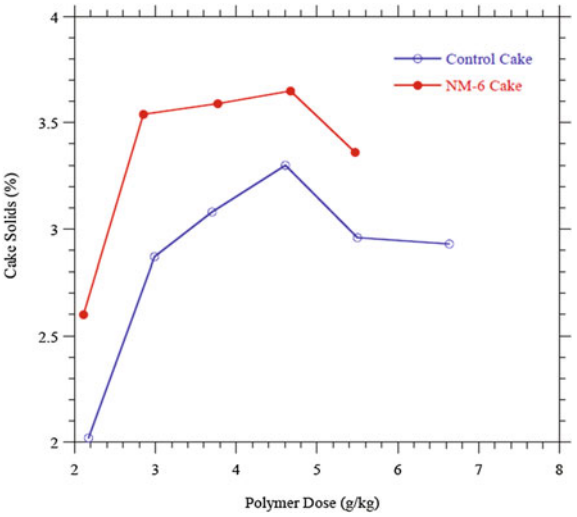

Fig. 5 Digested sludge cake solids as a function of 536K polymer dose with and without 2% NM-6 addition

shown in Fig. 14, was similar for the polymer and polymer/nanoparticle combination.

The results from the first series of polymer that have charge densities of medium, medium/high, and high, all with similar molecular weights demonstrate that the polymer type will impact the effectiveness of the cationic nanoparticle. In this case, the main role of the nanoparticle appears to be charge neutralization of the sludge particles, which would help reduce the polymer requirements for charge neutralization. With the higher charged polymer, the nanoparticles appear to have less of an effect.

giovanni.libralato@unina.it

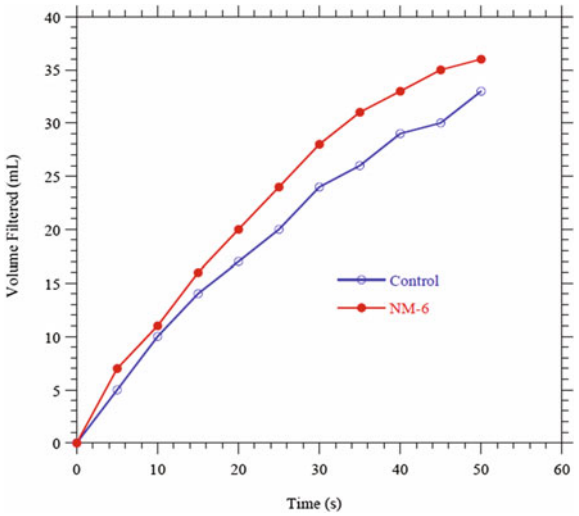

Fig. 6 Digested sludge time to filter for similar 536K polymer dose with and without 2% NM-6 addition

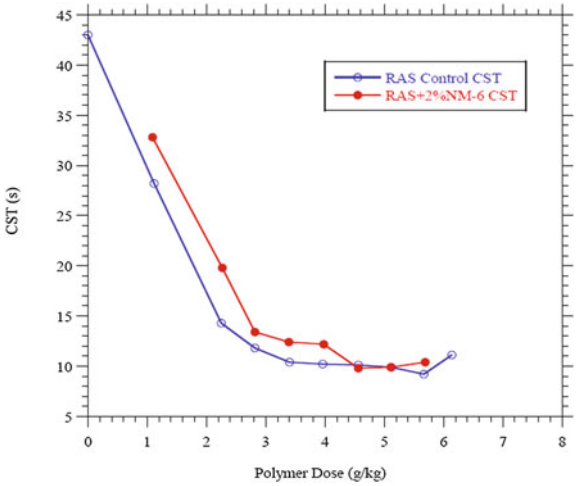

Fig. 7 RAS CST as a function of 650BC polymer dose with and without 2% NM-6 addition

A second series of tests were performed with the Betz emulsion polymers that had varying charge densities as described in Table 2. The CST-profile results from the low charge polymer (2682) are shown in Fig. 15. The cake solids profiles are shown in Fig. 16. Not much difference was measured with the nanoparticle compared to the polymer only trial, which was not expected. One complicating factor was the polymer dose for conditioning was very high, around 70 g/kg (or kg/ton), which is much higher than all previous experiments (and much higher than that seen in practice, typically 5–10 kg/ton DS). In addition, the actual polymer sample of the 2682 polymer had begun to separate in the bottle, which may have been a sign of deterioration in the polymer.

giovanni.libralato@unina.it

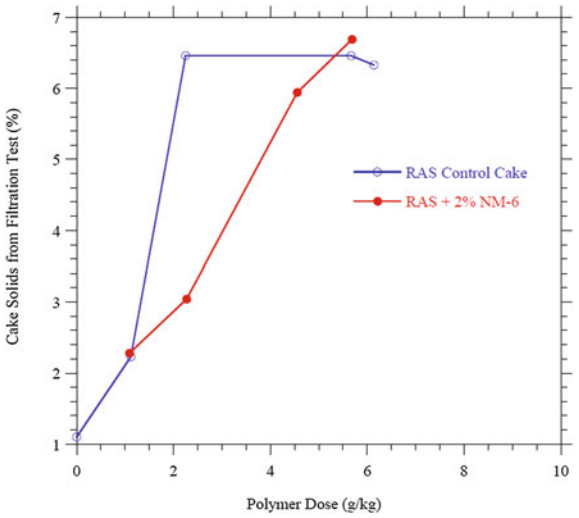

Fig. 8 RAS cake solids as a function of 650BC polymer dose with and without 2% NM-6 addition

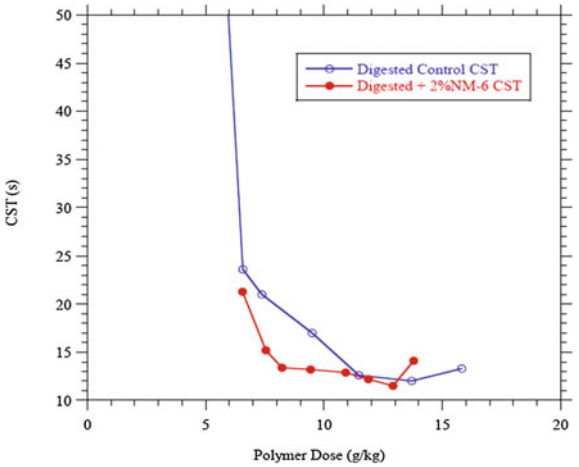

Fig. 9 Digested sludge CST as a function of 650BC polymer dose with and without 2% NM-6 addition

The second polymer in the series, 2680, had a medium charge density and high molecular weight, similar to 650BC. The CST-polymer dose profile is shown in Fig. 17. Addition of the NM-6 did not reduce the polymer demand to achieve the optimum dose, but it did lower the final CST for equivalent polymer dosages, suggesting an improvement in the dewaterability. The cake solids profile confirms the improved dewaterability as shown in Fig. 18. The cake solids with the NM-6 addition were higher than the polymer only controls by about 10–20% depending on the polymer dose. This is a substantial improvement. For a plant that is achieving cake solids of 25%, the same improvement could result in cake solids from 27 to 30% which is a large difference for a treatment process in terms of

giovanni.libralato@unina.it

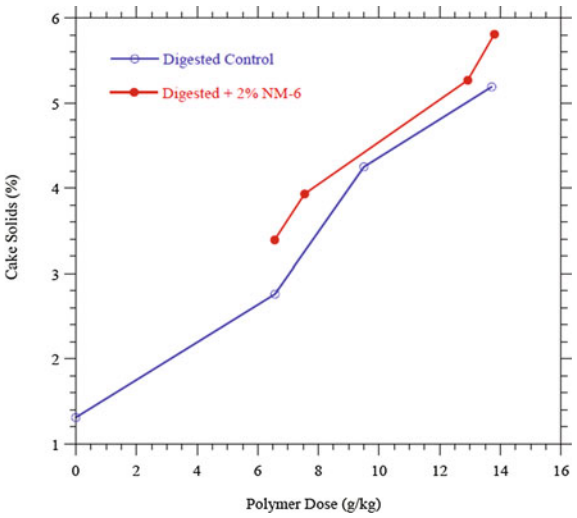

Fig. 10 Digested sludge cake solids as a function of 650BC polymer dose with and without 2% NM-6 addition

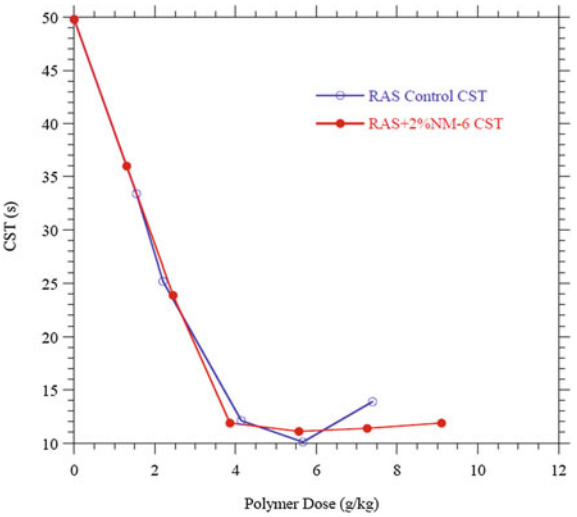

Fig. 11 RAS CST as a function of 8818 polymer dose with and without 2% NM-6 addition

hauling costs. The time to filter results, shown in Fig. 19, also show improved dewaterability through faster filtration times with the NM-6 addition.

The third polymer in this second series had a high charge and high molecular weight, similar to the Zetag 8818 polymer. Like the 8818 polymer, the addition of NM-6 did not have much of an effect on the CST-polymer dose profile as shown in Fig. 20. There were slight improvements in the dewaterability as measured by the cake solids and time to filter experiments, Figs. 21 and 22, respectively.

A set of experiments was performed to examine the effect of nanoparticles on filtrate quality as well as other usual dewatering parameters such as cake solids.

giovanni.libralato@unina.it

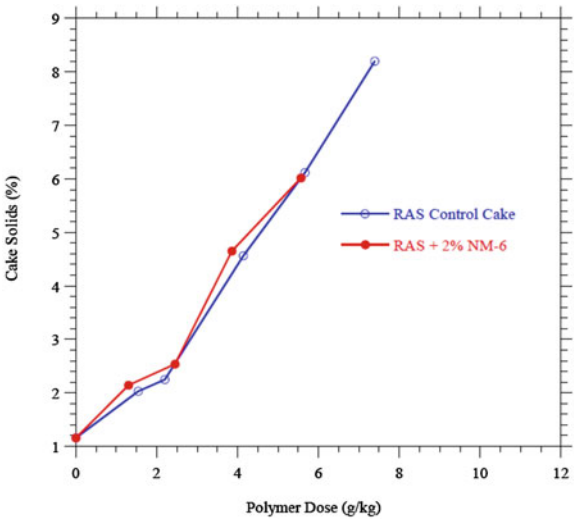

Fig. 12 RAS cake solids as a function of 8818 polymer dose with and without 2% NM-6 addition

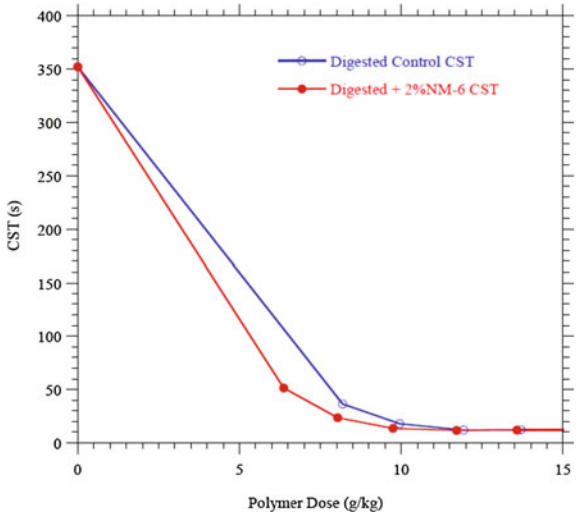

Fig. 13 Digested CST as a function of 8818 polymer dose with and without 2% NM-6 addition

In these tests, the nanoparticle was added during the conditioning step immediately before the polymer addition, and then after mixing of 2 min at 100 rpm, the sample was placed on belt filter press fabric for a free drainage test. The belt filter press filtrate was then collected and analyzed for TSS, and then the filtrate was filtered through a 1.5 μm nominal pore sized filter to collect the colloidal and soluble fraction.

Absorbance at 480 nm, and colloidal plus soluble (cs) or csCOD were measured on these samples. Absorbance at 480 nm provides a measure of the color which is an indicator of biomaterials such as humic-like constituents in the filtrate. This colloidal and soluble fraction is important for wastewater treatment since this

giovanni.libralato@unina.it

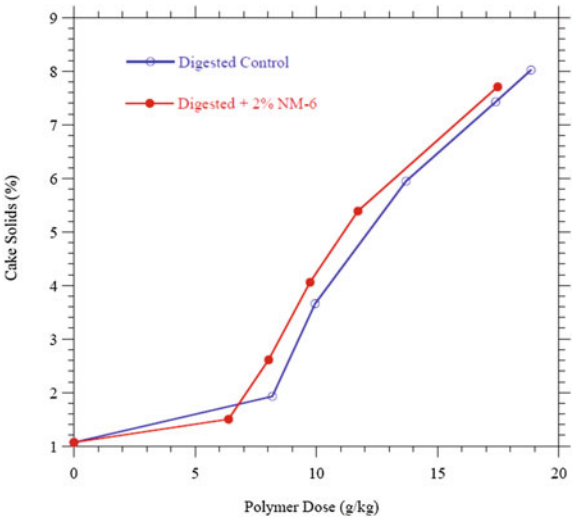

Fig. 14 Digested cake solids as a function of 8818 polymer dose with and without 2% NM-6 addition

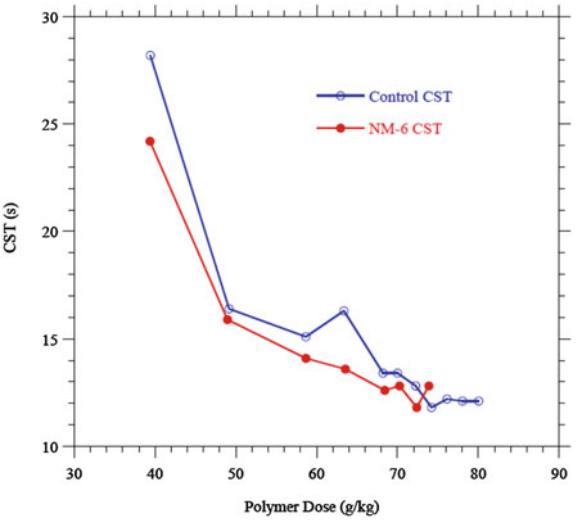

Fig. 15 Digested CST as a function of 2682 polymer dose with and without 2% NM-6 addition

fraction would be returned to the headworks of the treatment. It likely would not settle well and could become part of the effluent and represent additional treatment issues. The cake that formed on the belt during the free drainage test was then placed in a test tube and dewatered using a laboratory centrifuge for 10 min at 3000*g*.

NM-5 was added during the conditioning step at dosages of 1, 2, and 4% and compared to a control with no NM addition. The effect of different dosages on the CST at the optimum polymer dose is shown in Fig. 23 which shows that the CST was very similar for all the conditions.

giovanni.libralato@unina.it

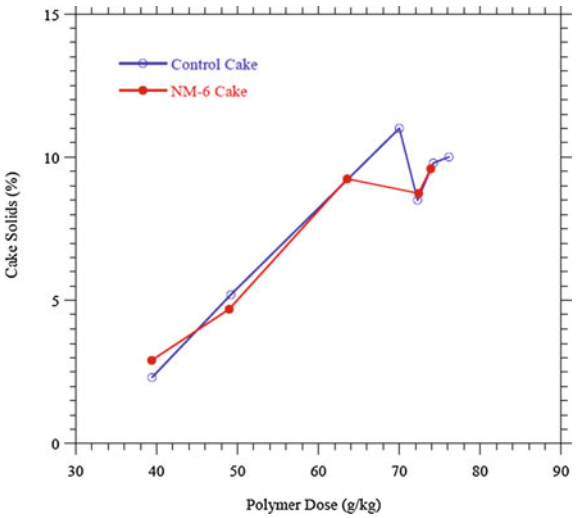

Fig. 16 Digested sludge cake as a function of 2682 polymer dose with and without 2% NM-6 addition

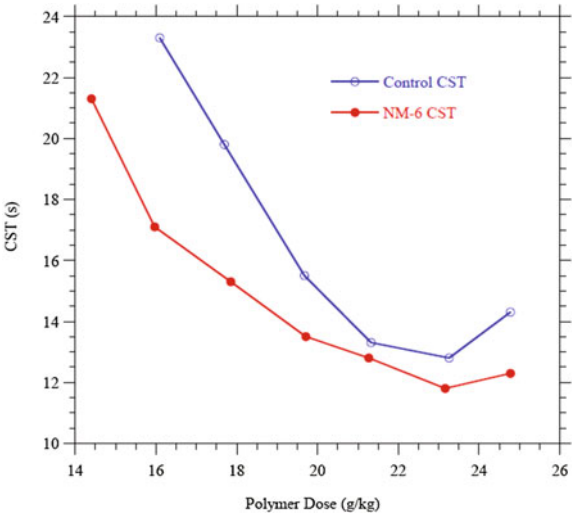

Fig. 17 Digested sludge cake solids as a function of 2680 polymer dose with and without 2% NM-6 addition

The lowest dosage of NM-5 reduced the filtrate TSS, but the higher dosages were similar to the control as shown in Fig. 24. Similarly, no appreciable trend was found for cake solids with the NM-5 addition, Fig. 25. At the dosages of 2 and 4%, the colloidal color measured as absorbance at 480 nm was reduced compared to the control, by up to about 20% as shown in Fig. 26. Finally, the filtrate colloidal and soluble COD also was not reduced by the addition of NM-5, shown in Fig. 27. Overall, addition of NM-5 did not have a consistent positive benefit on the filtrate characteristics during dewatering.

giovanni.libralato@unina.it

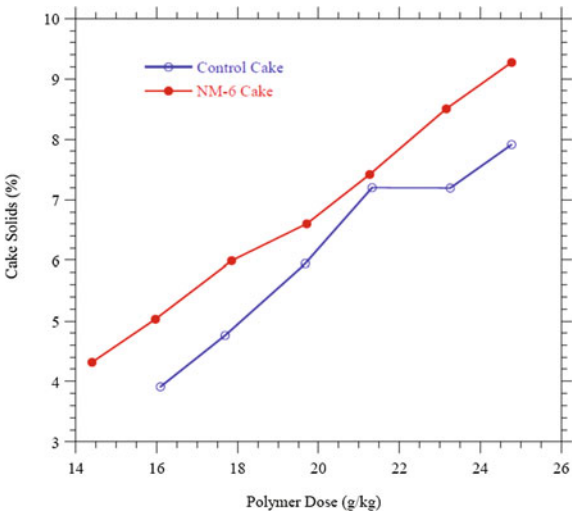

Fig. 18 Digested sludge cake solids as a function of 26SQ polymer dose with and without 2% NM-6 addition

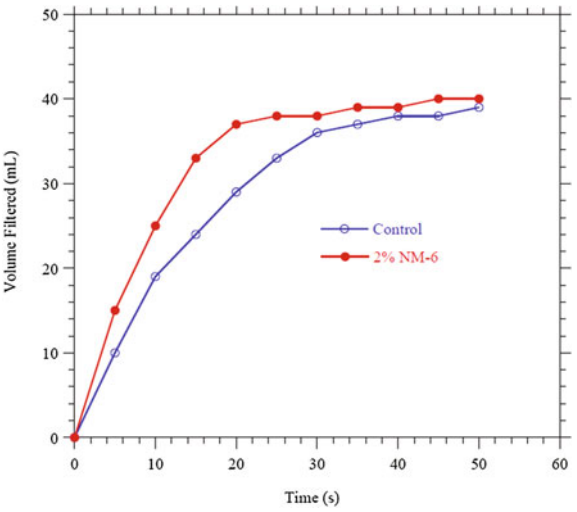

Fig. 19 Digested sludge TTF as a function of 2680 polymer dose with and without 2% NM-6 addition

The results from these dewatering tests demonstrated that polymer type has an impact on the efficacy of the nanoparticle in terms of its ability to improve conditioning and dewatering through a reduction in polymer demand, increase in cake solids or increase in the filtration rate. However, other factors such as shear and sludge characteristics play all an important role, such that no single parameter can be used to determine the best outcomes. The use of the cationic nanoparticle in combination with the lower charge density polymer resulted in consistent improvements compared to the higher charge density polymer, although in several cases the nanoparticles worked well with the higher charged. The results showed

giovanni.libralato@unina.it

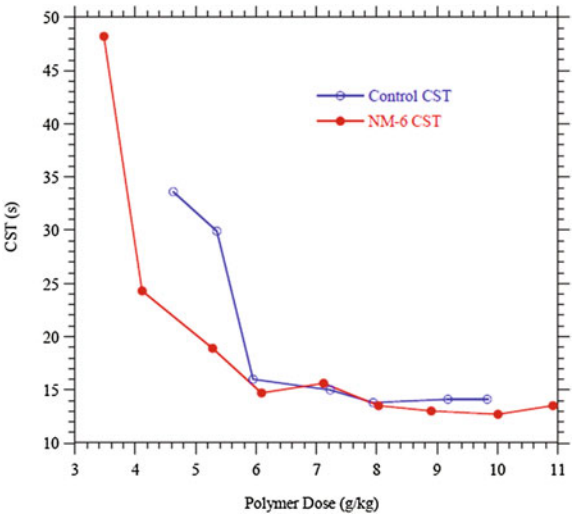

Fig. 20 Digested sludge CST as a function of 2688 polymer dose with and without 2% NM-6 addition

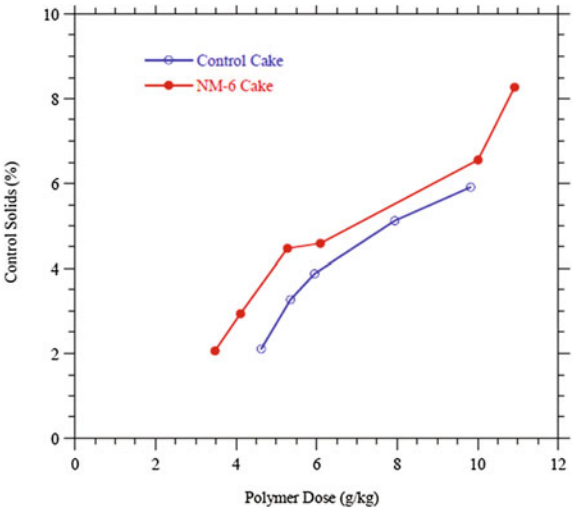

Fig. 21 Digested sludge cake solids as a function of 2688 polymer dose with and without 2% NM-6 addition

improvements that included lower polymer demand, increased cake solids and better filtration times.

The results fit well with expectations. Higgins et al. (2004) showed that higher charge density polymers do not use their charge as effectively as lower charge density polymers, meaning that they have excess charge that is not used in the conditioning process, except for very high shear conditions. In other words, if polymer dose was expressed in terms of an equivalent charge per gram of dry solids, high charge density polymers have greater polymer dosages than lower charged polymers. This may help explain why the use of nanoparticles with the

giovanni.libralato@unina.it

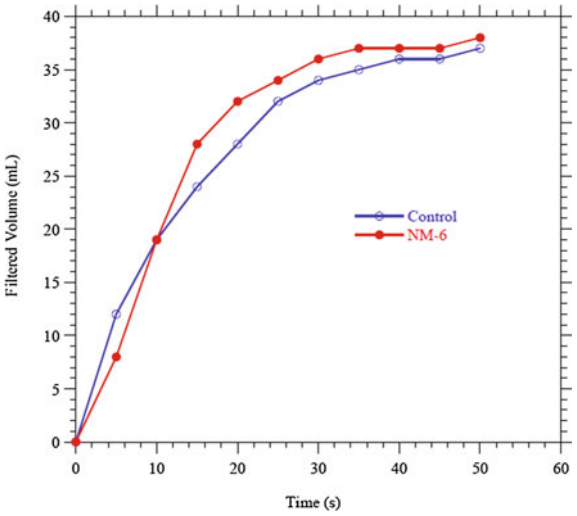

Fig. 22 Digested sludge time to filter as a function of 2688 polymer dose with and without 2% NM-6 addition

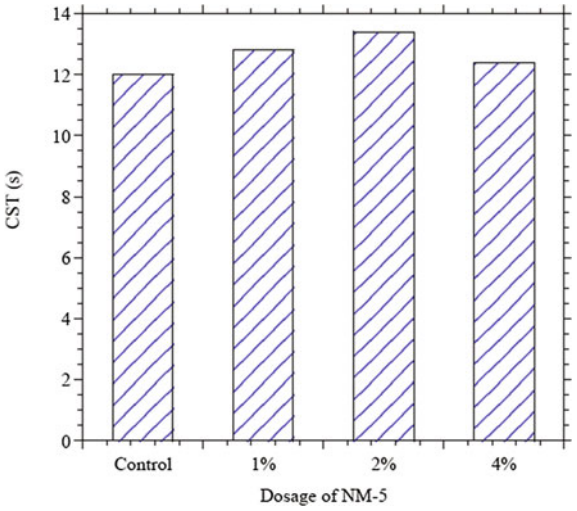

Fig. 23 Effect of NM-5 dosage on CST with Lewisburg biosolids

lower charged density polymers was more effective than those using higher charged densities polymers. The lower charged density polymers use more of their charge during the charge neutralization process (Higgins et al. 2004), and if the cationic nanoparticles play a role in charge neutralization, this should then have an impact on the polymer demand, which it did in the experiments.

These results with polymer charge density correlate well with the results related to the effect of shear. As shear increases, polymer dose typically increases as a result of floc breakup and the exposure of greater floc charge that must be neutralized (Novak and Lynch 1990; Murthy et al. 1997, 2003). In addition, as shear

giovanni.libralato@unina.it

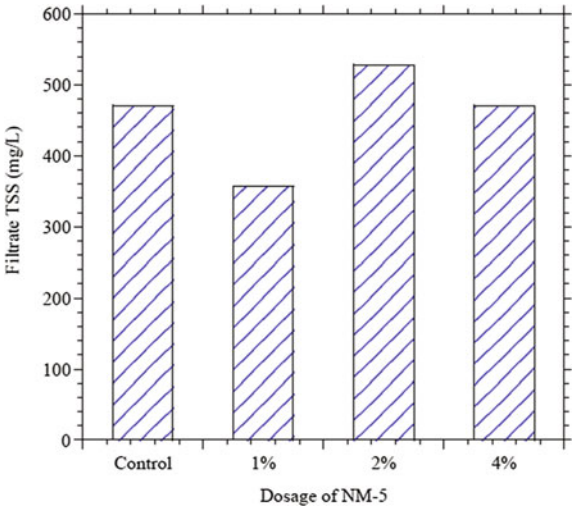

Fig. 24 Effect of NM-5 dosage on filtrate TSS with Lewisburg biosolids

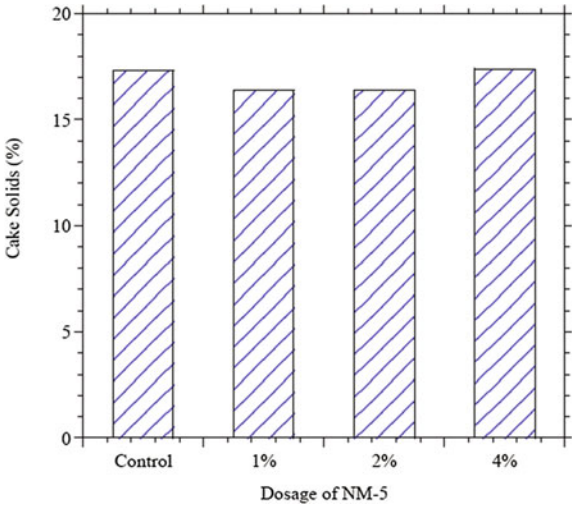

Fig. 25 Effect of NM-5 dosage on cake solids with Lewisburg biosolids

increases, polymer bridging becomes more important in order to hold the small particles within the floc together. The greater shear would lead to greater polymer demand, and as a result, the role of the charge neutralization may be less important, creating less of an opportunity for the nanoparticles to play a role. This is likely why in these experiments the researchers saw that the nanoparticles had less of an effect on conditioning and dewatering and odors with the high shear conditions compared to the lower shear conditions. Higgins et al. (2010) reported very similar findings for the use of alum and ferric chloride addition for the reduction in odors. With higher shear conditions, the addition of alum and ferric chloride was less

giovanni.libralato@unina.it

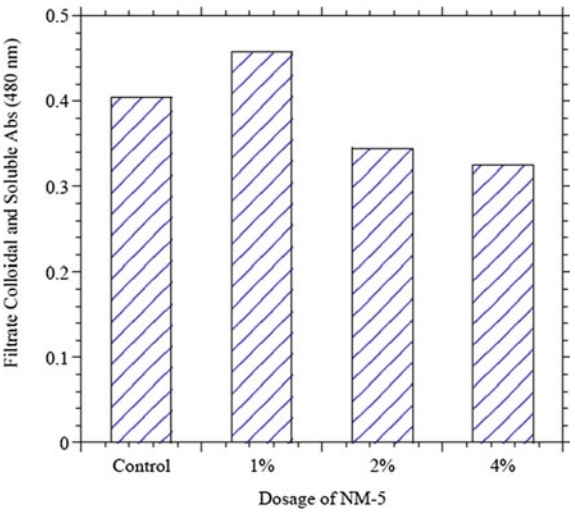

Fig. 26 Effect of NM-5 dosage on colloidal and soluble Abs with Lewisburg biosolids

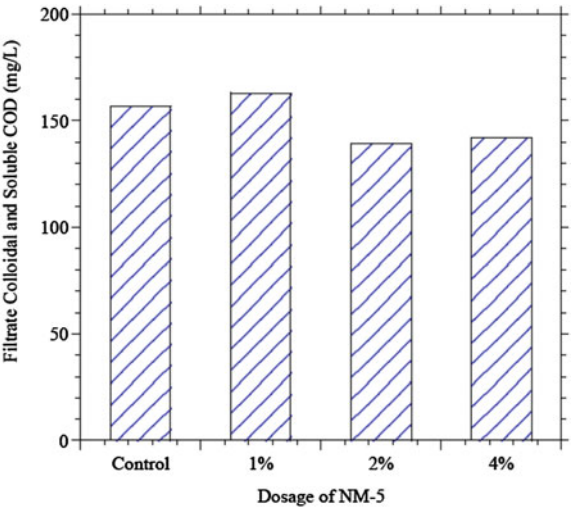

Fig. 27 Effect of NM-5 dosage on colloidal and soluble COD with Lewisburg biosolids

effective for dewatering and odors, and much higher dosages would be required for reducing odors.

However, the extent of dewatering benefits using the same nanoparticle and same or similar high charge density polymers varied during the screening study phase and detailed study period. It is not currently known if the plant made any modifications to operating conditions over this period. Additional studies may be required to understand the underlying factors that caused such differences. However, data from concurrent studies using polymers of varying charge densities indicated that nanoparticles are more effective in conjunction with lower than

giovanni.libralato@unina.it

higher charge density polymers. Data indicated also that a lower charge density polymer instead of a higher charge density polymer could be used for effective dewatering when used in conjunction with the nanoparticles.

The addition of NM-6 had a large positive impact on the filtrate quality, especially as measured by the filtrate TSS. It also increased the cake solids during dewatering. NM-11 resulted in a moderate improvement in the filtrate quality, as measured by filtrate TSS, while NM-5 had less of an impact. These results have provide the framework for understanding the conditions for which the addition of nanoparticles may (or may not) aid in the conditioning in dewatering process.

For the study evaluating the use of nanoparticles to reduce odors produced by the cake, ten different nanoparticles were tested under a range of conditions. They were added prior to polymer addition during the conditioning process as well as directly to the cake for odor control. The results of these tests follows:

- Three nanoparticles (NM-5, NM-6, and NM-7) worked well for conditioning and dewatering improvements and/or reduction in odorant concentrations;
- Additional testing was performed on NM-5, NM-6, and NM-7 to further understand their effectiveness for improving dewaterability, reducing polymer demand, and improving filtrate quality;
- NM-5 resulted in little improvement in dewatering parameters such as polymer dose, cake solids and filtrate quality. It did reduce TVOSC production when added during the conditioning step and was especially true for incubation at 25 °C. Addition directly to the cake did not have as much of an effect when compared to adding it during the conditioning step;
- NM-6 consistently improved conditioning and dewatering parameters such as reducing polymer demand, increasing cake solids, and improving filtrate quality. It seemed to have its best effect when added with the low and medium charge density polymers. Unfortunately, it did not have a consistent improvement in TVOSC production, and in some cases the addition of NM-6 at the dosages tested (2 and 4%) actually increased the TVOSC production;
- NM-7 addition had positive effects on dewatering, but had a greater effect on TVOSC production, especially when added directly to the cake after dewatering. In some cases, peak TVOSCs concentrations were 20–50% of control samples.

6 Conclusions

Results suggested that the addition of nanoparticles could help to improve dewatering in most cases for the cationic nanoparticles, but not in all cases. However, no clear pattern emerged on why some nanoparticles worked better than others especially when examining the NM characteristics such as Zeta potential, particle size and surface area. It is not clear why some nanoparticles worked and others did not especially when particles had similar charge and size. One interesting finding is that

giovanni.libralato@unina.it

NM-6, which was the one that improved dewatering most consistently, presented the smallest size of around 1 nm, thus being worthy of further additional study.

The overall objective of this research was to examine if nanoparticles held promise as additives that could improve conditioning, dewatering, and cake quality. The results are mixed, and suggest that with further development, it might be possible to develop nanoparticles as useful additives for this purpose. The work suggests that additional testing should be performed on defining the characteristics of nanoparticles that make them useful additives. For example, experiments could be performed in which the same nanoparticle is used, but its size is varied over a range such as 1, 50, and 100 nm to determine how size affects their effectiveness. Additional experiments could be performed varying charge, and specific surface area as well.

References

Adams GM, Witherspoon JR, Erdal ZK, Forbes RH, Hargreaves JR, Higgins MJ, McEwen DW, Novak JT (2007) Identifying and controlling the municipal wastewater odor environment phase 3: biosolids processing modifications for cake odor reduction. Water Environment Research Foundation, Report No.03-CTS-9T, Alexandria, VA

Andersen K, Lindgren E (1996) Important properties of colloidal silica in microparticulate systems. Nordic Pulp Paper Res J 11(1):15–21

Bernier JF, Begin B (1994) Experience of a microparticle retention system. Tappi J 77(11): 217–224

Cao J, Clasen P, Zhang WX (2005) Perchlorate reduction by nanoscale particles. J Nanoparticles Res 7:499–506

Chen Y, Higgins MJ, Murthy SN, Maas NA, Covert KJ, Toffey WE (2006) Production of odorous indole, skatole, p-cresol, toluene, styrene, and ethylbenzene in biosolids. J Residual Sci Technol 3:193–202

Chen YC, Forbes RH, Adams G, Witherspoon JR, Hargreaves R, Novak JT, Higgins M, Erdal Z, Morton R, Shea T, Abu-Orf M (2007) WERF odor study phase III: effect of alum addition on odorant production from anaerobically digested biosolids. In: Proceedings of water environment federation joint residuals and biosolids management conference, Denver, CO

Dentel SK, Gossett JM (1982) Effect of chemical coagulation on anaerobic digestibility of organic materials. Wat Res 16:707–718

Dixon LG, Field P (2004) Proceedings from the biosolids research summit. Water Environment Research Foundation Project Report 03-HHE-1; Water Environment Foundation Project Report: Alexandria, VA

Ganesh R, Liu B, Leong LYC, Kuo J, Jain M (2007) Removal of organic and inorganic contaminants from water using ferric oxide nanoparticles. J Nat Sci Sustainable Technol 1(4)

Ganesh R, Higgins MJ, Ou R, Skandan G (2009) Evaluation of nanoscale additives to improve sludge conditioning and dewatering. In: Proceedings of the water environment federation 23rd annual residuals and biosolids management conference, Portland, OR

Higgins MJ, Murthy SN, Striebig B, Hepner S, Yamani S, Yarosz DP, Toffey W (2002) Factors affecting odor production in Philadelphia Water Department Biosolids. In: Proceedings water environment federation odors and toxic air emissions 2002, Albuquerque, NM

giovanni.libralato@unina.it

Higgins MJ, Hamel K, Chen YC, Murthy SN, Barben EJ, Livadaros A, Travis M, Maas NA (2005) Part II of field research: impact of centrifuge torque and polymer dose on odor production from anaerobically digested biosolids. In: Proceedings of WEF/AWWA joint residuals and biosolids management conference, Nashville, TN

Higgins MJ, Chen YC, Yarosz DP, Murthy SN, Maas NA, Glindemann D, Novak JT (2006a) Cycling of volatile organic sulfur compounds in biosolids and its implications for odors. Water Env Res 78:243–252

Higgins MJ, Murthy SN, Chen YC (2006b) Understanding factors affecting conditioning and dewatering. Water Environment Research Foundation Report No. 01-CTS-1, Alexandria, VA

Higgins MJ, Adams G, Card T, Chen YC, Erdal Z, Forbes RH Jr, Hargreaves JR, McEwen D, Murthy SN, Novak JT, Witherspoon JR (2008) Role of protein, amino acids, and enzyme activity in odor production from anaerobically digested and dewatered biosolids. Water Env Res 80:127

Higgins MJ, Murthy SN, Chen YC (2010) Evaluation of aluminum and iron addition during conditioning and dewatering for odor control. Water Environment Research Foundation Report No. 03-CTS-9, Alexandria, VA

Honig DS, Harris EW, Pawlowska LM, O'Toole MP, Jackson LA (1993) Formation improvements with water soluble micropolymer systems. Tappi J 76(9):135–143

Lindstrom T, Hallgren H, Hedborg F (1989) Aluminum-based microparticulate retention aid systems. Nordic Pulp Paper Res J 4(2):99–103

Murthy SN, Novak JT, Buckley M (1997) Predicting polymer conditioning requirements in high pressure sludge dewatering devices. Mid-Atlantic Ind Hazard Waste 29:293–302

Murthy SN, Higgins MJ, Chen YC, Covert K, Maas NA, Toffey W (2003) The impact of dewatering equipment on odorant production from anaerobically digested biosolids. In: Proceedings of WEF annual conference (WEFTEC03), Los Angeles, CA

Novak JT, Lynch DP (1990) The effect of shear on conditioning: chemical requirements during mechanical sludge dewatering. Water Sci Tech 22:117–124

Novak JT, Adams G, Chen Y, Erdal Z, Forbes RH, Glindemann D, Hargreaves JR, Hentz L, Higgins MJ, Murthy SN, Witherspoon J (2006) Generation pattern of sulfur containing gases from anaerobically digested sludge cakes. Water Environ Res 78:821–827

Shelke K (2007) Tiny, invisible ingredients. For Food Procesing.com, The Digital Resource of Food Processing Magazine. http://www.foodprocessing.com/articles/2006/227.html?page=1

U.S. Patent 6020402 (2006) Silicone rubber compositions incorporating silicon-treated carbon blacks. WWICS (Woodrow Wilson International Center for Scholars). Project on Emerging Nanotechnologies. A Nanotechnology Consumer Products Inventory. http://www.nanotechproject.org/index.php?id=44

Wang ZS, Hung MT, Liu JC (2007) Sludge conditioning by using alumina nanoparticles and polyelectrolyte. Water Sci Technol 56(8):125–132

giovanni.libralato@unina.it

Presence, Behavior and Fate of Engineered Nanomaterials in Municipal Solid Waste Landfills

Ceyda Senem Uyguner-Demirel, Burak Demirel, Nadim K. Copty and Turgut T. Onay

Abstract As a result of extensive use of engineered nanomaterials (ENMs) in consumer products, significant amounts of ENMs are eventually released to the environment and find their way to wastewater treatment plants, incineration plants and landfills. Recent concerns about the potential impacts of these materials on the environment and human health, have diverted researchers' interest to investigate the behaviour of inorganic, metallic/metal oxide ENMs in conventional activated sludge wastewater treatment and anaerobic sewage sludge digestion systems. However, related information about the presence and fate of such ENMs during waste stabilization in municipal solid waste (MSW) landfills which remains a widely used method of solid waste management, is scarce in literature. Therefore, in this paper, recent information about the detection methods and fate of the most commonly used metal oxide ENMs such as TiO2, ZnO, Ag and SiO2 in MSW landfills was revealed. The complexity of the factors influencing ENMs retention and transport mechanisms was discussed. Future research needs relating to the fate of ENMs in MSW were also identified.

Keywords Engineered nanomaterials · Municipal solid waste · Landfill · Analytic techniques · Fate and transport · Numerical modeling

1 Introduction

Engineered nanomaterials (ENMs) are commonly used in numerous commercial products. As a result of increasing demand and consumption of ENMs, a greater amount of ENM-containing products eventually reach wastewater treatment plants,

C.S. Uyguner-Demirel · B. Demirel (✉) · N.K. Copty · T.T. Onay
Institute of Environmental Sciences, Boğaziçi University, 34342 Bebek, Istanbul, Turkey
e-mail: burak.demirel@boun.edu.tr

© Springer International Publishing AG 2017

G. Lofrano et al. (eds.), *Nanotechnologies for Environmental Remediation*,
DOI 10.1007/978-3-319-53162-5_12

giovanni.libralato@unina.it

incineration plants and landfills. The extensive use of ENMs in commercial consumer products and their eventual release to the environment through various pathways have recently raised concern about the potential impacts of these materials on the environment and human health. Life cycle analyses covering end-of-life stage studies of nanomaterials indicate that important impacts for the environment may arise (Asmatulu et al. 2012). Furthermore, sewage sludge, wastewater and waste incineration of ENM-containing products have been shown to be the major flows of ENMs to the environment (Gottschalk and Nowack 2011). The predictions for the release of large amounts of the most commonly used ENMs have recently been reported as well (Keller et al. 2013; Keller and Lazareva 2014). It is also noteworthy that the ENMs are now classified to be among the list of emerging contaminants, having potential to pose considerable challenges to conventional biological waste treatment systems (Marcoux et al. 2013; Sima et al. 2014; Han et al. 2014; Kinsinger et al. 2015).

Among the inorganic metallic/metal oxide ENMs commercially available, titanium dioxide (TiO_2), silver (Ag), and zinc oxide (ZnO) are the most frequently used materials (Yang et al. 2013a). Nano-TiO_2, which is widely used in production of paints, paper, plastics, cosmetics, is also the most commonly employed semiconductor photocatalyst (Macwan et al. 2011). Nano-Ag is used as an antimicrobial agent in domestic appliances, paints, medical applications, plastics and textiles (Mueller and Nowack 2008; Bystrzejewska-Piotrowska et al. 2009; Siripattanakul-Ratpukdi and Fürhacker 2014). Nano-ZnO is used in cosmetics, catalysts and UV-protection (Bystrzejewska-Piotrowska et al. 2009). In addition to TiO_2, Ag, and ZnO, nano copper oxide (CuO) are employed in the production of solar cells, lithium-ion batteries, gas sensors, bio-sensors, photodetectors, and magnetic storage media (Zhang et al. 2014). Nano aluminum oxide (Al_2O_3) is reported to be used in production of batteries, fire protection, metal and biosorbent, while nano silicon oxide (SiO_2) is used in fire-proof glass, UV-protection, varnish, ceramics, electronics, pharmaceutical products, dentistry and polishing (Bystrzejewska-Piotrowska et al. 2009). Nano cerium oxide (CeO_2) has been reported to be commercially used in cosmetics as UV-filters and in drugs (Strobel et al. 2015).

Despite the widespread use of ENMs in commercial products and their eventual disposal in sanitary landfills, the fate and behavior of ENMs in solid waste environments are still not well understood. Even though recent research efforts have examined the fate of inorganic, metal oxide ENMs on conventional activated sludge (AS) wastewater treatment and anaerobic digestion (AD) of sewage sludge systems, the information about the presence, fate and behavior of nano metal oxides in municipal solid waste (MSW) landfills is scarce. Therefore, in this paper, recent information about the presence, fate and behavior of the most commonly used metal oxide ENMs such as TiO_2, ZnO, Ag and SiO_2 in MSW landfills is discussed.

giovanni.libralato@unina.it

2 Fate and Behavior of Metal Oxide ENMs in Landfills

Sanitary landfilling is considered as an acceptable method for disposing both MSW and large portion of industrial wastes. However, there are several health and environmental concerns for the landfill gas and leachate emissions resulting from the operation of landfills. Therefore, an effort to improve the design and operation of landfills to minimize these impacts is very important. Currently, there are two types of landfill operations: conventional and bioreactor landfills.

Conventional sanitary landfills consist of cells and lifts with liners, drains, gas vents, leak detection systems and intermediate and final covers. Due to the inadequacy of conventional waste management, extensive lab-scale and full-scale investigations were carried out to answer the essential questions of low-emission landfilling. Anaerobic decomposition of solid waste causes significant environmental pollution by producing methane (an explosive, "greenhouse" gas) and harmful leachate, which can pollute the groundwater (Erses et al. 2008; Renou et al. 2008). According to some researchers, the long term environmental impact caused by MSW landfills may last for centuries (Kjeldsen et al. 2002).

Increasing attention is being given to the enhancement of waste stabilization by leachate recirculation to reduce the time required for waste degradation, improve leachate quality and enhance the rate of gas production and methane concentration for energy recovery. Bioreactor landfill systems as the modification of conventional landfill with the addition of leachate recirculation evolved to minimize environmental impacts with optimizing waste degradation. During the leachate recirculation, leachate is collected, stored and reinjected back into the landfill to promote in situ anaerobic biological treatment. The advantages of leachate recirculation have been demonstrated by many researchers that performed numerous lysimeters and field tests (Onay and Pohland 1998; San and Onay 2001; Erses and Onay 2003).

Besides the changes in landfill configuration, there is also increasing demand for more stringent regulations for monitoring landfills in addition to their design and operation. The most recent European regulations on waste management are primarily intended to reduce the use of landfilling, to control landfill emissions and their effects (including greenhouse effect) and to shorten the long term environmental impact (aftercare phase). In spite of extensive laws and regulations to reduce the waste quantity, considerable amounts of solid waste have to be expected in the future and landfilling will be the most commonly employed disposal method especially in the developing world since it is a comparatively simple and economic way for solid waste disposal. Moreover, landfilling is the most utilized ultimate disposal method for wastes that cannot be recovered (Aljaradin and Persson 2012).

It is evident that more ENM containing waste will enter landfills in the future. A recent study showed that 63–91% of over 260,000–309,000 metric tons of global ENM production in 2010 ended up in landfills (Keller et al. 2013). ENMs can enter into landfills and further into leachate through the sludge and ash generated during the wastewater treatment and incineration processes, respectively (Disalvo et al. 2008; Holder et al. 2013). Mueller and Nowak (2008) determined that the three

giovanni.libralato@unina.it

most commonly used ENMs including nano-silver, nano-titanium dioxide and carbon nano-tubes will be eventually released in landfills. Therefore, disposal of ENMs may generate problems through their release and fate on landfill gas or leachate. A recent study by Hennebert et al. (2013) investigated the presence of ENMs in various waste leachates. It showed the presence of significant amount of colloids in leachate with different elemental composition from natural ones. ENMs are considered as emerging contaminants that can be found in environment but are not included in monitoring programs because of the lack of information about their fate and behavior in environment (Marcoux et al. 2013). It should also be noted that ENMs containing products cannot be always named as free ENMs since they are surface modified, functionalized or coated to convey their implementer properties (Reinhart et al. 2010). Evaluation of the current literature shows that recent research activities have mostly focused on the eco-toxicity of ENMs. However, the fate of ENMs during waste stabilization in landfills, which play a crucial role in integrated waste management systems, remains mostly unknown.

Solid wastes disposed of in landfills can be an important source of heavy metals release to our environment (Kanmani and Gandhimathi 2013). Landfill conditions, on the other hand can affect the heavy metals impacts on microorganisms. At the beginning of landfilling, the initial stage represents the aerobic condition where the oxygen content in landfill gas is in the range of 0.1–1%. It was investigated that presence of oxygen is necessary for oxidative dissolution of ENMs which converts the ENMs to its heavy metal ion causing further toxicity to microorganisms during anaerobic digestion (Yang et al. 2012). A large number of studies have reported metals concentrations in landfills (e.g., Al-Wabel et al. 2011; Kanmani and Gandhimathi 2013; Karim et al. 2014). Even though trace amounts of metals are necessary for microorganisms, they can be inhibitory to microbial life above threshold concentrations and adversely affect degradation process. For example, nano-silver was found to decline the total gene copy numbers of methanogens. Moreover, release of silver ions from products containing nano-silver generates a concentration gradient which causes toxicity to the microorganisms (Yang et al. 2012).

The fate of ENMs in landfills depends highly on their properties, the waste composition and also the physicochemical conditions of landfill sites (Boldrin et al. 2014). The properties of ENMs including solubility, redox activity and their release sources to the environment affect ENMs fate in landfills. For example, TiO_2 is not soluble, whereas nano-Ag is soluble or TiO_2 is unreactive compared to reactive cerium oxide. The modification of the ENMs—containing product by adding a layer to achieve the desired feature of the product can change its physical, chemical and biological properties which differs from those of the ENMs. For example AlOOH or a SiO_2 layer which is added to the TiO_2 nano-particles in sunscreens can disrupt the incorporation of oxygen species (Nowack et al. 2012).

ENMs in landfills can either be released from liquid wastes including cosmetic, hair products, sunscreens and wastewater sludge or from solid wastes such as plastics, polymers or metals that they bound in them and incorporate to leachate. The ENMs bond on products can even be released because of extreme

giovanni.libralato@unina.it

environmental conditions in landfills such as low pH, high reducing condition. Sometimes abrasion and compaction in landfill can enhance the release of ENMs into the leachate. After entering the leachate, the composition of leachate plays an important role in the fate of ENMs. The organic matter and electrolyte concentration of leachates affect the mobility and therefore the fate of ENMs. It was reported that in old landfills, the high concentration of high molecular weight organics such as humic and fulvic acid can enhance the mobility of ENMs (Reinhart et al. 2010; Lozano and Berge 2012; Nowack et al. 2013). The presence of humic acid favored the mobility of single-walled carbon nano-tubes (Jaisi et al. 2008; Lozano and Berge 2012). On the other hand, in young leachates, most portions of organics are composed of volatile fatty acids, which can decrease the pH and thus increase the mobility of ENMs. Yang et al. (2012) investigated the total silver concentration in bioreactor loaded with 10 mg Ag/kg solids A decline in silver concentration was observed which may be attributed to the precipitation as AgS_2, sorption on solid particles or reaction with anions and functional groups such as Cl^- and CO_3^{2-} to form complexes (Yang et al. 2012).

ENMs disposed of in landfills can affect the microbial activities and therefore interrupt the biogas production. Yang et al. (2013b) investigated the effects of nano-Ag on methanogenesis and biogas production in sanitary landfills using MSW loaded in identical landfill bioreactors. Their results showed that the biogas production reduced by 78% when the bioreactors were exposed to 10 mg Ag/kg solids, whereas there was no significant difference between the control and the reactor with 1 mg Ag/kg solid. The total copy of 16S rRNA gene of methanogens was significantly interrupted by the action of nano-Ag, which resulted in low biogas production. Moreover, higher concentration of volatile fatty acids (VFAs) produced in reactor with 10 mg Ag/kg solids confirmed the inhibition of anaerobic digestion by nano-Ag (Yang et al. 2013b). In a recent study, the effects of nano-ZnO and nano-CeO_2 on biogas production from sludge were investigated. Addition of 1000 mg/L of ZnO inhibited the methanogenic activity, which reduced the biogas generation by 65.3%. Although 100, 500 and 1000 mg/L of CeO_2 decreased the biogas production, addition of 10 mg/L of CeO_2 enhanced the biogas production by 11% (Nguyen et al. 2015).

The above survey of the literature relating to the fate of metal oxide ENMs after their disposal in landfills reveals that this line of research remains in its early changes. Future research is needed to understand the behavior of ENMs in landfills and their impact on waste stabilization as well as the potential risks that they may cause to the environment, and public health (Reinhart et al. 2010).

3 Presence and Detection of Selected ENMs in Leachate

Quantification of ENMs in various matrixes is a topic of interest for researchers studying their potential health and environmental impacts. Different methods of analysis were reported in literature for their measurement and recovery (Hennebert

giovanni.libralato@unina.it

et al. 2013; Bolyard et al. 2013; Yang et al. 2012). However, studies show that there are difficulties in the determination and analysis of ENMs in landfill leachate. For the measurement of ENMs, sample preparation is a crucial step which requires significant attention. To date, there is no specifically defined method which is capable of routine monitoring of the existence of such particles in the environment or in complex matrix as leachates. Several aspects, including the properties of the particles (e.g., size, shape, aggregation state, surface characteristics, coatings) (Mudunkotuwa et al. 2012; Reed et al. 2012; Vogelsberger et al. 2008) and of the surrounding matrix (pH value, temperature, ionic strength) (Reed et al. 2012) as well as the concentration and the intensity/duration of the dissolution process, have to be considered for the determination of ENMs (Schmidt and Vogelsberger 2009).

For ENMs composed of metals or metal oxides, analytical techniques for their detection usually require digestion, followed by dissolution in aqueous media prior to analysis (Hennebert et al. 2013; Khosravi et al. 2012). Currently, there are a wide variety of methods for digesting metals in environmental samples, such as open hot-plate, microwave and alkaline fusion. Microwave assisted and open hot-plate acid digestion methods are widely used techniques for preparing solid samples for analysis (Szymczycha-Madeja and Mulak 2009; Bolyard et al. 2013). Using ammonium persulfate as a fusing reagent, the fusion method developed by Khosravi et al. (2012) achieved comparable Ti recoveries (>95%) from different forms of TiO_2 including anatase, rutile and mixed nano-sized crystals, and amorphous particles with microwave digestion and higher than open hotplate digestion with a mixture of HNO_3, H_2O_2 and HF.

The digestion process is normally carried out with various combinations and proportions of mineral acids, such as: HNO_3, HNO_3 + HCl, HNO_3 + HCl + HF, HNO_3 + HF, HNO_3 + $HClO_4$ (Szymczycha-Madeja and Mulak 2009; Larrea et al. 1997; Fabricius et al. 2014; Bolyard et al. 2013). Hydrofluoric acid, which is capable of dissolving silicates, may require the removal of excess hydrofluoric acid to prevent equipment damage or the use of specialized non-glass components during instrumental analysis. Moreover, hydrofluoric acid is hazardous and requires special handling such as the use of proper personal protection equipment and an adequate fume hood. It has been shown that either a mixture of hydrogen peroxide, nitric acid, and sulfuric acid or hydrogen peroxide, nitric acid, and hydrofluoric acid can sufficiently digest TiO_2 with recoveries greater that 95% (van Bussel et al. 2010; Packer et al. 2007).

In a recent work of Bolyard et al. (2013), background metal concentrations from nano-ZnO, TiO_2, and Ag in leachate fractions (total, <1500, and <1 nm) were quantified using inductively coupled plasma-optical emission spectrum (ICP-OES) subsequent to digestion of samples using concentrated nitric acid and 1:1 water/hydrochloric acid solution.

Fabricius et al. (2014) in their recent paper investigated sample preparation procedures required prior to inductively coupled plasma-mass spectroscopy (ICP-MS) measurements to quantify precisely the total concentration of some of the most commonly used and discussed nanoparticle suspensions (Ag, TiO_2, CeO_2, ZnO, Au). In their work nano-ZnO and Au were digested in a mixture of HNO_3

giovanni.libralato@unina.it

(1.1 mL ~65%) and HCl (0.3 mL ~30%), for nano-Ag HNO_3 (1.4 mL ~65%), for CeO_2 a mixture of HNO_3 (1.2 mL ~65%) and H_2O_2 (0.2 mL ~30%) was used. Digestion of nano-TiO_2 was conducted in H_2SO_4 (1.4 mL ~96%).

A method validation process for Ti determination from nano-TiO_2 in biological matrixes was presented by Nia et al. (2015) using a closed-vessel microwave digestion with a mixture HNO_3 and HF by quadrupole ICP-MS. The results demonstrated an accurate determination of Ti with a great accuracy at low concentration levels near the limit of quantification (LOQ) of 0.10 mg kg^{-1}. Durenkamp et al. (2016) investigated the quantification of nano-ZnO and nano-Ag in leachate, digestion with 5 mL conc. nitric acid/perchloric acid (87:13 v/v) was applied subsequent to analysis by ICP-OES for Zn and by ICP-MS for Ag.

Dulger et al. (2016) indicated very recently that using HNO_3 and HCl acid combination in digestion provided acceptable recoveries (75%) for Ti detection from nano-TiO_2 in real landfill leachate. The concentrations were measured by ICP-OES in individual samples containing 1, 10 and 100 mg/L of nano-TiO_2 resulted in recoveries of 87, 86, 84% for TiO_2 in deionized water.

It is important to note that once quantification of ENMs in landfill leachate is successfully accomplished with verified methods, critical knowledge about their potential transport and ultimate disposition could be attained. However, concerning quantification and characterization of ENM suspensions, the analytical tools available are not necessarily suitable for all nanomaterials. Understanding the properties of coated ENMs is also important because the coating can reduce the nanoparticle bioavailability, and limit the toxicological effects in the environment (Musee 2011). Considering that other engineered nanomaterials may have different density, surface coatings, or other properties, further research is required with different ENMs.

4 Modeling of ENM Retention and Transport in MSW

As noted earlier, the interest in the fate of nanomaterials in MSW has only materialized in recent years with the tremendous increase in the manufacturing of ENMs and their incorporation in a wide variety of consumer products. As such very few studies focusing on the mathematical modeling of the fate and transport of ENMs in MSW can be found in the literature at the present time. While the modeling of ENMs in MSW remains in its early stages, as a starting point the field can benefit from the considerable efforts that have been directed towards understanding the fate and transport of colloids in porous media such as soil or glass beads (see, for example, recent reviews by Sen and Khilar 2006; Bradford and Torkzaban 2008). The potential applicability of some of these earlier findings to ENMs in MSW stems from the fact that MSW can be treated as a partially water-saturated porous medium, albeit a dynamic one which is constantly changing in time as the MSW is stabilized.

giovanni.libralato@unina.it

Initial attempts to model the colloidal forces acting on a bare colloid with no surface coating in the presence of a solid surface (collector) or other colloids have often relied on the Derjaguin-Landau-Verwey-Overbeek (DLVO) theory (Elimelech et al. 1998). The underlying premise of this theory is that attachment of a colloid on the collector surface is dependent on the balance of forces acting on the colloid in the vicinity of the collector surface. The DLVO theory identifies the van der Waals forces as the main attractive force between a particle and the collector. The van der Waals forces result from the induced dipole which tends to attract the particle to the collector (deposition) or other particles (aggregation). The attractive van der Waals forces increase as the particle size increases and as the separation distance decreases (Phenrat and Lowry 2009). The main repulsive force as proposed by the DLVO theory is the electrostatic double layer repulsion. This repulsive force is function of the zeta potentials of the particle and collector and the separation distance. It is also function of the ionic strength of the solution. The electrostatic repulsive forces act to prevent the aggregation of colloids and their deposition on the collector.

Combining the electrostatic repulsion and the Van der Waals attractive forces results in the interactive energy plot depicted schematically in Fig. 1. Two energy minimums are observed. The primary minimum is located just next to the collector surface. However, for a particle to deposit under the primary minimum it must have sufficient energy to overcome the energy barrier. The DLVO theory also predicts a secondary minimum located outside the energy barrier. Particles can deposit or aggregate under this shallower minimum. Because particles often may not reach the

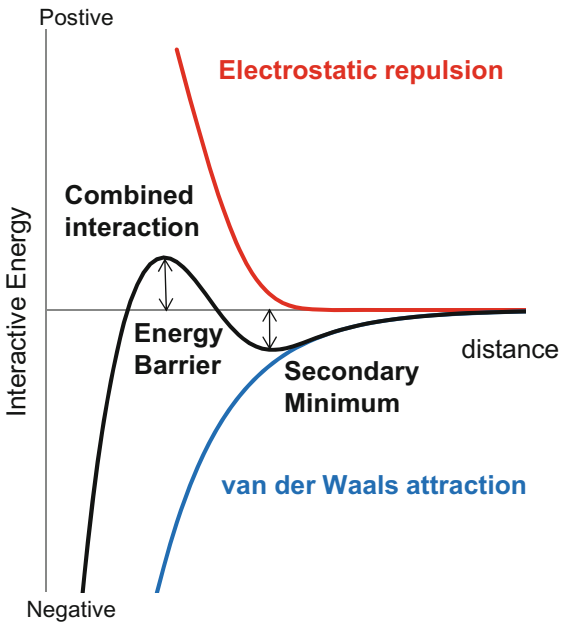

Fig. 1 Interactive energy between a particle and a collector as a function of separation distance based on the DLVO theory

giovanni.libralato@unina.it

collector surface for deposition within the primary minimum, deposition is quite likely to occur at the shallower second minimum. The shallow depth (interactive energy) of this minimum also means that particles may detach from this collector if the particle's Brownian energy or the gravitation forces (buoyancy), due to the particles density relative to the fluid, are large enough to overcome the article-collector attractive energy. The shear forcing or the hydrodynamic forces due to the flowing fluid is another mechanism that can detach a particle from a collector.

The shallow secondary minimum leading to the attachment of a particle on a collector and its potential detachment from the collector can have important consequences on ENM transport. These mechanisms show that detachment and re-suspension of ENMs is possible even after its deposition on a solid surface. Research has shown that the depth of the secondary minimum is strongly dependent on the ionic strength of the solution and in particularly the presence of divalent ions as opposed to monovalent ions in the solution. Specifically, the depth of the ionic depth is expected to increase with ionic strength. Given the high ionic strength expected in landfills, the secondary minimum may not be very shallow. At the same time, the moisture flow within the emplaced waste is relatively small resulting in low shear forces. Therefore, further experimentation would be needed to assess whether the external forces are indeed sufficient for the reversal of ENM deposition on the MSW and its re-suspension into the leachate. Other factors influencing the collector efficiency include particle size, fluid velocity, fluid pH, and soil matrix properties such as surface roughness (Lecoanet and Wiesner 2004; Mallouk et al. 2007; Yang et al. 2007; Saleh et al. 2008; Phenrat et al. 2009).

Although the DLVO theory has been useful for examining the interaction of a particle with a collector and the impact of this interaction on ENM mobility, this theory has been shown to be inadequate in some instances due to the presence of other forces that complicate particle/collector. The most notable force not included in this theory is the steric repulsion force for surface-coated particles. In many applications ENMs are not present in bare form but are surface-stabilized using for example some polymeric materials such as polyacrylic acid (PAA). The purpose of the surface coating is to prevent the particles from aggregating. This would result in an additional steric repulsion force when a particle approaches another particle or a collector that is not accounted for in the classical DLVO theory. The magnitude of the steric forces depends on the properties of the stabilization layer, specifically the surface concentration of the surface stabilizer and its charge density. Overall, the particle surface coating and the steric repulsion forces it creates prevents the deposition of particles within the primary minimum and weakens somewhat the secondary minimum and therefore can enhance the potential detachment of the particles from the collector. It is important to note that ENMs in MSW will likely remain within the MSW for a long time. The properties of the surface coating and the steric repulsion it provides can weaken over time, further complicating ENM-MSW interaction and, consequently, ENM transport.

Another mechanism not accounted for in the DLVO theory is the potential straining of the ENMs within the MSW. Straining is the deposition or capture of

giovanni.libralato@unina.it

particles in small areas within a porous medium. Potential straining processes have been discussed in detail by Bradford and Torkzaban (2008) within partially saturated porous media. These processes include wedging of particles in tight volumes between solids as well as on air-water interfaces and within the solid-water-air triple point (Bradford and Torkzaban 2008). Straining of colloids in partially saturated soils has been shown to be strongly dependent on the pore volume geometry and the capillary forces in the flowing fluid (Steenhuis et al. 2006). It is likely that these straining processes will also be present for ENMs in MSW and the waste's highly irregular pore geometry. Moreover, with decrease in moisture content of the waste, downward moisture movement will be restricted to smaller areas, further increasing the potential of straining. Straining, similar to particle deposition and detachment due to the attractive and repulsive forces described above, is likely to be partially reversible as the moisture content or pore volume within the waste change with time. Surface coating of the ENMs can also influence particle straining. Specifically, the repulsive forces of surface coated strained particles are likely to block other particles from being retained within the same pore volume (Bradford et al. 2003).

Besides the pore scale physiochemical processes that have been described above, there were some recent attempts to model ENM transport at a larger scale without the need to identify and model the actual pore scale physiochemical processes responsible for the ENM mobility. The most relevant study along this area is the study of Sakallioglu et al. (2016), which used a numerical model to simulate the kinetic attachment/detachment of the nano-ZnO in fresh MSW. The model was initially developed to model attachment of engineered nanoparticles in saturated porous media (Bradford et al. 2003; Torkzaban et al. 2010; Ersenkal et al. 2011). The model defines particle deposition and detachment kinetics as first order rate expressions:

$$\frac{\partial C}{\partial t} = -K_{dep}C + \frac{M_s}{V_w}K_{\mathrm{det}}S \tag{1}$$

where, C is the nano-ZnO concentration in suspension; S is the retained nano-ZnO concentration; K_{dep} and K_{det} are the deposition and detachment rate constants, respectively, that combine all potential processes occurring at the collector surface; M_s is the dry mass of MSW; V_s is the volume of moisture within the MSW; and t is time. A similar mass conservation equation can be written for the change in the retained nano-ZnO concentration:

$$\frac{\partial S}{\partial t} = \frac{V_w}{M_s}K_{dep}C - K_{\mathrm{det}}S \tag{2}$$

By solving the above system of equations for the two unknowns S and C and comparing to observed concentration data, estimates of the deposition/detachment parameters (K_{dep} and K_{det}) were determined. It was shown that the model was able to adequately simulate ENM deposition/retention within the MSW.

giovanni.libralato@unina.it

This review clearly demonstrates that, while significant work has been done in the area of colloid transport in porous media, there is a clear need to evaluate to what extent these mechanisms are also valid for ENMs in MSW.

5 Conclusions

As a result of increasing demand for nanomaterials to be used in commercial products, it is evident that more ENM containing waste will ultimately end up in sanitary landfills in the near future. However, even though ENMs are commercially employed in ever increasing amounts, we are still not well informed about the potential impacts of ENMs on the environment and human health. Particularly, the current state of scientific information about the behavior of ENMs in landfill environment needs to be significantly improved so that novel strategies can be developed and implemented to manage ENMs containing wastes within integrated solid waste management systems.

In this paper, the detection, behavior and transport mechanisms of inorganic metal oxide/metallic ENMs were discussed in landfill environment by reviewing the current scientific information available, with special focus on the fate of heavy metals in landfills and their potential impact on biochemical waste stabilization processes. Based on the assessment of literature, firstly it is important to note that once quantification of ENMs in landfill leachate is successfully accomplished with verified analytical methods, critical knowledge about their potential transport and disposition within the waste matrix can be attained. In order to simulate variations in landfill leachate characteristics over time and their subsequent effect on the fate of ENMs, different leachate samples from real landfills should also be studied.

It is also of paramount importance to determine the long-term behavior and fate of ENMs after they enter the landfill environment. It is clear that such studies are lacking in literature at the moment and future research should also focus on this particular topic, which is a quite difficult challenge for the scientists to deal with.

The physiochemical processes described in this paper clearly demonstrate the complexity of the factors influencing ENM retention and transport within MSW. While significant work has been done in the area of colloid transport in porous media, there is a clear need to evaluate to what extent these mechanisms are also valid for ENMs in MSW. In this regard, there is a need to conduct detailed experimental work for identifying the physical and biochemical factors influencing ENM transport in the waste matrix as well as develop and validate mathematical models that can adequately describe these processes.

Acknowledgements The authors express their gratitude to the Scientific and Technological Research Council of Turkey (TÜBİTAK) for their support for this work through project 112Y322.

giovanni.libralato@unina.it

References

Aljaradin M, Persson KM (2012) Environmental impact of municipal solid waste landfills in semi-arid climates—case study—Jordan. Open Waste Manag J 5:28–39

Al-Wabel MI, Al Yehya WS, Al-Farraj AS, El-Maghraby SE (2011) Characteristics of landfill leachates and bio-solids of municipal solid waste (MSW) in Riyadh City, Saudi Arabia. J Saudi Soc Agric Sci 10:65–70

Asmatulu E, Twomey J, Overcash M (2012) Life cycle and nano-products: end-of-life assessment. J Nanopart Res 14:720–727

Boldrin A, Hansen SF, Baun A, Hartmann NIB, Astrup TF (2014) Environmental exposure assessment framework for nanoparticles in solid waste. J Nanopart Res 16:2394–2412

Bolyard SC, Reinhart DR, Santra S (2013) Behavior of engineered nanoparticles in landfill leachate. Environ Sci Technol 47:8114–8122

Bradford SA, Torkzaban S (2008) Colloid transport and retention on unsaturated porous media: a review of interface-, collector-, and pore-scale processes and models. Vadose Zone J 7:667–681

Bradford SA, Simunek J, Bettahar M, van Genuchten MT, Yates SR (2003) Modeling colloid attachment, straining, and exclusion in saturated porous media. Environ Sci Technol 37:2242–2250

Bystrzejewska-Piotrowska G, Golimowski J, Urban PL (2009) Nanoparticles: their potential toxicity, waste and environmental management. Waste Manag 29:2587–2595

DiSalvo RM, Gary PE, McCollum GR (2008) Evaluating the impact of nanoparticles on wastewater collection and treatment systems in Virginia. Water jam 2008. Virginia Beach, Virginia, 7–11 Sept 2008

Dulger M, Sakallioglu T, Temizel I, Demirel B, Copty NK, Onay TT, Uyguner-Demirel CS, Karanfil T (2016) Leaching potential of nano-scale titanium dioxide in fresh municipal solid waste. Chemosphere 144:1567–1572

Durenkamp M, Pawlett M, Ritz K, Harris JA, Neal AL, McGrath SP (2016) Nanoparticles within WWTP sludges have minimal impact on leachate quality and soil microbial community structure and function. Environ Pollut 211:399–405

Elimelech M, Gregory J, Jia X, Williams RA (1998) Particle deposition and aggregation measurement, modeling, and simulation. Butterworth-Heinemann, Woburn, MA

Ersenkal DA, Ziylan A, Ince NH, Acar HY, Demirer M, Copty NK (2011) Impact of dilution on the transport of poly (acrylic acid) supported magnetite nanoparticles in porous media. J Contam Hydrol 126:248–257

Erses S, Onay TT (2003) In situ heavy metal attenuation in landfills under methanogenic conditions. J Hazard Mater 99:159–175

Erses AS, Onay TT, Yenigun O (2008) Comparison of aerobic and anaerobic degradation of municipal solid waste in bioreactor landfills. Bioresour Technol 99:5418–5426

Fabricius AL, Duester L, Meermann B, Ternes TA (2014) ICP-MS-based characterization of inorganic nanoparticles—sample preparation and off-line fractionation strategies. Anal Bioanal Chem 406:467–479

Gottschalk F, Nowack B (2011) The release of engineered nanomaterials to the environment. J Environ Monit 13:1145–1155

Han X, Geller B, Moniz K, Das P, Chippindale AK, Walker VK (2014) Monitoring the developmental impact of copper and nanoparticle exposure in Drosophila and their microbiomes. Sci Total Environ 487:822–829

Hennebert P, Avellan A, Yan J, Aguerre-Chariol O (2013) Experimental evidence of colloids and nanoparticles presence from 25 waste leachates. Waste Manag 33:1870–1881

Holder AL, Vegerano EP, Zhou S, Marr LC (2013) Nanomaterial disposal by incineration. Environ Sci Process Impacts 15:1652–1664

Jaisi DP, Saleh NB, Blake RE, Elimelech M (2008) Transport of single-walled carbon nanotubes in porous media: filtration mechanisms and reversibility. Environ Sci Technol 42:8317–8323

giovanni.libralato@unina.it

Kanmani S, Gandhimathi R (2013) Assessment of heavy metal contamination in soil due to leachate migration from an open dumping site. Appl Water Sci 3:193–205

Karim MR, Kuraoka M, Higuchi T, Sekine M, Imai T (2014) Assessment of heavy metal concentration from municipal solid waste open dumping sites in Bangladesh. J Hydrol Environ Res 2:41–49

Keller AA, Lazareva A (2014) Predicted releases of engineered nanomaterials: from global to regional to local. Environ Sci Technol Lett 1:65–70

Keller AA, McFerran S, Lazareva A, Suh S (2013) Global life cycle release of engineered nanomaterials. J Nanopart Res 15:1692–1708

Khosravi K, Hoque ME, Dimock B, Hintelmann H, Metcalfe CD (2012) A novel approach for determining total titanium from titanium dioxide nanoparticles suspended in water and biosolids by digestion with ammonium persulfate. Anal Chim Acta 713:86–91

Kinsinger N, Honda R, Keene V, Walker SL (2015) Titanium dioxide nanoparticle removal in primary prefiltration stages of water treatment: role of coating, natural organic matter, source water, and solution chemistry. Environ Eng Sci 32:292–300

Kjeldsen P, Barlaz MA, Rooker AP, Baun A, Ledin A, Christensen TH (2002) Present and long-term composition of MSW landfill leachate: a review. Crit Rev Environ Sci Technol 32:297–336

Larrea MT, Gómez-Pinilla I, Fariñas JC (1997) Microwave-assisted acid dissolution of sintered advanced ceramics for inductively coupled plasma atomic emission spectrometry. J Anal At Spectrom 12:1323–1332

Lecoanet HF, Wiesner MR (2004) Velocity effects on fullerene and oxide nanoparticle deposition in porous media. Environ Sci Technol 38:4377–4382

Lozano P, Berge ND (2012) Single-walled carbon nanotube behavior in representative mature leachate. Waste Manag 32:1699–1711

Macwan DP, Dave PN, Chaturvedi S (2011) A review on nano TiO_2 sol-gel type syntheses and its applications. J Mater Sci 46:3669–3686

Mallouk TE, Hydutsky BW, Mack EJ, Beckerman BB, Skluzacek JM (2007) Optimization of nano- and microiron transport through sand columns using polyelectrolyte mixtures. Environ Sci Technol 41:6418–6424

Marcoux MA, Matias M, Olivier F, Keck G (2013) Review and prospect of emerging contaminants in waste—key issues and challenges linked to their presence in waste treatment schemes: general aspects and focus on nanoparticles. Waste Manag 33:2147–2156

Mudunkotuwa IA, Rupasinghe T, Wu CM, Grassian VH (2012) Dissolution of ZnO nanoparticles at circumneutral pH: a study of size effects in the presence and absence of citric acid. Langmuir 28:396–403

Mueller NC, Nowack B (2008) Exposure modeling of engineered nanoparticles in the environment. Environ Sci Technol 42:4447–4453

Musee N (2011) Nanowastes and the environment: potential new waste management paradigm. Environ Int 37:112–128

Nguyen D, Visvanathan C, Jacob P, Jegatheesan V (2015) Effect of cerium (IV) oxide and zinc oxide particles on biogas production. Int Biodeterior Biodegradation 102:1–7

Nia Y, Millour S, Noël L, Krystek P, de Jong W, Guerin T (2015) Determination of Ti from TiO_2 nanoparticles in biological materials by different ICP-MS instruments: method validation and applications. J Nanomed Nanotechnol 6:1–8

Nowack B, Ranville JF, Diamond S, Gallego-Urrea JA, Matcalfe C, Rose J, Horne N, Koelmans AA, Klaine SJ (2012) Potential scenarios for nanomaterial release and subsequent alternation in the environment. Environ Toxicol Chem 31:50–59

Nowack B, David RM, Fissan H, Morris H, Shatkin JA, Stintz M, Zepp R, Brouwer D (2013) Potential release scenarios for carbon nanotubes used in composites. Environ Int 59:1–11

Onay TT, Pohland FG (1998) In situ nitrogen management in controlled landfills. Water Res 32:1383–1392

Packer AP, Lariviere D, Li CS, Chen M, Fawcett A, Nielsen K, Mattson K, Chatt A, Scriver C, Erhardt LS (2007) Validation of an inductively coupled plasma mass spectrometry (ICP-MS)

giovanni.libralato@unina.it

method for the determination of cerium, strontium, and titanium in ceramic materials used in radiological dispersal devices (RDDs). Anal Chim Acta 588:166–172

Phenrat T, Lowry GV (2009) Physicochemistry of polyelectrolyte coatings that increase stability, mobility and contaminant specificity of reactive nanoparticles used for groundwater remediation. In: Savage N, Diallo M, Duncan J, Street A, Sustich R, Andrew W (eds) Nanotechnology applications for clean water. Norwich, NY, USA, pp 249–267

Phenrat T, Kim H-J, Fagerlund F, Illanasekare T, Tilton RD, Lowry GV (2009) Particle size distribution, concentration and magnetic attraction affect transport of polymer-modified Fe^0 nanoparticles in sand columns. Environ Sci Technol 43:5079–5085

Reed RB, Ladner DA, Higgins CP, Westerhoff P, Ranville JF (2012) Solubility of nano-zinc oxide in environmentally and biologically important matrices. Environ Toxicol Chem 31:93–99

Reinhart D, Berge N, Santra S, Bolyard SC (2010) Emerging contaminants: nanomaterial fate in landfills. Waste Manag 30:2020–2021

Renou S, Givaudan JG, Poulain S, Dirassouyan F, Moulin P (2008) Landfill leachate treatement: review and opportunity. J Hazard Mater 150:468–493

Sakallioglu T, Bakirdoven M, Temizel I, Demirel B, Copty NK, Onay TT, Demirel CSU, Karanfil T (2016) Leaching of nano-ZnO in municipal solid waste. Under Rev J Hazard Mater

Saleh N, Kim H-J, Phenrat T, Matyjaszewski K, Tilton RD, Lowry GV (2008) Ionic strength and composition affect the mobility of surface-modified Fe^0 nanoparticles in water-saturated sand columns. Environ Sci Technol 42:3349–3355

San I, Onay TT (2001) Impact of various leachate recirculation regimes on municipal solid waste degradation. J Hazard Mater 87:259–271

Schmidt J, Vogelsberger W (2009) Aqueous long-term solubility of titania nanoparticles and titanium (IV) hydrolysis in a sodium chloride system studied by adsorptive stripping voltammetry. J Solution Chem 38:1267–1282

Sen TK, Khilar KC (2006) Review on subsurface colloids and colloid associated contaminant transport in saturated porous media. Adv Colloid Interface Sci 119:71–96

Sima L, Amador J, da Silva AK, Miller SM, Morse AN, Pellegring ML, Rock J, Wells MJM (2014) Emerging pollutants—part I: occurrence, fate and transport. Water Environ Res 86:1994–2035

Siripattanakul-Ratpukdi S, Fürhacker M (2014) Review: issues of silver nanoparticles in engineered environmental treatment systems. Water Air Soil Pollut 225:1939–1956

Steenhuis TS, Dathe A, Zevi Y, Smith JL, Gao B, Shaw SB, DeAlwis D, Amaro-Garcia S, Fehrman R, Cakmak ME, Toevs IC, Liu BM, Beyer SM, Crist JT, Hay AG, Richards BK, DiCarlo D, McCarthy JF (2006) Biocolloid retention in partially saturated soils. Biologia 61: S229–S233

Strobel C, Oehring H, Herrmann R, Förster M, Reller A, Hilger I (2015) Fate of cerium dioxide nanoparticles in endothelial cells: exocytosis. J Nanopart Res 17:206–219

Szymczycha-Madeja A, Mulak W (2009) Comparison of various digestion procedures in chemical analysis of spent hydrodesulphurization catalyst. J Hazard Mater 164:776–780

Torkzaban S, Kim Y, Mulvihill M, Wan J, Tokunaga TK (2010) Transport and deposition of functionalized CdTe nanoparticles in saturated porous media. J Contam Hydrol 118:208–217

van Bussel W, Kerkhof F, van Kessel T, Lamers H, Nous D, Verdonk H, Verhoeven B, Boer N, Toonen H (2010) Accurate determination of titanium as titanium dioxide for limited sample size digestibility studies of feed and food matrices by inductively coupled plasma optical emission spectrometry with real-time simultaneous internal standardization. At Spectrosc 31:81–88

Vogelsberger W, Schmidt J, Roelofs F (2008) Dissolution kinetics of oxidic nanoparticles: the observation of an unusual behavior. Colloids Surf A 324:51–57

Yang GCC, Tu H-C, Hung C-H (2007) Stability of nano-iron slurries and their transport in the subsurface. Sep Purif Technol 58:166–172

Yang Y, Xu M, Wall J, Hu Z (2012) Nanosilver impact on methanogenesis and biogas production from municipal solid waste. Waste Manag 32:816–825

giovanni.libralato@unina.it

Yang Y, Zhang C, Hu Z (2013a) Impact of metallic and metal oxide nanoparticles on wastewater treatment and anaerobic digestion. Environ Sci Process Impacts 15:39–48

Yang Y, Gajaraj S, Wall JD, Hu Z (2013b) A comparison of nanosilver and silver ion effects on bioreactor landfill operations and methanogenic population dynamics. Water Res 47:3422–3430

Zhang Q, Zhang K, Xu D, Yang G, Huang H, Nie F, Liu C, Yang S (2014) CuO nanostructures: synthesis, characterization, growth mechanisms, fundamental properties, and applications. Prog Mater Sci 60:208–337

giovanni.libralato@unina.it